Publication Date: June 1, 1969 | doi: 10.1021/ba-1969-0080.fw001

Chemical Reactions in Electrical Discharges

In Chemical Reactions in Electrical Discharges; Blaustein, B.;
Advances in Chemistry; American Chemical Society: Washington, DC, 1969.

Publication Date: June 1, 1969 | doi: 10.1021/ba-1969-0080.fw001

In Chemical Reactions in Electrical Discharges; Blaustein, B.;
Advances in Chemistry; American Chemical Society: Washington, DC, 1969.

Chemical Reactions in Electrical Discharges

A symposium co-sponsored by the Division of Fuel Chemistry and the Division of Physical Chemistry at the 153rd Meeting of the American Chemical Society, Miami Beach, Fla., April 11-13, 1967.

Bernard D. Blaustein

Symposium Chairman

ADVANCES IN CHEMISTRY SERIES 80

AMERICAN CHEMICAL SOCIETY

WASHINGTON, D. C. 1969

Publication Date: June 1, 1969 | doi: 10.1021/ba-1969-0080.fw001

Publication Date: June 1, 1969 | doi: 10.1021/ba-1969-0080.fw001

Library of Congress Catalog Card 70-76951

PRINTED IN THE UNITED STATES OF AMERICA

Advances in Chemistry Series

Robert F. Gould, *Editor*

Advisory Board

AMERICAN CHEMICAL SOCIETY PUBLICATIONS

Publication Date: June 1, 1969 | doi: 10.1021/ba-1969-0080.fw001

In Chemical Reactions in Electrical Discharges; Blaustein, B.;
Advances in Chemistry; American Chemical Society: Washington, DC, 1969.

Publication Date: June 1, 1969 | doi: 10.1021/ba-1969-0080.fw001

FOREWORD

ADVANCES IN CHEMISTRY SERIES was founded in 1949 by the American Chemical Society as an outlet for symposia and collections of data in special areas of topical interest that could not be accommodated in the Society's journals. It provides a medium for symposia that would otherwise be fragmented, their papers distributed among several journals or not published at all. Papers are refereed critically according to ACS editorial standards and receive the careful attention and processing characteristic of ACS publications. Papers published in ADVANCES IN CHEMISTRY SERIES are original contributions not published elsewhere in whole or major part and include reports of research as well as reviews since symposia may embrace both types of presentation.

In Chemical Reactions in Electrical Discharges; Blaustein, B.;
Advances in Chemistry; American Chemical Society: Washington, DC, 1969.

PREFACE

As far as we are aware, this symposium on "Chemical Reactions in Electrical Discharges" was the first ever held on this topic. There was a surprisingly large amount of interest shown in this symposium, before, during, and after the meeting. This is good evidence that activity in this field of chemistry is growing. This volume contains almost all the papers that were presented in the symposium. In addition, three other papers are included although they were not presented as talks.

The work described in this volume demonstrates that many interesting chemical reactions can be carried out in electrical discharges. It is evident, too, that this symposium has shown how little is known concerning the importance and interrelationships of the many physical and chemical variables involved in the very complex discharge reactions; the mechanisms by which these reactions occur are essentially unknown. This is one of the areas where work should be concentrated in the near future.

In arranging this symposium, we tried to cover as wide a range of relevant topics as possible. It was intentional that physicists, chemists, and engineers were all brought together for this meeting. Even though the term is used perhaps too much these days, it can truly be said that this area of chemistry is interdisciplinary. Collaboration between workers in the different disciplines will be necessary for progress to be made in this field. From a theoretical viewpoint, the subject is as much physics as chemistry. From a practical standpoint, the chemists and physicists will have to work with the engineers in order to make discharges useful industrial processes.

Lastly, I would like to acknowledge the very helpful assistance given me in organizing this symposium by the program chairman of the Division of Fuel Chemistry, Irving Wender; and the financial support for several speakers furnished by the United States Air Force Office of Scientific Research, Department of Defense.

BERNARD D. BLAUSTEIN

Pittsburgh Coal Research Center
U.S. Bureau of Mines
Pittsburgh, Pa.

August 1967

Publication Date: June 1, 1969 | doi: 10.1021/ba-1969-0080.pr001

Chemical Physics of Discharges

WADE L. FITE

Department of Physics, University of Pittsburgh, Pittsburgh, Pa.

This introductory paper to the symposium reviews some of the basic physical processes operating to provide the chemical environment found in low pressure gas discharges. Electron collisions with neutrals are first treated as a basis for understanding the appearance of high electron temperatures, and then ambipolar diffusion is discussed as a plasma loss mechanism. Gas-phase electron production and loss mechanisms are then enumerated and the balance of electrons, positive ions and negative ions in a discharge is considered. Electron-impact excitation processes are enumerated and compared, and the consideration of wall effects concludes the discussion of microscopic processes. The role of plasma polarization as a macroscopic process is discussed and the paper ends with a comparison of active discharges and discharge afterglows.

Publication Date: June 1, 1969 | doi: 10.1021/ba-1969-0080.ch001

Gas discharge as a chemical tool is of interest for the environment which it provides, an environment which in many respects is very close to and in others very far away from thermal and chemical equilibrium. For example, while the electrons and the heavy particles both have velocity distributions very close to the equilibrium Maxwell-Boltzmann distribution, the temperatures of the two groups of particles are widely disparate; while the temperature of both the atoms and molecules present in a hydrogen discharge is very close to room temperature, the dissociation fraction as evidenced by modulated beam mass spectrometry is that which would be expected for hydrogen in equilibrium to 4000°K.!

Achieving such a peculiar environment is a result of the physical processes occurring to sustain the electrical characteristics of the discharge and of the chemical processes both in the gas phase and at walls involving both the ions and the neutral particles.

In attempting to understand discharges, one would first like to understand the microscopic processes and then construct a complete and

In Chemical Reactions in Electrical Discharges; Blaustein, B.;
Advances in Chemistry; American Chemical Society: Washington, DC, 1969.

accurate synthesis to describe the macroscopic characteristics. This approach of course requires detailed knowledge of all the processes with their rates and cross sections, knowledge which is simply not in hand. Even if it were available, the complexities of such constructions are enormous and one probably will always be forced to formulate macroscopic descriptions and work toward a juncture of the macroscopic viewpoints with the microscopic constructions.

In this brief review, the microscopic point of view will be used primarily. Also in view of the fact that the other participants at this symposium will discuss extensively the heavy particle aspects of discharges; *i.e.*, the chemistry, it would appear appropriate in this report to emphasize the role of the electron in discharges. In the final analysis the electron is the *sine qua non* of a gas discharge, the agent which transfers the energy from an electrical power supply to the gas, the producer of the ions which will engage in the ion chemistry, and the exciter of molecules which will dissociate to form the free radicals from whence originate the chemical chain processes.

No attempt will be made in this review either to be complete or particularly current. The aim here is to summarize in a rudimentary way a few of the elementary physical processes without reference either to any specific type of discharge or to any particular gas in the discharge tube.

Publication Date: June 1, 1969 | doi: 10.1021/ba-1969-0080.ch001

Electron Motion and Behavior

Assumed that a gas is enclosed in a container and that a free electron has been produced—perhaps by a cosmic ray, or by the radiation from the experimenter's watch dial or from a piece of uranium glass in a graded seal, or by cold cathode emission by the very strong electric fields around a sharp point on an electrode in the discharge tube—if a d.c. electric field is imposed, the electron will respond according to Newton's law,

$$\dot{\vec{v}} = \frac{q}{m}\vec{E} \tag{1}$$

and begin to accelerate in free fall. This acceleration will continue until the electron has a collision with a gas molecule. If the energy of the electron at the time of collision is very low, only elastic scattering will be admitted. At higher energies large amounts of energy can be lost by the electron in exciting the molecule to high-lying states of internal energy and at higher energies yet, ionization can occur. The latter process is, of course, essential to achieve the electron multiplication and convert the gas with a single electron in it into a gaseous medium of high electrical conductivity.

In Chemical Reactions in Electrical Discharges; Blaustein, B.;
Advances in Chemistry; American Chemical Society: Washington, DC, 1969.

Since each type of collision has separate consequences for the discharge we consider them in turn. The collisions are of course statistical and we must incorporate statistics with particle mechanics in their treatment.

Elastic Collisions: Transfer of Energy. In elastic collisions of electrons with heavy gas molecules, two effects are of importance. First there is a redistribution of directions of travel of the electrons and second there is a very slight loss of energy (and therefore speed) as a very small amount of momentum and energy are transferred to the molecule by the electron.

At low energies; *i.e.*, a few e.v. and less, electron scattering tends to be isotropic in angle in the center of mass coordinates. This implies that if we examine many electrons immediately after they have had a collision the average vector velocity will be zero, but of course the average scalar speed will not be zero. The probability per unit time that an electron will have a collision (*i.e.*, the collision frequency) is given by

$$Z(c) = nQ(c)c \tag{2}$$

where n is the number density of molecules, c is the electron's speed and $Q(c)$ is the total cross section for elastic collisions. The cross section generally diminishes with increasing speed, although resonances in scattering impart considerable structure in the functional form of the cross section in the case of most gases.

We suppose that an electric field, E, is imposed in the z direction, and inquire about the component of velocity in the z direction, averaged over all electrons, $<v_z>$, which is identical to $<\vec{v}>$. Since each electron responds to the field in the same way, the average acceleration due to the field is that of each electron separately. Further, because the average velocity is zero following a collision, the loss of average velocity because of collisions is to good approximation just the product of the average collision frequency $<Z>$ and the average velocity. Thus, we can write that for the average velocity in the z direction

$$\frac{d<v_z>}{dt} = \frac{q}{m} E - <Z><v_z>. \tag{3}$$

When the steady state is achieved the left side vanishes, which implies that the pickup of directed velocity from the field is just balanced by the loss of directed velocity because of the randomization of direction of motion by the collisions. Under steady state collisions, then,

$$<v_z> = \frac{q}{m} \cdot \frac{1}{<Z>} \cdot E = \mu E \tag{4}$$

where μ is designated the mobility.

Publication Date: June 1, 1969 | doi: 10.1021/ba-1969-0080.ch001

In Chemical Reactions in Electrical Discharges; Blaustein, B.;
Advances in Chemistry; American Chemical Society: Washington, DC, 1969.

Equation 4 can be re-written in terms of Equation 2 as

$$\langle v_z \rangle = \frac{q}{m} \cdot \frac{1}{\langle cQ(c) \rangle} \cdot \frac{E}{n}. \tag{5}$$

In this expression the second term gives all the information about the interaction between the electron and the particular gas molecule and the third term contains the parameters available to the experimenter; *i.e.*, the electron field and the gas number density. Since the number density is proportional to the gas pressure, the experimental quantity of major relevance is the ratio E/p.

Randomization of directions of velocity says nothing whatever about average speeds of the particles. For this we turn to other considerations. Conservation of momentum requires that the energy loss from an electron of mass m and kinetic energy W in collision with a heavy particle of mass M is given by

$$\Delta W = W \frac{2m}{M} (1\text{-}\cos\theta) \tag{6}$$

where θ is the angle of deflection of the electron in the collision. If the scattering is isotropic (as it closely approximates at low energies) then the energy loss in a collision averaged over angle is

$$\overline{\Delta W} = \frac{2m}{M} W = hW \tag{7}$$

where for convenience we let $2m/M = h$.

We would expect a steady state ultimately to be achieved between the electron energy picked up from the electric field between collisions and the energy transmitted from the electron to the heavy particles through the collisions. We proceed to evaluate these separately. For simplicity we assume that the collision frequency is independent of speed of the electrons.

Since the electric field acts only in the z direction, all the increase in kinetic energy of an electron will occur through increasing the z component of its velocity which is given by

$$v_z = v_{oz} + at \tag{8}$$

where v_{oz} is the value of v_z immediately following the collision and t is the time elapsed since the last collision and $a = (q/m)E$. The energy picked up will be

$$\Delta W = qE \int dz = ma \int v_z dt = ma \{ v_{oz} t + \tfrac{1}{2} a t^2 \}. \tag{9}$$

If we now average over all angles of direction of motion immediately following the last collision, $\overline{v_{oz}} = 0$, so that

$$\overline{\Delta W} = \tfrac{1}{2} m a^2 t^2. \tag{10}$$

Publication Date: June 1, 1969 | doi: 10.1021/ba-1969-0080.ch001

If we now average over all collision times Equation 10 becomes

$$\overline{\Delta W}_{av} = \tfrac{1}{2}ma^2(t^2)_{av}. \tag{11}$$

To find $(t^2)_{av}$, we assume that collisions are random events and the collision frequency is independent of speed. We can then write that the probability of a collision occurring in the interval t to $t + dt$ following the preceding collision is

$$p(t)dt = Ze^{-zt}dt \tag{12}$$

for which the average value of t^2 is $2\tau^2$ where $\tau = 1/Z$ is the mean collision time. Equation 11 then becomes

$$\overline{\Delta W}_{av} = ma^2\tau^2. \tag{13}$$

If we also average over all speeds of electrons and neglect some of the finer points of statistics, Equation 13 becomes

$$<\overline{\Delta W}_{av}> \simeq ma^2 \frac{\lambda^2}{(\bar{c})^2}. \tag{14}$$

where λ is the mean free path and $\bar{c}$ is the mean speed of the electrons.

This quantity, in the steady state, will equal the right hand side of Equation 7 averaged over all electrons. If we let $W \simeq \frac{1}{2}m(c)^2$

$$\tfrac{1}{2}hm(\bar{c})^2 \simeq ma^2 \frac{\lambda^2}{(\bar{c})^2}. \tag{15}$$

Thus, we would expect that the mean speed would be given by

$$(\bar{c})^4 \simeq 2\frac{a^2\lambda^2}{h} \tag{16}$$

and the mean energy of the electrons in the steady state by

$$\tfrac{1}{2}m(\bar{c})^2 \simeq \tfrac{1}{2}m\overline{(c^2)} \simeq \tfrac{1}{2}\sqrt{\frac{M}{m}}\,qE\lambda. \tag{17}$$

The remarkable aspect of this result comes on the insertion of numbers in Equation 17. If for example, one has electrons moving through a gas with $M \sim 30$ a.m.u., at pressures giving $\lambda \sim 1$ mm.—*i.e.*, p $\sim$ .25 torr —then the mean energy in e.v. is around 25 times the field strength in volts/cm. With as little as a few tenths of volts/cm. fields, mean electron energies are several e.v. We can thus understand the appearance of high electron "temperatures" in gas discharges.

It can be shown that if one assumes that only elastic collisions occur one can obtain an approximate solution of the Boltzmann equation for the distribution of speeds. The result is not the Maxwell-Boltzmann dis-

Publication Date: June 1, 1969 | doi: 10.1021/ba-1969-0080.ch001

In Chemical Reactions in Electrical Discharges; Blaustein, B.;
Advances in Chemistry; American Chemical Society: Washington, DC, 1969.

tribution, but rather that known as the Druyvesteyn distribution whose dependence on speed is given by

$$f(c)dc \propto c^2 e^{-\frac{3hc^4}{8\lambda^2 a^2}} dc. \tag{18}$$

This distribution function is similar in shape to the Maxwell-Boltzmann distribution for a given mean speed, except that the most probable speed is slightly higher and the high energy tail is diminished in the Druyvesteyn distribution. Nonetheless, the distributions are sufficiently similar that one can, to good approximation, think of the electrons as having a temperature in the Maxwellian sense which is much higher than the neutral gas temperature—*i.e.*, typically 30,000°K. *vs.* 300°K. It is this dichotomy of temperatures which is perhaps the most striking of the non-equilibrium aspects of a gas discharge.

This general effect of collisions randomizing the direction of motion of electrons which have picked up energy from the field between collisions has another important manifestation. It is responsible for the operation of microwave electrodeless discharges. If we consider an electron moving in an a.c. field which is of the form $E(t) = E_0 \cos \omega t$, then Newton's law for the electron becomes, in the absence of collisions,

$$v = \frac{q}{m} E_0 \cos\omega t \tag{19}$$

which solves to give

$$v = \frac{qE_0}{m\omega} \sin\omega t \text{ and } x = -\frac{qE_0}{m\omega^2} \cos\omega t. \tag{20}$$

The rate of energy pickup from the field—*i.e.*, the power, P—is given by

$$P = q\mathrm{E}v = \frac{q^2 E_0^2}{m\omega} \cos\omega t \sin\omega t, \tag{21}$$

which, it is noted can be negative as well as positive. If we consider the total power pickup over a complete cycle, the sine-cosine product integrates to zero, indicating that there is no net transferral of energy from the electric field to the electron. This is of course a result of the fact that the applied field and the electron velocity are 90° out of phase.

Furthermore, we can note from Equation 20 that the maximum electron velocity will be $qE_0/m\omega$ and the maximum kinetic energy will be

$$W_{\max} = \tfrac{1}{2} \frac{q^2 E_0^2}{m\omega^2}. \tag{22}$$

It is noted that if one has a field oscillating at say 10^9 c.p.s. and a maximum field strength of say 300 volts/cm., Equation 22 indicates that the maximum kinetic energy of the freely oscillating electron will be only

Publication Date: June 1, 1969 | doi: 10.1021/ba-1969-0080.ch001

about 2 e.v. This is insufficient energy to ionize gases, and yet breakdown will occur for this type of field.

Collisions are responsible for build-up of energy to the point where ionization can occur. An electron will be accelerated by the field during a portion of its cycle and then be deflected in a collision. Then energy parallel to the electric field is thus converted to energy perpendicular to the field. The field then proceeds to give the electron additional energy in the direction of the field. Energy is pumped from kinetic energy of motion parallel to the field to kinetic energy in all directions.

If we write Newton's law for an electron, adding a collision term, we are left with Equation 3, except now, E is time-dependent. Writing $E = E_o \cos\omega t$

$$\frac{d\langle v\rangle}{dt} = \frac{qE_o}{m}\cos\omega t - Z\langle v\rangle \tag{23}$$

The power delivered to an electron by the field, averaged over a cycle, is

$$P = \tfrac{1}{2}\frac{q^2E_o^2}{m}\frac{Z}{Z^2+\omega^2} \tag{24}$$

This equation shows directly the role of collisions of electrons in conversion of electrical energy to energy of the gas.

Again if this power gain is equated to the loss of energy of electrons in elastic collisions with the gas molecules, as would occur in the steady state, then

$$h \cdot \tfrac{1}{2}m(\bar{c})^2 \cdot Z \simeq \frac{q^2E_o^2}{m}\frac{Z}{Z^2+\omega^2} \tag{25}$$

or since $Z = \dfrac{\bar{c}}{\lambda}$

$$\tfrac{1}{2}m(\bar{c})^2 \simeq \frac{\lambda a}{h}\left\{\sqrt{1+\frac{\lambda^2\omega^2}{a^2h}} - \frac{\lambda\omega}{a\sqrt{h}}\right\} \tag{26}$$

where $a \equiv \dfrac{qE_o}{m}$.

From Equation 26 one would expect the electron "temperature" for fixed E_o to diminish with increasing frequency, but for pressures of the order of one torr and gas masses of around 30 a.m.u. the electron temperature will remain near the d.c. value for frequencies usually employed for gas discharge work.

It must be pointed out that considering only elastic collisions in deriving an electron temperature of several e.v. is unrealistic for molecular gases of interest to the chemist. Inelastic collisions leading to excitation of rotational, vibrational, and low-lying electronic states in molecules can enter the picture in major ways. Understanding in detail the way in which an electron energy distribution is established in most real cases of

Publication Date: June 1, 1969 | doi: 10.1021/ba-1969-0080.ch001

In Chemical Reactions in Electrical Discharges; Blaustein, B.;
Advances in Chemistry; American Chemical Society: Washington, DC, 1969.

interest is an incredibly difficult matter. In general, however, something resembling a Maxwellian distribution is established and it is common to speak of "electron temperature" which typically ranges around 2 or 3 e.v.

Elastic Collisions and Diffusion. Since in either d.c. or a.c. discharges, the electrons will have high temperatures, one can expect that all the manifestations of a kinetic temperature will be present. Particularly important among these is diffusion through elastic collisions. If only electrons are present in a neutral gas they will tend to diffuse as would any other gaseous component with a current density

$$\vec{S}_e = n\langle\vec{v}_e\rangle = -D_e \nabla n_e \tag{27}$$

where n_e is the number density of the electrons and D_e is the diffusion coefficient of the electrons through the gas. If a field is also superposed, the current density will contain a mobility term as well so that

$$\vec{S}_e = -D_e \nabla n_e - n_e \mu_e \vec{E} \tag{28}$$

where the minus sign in the second term indicates that because of the negative charge on the electrons, their motion will try to be in the direction opposite to that of the applied field. μ_e is taken to be a positive number. Whether the electron motion is diffusion-dominated or field dominated depends on whether the first term is larger than or smaller than the second.

In a gas discharge, the electrons will have produced ions and these also will tend to diffuse through the neutral gas as well as respond to any electric fields. The current density of ions will be given therefore by a similar equation

$$\vec{S}_+ = -D_+ \nabla n_+ + n_+ \mu_+ \vec{E}. \tag{29}$$

From Equation 4 the mobility of either type of particle is

$$\mu = \frac{q}{m\langle Z\rangle} \tag{30}$$

and from kinetic theory, the diffusion coefficient is given by

$$D = \frac{kT}{m\langle Z\rangle}. \tag{31}$$

Since both these parameters have the mass appearing in the denominator the electron will diffuse and respond to an electric field much more rapidly than will the heavy ions.

The case of major interest for discharge physics is that where the number density of ions is very nearly equal to that of the electrons. Clearly because the electron mass is very light these will try to diffuse away from the ions. However, as soon as they do this, an electric field is

Publication Date: June 1, 1969 | doi: 10.1021/ba-1969-0080.ch001

In Chemical Reactions in Electrical Discharges; Blaustein, B.;
Advances in Chemistry; American Chemical Society: Washington, DC, 1969.

set up between the electrons and ions so that the electrons are held back by the ions and the ions are dragged along by the electrons. We would thus expect that the current fluxes S_e and S_+ would be equal.

If we set $S_e \doteq S_+ \equiv S$, and $n_e = n_+ \equiv n$, to indicate an electrically neutral plasma, Equations 28 and 29 can be combined to eliminate the electric field with the result that

$$S = -D_a \nabla n \tag{32}$$

where

$$D_a = \frac{\frac{D_+}{\mu_+} + \frac{D_e}{\mu_e}}{\frac{1}{\mu_+} + \frac{1}{\mu_e}}. \tag{33}$$

Since $\frac{D_+}{\mu_+} = \frac{kT_+}{q_+}$ and $\frac{D_e}{\mu_e} = \frac{kT_e}{\mu_e}$ and $\frac{1}{\mu_+} >> \frac{1}{\mu_e}$ we can write

$$D_a \simeq \frac{k\mu_+}{e}(T_+ + T_e) \tag{34}$$

or

$$D_a \cong \frac{k\mu_+ T_+}{e}\left(1 + \frac{T_e}{T_+}\right) = D_+\left(1 + \frac{T_e}{T_+}\right). \tag{35}$$

If the electron temperature is equal to the ion temperature, as in the case of late in an afterglow, the ambipolar diffusion coefficient is just twice the value of D_+. In the active discharge, however, as we have seen T_e will be large, perhaps of the order of 30,000°K. On the other hand the ion temperature will deviate little from the neutral gas temperature. The reason is that the ion mass is comparable with the neutral gas temperature; thus, by arguments similar to those leading to Equation 7 the ion will in a single collision be able to give to the neutral gas virtually all of the energy it picks up from the field between collisions. The temperature of the ions will therefore remain very close to the neutral gas temperature, and the ratio T_e/T_+ will be of the order of 100 typically in an active discharge. Thus, ambipolar diffusion will proceed much more rapidly than would diffusion of free ions.

By the same token ambipolar diffusion will be slower than would be diffusion of free electrons. The drag on the electrons by the ions inhibits their diffusion and tends to keep the electrons in the gas and away from the walls where they would be lost from the discharge.

Electron Loss Processes. Ambipolar diffusion to the walls is an important mechanism for loss of electrons from the discharge. It is appropriate to enumerate other electron loss mechanisms and then balance these against the various production mechanisms operative in a sustained discharge.

Publication Date: June 1, 1969 | doi: 10.1021/ba-1969-0080.ch001

In Chemical Reactions in Electrical Discharges; Blaustein, B.;
Advances in Chemistry; American Chemical Society: Washington, DC, 1969.

Foremost among the gas-phase mechanisms for electron loss is recombination between electrons and ions. Under the usual gas discharge conditions molecular ions are present (even in the inert gases, diatomic molecular ions exist stably), and the reaction process is that of dissociative recombination; *i.e.*,

$$e + AB^+ \rightarrow A + B. \tag{36}$$

The process is strictly two-body, since the two products can conserve energy and momentum, and the rate of electron density loss can be described by

$$\frac{dn_e}{dt} = -\alpha_d n_e n_+, \tag{37}$$

where α_d is the dissociative recombination coefficient, values for which are typically of the order of 10^{-7} cc. sec.$^{-1}$. Since the plasma is almost electrically neutral, the electron and ion densities are almost equal and Equation 37 can be rewritten

$$\frac{dn_e}{dt} \simeq -\alpha_d n_e^2 \tag{38}$$

At number densities of the order of 10^{10} cm.$^{-3}$, the lifetime of an electron against recombination is around a millisecond.

At electron densities of the order of 10^{12} cm.$^{-3}$, a second recombination process becomes of consequence. This is three-body recombination with an electron as the third body; *i.e.*,

$$A^+ + e + e \rightarrow A + e. \tag{39}$$

Since the atom A is preferentially formed either directly or in subsequent electron interactions in an excited state which can radiate, this process is often designated as collisional-radiative recombination. For most laboratory gas discharges in which $n_e \sim 10^{10}$ cm.$^{-3}$, this process is not of consequence.

Radiative recombination; *i.e.*,

$$A^+ + e \rightarrow A + h\nu \tag{40}$$

occurs so slowly as to be negligible. Typically the radiative recombination coefficient is five orders of magnitude below that for dissociative recombination. Other recombination processes are of comparable magnitude and are negligible.

Electrons can also be lost through attachment to form negative ions in those gases for which stable negative ions exist. Three-body attachment,

$$e + A + B \rightarrow A + B^- \tag{41}$$

Publication Date: June 1, 1969 | doi: 10.1021/ba-1969-0080.ch001

can exist at all energies and occurs with rate coefficients of the order of 10^{-30} cm.^{6} sec.$^{-1}$ which is equivalent to an electron lifetime in typical discharge conditions of the order of 1 millisecond. Three-body attachment can compete for electrons with dissociative recombination.

A second attachment process is dissociative attachment to molecules; *i.e.*,

$$e + AB \rightarrow A + B^- . \qquad (42)$$

This process usually requires the electron to have an energy of a few e.v. in order to proceed, but of course this energy is provided by the high electron temperature in a gas discharge. In general the rate coefficients for this process can range as high as 10^{-10} cc. sec.$^{-1}$ for groundstate molecules and some evidence is in hand suggesting that the process can proceed much more rapidly if the molecule is vibrationally and/or rotationally excited. Even with a rate of 10^{-10} cc. sec.$^{-1}$, in a gas discharge at a fraction of a torr, the electron lifetime against dissociative attachment is of the order of a microsecond and therefore this process can completely overwhelm dissociative recombination as an electron loss mechanism.

However, it is wrong to suppose that such a rapid attachment process will describe the rate of removal of electrons. The reason is that when an electron recombines with an ion, the electron becomes tightly bound in an atom with an energy of 10 e.v. or more, while in forming a negative ion the electron binding energy is an order of magnitude less. Numerous processes in the discharge operate to liberate the electron from the negative ion, among these being photodetachment ($h\nu + B^- \rightarrow B + e$), associative detachment ($A + B^- \rightarrow AB + e$) and electron-impact neutralization $e + B^- \rightarrow 2e + B$. Of these various processes it appears that the most important for usual gas discharges will be associative detachment. Rates in several cases have been measured by the group of E. E. Ferguson (*1*) at values of the order of 10^{-10} cc. sec.$^{-1}$. The rapidity of both negative ion destruction and negative ion formation through dissociative attachment implies that a steady state is quickly achieved between the electron negative ion concentrations. As dissociative recombination operates on the electrons in this steady state situation and mutual neutralization occurs between positive and negative ions, it is straightforward to show that the loss of electron density in the plasma is described by Equation 38 where

$$\alpha = \text{effective recombination coefficient} = \alpha_d + \lambda\alpha_i \qquad (43)$$

where α_d is the electron-ion dissociative recombination coefficient, α_i is the coefficient for mutual neutralization between positive and negative ions and λ is the ratio of negative ions to electrons. Thus, electron loss is enhanced by electron attachment followed by mutual neutralization,

Publication Date: June 1, 1969 | doi: 10.1021/ba-1969-0080.ch001

In Chemical Reactions in Electrical Discharges; Blaustein, B.;
Advances in Chemistry; American Chemical Society: Washington, DC, 1969.

the actual rate being dependent on the steady state ratio of concentration of negative ions to that of electrons.

Electron Production Processes. The important electron production processes occur in the gas phase and, in the case of discharges with electrodes, at electrode surfaces. The major surface processes are: (a) secondary electron emission on ion impact at the cathode, (b) field emission at sharp points on electrodes, and (c) thermionic emission in the case of arc-type discharges where electrodes become strongly heated. These are the sources of the primary electrons in d.c. and low frequency discharges.

The large bulk of electrons in discharges are secondary electrons made in the gas phase. A process always operative in gas discharges is simple electron-impact ionization,

$$e + A \rightarrow 2e + A^+ \tag{44}$$

where A is a groundstate neutral molecule or atom. Since only electrons in the rapidly diminishing high-energy tail of the electron energy distribution have sufficient energy to ionize, and since for the first few e.v. above threshold ionization cross sections are approximately linear with energy, the rate coefficient for ionization

$$\eta = \frac{2}{m}\int_{E_o}^{\infty} E^{1/2}Q(E)f(E)\,dE \cong \frac{2}{m}\left(\frac{dQ}{dE}\right)\int_{E_o}^{\infty} E^{1/2}(E - E_o)f(E)\,dE, \tag{45}$$

where E_o is the ionization threshold and $f(E)$ is the electron energy distribution function. If we equate electron production rate to the rate of loss through diffusion and recombination, we have the plasma balance equation for the steady state discharge,

$$D_a \nabla^2 n_e = \eta n_e n_o + \alpha n_e^2 \tag{46}$$

where n_o is the number density of neutrals in the discharge. This equation can be solved using the boundary conditions that $n_e = 0$ at the walls to determine the spatial distribution of electrons.

Electron-impact Excitation. The high temperature electrons in a plasma are able to excite as well as ionize neutral atoms and molecules in the discharge. The thresholds for excitation are lower than for ionization and the cross sections for excitation rise more rapidly with energy above the threshold energy than do those for ionization, and therefore the tail of the electron energy distribution can be more effective in producing excitation than in producing ionization. The excitation on electron impact is largely responsible for the light issuing from a discharge and is responsible for the production of active neutral species of chemical interest in a gas discharge.

Publication Date: June 1, 1969 | doi: 10.1021/ba-1969-0080.ch001

In Chemical Reactions in Electrical Discharges; Blaustein, B.;
Advances in Chemistry; American Chemical Society: Washington, DC, 1969.

The effects of simple excitation,

$$e + A \rightarrow e + A^* \tag{47}$$

depend on the lifetime of the excited state A*. For radiating states the lifetime is of the order of 10^{-8} seconds and little can occur before a photon is emitted returning the atom to some lower state. For most radiation the light will simply escape. If the radiation takes place to the ground-state, then the photon can be re-absorbed by a neighboring atom or molecule which is then excited. This is a phenomenon of resonance radiation absorption. Under these circumstances the photon must diffuse out of the gas discharge. Since in general the time of transit of a photon between particles is small compared with the mean life of the excited atom, having a resonance radiation photon in a discharge is effectively equivalent to having an excited atom whose lifetime is equal to the time required for the photon to escape the discharge which can be several times longer than the natural lifetime of the excited state.

In addition to the "equivalent metastable neutrals" from resonance radiation entrapment, excitation can lead to true metastable states; *i.e.*, states whose lifetime against radiative decay is long (microseconds to seconds and more). These metastable neutrals will be destroyed by collision processes in the gas discharge.

Neutrals with high electronic excitation can be very effectively ionized by both electrons and photons in the discharge, and they can ionize a neutral whose ionization potential is lower than the excitation energy (Penning ionization). These processes can contribute substantially to the plasma electron balance. Of perhaps more interest from the point of view of chemistry is the conjecture that excited neutrals may be able to engage in reactions which are forbidden to ground-state neutrals. The question of the extent to which "activation energy" can be provided by internal energy alone appears not well established and is a question to which molecular beam experiments may provide the answer.

If the particle to be excited is a molecule, the possibility of dissociative decay is open; *i.e.*,

$$e + AB \rightarrow e + (AB)^* \rightarrow e + A + B. \tag{48}$$

For this process to occur it is of course necessary for the electron energy and the energy of excitation achieved within the limits of Franck-Condon transition must exceed the dissociation energy. Not only is this a very effective mechanism for the formation of free radicals in a discharge, but further the fragments are usually formed with kinetic energies appreciably higher than the ambient thermal energies.

It would appear that the elemental gas-phase process of major importance to gas discharge chemistry is electron impact excitation, for this

Publication Date: June 1, 1969 | doi: 10.1021/ba-1969-0080.ch001

In Chemical Reactions in Electrical Discharges; Blaustein, B.;
Advances in Chemistry; American Chemical Society: Washington, DC, 1969.

produces the free radicals (and perhaps the excited molecules and atoms) which are the starting reactants in the neutral chemical chains operating in the gas discharge.

Unfortunately at this point, detailed understanding of excitation processes is far from complete even in the case of the very simplest molecules. It is virtually impossible to predict except in a qualitative way active reactants that will be created in a gas discharge through the basic electron-impact excitation processes.

Wall Effects. In d.c. discharges where steady fields tend to drain the electrons toward the anode and ions toward the cathode, production of new primary electrons at the cathode is essential to the sustenance of the discharge. If the cathode is very hot, as in an arc discharge, thermionic emission of electrons provides these new electrons. In cold cathode discharges, obtaining new primary electrons depends on interactions between the discharge and the surface. The most important such interaction is the emission of secondary electrons by a metal which is struck with an energetic positive ion. In a glow discharge, ions drifting toward the cathode pick up energies of the order of 100 e.v. or more in the cathode dark space and eject electrons with an efficiency in the range from 10^{-2} to 10^{-1} typically. Other processes, usually of less import, are photoemission by ultraviolet photons produced in the plasma and by electron ejection on impact of a metastable neutral whose excitation energy exceeds the work function of the material.

At insulating walls or conducting walls which are electrically isolated charges of one sign can be captured and held until charges of the opposite sign move in from the plasma to neutralize them. At electrode walls charge can be taken directly into the external circuitry of the discharge.

The major wall effects from the point of view of discharge chemistry deal not with electron production and loss mechanisms but with the surface catalytic effects of walls. Regretably the present state of knowledge of such wall effects is in particularly bad shape. To illustrate this statement, we can consider the problem of producing beams of hydrogen atoms in borosilicate glass radiofrequency electrodeless discharge sources for atomic beam experiments. It is the author's experience that very poor dissociation (of the order of 10%) is achieved if one puts moderately clean H_2 into a clean vessel. If one adds a few percent of O_2 to the gas the dissociation improves, perhaps achieving of the order of 50%. If one removes the H_2 altogether and runs a discharge in O_2 for a few minutes, then removes the O_2 and replaces it with only H_2, the dissociation fraction commonly reaches 90% and more and the source continues to operate for up to several hours at high (although deteriorating) dissociation. Evidently running the discharge in O_2 does something to cause the walls to lose their ability to recombine the atoms back into molecules. Some workers

Publication Date: June 1, 1969 | doi: 10.1021/ba-1969-0080.ch001

In Chemical Reactions in Electrical Discharges; Blaustein, B.;
Advances in Chemistry; American Chemical Society: Washington, DC, 1969.

condition the interior walls of such sources in other ways and several chemicals painted on the inside of the discharge tube prior to use are alleged to improve dissociation of H_2.

In the opinion of the writer, our abysmally poor understanding of adsorption of gas discharge products by discharge tube walls and the catalysis of reactions by these walls is the major blind spot in understanding of the chemistry which occurs in discharges.

Plasma Polarization

From the point of view of both the electrical and chemical properties of a discharge, perhaps the most important macroscopic consequence of a plasma state is the shielding which it provides against electrical fields. With highly mobile electrons and ions present, any attempt to apply a field will be nullified in great measure by the polarization of the plasma, and the field will be able to be felt only near the edges of the plasma.

Recalling that the electrons can be thought of as being in thermal equilibrium with themselves, the electron density will be given by

$$n = n_0 e^{\frac{e\phi}{kT_e}} \tag{49}$$

where ϕ is the electrical potential and n_0 is the electron number density deep in the plasma where we choose to call the value of $\phi = 0$. If we consider a one-dimensional case, Maxwell's first equation states that

$$\frac{d^2\phi}{dx^2} = 4\pi e(n_e - n_+). \tag{50}$$

If we assume that the ions are stationary (a good approximation for say a radio-frequency discharge where because of their large mass the ions will not respond to the rapidly changing field), then $n_+ = n_0$, and deep in the plasma where $e\phi/kT_e$ is small the exponential can be expanded in a Taylor series. Equation 49 then becomes

$$\frac{d^2\phi}{dx^2} \simeq 4\pi e n_0 \left(1 + \frac{e\phi}{kT_e} - 1\right) = \frac{1}{\lambda_D{}^2}\phi \tag{51}$$

where

$$\lambda_D = \left(\frac{kT_e}{4\pi n e^2}\right)^{1/2} \tag{52}$$

is the Debye length.

The solution,

$$\phi \propto e^{-\frac{x}{\lambda_0}} \tag{53}$$

Publication Date: June 1, 1969 | doi: 10.1021/ba-1969-0080.ch001

In Chemical Reactions in Electrical Discharges; Blaustein, B.;
Advances in Chemistry; American Chemical Society: Washington, DC, 1969.

indicates that both the potential and the electric field will decay exponentially with the Debye length describing the decay. For a plasma of $T_e = 2.5$ e.v. and a number density 10^{10} cm.$^{-3}$, the Debye length is approximately 10^{-2} cm. Obviously the polarization of the plasma enormously inhibits the electrical fields in the interior a discharge and is the cause of the weak-field condition which exists in the interior of RF. discharges. Similarly it is the plasma polarization which is responsible for the electrical fields throughout the bulk of the positive column of a d.c. glow discharge being weak and for the major share of the potential drop across the tube occurring near the cathode.

In view of the small fields within a well developed plasma and the fact that ions can readily transfer kinetic energy to the neutral molecules, one expects that the ion and neutral kinetic temperatures will be very similar and only slightly higher than the temperature of the walls of the discharge. As we have seen before electron temperatures can be high even in quite weak fields owing to the poor exchange of energy between electrons and heavy particles.

Publication Date: June 1, 1969 | doi: 10.1021/ba-1969-0080.ch001

Afterglows

When one removes the electrical power from a discharge and the gas begins its decay back to quiescent neutrality, one speaks of the afterglow regime. Afterglows are commonly produced in either of two ways: by removing the electrical power from a discharge in a closed discharge tube or by allowing the gas to flow in a rapidly pumped tube away from the region where the electrical power is applied.

In either experimental method the principal mechanism for maintaining a high electron temperature is removed. Under most circumstances the electrons will cool in elastic collisions with the neutral gas with temperature decay times of the order of 10 μsec. Excited states will decay according to their various lifetimes and at times of the order of a msec. one is left only with those species whose decay constants are slow.

Among the last species to go are the positive ions and electrons (and negative ions if the gas permits formation of negative ions). As they decay through both recombination and ambipolar diffusion to the walls, one has an optimum experimental arrangement for the study of the recombination processes themselves. Most of the recombination rate coefficient results have come from such afterglow experiments.

The afterglow presents a unique environment for the study of the ion chemistry of discharges also. In the absence of electron-impact ion production processes, the separate charge transfer and ion-molecule reaction processes can be displayed through mass spectrometric monitoring of the afterglow and in fact the large bulk of the thermal energy

In Chemical Reactions in Electrical Discharges; Blaustein, B.;
Advances in Chemistry; American Chemical Society: Washington, DC, 1969.

ion-neutral reaction rate data have been so obtained. Ferguson *et al.* (*2*) will discuss the results of such experiments.

Additionally mass spectrometry of afterglows reveals processes leading to the formation of very heavy complex ions and ion clusters which presumably are so weakly bound that they cannot exist in appreciable numbers in the fierce environment of an active discharge but which may very well exist in nature, for example in the earth's upper atmosphere (*3*).

Lastly, the flowing afterglow has been particularly significant as a contributor to our knowledge about neutral free radical reactions. In typical experiments the discharge through a suitable gas mixture is used to produce a copious supply of some particular reactants. By observing spectroscopically the spatial decay of a given species downstream in the afterglow one obtains information on the rate of reaction for the species. Kaufman (*4*) has been one of the leaders in this type of experimentation which is a major source of information on discharge chemistry.

It would be incorrect to suppose that afterglows are always simple. Long-lived metastable neutrals and ions introduce interpretational complexities and processes such as transfer of vibrational energy to kinetic energy of electrons can operate to keep electron temperatures from decaying as rapidly as would be desirable. However, study of the chemical physics of afterglows is at present among the most powerful ways to learn about the chemistry of gas discharges.

Publication Date: June 1, 1969 | doi: 10.1021/ba-1969-0080.ch001

Literature Cited

(1) Fehsenfeld, F. C., Ferguson, E. E., Schmeltekopf, A. L., *J. Chem. Phys.* **45**, 1844 (1966).
(2) Ferguson, E. E., Fehsenfeld, F. C., Schmeltekopf, A. L., ADVAN. CHEM. SER. **80**, 83 (1969).
(3) Fite, W. L., Rutherford, J. A., *Disc. Faraday Soc.* **37**, 192 (1964).
(4) Kaufman, Frederic, ADVAN. CHEM. SER. **80**, 29 (1969).

RECEIVED May 2, 1967.

2

Basic Parameters for Electrical Discharges in Gases

A. V. PHELPS

Westinghouse Research Laboratories, Pittsburgh, Pa.

Publication Date: June 1, 1969 | doi: 10.1021/ba-1969-0080.ch002

Combinations of the experimental parameters of electric field strength, frequency, gas density, container dimension, fractional ionization, and duration of applied voltage can be used to relate experimental data for electrical breakdown and for steady state discharges in simple gases over a wide range of these parameters. It is important that studies of the chemical effects of electrical discharges make use of these combinations of parameters and discover the additional parameters appropriate to the chemical aspects of the discharges.

Electrical discharges have been studied over a wide range of experimental conditions, ranging from d.c. to microwave frequencies for the applied electrical fields; pressures from a fraction of a torr to many atmospheres; power levels from a few watts to several megawatts; effective residence times of reacting species from a few microseconds to many seconds; and gases of a wide variety of compositions. It is therefore of interest to consider briefly the applicability of basic combinations of experimental parameters developed in connection with the study of simple gases (*6*, *16*, *17*, *22*, *35*, *42*, *57*) and to speculate as to others which might be investigated further. The use of these combinations leads to scaling laws which may be of use in predicting the properties of various discharges. Obviously, the present comments will be very qualitative and many will have to be tested against past and future experiments in which careful measurements are made of such quantities as the electric field strength, current density, electron density and temperature, gas temperature, gas flow rates, etc. Although numerous references are given, there are many other references which could have been cited.

In Chemical Reactions in Electrical Discharges; Blaustein, B.;
Advances in Chemistry; American Chemical Society: Washington, DC, 1969.

We now consider some specific combinations of experimental parameters and some examples of their application.

Electric Field to Gas Density Parameter

Fite (*21*), Kaufman (*29*), and Lunt (*37*) have all pointed out that theory shows (*35, 57*) that provided the degree of ionization and excitation of the gas is low the electron transport coefficients and rate coefficients for reactions caused by electrons in the presence of a d.c. electric field E and for a given gas mixture depend only on the value of E/N where N is the total gas density. We have used the E/N rather than the usual E/p because it is the gas density rather than the pressure p that is important and because we are concerned with a wide range of gas temperatures. The E/N value required to produce a given reaction rate coefficient varies considerably with the gas. As an indication of this we note that to obtain a mean electron energy of 1.5 e.v. in pure Ar one requires an E/N value of only 3×10^{-18} volts-cm.^{2} whereas to obtain the same mean electron energy in a highly polar gas such as H_2O one requires an E/N of 6×10^{-16} volts-cm.^{2}. These differences are because of the fact that at these energies in pure Ar the electrons lose energy only through the recoil of the heavy argon atoms in an elastic collision whereas in H_2O the electrons lose energy very rapidly owing to the excitation of rotational and vibrational states of the molecule. Because of the large cross sections for rotational and vibrational excitation of some molecular gases, small admixtures of molecular gases in the rare gases cause large charges in the mean electron energy and in the electron transport coefficients at fixed E/N.

The E/N parameter has been used by many workers (*16, 17, 34, 35, 41, 50, 57*) to compare measurements of the rate coefficients for the ionization of atoms and molecules by electron impact. However, only a few attempts have been made to obtain the data necessary to correlate experimental rate coefficients for chemical reactions such as molecular dissociation (*29, 36, 37*). Correlations of this kind are essential to the understanding of and prediction of the rates of chemical reactions in electrical discharges under various experimental conditions.

Effective Electric Field Strength

The concept of effective electric field strength was originally developed (*6, 42*) to take into account the observed frequency dependence of the electric field strength required for gas breakdown. However, this concept is of great general utility for reasonably homogeneous discharges since it allows one to compare the effect on the electrons of an applied

Publication Date: June 1, 1969 | doi: 10.1021/ba-1969-0080.ch002

In Chemical Reactions in Electrical Discharges; Blaustein, B.;
Advances in Chemistry; American Chemical Society: Washington, DC, 1969.

electric field of any frequency to the effect produced by an equivalent d.c. applied field. The effective d.c. electric field E_e is related to the r.m.s. value of the applied field E by

$$E_e = \frac{E}{(1 + \omega^2/\nu_e^2)^{1/2}}$$

where ν_e is the effective frequency of electron collisions with gas molecules and ω is the radian frequency of the applied field. Typically the electron collision frequency under discharge conditions (*19, 26, 41*) is $10^{-7}N\text{sec.}^{-1}$, so that at a pressure of 1 torr at 300°K. the quantity $\omega/\nu_e = 1$ at a frequency of 500 MHz. At significantly lower frequencies; *i.e.*, below 150 MHz., $E_e = E$ and the rate at which energy is absorbed by electrons from the electric field is independent of the frequency. The effective field relation has been found (*6, 12, 42*) to be good for helium and hydrogen under gas breakdown conditions; *i.e.*, high values of E_e/N. The effective field concept is particularly useful for the accurate prediction of quantities which vary slowly with E_e/N; *i.e.*, electron drift velocity, average electron energy, discharge maintenance field strengths and some reaction rate coefficients. The effective field relation is least accurate at low ω/N in gases such as argon and methane where the cross section for momentum transfer collisions between electrons and gas molecules is a rapidly increasing function of electron energy over much of the energy range of interest. The effective field relation may also be somewhat inaccurate for ω/N values such that the electron energy distribution function relaxes significantly during one cycle of the field (*25*). In this case only those rate coefficients which vary as $(E_e/N)^2$ will be accurately scaled using the r.m.s. value of the applied frequency. In cases where the effective field concept is not sufficiently accurate, the results of measurements of rate coefficients, etc., at various ω and N in a given gas can be shown to depend upon the parameters E/N and ω/N.

Breakdown Parameters

This is the most widely investigated (*6, 16, 34, 35, 42, 43, 50, 57*) of the aspects of electrical discharges and will be discussed only very briefly. The results of breakdown measurements using slowly rising d.c. voltage and electrode gaps with a spacing which is small compared with the distance to side walls are usually given in the form of Paschen curves (*35, 43, 57*) of breakdown voltage as a function of the product of pressure (more correctly, gas density) gap spacing, d. By dividing the breakdown voltage by the Nd product one can express the result as the E/N value required to cause breakdown for a given value of Nd. The importance of

Publication Date: June 1, 1969 | doi: 10.1021/ba-1969-0080.ch002

In Chemical Reactions in Electrical Discharges; Blaustein, B.;
Advances in Chemistry; American Chemical Society: Washington, DC, 1969.

the Nd product can be shown (*34, 35, 43*) to result from the requirement that each electron produce enough positive ions or excited molecules to cause the release of an additional electron from the cathode. Other experimental parameters, such as those describing the shapes of the electrodes and the sensitivity of the experiment for the detection of breakdown must be considered in precise work but are often of secondary importance for Nd values near and above that of the Paschen minimum. When the voltage is applied in the form of a short pulse of length Δt, the product $N\Delta t$ must be included in the list of significant parameters (*34, 43, 50*) since the ionization must be produced in a time Δt with a rate coefficient set by E/N. In the limit of very short pulses the Nd parameter becomes unimportant (*20, 50*). At low a.c. frequencies the parameters required to correlate breakdown data for a given gas are same as for d.c. breakdown except that it is often necessary to take into account the statistical effects arising when the number of electrons available for initiating breakdown is low (*34, 43, 50*). When the number of electrons initially present is high enough to cause space charge distortion of the applied field, an additional parameter is required—*e.g.*, the prebreakdown current (*16*).

Gas breakdown in the presence of very high frequency electric fields of slowly increasing amplitude is often determined by the condition that the rate of electron production equals the rate of loss by diffusion to the container wall (*6, 42*). As indicated above the rate coefficient for ionization can often be expressed as a function of E_e/N although more correctly (*42*), it is a function of E/N and ω/N or $N\lambda$, where λ is the wavelength corresponding to ω. The balance between the ionization rate and the diffusion loss introduces (*6, 21, 29, 42*) the parameter $N\Lambda$ where Λ is the "diffusion length" and for an infinite cylinder is the radius divided by 2.4. Note that the reflection coefficient for ions and electrons at all surfaces investigated are small—*i.e.*, less than 1% and 50%, respectively—so that the diffusion losses may be calculated on the assumption of zero concentration at the wall. The parameters E/N, $N\lambda$, and $N\Lambda$ or combinations of these, such as $E\Lambda$, $N\lambda$, and $N\Lambda$, have been used to correlate experimental data for a given gas and a wide range of λ and N (*6, 42*), including very high gas densities (*25*). When the microwave energy is pulsed, the product $N\Delta t$ becomes important (*20, 25*).

Other special cases of possible interest to chemists are the breakdown in long narrow tubes where diffusion losses are important and breakdown in gases where electron attachment to the gas is the dominant electron loss process. An example of the latter case is the breakdown of SF_6 which occurs very close to the E/N value at which the rate coefficients for attachment and ionization are equal (*4, 43, 49*).

Publication Date: June 1, 1969 | doi: 10.1021/ba-1969-0080.ch002

In Chemical Reactions in Electrical Discharges; Blaustein, B.;
Advances in Chemistry; American Chemical Society: Washington, DC, 1969.

Discharge Maintenance Parameters

We are concerned here with the general question of the electric field strength required to maintain a given electron density or current density in a volume reasonably far removed from electrodes such as the cathode and anode of a d.c. discharge. At moderate degrees of ionization the steady state discharge conditions are determined by a balance between the rate coefficient for ionization by electrons and the effective first order rate coefficient for loss of electrons by diffusion to the walls or by field controlled flow of electrons and ions to electrodes. Several authors show how the dependence of the ionization rate coefficient and the effective electron temperature on E_e/N can be used to predict the E_e/N or electron temperature required to maintain a d.c. positive column (*10, 16, 17, 21, 22, 35*) or a microwave plasma (*29, 33, 52*) for various values of $N\Lambda$. Note that this is the same condition as for the diffusion controlled breakdown discussed above except that the diffusion loss rate for the electrons has been lowered drastically by space charge effects (*21*). The lower loss rate means that the ionization rate coefficient required to maintain the discharge is lowered—*i.e.*, that the E_e/N required is lowered. Because of the similarity of the breakdown and diffusion controlled plasma conditions the same parameter may be used to compare results from given gas but different experimental conditions—*i.e.*, E/N, $N\Lambda$, and $N\lambda$. At high gas flow rates it is necessary to add a parameter which includes the gas residence time Δt—*e.g.*, $N\Delta t$.

Since the production and loss rates for a diffusion controlled plasma are the same order in the electron concentration in this approximation, the electron concentration and the discharge current would appear to be indeterminate. In fact, they are determined (*10, 17, 22*) by the interaction between the discharge and the electrical circuitry—*i.e.*, the power supply with its impedance or the microwave oscillator and coupling device. In general, the larger the discharge current the lower the electric field strength available for the discharge. In the case of d.c. or low frequency a.c. discharges, a large fraction of the applied voltage is often necessary to release the required electron current from the cathode and to satisfy space charge relations at the cathode and anode (*10, 22, 35, 56*).

The simple model of a diffusion controlled or wall stabilized plasma discussed above must be modified to take into account departure of the effective diffusion rate coefficient from the ambipolar value (*2, 3, 11, 52*) when the electron concentration is low enough such that the Debye length λ_D for the plasma (*21*) is comparable with a diffusion length Λ characteristic of the discharge dimensions. Although the results of theoretical treatments of this problem are still given in terms of numerical coefficients for particular gases, an empirical expression can be given

In Chemical Reactions in Electrical Discharges; Blaustein, B.;
Advances in Chemistry; American Chemical Society: Washington, DC, 1969.

which fits the available calculations (*2, 11*) for conditions in which the effective electron temperature is much larger than the gas temperature. Thus, the ratio of the effective diffusion coefficient in the presence of space charge, D_s, to the diffusion coefficient for free electrons, D_e, is given by (*48*)

$$\ln D_s/D_e = [1 + (\lambda_D/\Lambda)^{0.76}]^{-1} \ln \mu_+/\mu_e$$

where μ_+ and μ_e are the mobilities of the positive ions and electrons, respectively. Further modification of the ambipolar diffusion theory is necessary when negative ions are present (*5, 47, 54*). The net effect of these departures from the ambipolar limit is to require that the description of a discharge include additional parameters—*i.e.*, λ_D/Λ and the ratio of the electron and negative ion densities n/N_-.

Publication Date: June 1, 1969 | doi: 10.1021/ba-1969-0080.ch002

Additional parameters may be required to describe the discharge when ionization and electron loss processes which are effectively second and higher order in the electron concentration become important at the higher degrees of ionization of the gas. Two such processes are cumulative ionization—*i.e.*, the ionization of excited state of molecules or atoms by electrons, and electron-ion recombination by either second or third order processes. When the rates of these processes are comparable with the rates of ionization by electron impact and loss by diffusion, they cause only small changes in the E_e/N (*22, 58*). When the rates of these "nonlinear" processes become large, they tend to constrict the discharge as discussed below. A second such process is the Maxwellianization of the electron energy distribution and the consequent higher ionization rate which results from energy sharing collisions between electrons (*15, 38, 44*). Another complicating feature of many low pressure discharges is the presence of either stationary or moving non-uniformities—*i.e.*, striations (*16, 22, 35*).

Because of the rapid variation of the ionization rate coefficient with E_e/N and because one is generally concerned with moderately large discharge currents, the effect of these parameters on E_e/N is generally small. Thus, the simple theories of the d.c. positive column are often very useful in estimating such quantities as E_e/N using the appropriate values of $N\Lambda$ for the diffusion controlled, wall stabilized plasma. As an example, we consider data for a discharge in H_2 for which $N\Lambda = 3 \times 10^{16}$ cm.^{2} and $n/N \sim 10^{-7}$. Theory and experiment (*10, 18, 22, 29*) for a d.c. discharge near the ambipolar limit give 5×10^{-16} volts cm.^{2} as the E/N value required to maintain the discharge. For a microwave discharge at the same $N\Lambda$ and n/N, theory gives the same value for E_e/N and experiment requires a slightly larger value of E_e/N (*52*). In the limit of low n/N—*i.e.*, microwave breakdown—the E_e/N value required is only 10^{-15} volts-cm.^{2} (*52*). Also, a 10 amp. arc ($n/N \sim 10^{-3}$) in H_2 at one atmosphere

In Chemical Reactions in Electrical Discharges; Blaustein, B.;
Advances in Chemistry; American Chemical Society: Washington, DC, 1969.

pressure (*10*) operates at $E/N = 3 \times 10^{-16}$ volts-cm.^{2} for the same $N\Lambda$. While such quantities as the electron mobility or electrical conductivity per unit charge are essentially constant over this range of E_e/N, the mean electron energy varies approximately linearly with E_e/N, the rate coefficient for dissociation of the hydrogen varies by a factor of about 100, and the rate coefficient for ionization by electron impact varies by many orders of magnitude. It must be kept in mind that the gas temperature and the fractional ionization are very high in the 10 amp. arc so that ionization rate coefficients calculated for the room temperature gas are too small. Also the gas is highly dissociated at the center of the arc.

Parameters Determining Constriction of the Discharge

A poorly understood feature of electrical discharge is the phenomenon of constriction of the current channel which is often observed at high gas pressures (*1, 7, 8, 9, 23, 31, 32, 39, 40, 55, 59*). Several effects are present which tend to cause a narrowing of the conducting channel. They are:

(a) Magnetic forces resulting from the current flowing through the arc. These effects are expected to be most important at high currents (*55*).

(b) Thermal gradients which result from the flow of heat from the center of the arc to the wall (*39, 40*) result in a reduced gas density and higher E/N at the center of the arc. If the rate coefficient for ionization increases sufficiently rapidly with E/N then the higher ionization rate more than compensates for the faster diffusion loss of a narrower conducting column. The ionization rate of a hot gas may be higher than that of a cold gas because of chemionization (*27*) or because of ionizing collisions between atoms or molecules (*30*).

(c) Cumulative ionization. Cumulative ionization refers to the ionization of excited atoms or molecules which have been produced by electron impact. Because this process is proportional to the square of the current density, it leads to higher rates of ionization in the regions of higher current density and tends to contrast the discharge.

(d) Electron-ion recombination. Some authors (*31*) propose that the recombination of electrons and ions at large radii leads to constriction of the discharge.

(e) Electron-electron interaction. Since collisions among electrons tend to make electron energy distribution functions more Maxwellian and to increase the excitation and ionization rate coefficients, the ionization rate near the center of a discharge will be higher and will tend to constrict the discharge (*24*).

Since diffusion of the electrons and ions tends to spread the discharge radially, one expects that constriction effects will set in at higher pressures for gases which have larger ambipolar diffusion coefficients as is observed (*39, 40*) for helium relative to the other rare gases.

Publication Date: June 1, 1969 | doi: 10.1021/ba-1969-0080.ch002

In Chemical Reactions in Electrical Discharges; Blaustein, B.;
Advances in Chemistry; American Chemical Society: Washington, DC, 1969.

Parameters Governing Excited State Concentrations

The usefulness of a gas discharge for the production of particular chemicals is often limited by the low gas densities and low power inputs which must be used to obtain a favorable yield (*37, 56*). Considerable effort is being devoted to the design of the gas flow arrangement in discharge reactors so as to obtain the desired products through rapid quenching of the discharge (*51, 56*). Here we wish to consider the parameters relevant to this problem from the point of view of whether the excited molecular species produced by electron impact react before their excitation energy reaches equilibrium with the translational energy of the gas molecules. The excited states are produced by electron-molecule collisions and are destroyed by excited molecule-ground state molecule collisions, by electron collisions, by wall collisions, or by spontaneous radiation. At reasonably high gas densities, spontaneous radiation and loss by diffusion to the wall will be unimportant, so that, for fixed E_e/N the degree of excitation will increase with the degree of ionization of the gas at low degrees of ionization and will be determined by the electron temperature at high degrees of ionization. The degree of ionization over which the transition occurs will depend critically on the excited state being considered and on the electron and gas temperatures. Most of the available data is concerned with excited vibrational states of the ground electronic state (*13, 45*) or with radiating state of atmospheric gases (*28*).

Recent studies (*18, 19, 26, 41, 53*) have shown that the rates of vibrational excitation of molecules by electron impact can be very large. These large cross sections may account for the large populations of vibrationally excited molecules observed (*46*) in flow systems. Because of these large cross sections a large fraction of the energy absorbed by the electrons from the electric field is transferred to the gas molecules in the form of vibrational excitation (*16, 18, 19*). At high gas pressures and translational temperatures, this vibrational energy is rapidly degraded to translational energy (*13, 45*). One potentially profitable area of future investigation is the effective utilization of this form of internal energy of the molecules before relaxation occurs. Alternatively, by choosing experimental conditions so as to keep the vibrational temperature near that of the electrons one can minimize the energy lost through this process.

Since the production of excited species in a stationary electrical discharge requires nonthermal electrons, one may be interested in the conditions for which the average electron energy is significantly above the average energy of the gas molecules. A simple, but not always useful answer, is that when the E_e/N is high enough so that the rate of electron

In Chemical Reactions in Electrical Discharges; Blaustein, B.;
Advances in Chemistry; American Chemical Society: Washington, DC, 1969.

energy gain from the electric field is comparable with the rate of energy gain from the gas molecules then the electrons become nonthermal. For pure Ar at 300°K. the mean electron energy is 10% higher than that of the gas for $E_e/N \sim 5 \times 10^{-21}$ volts-cm.^{2} whereas for a highly polar gas such as H_2O, the same increase in electron energy requires $E_e/N \sim 2 \times 10^{-16}$ volts-cm.^{2}.

The reason that the specification of the E_e/N value required to produce a given rise in average electron energy is not always useful, is that the increased energy the electrons gain from the electric field may cause a corresponding rise in the gas temperature. Since in a static system the excess thermal energy of the molecules is transported to the wall by a diffusion process, the temperature rise is proportional to the power input per unit volume times the square of the diffusion length or at a given E_e/N, to $(n/N)(N\Lambda)^2$. The average gas temperature rise can be kept low by flowing the gas or by pulsing the discharge as in an ozonizer (*14, 36*).

Summary

In the preceding discussion we have attempted to show that in spite of the variety of experimental arrangements used for electrical discharges, there are a relatively few combinations of experimental parameters which characterize the electrical characteristics of the more uniform portions of a discharge. These combinations, E/N, ω/N, $N\Lambda$, n/N and $N\Delta t$, have made possible quantitative comparisons of experimental data obtained for simple gases over a wide range of ω, N, n, Λ and Δt. It is expected that similar comparisons can be made of the electrical characteristics of more complex gases. The chemical behavior of these discharges depends directly upon these parameters and upon others such as the reactivity of the wall and the temperature of the gas. It is to be hoped that the search for the combinations of parameters appropriate to the chemical reactions occurring in the discharge (*36, 51, 56*) will be as fruitful as has been the search for the proper electrical parameters.

Acknowledgement

The author wishes to acknowledge helpful discussions of this paper with F. Kaufman.

Literature Cited

(1) Albrecht, G., Ecker, G., Muller, K. G., *Z. Naturforsh.* **17a,** 854 (1962).
(2) Allis, W. P., Rose, D. J., *Phys. Rev.* **93,** 84 (1954).
(3) Belousova, L. E., *Zhurnal Teknicheskoi Fiziki* **35,** 475 (1965); *Soviet Phys. Tech. Phys.* (English transl.) **10,** 369 (1965).

(4) Bhalla, M. S., Craggs, J. D., *Proc. Phys. Soc. (London)* **80,** 513 (1962).
(5) Biondi, M. A., *Phys. Rev.* **109,** 2005 (1958).
(6) Brown, S. C., "Introduction to Electrical Discharges in Gases," John Wiley and Sons, Inc., New York, 1966.
(7) Champion, K. S. W., *Proc. Phys. Soc. (London)* **B65,** 329 (1952).
(8) *Ibid.*, **B65,** 345 (1952).
(9) *Ibid.*, **B65,** 359 (1952).
(10) Cobine, J. D., "Gaseous Conductors," Chap. 9, Dover Publications, New York, 1958.
(11) Cohen, I. M., Krushal, M. D., *Phys. Fluids* **8,** 920 (1965).
(12) Cottingham, W. B., Buchsbaum, S. J., *Phys. Rev.* **130,** 1002 (1963).
(13) Cottrell, T. L., Day, M. A., "Molecular Relaxation Processes," Academic Press, New York, 1966.
(14) Cromwell, W. E., Manley, T. C., ADVAN. CHEM. SER. **21,** 304 (1959).
(15) Dreicer, H., *Phys. Rev.* **117,** 343 (1960).
(16) Druyvestyn, M. J., Penning, F. M., *Rev. Mod. Phys.* **12,** 87 (1940).
(17) Engel, A. von, *Ionized Gases,* 2nd ed., Oxford University Press, London, 1965.
(18) Engelhardt, A. G., Phelps, A. V., *Phys. Rev.* **131,** 2115 (1963).
(19) Engelhardt, A. G., Phelps, A. V., Risk, C. G., *Phys. Rev.* **135,** A1566 (1964).
(20) Felsenthal, P., Proud, J. M., *Phys. Rev.* **139,** A1796 (1965).
(21) Fite, W. L., ADVAN. CHEM. SER. **80,** 1 (1969).
(22) Francis, G., "Handbuch der Physik," Vol. 22, S. Flugge, ed., Springer-Verlag, Berlin, 1956.
(23) Gambling, W. A., Edels, H., *Brit. J. Appl. Phys.* **7,** 376 (1956).
(24) Golobovskii, Yu. B., Kagan, Yu. M., Lyagushchenko, R. I., *Opt. Spectr. (USSR) (English Transl.)* **20,** 317 (1966).
(25) Gould, L., Roberts, L. W., *J. Appl. Phys.* **27,** 1162 (1956).
(26) Hake, R. D., Jr., Phelps, A. V., *Phys. Rev.* **158,** 70 (June 5, 1967).
(27) Hand, C., Kistiakowsky, G. B., *J. Chem. Phys.* **37,** 1239 (1962).
(28) Hunten, P. M., McElroy, M. B., *Rev. of Geophys.* 4, 303 (1966).
(29) Kaufman, F., ADVAN. CHEM. SER. **80,** 29 (1969).
(30) Kelly, A. J., *J. Chem. Phys.* **45,** 1723 (1966).
(31) Kenty, C., *Phys. Rev.* **126,** 1235 (1962).
(32) King, L. A., *Appl. Sci. Res. (The Hauge)* **B5,** 189 (1955-6).
(33) Krasik, S., Alpert, D., McCoubrey, A. O., *Phys. Rev.* **76,** 722 (1949).
(34) Llewellyn-Jones, F., "Ionization and Breakdown in Gases," Methuen and Co., Ltd., London, 1957.
(35) Loeb, L. B., "Basic Processes in Gaseous Electronics," Chap. 8, Univ. of California Press, Berkeley, California, 1955.
(36) Lunt, R. W., ADVAN. CHEM. SER. **21,** 286 (1959).
(37) Lunt, R. W., ADVAN. CHEM. SER. **80,** 452 (1969).
(38) Maronne, T., *Phys. Rev.* **141,** 27 (1966).
(39) Massey, J. T., Cannon, S. M. J., *J. Appl. Phys.* **36,** 361 (1965).
(40) *Ibid.*, **36,** 373 (1965).
(41) McDaniel, E. W., "Collision Phenomena in Ionized Gases," Chap. 4, John Wiley and Sons, Inc., New York, 1964.
(42) McDonald, A. D., "Microwave Breakdown in Gases," John Wiley and Sons, Inc., New York, 1966.
(43) Meek, J. M., Craggs, J. D., "Electrical Breakdown of Gases," Oxford University Press, London, 1953.
(44) Megill, L. R., Cahn, J. H., *J. Geophys. Res.* **69,** 5041 (1964).
(45) Millikan, R. C., White, D. R., *J. Chem. Phys.* **39,** 3209 (1963).
(46) Morgan, J. E., Phillips, L. F., Schiff, H. I., *Discussions Faraday Soc.* **33,** 119 (1962).
(47) Oskam, H. J., *Phillips Res. Repts.* **13,** 335 (1958).

Publication Date: June 1, 1969 | doi: 10.1021/ba-1969-0080.ch002

In Chemical Reactions in Electrical Discharges; Blaustein, B.;
Advances in Chemistry; American Chemical Society: Washington, DC, 1969.

(48) Phelps, A. V., "Proceeding of the Conference on the Physics of Quantum Electronics," p. 546, P. Kelley, ed., McGraw-Hill Book Co., New York, 1966.
(49) Prasad, A. N., Craggs, J. D., "Atomic and Molecular Processes," Chap. 6, D. R. Bates, ed., Academic Press, New York, 1962.
(50) Raether, H., "Electron Avalanches and Breakdown in Gases," Butterworths, Washington, 1964.
(51) Rony, P. R., *Preprints Div., Fuel Chem. ACS* **11** (**2**), 107 (1967).
(52) Rose, D. J., Brown, S. C., *Phys. Rev.* **98**, 310 (1955).
(53) Schulz, G. J., *Phys. Rev.* **135**, A988 (1964).
(54) Seeliger, R., *Ann. Phys.* **6**, 93 (1949).
(55) Thonemann, P. C., Cowhig, W. T., *Proc. Phys. Soc. (London)* **B64**, 345 (1951).
(56) Thornton, J. D., ADVAN. CHEM. SER. **80**, 372 (1969).
(57) Townsend, J. S., "Electrons in Gases," Hutchinson's Scientific and Technical Publications, London, 1947.
(58) Walsh, P. J., Manning, G. W., Larson, D. A., *J. Appl. Phys.* **34**, 2273 (1963).
(59) Woolsey, G. A., "Proceeding of the 6th International Conference on Ionization Phenomena in Gases," Vol. **2**, p. 141, P. Hubert, ed., S.E.R.M.A., Paris, 1965.

RECEIVED June 5, 1967.

The Production of Atoms and Simple Radicals in Glow Discharges

FREDERICK KAUFMAN

University of Pittsburgh, Pittsburgh, Pa.

Publication Date: June 1, 1969 | doi: 10.1021/ba-1969-0080.ch003

The fundamental processes are briefly reviewed which produce and recombine electrons as well as atomic species in glow discharges of H_2, O_2, and N_2 at 1 torr pressure. Cross sections for electron impact ionization and dissociation are taken from the recent work of Phelps et al. *and approximate rate constants are deduced. The experimental fact that very little dissociation is produced in high frequency discharges of purified diatomic gases requires a very large recombination term, and it is concluded that surface recombination in and near the discharge region must be responsible. The well-substantiated "catalytic" dissociation brought on by small amounts of added impurities therefore appears to involve a modification of surface properties. Brief mention is made of the discharge chemistry of water vapor.*

The size and topical variety of this symposium clearly show that electrical discharges are finding increasing application in many areas of chemistry ranging from the production of simple atomic species such as H, O, or N from their diatomic molecules to the synthesis or specific decomposition of complex organic or inorganic compounds. It is true, unfortunately, that our understanding of the chemistry of discharge processes is still in a rudimentary state, that the field is more an art than a science, and thus represents one of the last frontiers of chemistry.

There is good reason for this unsatisfactory state of affairs. Glow discharges are complex phenomena in which gases at sub-atmospheric pressure are undergoing excitation and ionization by electron impact and so give rise to highly unequilibrated steady-state conditions where the effective temperature of free electrons is typically tens of thousands °K., that of electronically or vibrationally excited states may be thousands of

In Chemical Reactions in Electrical Discharges; Blaustein, B.;
Advances in Chemistry; American Chemical Society: Washington, DC, 1969.

°K., whereas the translational and rotational temperature will only be tens to hundreds of °K. above ambient. It should be clear, of course, that apart from the processes occurring at the electrodes, energy from the electric field is coupled to the gas almost entirely through the kinetic energy of free electrons which, because of their small mass, acquire energy rapidly from the field, lose it negligibly slowly in elastic collisions (the mean fractional energy loss per elastic collision equals $2\ m/M$ in the simplest classical model where m and M are the masses of the electron and of the molecule), and thus reach their steady-state distribution through various inelastic processes. In this manner, electrons become sufficiently energetic to ionize some of the neutral species and thereby balance their continuous loss by diffusion, attachment, and recombination. As the ionization potentials of most neutral gases are in the 10 to 20 e.v. range (230 to 460 kcal./mole), an appreciable fraction of the electrons has enough energy to produce electronic excitation (responsible for the emitted glow) and dissociation.

In the following sections, the mechanism of d.c. and a.c. glow discharges will be briefly described, with emphasis on high frequency electrodeless discharges ($f = 10^6$ to 10^{10} sec.$^{-1}$) and on the simple geometry often encountered in rapidly pumped steady-state flow systems at pressures near 1 torr. After a brief discussion of the rates and energy dependence of specific collision and diffusion processes, available experimental data will be brought to bear on the problem of H_2, N_2, and O_2 dissociation and of the chemistry of some more complicated systems.

Although there are several fine monographs available on electron impact phenomena and discharge physics (*3, 20, 22, 23*), they contain relatively little information on active high frequency discharges which is pertinent to the problem of dissociation and chemical reaction. The electron physics of microwave discharges is discussed in some review articles (*2, 13*).

Basic Physical Processes

General Mechanism and Frequency Dependence. Glow discharges are typically observed in the pressure range of about 0.1 to 10 torr. At much lower pressures, the electron mean free path is too long for gas collisions to be important, electrons pick up large amounts of energy from the d.c. or slow a.c. field and bombard the anode or the tube wall which may then fluoresce. At much higher pressures, the mean free path is very short, the breakdown field strength is very high, and when it is exceeded, local, highly ionized, but narrow pathways are created for the conduction of current—*i.e.*, spark filaments are formed. The normal d.c. glow discharge in a long cylindrical tube is characterized by many axially distinct

Publication Date: June 1, 1969 | doi: 10.1021/ba-1969-0080.ch003

In Chemical Reactions in Electrical Discharges; Blaustein, B.;
Advances in Chemistry; American Chemical Society: Washington, DC, 1969.

but radially fairly uniform regions of quite different optical and electrical properties such as the Aston Dark Space, Cathode Glow, Cathode Dark Space, Negative Glow, Faraday Dark Space, Positive Column, Anode Glow, and Anode Dark Space, in this order, between cathode and anode. The reason for this complexity is that quite different processes occur in the different regions as is also shown by a very non-uniform voltage rise between cathode and anode. Most of the potential difference is taken up in the "cathode fall" which comprises the first four regions enumerated above, is dependent on the cathode material as well as on the nature of the gas and on the natural variable E/N (volts cm.^{2}/molecules) where E is the field strength (volts/cm.) and N the total neutral density (molecules/cc.). The "cathode fall" and "anode fall" regions also have large gradients of electron and ion concentrations and a local imbalance of electrical charge. The positive column is simpler in nature (although striated positive columns are still poorly understood), has a small and constant axial voltage drop, and only a small imbalance of charge carriers, because, although electrons initially diffuse to the tube wall faster than ions, the resultant radial field prevents further charge separation and forces electrons and ions to diffuse equally fast. This process is called ambipolar diffusion and is further discussed below. The quantity E/N is a measure of the electron energy under conditions of steady-state drift, and takes on a well-defined, constant value in the positive column. To obtain a simple expression relating the electron energy, $\epsilon = \frac{1}{2}mv^2$, to E/N, we equate energy loss and gain per electron per second, $\frac{2m}{M}\frac{\epsilon v}{l} = eEw$, where l is the mean free path for electron-neutral collisions, e the electronic charge, and $w = \frac{2}{3}\frac{eEl}{mv}$ the electron drift velocity. One obtains $\epsilon = \frac{E}{N}\frac{eM^{1/2}}{2\Pi\sigma^2(3m)^{1/2}}$ where l was replaced by $1/(1/2^{1/2}\Pi\sigma^2 N)$ from simple kinetic theory.

The voltage drop along the positive column is also independent of the total current over a fairly wide range, and since the current, i, is carried mostly by the electrons whose drift velocity is about 100 times larger than that of the ions, $i = n_e ew = \frac{2}{3}\frac{e^2El}{mv}n_e$, which shows that the electron concentration, n_e, increases linearly with increasing current because E and v are constant. In its normal range of electron (and ion) concentrations of 10^8 to 10^{11} cm.$^{-3}$, the positive column of a d.c. glow discharge is diffusion-controlled and serves as the electrical connection between the cathode and anode regions.

In high frequency electrodeless discharges the complications of the cathode and anode regions are absent, the entire plasma is approximately

Publication Date: June 1, 1969 | doi: 10.1021/ba-1969-0080.ch003

In Chemical Reactions in Electrical Discharges; Blaustein, B.;
Advances in Chemistry; American Chemical Society: Washington, DC, 1969.

neutral and diffusion-controlled, and the discharge often resembles the positive column of an equivalent d.c. discharge. Yet, there are differences in its fundamental mechanism, especially at microwave frequencies. Free electrons oscillating in an alternating field can not derive power from the field on the average, because their motion is 90° out of phase with the field. They therefore acquire energy only because collisions with neutral molecules change their phase relationship with the field while at the same time representing a small fractional loss of the energy gained. Under the assumption that the a.c. frequency, f, is greater than the elastic collision frequency, ν_e, the maximum displacement, x, of an electron because of the high frequency field is given by $x = \frac{2eE}{m\omega^2}$ where $\omega = 2\Pi f$. In an active microwave discharge E is typically 30 volts/cm. and x is therefore less than 10^{-3} cm. when $f = 2.5 \times 10^9$ sec.$^{-1}$ (as in the widely used Raytheon Microtherm Generator). The corresponding maximum electron energy acquired during the cycle is eEx, about 0.02 e.v.—*i.e.*, the electrons slowly accumulate the energy necessary to undergo inelastic, ionizing collisions and to sustain the discharge. When elastic collisions are approximately accounted for, it is convenient to define an effective field strength, $E_e = E_o\left(\frac{\nu^2}{\nu^2 + \omega^2}\right)^{1/2}$ where E_o is the r.m.s. value of the applied field strength. The power gained from the field per electron is $\frac{e^2E_e^2}{m\nu}$ and per collision therefore $\frac{e^2E_e^2}{m\nu^2}$.

Diffusion of Charged Species. In the discharges of interest here, the concentration of charged species is greater than 10^8 cm.$^{-3}$ and a large fractional separation of electrons and positive ions becomes impossible, because it would set up a very large opposing field. The currents of electrons and ions reaching the wall must then be equal, $i_e = -D_e\nabla n - n\mu_eE'$, $i_+ = -D_+\nabla n + n\mu_+E'$ where $n = n_e = n_+$ is the electron density, ∇n the density gradient, D the diffusion coefficient, μ the mobility, and E' the field caused by the (small) space charge. The subscripts e and $+$ refer to electron and positive ion. Equating i_e and i_+ and eliminating E' one obtains

$$i = -\frac{D_e\mu_+ + D_+\mu_e}{\mu_+ + \mu_e}\triangle n = D_a\nabla n$$

which serves as the definition of the ambipolar diffusion coefficient, D_a. Substituting $\mu_e\frac{kT_e}{e}$ for D_e and the equivalent expression for D_+ one obtains

$$D_a = \frac{\mu_e\mu_+}{\mu_e + \mu_+}\frac{k}{e}(T_e + T_+)$$

Publication Date: June 1, 1969 | doi: 10.1021/ba-1969-0080.ch003

which approximately equals $\frac{\mu_+ k}{e}(T_e + T_+)$ or $D_+\left(1 + \frac{T_e}{T_+}\right)$ because the electron mobility μ_e, is much larger than the ionic mobility μ_+. In active glow discharges T_e/T_+ is typically 20 to 100, whereas in the afterglow the electrons thermalize rapidly and $T_e/T_+ = 1$. Thus, $D_a \approx 20$ to 100 D_+ in the active discharge, and 2 D_+ in the afterglow.

The disappearance of charged species by ambipolar diffusion in the absence of a source term is described by the diffusion equation $\frac{\delta n}{\delta t} = D_a \nabla^2 n$ where n is a function of r, θ, z, and t. The well known solution of this equation for the case of an infinite cylinder is $n(r,t) = \sum_{i=1}^{\infty} A_i J_o\left(\alpha_i \frac{r}{r_o}\right) e^{-k_i t}$ where α_i is the i th root of J_o, the Bessel function of zero order and $k_i = \left(\frac{\alpha_i}{r_o}\right)^2 D_a = \frac{D_a}{\Lambda^2}$. The diffusion length, Λ, therefore equals $\frac{r_o}{\alpha_1}$. The first few zeros of J_o are $\alpha_1 = 2.405$, $\alpha_2 = 5.520$, $\alpha_3 = 8.654$, $\alpha_4 = 11.792$ which shows that, as diffusion proceeds, the time decay will be increasingly governed by $k_1 = \left(\frac{2.405}{r_o}\right)^2 D_a$, the first (lowest) diffusion mode, because the next three higher modes are damped out more rapidly by factors of 5.3, 12.9, and 24. After a short transient, the diffusion-controlled electron decay or the diffusion controlled loss under steady-state conditions with a spatially well distributed source term can therefore be closely approximated by a first-order rate constant, $k = 5.78\ D_a/r_o^2$.

This analysis applies when there are only positive ions and electrons present. When negative ions are also present, their principal effect is to accelerate the ambipolar diffusion of the electrons, $(D_a)_e$, which now becomes approximately $(D_a)_e = (1 + \lambda)\ D_+\left(1 + \frac{T_e}{T_+}\right) + \lambda D_-\left(\frac{T_e}{T_+} - 1\right)$ which for active discharges $(T_e/T_+ >> 1)$ can be further approximated by $(1 + 2\lambda)\ T_e/T_+$, where $\lambda = n_-/n_e$, the concentration ratio of negative ions and electrons. It can be seen that for $\lambda > 1$ electrons will be lost much more rapidly by diffusion to the wall than in the absence of negative ions.

Electron-Ion and Ion-Ion Recombination. Although several radiative, two-body, and three-body recombination mechanisms exist, only the fastest ones will be mentioned here. These are the dissociative recombination of electrons and positive molecular ions as exemplified by $NO^+ + e \rightarrow N + O$ (where the products may be electronically excited), similar ion-ion reactions such as $I_2^+ + I^- \rightarrow I_2 + I$ or 3I, $NO^+ + NO_2^- \rightarrow$ neutral products, and three-body ion-ion recombinations such as $NO^+ + NO_2^- + M \rightarrow$ neutral products.

Publication Date: June 1, 1969 | doi: 10.1021/ba-1969-0080.ch003

In Chemical Reactions in Electrical Discharges; Blaustein, B.;
Advances in Chemistry; American Chemical Society: Washington, DC, 1969.

All of these processes have very large rate constants, owing to the long range coulombic attraction between reactants, if reasonable paths are available for the dissipation of the large exothermic reaction energy ($\sim$ 10 e.v.) such as dissociation and electronic excitation. The first of these three processes has been studied in greatest detail, especially by Biondi and co-workers (*1, 16*) who found a value of $2.9 \pm 0.3 \times 10^{-7}$ cc. molecule^{-1} sec.$^{-1}$ for the rate constant of $N_2^+ + e \rightarrow N + N$, for example. The generally observed range of 1 to 5×10^{-7} (6×10^{13} to 3×10^{14} liter mole^{-1} sec.$^{-1}$) means that at an electron and ion concentration 10^{11} cm.$^{-3}$, which is near the upper limit of charged particle densities encountered in glow discharges, the effective first order rate constant for electron removal under steady-state conditions will be 1 to 5×10^4 sec.$^{-1}$.

Two-body ion-ion recombinations have rate constants in the same general range, although few have been studied in detail, none with precise analysis of reactants and products. Some three-body ion-ion recombinations have recently been studied by Mahan and co-workers (*4, 21*) who found effective termolecular rate constants in the range 4×10^{-26} to 3×10^{-25} cm.^{6} molecule^{-2} sec.$^{-1}$ for $NO^+ + NO_2^- + M$ near 300°K. With an approximate $T^{-5/2}$ dependence, and at a total pressure of 1 torr, such processes would have effective first-order rate constants of ion removal in the 10 to 100 sec.$^{-1}$ range, too slow to be of importance.

Electron Attachment and Detachment. Only the fastest of the many possible processes need to be discussed here. Radiative attachment and photodetachment as well as three-body attachment processes are unlikely to be of importance. Dissociative attachment reactions such as $e + O_2 \rightarrow O^- + O$ have rate constants (*25*) which rise from zero at an electron energy threshold (4 to 9 e.v. for the formation of O^- from O_2, NO, or CO) to a maximum of 10^{-11} to 10^{-10} cc. molecule^{-1} sec.$^{-1}$ for electrons with 6 to 10 e.v. For average electron energies of 2 to 3 e.v. in an active discharge, the effective rate constant must therefore be lowered about 10-fold to a range of 10^{-12} to 10^{-11}. Moreover, several associative detachment reactions such as $O^- + O \rightarrow O_2 + e$, $O^- + N \rightarrow NO + e$, $O^- + H_2 \rightarrow H_2O + e$ have recently been found (*9*) to be very rapid ($k = 1$ to 5×10^{-10} cc. molecule^{-1} sec.$^{-1}$) under thermal conditions near 300°K. This further reduces the likelihood that negative ions are important species in rapidly pumped steady-state glow discharges of diatomic gases. In this regard, active discharges probably differ markedly from their corresponding afterglows or from drift tube experiments where electron attachment or secondary negative ion reactions produce various negative ions of low electron affinities.

Charge-Transfer and Ion-Molecule Reactions. Both positive and negative ion-molecule reactions have recently been studied by a variety of experimental methods, and consistent values for many rate constants

Publication Date: June 1, 1969 | doi: 10.1021/ba-1969-0080.ch003

have become available. Because of the strong ion-dipole or ion-induced dipole interaction, these reactions usually have little or no activation energy if they are exothermic, and often have rate constants near 10^{-9} cc. molecule^{-1} sec.$^{-1}$, in accord with the simple theory based on the polarizability of the neutral reactant. Some exceptions such as $O_2^+ + N_2 \rightarrow NO^+ + NO$ which is at least 10^{-6} times as fast (*10*) are probably caused by the large energy requirements for bond rearrangement which in the corresponding neutral four-center reaction gives rise to a large activation energy. Other unusually slow reactions such as $O^+ + N_2 \rightarrow NO^+ + N$ ($k \sim 2 \times 10^{-12}$) are less easily rationalized, particularly since k rises sharply when the reactant N_2 is vibrationally excited (*29*).

From the magnitude of 10^{-10} to 10^{-9} for many of the exothermic reactions it is clear that the effective first-order rate constant for the transformation of an ionic species by reaction with a major neutral constituent ($P = 1$ torr $\simeq 2 \times 10^{16}$ molecules cm.$^{-3}$ at the higher temperature of the discharge) is 2×10^6 to 2×10^7 sec.$^{-1}$—*i.e.*, such reactions will go to completion in a small fraction of the residence time in even the most rapidly pumped flow systems. Minor neutral constituents such as atomic species at 0.1 to 1 mole % will transform ionic species with rate constants of 10^3 to 10^5 sec.$^{-1}$, still much faster than the rate of traversal through most discharges whose average flow velocities are in the range 10^2 to 10^4 cm. sec.$^{-1}$ and whose lengths are 1 to 10 cm.

Electron Impact Ionization. As shown earlier in this paper, the electron loss term by ambipolar diffusion can be approximated by a first-order rate constant, $k = 5.78\ D_a/r_o^2$, which for an active discharge with $T_e/T_+ \sim 50$, $D_+ \sim 100$ cm.^{2} sec., and $r_o = 0.5$ cm., makes $k \sim 1 \times 10^5$ sec.$^{-1}$. Although it is conceivable that chemi-ionization will occur in which two electronically excited molecules with 5 to 10 e.v. energy react to produce ionization, such processes will normally be of very minor importance. Even with a large chemi-ionization rate constant of 10^{-10} cc. molecule^{-1} sec.$^{-1}$, a concentration of 5×10^{14} cm.$^{-3}$, 2 to 3 mole %, of such excited molecules would be required to balance the diffusional loss. It thus seems likely that electron impact ionization is the major source term for charged species in the discharge. Although this requires more than the ionization potential of the atom or molecule—*i.e.*, electron energies in excess of about 15 e.v.—the large electron velocity and its very high average temperature, T_e, can easily provide the required magnitude of the rate constant.

The ionization cross section of most atoms and simple molecules rises sharply from zero at the ionization potential and comes to a broad maximum of about 1 to 5×10^{-16} cm.^{2}/molecule at electron energies of 70 to 120 e.v. It normally reaches a value of 1×10^{-17} about 2 to 4 e.v.

Publication Date: June 1, 1969 | doi: 10.1021/ba-1969-0080.ch003

In Chemical Reactions in Electrical Discharges; Blaustein, B.;
Advances in Chemistry; American Chemical Society: Washington, DC, 1969.

above its ionization potential—*i.e.*, at electron energies of 12 to 17 e.v. For average electron energies of 2 to 3 e.v. in active glow discharges, this leads to total effective ionization rate constants of 10^{-11} to 10^{-10} cc. molecule^{-1} sec.$^{-1}$ if a Maxwell distribution is assumed. A somewhat lower range would be obtained for a Druyvesteyn distribution, but since the ratio, $\epsilon/\bar{\epsilon}$, of required to average energy is never very large, the error owing to the assumption of a Maxwell distribution should be fairly small.

An important, though infrequently applicable ionization mechanism is the direct ionization by collision with sufficiently energetic, metastable neutral species. This process, called Penning ionization, can occur only if the excitation energy of the metastable exceeds the ionization potential of the other reactant. For He, Ne, and Ar the excitation energy of the lowest triplet state is 19.80, 16.62, and 11.55 e.v. respectively, and since the rate constants for Penning reactions are often gas kinetic—*i.e.*, near 10^{-10} cc. molecule^{-1} sec.$^{-1}$, this process is likely to be the major ionization source in diatomic gases mixed with excess He or Ne but not with Ar.

Excitation and Dissociation. Molecules can have internal energy in the form of rotation, vibration, or electronic excitation, and they can therefore undergo inelastic collisions with electrons which leave the molecule in one of its many excited states. For the purpose of this review, rotational excitation need not be considered, because rotational energies are small, and the collisional exchange of translational and rotational energy is so rapid that rotational states are unlikely to be substantially out of kinetic temperature equilibrium. Vibration-translation interchange, however, is very inefficient, especially for strongly bound, homonuclear diatomic molecules, so that appreciable vibrational excitation can occur in glow discharges, and effective vibrational temperatures may be established which are intermediate between T_e and T_g. Electron impact excitation of vibrational energy is a highly specific process whose cross section can differ by two orders of magnitude from one molecule to another, because it depends on the existence of virtual negative ion states which decay into vibrationally excited ground-state molecules and slow electrons. This mechanism is particularly important in N_2, CO, and CO_2 which have large cross sections (1 to 5 $\times$ 10^{-16} cm.^{2}/molecule, $k = 5 \times 10^{-9}$ to 2×10^{-8} cc. molecule^{-1} sec.$^{-1}$ at electron energies of about 2 to 5 e.v.), but less so in H_2 and O_2 whose cross sections are smaller by a factor of 10 to 50 than those in N_2. The high vibrational temperature, T_v, of N_2 in glow discharges is likely to be responsible for much of its electronic excitation, because if T_v approaches T_e, the internal equilibration of vibrational states will produce appreciable concentrations of molecules with 5 to 8 e.v. of vibrational energy, consistent with some recent spectroscopic observations in active nitrogen (32) as well as electronically

Publication Date: June 1, 1969 | doi: 10.1021/ba-1969-0080.ch003

In Chemical Reactions in Electrical Discharges; Blaustein, B.;
Advances in Chemistry; American Chemical Society: Washington, DC, 1969.

excited molecules by the reverse process of the very fast quenching reactions of the $A^3\Sigma$ state of N_2 by N-atoms.

Electronically excited states can be formed directly by electron impact. When the corresponding radiative transition is allowed, the excitation cross section rises to a broad maximum and then slowly decreases, whereas for forbidden radiative transitions, the cross section is often sharply peaked at the corresponding energy and falls off rapidly at higher energies. Peak cross sections are often in the 10^{-17} to 10^{-18} cm.^{2}/molecule range which roughly corresponds to rate constants of 10^{-11} to 10^{-10} cc. molecule^{-1} sec.$^{-1}$ for transitions requiring 5 to 10 e.v., assuming average electrons energies of 2 to 3 e.v.

The principal mechanism for the direct dissociation of a molecule into neutral fragments by electron impact must, of course, be the initial formation of an electronic state with energy greater than D, the dissociation energy. This transition will take place within the limitations set by the Franck-Condon principle. The ensuing dissociation will normally come about in one of three principal ways: (a) the upper state is repulsive and dissociates upon its first pseudovibration—*i.e.*, in about 10^{-13} sec.; (b) the upper state is bound, but the molecule is formed on the repulsive part of its potential energy curve at a point above its dissociation energy, and will therefore dissociate on its first vibration, also in about 10^{-13} sec.; (c) the upper state is bound, the molecule is formed with less than the dissociation energy of that state, but there is another state of lower dissociation energy with which the first state may interact. Near the crossing point of the two potential energy curves, the states become mixed and there is a probability of crossing and subsequent dissociation. Depending on the degree of mixing, this pre-dissociation process may be much slower than the first two. The overall cross section and rate constant for dissociation will normally equal that of the primary excitation step—*i.e.*, there will be near unit probability for the subsequent dissociation, because collisional or radiative lifetimes of the excited states can not be shorter than about 10^{-7} to 10^{-8} seconds.

Publication Date: June 1, 1969 | doi: 10.1021/ba-1969-0080.ch003

Application to the Dissociation of Some Diatomic Molecules

Summary of Some Atom Production and Loss Processes. In the following sections much evidence will be cited for catalytic effects in the production of atomic species such as H, N, or O in glow discharges of their diatomic gases. The existence of such effects suggests large changes in the atom production or loss terms upon small variations in gas composition. The principal processes are therefore summarized in this section, and approximate ranges given for their rates. A cylindrical discharge

In Chemical Reactions in Electrical Discharges; Blaustein, B.;
Advances in Chemistry; American Chemical Society: Washington, DC, 1969.

tube of 1 cm. diameter, average electron concentration of 10^{11} cm.$^{-3}$, and electron energy of 2 to 3 e.v. are assumed corresponding to known conditions in microwave discharges (*28*) at input power levels of about 10 to 500 watt.

Production terms: (a) Electron impact dissociation *via* excited states depends on the existence of a dissociating or predissociating state at moderate excitation energy and is therefore quite variable. When the dissociation energy is relatively small, as in H_2 and O_2, and when states are available at 8 to 10 e.v. excitation threshold, an atom production rate of 10 to 100 torr/sec. can be calculated. For N_2 whose dissociation energy is larger, the rate will be only about 1/10 as large. It should be clear that this process must occur in active discharges, since electron impact ionization, which requires appreciably larger electron energies, is the principal source term for electron production. Therefore, since there are enough electrons present with 15 to 20 e.v. energy to balance the rapid ambipolar diffusion (and recombination) loss, there must be appreciably more with 8 to 12 e.v. for excitation-dissociation.

(b) Electron-Ion recombination at the wall (following ambipolar diffusion) or in the gas phase will also produce atomic species in reactions such as $e + O_2^+ \rightarrow 2\ O$, $e + N_2^+ \rightarrow N + N$, etc. It is clear that the upper limit to this atom production term is given by the total rate of ionization except for a possible factor of two from the stoichiometry of the dissociation. But as this surface recombination may also lead to the molecular product by the dissipation of energy to the surface, the dissociation rate caused by this process is likely to be lower than the corresponding ionization or equivalent ambipolar diffusion term—*i.e.*, $<$ 0.5 to 5 torr/sec. The gas-phase dissociative recombination will produce atoms at a rate of 0.1 to 0.3 torr/sec. at an electron density of 10^{11} cm.$^{-3}$ and much more slowly at lower densities.

(c) Ion-molecule reactions of primary ions may in exceptional cases be sufficiently exothermic to produce atomic species and ions of lower ionization potential such as in $H_2^+ + H_2 \rightarrow H_3^+ + H$, but the equivalent reactions for O_2 and N_2 are endothermic. When such a process is possible, its rate is again limited by the total rate of ionization, but should closely approach it if the neutral molecule is a major species as in the above H_2 reaction.

(d) Neutral-neutral dissociation reactions may also occur, but little can be said about them in general. As the kinetic temperature of all but the electrons is fairly low (300° to 800°K., mostly near 600°K.), two excited, metastable molecules would have to react to transfer their excitation to a predissociating state. Few such reactions are known, and their rate constants are likely to have upper limits in the 10^{-12} to 10^{-11} cc. molecule^{-1} sec^{-1}. range. If that were so, metastable mole fractions as high as 0.1% would only produce atoms at ratios of 0.02 to 0.2 torr/sec. Such states would also have to be optically metastable—*i.e.*, have radiative lifetimes longer than 0.01 sec.—and be resistant to collisional quenching —*i.e.*, have deactivation probability per collision lower than 10^{-4}.

Loss Terms: (a) Homogeneous gas-phase atom recombinations are three-body processes with rate constants near 10^{-32} cm.^{6} molecule^{-1} sec.$^{-1}$

Publication Date: June 1, 1969 | doi: 10.1021/ba-1969-0080.ch003

In Chemical Reactions in Electrical Discharges; Blaustein, B.;
Advances in Chemistry; American Chemical Society: Washington, DC, 1969.

so that even for atom mole fractions of 5%, such loss rates are near 0.01 torr/sec., negligibly small.

(b) Surface recombination is a well-known process, usually kinetically first order, and characterized by a rate constant, $k = \frac{\gamma c}{d}$, for a cylindrical tube of diameter d. Here γ is the recombination coefficient, the fraction of surface collisions leading to recombination, and c is the average molecular velocity of the atomic species. γ which is often as low as 10^{-5} outside the discharge for a well-cleaned or suitably poisoned surface, is likely to be 10^{-3} or larger in the active discharge. For $\gamma = 10^{-3}$, atom loss rates of 2 to 10 torr/sec. can be calculated, and for larger γ, these rates would be larger, but not proportionately so, because large radial concentration gradients would be produced and diffusion would become rate-controlling. Then, an effective first order rate constant, $k = D/\Lambda^2 = 5.8\ D/r^2$, would be applicable, similar to ambipolar diffusion, but with the smaller, molecular diffusion coefficient. For an atom mole fraction of 5%, the upper limit to the diffusional atom recombination rate will be 100 to 300 torr/sec., depending on the atomic species.

(c) Ion-molecule reactions can remove atomic species if the ion is polyatomic such as in $N + N_3^+ \rightarrow N_2 + N_2^+$ or the equivalent oxygen reaction. If the polyatomic ion is a major ionic species, and the reaction is a fast one, its rate at 5% atom mole fraction will be near 5 torr/sec. It will then be limited by the rate of regeneration of the polyatomic ion. Reactions of the type $O_2^+ + N \rightarrow NO^+ + O$ or $N_2^+ + O \rightarrow NO^+ + N$ are known to be fast (*10*), but as they replace one atomic species by another they need not be considered here.

(d) Neutral, bimolecular atom-molecule reactions such as $N + O_2 \rightarrow NO + O$ or $O + H_2 \rightarrow OH + H$ often have appreciable activation energies. Moreover, they, too, often shuffle atomic species and can not be considered loss terms. In the few applicable cases where this does not hold as in $O + N_2O \rightarrow 2\ NO$ or $N + N_2O \rightarrow N_2 + NO$, the reactions are known to be negligibly slow.

Hydrogen Discharges. The discussion of the electron collisional aspects of H_2, N_2, and O_2 discharges is greatly aided by the excellent papers by Phelps and co-workers in which elastic and inelastic collision cross sections are obtained by numerical solution of the Boltzmann transport equation and comparison with all available experimental data on electron transport coefficients. For H_2 and D_2 (*7*), the effective vibrational excitation cross section becomes appreciable (10^{-17} cm.^{2}) at about 1 e.v. and peaks near 5 e.v. at 8×10^{-17} cm.^{2}. For dissociation, a threshold at 8.85 e.v. and peak of 4.5×10^{-17} cm.^{2} at 16 to 17 e.v. was found to be consistent with the data. A recent measurement by Corrigan (*5*) of the dissociation cross section of H_2 is in good agreement with the above except for a larger peak of about 9×10^{-17} cm.^{2} at 16.5 e.v. For average electron energies, ϵ_k, of 3.0 or 2.0 e.v. (*28*), dissociation rate constants, k_d, of 11 or 2×10^{-10} cc. molecules^{-1} sec.$^{-1}$ can be calculated by summation

In Chemical Reactions in Electrical Discharges; Blaustein, B.;
Advances in Chemistry; American Chemical Society: Washington, DC, 1969.

of $Qvf(\epsilon)$ from $\epsilon = 0$ to ∞, using energy increments of 2 or 3 e.v., where Q is the appropriate cross section, v the electron velocity, and

$$f(\epsilon) = \frac{2}{\Pi^{1/2}} \left(\frac{\epsilon}{\epsilon_k}\right)^{1/2} e^{-\frac{\epsilon}{\epsilon_k}} \frac{d\epsilon}{\epsilon_k}$$

is the Maxwell distribution function. Such k_d's correspond to H-atom production rates of 200 or 40 torr/sec. An effective ionization rate constant, k_i, was similarly found to be 7×10^{-11} ($\epsilon_k = 3$ e.v.) or 6×10^{-12} ($\epsilon_k = 2$ e.v.), corresponding to ionization rates of 7 or 0.6 torr/sec., respectively. The latter should be approximately equal to the ambipolar diffusion loss, $5.8/r_0^2\ D_+T_e\ n_e/T_g$, which equals 9 or 6 torr/sec. if $D_+ =$ 700 cm.^{2}/sec. at 1 torr pressure. This crude calculation suggests that $\epsilon_k =$ 3 e.v. is a better choice than 2.0 e.v. It neglects the serious deviation from a Maxwell distribution which is to be expected.

More realistic estimates of k_d and k_i were obtained by Phelps by simultaneously adjusting E/N, ϵ_k, and using the appropriate rate coefficients to balance ionization against diffusion losses. This led to values of $\epsilon_k = 3.0$ e.v., $E/N = 1.1 \times 10^{-15}$ volts cm.^{2}/molecule and $k_i = 7 \times 10^{-11}$, in surprising agreement with the above. (The quantity ϵ_k is here defined to equal eD/μ, the ratio of diffusion coefficient to mobility. It is an experimentally determined measure of the electron energy even when the energy distribution is not Maxwellian.) With that E/N, an estimate of k_d can be obtained from Reference 15, Figure 8 by multiplying the excitation coefficient (8×10^{-17} cm.^{2}/molecule) by the drift velocity (1.5×10^7 cm./sec.) which gives $k_d = 1.2 \times 10^{-9}$, also in fortuitously good agreement with 1.1×10^{-9} above. This excitation coefficient includes other, non-dissociating processes, but since application of Corrigan's (5) larger dissociation cross section would increase the total excitation coefficient, its subsequent apportioning would not lead to serious discrepancies. It is Phelps's view that the high E/N portion of the inelastic collision frequency and the corresponding cross sections will have to be modified in view of recent work by Fletcher and Haydon (*11*).

Thus, a very large atom production term of about 200 torr/sec. is indicated by all available estimates. In addition, there is the source term because of electron-ion recombination at the wall, and because of the fast reaction $H_2^+ + H_2 \rightarrow H_3^+ + H$. Each of these can at most equal the ionization rate, so that their sum will contribute 10 to 20 torr/sec. of atomic hydrogen. All other source terms are negligible.

Surface recombination provides the only comparably large loss term in the discharge. For small γ, the first order rate constant, $k_s = \gamma c/d = 2 \times 10^5\ \gamma$, and the steady-state atom concentration, $[H]_{ss}$ is approximately $1 \times 10^{-3}/\gamma$. This shows that γ must always be relatively large, and that the diffusion controlled $k_s = 5.8\ D/r^2 =$ 2 to 4×10^4 sec.$^{-1}$

Publication Date: June 1, 1969 | doi: 10.1021/ba-1969-0080.ch003

In Chemical Reactions in Electrical Discharges; Blaustein, B.;
Advances in Chemistry; American Chemical Society: Washington, DC, 1969.

may be applicable which leads to an $(H)_{ss}$ of 0.5 to 1 $\times$ 10^{-2} torr, less than 1% mole fraction. When γ is lowered to 10^{-2}, $[H]_{ss} = 0.1$ torr, and under either condition the half-life for this formation is very short (3×10^{-5} or 3×10^{-4} sec.).

One is thus led to the interesting conclusion that the dissociation yield of such H_2 discharges is mainly controlled by surface recombination and that the surface in the discharge must be moderately to highly efficient for atom recombination. Moreover, the effect of small amounts of added gases such as H_2O or O_2 in increasing the yield must be through their influence on the surface efficiency, as they can not affect the principal production term and as no homogeneous loss mechanisms of proper magnitude are available. These conclusions are in general agreement with recent work by Goodyear and Von Engel (*14*) on radio frequency discharges at lower pressure and of different geometry.

The very large body of experimental work on the "catalytic" production of H when small amounts of H_2O or O_2 are added will not be reviewed here. The effect is unquestionably real—*i.e.*, factors of 10 or so in H-atom yield when switching from "dry" H_2 to H_2 containing 0.1 to 0.3% H_2O can be demonstrated routinely and reversibly. Rony and Hanson (*26, 27*) have recently questioned the existence of such an effect at a pressure of 0.075 torr and have reviewed the general subject. Our early experiments do not bear this out, as they show a large catalytic effect for added H_2O, but they do indicate that the effect is less pronounced at pressures below 0.1 torr. This trend can be expected if the above analysis is correct, because at low pressures, the production terms are decreased and the loss terms increased. Moreover, for a given discharge energy input, the surface should be hotter at low pressure, and this may nullify the deactivation which is probably caused by adsorbed water molecules. Several of the relevant experiments are now under way in our laboratory by D. A. Parkes, using Lyman-α absorption for the downstream measurement of [H].

Oxygen Discharges. Electron collision cross sections have been calculated by Hake and Phelps (*15*) from all available experimental data on electron drift velocity and other transport coefficients. The cross sections for vibrational excitation are much smaller than in H_2 and that process can probably be neglected. Electronic excitation is described by three processes with thresholds at 4.5, 8.0, and 9.7 e.v. The latter two are larger than the first, and should lead to dissociation, since the upper states have shallow potential energy minima at larger internuclear distances than the ground state. The combined cross section for the 8.0 and 9.7 e.v. excitation shows a broad first peak of 1.1×10^{-16} cm.^{2} at 12 to 15 e.v., then drops slightly and rises again to a second peak in the 50 to 100 e.v. range. With the assumption of an average electron energy, ϵ_k,

Publication Date: June 1, 1969 | doi: 10.1021/ba-1969-0080.ch003

In Chemical Reactions in Electrical Discharges; Blaustein, B.;
Advances in Chemistry; American Chemical Society: Washington, DC, 1969.

of 3.0 e.v. the effective dissociation rate constant, k_d, is about 2×10^{-9} cc. molecule^{-1} sec.$^{-1}$.

The corresponding ionization rate constant, k_i, was calculated to be 1.3×10^{-10} cc. molecule^{-1} sec.$^{-1}$. Fitting the O_2 data in a similar way to H_2, Phelps obtained $E/N = 9 \times 10^{-16}$ volts cm.^{2}/molecule, $\epsilon_k = 3.4$ e.v., $k_d = 1 \times 10^{-9}$, and $k_i = 1 \times 10^{-11}$ cc. molecule^{-1} sec.$^{-1}$, in fair agreement with the above except for the smaller k_i, but k_i is strongly dependent on E/N near 10^{-15} volts cm.^{2}/ molecule, so that a 20% increase of E/N would lead to a ten-fold increase of k_i.

An O-atom production rate of about 200 torr/sec. by dissociative electron impact is thus indicated, and all other production terms are negligible by comparison. Surface recombination of O-atoms is kinetically similar to that of H-atoms except for a lower diffusion coefficient and molecular velocity by a factor of three. Thus, the effective first order surface recombination rate constant is $6 \times 10^4 \gamma$ sec.$^{-1}$ for small γ and 5×10^3 sec.$^{-1}$ for γ approaching unity.

In pure O_2, as in N_2, there is another loss term which does not arise in H_2. The polyatomic ions O_3^+ and O_4^+ can react exothermically and rapidly *via* $O_4^+ + O \rightarrow O_3^+ + O \rightarrow O_2^+ + O_2$ to recombine O-atoms. To obtain an upper limit for this loss rate one may assume that O_4^+ is a major ion—*i.e.*, $[O_4^+] = 10^{11}$ cm.$^{-3}$, and that it is therefore regenerated by the bimolecular reaction $O_2 + O_2^+ \rightarrow O_4^+$. The latter assumption requires that the lifetime of the unstabilized O_4^+ collision complex be equal to or longer than the collision time, 3×10^{-7} sec., which seems excessively long for such a simple species. At its (unreasonable) maximum estimate, such a chain process may recombine O-atoms at twice the rate of $O_4^+ + O \rightarrow O_3^+ + O_2$—*i.e.*, with an effective first order rate constant of 200 sec.$^{-1}$ if both ion molecule reactions have rate constants of 10^{-9} cc. molecule^{-1} sec.$^{-1}$. Even so, it would not seriously limit O-atom production, since the corresponding $[O]_{ss} = 0.5$ torr $= 50\%$ mole fraction. Moreover, Knewstubb, Dawson, and Tickner (*19*) saw no O_4^+ in their mass-spectrometric study of d.c. O_2 discharges at 0.4 torr, though the weakly bound ion could have dissociated in the large electric field at the sampling orifice as Schmidt (*30*) suggests for N_4^+ in his mass-spectrometric study of nitrogen ions. The above mechanism does have the desirable property that it is easily quenched by small amounts of added gases such as N_2 or H_2 which are capable of transforming the oxygen ions into more stable ions such as NO^+ or H_3O^+, but it is unlikely to be important here.

The process $O^- + O \rightarrow O_2 + e$ is known to be fast (*9*) ($k = 1.5 \times 10^{-10}$) and it should follow the dissociative attachment step $e + O_2 \rightarrow O^- + O$ which has a threshold of 4.5 e.v. and a low maximum near 7 e.v. Insofar as O^- is formed mainly by this reaction and removed by its

Publication Date: June 1, 1969 | doi: 10.1021/ba-1969-0080.ch003

reverse, and the concentrations of electrons and ions are very much lower than those of neutral species, these steps leave [O] unchanged.

If the above large excitation-dissociation rates are approximately correct, the O-atom yield, as the H-atom yield in the preceding section, is principally controlled by surface recombination in the discharge. The smallest calculated $[O]_{ss}$ ($\gamma = 1$) is about 0.04 torr, 4% mole fraction, considerably larger than experimental values for pure O_2. A possible explanation of this discrepancy may lie in the surface properties immediately downstream from the discharge region. Active discharges have a sharp boundary as shown by their light emission, because electron loss processes are very fast. The corresponding transition of the surface from a region where γ is near unity to one where it is less than 10^{-4} is likely to be more gradual, and would provide a region in which large, highly localized surface loss terms could quickly reduce the atom concentration.

Experimentally, large catalytic effects by N_2, NO, or H_2 in the production of O-atoms in microwave discharges have been reported (*17, 18*). Very pure oxygen gave only 0.6% atoms (still lower yields of 0.3% were later obtained), but small additions (0.01 to 0.05%) of N_2, N_2O, or NO produced O-atoms at the rate of 40 to 45 per added N, and similar additions of H_2 produced 160 to 200 O-atoms per added H_2. In terms of the present interpretation, the large catalytic effect may be understandable for H_2 additions as caused by H_2O wall effects, but less so for nitrogen compounds which should not be strongly adsorbed at the surface. Conceivably, NO^+ or NO_2^+, strong Lewis acids, may be involved in poisoning the surface. Thus, our understanding of O_2 discharges is still in an unsatisfactory state. Further experiments are required in which particular attention should be given to the condition and characterization of the surface as well as to the immediate downstream region.

Nitrogen Discharges. The great complexity of "active nitrogen" is probably ascribable to its larger cross sections for vibrational excitation and to the existence of metastable electronically excited states below the dissociation limit of ground-state N_2. Consequently, extensive vibrational excitation persists for times much longer than those spent in the discharge zone, and chemiionization is observed in regions such as the "pink glow" well downstream of the discharge. The absence of the lowest triplet state, $A,^3\Sigma_u$, in active nitrogen (*36*) containing N-atoms indicates that these excited molecules are very efficiently quenched by N, and that vibrationally highly excited ground-state molecules are the principal carriers of excitation to the downstream region. Engelhardt, Phelps, and Risk (*8*) have determined the relevant elastic and inelastic electron collision cross sections. Some of the electronically excited states above the dissociation limit do not lead to predissociation, and therefore only the

Publication Date: June 1, 1969 | doi: 10.1021/ba-1969-0080.ch003

In Chemical Reactions in Electrical Discharges; Blaustein, B.;
Advances in Chemistry; American Chemical Society: Washington, DC, 1969.

state with threshold energy of 14 volts was used in the estimate of dissociation. Assuming an average electron energy, $\epsilon_k = 3$ e.v., and a maxwellian distribution, one obtains an effective dissociation rate constant, k_d, of 3×10^{-10} (60 torr/sec.) and a corresponding ionization rate constant, k_i, of 6×10^{-11}. The latter is larger (6 torr/sec.) than the corresponding ambipolar diffusion loss term (0.5 to 1 torr/sec.). The more realistic calculation by Phelps which simultaneously fits ϵ_k, E/N, and the known cross sections to make the ambipolar diffusion loss equal the rate of ionization gave $\epsilon_k = 2.2$ e.v., $E/N = 1.2 \times 10^{-15}$ volts cm.^{2}/molecule, $k_d = 3 \times 10^{-11}$ (6 torr/sec.), and $k_i = 3 \times 10^{-12}$. The dissociation rate is much lower than that of H_2 or O_2 and properly reflects the difficulty of producing extensive dissociation of N_2 in glow discharges. No other source terms of comparable magnitude are available. The principal loss processes include atom recombination at the surface which can be set equal to those of oxygen, because the molecular velocities are similar. The catalytic atom loss mechanism by $N_4^+ + N \rightarrow N_3^+ + N_2$, $N_3^+ + N \rightarrow N_2^+ + N_2$, and $N_2^+ + N_2 \rightarrow N_4^+$ has been suggested by Young *et al.* (*37*). The binding energy of N_4^+ is about 0.5 e.v. (*34*, *35*), but its direct, bimolecular formation is reported to be very slow (*12*). It must be expected that the association of such a simple complex will not be in its second-order (high pressure) limit at 1 torr pressure, and the catalytic loss process then becomes inoperative, as its rate is limited by a relatively slow three-body reaction. The balance of the main production and loss terms here predicts a minimum $[N]_{ss}$ of 0.1% when γ is near unity and the recombination in the close post-discharge region is neglected. When γ is sufficiently small to make $[N]_{ss}$ about 20 to 50 times larger, the corresponding surface recombination rate constant, k_s, is relatively small (100 sec.$^{-1}$) and the half-life for attaining steady-state may become longer than the residence time so that dissociation becomes source-controlled. This has been observed in recent experiments in our laboratory where two microwave discharges in series in rapidly pumped N_2 at 7 torr produced approximately twice the [N] of each one operating alone.

Experimentally, there is abundant evidence for "catalytic" effects as summarized by Young *et al.* (*38*), who studied the effectiveness of O_2, NO, and SF_6 added either before or immediately after a microwave discharge in highly purified, flowing N_2. All three gases were "catalytic" when added before, but only NO after the discharge, and SF_6 added before "produced" 230 N-atoms per SF_6 molecule. The ESR method employed may give erroneous results, however (*33*). At the present writing, these effects, as the similar ones in H_2 or O_2, can only be understood in terms of surface effects in the discharge. In addition, long-lived vibrational excitation is probably responsible for downstream "pink glow" chemiionization effects. The electron impact cross sections are largest

Publication Date: June 1, 1969 | doi: 10.1021/ba-1969-0080.ch003

In Chemical Reactions in Electrical Discharges; Blaustein, B.;
Advances in Chemistry; American Chemical Society: Washington, DC, 1969.

for the production of ground-state N_2 with relatively little vibrational excitation (*31*) (v = 1 to 4). If these states are extensively populated, the gas will leave the discharge with vibrational energy corresponding to a temperature of 5,000 to 10,000°K., but in a non-equilibrium distribution, lacking its proper complement of highly energetic molecules. These will be formed by vibration-vibration energy transfer which may be relatively slow at the higher levels where the anharmonicity is large.

Discharge Chemistry in More Complicated Systems

Although this is the area of greatest interest to most chemists, the necessary fundamental information is mostly lacking. Data on some triatomic molecules such as CO_2 (*15*) and H_2O (*24*) have been analyzed. Their active discharges will also contain diatomic molecules such as CO, O_2, OH, or H_2 as well as the free atoms. This means that reactions between the various neutral species must also be considered. These may be much slower than the electron impact processes and may require long residence times in the discharge to reach their steady state. The approach to full steady state may therefore be characterized by several time constants, very short ones for ionization and direct excitation or dissociation, and various superimposed longer ones due to reactions of neutral species requiring an energy of activation—*e.g.*, hydrogen abstraction from hydrocarbons which often has an E of 7 to 10 kcal./mole.

Glow discharges in water vapor are a good example of the chemical complexity of simple polyatomic systems. Their chemistry was long misrepresented on the assumption that dissociation to H and OH was the principal discharge reaction and that their recombination could be measured downstream. Space-resolved line absorption experiments on OH in a fast-flow steady-state system (*6*) showed, however, that negligible amounts of OH were present a few milliseconds downstream of the discharge, but that a little OH was produced further downstream by slow reactions such as $H + O_2 + M \rightarrow HO_2 + M$ and $H + HO_2 \rightarrow 2\ OH$. Thus, the discharge is an excellent source of H-atoms, but the further excitation-dissociation of OH is apparently so rapid that O-atoms are also formed, and the very fast reaction $O + OH \rightarrow O_2 + H$ accounts for the major discharge products which are H-atoms and O_2. When the dissociation of OH in the discharge is insufficient to produce the O-atoms needed in the above reaction, OH may leave the discharge, but will react rapidly by $2\ OH \rightarrow H_2O + O$ and $OH + O \rightarrow O_2 + H$ for an overall stoichiometry of $3\ OH \rightarrow H_2O + O_2 + H$. Should OH be extensively dissociated in the discharge as appears to be the case at pressures below 0.1 torr, O-atoms will persist, and the overall discharge products will consist of varying amounts of H, O, and O_2, with H always in great excess. It is

Publication Date: June 1, 1969 | doi: 10.1021/ba-1969-0080.ch003

In Chemical Reactions in Electrical Discharges; Blaustein, B.;
Advances in Chemistry; American Chemical Society: Washington, DC, 1969.

clear from this discussion that the primary electron energy and cross section data obtained from transport properties in pure H_2O are much less applicable in determining principal discharge products and their yields. The ionization threshold and cross sections in H_2O are similar to those in O_2. The excitation-dissociation cross sections have higher thresholds (12.0 and 12.6 e.v.), but rise more sharply with increasing electron energy, so that one would expect the primary ionization rate to be equal to that in O_2, and the primary dissociation rate to be lower if ϵ_k is comparable. All ions will be extensively hydrated, which should increase the rate constants of many bimolecular ion-molecule reactions and make it possible for association reactions to take place by simple two-body processes.

In conclusion, the varied aspects of glow discharge chemistry should be summarized once more. In the case of moderately complex reactants, one should have knowledge of many things in order to progress from a cookbook level to one of (partial) understanding: (a) Electron impact ionization and dissociation rates of reactants and other major species; (b) Surface recombination rates in the discharge; (c) Ion-molecule reaction rates involving major neutral species; (d) Neutral-neutral reaction rates and their temperature dependences in and out of the discharge. Much of the necessary information for (a), (c), and (d) is becoming available for many systems. The role of the surface, however, is little understood for electrically neutral reactants, even less so for charged species, and seems to be the present bottleneck.

Publication Date: June 1, 1969 | doi: 10.1021/ba-1969-0080.ch003

Acknowledgments

The author would like to thank A. V. Phelps for many interesting discussions and for calculations of important parameters.

Literature Cited

(1) Biondi, M. A., *Advan. Electron.* **18,** 67 (1963).
(2) Brown, S. C., *Handbuck der Physik* **22,** 531 (1956).
(3) Brown, S. C., "Introduction to Electrical Discharges in Gases," John Wiley & Sons, New York, 1966.
(4) Carlton, T. S., Mahan, B. H., *J. Chem. Phys.* **40,** 3683 (1964).
(5) Corrigan, S. J. B., *J. Chem. Phys.* **43,** 4381 (1966).
(6) DelGreco, F. P., Kaufman, F., *Discussions Faraday Soc.* **33,** 128 (1962).
(7) Engelhardt, A. G., Phelps, A. V., *Phys. Rev.* **131,** 2115 (1963).
(8) Engelhardt, A. G., Phelps, A. V., Risk, C. G., *Phys. Rev.* **135,** A1566 (1964).
(9) Fehsenfeld, F. C., Ferguson, E. E., Schmeltekopf, A. L., *J. Chem. Phys.* 44, 1844 (1966).
(10) Ferguson, E. E., Fehsenfeld, F. C., Golden, P. D., Schmeltekopf, A. L., *J. Geophys. Res.* **70,** 4323 (1965).
(11) Fletcher, J., Haydon, S. C., *Australian J. Phys.* **19,** 615 (1966).

(12) Giese, C. F., Maier, W. B., *J. Chem. Phys.* **35,** 1913 (1961).
(13) Goldstein, L., *Advan. Electron. Electron Phys.* **7,** 399 (1955).
(14) Goodyear, C. C., Von Engel, A., *Proc. Phys. Soc.* **79,** 732 (1962).
(15) Hake, R. D., Jr., Phelps, A. V., *Phys. Rev.* **158,** A70 (1967).
(16) Kasner, W. H., Biondi, M. A., *Phys. Rev.* **137,** A317 (1965).
(17) Kaufman, F., Kelso, J. R., *J. Chem. Phys.* **32,** 301 (1960).
(18) Kaufman, F., Kelso, J. R., "8th International Combustion Symposium," p. 230, Williams and Wilkins, Baltimore, Md., 1960.
(19) Knewstubb, P. F., Dawson, P. H., Tickner, A. W., *J. Chem. Phys.* **38,** 1031 (1963).
(20) Llewellyn-Jones, F., "The Glow Discharge," Methuen, London, 1966.
(21) Mahan, B. H., Person, J. C., *J. Chem. Phys.* **40,** 392 (1964).
(22) Massey, H. S. W., Burhop, E. H. S., "Electronic and Ionic Impact Phenomena," Oxford Univ. Press, London, England, 1952.
(23) McDaniel, E. W., "Collision Phenomena in Ionized Cases," John Wiley and Sons, New York, 1964.
(24) Phelps, A. V. (private communication).
(25) Rapp, D., Briglia, D. D., *J. Chem. Phys.* **43,** 1480 (1965).
(26) Rony, P. R., Hanson, D. N., *J. Chem. Phys.* 44, 2536 (1966).
(27) Rony, P. R., *Lawrence Radiation Lab. Rept.* **UCRL-16050** (April 1965).
(28) Rose, D. J., Brown, S. C., *Phys. Rev.* **98,** 310 (1955).
(29) Schmeltekopf, A. L., Fehsenfeld, F. C., Gilman, G. I., Ferguson, E. E., *Planetary Space Sci.* **15,** 401 (1967).
(30) Schmidt, M., *Beiträge d. Plasmaphysik* **3,** 147 (1966).
(31) Schulz, G. J., *Phys. Rev.* **135,** A988 (1964).
(32) Tanaka, Y., Innes, F. R., Jursa, A. S., Nakamura, M., *J. Chem. Phys.* **42,** 1183 (1965).
(33) Ultee, C. J., *J. Chem. Phys.* **41,** 281 (1964).
(34) Varney, R. N., *J. Chem. Phys.* **31,** 1314 (1958).
(35) *Ibid.*, **33,** 1709 (1960).
(36) Young, R. A., *Can. J. Chem.* 44, 1171 (1966).
(37) Young, R. A., Gatz, C. R., Sharpless, R. L., *J. Phys. Chem.* **69,** 1763 (1965).
(38) Young, R. A., Sharpless, R. L., Stringham, R., *J. Chem. Phys.* **40,** 117 (1964).

RECEIVED May 12, 1967. This work was supported by the National Science Foundation under Grant No. GP-5369.

4

Ionic Reactions in Corona Discharges of Atmospheric Gases

M. M. SHAHIN

Research Laboratories, Xerox Corporation, Rochester, N. Y.

Publication Date: June 1, 1969 | doi: 10.1021/ba-1969-0080.ch004

Mass spectrometric studies of positive corona discharges in various mixtures of nitrogen, oxygen, and water vapor, at pressures up to 40 torr, have provided evidence for the importance of water in these systems. Detailed studies of these discharges show many sequences of chemical reactions by which various ionic species undergo transformations which produce hydrated proton clusters such as $(H_2O)_nH^+$ *where* $n = 1, 2$, *etc., as final charge carriers. In various mixtures of nitrogen and oxygen, where water vapor is absent, it is shown that charge exchange reactions are by far the most important ionic reactions through which the primary ion is transformed. Reactions leading to the formation of various ions of oxides of nitrogen appear to be of secondary importance within the pressure range investigated.*

Mass spectrometric studies of electrical discharges have been carried out during the past decade by several workers (*4, 5, 6, 8, 9, 10*) in an attempt to identify the ionic precursors of a variety of neutral by-products which are formed in these systems. Such studies are expected to reveal the detailed chemistry of the many reactions that follow the formation of primary ions through the impact of energetic electrons on the neutral gas molecules, and end with the neutralization of the final form of the ion either in the gas-phase or at the electrodes or the walls of the discharge tube. Thus, the identification of these ionic reactions will, in many cases, demonstrate the mechanism of the production of the free-radicals which are the source of the neutral by-products. Further, such studies would be expected to provide information on the mechanisms of catalytic or inhibitory effects of trace quantities of certain compounds —*e.g.*, water vapor—on the formation of these products. Processes such as charge-exchange or ion-molecule reactions which occur with large

In Chemical Reactions in Electrical Discharges; Blaustein, B.;
Advances in Chemistry; American Chemical Society: Washington, DC, 1969.

cross sections and have been suspected to be responsible for such effects will thus be easily identified.

The complexity of electrical discharges, however, often makes the interpretation of mass spectrometric data very difficult. Specifically, the variations of electric field along and across the discharge tube in certain commonly used discharges often affect the abundance distribution of the various ionic species which are observed at the mass spectrometer (*5*, *6*). This is mainly caused by the complex dependence of the cross sections of both charge-exchange and ion-molecule reactions on ion energy as determined by the electric field within the discharge tube. Further complication arises from the formation of ion-sheaths around the walls of the discharge tube, through ambipolar diffusion. These may strongly influence the sampling of the discharge by the mass spectrometer. It is therefore essential that the system under investigation be well understood before the interpretation of the data is attempted.

In this paper, the results of mass spectrometric investigations on low pressure positive corona discharges established between two coaxially placed electrodes will be discussed. This form of discharge has been chosen primarily because its electrical properties are relatively simple and better understood. Further, the ion-sheath effects at the point of sampling are minimized because of the low level of ionization in these systems.

Publication Date: June 1, 1969 | doi: 10.1021/ba-1969-0080.ch004

Experimental

Detailed description of the apparatus has already been given (*10*). Figure 1 shows the schematic diagram of the apparatus. The corona discharge tube was constructed of a stainless-steel cylinder 4 inches long and ½-inch i.d. with a coaxial platinum wire of 3-mil diameter. The cylindrical tube wall contained a pinhole which was positioned along the axis of the quadrupole mass spectrometer and served as an ion-exit aperture. The pinhole was made by thinning the wall of the tube to a thickness of 1 to 2 mils before drilling a hole of 0.1 mm. This hole was later narrowed to the desired diameter by peening. The coaxial discharge tube is operated through a high-voltage d.c. power supply and the current is stabilized through the use of an external current limiting resistor, *R*. Electrons moving through the high field region present only at very close distances to the anode wire will gain energy from the field and cause ionization of the gas molecules in this region. Because of the symmetry of the electrodes, therefore, the system closely behaves as a line source of positive ions which are continuously regenerated. These ions will then move through the gas, perpendicular to the axis, undergoing various interactions before reaching the cathode. The small sampling port (10 to 100 microns in diameter) at the cathode allows a small portion of the ions to escape the discharge tube and be analyzed by a quadrupole mass spectrometer.

In Chemical Reactions in Electrical Discharges; Blaustein, B.;
Advances in Chemistry; American Chemical Society: Washington, DC, 1969.

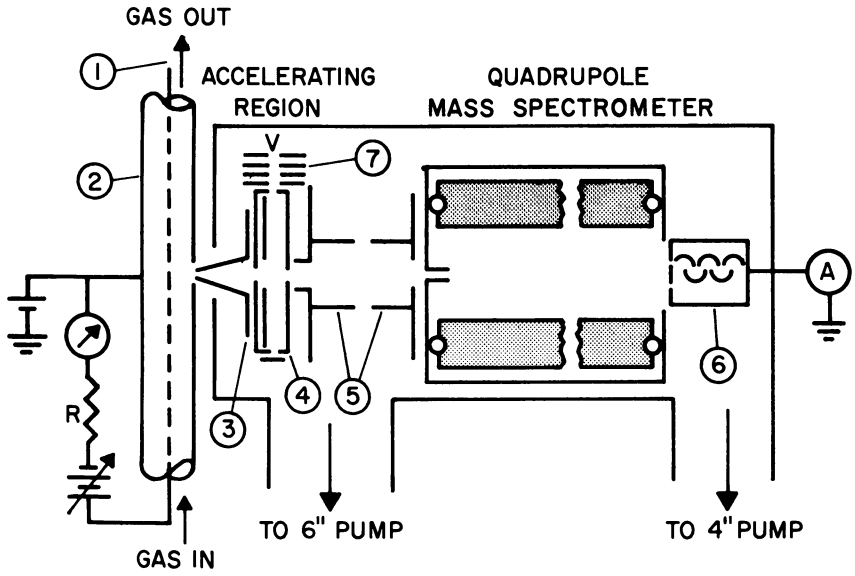

Figure 1. Schematic diagram of the discharge tube and mass spectrometer— (1) platinum wire anode; (2) cylindrical discharge tube; (3) extraction electrode; (4) mass spectrometer ionization chamber; (5) focussing electrodes; (6) electron multiplier; (7) electron-gun assembly. Typical voltages used on these electrodes during ion extraction from the discharge tube, are with respect to ground as follows: (2) + 50 volts; (3) − 50 volts; (4), and inner electrode, 0 volts; (5), part close to (4), − 25 volts; (5), part close to quadrupole, + 100 volts; quadrupole case, 0 volts

The form of the electric field within the discharge tube is rectangular hyperbolic before the discharge is established. As the discharge is formed, under sufficiently high current density, the presence of the positive space charge distorts this initial field, causing the latter to attain a constant value for the major distance between the electrodes (*12*). Experiments which are described here, however, are carried out mainly in low current region where the general form of the electric field within the discharge is expected to remain rectangular hyperbolic. Thus, $E_r = V/r \ln(b/a)$, where E_r is the electric field at a distance r from the central wire, V is the applied voltage and b and a are the radii of the cathode and anode respectively. The discharge current throughout these experiments were maintained constant to better than 10%. Under these conditions the reproducibility of the individual ion intensity measurement could be maintained to approximately 10% when the discharge gas pressure and composition remained unchanged.

Differential pumping of the sampling region and the mass spectrometer allows operation of the discharge tube between pressures ranging from less than 1 torr to atmospheric. An electron gun placed before the mass spectrometer serves as an independent ionizing source for monitoring the composition of the neutral discharge gas when no ions are extracted

Publication Date: June 1, 1969 | doi: 10.1021/ba-1969-0080.ch004

In Chemical Reactions in Electrical Discharges; Blaustein, B.;
Advances in Chemistry; American Chemical Society: Washington, DC, 1969.

from the discharge tube. For such analysis, calibration curves made on prepared gas mixtures, showing mass discrimination owing to the specific flow condition are used. A rapid flow of gas is maintained through the discharge tube to avoid appreciable accumulation of neutral by-products of the discharge. For this purpose a linear flow velocity is maintained such as to completely renew the gas within the tube in two seconds. In systems where the concentration of the electro-negative gas—*e.g.*, oxygen —is low, an external source of ionization through the use of a weak radioactive source—*e.g.*, ^{210}Po—is used to stabilize the discharge.

The general problem of mass spectrometric sampling from high pressure sources has recently been discussed by several workers (*1, 3, 7*). In systems where condensable gases are present, the temperature drop following the adiabatic expansion of the gas through the sampling nozzle may cause condensation if such gaseous components are present in sufficient concentrations. In the present experiments, the water content of the gases under investigation has been chosen below 5×10^{-2} mole %. Under these conditions, it can be demonstrated that such condensations make negligible contribution to the results. (Calculations based on the maximum number of collisions of an ion with water molecules present up to 10^{-1} mole % in an expanding gas, assuming cross sections of 10^{-13} cm.^{2}, show negligible contribution to the total collisions that such an ion and molecule will undergo within the discharge system. These calculations will be published elsewhere.)

Publication Date: June 1, 1969 | doi: 10.1021/ba-1969-0080.ch004

Results and Discussions

Earlier experiments (*8*) on corona discharges in air at atmospheric pressure clearly demonstrated the important role of trace quantities of water vapor in these systems. In nitrogen, oxygen, and their mixtures, where the water content exceeded 4 to 5×10^{-2} mole %, the dominant ionic species observed at the mass spectrometer were those corresponding to hydrated proton clusters, $(H_2O)_nH^+$. These species were apparently formed from the interaction of the primary ions with the water molecules in the system as they passed through the gas to the cathode. In order to determine the role of various reactions which lead to such clusters, low pressure experiments were designed with individual gaseous components —*e.g.*, O_2, N_2—and their corresponding mixtures with various quantities of water vapor. These experiments were expected to reveal the formation of intermediate species and their final conversion to hydrated protons.

Discharge in Nitrogen. Experiments with nitrogen at low pressures, containing various concentrations of water vapor show several intermediates which are formed through the reactions of nitrogen ions with water. The results of a typical experiment showing the relative abundances of various species reaching the mass spectrometer as the pressure of the discharge is varied, are shown in Figure 2. In this experiment, which was carried at low current density (1×10^{-8} amps./cm. length), where

In Chemical Reactions in Electrical Discharges; Blaustein, B.;
Advances in Chemistry; American Chemical Society: Washington, DC, 1969.

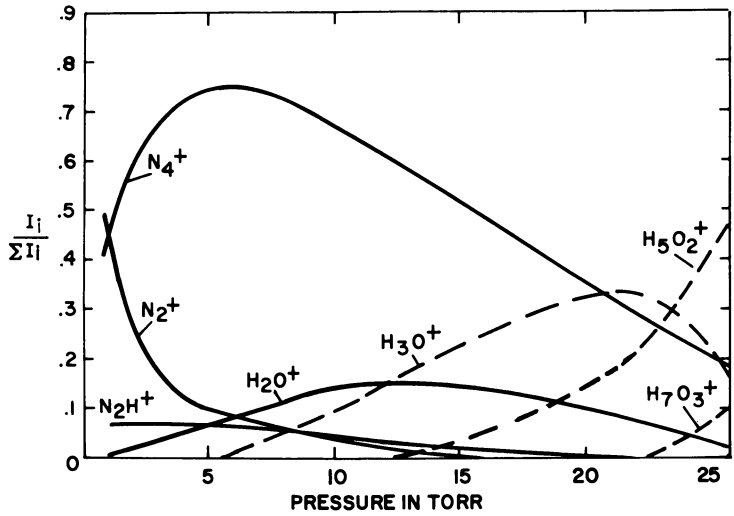

Figure 2. Variation of the relative abundance of different ions with pressure in a positive corona discharge in nitrogen containing 2.2 × 10^{-2} mole % of water vapor. Discharge current is 1 × 10^{-8} amps./cm. length. Discharge potential varied between 630 and 720 volts

the overall electric field is relatively low, it can be observed that as the pressure is increased, the abundance of the primary ion, N_2^+, is sharply reduced while those of the intermediate ions, namely, N_4^+, N_2H^+, and H_2O^+ rise to a maximum and then decrease as the tertiary ion H_3O^+ begins to appear. This latter ion also rises to a maximum at higher pressures as its more highly hydrated forms appear. Thus, the two reactions:

$$N_2^+ + H_2O \rightarrow N_2H^+ + OH, \Delta H \doteq -0.6 \text{ e.v.} \quad (1)$$

and

$$N_2^+ + H_2O \rightarrow H_2O^+ + N_2, \Delta H = -3.0 \text{ e.v.} \quad (2)$$

appear to provide species which can further react with water through Reactions 3 and 4 to form the hydrated proton:

$$N_2H^+ + H_2O \rightarrow H_3O^+ + N_2, \Delta H \doteq -3.4 \text{ e.v.} \quad (3)$$

$$H_2O_g^+ + H_2O_g \rightarrow H_3O_g^+ + OH, \Delta H = -1 \text{ e.v.} \quad (4)$$

The third and the major intermediate, namely N_4^+ which is formed through reaction of N_2^+ with neutral nitrogen molecule (*11*), apparently also undergoes reactions with water similar to Reactions 1 and 2 to form N_2H^+ and H_2O^+ ions. These reactions are also expected to be exothermic. The relative abundance of N_4^+ ion is found to be strongly dependent on the field strength within the discharge tube. Specifically, it is found that the relative abundance of N_4^+ decreases sharply at current densities above

Publication Date: June 1, 1969 | doi: 10.1021/ba-1969-0080.ch004

1×10^{-8} amp./cm. length, reaching a steady but lower value at around 1×10^{-7} amp./cm. length.

Two other intermediate species have been observed in this system. These ions, not shown in Figure 2, are N_4H^+ and N_3H^+. They apparently arise as a result of ion-molecule reactions involving N_4^+ and N_3^+ ions in the system with water molecules and are expected to undergo proton transfer reactions similar to Reaction 3, to yield H_3O^+.

Other ions observed were at $m/e = 32$ and 46. These ions are believed to arise from trace quantity of oxygen which is inevitably present in this system as a result of the decomposition of water. The ion of $m/e = 32$ is apparently O_2^+ while that of $m/e = 46$ is NO_2^+.

In a system of pure nitrogen where the water concentration was kept below 5×10^{-3} mole %, under similar discharge conditions as those presented in Figure 2, it was observed that the intensity of N_4^+ ion rapidly increased as the gas pressure was increased, reaching a plateau after a few mm. Hg pressure. This plateau corresponded to 95% of total ion intensity, with the remaining 5% being mainly owing to N_3^+ ion. This result indicates the presence of a low overall E/P between the two electrodes (*11*) in these low current experiments and the lack of any appreciable ion-sheath near the cathode.

Discharge in Oxygen. Figure 3 shows the pressure dependence of the relative abundance of various ionic species in a corona discharge in oxygen. This experiment shows several marked differences from those shown for nitrogen in Figure 2. The most striking feature is the presence of large abundances of hydrated forms of the primary ion, namely $O_2^+(H_2O)_{1,2}$ and their dependence on pressure. That the abundances of these ions appear to rise to a maximum and then decrease at higher pressures with the formation of hydrated protons strongly suggests their role in the intermediate processes. This evidence together with the appearance of $(H_2O)_2^+$ ions in the system, and the variation of its abundance with pressure—*i.e.*, rising to a maximum and then reducing at higher pressures—indicates the operation of an entirely new mechanism in this system for the formation of hydrated protons. Since the ionization potential (I.P.) of oxygen (12.07 e.v.) is lower than that of water (I.P. = 12.56 e.v.), a charge-exchange reaction similar to Reaction 2, for nitrogen does not appear probable. Nor is it likely that a reaction similar to that of Reaction 1, to form O_2H^+ would occur, as it appears to be endothermic. It is therefore probable that the hydrated form of the primary ion, especially the species containing two water molecules may be a precursor in the formation of the hydrated proton through the reactions:

$$O_2^+(H_2O)_2 \rightleftharpoons (H_2O)_2^+ + O_2 \quad (5)$$

$$(H_2O)_2^+ + O_2 \rightarrow (H_2O)H^+ + OH + O_2 \quad (6)$$

Publication Date: June 1, 1969 | doi: 10.1021/ba-1969-0080.ch004

In Chemical Reactions in Electrical Discharges; Blaustein, B.;
Advances in Chemistry; American Chemical Society: Washington, DC, 1969.

Reaction 5 is expected to be exothermic owing to the heat of hydration of H_2O^+ ion. It may also be possible, though unlikely, that any required energy for the reaction be supplied through the electric field in the discharge.

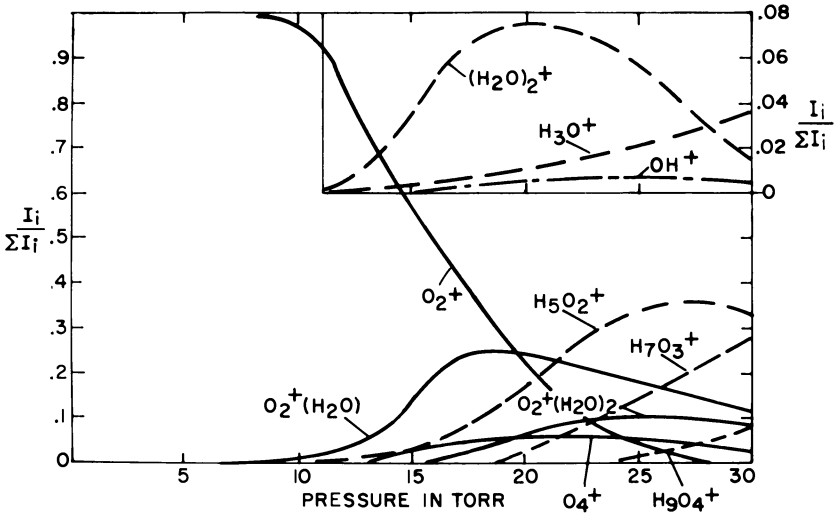

Figure 3. Variation of the relative abundance of different ions with pressure in a positive corona discharge in oxygen containing 2.0 × 10^{-2} mole % of water vapor. Discharge current is 1 × 10^{-8} amps./cm. length. Discharge potential varied between 630 and 750 volts

One other ionic species which may play a role in this system is O^+. However, since the I.P. of atomic oxygen (13.61 e.v.) is greater than that of oxygen, this species is not observed in this system as it most probably undergoes charge exchange with molecular oxygen at pressures used in these experiments. The reaction of O^+ with O_2 to give rise to O_3^+, if it occurs at all, is not observed in these experiments since ozone has also a higher I.P. (12.8 e.v.) than that of oxygen and therefore O_3^+ is similarly expected to undergo a charge-exchange reaction with O_2.

Three other ions were observed in minor relative abundance in this system. These ions are OH^+, H_2O^+, and $H_2O_2^+$. The relative yield of the OH^+ ion is shown in Figure 3 while the yields of H_2O^+ and $H_2O_2^+$, being somewhat smaller, are not indicated. It is believed that the first two of these ions arise from an ion-molecule reaction and a charge-exchange process between O^+ and water molecule respectively, and are detected only at higher discharge pressures where such reactions compete with direct charge transfer of O^+ to oxygen molecules. $H_2O_2^+$ ion, however,

Publication Date: June 1, 1969 | doi: 10.1021/ba-1969-0080.ch004

may appear as a result of an efficient charge transfer process between O_2^+ ion and the trace quantities of H_2O_2, apparently formed in the system.

In a system of pure oxygen, where the water content was kept below 5×10^{-3} mole %, only two ions, O_2^+ and O_4^+ were observed within the pressure range investigated. The abundance of O_4^+ ion rises sharply as the pressure is increased while that of O_2^+ decreases and both reach a plateau beyond a pressure of 20 torr in the discharge tube. The relative abundance of O_4^+ in this plateau region is closely related to the electric field within the discharge tube similar to that already described for N_4^+ ion.

Discharge in Nitrogen Containing 0.44 mole % Oxygen. In order to determine the role of oxygen in air discharges in the absence of water vapor, a number of experiments were carried out in nitrogen containing 0.44 mole % of oxygen. The lower limit of water vapor in these experiments was 5×10^{-3} mole %. Figure 4 shows the results of the relative abundance of various ionic species which are detected at the cathode as

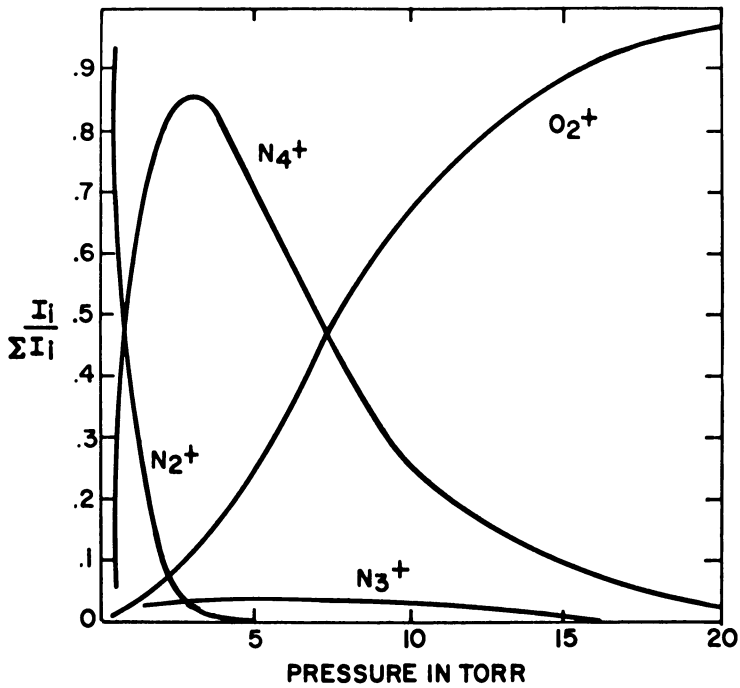

Figure 4. Variation of the relative abundance of different ions with pressure in a positive corona discharge in nitrogen containing 4.4 × 10^{-1} mole % of oxygen and less than 5 × 10^{-3} mole % of water vapor. Discharge current is 1 × 10^{-8} amps./cm. length. Discharge potential varied between 630 and 700 volts

Publication Date: June 1, 1969 | doi: 10.1021/ba-1969-0080.ch004

the pressure of the discharge is increased. These experiments clearly trace the history of the primary ionic species, namely N_2^+ as it is converted to N_4^+ and the latter undergoes charge-exchange with the trace quantity of oxygen present in this system. Thus, beyond a pressure of 20 torr in the discharge tube the charge carriers in this system are almost all O_2^+. The trace amount of N_3^+ observed in the system is also all removed beyond a pressure of 15 torr.

It is significant to note that within the pressure range investigated, no detectable nitric oxide ion is observed in this system. This indicates that neither the reaction $N_4^+ + O_2 \rightarrow NO^+ + NO + N_2$, nor $O_2^+ + N_2 \rightarrow NO^+ + NO$, occur to any appreciable extent, in spite of the fact that both these reactions are expected to be exothermic.

Experiments in which water was not excluded showed the appearance of many ionic intermediates of both pure oxygen and nitrogen and their mixtures. All these ions could be traced and their final conversion to hydrated protons followed.

Discharge in Air. Experiments in air in the absence of water vapor (less than 5×10^{-3} mole %) were carried out to determine the importance of ionic species of oxides of nitrogen in these systems. The results of these experiments are shown in Figure 5. As expected from the previous sections, O_2^+ ion appears as the most abundant ion in this system. Also as expected, O_4^+ ion appears in the system and as the pressure is increased, it becomes an important charge carrier and its relative abundance eventually reaches a plateau. Its relative abundance, however, is strongly dependent on the discharge current similar to that described for N_4^+ ion. The appearance of the ion $O_2^+(H_2O)$, hydrated form of molecular oxygen ion, in this system, indicates the high affinity of this ion for hydration as the gas contained less than 5×10^{-3} mole % water in the discharge tube.

Nitric oxide ion was the only important oxide of nitrogen found in the system under the experimental conditions used here. Its relative abundance remained constant as the discharge pressure was varied between 2 to 40 torr. The presence of NO^+ in these experiments and its absence in experiments carried out in nitrogen containing 0.44 mole % of oxygen may indicate that these ions are probably formed through the reaction

$$N_2^+ + O_2 \rightarrow NO^+ + NO, \Delta H = -4.5 \text{ e.v.} \quad (7)$$

Assuming that O_2^+ arises either through charge-exchange with N_2^+ ion or by direct electron impact on neutral oxygen molecule, one can use the data in these experiments to obtain a relative ratio of the rate-constants for the charge-exchange reaction of N_2^+ with oxygen to that of ion-molecule Reaction 7. This ratio is found to be equal to 8, a value

Publication Date: June 1, 1969 | doi: 10.1021/ba-1969-0080.ch004

which is lower than the ratio of the published values of these rate-constants (*2*). This indicates that possibly other reactions such as $N^+ + O_2 \rightarrow NO^+ + O$ and $O^+ + N_2 \rightarrow NO^+ + N$ or others involving neutral atomic species also contribute to the total yield of NO^+ ion.

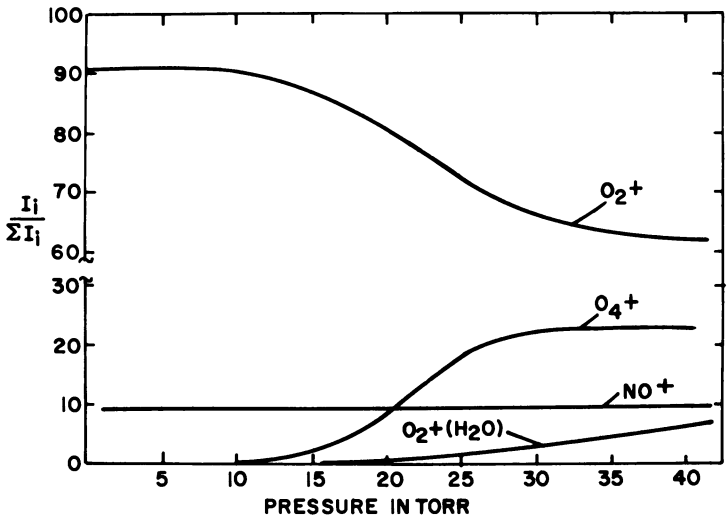

Figure 5. Variation of the relative abundance of different ions with pressure in a positive corona discharge in air with water concentration below 5×10^{-3} mole %. Discharge current is 1×10^{-8} amp./cm. length. Discharge potential varied between 630 and 800 volts

Conclusions

Mass spectrometric studies of low pressure positive d.c. corona discharges in atmospheric gases containing trace quantities of water vapor show a complex series of reactions with each component leading to the formation of hydrated protons in the system. In the case of nitrogen, intermediate species N_2H^+ and H_2O^+ are presumably formed through ion-molecule reaction and charge-exchange of N_2^+ and N_4^+ with water molecules. These species later form the hydrated proton through proton transfer reactions in subsequent collisions with water molecules. In moist gaseous oxygen, it appears that the hydrated form of the primary ion $O_2^+(H_2O)_2$, plays an important role in the conversion of the charge carriers to hydrated protons. It is suggested that this transformation may occur through the formation of the intermediate $(H_2O)_2^+$ which has been found in this system. In experiments where water vapor is excluded from the system, a concentration of 4.4×10^{-1} mole % oxygen can transform,

Publication Date: June 1, 1969 | doi: 10.1021/ba-1969-0080.ch004

In Chemical Reactions in Electrical Discharges; Blaustein, B.;
Advances in Chemistry; American Chemical Society: Washington, DC, 1969.

through charge-exchange reactions, all ionic species of nitrogen to O_2^+ at a discharge pressure of 20 torr, and that ion-molecule reactions leading to the formation of oxides of nitrogen are by far less probable within the pressure range investigated.

Acknowledgments

The author is indebted to W. Roth for his invaluable comments during the course of this work and to A. Friske for his assistance in experimental work.

Literature Cited

(1) Anderson, J. B., Anders, R. P., Fenn, J. B., "Advances in Atomic and Molecular Physics," p. 345, D. R. Bates, ed., Academic Press, New York, 1965.
(2) Ferguson, E. E., Fehsenfeld, F. C., Golddan, P. D., Schmeltekoff, A. L., *J. Geophys. Res.* **70,** 4323 (1965).
(3) Green, F. T., Milne, T. A., *J. Chem. Phys.* **39,** 3150 (1963).
(4) Knewstubb, P. F., Tickner, A. W., *J. Chem. Phys.* **36,** 684 (1962).
(5) *Ibid.*, **36,** 674 (1962).
(6) *Ibid.*, **37,** 2941 (1962).
(7) Leckenby, R. E., Robbins, E. J., Trevalion, P. A., *Proc. Roy. Soc. (London)* **A280,** 409 (1964).
(8) Shahin, M. M., *J. Chem. Phys.* **43,** 1798 (1965).
(9) Shahin, M. M., ADVAN. CHEM. SER. **58,** 315 (1966).
(10) Shahin, M. M., *J. Chem. Phys.* **45,** 2600 (1966).
(11) Varney, R. N., *J. Chem. Phys.* **31,** 1314 (1959).
(12) vonEngel, "Ionized Gases," 2nd ed., Oxford University Press, London. 1965.

RECEIVED April 20, 1967.

Ion-Molecule Reactions in Electric Discharge

J. L. FRANKLIN, P. K. GHOSH, and STANLEY STUDNIARZ

Rice University, Houston, Texas

Publication Date: June 1, 1969 | doi: 10.1021/ba-1969-0080.ch005

A brief review of the literature on reactions and reaction rates of ions with molecules in the gas phase is presented. Most of the studies have been made employing the ion source of a mass spectrometer as a reactor and this review necessarily emphasizes this aspect of the subject. Several studies of ion-molecule reactions in electric discharges have appeared in recent years and these are reviewed briefly. In addition, some unpublished investigations of ions in microwave discharges have been conducted in our laboratory and the results are presented briefly.

A large body of knowledge has been developed in recent years about the kinds of reactions that occur between ions and neutral molecules. The kinetics of ion-molecule reactions have been studied extensively and some are known to be dependent upon the relative velocity of ionic and neutral reactants. Most such information has been obtained employing the ion sources of mass spectrometers. Ions are present in discharges and are important to the support of the discharge and to the nature of the reactions occurring in it. Ions and excited species are usually formed by electron impact and disappear by diffusion to the walls and by recombination in the gas. The recombination reactions are understood very little. The ions themselves often have considerable energy, which affects the rates of their reactions. Discharge characteristics vary greatly with the kinds of discharges, so that the same reactions are not necessarily observable in all kinds of discharges. Several reactions that have been observed in discharges will be discussed.

Ion-Molecule Reactions

Before the development of good vacuum equipment and techniques, mass spectrometrists observed many ions occurring at masses well above

In Chemical Reactions in Electrical Discharges; Blaustein, B.;
Advances in Chemistry; American Chemical Society: Washington, DC, 1969.

those of the molecules admitted to the instrument. These interferred with the main interests of the experimenters at that time, although in a few instances it was recognized that reactions were occurring between primary ions and molecules. When good vacuum facilities became available in the early 1930s they were adapted to mass spectrometry and for a number of years every effort was made to maintain source pressures well below 10^{-6} torr to avoid collisions of primary ions with neutrals. However, in 1940, Mann, Hustrulid, and Tate (*67*) in studying water, observed an ion at mass 19, and by varying the pressure in their instrument, concluded that it was H_3O^+, probably formed by the reaction:

$$H_2O^+ + H_2O \rightarrow H_3O^+ + OH$$

During the middle 1950s, several groups of mass spectrometrists became curious as to the results that would be observed if source pressures were raised sufficiently to allow a few collisions to occur between ions and molecules. Several ions occurring at masses above those of the parent ion were observed. Because of this, a number of systematic studies were made and increasing interest and emphasis on reactions of ions with neutral molecules has developed, until at present some 50 to 100 papers per year are published on this subject alone.

Perhaps one of the strongest reasons for the interest in ion-molecule reactions is the fact that ions of unusual and unsuspected composition were observed. Most fascinating of these has been CH_5^+, which was completely unexpected, but which, nevertheless, is now well established as a stable ion. This ion was first announced by Tal'roze and Lyubimova (*94*), but it was also reported shortly after the Russians by several groups in this country (*22, 68, 89, 92*). Studies of secondary ions from a large number of molecules followed.

The earlier studies of secondary ions were largely limited to ions of masses greater than that of the parent ion, but subsequent studies have shown that many secondaries of lower mass also occur. In most instances, the fact that the ion resulted from collision rather than from impurities was demonstrated by varying the pressure in the ion source. If the ion intensity increased by the second power of the pressure, the ion clearly resulted from a collision. In some instances it would have been helpful to have available high resolution instruments for studying ion-molecule reactions. This would often have simplified the problem of establishing the composition of certain ions and thus have aided in separating impurities from primary product ions. There also have been occasions when it would have been advantageous to distinguish two ions of different composition, but nominally the same mass. Thus, Franklin *et al.* (*31*) in studying ion-molecule reactions in CH_3CN and C_2H_5CN faced the problem of determining the proportions of the ion of mass 26 that were CN

Publication Date: June 1, 1969 | doi: 10.1021/ba-1969-0080.ch005

In Chemical Reactions in Electrical Discharges; Blaustein, B.;
Advances in Chemistry; American Chemical Society: Washington, DC, 1969.

and C_2H_2; of mass 27 that were HCN and C_2H_3 and of mass 28 that were H_2CN and C_2H_4. Unfortunately few, if any, investigators interested in ion-molecule reactions have had high resolution equipment available to them and have had to make do without it. However, it seems probable that in the future high resolution instruments will play a more prominent part in ion-molecule reaction studies.

Having established that an ion was indeed the result of a collision, it was obviously of interest to ascertain the primary ion precursor of the secondary ion. Two methods have usually been used for this purpose. The method most often used was to measure the appearance potential of the secondary ion and compare it with appearance potentials of various primary ions occurring in the system in question. Obviously, the secondary ion must have the same appearance potential as its precursor, and where reasonable agreement of primary and secondary ion appearance potentials was found the reactant and product relationship was established. In some instances, it has been possible to reduce the electron energy to the point where only one or two primary ions were present. Under these conditions, it is often possible by comparing intensities of secondary ions with the disappearance of primaries to identify unequivocally the precursors of the various secondaries. Obviously both of these techniques suffer from certain difficulties. Where the primary ion spectrum is sufficiently complicated, or where the appearance potentials of several primary ions are sufficiently close together, it is difficult and often impossible to determine the precursor of a secondary ion satisfactorily. Further, comparison of primary and secondary appearance potentials usually serves to identify only the precursor of lowest appearance potential. Possible precursors of higher appearance potential are obscured and can only be detected by other means. Of course, it is also true that one cannot always simplify the primary spectrum sufficiently by reducing the electron energy to permit satisfactory identification of the precursor. As a result, in recent years a few mass spectrometrists following Lindholm (*62*) have employed a primary mass sorter to select the primary ion which is then injected into the gas with which reaction is desired.

Mass spectrometer ion sources are quite small chemical reactors. It can easily be shown that the reaction time of an ion in the source will normally be in the order of a microsecond, and unless the pressure in the source is well over 100 microns only a small fraction of the ions can undergo collision. It early became apparent that where secondary ions were observed they must, in most instances, have resulted at almost every collision of ion and neutral. Further, in many instances, the heats of formation of ions and neutrals were well established, and in all such instances it was possible to show that the reactions were exothermic. Indeed, it would be impossible under most circumstances to observe a

Publication Date: June 1, 1969 | doi: 10.1021/ba-1969-0080.ch005

In Chemical Reactions in Electrical Discharges; Blaustein, B.;
Advances in Chemistry; American Chemical Society: Washington, DC, 1969.

reaction to form secondary ions if the reaction were endothermic. Such endothermicity would appear as activation energy, which would greatly reduce the probability of reaction when the ion and molecule collide. (Later on we mention certain conditions in which this rule is violated, but under most circumstances it holds rigorously.) This rule is so seldom violated that it can be used as a means of helping to eliminate possible precursors of a secondary ion.

It was mentioned above that the secondary ions first observed occurred at masses above those of the parent. However, there was always an expectation that ions of lower mass might also be formed in collision reactions and as the pressure that could be tolerated in the ion source was increased it became apparent that such was indeed the case. For example, it was observed by Munson, Franklin, and Field (*79*) that the $C_2H_5^+$ ion from ethane and the $C_3H_7^+$ ion from propane, both present in the primary spectrum, increased with increasing pressure and indeed, in the case of propane the $C_3H_7^+$ ion increased from a very small proportion of the primary spectrum until it represented some 70% of all the ions present. Many secondary ions of mass less than the parent did not show such spectacular increases and other techniques were sought to establish these. One method of special interest was that attributed to Cermák (*6*). He employed electrons having energies too small to ionize in the ionization chamber. However, he employed a relatively high variable potential between the ion chamber and the trap anode, so that the electrons were accelerated in the anode region. Some of these electrons ionized molecules in the trap region and the resulting ions were repelled by the potential on the anode and drifted back into the ionization chamber. These primary ions could not be collected themselves, but they could undergo reaction with neutrals in the source and these could be collected. These ions were necessarily products of ion-molecule reactions and thus the method permitted an unequivocal distinction of secondary and primary ions of m/e less than that of the parent ion. Further, by varying the potential on the anode, it was possible to obtain appearance potentials for the secondary ions and from this to deduce the identity of their precursors.

A large number of reactions of ions with neutrals have now been identified and typical examples of the various classes of such bimolecular reactions are given in Tables I through VII.

Tables I–VI present examples of relatively simple reactions. However, reactions involving quite profound changes in structure and bond reorganizations have been observed by a number of investigators. Table VII shows several typical examples of such reactions. Certain of the reactions shown result in more than one set of products, all of which occur at the same appearance potential and thus involve the same pre-

Publication Date: June 1, 1969 | doi: 10.1021/ba-1969-0080.ch005

In Chemical Reactions in Electrical Discharges; Blaustein, B.;
Advances in Chemistry; American Chemical Society: Washington, DC, 1969.

cursor. One would expect that reactions of this kind would involve the formation of a relatively stable complex, which breaks up in ways dictated by the energy content of the complex. Unfortunately, no quantitative treatment of the break up of the complex has yet been published, so it is not now possible to predict the ratios of product ions where more than one product arises from a single reactant. It has, however, been observed by Lampe *et al.* (*59*) that the ratios of secondary ions from a collision complex will often be very similar to those of the same fragment ions in the primary mass spectrum of a compound having the same composition as the complex. Thus, they pointed out that the ratio of $C_3H_5^+/C_4H_7^+$ in the reaction of $C_2H_4^+$ with C_2H_4 was about the same as that observed in the mass spectra of the butenes. The literature contains only a few examples of simple condensation reactions. This is not surprising in view of the fact that every complex is formed with enough energy to decompose. Since most complexes can break up rapidly they will generally do so in a time which is short compared with that required to collect the ion. In a few instances such complexes have been observed to survive long enough to be measured. One example of this is given in Table VII. It might be mentioned that several apparently long-lived complexes were observed by Field (*20*) in his study of ethylene, but these in all cases turned out to depend upon the third or higher power of the pressure, and thus were in fact complexes that had been stabilized by collision or had resulted from the decomposition of a complex of higher molecular weight.

Although the preceding discussion has largely been devoted to ions formed as bimolecular reaction products, in the last few years many examples of ions formed with much higher pressure dependence have been observed. Thus, in his study of ethylene at pressures above 100 microns, Field (*20*) observed ions with pressure dependencies as high as about 6, although those exhibiting the highest pressure dependence were of such low intensity that the nature of the reactions involved could not be ascertained. Indeed, above about 3rd order the method of appearance potentials becomes completely useless, and the identification of precursors to a given product becomes very tenuous indeed. To form ions at high pressures in a region from which they can be collected, it is usually necessary to employ electrons of several hundred volts rather than the usual 60–70 volts employed in most mass spectrometry. Indeed, because of this problem, Kebarle and Hogg (*42, 48*) have employed alpha particles of high energy to provide primary ions. When ions are formed by high energy massive particles it is possible to operate at much higher pressures and Kebarle (*42, 48*) and Wexler *et al.* (*97*) and others have studied the ions formed at pressures up to about one atmosphere. Naturally, they have observed ions with a very high pressure dependence,

Publication Date: June 1, 1969 | doi: 10.1021/ba-1969-0080.ch005

In Chemical Reactions in Electrical Discharges; Blaustein, B.;
Advances in Chemistry; American Chemical Society: Washington, DC, 1969.

although they have not been able to establish the order of reaction. With such a system, Kebarle *et al.* (*43*, *49*) have observed ions having the general formula, $H^+(H_2O)_n$, with n varying from 1 to 7, and Wexler, *et al.* (*97*) have observed polymer ions from acetylene having up to 12 carbon atoms.

Table I. Atom Transfer Reactions

Reactions	*References*
$Kr^+ + D_2 \rightarrow KrD^+ + D$	*89*
$Xe^+ + CH_4 \rightarrow XeH^+ + CH_3$	*21*
$N_2^+ + D_2 \rightarrow N_2D + D$	*89, 91*
$CH_4^+ + C_3H_6 \rightarrow CH_5^+ + C_3H_5$	*27*
$D_2O^+ + nC_4H_{10} \rightarrow HD_2O^+ + C_4H_9$	*58*
$O^+ + N_2 \rightarrow NO^+ + N$	*18, 85*
$O^+ + CO_2 \rightarrow O_2^+ + CO$	*16*
$I^+ + CH_3I \rightarrow I_2^+ + CH_3$	*86*

Table II. Positive Atomic Ion Transfer Reactions

Reactions	*References*
$O_2^+ + H_2 \rightarrow H_2O^+ + O$	*46*
$H_2^+ + O_2 \rightarrow HO_2^+ + H$	*89, 91*
$HI^+ + CH_3I \rightarrow CH_3I_2^+ + H$	*86*
$C_2H_6^+ + D_2O \rightarrow HD_2O^+ + C_2H_5$	*58*
$O_2^+ + N \rightarrow NO^+ + O$	*35*
$O_2^+ + C_2H_2 \rightarrow C_2H_2O^+ + O$	*29*

Table III. Symmetrical Transfer Reactions

Reactions	*References*
$H_2^+ + H_2 \rightarrow H_3^+ + H$	*15, 91, 92*
$CH_4^+ + CH_4 \rightarrow CH_5^+ + CH_3$	*22, 68, 92, 94*
$H_2O^+ + H_2O \rightarrow H_3O^+ + OH$	*67*
$HCl^+ + HCl \rightarrow H_2Cl^+ + H$	*89*
$CH_2O_2^+ + CH_2O_2 \rightarrow CH_3O_2^+ + HCO_2$	*29*
$NH_3^+ + NH_3 \rightarrow NH_4^+ + NH_2$	*11, 13, 59*
$I_2^+ + I_2 \rightarrow I_3^+ + I$	*44*

Table IV. H^- and H_2^- Transfer Reactions

Reactions	*References*
$C_2H_5^+ + C_3H_8 \rightarrow C_2H_6 + C_3H_7^+$	*79*
$C_2H_4^+ + C_3H_8 \rightarrow C_2H_5 + C_3H_7^+$	*79*
$CH_3^+ + C_2H_6 \rightarrow C_2H_5^+ + CH_4$	*25*
$C_3H_5^+ + \text{neo-}C_5H_{12} \rightarrow tC_5H_{11}^+ + C_3H_6$	*25*
$C_2H_4^+ + C_3H_8 \rightarrow C_2H_6 + C_3H_6^+$	*79*
$C_3H_6^+ + iC_4H_{10} \rightarrow C_3H_8 + iC_4H_8^+$	*79*

Publication Date: June 1, 1969 | doi: 10.1021/ba-1969-0080.ch005

Table V. Some Reactions of Excited Ions

Reactions	*References*
$C_2H_6^{+*} + C_2H_6 \rightarrow C_2H_7^+ + C_2H_5$	*79*
$H_2^{+*} + He \rightarrow HeH^+ + H$	*96*
$N_2^{+*} + N_2 \rightarrow N_3^+ + N$	*47, 77, 88*
$O_2^{+*} + O_2 \rightarrow O_3^+ + O$	*8, 29*

Table VI. Charge Transfer Reactions

Reactions	*References*
$O^+ + O_2 \rightarrow O_2^+ + O$	*17*
$N_2^+ + O_2 \rightarrow N_2 + O_2^+$	*19*
$C_2H_2^+ + C_2H_4 \rightarrow C_2H_4^+ + C_2H_2$	*20*
$Xe^+ + C_2H_4 \rightarrow C_2H_4^+ + Xe$	*28*
$\rightarrow C_2H_2^+ + H_2^+ + Xe$	*28*
$Ar^+ + C_2H_4 \rightarrow C_2H_2^+ + H_2 + Ar$	*28*
$\rightarrow C_2H_3^+ + H + Ar$	*28*
$Ar^+ + CH_4 \rightarrow CH_3^+ + H + Ar$	*68, 69*
$F^+ + CO \rightarrow CO^+ + F$	*63*
$\rightarrow C^+ + O + F$	*63*

Table VII. Complex Rearrangements

Reactions	*References*
$CH_3^+ + CH_4 \rightarrow C_2H_5^+ + H_2$	*22, 68, 69, 91, 92*
$C_2H_4^+ + C_2H_4 \rightarrow C_3H_5^+ + CH_3$	*22, 42, 69*
$\rightarrow C_4H_7 + H$	*22, 42, 69*
$C_2H_2^+ + C_2H_2 \rightarrow C_4H_2^+ + H_2$	*23*
$\rightarrow C_4H_3^+ + H$	*23*
$C_4H_6^+ + C_4H_6 \rightarrow C_5H_7^+ + C_3H_5$	*1*
$\rightarrow C_6H_6^+ + C_2H_6$	*1*
$\rightarrow C_6H_7^+ + C_2H_5$	*1*
$\rightarrow C_6H_8^+ + C_2H_4$	*1*
$\rightarrow C_7H_9^+ + CH_3$	*1*
$O_2^+ + CH_4 \rightarrow CH_3O_2^+ + H$	*29*
$CH_4^+ + O_2 \rightarrow CH_3O^+ + OH$	*29*
$Xe^+ + CH_4 \rightarrow XeCH_3^+ + H$	*21*
$ArN_2^+ + N_2 \rightarrow Ar + N_4^+$	*77*
$C_3H_7I^+ + C_3H_7I \rightarrow C_6H_{14}I_2^+$	*87*

At pressures of several torr in an ion source, any primary ions formed will undergo many collisions and will have ample opportunity to react if they are capable of doing so. Field and Munson (*26, 76*) have taken advantage of this to carry out some very interesting studies of reactions of higher order. They observed that in very pure methane, the principal secondary ions CH_5^+ and $C_2H_5^+$ reached a plateau and remained constant with increases in pressure beyond about 0.5 torr. They observed also that if there were a small amount of impurity in the methane the intensities of these ions (CH_5^+ and $C_2H_5^+$) passed through a maximum around

Publication Date: June 1, 1969 | doi: 10.1021/ba-1969-0080.ch005

In Chemical Reactions in Electrical Discharges; Blaustein, B.;
Advances in Chemistry; American Chemical Society: Washington, DC, 1969.

a few 10ths torr and then declined steadily with further increases in pressure. The primary ions had very small probability of colliding with anything but methane and consequently the disappearance of the secondaries must be because of their reaction with the impurities, since it is demonstrated that they did not react with methane itself. It was a simple step from this to the addition of small amounts of a variety of materials to the methane plasma, with results that proved extremely interesting. When, for example, small amounts of long chain paraffin hydrocarbons, such as dodecane, were added to the methane plasma, the spectrum of ions from the high molecular weight paraffin was quite different from that obtained by electron impact. Such high molecular weight paraffins give only small intensities of ions above about the C_5 range under electron impact. However, in the methane plasma, ions of the general composition C_nH_{2n+1} formed at each carbon number from that of the parent down to C_4. No doubt ions of smaller mass are also formed, but these are not observable because of the interference from secondary and ternary ions from methane. Further, the largest of these ions is the one having the same carbon number as the parent molecule—*i.e.*, with dodecane, $C_{12}H_{25}^+$.

Field and Munson have studied a number of compounds by this method, and in many instances have obtained profound changes in the mass spectrum, produced by "chemical ionization," the term which they have given the processes (*26, 76*). They have concluded that for methane the principal reactions are probably as follows:

$$CH_5^+ + C_nH_{2n+2} \rightarrow CH_4 + H_2 + C_nH_{2n+1} \quad (2)$$

$$C_2H_5^+ + C_nH_{2n+2} \rightarrow C_2H_4 + H_2 + C_nH^+{}_{2n+1} \quad (3)$$

$$\rightarrow C_2H_6 + C_nH^+{}_{2n+1}$$

Although the previous discussion has been devoted entirely to reactions of positive ions, negative ions are also known to undergo reactions on collision. Relatively few of these reactions have been studied, largely because negative ions present some rather serious difficulties to the investigator. Some reactions of negative ions, however, have been carried out by Melton, Henglein, and others, and several typical reactions are given in Table IX.

Table VIII. Some Ions Formed by Processes of Order Higher Than 2

Reactant	*Ionic Product*	*Reference*
H_2O	$H^+(H_2O)_n$ $(1 < n < 8)$	*49*
NH_3	$H^+(NH_3)_n$ $(1 < n < 5)$	*43*
CH_4	$C_3H_5^+$, $C_3H_7^+$	*24*
C_2H_4	$C_4H_8^+$, $C_4H_6^+$	*20*

Publication Date: June 1, 1969 | doi: 10.1021/ba-1969-0080.ch005

Table IX. Negative Ion-Molecule Reactions

Reaction	*Reference*
$I_2^- + I_2 \rightarrow I_3^- + I$	*44*
$H^- + H_2O \rightarrow OH^- + H_2$	*80*
$HCO_2^- + N_2 \rightarrow CN^- + HNO_2$?	*70*
$O^- + CH_3I \rightarrow OI^- + CH_3$	*39*
$CN^- + C_2N_2 \rightarrow C_2N_2^- + CN$	*71*
$O^- + NO_2 \rightarrow NO_2^- + O$	*39*

Table X. Chemi-Ionization

Reaction	*Reference*
$He^* + He \rightarrow He_2^+ + e$	*45*
$He^* + Ar \rightarrow HeAr^+ + e$	*78*
$Ar^* + N_2 \rightarrow ArN_2^+ + N_2$	*77*
$N_2^* + N_2 \rightarrow N_4^+ + e$	*77*
$H_2^* + H_2 \rightarrow H_3^+ + H + e$	*50*
$CO^* + CO \rightarrow C_2O_2^+ + e$	*77*

Chemi-Ionization Reactions

Somewhat akin to ion-molecule reactions is a process first identified by Hornbeck and Molnar (*45*) for forming the rare gas diatomic ions. Hornbeck and Molnar observed diatomic ions of all the rare gases and found their intensities to vary as the square of the pressure. The appearance potentials of the diatomics proved to be 0.7 to 1.5 e.v. below the ionization potentials of the corresponding atom, and hence the diatomic ions were not derived from atomic ions. As a consequence, they proposed that excited atoms formed by electron impact reacted upon collision with a neutral atom to form a molecular ion and eject an electron, thus:

$$Ar^* + Ar \rightarrow Ar_2^+ + e$$

A number of investigators have subsequently studied this chemi-ionization reaction of the rare gases and have confirmed and extended Hornbeck and Molnar's observations. [Reactions by which ionization occurs as a result of forming a chemical bond are generally termed "chemi-ionization." This is to be distinguished from the term "chemical ionization," applied by Field and Munson (*26, 76*) to their high pressure ionic reactions as discussed above.] It has now been observed that all of the rare gases react with each other to form the heteronuclear diatomic ions (*78*). In addition, a number of ionic compounds of the rare gases with nitrogen, CO, O_2, methane, acetylene, and others have been reported. Chemi-ionization reactions are not necessarily limited to rare gases, however. Chemi-ionization products of excited mercury atoms with a number of compounds have been observed (*7*) and nitrogen and CO are known

Publication Date: June 1, 1969 | doi: 10.1021/ba-1969-0080.ch005

In Chemical Reactions in Electrical Discharges; Blaustein, B.;
Advances in Chemistry; American Chemical Society: Washington, DC, 1969.

to undergo chemi-ionization with their own ground-state species, forming respectively N_4^+ and $C_2O_2^+$ (77).

Reaction Rates

In the study of ion-molecule reactions the relative intensities of reactants and ionic product are immediately available and thus the reaction rate is readily determined. With the reaction $A^+ + M \rightarrow B^+ + S$, if M is much larger than A^+, the reaction rate is psuedo first order and the equation expressing the concentration of A^+ and B^+ is as follows:

$$\frac{A^+}{A_0^+} = e^{-kMt} \tag{4}$$

$$\frac{B^+}{A_0^+} = 1 - e^{-kMt} \tag{5}$$

where k is the reaction rate constant, t is time and A^+, B^+ and M are concentrations. A_0^+ is the initial concentration of A^+ and in simple reactions can be taken as the sum of A^+ and B^+.

At relatively low pressures (a few microns),

$$\frac{B^+}{A^+ + B^+} = kMt \tag{6}$$

A plot of $\frac{B^+}{A^+ + B^+}$ against M will yield a straight line whose slope is kt. If a continuous ion withdrawal is employed, the retention time in the source will be the time required for the primary ion to drift from the point of formation in the electron beam to the exit slit under the influence of the repeller potential. The time is thus:

$$\left(\frac{2md}{eE}\right)^{1/2}$$

where E is the field strength, m is the mass of the ion, and d the distance from the center of the electron beam to the ion exit slit. With the slope known, k can be calculated. A large number of rate constants have been determined in this way.

Lampe, Franklin and Field (59) discussed this problem of rates of ion molecule reactions at some length and surveyed the known data at that time. A few typical rate constants for second order ion-molecule reactions are given in Table XI. It will be observed that many of them are in the order of 10^{-9} cc./molecule/sec. However, values as small as 10^{-13} cc./molecule/sec. have been reported for some reactions. The values in the neighborhood of 10^{-9} cc./molecule/sec. represent reactions that must occur at essentially every collision in that they have cross sections considerably larger than ordinary collision cross sections. The values

Publication Date: June 1, 1969 | doi: 10.1021/ba-1969-0080.ch005

around 10^{-13} represent about the limit at which secondary ions can be measured with sufficient confidence to justify calculation. It is obvious that reactions of this kind occurring at relatively low pressures and in times of the order of a micro-second must be very fast reactions, and in fact, so fast that the activation energy must be either 0 or very small. As was mentioned before, ion-molecule reactions to be observable must not involve appreciable energy of activation. Stevenson and Schissler (*91, 92*) have confirmed this experimentally for a few reactions and the very fact that a reaction is observed precludes this possibility. It should be mentioned, however, that certain endothermic reactions can be forced to take place if the relative velocity of the reacting partners is sufficiently great. Giese and Maier (*33*) have shown that for the reaction $Ar^+ + CO \rightarrow Ar + C^+ + O$, which is endothermic by 6.62 for the $2P_{3/2}$ state and 6.44 e.v. for the $2P_{1/2}$ state of Ar^+, the threshold for the appearance of C^+ is:

$$\frac{6.44\ (M_{Ar} + M_{CO})}{M_{CO}} \text{ or } 15.65 \text{ e.v.}$$

Their measured values were in agreement with this relation.

Table XI. Some Second-Order Rate Constants

Reaction	10^{10}k, *cc./molecule sec.*	*Reference*
$D_2^+ + D_2 \rightarrow D_3^+ + D$	14.5	*91, 92*
$CH_4^+ + CH_4 \rightarrow CH_5^+ + CH_3$	10	*31, 36, 37, 93*
$H_2O^+ + H_2O \rightarrow H_3O^+ + OH$	12.7	*22, 58, 67*
$C_2H_3^+ + C_2H_6 \rightarrow C_3H_5^+ + CH_4$	14.5	*89*
$O_2^+ + CH_4 \rightarrow CH_3O_2^+ + H$	0.126	*29*
$CH_4^+ + O_2 \rightarrow CH_3O^+ + OH$	0.257	*29*

Although most rate measurements have been made at sufficiently low conversion (low pressure) for Equation 3 to apply, it has been shown that the psuedo first order rate laws (Equations 4 and 5) are obeyed over wide ranges of pressure, if subsequent reactions do not interfere. Thus, Field *et al.* (*24*) found the disappearance of CH_4^+ in methane to obey first law kinetics over a pressure range of about 0.1 to 400 microns. However, in certain systems, reactions of apparently higher order do occur. Actually, these are the result of a succession of reactions which show dependence upon a higher power of the pressure. Rates of reactions of such high order do not yield satisfactory rate constants, but it has been possible to determine rate constants for reactions of 3rd order, and Field (*20*) and several others have made approximate measurements of the rate constants for such third order processes. As is the case with the second order processes, these reaction rates are relatively high. For

Publication Date: June 1, 1969 | doi: 10.1021/ba-1969-0080.ch005

In Chemical Reactions in Electrical Discharges; Blaustein, B.;
Advances in Chemistry; American Chemical Society: Washington, DC, 1969.

example, in ethylene, Field determined several third order rate constants to be in the order of 10^{-27} cc.^{2} molecule^{-2} sec.$^{-1}$.

Although most of the measurements of rate constants in the literature were obtained with the source operating in a continuous mode employing a variation in pressure to establish the rate, some studies have been made in which retention time in the source was varied. Such measurements were originally made by Tal'roze and Frankevitch (*93*), but subsequent measurements have been made by Hand and von Weissenhoff (*36, 37*) and Franklin, Natalis, Wada, and Hierl (*31*), and others. In order to obtain a satisfactory variation of time, a pulsed mode is employed. In such an operation a pulse of electrons is fired through the gas. After it is stopped, the resulting ions can be retained in the source for a controlled period of time and then rapidly extracted by a pulse of high energy. By varying the delay time, the time of retention in the source is varied, and rate constants determined in the manner more usually employed by chemists in rate studies. Results obtained in this way generally agree rather well with those obtained by the pressure method, although some disagreements have been observed. One difference that may be of significance is that the ions in the pulsed mode will generally have approximately thermal energies whereas those reacting in the continuous mode will have variable energies, depending upon the point of their reaction in travelling from the electron beam to the exit slit.

The question of the effect of ionic energy on reaction rate has been one of considerable interest and the subject of a number of investigations, both theoretical and experimental. In their early work on ion-molecule reactions, Field, Franklin, and Lampe (*22*) observed that when they varied the field strength in the ion source in order to vary the retention time, the rate constants that they calculated for their ion-molecule reactions varied considerably. In general, they seemed to drop as the field strength increased, suggesting that the reaction rate constant decreased with the relative velocity of ions and neutrals. Other investigators have made similar observations. However, it appears that not all reactions show such reduction in rate constants with increasing relative velocity. Attempts to explain this have been made by a number of investigators. Field, Franklin, and Lampe (*22*) attempted to obtain the theoretical relations based upon a balance of polarization and centrifugal forces. Gioumousis and Stevenson (*34*) derived a more precise expression for the collision rate based upon Langevin's (*60*) treatment for polarizable systems. Gioumousis and Stevenson found the collision cross section to be:

$$\sigma = \frac{2\pi e}{v_i}\left(\frac{\alpha}{\mu}\right)^{1/2} \tag{7}$$

Publication Date: June 1, 1969 | doi: 10.1021/ba-1969-0080.ch005

where α is the polarizability of the neutral, v_i is the velocity of the ion, μ is the reduced mass and e the charge on the electron. Since

$$v_i = \left(\frac{2E}{m_i}\right)^{1/2}$$

σ will vary as $E^{-1/2}$. Further, since $k = \sigma v$

$$k = 2\pi e \left(\frac{\alpha}{\mu}\right)^{1/2} \tag{8}$$

and thus is independent of velocity or energy. This, unfortunately, did not agree with the observed rate behavior of a number of reactions, although it appears to hold for some. In attempting to solve this problem, Hamill and his associates (*4, 56*) have shown that ion-molecule reactions cannot be accurately treated as involving point particles. By considering the deformable neutral to exhibit a hard core to high energy collisions while being deformable in low energy collisions, these workers showed that for small ion energies σ obeyed the Gioumousis-Stevenson relation (Equation 7), but for large energy $\sigma \propto E_0^{-1}$ which agrees with experimental results. Theard and Hamill (*95*) and Moran and Hamill (*74*) have extended their treatment to ion-molecule reactions involving neutrals with permanent dipoles. They showed that at low relative velocities a cross section for the ion-permanent dipole interaction,

$$\sigma_D = \frac{\pi e \mu}{E_t} \tag{9}$$

must be added to the Langevin cross section. Here μ is dipole moment and E_t is the translational energy of the reacting system in center of mass coordinates.

No attempt will be made here to review all of the studies of the effect of energy upon the rates of ion-molecule reactions. However, several investigators who have made especially important contributions should be mentioned. In addition to the work of Hamill discussed above, important studies have been made by Futrell and Abramson (*32*), Giese and Maier (*33*), Friedman (*51, 72, 73*), and Light and Horrocks (*61*).

It should be pointed out that if the relative velocities of ions and neutrals become sufficiently high other reactions begin to occur as a result of the different forces coming into play. Thus, a fast moving ion passing a molecule with sufficient velocity may simply strip off a peripheral atom, leaving the partially denuded entity behind. Such stripping reactions have been studied by Henglein (*38*) and Koski (*3*), who found that they obey quite different rules from those above. It thus appears that a complete theory of the rates of ion-molecule reactions has not been developed, but there is little doubt that to a first approximation the equation of Gioumousis and Stevenson gives fairly good results.

Publication Date: June 1, 1969 | doi: 10.1021/ba-1969-0080.ch005

In Chemical Reactions in Electrical Discharges; Blaustein, B.;
Advances in Chemistry; American Chemical Society: Washington, DC, 1969.

Ions in Electric Discharges

An electric discharge, of course, involves ions and electrons and the ions present can be sampled and analyzed by mass spectrometry. Such studies have been undertaken by a number of investigators and some progress is being made toward understanding the chemical behavior of ions in various discharges. The problem is complicated by the fact that there are several kinds of electric discharge, each of which has its own physical and chemical characteristics. Of these, the type most often studied is the direct current glow discharge, but corona and high frequency and micro-wave discharges have also received some attention.

In order to analyze the ionic content of a discharge it is necessary to transfer the ions from the discharge into the mass analyzer. While this is not a particularly serious problem at pressures below 10 microns, the difficulty becomes more acute as the pressure increases. This is attributable to the fact that electrons and ions diffuse to the walls at different rates, so that an electric gradient is established which alters the distribution of energy of the various charged species. Ordinarily a sheath of electrons or ions is formed at any surface, including that of a sampling probe and ions or electrons must have, or be given enough energy to pass through this sheath in order to be sampled. However, if the energy is sufficiently high some ions may be decomposed by collision. The result then is that there is often considerable uncertainty as to the quantitative correspondence of the ion distribution reported by the mass spectrometer with the actual distribution in the discharge. Further, while there is little doubt that the ions observed were actually present, there is always some question as to the presence of ions that might be expected, but that are not observed.

An added complication that must be taken into account, especially in glow discharges, is that different portions of the discharge have different characteristics. Thus, the negative glow and positive column have quite different electric fields, the ions and electrons present have different energies and the distribution of ions in the two regions is different.

In spite of these reservations, considerable information has been obtained concerning the ions present in certain discharges and some understanding of the reactions occurring is beginning to develop.

In the glow discharge, the regions most studied have been the negative glow and the positive column. Both are regions of nearly equal positive and negative ion concentration, although the ion concentration in the negative glow is usually greater (often 10–100 times) than that in the positive column. Further, the electric field in the negative glow is considerably greater than that of the positive column, through which the ions drift with relatively small energies.

Publication Date: June 1, 1969 | doi: 10.1021/ba-1969-0080.ch005

In Chemical Reactions in Electrical Discharges; Blaustein, B.;
Advances in Chemistry; American Chemical Society: Washington, DC, 1969.

Discharges in the rare gases, of course, always contain atomic ions and, at sufficiently high pressures, diatomic ions as well. The latter can be produced by two possible reactions, typified by helium:

$$He^* + He \rightarrow He_2^+ + e \quad (10)$$

$$He^+ + 2He \rightarrow He_2^+ + He \quad (11)$$

Since the formation of He* is an excitation process, it will occur over a relatively small energy range with electrons of energy close to the ionization potential of He. Thus, it would be expected to predominate in the positive column of a glow discharge. This has been observed by Morris (*75*) and by Pahl (*82, 83*).

In order for Reaction 11 to be observed relatively high pressures are required. The third order rate constant has been found by Phelps and Brown (*84*) to be 6.3×10^{-32} cc.^{2}/molecule^2 sec. and the time of the ion in the plasma will probably not exceed 10^{-5} sec. Thus, for He_2^+/He^+ to be approximately 0.1 by Reaction 11 the pressure must be approximately 30–40 torr. Thus, the formation of the diatomic ion by the three-body process will decrease very rapidly with decreasing pressures and will be negligible below 0.1 torr. Knewstubb and Tickner (*53, 54*) have studied the ions of the rare gases in both the negative glow and the positive column of a d.c. glow discharge. They find the ratio Ar_2^+/Ar^+ to be much less in the negative glow than in the positive column, and conclude that the diatomic ion is formed principally by the three-body process in the negative glow, but that the chemi-ionization reaction predominates in the positive column. Similar considerations apply to the other rare gases.

In our laboratory a microwave discharge was generated in helium by a 100 watt Raytheon microtherm generator and sampled through a pinhole leak at the apex of a conical probe into a quadrupole mass filter. Typical variations in the intensities of He^+ and He_2^+ with pressure are given in Figure 1. If the He_2^+ is formed by the three-body process (Equation 11) the rate constant would have to be about 10^{-28} cc.^{2}/molecule^2/sec. which far exceeds the measured value (*84*). We conclude then that the diatomic ion is formed principally by the chemi-ionization process (Equation 10).

Of perhaps greater interest are the ionic processes occurring in more complex gases. Thus, glow discharges in hydrogen (*5, 66*) and in H_2–D_2 mixtures (*2*) showed the formation of H_3^+ or H_3^+–D_3^+ mixtures, which increased in concentration with pressure at the expense of the diatomic ion. In an effort to interpret the behavior of the discharge in hydrogen, Eyring, Hirschfelder, and Taylor (*15*) considered the reaction forming H_3^+ to be:

$$H_2^+ + H_2 \rightarrow H_3^+ + H \quad (12)$$

Publication Date: June 1, 1969 | doi: 10.1021/ba-1969-0080.ch005

In Chemical Reactions in Electrical Discharges; Blaustein, B.;
Advances in Chemistry; American Chemical Society: Washington, DC, 1969.

They took the activation energy for the reaction to arise from the balance of centrifugal force and polarization attraction acting in opposite directions. The resulting rate constant for the reaction is identical with that given by Equation 8. Subsequent studies of this reaction in a mass spectrometer ion source (*92*) have established this reaction beyond doubt, and have shown that the reaction rate is given approximately by the above relation of Eyring *et al.* Recent studies by Ortenburger *et al.* (*81*) employing a high frequency discharge have shown that Reaction 8 occurs under these conditions as well.

Studies of ions in the negative glow and Faraday dark space of a glow discharge in water vapor at 0.4 torr have been made by Knewstubb

Publication Date: June 1, 1969 | doi: 10.1021/ba-1969-0080.ch005

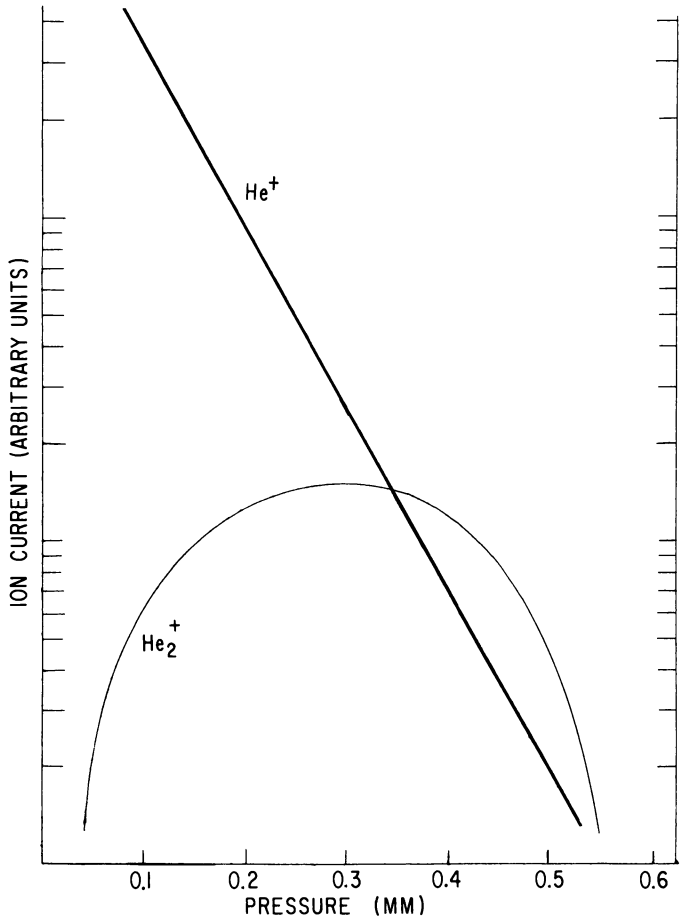

Figure 1. Effect of pressure on ion abundances in a microwave discharge in helium

and Tickner (*55*). They found the maximum ion intensity to occur in the negative glow. There was little H_2O^+ present, but a series of solvated protons was observed having the general composition $H^+(H_2O)_n$ with n varying from one to five. Mass spectrometer studies have established Reaction 1 (*58, 69, 94*) and more recent studies have detected the more highly solvated species (*43, 49*). The results of the discharge studies showed the first four water molecules to be more strongly bonded to the proton than succeeding molecules and this has been substantiated by the work of Kebarle (*43, 49*), previously discussed.

Similar studies have been made of ions in a glow discharge in ammonia (*10*) with similar results. The negative glow at 0.4 torr was found to contain the ions $H^+(NH_3)_n$ with n from 1 to 5, with NH_4^+ being formed in highest concentration in the negative glow, but with $H^+(NH_3)_4$ predominating in the Faraday dark space. The multipli-solvated proton has also been observed in the ion source of a mass spectrometer at elevated pressure (*41, 42*).

Knewstubb (*52*) also mentions the observation of ions in a glow discharge in methane in which the ions $C_2H_5^+$ and CH_5^+ predominated, and in which some 40% of the ions present contained three or more carbon atoms. Munson and Field (*26, 76*) (*see* above) showed that CH_5^+ and $C_2H_5^+$ did not react with methane and that ions having more than 2 carbon atoms were present in small proportions in pure methane at pressures below 2 torr. This suggests that the ions of higher mass reported by Knewstubb (*52*) originated either from impurities in the methane employed or, more probably, from molecules such as acetylene or ethylene formed by the action of the discharge on methane.

Nitrogen has been the subject of several investigations employing both mass spectrometer ionization chambers and discharges for the production of ions. The ions of greatest interest are N_3^+ and N_4^+. The mass spectrometer studies have shown N_3^+ to be formed by the reaction:

$$N_2^{+*} + N_2 \rightarrow N_3^+ + N \qquad (13)$$

where N_2^{+*} implies an excited ion having an appearance potential of about 21–22 e.v. (*8, 77, 88*). N_4^+ has been found to result from the reaction (*47*):

$$N_2^+ + 2N_2 \rightarrow N_4^+ + N_2 \qquad (14)$$

In addition, Munson *et al.* (*77*) showed that under certain conditions N_4^+ is formed by the chemi-ionization reaction:

$$N_2^* + N_2 \rightarrow N_4^+ + e \qquad (15)$$

Both ions have been observed in electric discharges in nitrogen. Luhr (*65*) and Dreeskamp (*14*) found N_3^+, but it appeared to be formed only

In Chemical Reactions in Electrical Discharges; Blaustein, B.;
Advances in Chemistry; American Chemical Society: Washington, DC, 1969.

in the drift space following the discharge. It was thought to result from the reaction

$$N^+ + 2N_2 \rightarrow N_3^+ + N_2 \quad (16)$$

Shahin (*90*) has reported N_3^+ formed in a glow discharge at 0.3 torr in nitrogen as well as N_4^+ in a corona discharge in a mixture of nitrogen and water vapor. The relative intensity of N_4^+ passed through a maximum at about 10 torr, then slowly declined at higher pressures. Shahin attributed the formation of the ion to the reaction:

$$N_2^+ + N_2 \rightarrow N_4^+ \quad (17)$$

In the same system, he observed H_2O^+, H_3O^+, $H_5O_2^+$, and N_2H^+ ions, all apparently resulting, at least in part, from reaction of N_2^+ with water.

In this laboratory nitrogen has been passed through a microwave discharge at pressures of 0.01 to 0.3 torr and the plasma sampled into a quadrupole mass filter where the ions were separated and analyzed.

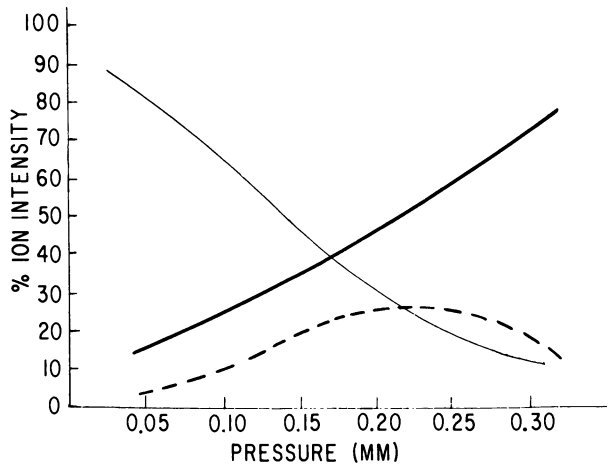

Figure 2. Effect of pressure on relative abundances of ions in a microwave discharge in nitrogen

N_4^+
N^+
N_3^+

The results are given in Figure 2. N_4^+ was not observed at any condition studied. Figure 3 shows the variation of the intensities of these ions with nominal power input at a pressure of 0.15 torr. The decrease in intensity with decreasing power is reminiscent of an ionization efficiency curve and suggests that the average electron energy decreased with decreasing power input. This is not the case, however. We have found (*30*) that the

Publication Date: June 1, 1969 | doi: 10.1021/ba-1969-0080.ch005

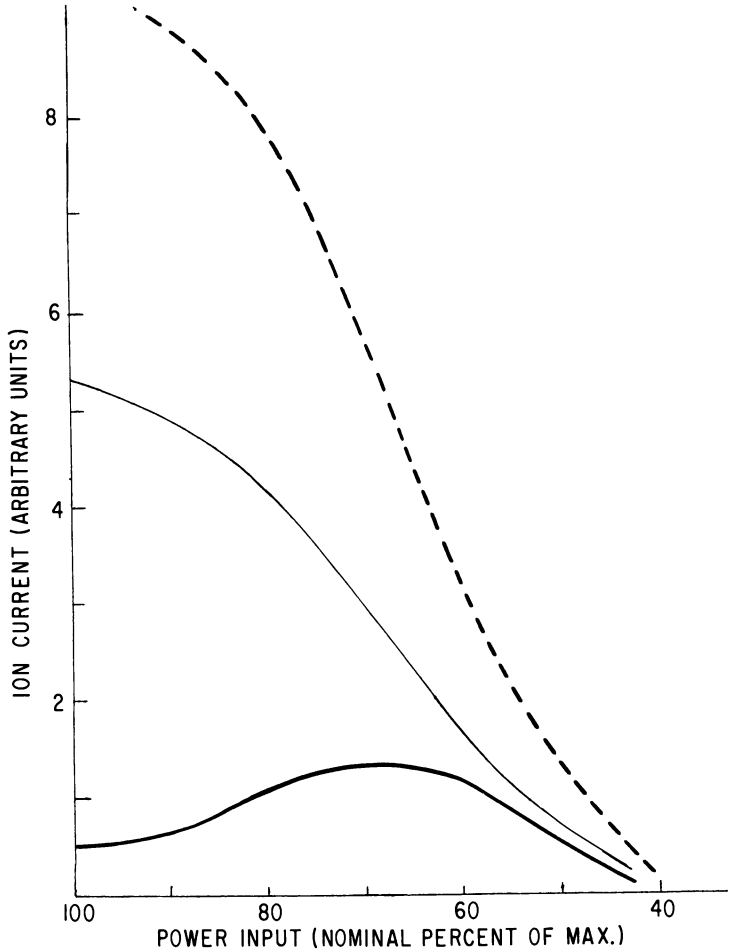

Figure 3. Effect of power input on the abundance of ions in a microwave discharge in nitrogen

energy of electrons in this discharge is independent of power input and that ion and electron density decrease with decreasing power and with increasing pressure. Electron energy also decreases somewhat with increasing pressure. The concentration of N atoms increases with both pressure and power input. We conclude, therefore, that N^+, which is formed at low pressures in about the same ratio to N_2^+ as in a mass spectrometer must be formed in increasing amounts by the reaction

$$N_2^+ + N \rightarrow N^+ + N_2 \qquad (18)$$

In Chemical Reactions in Electrical Discharges; Blaustein, B.;
Advances in Chemistry; American Chemical Society: Washington, DC, 1969.

as the pressure or power is increased. The concentration of N_3^+ is much too great to be accounted for by Reaction 16. Further, Reaction 13 cannot account for the major part of the N_3^+ formed because the N_2^+ is present (at least in a mass spectrometer source) in rather small amounts —*i.e.*, approximately 1% of the N_2^+. We conclude that the ion is probably formed by a chemi-ionization process

$$N^* + N_2 \rightarrow N_3^+ + e \tag{19}$$

Such a reaction would be expected to proceed at a sufficient rate to account for the N_3^+ observed. The decrease in N_3^+ at elevated pressures is probably explainable either by collisional decomposition in the sheath or by the exothermic reaction

$$N_3^+ + N \rightarrow N_2^+ + N_2 \tag{20}$$

We consider the latter to be the more probable in view of the decrease in N_3^+ intensity at high power input.

The absence of N_4^+ is puzzling, since it has been observed in some discharges. It is possible that the ion is decomposed by collision in passing through the sampling aperture. This seems improbable, however, since N_4^+ is held together by a bond of about 1.5 e.v. energy. This is about the same strength as the bond in He_2^+, which we observe. Conceivably, the ion may appear at higher pressures, but some alterations in our sampling probe will be necessary to achieve this.

Several investigations of ions in glow discharges in oxygen have been reported. O^+ and O_2^+ were reported by Knewstubb (*52*), Luhr (*64*), and Dickenson and Sayers (*12*). In addition, O_3^+ and O_4^+ (*12*) have been reported.

In our studies of oxygen in the pressure range 0.01 to 0.3 torr, using a microwave discharge only O^+ and O_2^+ were found. Both ions dropped in intensity exponentially with increasing pressure, but the O^+ dropped slightly less rapidly than did O_2^+. The drop in O^+ with increasing pressure may be because of the fact that O^+ can react with O_2 by charge exchange.

$$O^+ + O_2 \rightarrow O_2^+ + O \tag{21}$$

This would account for the drop in O^+ intensity at conditions at which N^+ (which cannot undergo loss by charge exchange) remains constant. In the same pressure range, O_2^+ drops in intensity to about the same extent as does N_2^+, which can disappear by charge exchange with N.

In a mass spectrometer ion chamber O_3^+ and O_4^+ are found in rather small intensities, apparently formed by the reactions:

$$O_2^+(^2\pi_u) + C_2 \rightleftarrows O_4^{+*} \rightarrow O_3^+ + O \tag{22}$$

$$O_4^{+*} + O_2 \rightarrow O_4^+ + O_2 \tag{23}$$

Publication Date: June 1, 1969 | doi: 10.1021/ba-1969-0080.ch005

In Chemical Reactions in Electrical Discharges; Blaustein, B.;
Advances in Chemistry; American Chemical Society: Washington, DC, 1969.

The latter is very faint, however. The ionization potential of O_3 is slightly greater than that of O_2 (*9, 40*), so O_3^+ can react with O_2 as follows:

$$O_3^+ + O_2 \rightarrow O_2^+ + O_3 \qquad (24)$$

No doubt this accounts for the failure to observe O_3^+. The absence of O_4^+ may be merely a matter of sensitivity.

In our laboratory we have also studied the ions formed in a microwave discharge in a mixture of nitrogen and oxygen at a constant pressure of about 0.1 torr. As might be expected, the intensities of N_2^+ and N^+ decreased and those of O_2^+ and O^+ increased as the proportion of nitrogen decreased and that of oxygen increased. NO^+ was very intense over the range of 10 to 75% oxygen in the mixture. This is not surprising, since N^+, N_2^+, and N_3^+ reacting with O_2 or O and O^+, and O_2^+ reacting with N or N_2 are capable of producing NO^+. Further, NO is produced in the discharge and no doubt is ionized by electron impact.

Small amounts of NO_2^+ ions were observed in all of the mixtures studied, and small amounts of N_2O^+ were found in the nitrogen rich mixtures, but disappeared when the proportion of nitrogen in the mixture dropped below 75%. The manner of their formation is not known, but from their very small intensity we infer that they are probably formed by third order processes. It is surprising that no N_3^+ ion was observed when oxygen was present. Presumably it is capable of reacting in several ways with O_2 or O, and so is destroyed as fast as it is formed. The system O_2–N_2 is of great interest and will be studied further.

Publication Date: June 1, 1969 | doi: 10.1021/ba-1969-0080.ch005

Acknowledgment

This research was supported by Project SQUID of the Navy under Grant NONR 3623 S-21, which we acknowledge with gratitude.

Literature Cited

(1) Barker, R., Williams, R. R., Jr., Hamill, W. H., *Proc. Meeting ASTM (Am. Soc. Testing Materials) Mass Spectrometry, New Orleans, La.*, **Committee E-14** (June 2–6, 1958).
(2) Beckey, H. D., Dreeskamp, H., *Z. Naturforsch* **9a**, 735 (1954).
(3) Berta, M. A., Ellis, B. Y., Koski, W. S., ADVAN. CHEM. SER. **58**, 63 (1966).
(4) Boelrijk, N., Hamill, W. H., *J. Am. Chem. Soc.* **84**. 730 (1962).
(5) Braesfield, C. J., *Phys. Rev.* **31**, 52 (1928).
(6) Cermak, V., Herman, Z., *Collection Czechoslov. Chem. Commun.* **27**, 406 (1962).
(7) Cermak, P., Herman, Z., *Proc. 10th Ann. Conf. Mass Spectrometry, New Orleans, La.*, p. 358 (1962).
(8) Curran, R. K., *J. Chem. Phys.* **38**, 2974 (1963).
(9) *Ibid.*, **35**, 1849 (1961).
(10) Dawson, P. H., Tickner, A. W., *J. Chem. Phys.* **40**, 3745 (1964).

(11) Derwish, G. A. W., Galli, A., Giardini-Guidoni, A., Volpi, G. G., *J. Chem. Phys.* **39,** 1599 (1963).
(12) Dickenson, P. H. G., Sayers, J., *Proc. Phys. Soc. (London)* **A76,** 137 (1960).
(13) Dorfman, L. M., Noble, P. C., *J. Phys. Chem.* **63,** 980 (1959).
(14) Dreeskamp, H., *Z. Naturforsch* **12a,** 876 (1958).
(15) Eyring, H., Hirschfelder, J. O., Taylor, H. S., *J. Chem. Phys.* 4, 479 (1936).
(16) Fehsenfeld, F. C., Ferguson, E. E., Schmeltekopf, A. L., *J. Chem. Phys.* 44, 3022 (1966).
(17) Fehsenfeld, F. C., Goldan, P. D., Schmeltekopf, A. L., Ferguson, E. E., *Planetary Space Sci.* **13,** 579 (1965).
(18) Fehsenfeld, F. C., Schmeltekopf, A. L., Ferguson, E. E., *Planetary Space Sci.* **13,** 219 (1965).
(19) *Ibid.*, **13,** 919 (1965).
(20) Field, F. H., *J. Am. Chem. Soc.* **83,** 1523 (1961).
(21) Field, F. H., Franklin, J. L., *J. Am. Chem. Soc.* **83,** 4509 (1961).
(22) Field, F. H., Franklin, J. L., Lampe, F. W., *J. Am. Chem. Soc.* **79,** 2419 (1957).
(23) Field, F. H., Franklin, J. L., Lampe, F. W., *J. Am. Chem. Soc.* **79,** 2665 (1957).
(24) Field, F. H., Franklin, J. L., Munson, M. S. B., *J. Am. Chem. Soc.* **85,** 3575 (1963).
(25) Field, F. H., Lampe, F. W., *J. Am. Chem. Soc.* **80,** 5587 (1958).
(26) Field, F. H., Munson, M. S. B., Becker, D. A., ADVAN. CHEM. SER. **58,** 167 (1966).
(27) Frankevich, E. L., Tal'roze, V. L., *Dokl. Akad. Nauk SSSR* **119,** 1174 (1958).
(28) Franklin, J. L., Field, F. H., *J. Am. Chem. Soc.* **83,** 3555 (1961).
(29) Franklin, J. L., Munson, M. S. B., *Proc. Tenth Intern. Symposium Combustion*, The Combustion Institute, p. 561 (1965).
(30) Franklin, J. L., Studniarz, S. A., Ghosh, P. K., *J. Appl. Phys.* **39,** 2052 (1968).
(31) Franklin, J. L., Wada, Y., Natalis, P., Hierl, P. M., *J. Phys. Chem.* **70,** 2353 (1966).
(32) Futrell, J. H., Abramson, F. P., ADVAN. CHEM. SER. **58,** 107 (1966).
(33) Giese, C. F., Maier, W. B., *J. Chem. Phys.* **39,** 197 (1963).
(34) Gioumousis, G., Stevenson, D. P., *J. Chem. Phys.* **29,** 294 (1958).
(35) Goldan, P. D., Schmeltekopf, A. L., Fehsenfeld, F. C., Schiff, H. I., Ferguson, E. E., *J. Chem. Phys.* 44, 4095 (1966).
(36) Hand, C. W., von Weyssenhoff, H., *Can. J. Chem.* **42,** 195 (1964).
(37) *Ibid.*, **42,** 2385 (1964).
(38) Henglein, A., ADVAN. CHEM. SER. **58,** 63 (1966).
(39) Henglein, A., Muccini, G. A., *J. Chem. Phys.* **31,** 1426 (1959).
(40) Herron, J. T., Schiff, H. I., *J. Chem. Phys.* **24,** 1266 (1956).
(41) Hogg, A. M., Haynes, R. M., Kebarle, P., *J. Am. Chem. Soc.* **88,** 28 (1966).
(42) Hogg, A. M., Kebarle, P., *J. Chem. Phys.* **43,** 449 (1965).
(43) *Ibid.*, **43,** 498 (1965).
(44) Hogness, T. R., Harkness, R. W., *Phys. Rev.* **32,** 784 (1928).
(45) Hornbeck, J. A., Molnar, J. P., *Phys. Rev.* **84,** 621 (1951).
(46) Hutchinson, D. A., *Paper presented at ACS (Am. Chem. Soc.) Meeting, Minneapolis, Minnesota* (September, 1955).
(47) Junk, G., Svec, H. J., *J. Am. Chem. Soc.* **80,** 2908 (1958).
(48) Kebarle, P., Hogg, A. M., *J. Chem. Phys.* **42,** 668 (1965).
(49) *Ibid.*, **42,** 798 (1965).

Publication Date: June 1, 1969 | doi: 10.1021/ba-1969-0080.ch005

(50) Keenan, D. J., Clarke, E. M., *Proc. 14th Ann. Conf. Mass Spectrometry, Dallas, Texas,* p. 42 (May 22–27, 1966).
(51) Klein, F. S., Friedman, L., *J. Chem. Phys.* **41,** 1789 (1964).
(52) Knewstubb, P. F., "Mass Spectrometry of Organic Ions," p. 284, Academic Press, New York, 1963.
(53) Knewstubb, P. F., Tickner, A. W., *J. Chem. Phys.* **36,** 674 (1962).
(54) *Ibid.*, **36,** 684 (1962).
(55) *Ibid.*, **38,** 464 (1963).
(56) Kubose, D. A., Hamill, W. H., *J. Am. Chem. Soc.* **85,** 125 (1963).
(57) Lampe, F. W., Field, F. H., *Tetrahedron* **7,** 189 (1959).
(58) Lampe, F. W., Field, F. H., Franklin, J. L., *J. Am. Chem. Soc.* **79,** 6132 (1957).
(59) Lampe, F. W., Franklin, J. L., Field, F. H., "Progress in Reaction Kinetics," Vol. 1, p. 69, Pergamon Press, New York, 1961.
(60) Langevin, P., *Ann. Chim. Phys.* **5,** 245 (1905).
(61) Light, J. C., Horrocks, J., *Proc. Phys. Soc.* **84,** 527 (1964).
(62) Lindholm, E., ADVAN. CHEM. SER. **58,** 1 (1966).
(63) Lindholm, E., *Arkiv Fysik* **8,** 433 (1954).
(64) Luhr, O., *Phys. Rev.* **38,** 1730 (1931).
(65) *Ibid.*, 44, 459 (1933).
(66) Luhr, O., *J. Chem. Phys.* **3,** 146 (1935).
(67) Mann, M. M., Hustrulid, A., Tate, J. T., *Phys. Rev.* **58,** 340 (1940).
(68) Meisels, G. G., Hamill, W. H., Williams, R. R., Jr., *J. Chem. Phys.* **25,** 790 (1956).
(69) Meisels, G. G., Hamill, W. H., Williams, R. R., Jr., *J. Phys. Chem.* **61,** 1456 (1957).
(70) Melton, C. E., Ropp, G. A., *J. Am. Chem. Soc.* **80,** 5573 (1958).
(71) Melton, C. E., Rudolph, P. S., *J. Chem. Phys.* **33,** 1594 (1960).
(72) Moran, T. F., Friedman, L., *J. Chem. Phys.* **39,** 2491 (1963).
(73) *Ibid.*, **42,** 2391 (1965).
(74) Moran, T. F., Hamill, W. H., *J. Chem. Phys.* **39,** 1413 (1963).
(75) Morris, D., *Proc. Phys. Soc. (London)* **A68,** 11 (1955).
(76) Munson, M. S. B., Field, F. H., *J. Am. Chem. Soc.* **88,** 2621 (1966).
(77) Munson, M. S. B., Field, F. H., Franklin, J. L., *J. Chem. Phys.* **37,** 1790 (1962).
(78) Munson, M. S. B., Franklin, J. L., Field, F. H., *J. Phys. Chem.* **67,** 1541 (1963).
(79) *Ibid.*, **68,** 3098 (1964).
(80) Muschlitz, E. E., *J. Appl. Phys.* **28,** 1414 (1957).
(81) Ortenburger, I. B., Hertzberg, M., Ogg, R. A., *J. Chem. Phys.* **33,** 579 (1960).
(82) Pahl, M., *Z. Naturforsch.* **14a,** 239 (1959).
(83) Pahl, M., Weimer, U., *Z. Naturforsch.* **13a,** 753 (1958).
(84) Phelps, A. V., Brown, S. C., *Phys. Rev.* **86,** 102 (1952).
(85) Potter, R. F., *J. Chem. Phys.* **23,** 2462 (1955).
(86) Pottie, R. F., Barker, R., Hamill, W. H., *Radiation Res.* **10,** 664 (1940).
(87) Pottie, R. F., Hamill, W. H., *J. Phys. Chem.* **63,** 877 (1959).
(88) Saporoschenko, M., *Phys. Rev.* **111,** 1550 (1958).
(89) Schissler, D. O., Stevenson, D. P., *J. Chem. Phys.* **24,** 926 (1956).
(90) Shahin, M. M., ADVAN. CHEM. SER. **58,** 315 (1966).
(91) Stevenson, D. P., *J. Phys. Chem.* **61,** 1453 (1957).
(92) Stevenson, D. P., Schissler, D. O., *J. Chem. Phys.* **23,** 1353 (1955).
(93) Tal'roze, V. L., Frankevich, E. L., *J. Phys. Chem. USSR* **34,** 1275 (1960).
(94) Tal'roze, V. L., Lyubimova, A. K., *Dokl. Akad. Nauk SSSR* **86,** 909 (1952).

Publication Date: June 1, 1969 | doi: 10.1021/ba-1969-0080.ch005

(95) Theard, L. P., Hamill, W. H., *J. Am. Chem. Soc.* **84,** 1134 (1962).
(96) von Koch, H., Friedman, L., *J. Chem. Phys.* **38,** 115 (1963).
(97) Wexler, S., Lifschitz, Assa, Guattrochi, A., ADVAN. CHEM. SER. **58,** 193 (1966).

RECEIVED March 6, 1967.

Ion–Molecule Reaction Rates Measured in a Discharge Afterglow

E. E. FERGUSON, F. C. FEHSENFELD, and A. L. SCHMELTEKOPF

Aeronomy Laboratory, Environmental Science Services Administration, Boulder, Colo.

Publication Date: June 1, 1969 | doi: 10.1021/ba-1969-0080.ch006

The application of a flowing afterglow technique to the measurement of thermal energy ion-molecule reactions is briefly discussed. The flowing afterglow system has the advantage of producing reactant species in their ground electronic and vibrational states in many cases and, additionally, allows the measurement of reactions of ions with unstable neutrals such as O, H, N, and O_3. Reactions observed in CO_2 and Ar–H_2 systems are shown to be consistent with ion composition studies in discharges in these gases. Several associative-detachment reactions, including $O^- + O \rightarrow O_2 + e$, $H^- + H \rightarrow H_2 + e$, and $O^- + H_2 \rightarrow H_2O + e$ are found to have large rate constants and such reactions may be important in determining negative ion concentrations in certain discharges.

A flowing afterglow system has been utilized for the past several years in the ESSA Laboratories in Boulder, Colorado, for the measurement of reaction rate constants at 300°K. for both positive and negative ions reacting with both stable and unstable neutral species (*5, 6, 7, 8, 9, 10, 11*). Figure 1 illustrates one version of the flowing afterglow tube which has been utilized. A tube of about 1 meter in length and 8 cm. in diameter serves as the reaction vessel. A gas, usually helium, is introduced at one end of the tube and exhausted at the other end at a rate of around 200 atm. cc./sec., the helium pressure being typically $\sim$ 0.3 torr. The helium is ionized by a pulsed d.c. discharge producing about 10^{10} He^+ ions and $He(2^3S)$ metastable atoms per cc. Positive ions are produced in most cases by adding a relatively small concentration of neutral gas into the helium afterglow by means of a small nozzle. The positive ions are products of He^+ and $He(2^3S)$ reactions with the added neutral. The reactions

In Chemical Reactions in Electrical Discharges; Blaustein, B.;
Advances in Chemistry; American Chemical Society: Washington, DC, 1969.

of these ions with a second neutral added at a second downstream nozzle are then measured. The ion composition of the afterglow is monitored by means of a frequency scanned quadrupole mass spectrometer covering the mass range 1–200 a.m.u. The rate of disappearance of a reactant ion with neutral reactant addition leads directly to a reaction rate constant. Our estimate of the reliability of the rate constants so determined is ±30% in favorable cases. Our experience in comparing our rate constants with other measured rate constants generally supports this estimate.

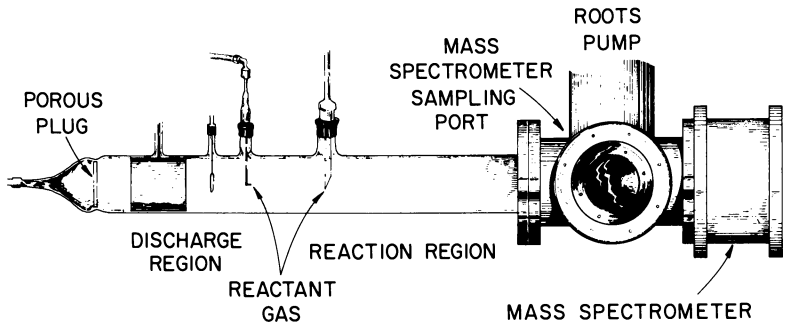

Figure 1. Flowing afterglow reaction system

Experimental

This experimental scheme mentioned above has many variations. We have, for example, successfully used borosilicate glass and quartz reaction tubes as well as stainless steel, and microwave and electron beam ionization as well as the d.c. discharge. We sometimes find it desirable to produce reactant ions by adding a suitable gas through the discharge with the helium rather than downstream in the afterglow, particularly in the case of certain negative ions such as O^- and H^-, which are readily created by dissociative-attachment by fast electrons in the discharge. We sometimes use carrier gases other than helium, particularly argon. Very recently a modified flowing afterglow system has been operated in the temperature range, 80° to 600°K.

Some of the important features of the flowing afterglow experimental technique are the following:

(1) The reactant ions in many cases are known to be in their ground states, either because of the reaction which produces them or by virtue of superelastic electron collisions in the plasma prior to neutral reactant addition. Stable neutral reactant species are added without being subjected to discharge or excitation conditions so that they can be assumed to be neither vibrationally nor electronically excited. On the other hand, some selective excitation is possible. For example, the reaction

$$O^+(^4S) + N_2(^1\Sigma) \rightarrow NO^+(^1\Sigma) + N(^4S) + 1.1 \text{ e.v.} \qquad (1)$$

In Chemical Reactions in Electrical Discharges; Blaustein, B.;
Advances in Chemistry; American Chemical Society: Washington, DC, 1969.

has been measured (*27, 28*) as a function of vibrational temperature from 300° to 6000°K.

(2) It is possible to add chemically unstable neutral reactants into the afterglow so that reactions such as

$$N_2^+ + O \rightarrow NO^+ + N, \quad (2)$$

$$O_2^+ + N \rightarrow NO^+ + O, \quad (3)$$

$$O^- + O \rightarrow O_2 + e, \quad (4)$$

and

$$O^- + O_3 \rightarrow O_3^- + O \quad (5)$$

have been studied in this system. The importance of this fairly unusual capability of the flowing afterglow system for discharge reaction studies is clear, particularly in view of Kaufman's discussion on the production of atoms and unstable neutrals (*18*).

(3) The difficulty of resolving concurrent reactions does not arise, as it does in mass spectrometer ion sources, and we have measured the reaction

$$CO_2^+ + H_2 \rightarrow CO_2H^+ + H \quad (6)$$

without complication from the reaction

$$H_2^+ + CO_2 \rightarrow CO_2H^+ + H, \quad (7)$$

since H_2 is not ionized in the flowing afterglow arrangement (*12*).

Thermal Energy Charge-Transfer Reactions

The flowing afterglow system is well suited to exothermic charge-transfer reaction measurements, since the neutral reactant, necessarily of lower ionization potential, does not go through the ionization region and hence is not selectively ionized as would be the case in some experimental arrangements used for ion-molecule reaction studies. For positive ions, either atomic or molecular, charge-transfer to molecular neutrals is usually fast (barring occurrence of a fast competitive exothermic rearrangement reaction). Many examples of such fast charge-transfers have been observed and only very few exceptions. Examples of the latter are the reactions between $He^+ + H_2$, which is observed not to have a rate constant as large as 10^{-13} cc./sec., and $Ne^+ + N_2$ which has a rate constant $< 10^{-12}$ cc./sec. Ar^+, CO^+, CO_2^+, N_2^+, N^+, and H_2O^+ all charge-transfer with O_2 to produce O_2^+ with rate constants greater than 10^{-10} cc./sec. (or cross sections greater than 20 A.^{2}) as a more typical finding.

The situation appears to be the same for negative ion charge-transfer although much less data is available in this case. Table I gives a few examples of some very recent measurements of negative ion charge-transfers which might be important in some gas discharge applications. It is of interest to note in Table I that some recent measurements of

Publication Date: June 1, 1969 | doi: 10.1021/ba-1969-0080.ch006

In Chemical Reactions in Electrical Discharges; Blaustein, B.;
Advances in Chemistry; American Chemical Society: Washington, DC, 1969.

Rutherford and Turner (*25, 26*) in crossed beam experiments at much higher energies yield similar rate constants in several cases. This suggests that the rate constants are not likely to change drastically with temperature over the range of temperatures of interest in gas discharges. Also the $O^- + NO_2$ charge-transfer measurement of Paulson's (*22*), which is in good agreement with the 300°K. flowing afterglow measurement, was made at an average ion energy of 2 e.v. in a mass spectrometer ion source. The fast charge-transfer of O^- with NO_2 agrees with earlier results of Curran (*2*), Henglein and Muccini (*17*), and Paulson (*22*). The slow charge-transfer of Cl^- with NO_2 does not agree with Curran's (*2*) estimate that Cl^- charge-transfers with NO_2 with a cross section in the range 8 to 70 A.^{2} at low energy. At present we are not sure whether the Cl^- (and F^-) charge-transfer with NO_2 does not go at all or is merely exceptionally slow. This is an important point to be established in further investigations since Curran's report of Cl^- charge-transfer with NO_2 is the basis for the generally accepted 3.6 e.v. lower limit on the electron affinity of NO_2.

Table I. Laboratory Rate Constants

	k (cc./sec.) $\times 10^{-9}$			
Reaction	*FA(300°K.)*	*Beam*[a]		*MS*[b] *E = 2 e.v.*
$O^- + O_3 \rightarrow O_3^- + O$	0.53			
$O_2^- + O_3 \rightarrow O_3^- + O_2$	0.40			
$O^- + NO_2 \rightarrow NO_2^- + O$	1.2	3	2 e.v.	1
$O_2^- + NO_2 \rightarrow NO_2^- + O_2$	0.8	2	2 e.v.	
$H^- + NO_2 \rightarrow NO_2^- + H$	2.9	0.5	25 e.v.	
$OH^- + NO_2 \rightarrow NO_2^- + OH$	1.0	3	2 e.v.	
$NH_2^- + NO_2 \rightarrow NO_2^- + NH_2$	1.0			
$F^- + NO_2 \rightarrow NO_2^- + F$	≤ 0.025	~ 0.015	3 e.v.	
$Cl^- + NO_2 \rightarrow NO_2^- + Cl$	≤ 0.006	Slow $>$	5 e.v.	

[a] J. A. Rutherford and B. R. Turner, Refs. *25, 26.*
[b] J. F. Paulson, Ref. *22.*

The finding of generally large charge-transfer rate constants contradicts most theoretical predictions which had assumed that charge-transfer would be slow except in unusual cases involving fortuitous energy resonances. In the absence of experimental data one would certainly predict that exothermic charge-transfer to a molecular neutral will more likely be fairly fast than slow.

Ion-Atom Interchange Reactions

The most commonly studied ion-molecule reactions have involved changes in molecular configuration. Typical examples are

In Chemical Reactions in Electrical Discharges; Blaustein, B.;
Advances in Chemistry; American Chemical Society: Washington, DC, 1969.

$$C^+ + O_2 \rightarrow CO^+ + O, \quad (8)$$

whose rate constant, 1.1×10^{-9} cc./sec., from flowing afterglow experiments (*9*) agrees with an earlier value 9×10^{-10} cc./sec. measured in a mass spectrometer ion source by Franklin and Munson (*15*); the reaction

$$O^+ + CO_2 \rightarrow O_2^+ + CO \quad (9)$$

with a rate constant of 1.2×10^{-9} cc./sec. from both flowing afterglow (*7*) and mass spectrometer ion source measurements (*23*); and

$$C^+ + CO_2 \rightarrow CO^+ + CO \quad (10)$$

with a rate constant 1.9×10^{-9} cc./sec.

Such reactions also seem to be more often fast than slow. One of the slowest exothermic ion-molecule reactions (again barring cases where fast charge-transfer competes) is

$$O^+ + N_2 \rightarrow NO^+ + N, \quad (11)$$

with a rate constant 1.3×10^{-12} cc./sec.[19]. This rate constant increases (*27, 28*) to about 5×10^{-11} cc./sec. for an N_2 vibrational temperature of 6000°K. and also increases with O^+ kinetic energy (*16, 29*).

No case of a fast ion-atom interchange reaction involving the breaking of two bonds has so far been reported. The exothermic reaction

$$O_2^+ + N_2 \rightarrow NO^+ + NO \quad (12)$$

has a rate constant less than 10^{-15} cc./sec., for example (*14*).

Associative Detachment Reactions

A number of associative detachment reactions have been recently measured to be fast in the flowing afterglow system—*i.e.*, $k > 10^{-10}$ cc./sec.—including those shown in Table II. The most recent flowing afterglow rate constant determinations are somewhat lower than the earlier published values, which are also included in Table II. Moruzzi and Phelps (*20, 24*) have measured some of the same associative detachment reactions in drift tube experiments at Westinghouse and their results are included in Table II. The flowing afterglow and drift tube results agree within better than a factor of two in each case. Moruzzi and Phelps are also able to obtain information on the energy dependence of these rate constants in the drift tube studies.

Several exothermic associative detachment reactions do not occur at measurable rates ($k < 10^{-12}$ cc./sec.), an example being

$$O^- + N_2 \rightarrow N_2O + e + 0.2 \text{ e.v.} \quad (13)$$

Publication Date: June 1, 1969 | doi: 10.1021/ba-1969-0080.ch006

In Chemical Reactions in Electrical Discharges; Blaustein, B.;
Advances in Chemistry; American Chemical Society: Washington, DC, 1969.

Table II. Laboratory Rate Constants

Reaction	k (cc./sec.) $\times 10^{-9}$ FA(300°K.)	FA(300°K.)[a]	DT.[b]
$O^- + O \rightarrow O_2 + e$	0.14		
$OH^- + O \rightarrow HO_2 + e$	0.20		
$OH^- + H \rightarrow H_2O + e$	1.0		
$H^- + H \rightarrow H_2 + e$	1.3		
$Cl^- + H \rightarrow HCl + e$	0.9		
$CN^- + H \rightarrow HCN + e$	0.8		
$O^- + H_2 \rightarrow H_2O + e$	0.6	(1.5)	1.0
$O^- + CO \rightarrow CO_2 + e$	0.44	(~0.5)	0.8
$O^- + NO \rightarrow NO_2 + e$	0.16	(0.5)	0.15

[a] F. C. Fehsenfeld, E. E. Ferguson, and A. L. Schmeltekopf, Ref. *11*.
[b] J. L. Moruzzi and A. V. Phelps, Refs. *20*, *24*.

Publication Date: June 1, 1969 | doi: 10.1021/ba-1969-0080.ch006

Ion-Molecule Reactions in Discharges

One obvious application of measured rate constants to the qualitative interpretation of the ion composition of a gas discharge is the case of the CO_2 discharge ion composition measured by Dawson and Tickner (*3*). Dawson and Tickner observed the dominant ions in a glow discharge in CO_2 to be O_2^+ and CO_2^+. This is quite reasonable in view of the known occurrence of Reactions 8, 9, and 10 above, together with the fast charge-transfer of CO^+ with CO_2 to produce CO_2^+. The results of these reactions are graphically illustrated in Figure 2, which shows that all of the ions, C^+, O^+, and CO^+, do convert to O_2^+ and CO_2^+ by reaction with CO_2 in the ~6 milliseconds reaction time in the flowing afterglow. If sufficient molecular oxygen were added, one would expect the dominant ion to become O_2^+ alone, since CO_2^+ is known to charge-transfer rapidly with O_2 (*21*). As a matter of interest, these same reactions dominate the Martian ion chemistry (*21*), since the Martian atmosphere is largely CO_2.

In a like manner Figure 3, showing ion composition in an Ar–H_2 afterglow (*12*), suggests that the ion-molecule chemistry is such that the dominant ion is H_3^+, and this would very likely be true for certain active discharge conditions as well. This has recently been shown to be the case for the negative glow of a discharge in an H_2 + 8.7% Ar mixture at 0.3 torr pressure (*4*).

An example of the possible importance of associative detachment reactions in discharges was noted many years ago by Massey (*19*), who speculated that the low negative ion density in oxygen discharges (relative to iodine discharges for example) might be attributed to electron detachment by the reaction $O^- + O \rightarrow O_2 + e$. In iodine the analogous reaction $I^- + I \rightarrow I_2 + e$ is endothermic. In view of the subsequent finding that the O^- reaction is indeed fast (Table II), Massey's suggestion

In Chemical Reactions in Electrical Discharges; Blaustein, B.;
Advances in Chemistry; American Chemical Society: Washington, DC, 1969.

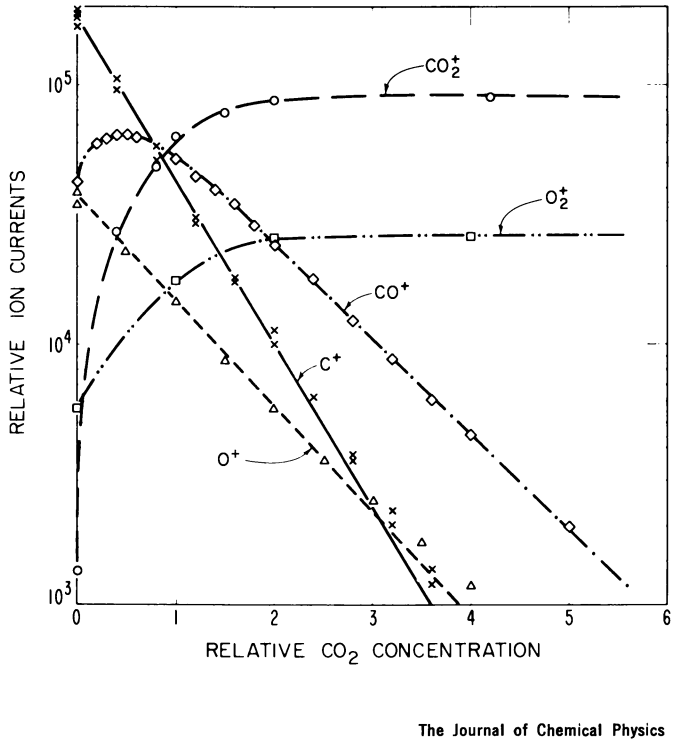

Figure 2. Ion reactions with CO_2

takes on renewed interest. The same argument could be applied to H_2 discharges in view of the rapidity of the reaction $H^- + H \rightarrow H_2 + e$, and in the case of other gases as suggested by Table II.

It has been observed that the electron density decay in the afterglow of microwave discharges in oxygen is anomalously slow in view of the known electron attachment cross sections for oxygen. Biondi (*1*) has suggested that this might be explained if a species capable of causing electron detachment is produced in substantial numbers in the discharge. We have recently (*13*) found the reaction

$$O_2^- + O \rightarrow O_3 + e + 0.5 \text{ e.v.} \qquad (14)$$

to be very efficient ($k_{14} = 3.3 \times 10^{-10}$ cc./ sec.) and it may well be that this is the detachment process involved.

It is not unlikely that the reaction

$$O^- + O_2\ (a^1\Delta_g) \rightarrow O_3 + e + 0.5 \text{ e.v.} \qquad (15)$$

is also fast, in view of the fairly general occurrence of fast associative

Publication Date: June 1, 1969 | doi: 10.1021/ba-1969-0080.ch006

detachment reactions, and this process might be important in oxygen discharges in certain cases.

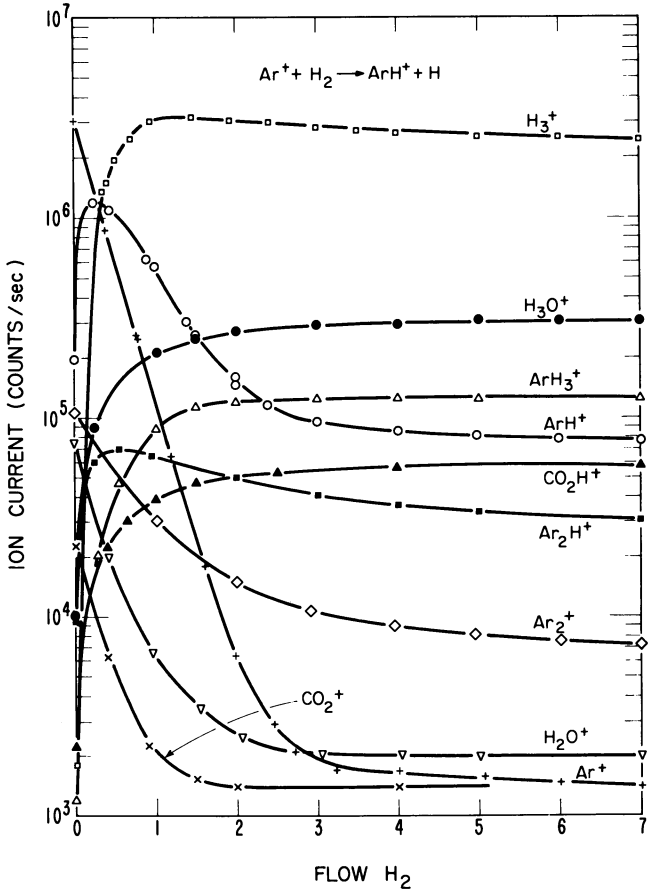

Figure 3. Ion reactions in an Ar–H_2 system

Conclusions

The growing body of quantitative ion-molecule reaction rate data now available should allow in favorable cases prediction and in many cases correlation of observed ion compositions of gas discharges with known ion-molecule chemistry.

Literature Cited

(1) Biondi, M. A., *Advan. Electron. Electron Phys.* **18,** 132 (1963).
(2) Curran, R. K., *Phys. Rev.* **125,** 910 (1962).

Publication Date: June 1, 1969 | doi: 10.1021/ba-1969-0080.ch006

(3) Dawson, P. H., Tickner, A. W., *Proc. Intern. Conf. Ionization Phenomena Gases, 6th, Paris, France* **2**, 79 (1963).
(4) Dawson, P. H., Tickner, A. W., *J. Chem. Phys.* **45**, 4330 (1966).
(5) Fehsenfeld, F. C., Goldan, P. D., Schmeltekopf, A. L., Schiff, H. I., Ferguson, E. E., *J. Chem. Phys.* 44, 4087 (1966).
(6) *Ibid.*, 44, 4095 (1966).
(7) Fehsenfeld, F. C., Schmeltekopf, A. L., Ferguson, E. E., *J. Chem. Phys.* 44, 3022 (1966).
(8) *Ibid.*, 44, 4537 (1966); erratum **46**, 2019 (1967).
(9) *Ibid.*, **45**, 23 (1966).
(10) *Ibid.*, **45**, 404 (1966).
(11) *Ibid.*, **45**, 1844 (1966).
(12) *Ibid.*, **46**, 2802 (1967).
(13) Fehsenfeld, F. C., Schmeltekopf, A. L., Schiff, H. I., Ferguson, E. E., *Planet. Space Sci.* **15**, 373 (1967).
(14) Ferguson, E. E., Fehsenfeld, F. C., Goldan, P. D., Schmeltekopf, A. L., *J. Geophys. Res.* **70**, 4323 (1965).
(15) Franklin, J. L., Munson, M. S. B., "Tenth International Symposium on Combustion," p. 561, Combustion Institute, Pittsburgh, Pa., 1965.
(16) Giese, C. F., ADVAN. CHEM. SER. **58**, 20 (1966).
(17) Henglein, A., Muccini, G. A., *J. Chem. Phys.* **31**, 1426 (1959).
(18) Kaufman, F., ADVAN. CHEM. SER. **80**, 29 (1969).
(19) Massey, H. S. W., "Negative Ions," 2nd ed., Cambridge University Press, Cambridge, 1950.
(20) Moruzzi, J. L., Phelps, A. V., *J. Chem. Phys.* **45**, 4617 (1966).
(21) Norton, R. B., Ferguson, E. E., Fehsenfeld, F. C., Schmeltekopf, A. L., *Planet. Space Sci.* **14**, 969 (1966).
(22) Paulson, J. F., ADVAN. CHEM. SER. **58**, 28 (1966).
(23) Paulson, J. L., Mosher, R. L., Dale, F., *J. Chem. Phys.* 44, 3025 (1966).
(24) Phelps, A. V. (private communication).
(25) Rutherford, J. A., Turner, B. R., *G. A. Rept.* **7649** (Feb. 23, 1967).
(26) Rutherford, J. A., Turner, B. R., *J. Geophys. Res.* **72**, 3795 (1967).
(27) Schmeltekopf, A. L., Fehsenfeld, F. C., Gilman, G. I., Ferguson, E. E., *Planet. Space Sci.* **15**, 401 (1967).
(28) Schmeltekopf, A. L., Fehsenfeld, F. C., Gilman, G. I., Ferguson, E. E., *J. Chem. Phys.* (April 1, 1968).
(29) Stebbings, R. F., Turner, B. R., Rutherford, J. A., *J. Geophys. Res.* **71**, 771 (1966).

RECEIVED April 24, 1967. This work was supported in part by the Defense Atomic Support Agency.

7

The Collection of Positive Ions and Electrons by a Screened Probe in the Neon Negative Glow

M. J. VASILE and R. F. POTTIE

Division of Applied Chemistry, National Research Council, Ottawa, Canada

Publication Date: June 1, 1969 | doi: 10.1021/ba-1969-0080.ch007

The concentrations of ions and electrons in the negative glow of a neon discharge have been measured by using a flat screened probe. The results show that three distinct groups of electrons are present: primary (100 $\leqslant$ E $\leqslant$ 375 e.v.), secondary (4 e.v.), and ultimate electrons (0.2 e.v.). The positive ion concentration is approximately equal to the concentration of ultimate electrons. The primary electron flux was found to decrease exponentially from the cathode edge of the negative glow. The distribution of energy among the secondary electrons is approximately Maxwellian for pure neon discharges, but not so for a mixture of 0.07% xenon in neon. Some conclusions are drawn with regard to the presence of metastable neon atoms in the negative glow.

The collection of ions and electrons by small probes placed within the plasma of a gas discharge has received considerable attention over the past four decades. A major advance in measurement technique was reported by Boyd (*2*) in 1950 with the introduction of a small screened flat probe. The new technique made it possible to separate the collected currents into the ion and electron components. As a result it became possible to measure their concentrations separately and to extend the range of measured electron velocities to beyond the ionization potential of the discharged gas with no interference from positive ion current. The method was extended by Boyd and co-workers (*3*) and by Pringle and Farvis (*10*) to the measurement of ions and electrons in both the positive column and negative glow in various gases. Despite the apparent success of these studies, little or no use has been made of this technique by other workers in the field.

In Chemical Reactions in Electrical Discharges; Blaustein, B.;
Advances in Chemistry; American Chemical Society: Washington, DC, 1969.

Previous work in this laboratory (*4, 5*) had established the usefulness of a mass spectrometer to obtain relative ion concentrations in the various regions of glow discharges. The work reported here is an extension of these earlier studies and represents an attempt to (*a*) measure the absolute concentrations of ions and electrons in conjunction with the mass spectrometric studies and, (*b*) to determine the electron energy distributions, particularly in the negative glow to assist in the interpretation of processes that result in the production of ions.

Experimental

Apparatus. In order to reduce undue disturbance of the discharge, an essential characteristic of a probe is small size. The probe consisted of a fine wire grid that was spot welded to a 5 × 5 mm. platinum frame which was mounted on a borosilicate glass plate. A 1/8-inch circular hole in the glass plate defined the current reaching the platinum collector (0.010 inch thick) mounted below it. A mica insulator shielded the collector from the discharge. The glass plate was 1 mm. thick, and the grid was a stainless steel mesh (0.001 inch diameter wires) with an optical transparency of 42%. The effective area of the collector was computed to be 3.33×10^{-6} meter^2. The probe parts were cemented together with "Gevac" and the platinum leads (0.01 inch diameter) from the electrodes were supported and insulated by means of a ceramic rod with two channels for the leads. The ceramic rod extended through a side-arm of the discharge tube so that it could be rotated or moved radially by means of a magnetic slug. An assembly drawing of the probe is shown in Figure 1. Impedance measurements showed that the resistance between the collector and grid was greater than 10^{13} ohms.

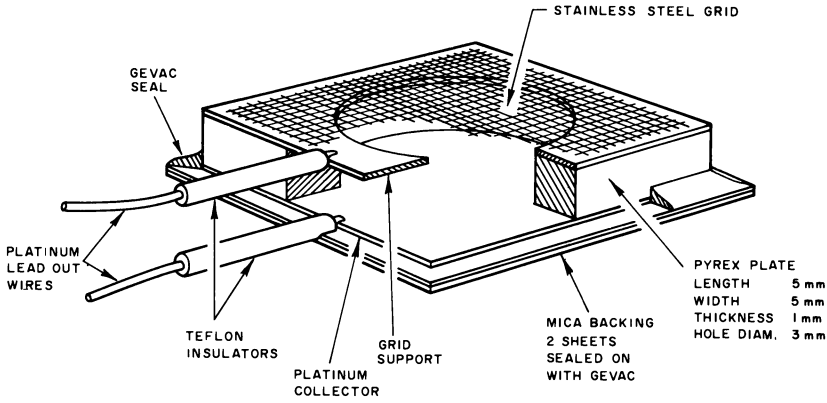

Figure 1. Assembly drawing of the screened probe; double-channel ceramic rod not shown

The borosilicate glass discharge tube was 50 cm. long and 5.5 cm. in diameter. The electrodes were polished stainless steel discs, 5 cm. in

Publication Date: June 1, 1969 | doi: 10.1021/ba-1969-0080.ch007

diameter and the cathode could be moved magnetically over a distance of 30 cm. The entire discharge tube, including side-arms, could be baked to temperatures greater than 350°C. Metal bellows valves were used for all openings into the discharge tube and the normal background pressure of 2×10^{-7} torr was achieved with a silicone oil diffusion pump.

The gases were of assayed research grade and periodic checks were made for impurities by mass spectrometry. The operating gas was admitted to the discharge tube *via* a Granville-Phillips variable leak valve, the pressure being measured with a Decker diaphragm gauge. A small flow was maintained through the discharge tube during operations by means of a needle valve to the pumps. The exit pressure was about 10^{-2} torr. Preliminary discharges of about one hour duration were always carried out before measurements were taken. The tube was then evacuated and a fresh gas sample was admitted for the experiment.

All results reported here were taken with a gas pressure of 0.28 torr and a discharge current of 0.250 ma.

Publication Date: June 1, 1969 | doi: 10.1021/ba-1969-0080.ch007

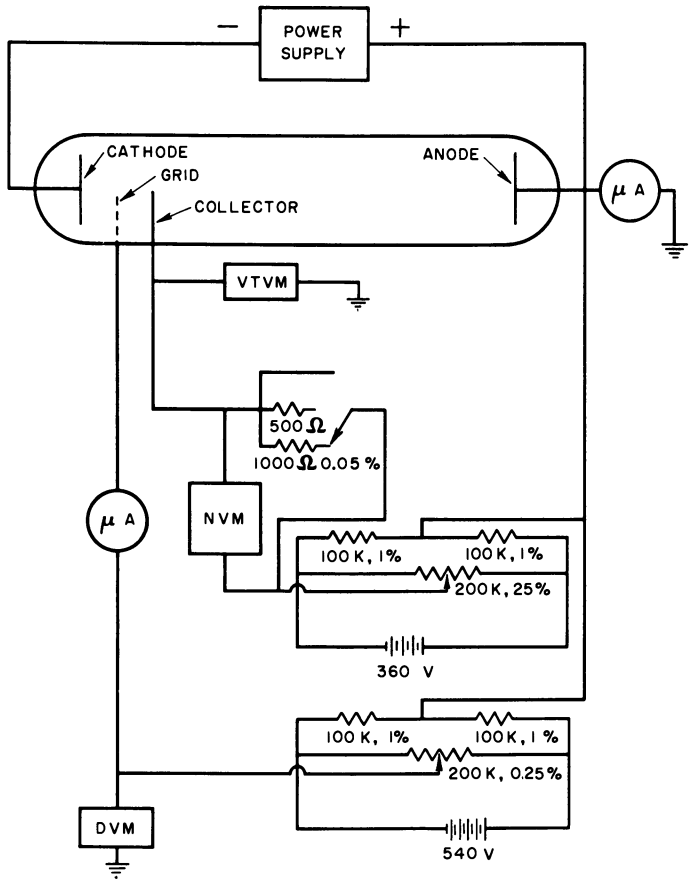

Figure 2. Apparatus and schematic diagram

A schematic diagram of the discharge tube and electrical circuit is given in Figure 2. The potentials of the grid and collector relative to the grounded anode could be controlled independently so that either one could be positive or negative with respect to the anode. The collector current passing through precision resistors (0.05%) was measured with a 1 megohm impedance nanovoltmeter which was isolated from ground. The minimum detectable current was 10^{-10} A. The potential of the collector was measured with a vacuum tube voltmeter, while a digital voltmeter was used for measurement of the grid potential. Grid and discharge currents were monitored by d.c. microammeters. Discharge power was provided by a commercial d.c. power supply.

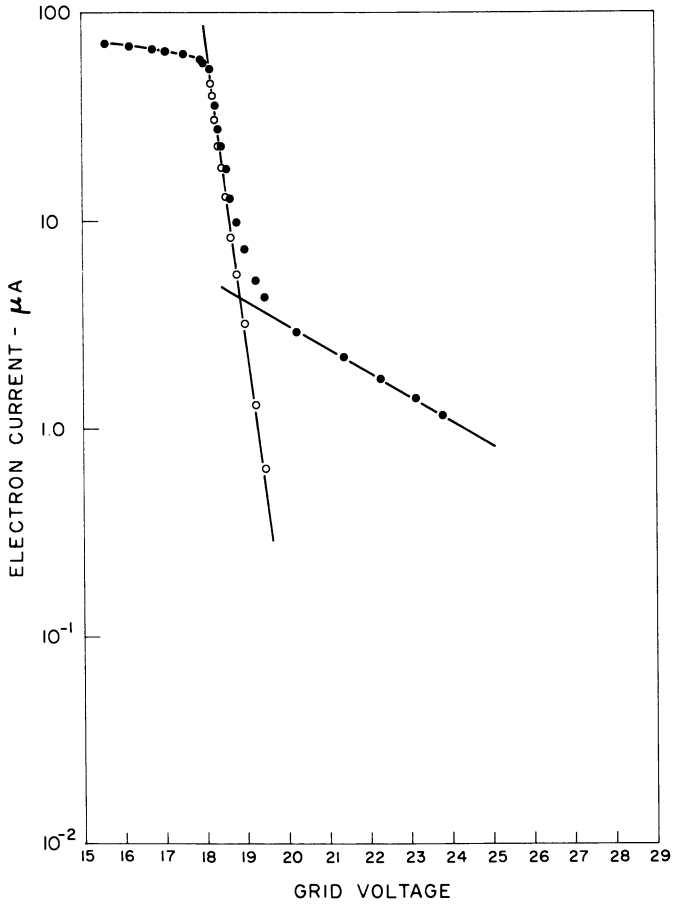

Figure 3. Collection of electrons in pure neon, distance from grid to cathode = 3.3 cm., probe facing the anode. The abscissa has units of negative volts, measured with respect to the anode (ground). The space potential is approximately −18.2 volts

Publication Date: June 1, 1969 | doi: 10.1021/ba-1969-0080.ch007

Results. COLLECTION OF LOW ENERGY ELECTRONS. Figure 3 is a typical semilogarithmic plot of the electron current, showing two straight line segments for the thermal and secondary electrons respectively. The closed circles are the experimental points. The open circles are the difference between the secondary electron component of the total current, and the total electron current. This difference is the component of the total current caused by thermal electrons only. The space potential was obtained from extrapolation of the saturation current to the rising portion of the curve. The gas was pure neon and the probe was near the position of maximum thermal electron concentration in the negative glow. The electron temperatures of the Maxwellian distributions were 0.293 and 3.79 e.v. for the thermal and secondary electrons, and their concentrations were 95.8×10^{13}/meter^3 and 2.8×10^{13}/meter^3 respectively, assuming collection of the random current at the space potential (*6*, *8*). The small electron residual current that was always observed at higher retardation potentials was subtracted from the total electron current. The collector potential was +70 volts with respect to the anode.

COLLECTION OF POSITIVE IONS. The collector potential was maintained at −70 volts and the grid voltage was varied from −70 volts to well above the space potential for the collection of positive ions. The method of calculation of the random positive ion current differed somewhat from previous approaches and is given briefly below.

The potential relative to the space potential at which a positive ion sheath can form is a function of electron energy, ion mobility and the pressure of gas (*2*). As the grid is made more negative than the space potential, the positive ion current to the probe increases because of field penetration into the plasma until a sheath is formed. At this point the current collected by the probe is equal to the random space current modified by field penetration of the sheath boundary. If the grid is made still more negative, additional ion currents measured by the probe are because of edge effects and further field penetration. We have found that for a favorable region in gas pressure, (0.1-1 torr), a log-log plot of probe current *vs.* grid voltage will show a pronounced break at the potential required for sheath formation. Under these conditions, the saturation current so obtained can be corrected for field penetration of the sheath according to an expression by Schultz and Brown (*12*).

$$J_d = n_o q \left(\frac{kT_e}{M\epsilon}\right)^{1/2} \tag{1}$$

in which J_d is the random current density, modified by field penetration of the sheath edge ,n_o is the ion concentration in the undisturbed plasma, T_e is the electron temperature, ϵ is the base of natural logarithms, q is the electronic charge, and M is the mass of the ion.

In our experiments we find two groups of low energy electrons so that we must use an average electron temperature.
Thus:

$$i_{\text{probe}} = J_d \cdot A = An_o q \left(\frac{k}{M\epsilon}\right)^{1/2} [f_1 \sqrt{T_{e_1}} + f_2 \sqrt{T_{e_2}}] \tag{2}$$

In Chemical Reactions in Electrical Discharges; Blaustein, B.;
Advances in Chemistry; American Chemical Society: Washington, DC, 1969.

In this equation, A = probe area—assumed to be the sheath area, and f_1 and f_2 are the fractions of electrons which have temperature T_{e_1} and T_{e_2} respectively.

Thus, in Figure 4 the log-log plot shows a pronounced break which leads to a value of $n_o = 90 \times 10^{13}$/meter^3, in good agreement with the value of the electron concentration obtained from the data of Figure 3 for the same probe position. The use of Equation 1 combined with the

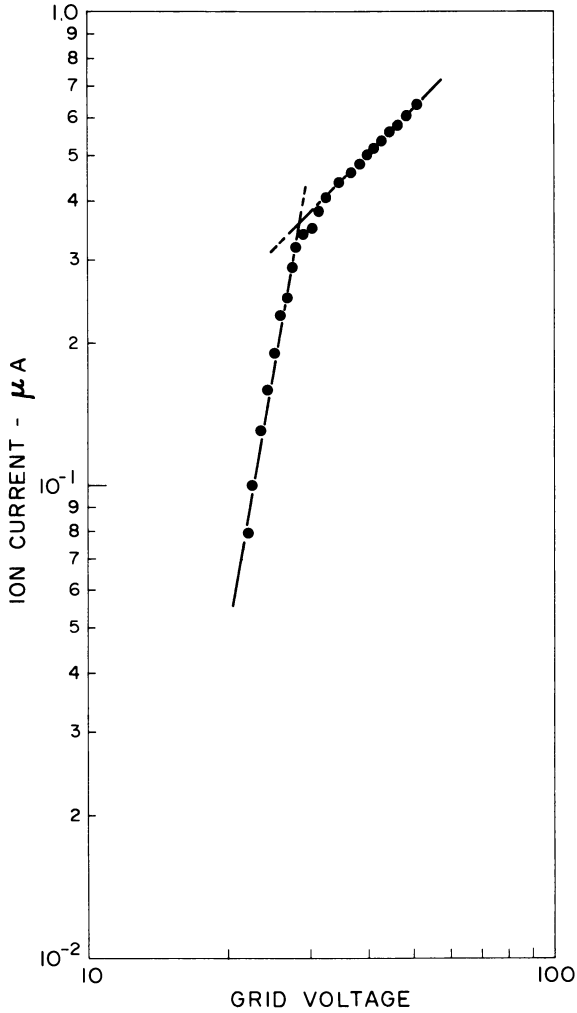

Figure 4. Collection of ions in pure neon. Distance from the grid to cathode = 3.3 cm., probe facing the anode. The abscissa has units of negative volts, measured with respect to the anode (ground)

Publication Date: June 1, 1969 | doi: 10.1021/ba-1969-0080.ch007

equation for collection of the saturation current of the electrons at the space potentials (*6, 8*), leads to the ratio of saturation currents (*12*):

$$\frac{J_e}{J_d} = \left(\frac{\epsilon M}{2\pi m}\right)^{1/2} \tag{3}$$

This ratio is 125.5 for neon, which compares favorable with the value of 129.5 that is obtained as the average ratio for all data obtained in this study.

Axial Variation in Ions and Low Energy Electrons. The observed ion and electron concentrations as a function of axial distance from the cathode are given in Figure 5 for the probe facing the anode. There is a slight displacement between the maxima for the two distributions and this may reflect a penetration of the field from the cathode dark space. However, the results show that a true plasma is present in the negative glow, since to a good approximation the concentration of electrons equals the concentration of ions. The secondary electron current was relatively insensitive to position of the probe and gave an average concentration of $2.5 \pm 0.5 \times 10^{13}$/meter^3 with electron temperatures in the range of 3.5 to 4.0 e.v. The rising portion of the secondary electron curve marks the anode edge of the negative glow. At this point the electric field begins to accelerate thermal electrons to the secondary electron velocities. For example at $d = 6.6$ cm., the secondary electrons account for almost 30% of the total electron current.

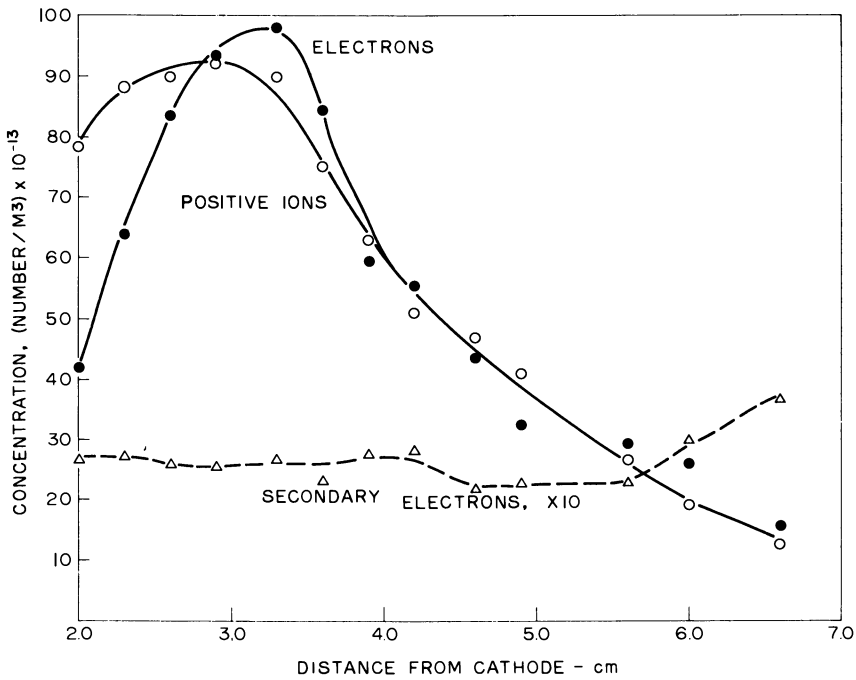

Figure 5. Axial concentration profiles of ions and electrons in the negative glow; probe facing the anode, pure neon discharge

Publication Date: June 1, 1969 | doi: 10.1021/ba-1969-0080.ch007

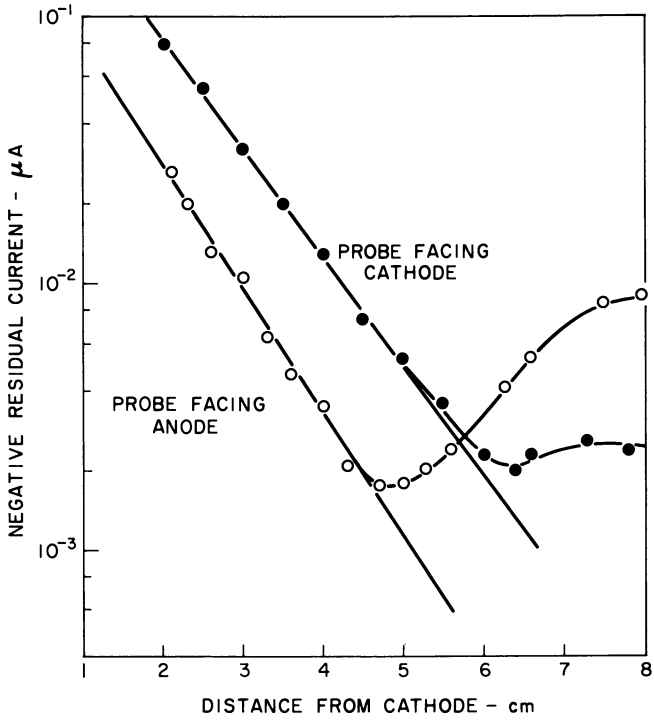

Figure 6. Variation in residual negative current vs. *distance from the cathode for a pure neon discharge*

The measurement of ions or electrons at any point in the negative glow could be reproduced to better than 5% on successive experiments. However, the day to day fluctuations in the discharge increased the concentration uncertainties to something like 10 to 15%. The reproducibility in the residual electron current discussed in the next section was somewhat better than this, and the slope of the line gave cross sections that differed by less than 5% over a period of several weeks.

Residual Electron Current. Small residual electron currents were observed for all probe positions and orientations. These are summarized in Figure 6 for pure neon. These minimum currents were constant for a range of −35 to −50 volts in grid potential. For grid voltages in excess of −50 volts there was a gradual rise in the current, presumably as a result of grid emission by the bombardment of positive ions. We find in Figure 6 that the residual current decreases exponentially throughout the negative glow with increasing distance from the cathode for both orientations of the probe surface. Additionally, there is a reduction by almost a factor of 5 for the probe facing the anode *vs.* cathode position. We have also observed no variation in the residual current as a function of radial position from the center to a point only 0.6 cm. from the wall. The current increases slowly with axial distance in the Faraday dark space ($d > 5$ cm.) and reaches a plateau in the positive column.

Publication Date: June 1, 1969 | doi: 10.1021/ba-1969-0080.ch007

The effect of adding 0.07% xenon to neon is seen in Figure 7. The residual current drops and there is a steeper slope to the exponential part of the curve. In addition, a smaller increase is observed in the Faraday dark space.

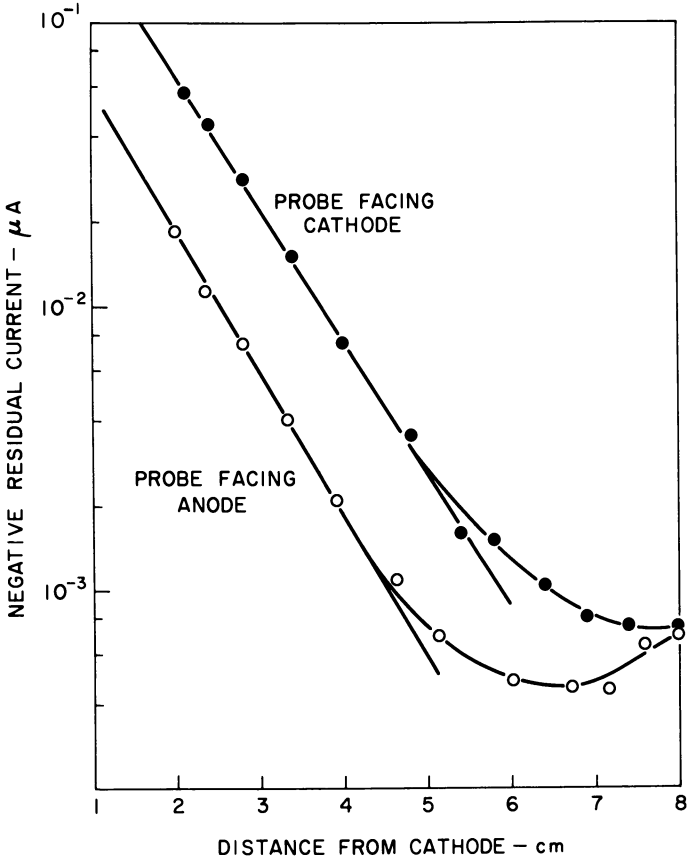

Figure 7. Variation in residual negative current vs. *distance from the cathode for 0.07% Xe in neon*

ENERGY DISTRIBUTION OF SECONDARY ELECTRONS. From Figure 3 we see that the energy distribution of secondary electrons is essentially Maxwellian in pure neon, at the indicated probe position. However, as the axial distance was increased a successively greater loss of electrons whose energies exceed about 10 e.v. occurred, although the distribution was not radically altered from Maxwellian. In the case of the mixture there is almost a complete depletion of secondary electrons above 12 e.v., and there are considerable deficiencies relative to a Maxwellian distribution beginning only 5 e.v. above the space potential. The energy distribution of secondary electrons in the mixture was not Maxwellian, especially at energies above 5–6 e.v.

Publication Date: June 1, 1969 | doi: 10.1021/ba-1969-0080.ch007

In Chemical Reactions in Electrical Discharges; Blaustein, B.;
Advances in Chemistry; American Chemical Society: Washington, DC, 1969.

The data are summarized in Figure 8. The energy distribution curves for the secondary electrons in the range $4 \leqslant E < 20$ e.v. were calculated from the experimental measurements according to the method of Medicus (7). The Maxwellian energy distributions shown are the distributions which correspond to the straight line fit obtained from the data in the energy range $0 \leqslant E \leqslant 5$ e.v. in the case of the mixture, and $0 \leqslant E \leqslant 8$ e.v. for pure neon. The calculated energy distributions and the Max-

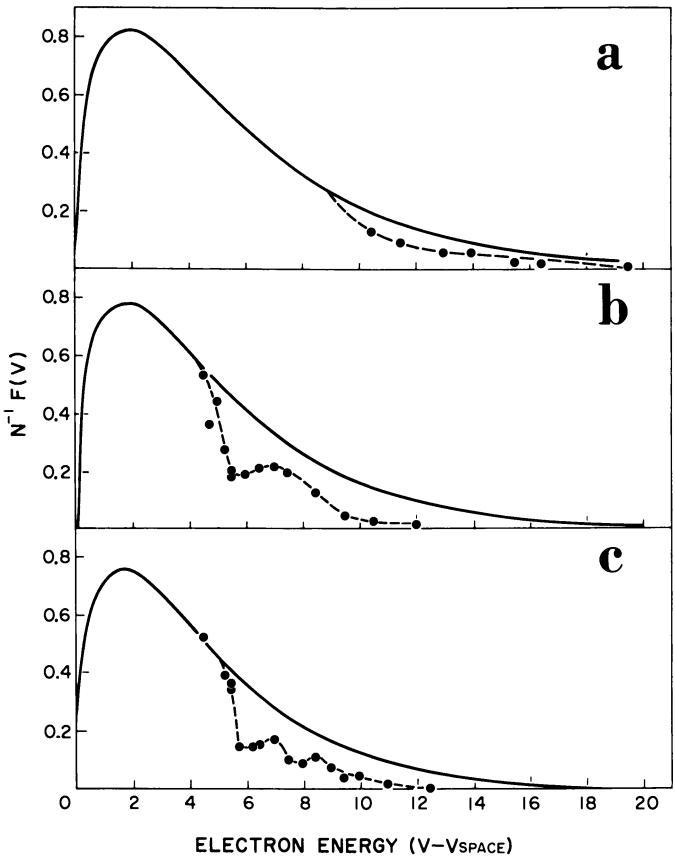

Figure 8. Energy distribution functions of secondary electrons calculated by Medicus' method for $E \geq 4$ e.v. The solid curve is the Maxwellian distribution corresponding to the best semilog straight line fit obtained from the data for $0 \leq E \leq 6$ e.v.

(a) neon discharge, $d = 2.3$ cm., Maxw. distribution calculated for $E = 3.73$ e.v.

(b) mixture 0.07% Xenon in neon, $d = 2.2$ cm. Maxwellian distribution calculated for $E = 3.36$ e.v.

(c) mixture, $d = 3.0$ cm., Maxwellian distribution calculated for $E = 3.11$ e.v.

Probe faces the anode for all the above configurations

Publication Date: June 1, 1969 | doi: 10.1021/ba-1969-0080.ch007

wellian distributions coincided at the electron energies indicated in Figure 8. The fluctuations in the curves for the mixture were reproducible and are similar in appearance to the structural features that were observed by Twiddy (*14*) in the cathode region of rare gas discharges. It is apparent that xenon effectively reduces the higher energy secondary electrons, even at 0.07% concentration. Twiddy (*15*) has shown that there is a similar loss of energetic electrons in the positive column of an argon–neon mixture.

Discussion

Since the production of ions and low energy electrons in the negative glow is governed largely by the rate of arrival of high energy electrons from the cathode dark space it is obvious that the direct observation of these high energy electrons offers an important method for interpreting the processes of ionization in the negative glow. A possible means of making such a measurement is to consider the negative residual currents collected by the screened probe when it faces the cathode. These currents could arise from several processes:

(a) Direct collection of high energy electrons.
(b) Grid emission by high energy electrons.
(c) Grid emission by bombardment of positive ions.
(d) Grid emission by metastable atom impact.
(e) Grid emission by photon impact.

Rotation of the probe to face the anode caused a 2/3 reduction in the residual current. One would not expect processes (c), (d), and (e) to depend markedly on probe orientation so that these processes probably account for less than 1/3 of the total residual negative current when the probe faces the cathode. Furthermore, neither the positive ion density nor the visible photon intensity decays exponentially, so that processes (c) and (e) are similarly rejected as a major source of current for the anode orientation. We conclude that the major causes of the negative residual current in the negative glow are processes (a) and (b) for the probe facing the cathode. We cannot distinguish between (a) and (b), nor is it possible to calculate the density of such high energy electrons without knowledge of their velocities.

The observed exponential decrease in i_e residual through the negative glow of pure neon (Figure 5) can be written as:

$$i_d = i_o \exp\left(-\sigma n(d - d_0)\right) \tag{4}$$

in which i_o is the residual current at d_o cm. from the cathode, d is the distance of the probe surface from the cathode at a second cathode position and n is the concentration of neon atoms, σ has the dimensions of cm.^{2} and as a first approximation, is an experimental cross section for loss of high energy electrons. From the slope of the exponential curve in

Publication Date: June 1, 1969 | doi: 10.1021/ba-1969-0080.ch007

In Chemical Reactions in Electrical Discharges; Blaustein, B.;
Advances in Chemistry; American Chemical Society: Washington, DC, 1969.

Figure 5 we calculate that $\sigma = 8.7 \times 10^{-17}$ cm.^{2}. This is a reasonable value since the cross section for ionization of neon (*11*) by 100 e.v. electrons is 8.6×10^{-17} cm.^{2}.

The addition of 0.07% xenon brings about a 30% reduction in the negative residual current and the exponential slope increases so that experimentally $\sigma = 1.03 \times 10^{-16}$ cm.^{2}. This cannot be accounted for by assuming that the only additional loss is that arising from the ionization of xenon. At a concentration of only 7×10^{-2} atom %, this would imply a cross section for ionization of xenon equal to 228×10^{-16} cm.^{2}—about a factor of 40 higher than the known σ_i of xenon (*11*) for 100 e.v. electrons. A more reasonable inference is that the loss of neon metastables by the Penning reaction:

$$Ne^* \ (^3P_{2,0}) + Xe \rightarrow Xe^+ + Ne + e^- \qquad (5)$$

is responsible for the lower values of i_e residual. The new slope more nearly reflects the actual decrease of high energy electrons in neon, since the component of secondary emission by metastable neon atoms has been removed from the negative residual current. Excitation as well as ionization can result from impact of a high energy electron, and a cross section of the order of 1×10^{-16} cm.^{2} is of the expected magnitude for electrons in the energy range $100 \leqslant E \leqslant 375$ e.v.

It would be expected that the addition of a small amount of xenon would not significantly change either the cathode fall or the number of directed high energy electrons passing into the negative glow. Thus, if one assumes that the reduction in the residual electron current is caused by Reaction 5 it is possible to obtain an approximate value for the concentration of metastables in the beginning of the negative glow.

Referring to Figures 6 and 7, for $d = 2$ cm., $-\Delta_i$, the reduction in the residual current is 0.02 μA. If the neon metastables have thermal velocities, and if one considers a reasonable yield of about 0.03 for the grid emission (geometric factor x efficiency), then a minimum concentration of 1×10^{15}/meter^3 is obtained for the metastables. It is then possible to calculate the reactive collision frequency between Ne* and Xe by assuming the same cross section for deactivation as Sholette and Muschlitz (*13*) observed for the He*–Xe Penning reaction, namely 12×10^{-16} cm.^{2}. This results in a calculated lifetime for the neon metastables of 0.5×10^{-3} sec. This is somewhat shorter than the lifetime of 0.875×10^{-3} sec. measured by Blevis *et al.* (*1*) for the decay of Ne($^3P_2$) in pure neon, and that found by Phelps and Molnar (*9*), to be approximately 3×10^{-3} sec. at 300°K. and 0.3 torr. We conclude that xenon can intercept the metastable neon atoms in the required time and that our assignment of the Penning reaction is reasonably justified as a major contributing cause of the reduction in the residual negative current. Similar

Publication Date: June 1, 1969 | doi: 10.1021/ba-1969-0080.ch007

In Chemical Reactions in Electrical Discharges; Blaustein, B.;
Advances in Chemistry; American Chemical Society: Washington, DC, 1969.

arguments can be used to account for the decrease in the residual current when the probe faces the anode. The effect is even more marked in this case, particularly at the beginning of the positive column.

Acknowledgement

We express our gratitude to Paul Lightman for the design and construction of the discharge apparatus, for his work on the preliminary stage of this study, and for many stimulating discussions on associated problems in electrical discharges.

Literature Cited

(1) Blevis, B. C., Anderson, J. M., McKay, R. W., *Can. J. Phys.* **35,** 941 (1957).
(2) Boyd, R. L. F., *Proc. Roy. Soc.* **A 201,** 329 (1950).
(3) Boyd, R. L. F., Twiddy, N. D., *Nature* **173,** 633 (1954).
(4) Knewstubb, P. F., Tickner, A. W., *J. Chem. Phys.* **36,** 674 (1962).
(5) *Ibid.*, **36,** 684 (1962).
(6) Langmuir, I., Mott-Smith, H., *G.E. Review* **27,** 449 (1924).
(7) Medicus, G., *J. Applied Phys.* **27,** 1242 (1956).
(8) Mott-Smith, H., Langmuir, I., *Phys. Rev.* **28,** 727 (1926).
(9) Phelps, A. V., Molnar, J. P., *Phys. Rev.* **89,** 1202 (1953).
(10) Pringle, D. H., Farvis, W. E. J., *Proc. Phys. Soc.* **68,** 836 (1955).
(11) Rapp, D., Englander-Golden, P., *J. Chem. Phys.* **43,** 1464 (1965).
(12) Schultz, G. J., Brown, S. C., *Phys. Rev.* **98,** 1642 (1955).
(13) Sholette, W. P., Muschlitz, E. E., *J. Chem. Phys.* **36,** 3368 (1962).
(14) Twiddy, N. D., *Proc. Roy. Soc.* **A 262,** 379 (1961).
(15) *Ibid.*, **A 275,** 338 (1963).

RECEIVED June 19, 1967. Work performed under the auspices of the National Research Council (publication No. **9902**).

Reactions of $N_2(A^3\Sigma_u^+)$

ROBERT A. YOUNG[1] and GILBERT A. ST. JOHN

Stanford Research Institute, Menlo Park, Calif. 94025

Publication Date: June 1, 1969 | doi: 10.1021/ba-1969-0080.ch008

The interaction of $N_2(A^3\Sigma_u^+)$ with atomic nitrogen and NO was studied by observing the steady state and transient behavior of Vegard-Kaplan band emission from $N_2(A^3\Sigma_u^+)$ excited in a Tesla-type discharge in flowing nitrogen. $N_2(A^3\Sigma_u^+)$ was deactivated by N

$$N_2(A^3\Sigma_u^+) + N \rightarrow N_2^* + N$$

with a rate coefficient of 5×10^{-11} cc./sec. and by NO

$$N_2(A^3\Sigma_u^+) + NO \rightarrow N_2(X^1\Sigma) + NO^*$$

with a rate coefficient of 7×10^{-11} cc./sec. NO was excited to the $A^2\Sigma_{v'=0}$ level by $N_2(A^3\Sigma_u^+)_{v'=0,1}$ with a rate coefficient of 3×10^{-11} cc./sec. and the $A^2\Sigma^+_{v'=3}$ level of NO was excited by $N_2(A^3\Sigma_u^+)_{v'=1}$ with a rate coefficient of 1.3×10^{-12} cc./sec.

The chemical effects occurring in an electrical discharge are the consequence of the injection of energy into a neutral gas from an applied electrical field by way of electron impact processes. Collisions of energetic electrons with neutral species produce ionization, fragmentation of molecules, and electronic, vibrational, and rotational excitation of the neutral gas.

Reactions of the positive ions, free radicals, and excited species with the unexcited gas are, of course, favored over reactions between the species generated by electron impact because of the much larger density of the original neutral, unexcited gas. In many cases, however, the neutral gas is inert even to energy rich species and then reaction between minor constituents, either those produced by electron impact or others purposely added to the gas, predominates and can be studied.

Discharges in molecular nitrogen have been studied for almost a century. This is partially because it is so readily available, and partially

[1] Present address: Physics Department, York Univ., Toronto, Ontario, Canada.

In Chemical Reactions in Electrical Discharges; Blaustein, B.;
Advances in Chemistry; American Chemical Society: Washington, DC, 1969.

because N_2 is so inert that reaction between electron impact produced species predominates. Despite this long period of study, the phenomena occurring in discharged nitrogen are poorly understood.

The ionic phenomena occurring in a pure N_2 discharge are evidently relatively simple. Since N_2 does not form a stable negative ion, electrons are removed by N_2^+ dissociative recombination. However, N_3^+ and N_4^+ ions are also observed and are probably produced by reactions of N and N_2 with N_2^+.

The recombination of nitrogen atoms, originally produced by the discharge, gives rise to phenomena of remarkable complexity. Perhaps the best known is the Lewis-Rayleigh afterglow. This afterglow consists entirely of the 1st positive bands of N_2 and reflects a peculiar vibrational population distribution in the emitting state. Since this state cannot be directly formed from unexcited atoms, it is necessary to postulate subsequent events causing the originally formed molecules to make nonradiative transitions to the radiating state.

The processes involved in the afterglow, following the initial atom recombination, necessarily involve excited N_2. Hence, to understand this phenomenon, it is essential to study the behavior of these excited N_2 molecules and, in particular, those processes which alter its quantum state while removing little energy. Although the excitation of the Lewis-Rayleigh afterglow requires a quantum state change with little energy removal, the complete dissipation of the energy of nitrogen atom recombination requires either large energy removal from N_2 in the $A^3\Sigma_u^+$ metastable state (radiative lifetime 10–12 sec.) directly to produce unexcited N_2, or a large internuclear-change-small-energy-removal transition horizontally on the potential diagram of N_2 so as to place the molecule on the vibrational ladder leading to unexcited N_2. The $A^3\Sigma_u^+$ state is singled out in this consideration of recombination energy degradation because (1) almost all the emission during atom recombination terminates on this level, and (2) direct recombination into the $A^3\Sigma_u^+$ state is, by statistical weight, 1/3 of the total recombination flux. Other considerations make it likely that a much larger fraction of the successful recombination events pass through the $A^3\Sigma_u^+$ state.

If the $N_2(A^3\Sigma_u^+)$ molecules formed by recombination are removed only by radiation, this emission should be intense in the Lewis-Rayleigh afterglow. However, this emission has never been observed as a consequence of atom recombination. To account for this, collisional deactivation must occur rapidly. However, emissions from $N_2(A^3\Sigma_u^+)$ have been observed in appropriate nitrogen discharges and in very high pressure, short lifetime afterglow. The major difference between those situations where emission is observed and where emission is not observed appears to be in the concentration of atomic nitrogen. Hence, a working hypothe-

Publication Date: June 1, 1969 | doi: 10.1021/ba-1969-0080.ch008

In Chemical Reactions in Electrical Discharges; Blaustein, B.;
Advances in Chemistry; American Chemical Society: Washington, DC, 1969.

sis (*8*) is that $N_2(A^3\Sigma_u^+)$ is converted to another state of N_2 in a process involving atomic nitrogen—*i.e.*,

$$N_2(A^3\Sigma_u^+) + N \rightarrow N_2^* + N$$

To study this process it is desirable to produce a detectable (by emission) amount of $N_2(A^3\Sigma_u^+)$ and study its behavior as the concentration of atomic nitrogen is increased. It is also advantageous to find other compounds which essentially remove all the energy residing in $N_2(A^3\Sigma_u^+)$ and thereby short circuit the flow of energy through $N_2(A^3\Sigma_u^+)$ to other states of N_2. Finally, if the molecules which abstract all the energy from $N_2(A^3\Sigma_u^+)$ rapidly radiate, then this energy can have no further effect within the system. A by-product of such a phenomenon is the development of a sensitive detector of the energy entering the $A^3\Sigma_u^+$ state of N_2.

Experimental

Figure 1 shows the experimental setup. Nitrogen was excited by a pulsed 150-kc., 5-kv. oscillator (of the type used in high-voltage supplies) in a 5-liter quartz bulb with exterior electrodes of silver-conducting paint applied above and below the center plane of the bulb with a radius of approximately half that of the bulb. A 1/2-meter Jarrell-Ash Seya-Namioka monochrometer was used to scan the discharge spectrum or to isolate bands for decay measurements. The signal from the photomultiplier used to detect emission leaving the exit slit of the monochrometer was very low, and an Enhancetron signal integration unit (Nuclear Data Inc., Palatine, Ill.) was used to abstract the decaying signal from the noise.

Prepurified nitrogen was passed through a liquid nitrogen trap, then through heated titanium-zirconium and two additional liquid nitrogen

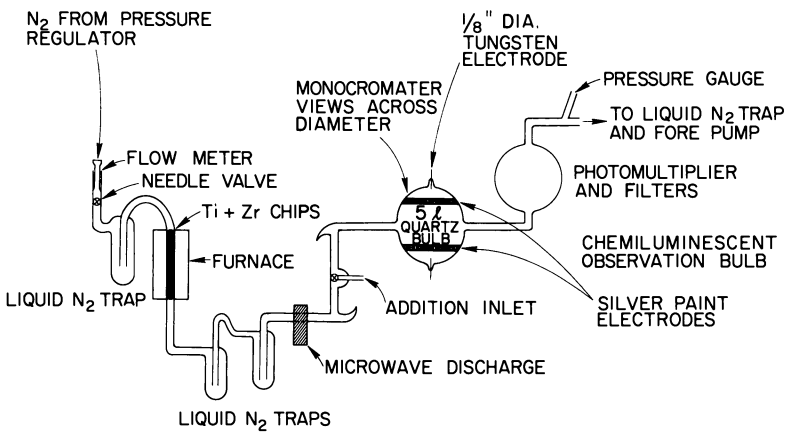

Figure 1. System used for studying the effects of gases on $N_2(A^3\Sigma_u^+)$ *radiation*

traps, past a microwave excitation section, an NO titration inlet, and finally into the 5-liter observation bulb, from which it was exhausted by a mechanical vacuum pump at approximately 1000 cc./sec. A filtered photomultiplier downstream from the bulb observed the N_2 first positive bands resulting from atom recombination (9). This permitted the atom concentration to be computed after calibration against an NO titration (9).

Interaction Of $N_2(A^3\Sigma_u^+)$ With N

Results and Discussion. Figure 2 shows spectrometer scans of the discharge. In Figure 2(a) the N_2 second positive and NO γ bands predominate below 3000 A. The β bands were the only other system of NO detected, and these were very weak. If the microwave discharge is adjusted to produce a small quanity of atomic nitrogen, the NO bands can be suppressed almost entirely. [*See* Figure 2(b)]. Although the Vegard-Kaplan bands are also reduced, the second positive bands remain relatively unchanged. Addition of NO causes a large increase in the intensity of the NO γ bands [*See* Figure 2(c)].

In Figure 3 the transient behavior of the Vegard-Kaplan band intensity, I, is shown. The rise of I with time t when the RF excitation is turned on is given by $I = I_o(1 - e^{-t/\tau})$ and the decay is given by $I = I_o e^{-t/\tau}$, where τ has the same value in both expressions. On the assumption that $N_2(A^3\Sigma_u^+)$ (called N_2* hereafter) decays more slowly than any of its sources, τ represents the actual lifetime of N_2*. All τ's so far measured are much larger than the characteristic decay of electron excitation ($\approx$0.1 msec.).

The value of $1/\tau$ for N_2* in the zero vibrational level *vs.* [N] is plotted in Figure 4 for a variety of conditions. The linear dependence of $1/\tau$ on [N] implies a reaction such as

$$N_2^* + N \rightarrow N_2^{**} + N \qquad (1)$$

and the slope of Figure 4 is $k_1 = 5 \times 10^{-11}$ cc./sec. The intercept in Figure 4, representing $1/\tau$ for zero added nitrogen atoms, gives a τ much shorter than that caused by radiation. Although atoms were not added from the upstream source, they were present because of the RF discharge. Measurements of the atom concentration when only RF excitation is occurring indicate that Reaction 1 accounts for the short lifetime of N_2* when atoms are not added. This value of k_1 agrees with the value deduced by Wray from studies in shock-heated N—N_2 mixtures (6).

Figure 4 indicates that the lifetime of N_2* is independent of pressure and that k_1 is independent of the presence of He. However, with small amounts of N_2 in rare gases the concentrations of N produced by the RF discharge is smaller and hence the lifetime of N_2* without adding N is larger.

Publication Date: June 1, 1969 | doi: 10.1021/ba-1969-0080.ch008

In Chemical Reactions in Electrical Discharges; Blaustein, B.;
Advances in Chemistry; American Chemical Society: Washington, DC, 1969.

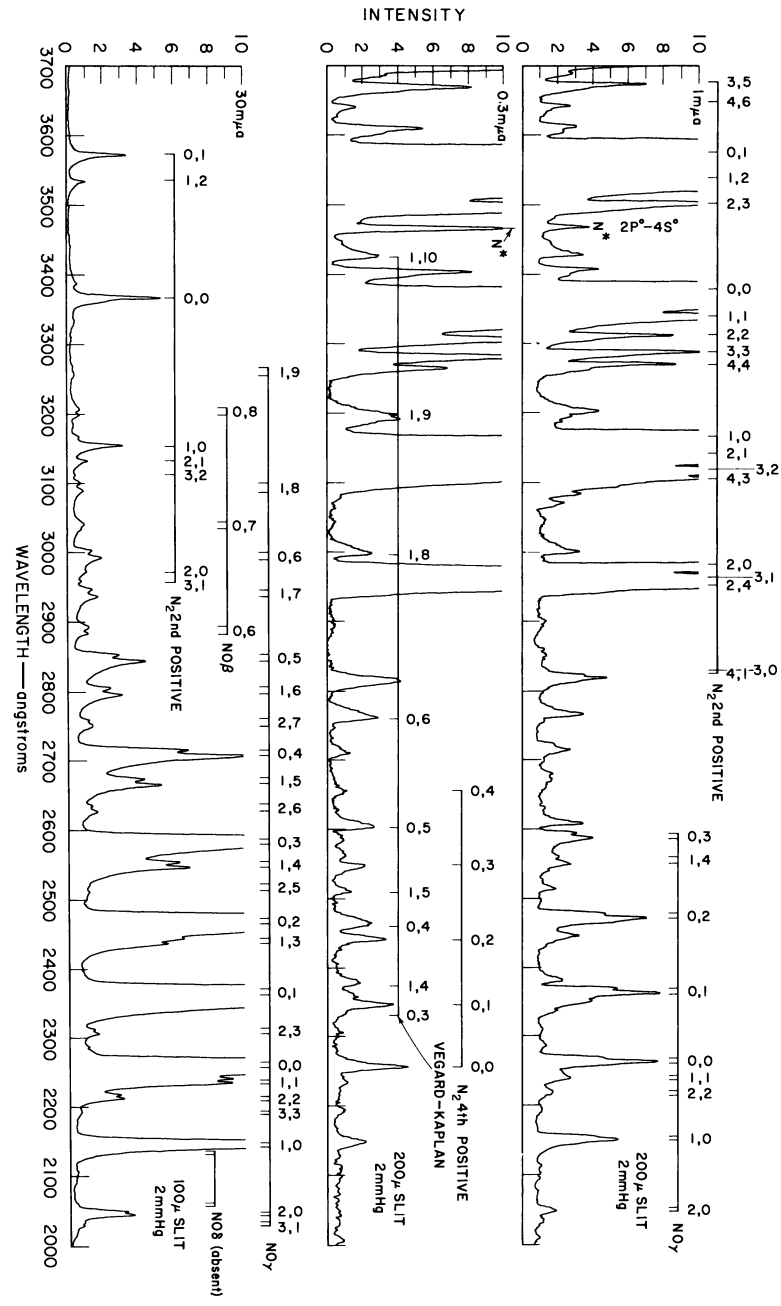

Figure 2. Spectrometer scans of the steady-state intensities under RF excitation: (a) purified nitrogen; (b) purified nitrogen plus ~0.01% N atoms; (c) purified nitrogen plus ~0.01% NO. Note changes of scale

Publication Date: June 1, 1969 | doi: 10.1021/ba-1969-0080.ch008

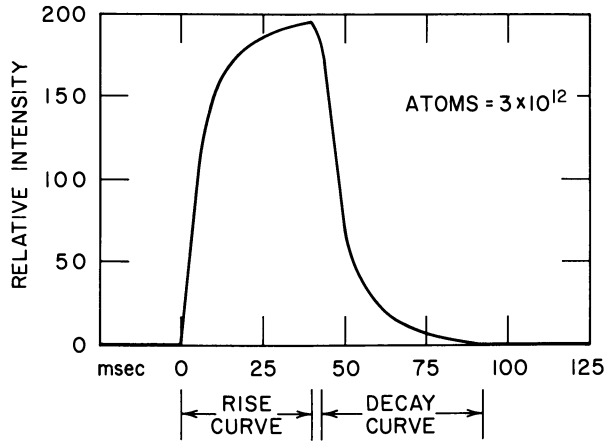

Figure 3. Transient behavior of the Vegard-Kaplan bands stimulated by a pulsed RF discharge. The vertical scale is relative intensity

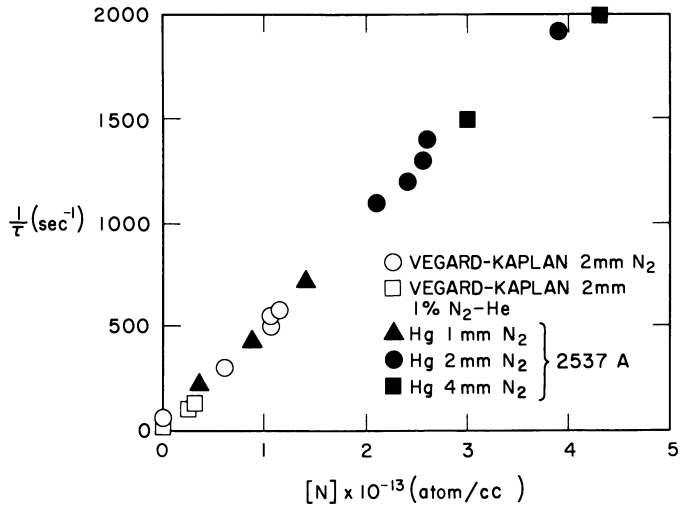

Figure 4. Reciprocal of lifetimes vs. *nitrogen atom concentrations*

(○) Vegard-Kaplan 2 mm. N_2, (□) Vegard-Kaplan 2 mm. 1% N_2-He, (▲) Hg (2537 A.) 1 mm. N_2, (●) Hg (2537 A.) 2 mm. N_2, (■) Hg (2537 A.) Hg 4 mm. N_2. Slope = k × 10^{-11} cc./sec.

Several points in Figure 4 represent the decay times of the 2537 A. line of Hg because of the exchange of energy between N_2* and Hg. The details of this energy transfer will be reported in another paper of this series. Since, at small Hg additions, the lifetime of N_2* is not appre-

Publication Date: June 1, 1969 | doi: 10.1021/ba-1969-0080.ch008

ciably affected (especially if [N] is large), it can be used to measure τ. The 2537 A. radiation was much more detectable than the Vegard-Kaplan bands, and was used when [N] was large.

In Figure 5 the ratio of steady-state intensities of the Vegard-Kaplan bands from $v' = 0$ and 1 with and without added nitrogen atoms are plotted *vs.* the number density of N in the RF excitation bulb. This ratio is linearly dependent on [N] and has a larger slope for $v' = 1$ than for $v' = 0$. This linear behavior is expected if N destroys N_2* in Process 1. The slopes of the lines in Figure 5 are $\tau_0 k_1$ where τ_0 is the lifetime of N_2* when N is not added. Using measured values of τ_0 (Figure 4) gives a value for k_1 approximately the same as that obtained from Figure 4. The ratio of the slopes of the lines in Figure 5 for $v' = 1$ and $v' = 0$ give $k_1(1)/k_1(0) = 1.3$. Here the numbers in parentheses indicate the vibrational level of N_2* in Reaction 1. This is another example of the importance of vibrational energy in determining the rate coefficient of reactions.

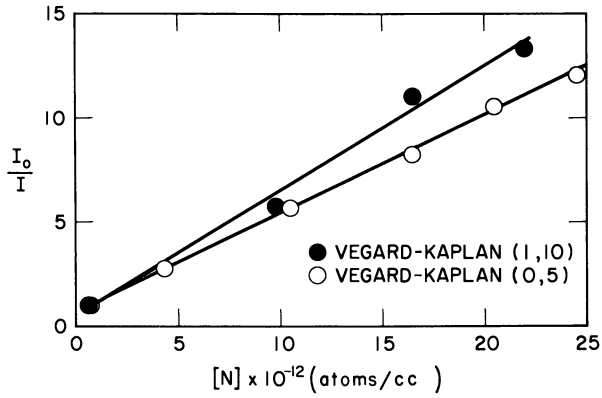

Figure 5. Reciprocal relative steady-state intensities vs. nitrogen atom concentrations

(○) Vegard-Kaplan (0,5), (●) Vegard-Kaplan (1,10)

Reaction 1 implies that nitrogen atoms are not removed in the quenching of N_2*. The number of atoms destroyed in passing through the discharge, when compared with the number of N_2* removed by reaction with nitrogen atoms, indicates that atoms are conserved in the processes quenching N_2*. The rate at which N_2* was destroyed was determined from absolute measurements of the Vegard-Kaplan band intensity, the Vegard-Kaplan radiative lifetime, relative Frank-Condon factors for the Vegard-Kaplan bands, and actual lifetimes of N_2* when nitrogen atoms were present. It is well known, and was observed in this experiment, that the recombination of N is accelerated in a discharge. The

In Chemical Reactions in Electrical Discharges; Blaustein, B.;
Advances in Chemistry; American Chemical Society: Washington, DC, 1969.

number of atoms destroyed, however, was orders of magnitude less than required to account for the number of N_2* destroyed if each N_2* removed one nitrogen atom.

Interactions of $N_2(A^3\Sigma_u^+)$ With NO

Results. Figure 6 shows the decay rate, when the exciting discharge is turned off, of the 0,3 NO γ bands and the 0,5 Vegard-Kaplan band as a function of atomic nitrogen added by the upstream microwave discharge.

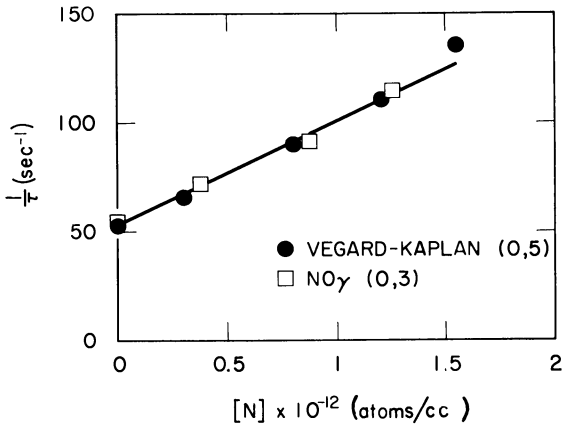

Figure 6. The dependence of the rate of decay of $N_2(A^3\Sigma_u^+)$ and $NO(A^2\Sigma^+)$ as a function of the atomic-nitrogen concentration

□, NO (0,3); ●, Vegard-Kaplan (0,5). Pressure is 1.0 mm.

Figures 7 and 8 show the intensity of the 0,5 Vegard-Kaplan band, the 0,3 NO γ band, and the 0,6 NO β band in the discharge bulb as a function of the NO concentration that would have existed in the stream if no destruction of NO occurred. Also shown are the responses of the yellow photomultiplier and the ultraviolet photomultiplier, both of which are located at the downstream bulb. Figure 7 represents effects occurring at high discharge power, where [N] and [O] are more easily followed. Phenomena beyond the null (at [NO] $\approx 3.5 \times 10^{12}$) are complex in Figure 7 but simplified in Figure 8, where the excitation power is low. The broken lines in Figure 8 represent behavior expected at low [NO].

Spectrometer scans of the discharge without adding NO and on the plateau of Figures 7 and 8 are shown in Figure 2.

Figure 9 is a plot of the area intensity ratio of 0,3 NO γ/0,5 Vegard-Kaplan bands as a function of NO added beyond the null and as a function of the relative response of the yellow phototube to the NO_2 con-

Publication Date: June 1, 1969 | doi: 10.1021/ba-1969-0080.ch008

tinuum. Figure 10 is similar to Figure 4 but involves the 1,10 Vegard-Kaplan band and the 3,0 NO γ band.

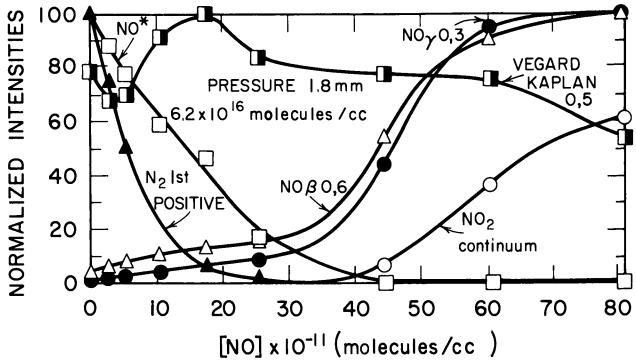

Figure 7. The dependence of emission intensities on NO concentration:

*□, the NO*β bands; ▲, the N_2 1st positive bands; ○, the NO_2 continuum (all excited in the downstream observation bulb); ●, the 0,3 NO band; △, the 0,6 NO β band; and ◨, the 0,5 Vegard-Kaplan band excited in the Tesla discharge bulb. Pressure is 1.8 mm. 6.2 × 10^{16} molecules/cc.*

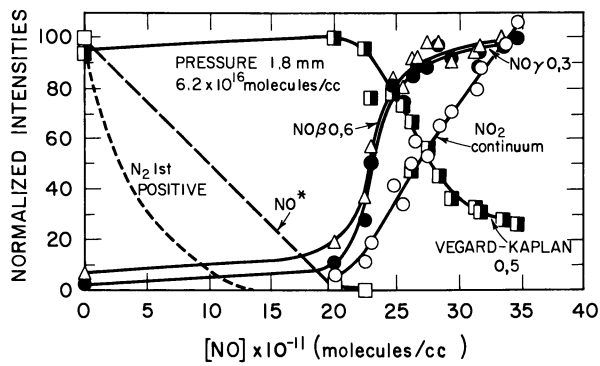

Figure 8. The dependence of emission intensities on NO concentration:

●, the 0,3 NO band; △, the 0,6 NO β band; ◨, the 0,5 Vegard-Kaplan band excited in the Tesla discharge bulb; the two dashed curves indicate the expected dependence of the N_2 1st positive bands and the NO β bands excited by chemiluminescence. Pressure is 1.8 mm. 6.2 × 10^{16} molecules/cc.

Publication Date: June 1, 1969 | doi: 10.1021/ba-1969-0080.ch008

In Chemical Reactions in Electrical Discharges; Blaustein, B.;
Advances in Chemistry; American Chemical Society: Washington, DC, 1969.

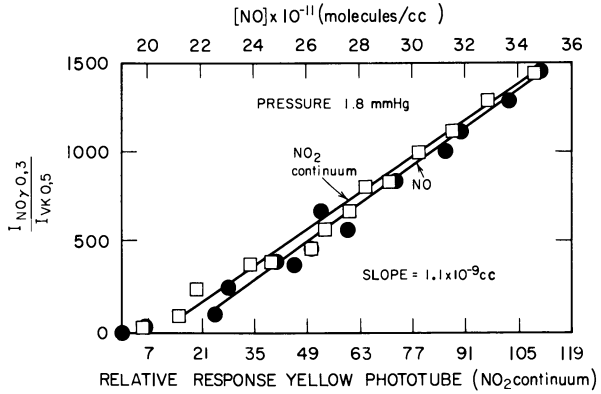

Figure 9. The relative photomultiplier response to the $NO_\gamma(0,3)$ and $N_2(0,5)$ Vegard-Kaplan bands as a function of both [NO] and the response of the yellow photomultiplier

□, NO_2 continuum; ●, NO. Pressure is 1.8 mm. Slope is 1.1×10^{-9} cc.

Discussion. The preceding observations will be shown to indicate the occurrence of

$$NO(X^2\pi) + N_2(A^3\Sigma_u^+) \rightarrow NO(A^2\Sigma^+) + N_2(X^1\Sigma) \qquad (2)$$

as hypothesized by others (*2*).

The initial decrease of the signals from the yellow downstream photomultiplier is caused by NO titration of nitrogen atoms produced in the exciting discharge—*i.e.*,

$$N + NO \rightarrow N_2 + O. \qquad (3)$$

The null point represents the complete conversion of nitrogen atoms to oxygen atoms. The concentration of these atoms derived from the amount of NO added to reach this null is consistent with the intensity of the 1st positive bands before NO addition. The linear rise of the yellow sensitive photomultiplier after null is caused by

$$NO + O \rightarrow NO_2 + h\nu \qquad (4)$$

and indicates that O is essentially constant.

There is an initial slow increase of the NO γ and β bands in the excitation bulb because of the slow increase in the actual steady-state concentration of NO which is maintained by

$$N + O + M \rightarrow NO + M, \qquad (5)$$

and Reaction 3—*i.e.*,

$$[NO] = k_5/k_3[O][M]$$

Publication Date: June 1, 1969 | doi: 10.1021/ba-1969-0080.ch008

Reaction of NO with O by

$$NO + O + M \rightarrow NO_2 + M \quad (6)$$

$$NO_2 + O \rightarrow NO + O_2 \quad (7)$$

does not alter the concentration of NO. When [N] goes to zero this steady state cannot be maintained and NO in the stream increases as expected for no reactions of NO. In the reaction time available Reactions 4 and 6 do not significantly alter either [O] or [NO].

As [NO] increases sharply after the removal of N, the NO γ and β bands increase sharply in the discharge and the N_2 Vegard-Kaplan bands decrease rapidly when the excitation discharge is operating at low power. Since

$$I_{vk} = [N_2(A^3\Sigma_u^+)]/\tau_{vk} \quad (8)$$

$$I_\gamma = [NO(A^2\Sigma^+)]/\tau_\gamma \quad (9)$$

for excitation in the discharge bulb and

$$I_{no_2} = K_{no_2}[NO][O] \quad (10)$$

for chemiluminescent excitation in the downstream bulb, Reaction 2 implies

$$\begin{aligned} I_\gamma &= k_2[NO][N_2(A^3\Sigma_u^+)] \\ &= k_2[NO]I_{vk}\tau_{vk} \\ &= (k_2 I_{no_2} I_{vk}\tau_{vk}/[O]K_{no_2}), \end{aligned} \quad (11)$$

if $NO(A^2\Sigma^+)$ is only deactivated by emission.

Since [O] is constant,

$$I_\gamma/I_{vk} \propto I_{no_2} \quad (12)$$

This is true, as Figures 9 and 10 show. In these graphs, intensities are not absolute, but relative.

To obtain k_2 from Equation 11, we must experimentally relate the emission intensities more directly to the concentration of the emitting state. If $I_\gamma(0,3)$ represents the absolute intensity of the 0,3 γ band of NO and similarly for the Vegard-Kaplan bands, then Equation 11 becomes

$$I_\gamma(0,3)/f_\gamma(0,3) = \{k_2[NO]\tau_{vk}I_{vk}(0,5)/f_{vk}(0,5)\beta\} \quad (13)$$

where $f_\gamma(0,3)$ is the fraction of all emission from the $v' = 0$ level which terminates on the $v'' = 3$ level and similarly for $f_{vk}(0,5)$, τ_{vk} is the radiative lifetime of the $A^3\Sigma_u^+$ state and β represents the fraction of all $N_2(A^3\Sigma_u^+)$ which are in $v' = 0$. Only $v' = 1$ and 0 are detected by their emission, and β is found to be 1/2 and relatively constant. Then

$$k_2 = [f_{vk}(0,5)/f_\gamma(0,3)\tau_{vk}]\beta\{I_\gamma(0,3)/I_{vk}(0,5)[NO]\}. \quad (14)$$

Publication Date: June 1, 1969 | doi: 10.1021/ba-1969-0080.ch008

In Chemical Reactions in Electrical Discharges; Blaustein, B.;
Advances in Chemistry; American Chemical Society: Washington, DC, 1969.

The parameters in brackets depend only on the internal characteristics of the molecules and have previously been measured (*1, 4, 5*) as $\tau_{vk} =$ 12 sec., $f_{vk}(0,5) = 0.13$, and $f_\gamma(0,3) = 0.16$. Hence,

$$k_2 = 0.03\ I_\gamma(0,3)/[\mathrm{NO}]I_{vk}(0,5). \qquad (15)$$

To obtain k_2, only the relative intensity of $I_\gamma(0,3)$ and $I_{vk}(0,5)$ are required. The relative intensity of these bands is equal to their relative signal level modified by the relative response of the detection system as previously measured (*7*). Hence, k_2 is 0.03 times the slope of the line in Figure 4—*i.e.*,

$$k_2 = 0.03(1.1 \times 10^{-9}) = 3 \times 10^{-11}\ \text{cc./sec.} \qquad (16)$$

This rate is much larger than that reported by Dugan (*3*).

The existence of the β bands and emission from higher vibrational levels of the NO($A^2\Sigma^+$) state indicate that this rate is a lower bound to the rate of energy transfer from $N_2(A^3\Sigma_u^+)$ to NO(X^2H). From spectra such as those shown in Figure 2 and the appropriate transition probabilities (*4*) it is found that the normalized fraction of emission from $NO(A^2\Sigma^+)_{v'=0,1,2,3}$ is 0.67, 0.26, 0.05, 0.02. Hence, the total rate for excitation of NO to the $A^3\Sigma^+$ level is 4.5×10^{-11} cc./sec.

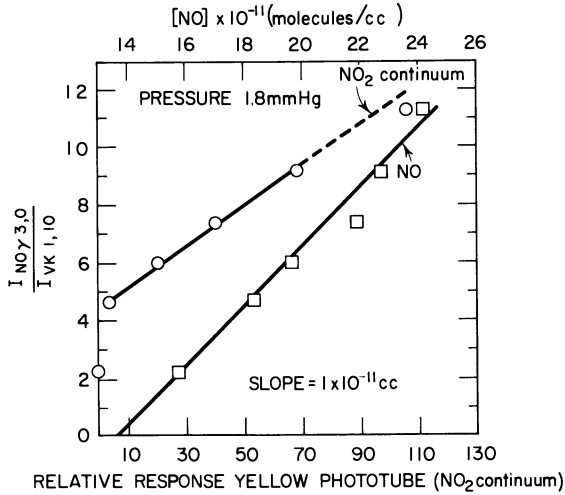

Figure 10. The relative response to the $NO_\gamma(3,0)$ and $N_2(1,10)$ Vegard-Kaplan bands as a function of both [NO] and the response of the yellow photomultiplier

○, NO_2 continuum; □, NO. Pressure is 1.8 mm. Slope is 1 × 10^{-11} cc.

Publication Date: June 1, 1969 | doi: 10.1021/ba-1969-0080.ch008

In similar fashion the spectral measurements of Figure 2 show that the NO β band from the $B^2H_{v'=0}$ state are 0.06 as intense as γ bands from the $A^2\Sigma^+_{v'=0}$ state. Hence their rate coefficient for excitation by $N_2(A^3\Sigma_u^+)_{v'=0,1}$ is 1.8×10^{-12} cc./sec. Then, the total observed rate coefficient for excitation of NO by $N_2(A^3\Sigma_u^+)_{v'=0,1}$ is 4.8×10^{-11} cc./sec.

The $NO(A^2\Sigma^+)_{v'=3}$ level can only be excited by $N_2(A^3\Sigma_u^+)v = 1$, while the $v' = 2$, 1, and 0 levels can be excited by $N_2(A^3\Sigma_u^+)v = 0,1$. Using the data in Figure 10 we can obtain the rate coefficient of

$$N_2(A^3\Sigma_u^+)v' = 1 + NO(X^2H) \rightarrow N_2(X^1\Sigma) + NO(A^2\Sigma^+)v = 3 \quad (17)$$

as $k_2(1,3) = 1.3 \times 10^{-12}$ cc./sec.

The total rate of de-excitation of $N_2(A^3\Sigma_u^+)$ can be estimated since we know, in the absence of NO, its deactivation rate is $1/\tau = 50$/sec. and the intensity of the Vegard-Kaplan bands is reduced by one-half when [NO] $\approx 7 \times 10^{11}$ molecules/cc.—*i.e.*, $50 = k_2'(7 \times 10^{11})$—*i.e.*,

$$k_2' = 7 \times 10^{11} \text{ cc./sec.} \quad (18)$$

or essentially 2/3 of all the deactivated $N_2(A^3\Sigma_u^+)$ leads to excitation of NO.

Literature Cited

(1) Brennan, W. R., Ph.D. thesis, Harvard University (September 1964).
(2) Callear, A. B., Smith, I. W. M., *Trans. Faraday Soc.* **61**, 2383 (1965).
(3) Dugan, C. H., Thesis, Harvard University (June 1963).
(4) Nicholls, R. W., *Ann. Geophys.* **20**, 144 (1964).
(5) Wentick, T., Jr., Isaacson, L., *J. Chem. Phys.* **46**, 822 (1967).
(6) Wray, K. L., *J. Chem. Phys.* 44, 623 (1966).
(7) Young, R. A., Sharpless, R. L., *J. Chem. Phys.* **39**, 1071 (1963).
(8) Young, R. A., *Can. J. Chem.* 44, 1171 (1966).
(9) Young, R. A., Black, G., *J. Chem. Phys.* 44, 3741 (1966).

RECEIVED July 7, 1967. This work was performed under the auspices of the U. S. Army Research Office (Durham, North Carolina), Contract No. DA-31-124-ARO(D)-104.

9

Chemiluminescent Reactions of Excited Helium with Nitrogen and Oxygen

MARK CHER and C. S. HOLLINGSWORTH

North American Aviation Science Center, Thousand Oaks, Calif. 91360

Publication Date: June 1, 1969 | doi: 10.1021/ba-1969-0080.ch009

Active species created in a fast flow of helium by a microwave discharge react outside the discharge with nitrogen or oxygen causing the emission of visible bands of N_2^+ and O_2^+. The emission intensity in the "flame" zone decays exponentially with distance, and the decay coefficient depends on both the flow rate of helium and the flow rate of the added gas. A mathematical analysis is developed to predict the intensity dependence on distance and flow parameters. Comparison of experimental and theoretical results permits the calculation of the rate constants for the reactions populating the emitting states and the diffusion coefficients of the excited helium species. Evidence is presented to suggest that the dominant reactive species is the metastable He atom in the 2^3S state.

Long-lived reactive species, produced when helium gas is subjected to an electrical discharge, react with many other gases and generate characteristic emissions of visible light. The nature of some of these chemiluminescent reactions has been discussed recently in a number of papers (*3, 4, 5, 9, 16*). The reaction with nitrogen gas produces an intense bright blue flame consisting of the first negative system of $N_2^+(B^2\Sigma_u^+ \rightarrow X^2\Sigma_g^+)$. With oxygen a bright yellow-green flame is observed owing to the excitation of both the first negative system of $O_2^+(b^4\Sigma_g^- \rightarrow a^4\Pi_u)$ and the second negative system of $O_2^+(A^2\Pi_u \rightarrow X^2\Pi_g)$. In this paper we report the results of our measurements of the spatial variation of the emission intensity in a fast flow system for various flow conditions, and show how these measurements can be used to evaluate the rate constants for the reactions populating the emitting states.

In Chemical Reactions in Electrical Discharges; Blaustein, B.;
Advances in Chemistry; American Chemical Society: Washington, DC, 1969.

Apparatus

The reaction cell and associated equipment are shown schematically in Figure 1. The reaction cell consisted of a pair of concentric borosilicate tubes. The inner tube, which carried the helium gas, was 0.955 cm. i.d. and 55 cm. long. The titrating gas was introduced into the helium stream *via* the outer tube through a 0.2 mm. inlet gap in the inner tube. High velocity flows of about 10^4 cm./sec. were maintained by three mechanical pumps connected in parallel, each of which was rated at 425 liters/min. The flow rates of the gases were measured using a pair of calibrated critical velocity orifice flow meters described by Andersen and Friedman (*1*). The pressure in the reaction cell was taken as the average value measured by two oil manometers located approximately 20 cm. upstream and 35 cm. downstream from the inlet gap. The observed pressure drop between the two manometers was approximately 75% of the average pressure.

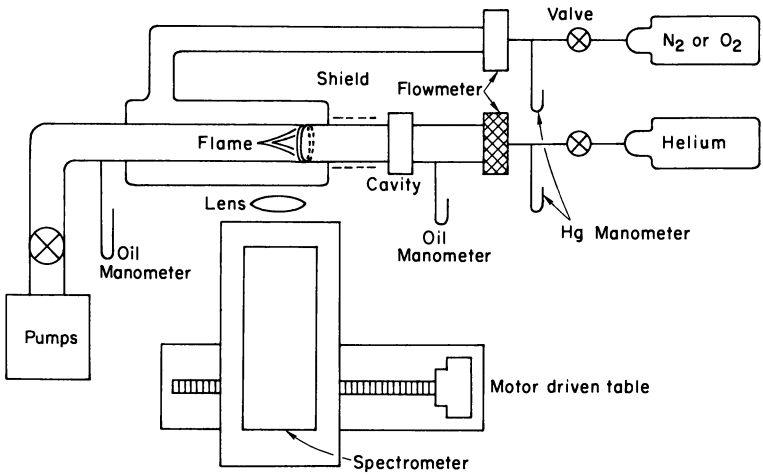

Figure 1. Schematic Diagram of Apparatus

The discharge in the helium stream was excited by a 2450 Mc./sec. cavity of the Evenson type (*7*) powered by a 125 watt Raytheon diathermy unit. The cavity was located 10.5 cm. upstream of the inlet gap. A metal shield excluded the active discharge from extending into the flame zone. At high helium flow rates and in the absence of added gases a pale pink afterglow primarily caused by atomic helium lines could be observed visually in the flame zone.

Spectra and intensity measurements were made with a 0.5 meter Jarrell-Ash Ebert spectrophotometer using an RCA 1P21 photomultiplier tube. A pair of large condensing lenses served to focus the image of a cross section of the flame on the entrance slit. The spectrophotometer was mounted on a table which could be moved at constant speed parallel to the axis of the reaction cell. In this way the intensity of the flame was recorded as a function of distance along the tube.

In Chemical Reactions in Electrical Discharges; Blaustein, B.;
Advances in Chemistry; American Chemical Society: Washington, DC, 1969.

The temperature in the reaction zone was calculated from the relative emission intensity of the rotational lines in the R branch of the O–O band of N_2^+ (*11*). Rotational quantum number assignments and the rotational constant for the B state of N_2^+ were obtained from the work of Coster and Brons (*6*). A check on the spectroscopic temperature was made using a very thin (0.0006 inches) bare thermocouple wire inserted in the middle of the reaction zone. Within experimental error the two methods were in good agreement at temperatures below 500°K. Above 500°K. the indicated thermocouple temperature was significantly lower than the spectroscopic temperature. Heat transfer problems probably accounted for the difference. The temperature in the reaction zone was not constant but decreased steadily because of the losses through the walls. The gradient was particularly large at the high temperatures obtained at the higher flow rates. For example, at a helium flow rate of 4.6×10^{-3} moles/sec., the temperature dropped approximately 225°K. in 6 cm., while at a flow rate of 3.1×10^{-3} moles/sec., the drop was only 100°K. in 6 cm. The observed temperature was found to be determined primarily by conditions in the helium discharge and was nearly independent of the flow rate of nitrogen and the nature of the added gas. Thus, for a given helium flow we can apply the temperature calculated from the nitrogen emission spectrum in the studies of reactions of other gases.

All gases were taken directly from the commercially available high pressure cylinders. Typical stated concentration of impurities in the helium tanks (Matheson Ultra High Purity) was 14 p.p.m., with neon being the major contaminant at 11 p.p.m.

Interpretation of Data

We assume that an excited helium species X^* reacts with N_2 or O_2 to give the electronically excited N_2^{+*} or O_2^{+*}, and the latter immediately decays by emission of a quantum of light, as indicated by Reactions 1 and 2

$$X^* + N_2 \rightarrow N_2^{+*} + X \quad (1)$$

$$N_2^{+*} \rightarrow N_2^+ + h\nu \quad (2)$$

At this point the identity of X^* remains unspecified. X^* could be, for example, the metastable 2^3S helium atom, in which case X represents a ground state He atom plus an electron. Alternatively X^* could be the He_2^+ molecule-ion, and X would then represent two ground state helium atoms. For simplicity we assume that under any one set of conditions only one excited helium species is dominant, although we can expect several processes occurring simultaneously. The natural lifetime of N_2^{+*} or O_2^{+*} is short compared with the time scale of the experiment, and thus the emission intensity is proportional to the rate of Reaction 1. If the concentration of nitrogen is uniform and constant along the tube, which should be the case after some distance of travel, the intensity

Publication Date: June 1, 1969 | doi: 10.1021/ba-1969-0080.ch009

becomes proportional to the concentration of X*. We therefore need to derive an expression for the concentration of X* as a function of position.

We consider a semi-infinite cylinder of radius r_0. Let n be the concentration of X* and N the concentration of the added gas, say N_2. We assume that the two major mechanisms responsible for the decay of n are diffusion of X* to the walls where $n = 0$ and the chemical reaction represented by Equation 1. Under these conditions the rate of change of n is given by

$$u\frac{\partial n}{\partial x} = D\nabla^2 n - kNn \tag{3}$$

where u is the stream flow velocity, x is the axial coordinate, D is the diffusion coefficient of X*, and k is the specific rate constant for Reaction 1. Since transport along the axial direction by convection is much greater than by diffusion, we need only consider radial diffusion, and for this case the solution of the axial part of Equation 3 assuming a constant average flow velocity u_0 is (*10*)

$$\bar{n}(x) = n_0 \exp\left[-\left(\frac{D}{\Lambda^2} + kN\right)\frac{x}{u_0}\right]. \tag{4}$$

Λ, the characteristic diffusion length is given by $\Lambda = r_0/2.405$, and is obtained from the solution of the radial part of Equation 3 using the assumed boundary condition $n = 0$ at the walls (*12*). The radial dependence of $\bar{n}(x)$ is taken care of by the experimental arrangement, since the photomultiplier tube views an entire cross section of the flame, and its response is proportional to the integrated average intensity. The average flow velocity u_0 and the concentration N are calculated by Equations 5 and 6

$$u_0 = RT\Sigma F/p\pi r_0^2 \tag{5}$$

$$N = (F_N/\Sigma F)(p/RT) \tag{6}$$

where p is the pressure, T is the temperature, F_N is the flow rate of the added gas in moles/sec., and ΣF is the total flow rate, which in these experiments is essentially equal to the flow rate of helium. If the emitted intensity $I(x)$ is proportional to $n(x)$, it follows that a plot of $\ln I$ *vs.* x should be a straight line with slope

$$-\frac{d\ln I}{dx} \equiv S = \frac{(D_0p_0)(2.405)^2\pi}{760\Sigma FRT} + k\pi\left(\frac{pr_0}{760\Sigma FRT}\right)^2 F_N \tag{7}$$

In Equation 7 we make use of the fact that D is inversely proportional to pressure and (D_0p_0) is the diffusion coefficient at pressure 1 mm. Hg. Using Equation 7 it should be possible to evaluate k and D_0p_0 from the predicted linear dependence of S on the flow rate of added gas F_N.

Publication Date: June 1, 1969 | doi: 10.1021/ba-1969-0080.ch009

In Chemical Reactions in Electrical Discharges; Blaustein, B.;
Advances in Chemistry; American Chemical Society: Washington, DC, 1969.

In the derivation of Equations 4 and 7 we have used a constant average flow velocity u_o and neglected to allow for the parabolic velocity profile that must exist under our laminar flow conditions. If we let u in Equation 3 be a parabolic function of r, namely $u = 2u_o(1 - r^2/r_o^2)$, then the equation becomes considerably more complicated, and this case does not appear to have been heretofore treated satisfactorily. The solution is worked out in the appendix and the final result is shown in Equation 8

$$S = \frac{(D_o p_o)\pi}{760\Sigma FRT}\left(\frac{\lambda_o^2}{2}\right) + k\pi\left(\frac{pr_o}{760\Sigma FRT}\right)^2\left(\frac{1+\epsilon_1}{2}\right)F_N - k^2\pi\left(\frac{pr_o}{D_o p_o}\right)\left(\frac{pr_o}{760\Sigma FRT}\right)^3\frac{\epsilon_2}{2}F_N^2 \quad (8)$$

where $\lambda_o = 2.710$, $\epsilon_1 = 0.237$ and $\epsilon_2 = 0.00115$. Except for the value of the empirical constants and the appearance of the quadratic third term, which turns out to be essentially negligible, Equations 7 and 8 are similar. Thus, the effect of considering the parabolic flow field in the tube is to increase all the values of $D_o p_o$ and k over those obtained in the simpler treatment by factors of 1.58 and 1.62, respectively.

Results

Measurements of intensity *vs.* distance were recorded for nitrogen at 3914 A. and for oxygen at 5586 A. and 4116 A. These wave lengths are the heads of intense vibrational bands of the first negative system of N_2^+ and the first and second negative systems of O_2^+. Flames were 5–20 cm. in length, and over this distance the intensity varied by factors of 100 or more. Typical plots of the logarithm of the intensity *vs.* distance for various nitrogen flow rates at constant helium flow rate are shown in Figure 2. These results demonstrate both the linear behavior and the increased rate of decay of intensity with increasing flow rate of added gas, as predicted by Equations 7 and 8. Rates of decay of intensity S for various flow rates of helium were plotted against the flow rate of added gas, and the results are shown in Figures 3 and 4. A linear dependence is obtained for nitrogen, but for oxygen some downward curvature is evident. The quantities k/T^2 and $D_o p_o/T$ were calculated from the slopes and intercepts (initial slopes in the oxygen experiments) using Equation 8, neglecting the quadratic third term, and the results are shown in Table I. From the values of k/T^2 and $D_o p_o/T$ obtained in this way, the magnitude of the third term was then calculated for the largest value of F_N used, and it was shown that the ratio of this term to the first two terms was less than 1% for nitrogen and 4% for oxygen. Taking an average value of the temperature in the reaction zone from the spectro-

Publication Date: June 1, 1969 | doi: 10.1021/ba-1969-0080.ch009

scopic measurements, we then calculate absolute values of k and D_0p_0. The magnitudes of the rate constants are in the range of 10^{-10} cc. molecule^{-1} sec.$^{-1}$. Thus, these reactions are very fast indeed, being of the order of the collision frequency. The rate constant for the reaction with N_2 is about one-third as large as those for the reaction with O_2. Qualitatively this is observed, since the nitrogen flames are generally longer than the oxygen flames. The small difference in the rate constants for the oxygen reaction, as determined from the data at the two wave lengths, is real and not caused by experimental error. This is shown by the fact that in a given flame the first negative band system decays with distance slightly more rapidly than the second band system.

The unusual square dependence of the rate constants on temperature shown in Table I is found in both sets of reactions. The diffusion coefficient D_0p_0 of the excited helium species shows a similar temperature behavior. The magnitude is reasonable for any one of the excited helium species (*13*), and it is interesting that essentially the same value is obtained for both sets of reactions.

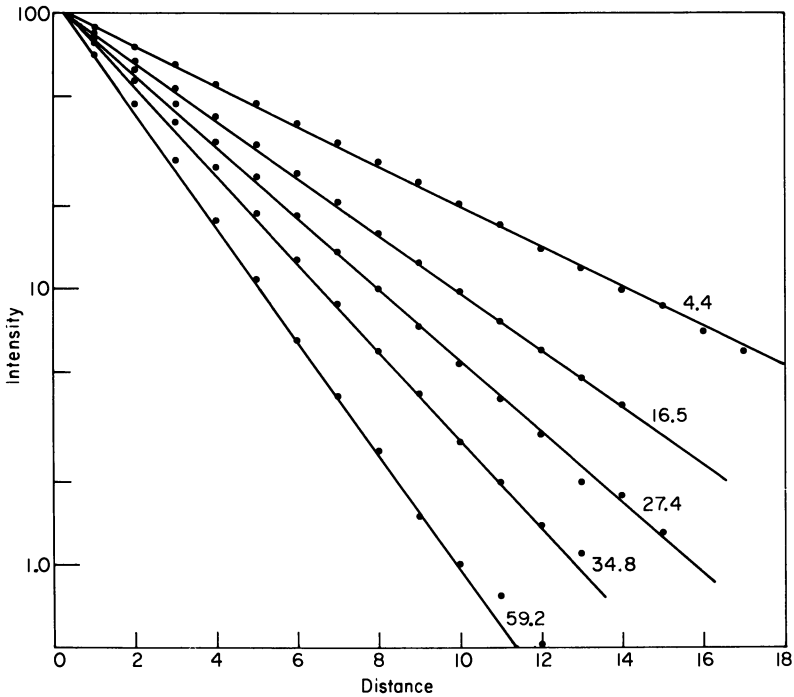

Figure 2. Intensity vs. distance plots for nitrogen titration at 3914 A. $F_{He} = 16.1 \times 10^{-4}$ moles/sec. The intensity was normalized to 100 arbitrary units in all runs. Distance scale: 1 unit = 0.531 cm. The number in each run refers to the pressure of nitrogen upstream of the flowmeter orifice and is approximately proportional to the flow rate of nitrogen

Discussion

The experimental data obtained in the nitrogen titrations fit the equations predicted by the model remarkably well, as evidenced by the results in Figures 2 and 3. In the oxygen titrations, the results are not as good; while the intensity curves obey the exponential decay law (Equation 4), the decay coefficient S shows a greater downward curvature than we would predict on the basis of Equation 8. A likely explanation is that photo-ionization and excitation of the oxygen by trapped 587 A. resonance radiation from the helium discharge acts as an additional source of excited molecules, and consequently the intensity of the emitted light decays less rapidly than expected at higher flow rates (and hence concentration) of added gas. Evidence for this effect is provided by our early experiments which were carried out with only one-third the ultimate pumping capacity. These experiments showed greater deviations from

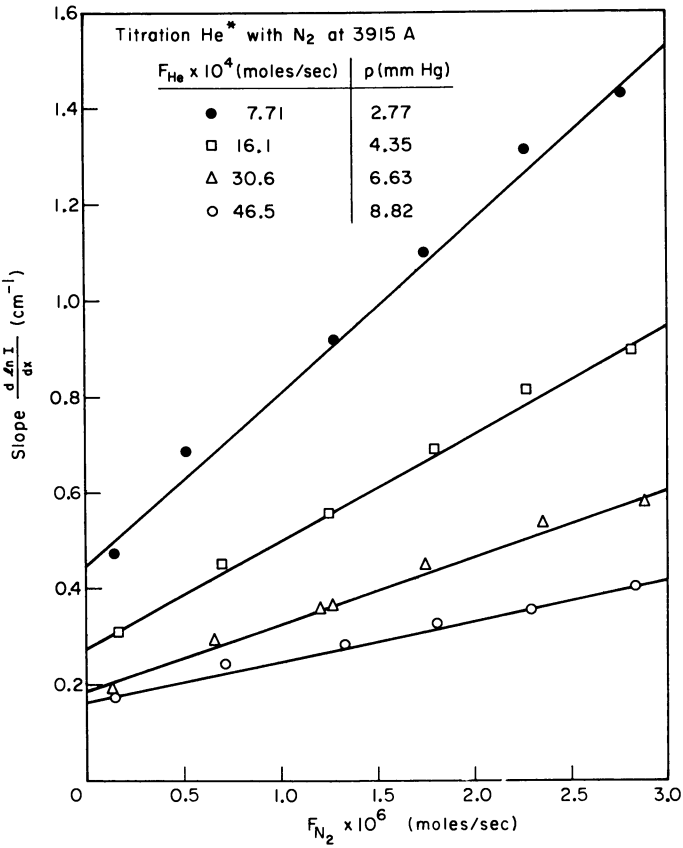

Figure 3. Plot of $-d\ln I/dx$ vs. flow rate of nitrogen

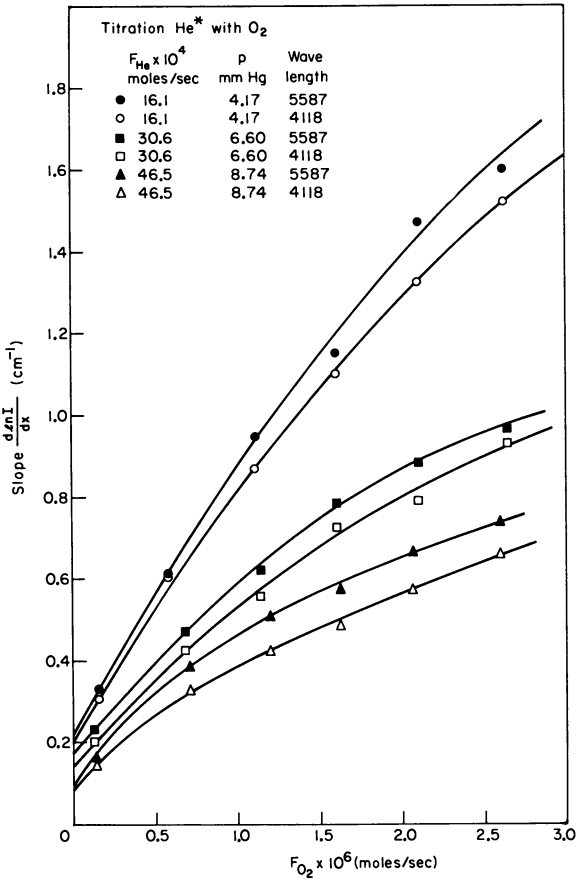

Figure 4. Plot of $-d\ln I/dx$ vs. flow rate of oxygen

linearity in both the oxygen and nitrogen systems, presumably because the resonance light is more efficiently absorbed at the resulting higher pressures. This indeed is the rationale for taking initial slopes to compute rate constants. Ferguson and co-workers (*10*) report direct evidence of the photo-ionization effect, although they find that the effect in oxygen is smaller than in nitrogen.

The square dependence on temperature for the rate constants of both reactions is quite surprising, and we cannot explain it. It is difficult to believe that these fast reactions involving highly excited species should have activation energies associated with them, although one could certainly draw Arrhenius plots from the data. Because of the scatter of the data in Table I and the uncertainties introduced by the temperature gradient in the reaction zone we cannot rule out the possibility of a

In Chemical Reactions in Electrical Discharges; Blaustein, B.;
Advances in Chemistry; American Chemical Society: Washington, DC, 1969.

somewhat less steep functional dependence on temperature. Additional experiments in which the gradient is removed will be required to establish more accurately the temperature coefficient. It should be noted that the determination of the temperature dependence comes out naturally from the mathematical model and the data of Figures 3 and 4 and does not depend on the measurement or knowledge of the actual temperature in the reaction zone. However, the solution of Equation 3 is based on the assumption of constant u_0 and N, and both of these quantities depend on the ratio of temperature and pressure—*i.e.*, density—as shown by Equations 5 and 6. The effect of the temperature gradient in the reaction zone is fortunately partially compensated by a corresponding drop in pressure because of the viscous drag. The net effect cannot be too serious in view of the excellent fit to the predicted exponential decay of intensity. Owing to the uncertainty in the temperature of the reaction because of the gradient, the error in the absolute value of k may be as large as 50%, whereas k/T^2 is probably accurate to within 20%.

Table I. Rate Constants and Diffusion Coefficients for the Reactions of Excited Helium with Nitrogen and Oxygen

Run	$F_{He} \times 10^4$ *moles/sec.*	p *mm. Hg*	T °K.	$\frac{k}{T^2} \times 10^{16}$	$k \times 10^{10}$ *cc./molecule-sec.*	$\frac{D_0 p_0}{T}$	$D_0 p_0 \times 10^2$ *cm.² mm. Hg/sec.*
			Titration with N_2 at 3914 A.				
1	7.70	2.77	399	4.2	0.66	1.8	7.3
2	16.1	4.35	440	4.5	0.87	2.4	11
3	30.6	6.63	525	4.3	1.2	3.0	16
4	46.5	8.82	660	3.4	1.5	4.2	28
			Average	4.1			
			Titration with O_2 at 5586 A. (1st. Neg.)				
1	16.1	4.17	440	14	2.7	2.0	8.6
2	30.6	6.60	525	12	3.4	3.1	16
3	46.5	8.74	660	13	5.8	3.1	20
			Average	13			
			Titration with O_2 at 4116 A. (2nd. Neg.)				
1	16.1	4.17	440	13	2.5	1.9	8.4
2	30.6	6.60	525	11	3.1	2.6	14
3	46.5	8.74	660	12	5.1	2.5	17
			Average	12			

A question may be raised concerning the significance of an equilibrium Boltzmann rotational temperature for N_2^+, and the propriety of equating it to the temperature of the gas stream, since under the condi-

In Chemical Reactions in Electrical Discharges; Blaustein, B.;
Advances in Chemistry; American Chemical Society: Washington, DC, 1969.

tions of our experiments excited N_2^+ suffers two to five collisions during its radiative lifetime of 6.6×10^{-8} secs. (*2*). The answer must be that either these very few collisions are sufficient to attain rotational equilibrium, or else the excited N_2^+ is produced in Reaction 1 at the same rotational temperature as the neutral N_2. In a reactive collision between N_2 and $He(2^3S)$ neither the He nor the Penning electron can carry away much orbital angular momentum, and thus the second possibility appears quite reasonable.

So far we have not considered the identity of the excited helium species X*. Collins and Robertson (*3*) have shown that the upper state of N_2^+ giving rise to the blue emission is populated by reaction of N_2 with both metastable 2^3S He and He_2^+. Similarly, they have shown that 2^3S He reacts with O_2 to populate the upper state of both band systems of O_2^+, while He_2^+ reacts with O_2 to populate only the upper state of the 5586 A. system.

In our experiments with O_2 we obtain rate constants which are almost the same whether we monitor the 5586 A. or the 4116 A. band systems. Also the diffusion coefficients appear to be the same in both oxygen and nitrogen titrations. These observations suggest that under our conditions metastable 2^3S He is responsible for most of the reactions leading to emission. If He_2^+ were contributing significantly to the reaction populating the upper state of the 5586 A. system, we would expect the differences between the results at the two wave lengths in oxygen to be a function of total pressure, since the population of He_2^+ is proportional to the square of the total pressure. This is not found. The small difference between the results at the two wave lengths shows that the reaction of He_2^+ cannot be excluded completely, however, and we would predict qualitatively that the rate constant for the reaction of He_2^+ with O_2 is larger than the corresponding rate constant for the reaction of 2^3S He. Quantitative comparisons for these reactions are not available. An independent check on the identity of the excited helium species and the magnitude of the rate constants could be obtained by following the decay of the 2^3S helium concentration using absorption measurements. Such experiments are being planned, and the results will be reported in future publications.

There are very few measurements of the rate constants for these reactions with which we may compare our results. Sholette and Muschlitz (*17*) give values of 19×10^{-11} cc. molecule^{-1} sec.$^{-1}$ and 9×10^{-11} cc. molecule^{-1} sec.$^{-1}$ for Reactions 9 and 10

$$He(2^3S) + O_2 \rightarrow He + O_2^+ + e^- \quad (9)$$

$$He(2^3S) + N_2 \rightarrow He + N_2^+ + e^- \quad (10)$$

Publication Date: June 1, 1969 | doi: 10.1021/ba-1969-0080.ch009

In Chemical Reactions in Electrical Discharges; Blaustein, B.;
Advances in Chemistry; American Chemical Society: Washington, DC, 1969.

while Fehsenfeld and co-workers (8) report 6×10^{-10} cc. molecule^{-1} sec.$^{-1}$ for Reaction 11

$$He_2^+ + N_2 \rightarrow 2He + N_2^+ \qquad (11)$$

Our results extrapolated to 300°K. give values of 11×10^{-11} and 4×10^{-11} cc. molecule^{-1} sec.$^{-1}$ for Reactions 9 and 10 in reasonable agreement with those of Sholette and Muschlitz.

Acknowledgments

The authors are grateful to D. A. McQuarrie for his help with the mathematical analysis and to G. Lauer for supplying the computer program.

Appendix

The Effect of a Parabolic Velocity Profile on the Concentration Distribution of Excited Species

We consider the differential equation

$$2u_o\left(1 - \frac{r^2}{r_o^2}\right)\frac{\partial n}{\partial x} = D\left(\frac{\partial^2 n}{\partial r^2} + \frac{1}{r}\frac{\partial n}{\partial r}\right) - \alpha n; \quad \alpha = kN \qquad (A\text{-}1)$$

This equation differs from Equation 3 in that the flow velocity u is given by $u = 2u_o\ (1 - r^2/r_o^2)$; u_o is as before the average flow velocity, and r_o is the tube radius. As usual we let $n(r,x) = X(x)R(r)$, substitute into Equation A-1, separate variables, and obtain two ordinary differential equations for $X(x)$ and $R(r)$, which are related by a separation constant b^2.

$$\frac{2u_o}{D}\frac{1}{X}\frac{dX}{dx} = -\frac{1}{b^2} \qquad (A\text{-}2)$$

$$\frac{d^2R}{dr^2} + \frac{1}{r}\frac{dR}{dr} + \left(\frac{1}{b^2} - \frac{\alpha}{D} - \frac{r^2}{r_o^2 b^2}\right)R = 0 \qquad (A\text{-}3)$$

The solution of Equation A-2 follows immediately

$$X(x) = C\exp\left[-\left(\frac{D}{\Lambda^2} + \alpha\right)\frac{x}{2u_o}\right] = C\exp\left[-\left(\frac{D\lambda^2}{r_o^2} + kN\right)\frac{x}{2u_o}\right] \qquad (A\text{-}4)$$

where C is a constant, and Λ and λ are parameters (independent of r and x) defined by

$$\frac{1}{\Lambda^2} \equiv \frac{\lambda^2}{r_o^2} = \frac{1}{b^2} - \frac{\alpha}{D} \qquad (A\text{-}5)$$

In Chemical Reactions in Electrical Discharges; Blaustein, B.;
Advances in Chemistry; American Chemical Society: Washington, DC, 1969.

Whereas in the solution of Equation 3 $1/\Lambda^2 = (2.405)^2/r_o^2$, and λ is simply the number 2.405 corresponding to the first zero of the Bessel function $J_o(r\lambda/r_o)$ evaluated at $r = r_o$, in the more complicated case of Equation A-1 λ turns out to be function of α and hence a function of N. The problem is to find this dependence.

We define a new variable

$$y = \frac{r}{\Lambda} = \frac{r\lambda}{r_o} \tag{A-6}$$

and simplify Equation A-3 to the non-dimensional form

$$\frac{d^2R}{dy^2} + \frac{1}{y}\frac{dR}{dy} + \left(1 - \frac{\beta^2}{\lambda^2}\, y^2\right)R = 0 \tag{A-7}$$

where R is now a function of y, and

$$\beta^2 = 1 + \frac{\alpha r_o^2}{D\lambda^2} = 1 + \frac{kr_o^2N}{D\lambda^2} \tag{A-8}$$

Equation A-7 can be reduced to the confluent hypergeometric differential equation (*14*)

$$z\frac{d^2G}{dz^2} + (1 - z)\frac{dG}{dz} - aG = 0$$

where

$$z = \beta\lambda r^2/r_o^2$$

$$a = (1/2) - (\lambda/4\beta)$$

$$G(z) = R\left(\frac{r\lambda}{r_o}\right)\exp[\beta\lambda r^2/2r_o^2]$$

and its solution in terms of the real variable r is (*14*)

$$R\left(\frac{r\lambda}{r_o}\right) = \exp[-\beta\lambda r^2/2r_o^2]\,{}_1F_1\left(\frac{1}{2} - \frac{\lambda}{4\beta}, 1; \frac{\beta\lambda r^2}{r_o^2}\right) \tag{A-9}$$

Here ${}_1F_1(a,1;z)$ represents the confluent hypergeometric function

$${}_1F_1(a, 1; z) = \sum_{j=0}^{\infty} \frac{a(a+1)\cdots(a+j-1)}{(j!)^2}\, z^j$$

The boundary condition $n = 0$ at the wall of the tube requires

$${}_1F_1\left(\frac{1}{2} - \frac{\lambda}{4\beta}, 1; \beta\lambda\right) = 0 \tag{A-10}$$

The solution of this equation gives λ as a function of β, which in turn is a function of N. The first three roots of Equation A-10 were solved numerically for several values of β in the range 1 to 2.5, and the results are shown in Table II. It is interesting to note that the first three solu-

In Chemical Reactions in Electrical Discharges; Blaustein, B.;
Advances in Chemistry; American Chemical Society: Washington, DC, 1969.

tions for the special case $\beta = 1$ (*i.e.*, no chemical reaction as $N = 0$) were obtained by Nusselt (*15*) in 1910 in connection with a heat flow problem, and he found values of λ equal to 2.705, 6.66, and 10.3. Although the complete solution of Equation A-1 involves an infinite sum of exponentials of the kind represented by Equation A-4, each corresponding to a root of Equation A-10, only the first root contributes substantially to the sum. Consequently, we shall ignore all roots except the first, and hereafter λ refers only to the first root.

Table II. The First Roots of Equation A-10 as a Function of β

β	$\lambda^{(1)}$	$\lambda^{(2)}$	$\lambda^{(3)}$
1.000	2.7044	6.679	10.673
1.100	2.7776	7.017	11.320
1.250	2.9090	7.656	12.561
1.375	3.0408	8.301	13.759
1.500	3.1947	9.013	15.001
1.625	3.3715	9.752	16.250
1.750	3.5699	10.500	17.500
2.000	4.0178	12.000	20.000
2.250	4.5032	13.500	22.500
2.500	5.0004	15.000	25.000

To obtain the dependence of λ^2 on N we plot λ^2 *vs.* $\lambda^2(\beta^2 - 1)$, and this is shown in Figure 5. This plot is suggested by the fact that according to Equation A-8 N is proportional to $\lambda^2(\beta^2 - 1)$. Experimental results using the approximate Equation 7 indicated that the range of $\lambda^2(\beta^2 - 1)$ was between 0 and 48, corresponding to a range of β between 1 and 2. A quadratic fit over this range was computed by the method of least squares. The results are expressed by the empirical relation

$$\lambda^2 = \lambda_o^2 + \epsilon_1\lambda^2(\beta^2 - 1) - \epsilon_2\lambda^4(\beta^2 - 1)^2 \qquad \text{(A-11)}$$

with

$$\lambda_o^2 = 7.3428$$

$$\epsilon_1 = 0.2372$$

$$\epsilon_2 = 0.001150$$

The standard deviation of the empirical curve from the actual curve is 2.29%. Using Equation A-8, Equation A-11 becomes

$$\lambda^2 = \lambda_o^2 + \epsilon_1 \frac{kr_o^2}{D} N - \epsilon_2 \frac{k^2 r_o^4}{D^2} N^2 \qquad \text{(A-12)}$$

Substituting Equation A-12 into Equation A-4, we obtain the desired axial dependence of n, denoted by $\overline{n}(x)$, as shown by Equation A-13.

Publication Date: June 1, 1969 | doi: 10.1021/ba-1969-0080.ch009

$$\bar{n}(x) = n_o \exp\left\{-\left[\frac{D\lambda_o^2}{2r_o^2} + \left(\frac{1+\epsilon_1}{2}\right)kN - \frac{\epsilon_2 k^2 r_o^2}{2D} N^2\right]\frac{x}{u_o}\right\} \quad \text{(A-13)}$$

Here n_o is a constant obtained by formally averaging out the r dependence of $n(r,x)$. Using Equations 5 and 6, taking logarithms and computing $S \equiv \frac{d \ln n}{dx}$, we arrive finally at Equation 8.

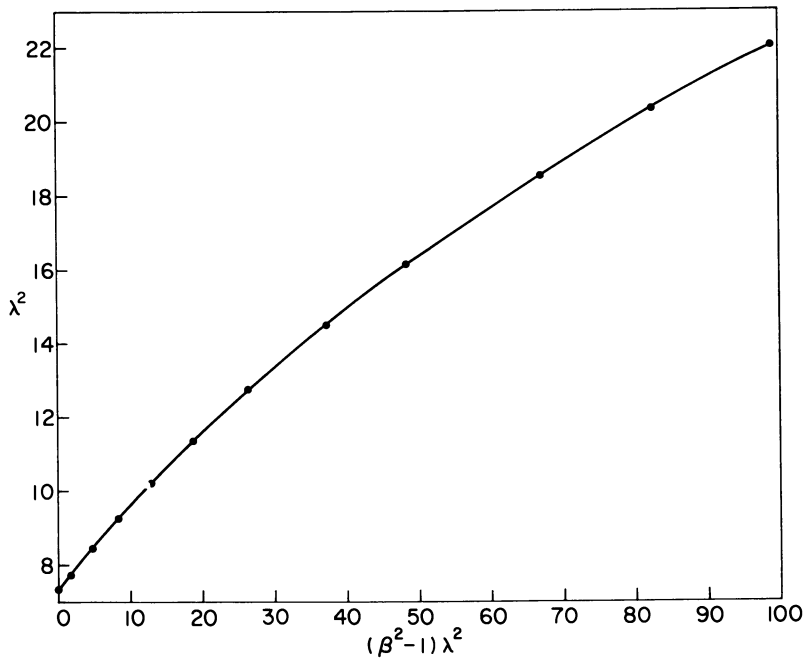

Figure 5. Plot of λ^2 *vs. the function* $(\beta^2 - 1)\lambda^2$. *See the appendix for explanation. Note that the points are not experimental points; they are calculated from the data in Table II and are shown only to aid in the plotting*

Literature Cited

(1) Andersen, J. W., Friedman, R., *Rev. Sci. Inst.* **20,** 61 (1949).
(2) Bennett, R. G., Dalby, F. W., *J. Chem. Phys.* **31,** 434 (1959).
(3) Collins, C. B., Robertson, W. W., *J. Chem. Phys.* **40,** 701 (1964).
(4) *Ibid.*, **40,** 2202 (1964).
(5) *Ibid.*, **40,** 2208 (1964).
(6) Coster, D., Brons, H. H., *Z. Physik.* **73,** 747 (1931).
(7) Fehsenfeld, F. C., Evenson, K. M., Broida, H. P., *Rev. Sci. Inst.* **36,** 294 (1965).
(8) Fehsenfeld, F. C., Schmeltekopf, A. L., Goldan, P. D., Schiff, H. I., Ferguson, E. E., *J. Chem. Phys.* **44,** 4087 (1966).
(9) Ferguson, E. E., Fehsenfeld, F. C., Goldan, P. D., Schmeltekopf, A. L., Schiff, H. I., *Planetary Space Sci.* **13,** 823 (1965).

In Chemical Reactions in Electrical Discharges; Blaustein, B.;
Advances in Chemistry; American Chemical Society: Washington, DC, 1969.

(10) Goldan, P. D., Schmeltekopf, A. L., Fehsenfeld, F. C., Ferguson, E. E., J. Chem. Phys. 44, 4095 (1966).
(11) Herzberg, G., "Spectra of Diatomic Molecules," 2nd ed., p. 204, D. Van Nostrand Co., Princeton, N. J., 1950.
(12) McDaniel, E. W., "Collision Processes in Ionized Gases," p. 503, John Wiley and Sons, Inc., New York, 1960.
(13) *Ibid.*, p. 516 (1960).
(14) Murphy, G. M., "Ordinary Differential Equations and their Solutions," p. 342, D. Van Nostrand Co., Princeton, N. J., 1960.
(15) Nusselt, W., Z. *Ing.* **54**, 1154 (1910).
(16) Schmeltekopf, A. L., Broida, H. P., *J. Chem. Phys.* **39**, 1261 (1963).
(17) Sholette, W. P., Muschlitz, E. E., *J. Chem. Phys.* **36**, 3368 (1965).

RECEIVED June 5, 1967.

Chemical Equilibrium in Electrically Excited Gases

M. MANES[1]

Mellon Institute, Pittsburgh, Pa.

Publication Date: June 1, 1969 | doi: 10.1021/ba-1969-0080.ch010

A model chemical reaction system is assumed, in which energy is separately conserved within each degree of freedom of each molecular species, each such degree of freedom therefore having in effect its own "temperature." A statistical mechanical treatment of this model shows that the composition behavior at any fixed set of "temperatures" is the same as for an equilibrium system—i.e., *the conventional expression for the equilibrium constant is retained—although the expressions for the magnitude and temperature dependence of the equilibrium constant become quite complex and no attempt is made to evaluate them. It is suggested that the model may simulate the behavior of chemical reactions in nonequilibrium steady-state electrical discharges, and therefore that such systems may resemble equilibrium systems in their responses to composition perturbations from the steady state.*

The formation of methane, water, ethane, and acetylene from mixtures of carbon monoxide and hydrogen in microwave discharges have been observed by Blaustein and Fu (*1*). Such systems obviously are not in equilibrium with respect to energy exchange with their surroundings. Moreover, the acetylene yields that were obtained are not found in normal systems at thermal equilibrium except at considerably higher temperatures than was estimated. Nevertheless, the response of these systems to composition changes—*e.g.*, removal of individual components by cold-finger condensation—is in keeping with Le Chatelier's principle applied to equilibrium systems. These systems therefore raise the ques-

[1] Present address: Kent State University, Kent, Ohio.

In Chemical Reactions in Electrical Discharges; Blaustein, B.;
Advances in Chemistry; American Chemical Society: Washington, DC, 1969.

tion of whether or not chemical equilibrium can exist (at least in the sense that the activity products for the individual chemical reactions will be approximately constant over some reasonably wide range of composition) when the system itself is at some excited steady state. One approach is to consider excited steady-state systems in which equilibrium does not exist between the individual degrees of freedom. Since such systems are outside the domain of classical thermodynamics, we consider a model system and see whether or not a relation similar to the customary expression for the equilibrium constant can be derived from statistical mechanics.

Our model system will be a multicomponent system in which: (1) a single chemical reaction can take place (generalization to multireaction systems is quite straightforward); (2) equilibrium exists within each degree of freedom (translational, rotational, vibrational, and electronic); and (3) equilibrium does not necessarily exist between different degrees of freedom. The assumptions state in effect that a "temperature" may be said to exist for each degree of freedom, but not necessarily for the system as a whole. It could be further assumed that the translational degrees of freedom are well equilibrated, in which case they would be a measure of the conventional temperature. The model could be a reasonable one for an electrically excited system. One can imagine, for example, that a hierarchy of excitation "temperature" exists at the steady state between the individual degrees of freedom, each receiving and emitting energy at equal rates. It should be emphasized that we do not yet know the extent to which our model simulates real systems. However, since it is at least a step in this direction, let us examine its consequences.

The derivation of the equilibrium constant expression for a multicomponent system will require the use of an appropriate modification of the single-molecule partition function, which we shall first derive. Consider a one-component system in which the index j specifies the energy level of the molecule. If we assume the energies of the individual degrees of freedom to be additive, then the energy ϵ_j of the j'th state is the sum of the energies $\epsilon_{j1}, \epsilon_{j2}, \ldots \epsilon_{jd}$ of the individual "substates" of the d degrees of freedom available to the molecule, where ϵ_{jk} is the contribution of the k'th degree of freedom to the j'th energy level. The index j may be considered as an abbreviation for the set $j_1, \ldots j_d$ of energy substates which have the corresponding energies $\epsilon_{j1}, \ldots, \epsilon_{jd}$; two such sets are identical only when they have every j_k (and ϵ_{jk}) in common. The statistical weight, g_j of the molecule is the product of the statistical weights g_{jk} of the individual substates within the set that makes up j. Assuming corrected Boltzmann statistics (2), the number of states, t, available to a system of N identical particles, each with d degrees of freedom, is

Publication Date: June 1, 1969 | doi: 10.1021/ba-1969-0080.ch010

In Chemical Reactions in Electrical Discharges; Blaustein, B.;
Advances in Chemistry; American Chemical Society: Washington, DC, 1969.

$$t = \prod_j \frac{g_j^{N_j}}{N_j!} = \prod_{j_k} \frac{g_{jk}^{N_j}}{N_j!} \tag{1}$$

We want the most probable distribution subject to the constraints:

$$\Sigma N_j = N \qquad (\alpha) \tag{2}$$

$$\sum_j N_{j\epsilon_{jk}} = \mathrm{E}_k;\ k = 1, \ldots, d(-\beta_1, \ldots, -\beta_d) \tag{3}$$

where the corresponding Lagrangian multipliers are in parentheses. The constraints of Equation 3 express our assumption that equilibrium is attained in energy exchange within each degree of freedom but not between degrees of freedom. The usual application of Lagrange's method of undetermined multipliers leads to the equation

$$\frac{N_j}{N} = e^{\alpha} g_j \prod_k e^{-\beta_k \epsilon_{jk}} = e^{\alpha} \prod_k g_{jk} e^{-\beta_k \epsilon_{jk}} \tag{4}$$

and summing over N_j gives

$$N = e^{\alpha} \sum_j \prod_k g_{jk} e^{-\beta_k \epsilon_{jk}} \tag{5}$$

Let us now define the single-particle partition function, q_k, for the k'th degree of freedom as

$$q_k = \sum_j g_{jk} e^{-\beta_k \epsilon_{jk}} \tag{6}$$

The assumption of additivity of energies allows us to write, for the molecule,

$$q^* = \prod_k q_k \tag{7}$$

which is analogous to the partition function of a normal molecule except that there is a separate β for each degree of freedom; the asterisk indicates lack of equilibrium between the individual degrees of freedom. (We can identify β with $1/kT$ only for those degrees of freedom that are equilibrated to the conventional temperature). Returning now to Equation 5 we see that

$$\sum_j \prod_k g_{jk} e^{-\beta_k \epsilon_{jk}} = \prod_k \sum_j g_{jk} e^{-\beta_k \epsilon_{jk}} = q^*. \tag{8}$$

The first equality follows from the fact that the summation over j indicates that the products are to be taken over all possible combinations of the available substates, and the second equality follows from Equation 6.

Before proceeding to the multicomponent case we digress to consider briefly the consequences of the nonequilibrium assumption on the distri-

Publication Date: June 1, 1969 | doi: 10.1021/ba-1969-0080.ch010

In Chemical Reactions in Electrical Discharges; Blaustein, B.;
Advances in Chemistry; American Chemical Society: Washington, DC, 1969.

bution of states. Returning to Equations 4 and 5 we find that $e^{\alpha} = N/q^*$ and that

$$\frac{N_j}{N} = \frac{\Pi g_{jk} e^{-\beta_k \epsilon_{jk}}}{q^*} \cdot \tag{9}$$

The distribution of the sublevels of each degree of freedom may be found by noting that $P(j)$ $(= N_j/N)$, the probability of finding the j'th level, is the product of the probabilities of finding each of the d sublevels—*i.e.*,

$$P(j) = P(j_1)P(j_2) \ldots P(j_d) = \prod_k \frac{g_{jk} e^{-\beta_k \epsilon_{jk}}}{q_k} \tag{10}$$

or

$$P(j_k) = \frac{g_{jk} e^{-\beta_k \epsilon_{jk}}}{q_k} \tag{11}$$

The individual substates, therefore, follow the Boltzmann distribution, each with its own value of β_k.

Consider now the case of a chemical reaction at a nonequilibrium steady state. For simplicity, we consider the reaction

$$A + xB = AB_x$$

i.e., the association of 1 atom of A with x atoms of B to form the compound AB_x (which for ease of notation we shall call C). Then, following the derivation in Davidson's text (2) (with a slight change in notation) we write

$$t = \prod_j \frac{(g_j^A)^{N_j^A}}{N_j^A!} \cdot \prod_j \frac{(g_j^B)^{N_j^B}}{N_j^B!} \cdot \prod_j \frac{(g_j^C)^{N_j^C}}{N_j^C!} \tag{12}$$

where the superscript letters refer to the individual molecular species and are not to be read as exponents. The index j again refers to individual (total) energy states; the use of a single index for all three molecular species is for simplicity of notation, it being understood that different molecular species in general have completely different sets of energetic states. We now maximize $ln\ t$ subject to the constraints

$$\Sigma N_j^A + \Sigma N_j^C = n_A \qquad (\alpha^A) \tag{13}$$

$$x\,\Sigma N_j^C + \Sigma N_j^B = n_B \qquad (\alpha^B) \quad , \tag{14}$$

where n_A and n_B are the total number of atoms of A and B in the system; this gives the Lagrangian multipliers α^A and α^B shown in parentheses. These are the same constraints as in the conventional derivation for an equilibrium systems. The energy constraints are

$$\Sigma_{j_A} N_j^A \epsilon_{jk}^A = E_k^A;\ k = 1, \ldots, d_A (-\beta_k^A) \tag{15}$$

In Chemical Reactions in Electrical Discharges; Blaustein, B.;
Advances in Chemistry; American Chemical Society: Washington, DC, 1969.

$$\sum_{j_B} N_j^B \epsilon_{jk}^B = E_k^B;\ k = 1, \ldots, d_B(-\beta_k^B) \tag{16}$$

$$\sum_{j_C} N_j^C \epsilon_{jk}^C = E_k^C;\ k = 1, \ldots, d_C(-\beta_k^C) \tag{17}$$

where E_k^A, etc., are the total energies in each degree of freedom of the corresponding molecular species (the k'th degree of freedom in A, B, and C being in general completely different), d_A is the number of degrees of freedom in A, etc., and the β_k^A, etc., are the corresponding sets of Lagrangian multipliers, one for each degree of freedom in each molecular species.

We now maximize $\ln t$ with respect to variation of each of the N_j^A, N_j^B, and N_j^C, leading to the equations

$$\frac{\partial \ln t}{\partial N_j^A} + \alpha^A - \sum_{k=1}^{d_A} \beta_k^A \epsilon_{jk}^A = 0 \tag{18}$$

$$\frac{\partial \ln t}{\partial N_j^B} + \alpha^B - \sum_{k=1}^{d_B} \beta_k^B \epsilon_{jk}^B = 0 \tag{19}$$

$$\frac{\partial \ln t}{\partial N_j^C} + \alpha^A + x\alpha^B - \sum_{k=1}^{d_C} \beta_k^C \epsilon_{jk}^C = 0 \tag{20}$$

whence

$$N_j^A = e^{\alpha^A} g_j^A \prod_k e^{-\beta_k^A \epsilon_{jk}^A} \tag{21}$$

$$= e^{\alpha^A} \prod_k g_{jk}^A e^{-\beta_k^A \epsilon_{jk}^A} \tag{22}$$

and

$$N_A = \sum N_j^A = e^{\alpha^A} q_A^*, \tag{23}$$

the last substitution being exactly the same as in Equation 8. By quite analogous reasoning we find

$$N_B = e^{\alpha^B} q_B^* \tag{24}$$

and

$$N_C = e^{\alpha^A} e^{x\alpha^B} q_C^*, \tag{25}$$

leading to the relation

$$\frac{(N_A)(N_B)^x}{N_C} = \frac{q_A^* (q_B^*)^x}{q_C^*}. \tag{26}$$

One can in quite straightforward fashion generalize the foregoing derivation to the general reaction

$$aA + bB + \ldots \rightarrow mM + nN + \ldots$$

(when A, B, etc., are quite general molecular species) to find

Publication Date: June 1, 1969 | doi: 10.1021/ba-1969-0080.ch010

$$\frac{N_M{}^m N_N{}^n \cdots}{N_A{}^a N_B{}^b \cdots} = \frac{(q_M{}^*)^m (q_N{}^*)^n \cdots}{(q_A{}^*)^a (q_B{}^*)^b \cdots} \tag{27}$$

where the energy states in all of the molecules are calculated using the energy of the separated atoms as the common zero of energy. We cannot separate out an expression of the form $e^{-\Delta E/kT}$ (a convenient operation for equilibrium systems) because we do not have a single temperature in the system. Moreover, we would expect q^* to be very difficult to evaluate. Nevertheless, Equation 24 will suit our purpose.

To the extent that the $q_A{}^*$, etc., are independent of composition, the steady-state composition at any "temperature"—*i.e.*, any fixed distribution of energy over the individual degrees of freedom—will satisfy a conventional equilibrium constant. It is, however, not necessary that the product on the right of Equation 27 be strictly constant, but only that its composition dependence should be of the same order of sensitivity as the corresponding "constant" in an equilibrium plasma. (Equilibrium compositions in an equilibrium plasma have been estimated, for example, by Zeleznik and Gordon (*3*).) This would suffice to account for the observations of Blaustein and Fu (*1*), with the added proviso that the "temperature" should not change radically with composition changes (which in some real systems could happen). It therefore seems reasonable to expect that excited systems should be found that behave as equilibrium systems to composition changes although one cannot claim such behavior for all such systems.

The crucial point appears to be that the composition dependence in Equation 27 follows, in the statistical mechanical derivation (*2*), from the constraint that the total number of each kind of atom in the system remains constant, a constraint that is not relaxed in the excited steady-state system. The normal temperature dependence of the equilibrium constant in equilibrium systems is, however, dependent on the equilibration of all of the degrees of freedom. The relaxation of this assumption in excited systems results in the loss of the classical thermodynamic temperature dependence of the equilibrium constant (with which Blaustein and Fu (*1*) were not concerned) while retaining the composition dependence.

Acknowledgments

I thank Bernard D. Blaustein and Yuan C. Fu for bringing this problem to my attention; G. C. Stey for helpful discussions; and the Pittsburgh Activated Carbon Company for partial support.

Publication Date: June 1, 1969 | doi: 10.1021/ba-1969-0080.ch010

Literature Cited

(1) Blaustein, B. D., Fu, Y. C., ADVAN. CHEM. SER. **80,** 250 (1969).
(2) Davidson, Norman, "Statistical Mechanics," p. 97, McGraw-Hill, New York, New York, 1962.
(3) Zeleznik, Frank J., Gordon, Sanford, *Can. J. Physics* 44, 1877 (1966).

RECEIVED May 12, 1967.

11

Radiation Chemistry and Electric Discharge Chemistry: Comparison and Contrast

MILTON BURTON and KOICHI FUNABASHI

Department of Chemistry and the Radiation Laboratory, University of Notre Dame, Notre Dame, Ind. 46556

Publication Date: June 1, 1969 | doi: 10.1021/ba-1969-0080.ch011

*Comparison of radiation chemistry and electric discharge chemistry necessarily involves emphasis on the roles played by thermal energy and vibrational energy. Except for noting the assumption that in a discharge tube most of the initial products of electron impact are neutral excited states —*i.e., *"high-temperature" states—no detailed characterization is presented of the type of electric discharge to which comparison is made. Elementary processes of the radiation chemistry of condensed systems are properly comparable with those of the discharge chemistry of gases, particularly with those processes involving slow electrons. In the case of methane, cited as an example, relatively efficient production of acetylene in discharge processes is attributed to production in secondary processes of vibrationally excited intermediate species such as cannot be produced in the radiation chemistry of gases.*

Studies in the chemistry of the electric discharge are confined mostly to the gaseous state; the energy deposition responsible for the effects observed is, for the main part, exclusively by relatively low-energy electrons. Radiation chemistry, on the other hand, encompasses the study of the effects of high-energy particles or radiations (including radioactive "emanations") on matter in any degree of aggregation or attenuation.

In an over-all sense the most important physical distinction between radiation chemistry and electric-discharge chemistry (hereafter called discharge chemistry) is that in the former the energetic particles—*e.g.*, electrons—are produced initially with high energy and lose that energy in interactions with the molecular system until finally the energy is reduced to a point where the particles are no longer energetically important.

In Chemical Reactions in Electrical Discharges; Blaustein, B.;
Advances in Chemistry; American Chemical Society: Washington, DC, 1969.

In discharge chemistry, by contrast, the electron is produced with small energy, gains energy from the field, loses a substantial fraction in an occasional impact and regains energy from the field in a series of energy-gain, energy-loss cycles.

Radiation chemistry and discharge chemistry have in common the feature that they are extremely complicated. Further, if one were to divide chemistry into two areas, in the first of which the individual features could conceivably be accurately measured and in the second of which only qualitative features are discernible, both would appear to belong in the first category. Nevertheless, in spite of the fact that individual features can be quantitatively studied, the synthesis of the understanding of the individual items into a complete theory is still so remote as to rouse the suspicion that, if neither belongs in the second category, it should not yet be admitted to the first.

Publication Date: June 1, 1969 | doi: 10.1021/ba-1969-0080.ch011

In both these branches of chemistry, specific processes can be isolated and measured very accurately and, indeed, it is possible to devise accurate theories regarding the facts observed. Aspects susceptible to exact quantitative and theoretical treatment can be isolated and studied by a variety of techniques including cloud-chamber experiments, molecular-beam studies, microwave and optical (including ultraviolet and infrared) spectroscopy, ion-molecule reactions (in the mass spectrometer), and photochemistry. Certainly, each of these types of study is capable of very great precision. Unfortunately, the synthesis of our knowledge of the elementary processes involved in a particular branch of reaction kinetics (even though we may know them all) into a theory of over-all effects is not simply a process of algebraic summation of the details. Complicated interactions are involved. In lieu of a knowledge of these interactions necessary to the formulation of a proper theory, we use a device which the physical scientist deplores when employed by the natural scientist—*i.e.*, we measure accurately and proceed by qualitative arguments to essentially qualitative conclusions. We compare details and note that certain features are exclusively present in one case or the other, that they do not add up in the same way, and that the effects to be expected in the two cases should be essentially different—as indeed they are, or we would not have begun the comparison in the first place.

On the other hand, if we are to understand radiation chemistry and discharge chemistry at all we must understand them in terms of elementary process, instead of in terms of over-all effects which can be so readily observed. We establish the reality of such elementary processes for the most part on an essentially intuitive basis. We are of the opinion that we know that certain elementary processes occur in radiation chemistry or in discharge chemistry because of observations made, for example, in cloud-chamber experiments or in mass spectroscopy. We conclude

In Chemical Reactions in Electrical Discharges; Blaustein, B.;
Advances in Chemistry; American Chemical Society: Washington, DC, 1969.

that many of the processes which occur in radiation chemistry are common to discharge chemistry. If there is a major point in this presentation, it is that for purposes of comparison of radiation chemistry and discharge chemistry we are forced into comparison of details. However, we cannot synthesize the totality of effects from the components because not only do the components have their own individual features, if studied separately by more sophisticated methods of physical science, but also these components interact in ways which have not been thoroughly examined and for which a theory is yet lacking. What we do (and this may be common to more than one branch of science) is to seek more components in what may be a vain hope that if we break down the totality of effects into a sufficient number of small components, each of which is understood, we ultimately can arrive at a situation where all that would be required would be to add together the totality of components.

Suppose we could assume both radiation chemistry and discharge chemistry to be sufficiently developed so that we could examine the components in this kind of detail. The next step would be to make the contrasts suggested in the title of this article. We would select components which in our opinion contribute the major characteristic of the particular branch. We would compare them with each other. We would compare the specifically important and contrasting ways in which they interact in the two cases. Such procedure would appear to be very logical indeed.

Unfortunately, the simple fact is that in radiation chemistry, which has now been elaborately studied by a larger and larger group of very competent scientists for the last 20 years or so, the details are not thoroughly understood. There is even a question whether any of them are well understood although there is no question that there is very much study of these individual effects and that new ones are being found. It is the very complexity of the number of phenomena in radiation chemistry which makes it difficult to develop a theory which is adequate for purposes of comparison with the chemistry of the electric discharge.

The chemistry of the electric discharge is confined essentially to the chemistry of the gaseous state. If we were to compare only gaseous-state radiation chemistry with discharge chemistry, we would neglect some of the most significant special aspects and applications and potential applications of radiation chemistry. Further, we must consider the radiation chemistry of condensed systems if we are to understand similarities to the chemistry of the electric discharge. In the latter, we are concerned almost exclusively with the effects of low-energy electrons—*i.e.*, with energies less than the ionization potential of the gas traversed. In radiation chemistry of non-polar liquids the ions initially produced may be neutralized before any significant amount of chemical change occurs.

Publication Date: June 1, 1969 | doi: 10.1021/ba-1969-0080.ch011

In Chemical Reactions in Electrical Discharges; Blaustein, B.;
Advances in Chemistry; American Chemical Society: Washington, DC, 1969.

Of course, there are important exceptions particularly when chain processes can occur. Thus, in *cis-trans* isomerization processes, even though the number of charges separated is very small, the chain length involved may be so long that the few ions initially separated play the dominant role; *cf.* Ref. *10.* Neutral excited species produced in that way as well as those produced in an initial excitation act may be presumed to behave much as do any electronically excited species produced in electric discharge processes in gases. On the other hand, in the radiation chemistry of gases, because of great charge separation, the charged species initially produced have an opportunity to react as such before the neutralization process; such processes make an unimportant contribution to discharge chemistry.

Finally, another obvious point, nevertheless worthy of emphasis, is that there are a variety of electric discharges and a variety of regions in each such discharge. Each has its peculiar characteristics. In this paper we consider the consequences of their single common feature: electrons are moving through them under the influence of an external field.

Publication Date: June 1, 1969 | doi: 10.1021/ba-1969-0080.ch011

Elementary Processes

With apology for an attempt at comparison and contrast clearly stated, and with the implicit reservations indicated, it is appropriate to consider the major differences between radiation chemistry (*5*) and discharge chemistry.

The over-all results in radiation chemistry can be expected to differ from those in discharge chemistry because of two essentially different groups of facts, namely those associated with the initial physical aspects and those associated with what, for convenience, we hereinafter call chemical physics, namely those processes in the exposed material which involve the actual production and distribution of different excited states. The classes of effects are summarized in Tables I and II.

As Table I indicates, there is a far wider range of energy source in radiation chemistry than there is in discharge chemistry. In the latter, high-voltage gaps are the principal source of energy while in radiation chemistry there is an important array of different types of sources, some of which are steady in action, some of which are pulsed, some of which involve very light particles such as electrons, and others of which involve very heavy ions such as those characteristic of fission recoils. Each has its own characteristic effects and should be examined in detail. We do not, for the purposes of this article, consider effects of fission recoils, which are certainly somewhat special. Instead, we limit our considerations to the effects of fast electrons, either initially produced as in a high voltage machine or secondarily by the interaction of x or gamma rays

In Chemical Reactions in Electrical Discharges; Blaustein, B.;
Advances in Chemistry; American Chemical Society: Washington, DC, 1969.

with the matter traversed. As for alpha particles or heavy ions such as may be produced in a cyclotron, there can in that case be an effect related to "linear energy transfer," which is important in condensed systems but is not significant in cases such as are discussed in this article, where for purposes of comparison with the effects of the electric discharge we must limit ourselves to gases. (Linear energy transfer, abbreviated as LET by radiation chemists, is the differential deposition of energy per unit distance traversed by the energetic particle—*i.e.*, dE/dx.) Even in the case of such heavy ions, most of the effects are produced by high-voltage secondary electrons and those effects produced by the ions themselves in dispersed media are not significantly different from the effects of electrons. However, one point must be emphasized. Most of the actual work in radiation chemistry is done at temperatures which are not significantly higher than room temperature. In recent years an increasing amount of work has been done at temperatures considerably below room temperature. Relatively little work has been done at temperatures far in excess of room temperatures primarily because the results cannot be easily disengaged from the effects of radiation itself. In the case of discharge chemistry the facts are essentially different. High temperature is a natural complement of electric discharge and the effort in this case is to understand the effect of the electric discharge as something different from, and additional to, the effect of temperature. This important point must be carefully considered in any attempt at understanding of the effects observed.

Publication Date: June 1, 1969 | doi: 10.1021/ba-1969-0080.ch011

Table I. Initial Physical Aspects

	Radiation Chemistry	*Discharge Chemistry*
Sources of energy	Natural radioactivity High-energy machines Nuclear reactors Artificial radioactivity	High-voltage gaps
Initial energetic species	α, β, γ, x rays; electrons, atomic nuclei, fast neutrons, heavy ions	Electrons
Major effective energetic species (primaries)	Electrons	Electrons
Energy per "primary"	$>$ 500 Kev. initially	$<$ 15 e.v.
Energy distribution of "primaries"	$<$ 2 Mev. *see* Figure 1	$<$ 15 e.v. *see* Figure 2
Electrons per primary electron	$\sim 10^4$	~ 1

In general in radiation chemistry, the energy of any important primary particle (which we henceforth consider to be an electron) is greater than $\sim$ 500 Kev. and in discharge chemistry $<$ 15 e.v. The former value

In Chemical Reactions in Electrical Discharges; Blaustein, B.;
Advances in Chemistry; American Chemical Society: Washington, DC, 1969.

Table II. Chemical Physics

	Radiation Chemistry	*Discharge Chemistry*
Ratio: Initial ionization processes to initial excitation processes	~ 0.5	→ 0
Ratio: Permitted processes to forbidden processes	Order of 1:1	~ 0:1
Charge separation	Depends on state	High
Track effects	Existent in condensed systems	Non-existent
Local temperature	No significant effect	May have dominant effect
Time scale of events	Dominant role	Note role of "forbidden states"
Secondary events involving "primaries"	Produce ions and excited species	Mainly production of vibrationally and electronically excited species

Publication Date: June 1, 1969 | doi: 10.1021/ba-1969-0080.ch011

is qualitative. It can vary considerably. The important point to note is that it is in a very high energy range. By contrast, in discharge chemistry it is unlikely that there are many electrons present with energy greater than the ionization potential of the medium traversed. Further, the numbers of particles of various energies follow quite different distribution laws in the two cases. In radiation chemistry the particles of high energy produce electrons of low energy which in turn produce electrons of lower energy and the result is that there is a minimum number of particles present of high energy and a very large number of charged particles present at low energy. The representative curve shown in Figure 1 is deliberately cut off without an attempt to go exhaustively into the very low-energy range—*i.e.*, below ionization potential—because many factors, such as the peculiar excitation levels of the medium traversed, will determine that distribution. By contrast, in discharge chemistry, as shown in Figure 2, the maximum in the number of electrons is at an intermediate energy below the ionization potential. Figure 2 is not intended to be theoretically precise. The approximate form given is correct but to what degree this form may be skewed as a result of interaction of the electrons with the molecular system is a matter which is not the proper subject of this article. There are many subtleties connected with the shape of the curve in Figure 1; the important point is that this shape is related to the fact that something of the order of 10^4 electrons is produced per primary electron involved in the case of radiation chemistry and that all these production processes are chemically important. On the other hand, although secondary generation of electrons is of central importance in

In Chemical Reactions in Electrical Discharges; Blaustein, B.;
Advances in Chemistry; American Chemical Society: Washington, DC, 1969.

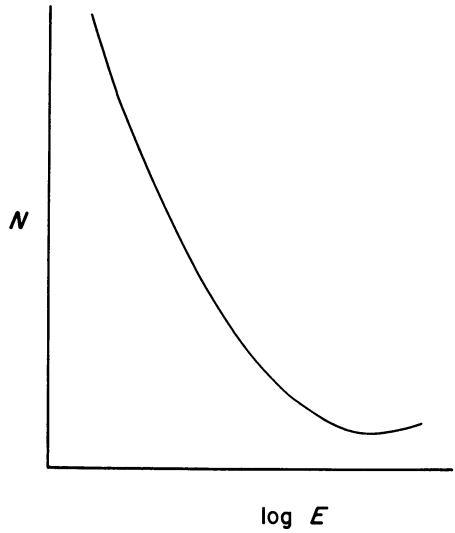

Figure 1. Steady-state electron energy distribution function for a system under high-energy irradiation (schematic). Mono-energetic 1 Mev. electrons are considered to be generated uniformly in space and constantly in time. N *represents the flux of electrons traversing a small spherical probe per unit cross-sectional area of the probe, per unit time per unit energy range of the spectrum.* E *is the energy of the electrons. (*Cf. *Ref. 28 for high-energy cases)*

the maintenance of an electric discharge, it makes an insignificant contribution to the totality of phenomena involved in the chemistry itself.

In radiation chemistry the direction of energy flow as far as the individual electron is concerned is always downhill. It loses energy; it never gains a significant amount of energy from the medium. In all cases where the electron energy is reduced below kT in an excitation or ionization process it does pick up energy from the medium by collision. This fact has important consequences for the theory of electron diffusion. In discharge chemistry, every time an electron gives up energy to the medium in the form of excitation it is free to accept more energy from the field and does so continuously (irrespective of the occurrence of minor losses to the molecules of the medium traversed) until it reaches an energy adequate to produce excitation of some species with which it interacts. Thereupon, its energy is reduced effectively to zero and commences once again to acquire energy from the field. The ways in which this energy is transferred from the field to the electron to the molecules

Publication Date: June 1, 1969 | doi: 10.1021/ba-1969-0080.ch011

with which collisions occur is the substance of the physical theory of discharge chemistry. The way in which the molecule is excited and comes ultimately to react is the substance of the theory of the chemistry of the electric discharge.

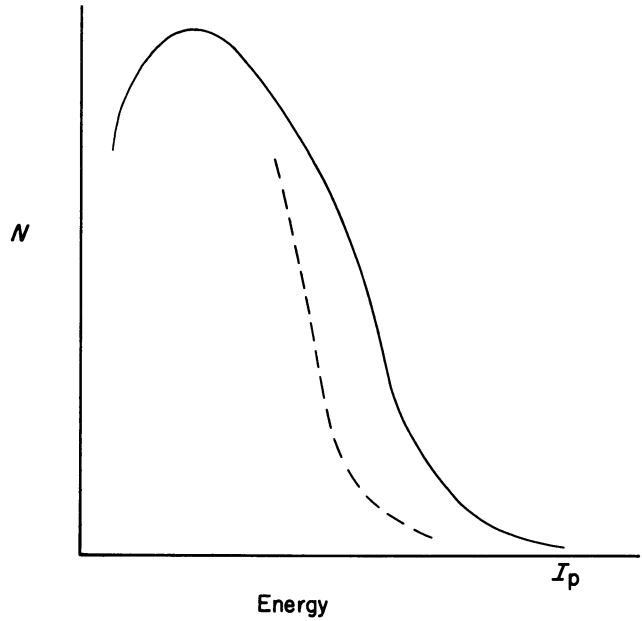

Figure 2. Schematic electron energy distribution function for a discharge tube (based on interpretation of theoretical calculations for H_2 gas (1)). The dashed line indicates the further possibility that the distribution function may be skewed in the direction of lower energy as the result of vibrational excitation processes

In radiation chemistry of condensed systems there is some question as to the mechanism of the processes by which energy is deposited. Even if one can consider the initial deposition of energy to be in a specific molecule, the energy deposited is in general so great that it can overlie a number of molecules and be held to be non-localized in the first step worthy of consideration. It is only thereafter that the energy becomes localized in a single molecule. However, in a dispersed system the molecules are spatially far from each other so that whatever energy is deposited in the molecule involves only that molecule in an initial act. The way that the radiation chemistry of gases differs from the discharge chemistry of gases is simply in the amount of energy which can be initially deposited in molecules. In radiation chemistry, the amount of energy which can be deposited in a molecule can far exceed its lowest ionization

potential. In discharge chemistry, on the contrary, the energy deposited in the molecule is generally lower than that required to produce ionization and, according to very reasonable theory, can be in general lower than that required to produce excitation even to the lowest single state (*17*). An important point to mention in this connection is that the theory of radiation chemistry definitely includes the idea of super-excited states of molecules (*20*), namely those which are initially excited to energies exceeding the ionization potential and which remain excited nevertheless. They auto-ionize, yielding parent ions and electrons, or dissociate into ion fragments, radicals and electrons or may even dissociate into radicals or excited molecules in a primary act. In discharge chemistry, on the contrary, super-excited states are hardly to be considered. Quite the contrary, discharge chemistry is almost exclusively confined to species in their lowest electronically excited states but by no means to those devoid of additional vibrational and rotational energy.

Publication Date: June 1, 1969 | doi: 10.1021/ba-1969-0080.ch011

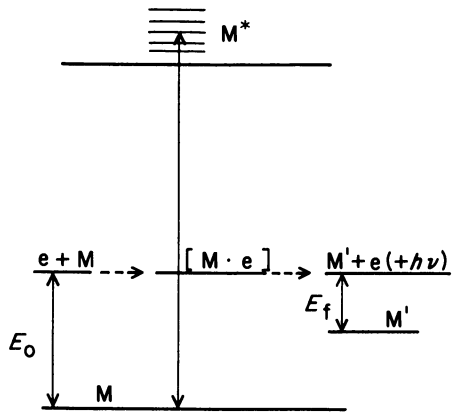

Figure 3. Schematic diagram indicating mechanism of vibrational excitation in electron encounter. An electron possessing energy E_0 *inadequate to cause an electronic excitation of the molecule M interacts with M, at that lower energy, to form an intermediate* [M · e], *a "virtual negative ion," of fairly long duration which dissociates to yield a vibrationally excited intermediate M' and an electron. The possibility of some light emission* ($h\nu$) *is indicated. At the end of the process, the electron possesses energy* $E_f - h\nu$ *and the vibrational energy of M' is* $E_0 - E_f$

The relative roles of initial ionization and initial excitation are shown in Table II. In radiation chemistry, the amount of initial ionization is

about the same as that of initial excitation with the latter possibly greater than the former by a factor of about 2. In discharge chemistry, on the other hand, the contribution of ionization to the totality of chemical phenomena is so small that by comparison with initial excitation processes it may be considered practically negligible.

Perhaps one quarter of the phenomena produced by the energetic electrons in radiation chemistry can be considered to be those produced by relatively high-energy electrons—*i.e.*, about 75 e.v. or more. In their interaction with molecules of the systems traversed, these electrons do not behave essentially differently from photons except that they are more random in their effects. In general, the transitions which occur are the optically allowed ones. However, as the energy decreases, the probability of optically forbidden transitions increases. Further, when the electrons are travelling at sufficiently low velocity, they can be involved in intermediate long-time interactions with the molecules (*3, 6, 7, 11, 27, 29*). Consequently, it must not be presumed that the transitions excited necessarily obey Franck-Condon restrictions—*i.e.*, the excitation can occur from a ground state to a state the geometric configuration of which does not correspond to that of the ground state (the excitation is non-vertical). The energy required for such a process may be much less than that required for a vertical transition whether it be optically permitted or not. In discharge chemistry, practically all the excitations have this character; the states preferentially excited are "forbidden states" of configuration not corresponding to the ground state. In addition, from a rather elementary but correct point of view it can be expected that an intermediate, short-lived, charged species produced in a process of electron impact in discharge chemistry dissociates into an electron and a vibrationally excited molecule with "temperature" far in excess of the ambient. Previously, the cross section for rotational-vibrational excitation in electron impact has been considered to be low because of great mass differences between the electron and the molecule involved. The new view (*3, 6, 7, 11, 27, 29*) of the long-time interaction of the electron and the molecule eliminates the necessity for consideration of processes in which the only interaction which can occur is by momentum transfer. The precise processes involved are still not thoroughly developed but one clear point is that in certain cases resonance can be involved and that electrons of certain specific energies have a higher probability of transferring energy in this way than do others. (As an example, in the case of the nitrogen molecule the probability for excitation of vibration attains a series of maxima for electrons centering $\sim$ 2.3 e.v. energy; *cf.* Reference 27.) In general, although the resonance processes are favored and are most dramatic, such excitation of vibrational states as a result of formation of a "virtual negative ion" always occurs in amount sufficient to

Publication Date: June 1, 1969 | doi: 10.1021/ba-1969-0080.ch011

In Chemical Reactions in Electrical Discharges; Blaustein, B.;
Advances in Chemistry; American Chemical Society: Washington, DC, 1969.

cause significant temperature rise of the gas in the electric discharge; processes of a non-resonant nature may be equally important. Although similar processes occur as terminal events in radiation chemistry, they play a relatively unimportant role.

An effect opposite to those of non-vertical transitions is the Ramsauer effect (*21*). When a molecule, such as methane, has essentially rare gas configuration, it may be transparent to low-energy electrons (*2*). Thus, the probability is that the electrons in certain velocity ranges either travel a great distance without interaction with molecules—*e.g.*, low-energy electrons in radiation chemistry—or are raised to energies significantly higher than these "window energies" very rapidly by an electric field, as in discharge chemistry. In such case, it is not necessarily true that excitation of the lowest energy states is favored. It may be that higher excitations can occur with increased probability in cases where the Ramsauer effect is to be expected. However, it would not be expected that any significant fraction of electrons of energy approaching the ionization potential would be thereby produced. In the discharge chemistry of methane, the effect prior to setting up of the steady state is unimportant. Some transient present is readily ionized and thereafter electrons are produced until the steady state is attained. The steady state involves the existence of a variety of species of excited molecules and of various intermediates as well as the small number of ions required to maintain the discharge. Intermediate free-radical species themselves can be preferentially acted upon by an electron and the probability of that interaction is large (*16*). This fact, not elsewhere discussed, cannot be ignored nor can the fact be ignored that such interaction with the intermediates can result in optically forbidden transitions (*17*). Thus, in a qualitative way one can expect that in the discharge chemistry of any species (and particularly in the case of those which show a Ramsauer effect), there will be present highly excited free radicals in vibrational states which cannot be produced in important number in ordinary optical processes.

There are certain effects present in the radiation chemistry of condensed systems which might well be mentioned even though they are not to be expected in gases. For example, in glasses at low temperature and in liquids which contain suitable acceptors the process of ionization may lead to a significant amount of long-time charge separation (*9*). Even when no generally recognized acceptor is around, there may be prolonged charge separation as a result of charge trapping (*4, 8*). It simplifies the considerations of this article that factors like this do not have to be considered in the radiation chemistry of gases. Strangely enough, however, such factors must be considered in the discharge chemistry of gases because electrons and ions involved may be pulled signifi-

Publication Date: June 1, 1969 | doi: 10.1021/ba-1969-0080.ch011

In Chemical Reactions in Electrical Discharges; Blaustein, B.;
Advances in Chemistry; American Chemical Society: Washington, DC, 1969.

cantly far apart by the field. Were it not so, electric discharge chemistry would not exist. On the other hand, a track effect, while important in the radiation chemistry of condensed systems, is non-existent in attenuated gases (although it is doubtless to be expected in gases at sufficiently high pressure (*22*)). Neither do track effects exist in discharge chemistry at all, so that, in this one respect, the radiation chemistry of gases and the discharge chemistry of gases are similar.

The idea that at certain particular resonance energies electrons can transfer a significant amount of energy into vibrational excitation is discussed in previous paragraphs. However, these energies are usually very low. Most of the energy transferred in radiation chemistry is transferred from electrons of higher energy. The consequence is that in radiation chemistry a relatively small fraction of the energy is transformed into heat. In discharge chemistry, practically all the electrons effective in energizing molecules of radical intermediates are at low energy and some of them surely are at resonance energies (*26*) for the specific species involved. Thus, unlike the case in radiation chemistry, one can expect that high temperatures can ensue and, even if the average temperature is not high, the intermediates of interest are always at "high temperature" —*e.g.*, 10,000° to 45,000°K.—and act like very high temperature bodies indeed; *cf.* the case of methane discussed in the next section.

In radiation chemistry the molecules primarily excited or ionized pass through an array of states before they enter into the final chemically important step. The time elapsed can be of the order of a microsecond although shorter and longer times are by no means excluded. These times become of considerable importance in the case of condensed systems. In discharge chemistry, the time scale of events plays no significant role except that it should be noted that, because most of the species are excited to optically forbidden levels, they do survive long enough without losing energy (by luminescence) so that they can enter into chemically significant interactions. In this respect, the time scale is very important. Discharge chemistry can be expected on this basis to be energetically more efficient because the energy put into a molecule is very unlikely to be squandered in light emission.

Finally, there is one additional respect in which the chemical physics of radiation chemistry differs from that of discharge chemistry. The probability, in radiation chemistry, that a molecule may suffer a second interaction or that a product from a molecule which has been decomposed may itself be acted upon by an exciting species is extremly small—except in cases where the radiation is so intense that it is hardly of present theoretical or experimental interest. In discharge chemistry, the probability of such processes is very high indeed. Thus, the effect of successive excitations must be considered and it must also be considered possible

Publication Date: June 1, 1969 | doi: 10.1021/ba-1969-0080.ch011

In Chemical Reactions in Electrical Discharges; Blaustein, B.;
Advances in Chemistry; American Chemical Society: Washington, DC, 1969.

that a species can be excited by a ladder of forbidden events to an energy level at which a process of interest can occur (*17*).

A "Simple" Case: Methane

The case of methane affords an unequivocal example of the contrasting chemical effects of high-energy radiation and of the electric discharge.

In the study of the effects of high-energy radiation on pure methane at atmospheric pressure a variety of radiations (such as 10 Mev. protons, ^{60}Co gammas and 4 Mev. electrons) have been used. Product yields—*i.e.*, in *G*, the 100 e.v. yield—are generally low. However, even though there may be some disagreement as to whether C_2H_2 is produced at all (*15*), it is clear that $G(C_2H_2)$ is not high and does not significantly exceed 0.02 (*12*). In explanation of the yields of other products there is a number of discussions in the literature which emphasize the role of ions and of charge and proton transfer on the one hand and of excitation on the other; there is also some opinion that both may be involved. In general, *G* values of whatever products are reported—*e.g.*, ethane, propane, and ethylene—run around 2 or less.

The situation in regard to the effect of the electric discharge is quite different. Although ethane and ethylene are well known among the products at low pressure, the yield of acetylene becomes dominant as the pressure is raised to atmospheric. Wiener and Burton (*30*) reported maximum $G(C_2H_2) \sim 2.4$ for experiments in which gas at about atmospheric pressure is passed through a d.c. discharge. Earlier Schoch (*25*) had reported $G(C_2H_2) \sim 24$ for data extrapolated to infinitesimal conversion. This high value is to be compared with the theoretical limit of 51.2 set by thermochemistry (*30*). The precise values are unimportant to this discussion—but they are extraordinarily high when compared with the values characteristic of radiation chemistry and the products are certainly different. Whether the effect is to be attributed to successive forbidden excitations and consequent reactions of intermediate free radicals (*18*), to an ionic chain process such as reported by Hentz, Shima, and Burton (*10*) or to some special temperature effect producible in a discharge (*19*) is an interesting question. Experiments by Il'in and Eremin (*13, 14*) clearly show that preheating to an adequate temperature —*e.g.*, 700°C.—increases the yield of C_2H_2 per unit energy input in an electric discharge. Schmellenmeier and his colleagues (*23, 24*) found that in low-pressure (20–30 mm.) discharges in methane, acetylene yield is increased as the result of accompanying lowering of temperature to 1500°K. (compared with 5000°K. at normal pressure) and thus minimizing decomposition of C_2H_2. Maximum yield of C_2H_2 could be made to correspond almost to complete conversion (*24*). One interpretation of such

Publication Date: June 1, 1969 | doi: 10.1021/ba-1969-0080.ch011

In Chemical Reactions in Electrical Discharges; Blaustein, B.;
Advances in Chemistry; American Chemical Society: Washington, DC, 1969.

results is that heat (from the discharge) does contribute to the production of states which can lead in thermoneutral processes or even exothermally to production of acetylene. The latter, however, must be permitted to escape the discharge before it, itself, is caused to decompose. The way in which this heat is employed is itself a most interesting problem. It may be to provide a variety of lower states (of parent methane or of free radicals) which can yield low-lying electronically excited states (in optically forbidden processes), it may be to provide energy of activation for processes involving free radicals (alone or in interaction with molecules), it may be to favor a chain reaction or it may be ascribed to a more subtle process—*e.g.*, purely vibrational excitation—particularly characteristic of electric discharge.

The theoretical indication of the importance of the processes of vibrational excitation in discharge chemistry is so impressive that there is an accompanying tendency to ascribe all the chemistry observed to such temperature effects rather than to processes of electronic excitation, which seem to be energetically so much less efficient (as in radiation chemistry). However, electronic excitation is a reality in discharge processes for, without it, production of charged species (in compensation for neutralization processes) necessary for maintenance of the discharge would be non-existent. The problem which is central in discharge chemistry is the question of the relative degrees of contribution of the two types of excitation. Certainly, one interesting hypothesis to explain the strange efficiency of discharge chemistry in production of acetylene from methane is that it is all attributable to the extraordinarily efficient use of thermal energy, as in a reaction sequence like

$$CH_4 \xrightarrow{e\text{-w}\rightarrow} \begin{cases} CH_3 + H \\ CH_2 + H_2 \end{cases}$$

$$H + CH_4 \rightarrow CH_3 + H_2$$

$$CH_3 \xrightarrow{e\text{-w}\rightarrow} CH_3'$$

$$CH_2 \xrightarrow{e\text{-w}\rightarrow} CH_2'$$

$$CH_3' + CH_4 \rightarrow CH_2 + CH_3 + H_2$$

$$CH_2' + CH_4 \rightarrow C_2H_2 + 2H_2$$

where the symbol $\xrightarrow{e\text{-w}\rightarrow}$ in this case indicates excitation by an electron of appropriate energy and the prime sign indicates a species vibrationally excited to temperature levels far exceeding the ambient and thus able to enter into processes neither envisaged nor expected in ordinary thermal kinetics. Whether or not these specific steps are correct, ideas like this

Publication Date: June 1, 1969 | doi: 10.1021/ba-1969-0080.ch011

In Chemical Reactions in Electrical Discharges; Blaustein, B.;
Advances in Chemistry; American Chemical Society: Washington, DC, 1969.

appear reasonable. Experimental evidence on the basis of which they can be accepted or rejected does not yet appear to be developed. However, the importance of this possible, and very different, type of reaction in chemical dynamics merits detailed experimental and theoretical study.

Conclusion

Radiation chemistry and electric discharge chemistry share one grand aspect. They are "brute-force" methods of studying the effects of energy input in chemical reactions. In both, energy is introduced in a variety of ways by species of a wide range of energy—although the two ranges of energy involved are considerably different.

If a real synthesis of the elementary processes involved into an understanding of these two branches of kinetics is at all possible, it is first necessary to know in greater detail what is being synthesized.

In both radiation chemistry and discharge chemistry we are concerned with the effects of electrons of a great variety of energies. More must be known in detail about the precise behavior of the mono-energetic electrons; this knowledge must be both theoretical and experimental. In this case we can guess that the experiments may be even more difficult than the theory. Certainly, the problem of studying the effects of mono-energetic high-energy electrons will prove to be difficult. Fortunately, in that case we are less concerned with problems of scattering than we are in the experiments with low-energy electrons. In that area beginnings have already been made. Detailed investigations, yet to be undertaken, on a great variety of compounds may yield some type of speculative understanding.

Finally, repeated attention has been addressed to the curious way temperature is introduced into discharge chemistry particularly. The theory on the basis of which the special chemical effects of the electrical discharge are to be explained may derive from these peculiar temperature effects. In this respect, the pioneering investigations by Il'in and Eremin (*13*, *14*) on the effects of temperature in the discharge chemistry of methane are particularly important. Unfortunately, information of this type can be interpreted in a great variety of ways and the detailed implications of their results must be more elaborately studied, particularly experimentally. In the same direction it is required to do temperature studies in radiation chemistry. A problem crying for investigation is the effect of temperature on the radiation chemistry of some simple compound such as methane. Perhaps, if such a "brute-force" set of investigations were attempted, it might turn out that radiation chemistry and discharge chemistry are not so greatly apart—although neither of them would be satisfactorily explained or understood in detail. At the moment

Publication Date: June 1, 1969 | doi: 10.1021/ba-1969-0080.ch011

the aesthetically most attractive hypothesis seems to involve the special role of the very highly excited vibrational states which seem peculiar to the possibilities of the electric discharge.

This is a particularly good place to emphasize a point implied by the Introduction. Although the special importance of vibrationally highly excited species in discharge chemistry may be easily invoked, we must at the same time not neglect the totality of phenomena in which they may be involved and affected by all the conditions and by all the intermediate species peculiar to the electric discharge.

Literature Cited

(1) Baraff, G. A., Buchsbaum, S. J., *Phys. Rev.* **130**, 1007 (1962).
(2) Bullard, E. C., Massey, H. S. W., *Proc. Roy. Soc.* **A133**, 637 (1931).
(3) Burke, P. G., *Advan. Phys.* **14**, 521 (1965).
(4) Burton, M., Dillon, M., Rein, R., *J. Chem. Phys.* **41**, 2228 (1964).
(5) Burton, M., Funabashi, K., Hentz, R. R., Ludwig, P. K., Magee, J. L., Mozumder, A., "Storage and Transfer of Energy by Molecules," Vol. I, G. M. Burnett and A. M. North, Eds., John Wiley and Sons, London, 1969.
(6) Chen, J. C. Y., Magee, J. L., *J. Chem. Phys.* **36**, 1407 (1962).
(7) Craggs, J. D., Massey, H. S. W., *Handbuch d. Physik* **37**, 314 (1959).
(8) Funabashi, K., Herley, P. J., Burton, M., *J. Chem. Phys.* **43**, 3939 (1965).
(9) Gallivan, J. B., Hamill, W. H., *J. Chem. Phys.* 44, 1279 (1966).
(10) Hentz, R. R., Shima, K., Burton, M. *J. Phys. Chem.* **71**, 461 (1967).
(11) Herzenberg, A., Mandl, F., *Proc. Roy. Soc. (London)* **A270**, 48 (1962).
(12) Hummel, R. W., *J. Phys. Chem.* **70**, 2685 (1966).
(13) Il'in, D. T., Eremin, E. N., *Zh. Prikl. Khim.* **35**, 2064 (1962).
(14) *Ibid.*, **35**, 2496 (1962).
(15) Johnsen, R. H., *J. Phys. Chem.* **69**, 3218 (1965).
(16) Kuppermann, A., Burton, M., *Radiation Research* **10**, 636 (1959).
(17) Magee, J. L., Burton, M., *J. Chem. Phys.* **23**, 2194 (1955).
(18) *Ibid.*, **23**, 2195(1955).
(19) Peters, K., Wagner, O. H., *Z. physik. Chem.* **A153**, 161 (1931).
(20) Platzman, R. L., *Radiation Research* **17**, 419 (1962).
(21) Ramsauer, P., *Ann. Physik Leipzig* **64**, 513 (1921).
(22) Samuel, A., *J. Phys. Chem.* **66**, 242 (1962).
(23) Schmellenmeier, H., Roth, L., Schirrwitz, H., Wolff, J., *Chem. Tech. (Berlin)* **16 (1)**, 33 (1964).
(24) *Ibid.*, **15 (10)**, 580 (1963).
(25) Schoch, E. P., *et al.*, "Acetylene from Hydrocarbons," University of Texas Publication, No. 5011, June 1, 1950.
(26) Schulz, G. J., *Phys. Rev.* **135**, A988 (1964).
(27) *Ibid.*, **136**, A650 (1964).
(28) Spencer, L. V., Fano, U., *Phys. Rev.* **93**, 1172 (1954).
(29) Taylor, H. S., Nazaroff, G. V., Golebiewski, A., *J. Chem. Phys.* **45**, 2872 (1966).
(30) Wiener, H., Burton, M., *J. Am. Chem. Soc.* **75**, 5815 (1953).

RECEIVED May 12, 1967. The Radiation Laboratory is operated by the University of Notre Dame under contract with the Atomic Energy Commission. This is AEC document No. COO-38-511.

12

Inorganic Synthesis with Electric Discharges

WILLIAM L. JOLLY

University of California and the Inorganic Materials Research Division, Lawrence Radiation Laboratory, Berkeley, Calif.

Publication Date: June 1, 1969 | doi: 10.1021/ba-1969-0080.ch012

Electric discharge reactions which yield thermodynamically unstable products are of interest to synthetic chemists, because such products are often difficult to prepare by other methods. Many fascinating compounds of unusual structure have been isolated from discharge reactions. Although such syntheses usually have low efficiencies, they are nevertheless of interest to chemists who hope to discover new types of compounds. In this review, some of the available data are systematized, and likely directions for future research are indicated.

Electric discharge reactions often yield thermodynamically unstable products, of unusual structure, that are difficult to prepare by other methods (*28, 30*). Such reactions are of great interest to chemists who hope to discover new types of compounds. Nevertheless, electric discharges are not yet a favorite laboratory technique among synthetic chemists. There are three reasons for this unpopularity of electric discharges. (a) In contrast to conventional synthetic equipment (flasks, heaters, stirrers, etc.), electric discharge apparatus is fairly complicated and time-consuming in use. (b) Apparatus large enough to give decent yields of product is fairly expensive. (c) The art of predicting the course of discharge reactions is primitive and unreliable. It is to be hoped that the first two problems can be solved by electrical engineers and apparatus manufacturers. The third problem must be solved by physical and synthetic chemists. In this review, we shall try to systematize briefly the available knowledge and to point out likely directions for future research.

Conversion of Simple Molecules into Higher Homologs

The simplest hydrides and halides of boron, silicon, germanium, phosphorus, and arsenic can be decomposed in electric discharges to form

In Chemical Reactions in Electrical Discharges; Blaustein, B.;
Advances in Chemistry; American Chemical Society: Washington, DC, 1969.

mixtures of the corresponding higher molecular weight compounds. The energetics and experimental technique for the hydride reactions are quite different from those for the halide reactions, and we shall discuss these two classes of reactions separately.

Hydrides. The decomposition of a simple hydride into hydrogen and a higher hydride is an exothermic process; therefore, when the reaction products leave the discharge zone there is no tendency for back-reaction to the starting material. Of course, inasmuch as reactions of molecular hydrogen are generally quite slow at ordinary temperatures, it is unlikely that any appreciable back-reaction would occur even if the decomposition were endothermic. The absence of back-reaction simplifies the experimental procedure, because there is no need to rapidly quench the reaction products and no need to remove the hydrogen from the vapors leaving the discharge.

The usual procedure in preparations of polysilanes and polygermanes is to circulate the simple hydride through an ozonizer-type discharge until practically all of it has decomposed and the gas being circulated is principally hydrogen. The product hydrides are trapped out in a suitable cold trap in the gas circuit. If the desired product vapors were allowed to circulate continually through the discharge, the product would

Publication Date: June 1, 1969 | doi: 10.1021/ba-1969-0080.ch012

Table I. Electric Discharge Syntheses of Volatile Hydrides

Starting Material	*Electric Discharge*	*Products Isolated*	*References*
SiH_4	Ozonizer	Si_2H_6, Si_3H_8, Si_4H_{10},[a] Si_5H_{12},[a] Si_6H_{14},[a] Si_7H_{16},[a] Si_8H_{18}	*15, 53*
GeH_4	Ozonizer	Ge_2H_6, Ge_3H_8, Ge_4H_{10},[a] Ge_5H_{12},[a] Ge_6H_{14},[a] Ge_7H_{16},[a] Ge_8H_{18}, Ge_9H_{20}	*7, 8, 15, 16*
AsH_3	Ozonizer	As_2H_4	
B_2H_6	Ozonizer; Glow discharge between Cu electrodes	B_4H_{10}, B_5H_9, B_5H_{11}, B_6H_{10}, B_9H_{15}	*14, 34*
B_5H_9 ($+ H_2$)	Glow discharge between Cu electrodes	$B_{10}H_{16} + \ldots$	*20, 21*
B_5H_9 ($+ B_2H_6 + H_2$)	Glow discharge between Cu electrodes	$B_8H_{12} + \ldots$	*10*
$B_{10}H_{14}$ ($+ H_2$)	Glow discharge between Cu electrodes	$B_{20}H_{16} + \ldots$	*13*

[a] Isomers observed.

In Chemical Reactions in Electrical Discharges; Blaustein, B.;
Advances in Chemistry; American Chemical Society: Washington, DC, 1969.

eventually be decomposed completely to hydrogen and a very high molecular weight, essentially non-volatile, product. The average molecular weight of the product can be adjusted by varying the cold trap temperature—the colder the trap, the lower the average molecular weight.

In Table I, some of the higher molecular weight hydrides which have been prepared from simple hydrides are listed.

Halides. When the volatile halides $SiCl_4$, $GeCl_4$, and BCl_3 are passed through a glow discharge at low pressure, the higher homologs, Si_2Cl_6, Ge_2Cl_6, and B_2Cl_4, are formed along with elementary chlorine. These higher halides may be isolated if the vapors emerging from the discharge are passed through suitable cold traps for separating the halides from chlorine by fractional condensation. However, a great deal of back-reaction occurs, and the yields are low. If the apparatus is modified so that a suitable reducing agent is present in the discharge zone or immediately after the discharge zone, the yields are greatly improved. Mercury and copper wool have been found to be very effective reducing agents for this purpose.

The effectiveness of including a reducing agent in the apparatus is shown dramatically by experiments with PCl_3. If a glow discharge is established in a stream of PCl_3 vapor in the absence of a reducing agent, the vapor leaving the PCl_3 discharge contains PCl_5 and probably one or more of the following species: P, P_2, or PCl. No P_2Cl_4 is obtained, even by fractional condensation of the vapors. However, by including a reducing agent (hydrogen, mercury, copper, or phosphorus) in or near the discharge, fairly good yields of P_2Cl_4 have been obtained.

A brief summary of some electric discharge halide syntheses is given in Table II.

Conversion of Mixtures into More Complicated Molecules

When a binary mixture of relatively simple molecules is subjected to an electric discharge, various types of reactions are possible, including simple coupling with the elimination of fragments, and the transfer of an atom or group from one species to another.

Hydrides. When mixtures of relatively simple hydrides are passed through an electric discharge, higher molecular weight ternary hydrides are formed. For example, by passing a mixture of SiH_4 and PH_3 through an ozonizer discharge, one obtains a mixture of the compounds SiH_3PH_2, $Si_2H_5PH_2$, and $(SiH_3)_2PH$, as well as P_2H_4 and various polysilanes (*9*, *17*). The ozonizer (or silent electric discharge) is mild in its action on molecules, and it does not cause drastic fragmentation and rearrangement. There is some evidence that, by the judicious choice of reagents, it can be used for the preparation of specific isomers (*18*). Thus, a mixture of

Publication Date: June 1, 1969 | doi: 10.1021/ba-1969-0080.ch012

SiH_3PH_2 and SiH_4 yields $(SiH_3)_2PH$, and a mixture of Si_2H_6 and PH_3 yields $Si_2H_5PH_2$. The conversion of acetylene-boron hydride mixtures into carboranes involves relatively deep-seated molecular rearrangements. The ozonizer is fairly inefficient in effecting such reactions, and the more powerful glow discharge between copper electrodes is preferred for such purposes (*19*).

Table II. Electric Discharge Syntheses of Halides

Starting Material	*Reducing Agent*	*Products Isolated*	*References*
BCl_3	none	B_2Cl_4	
	Hg	B_2Cl_4	*59, 60*
	Zn	B_2Cl_4	*56*
	Cu	B_2Cl_4	*61*
BI_3	none	B_2I_4, B_xI_y, $(BI)_x$	*46*
AlI_3	none	$(AlI)_x$	*47*
$SiCl_4$	Hg	Si_nCl_{2n+2}	*58*
	Si	Si_nCl_{2n+2}	*31*
$GeCl_4$	none	Ge_2Cl_6	*27, 50*
	Cu	Ge_2Cl_6	*29*
PCl_3	none	P_xCl_y, PCl_5	*29*
	H_2	P_2Cl_4	*44*
	Hg	P_2Cl_4	*12*
	Cu	P_2Cl_4	*29*
	P_4	P_2Cl_4	*44*
$TiCl_4$	H_2	$TiCl_3$	*26*

A summary of some electric discharge syntheses of ternary hydrides is given in Table III.

Halides. The author is aware of only one example of the preparation of a ternary halide in an electric discharge. Massey and Urch (*36*) obtained a very small sample of impure $SiCl_3BCl_2$ as a by-product from the mercury discharge synthesis of B_2Cl_4. The silicon probably originated from the quartz discharge cell used. It appears that the essentially unexplored study of mixtures of halides in electric discharges is worthy of study.

Fluorides. Some remarkable compounds have been prepared by subjecting mixtures of various species with elementary fluorine to glow discharges. Both static and circulating systems have been employed, and the products of the reactions have been effectively removed from the possible destructive action of the discharge by holding the discharge tube at a temperature low enough to cause the condensation of the product. Thus, by subjecting mixtures of oxygen and fluorine to the action of a glow discharge between copper electrodes at 60°–77°K., the compounds O_2F_2 (*43*), O_3F_2 (*2, 3, 32 33*), O_4F_2 (*23*), O_5F_2 (*57*), and O_6F_2 (*57*) have

Publication Date: June 1, 1969 | doi: 10.1021/ba-1969-0080.ch012

been prepared. The higher members of this series are extremely unstable compounds that decompose to their elements even at 90°K. Using a similar apparatus at 86°K., krypton and fluorine have yielded the very re-

Table III. Electric Discharge Syntheses of Ternary Hydrides

Reagents	*Electric Discharge*	*Products Isolated*	*References*
$SiH_4 + GeH_4$	Ozonizer	SiH_3GeH_3	*54*
$SiH_4 + PH_3$	Ozonizer	SiH_3PH_2, $Si_2H_5PH_2$, $(SiH_3)_2PH$	*9, 17*
$Si_2H_6 + PH_3$	Ozonizer	$Si_2H_5PH_2$	*18*
$SiH_3PH_2 + SiH_4$	Ozonizer	$(SiH_3)_2PH$	*18*
$SiH_4 + AsH_3$	Ozonizer	SiH_3AsH_2, Si_2AsH_7	*9*
$GeH_4 + PH_3$	Ozonizer	GeH_3PH_2, Ge_2PH_7, Ge_3PH_9, GeP_2H_6	*9*
$GeH_4 + AsH_3$	Ozonizer	GeH_3AsH_2	*9*
$SiH_4 + CH_3OCH_3$	Ozonizer	$CH_3Si_2H_5$	*1*
$B_5H_9 + C_2H_2$	Ozonizer	$B_3C_2H_5$, *sym*-$B_4C_2H_6$, *unsym*-$B_4C_2H_6$, $B_5C_2H_7$	*48, 49*
$B_2H_6 + C_2H_2$	Glow discharge between Cu electrodes	$B_3C_2H_5$, *sym*-$B_4C_2H_6$, $B_5C_2H_7$ + methyl derivs.	*19*

active species KrF_2 (*22, 45*). Recently, the unusual compound $NF_4^+AsF_6^-$ was prepared by subjecting a mixture of NF_3, AsF_5, and F_2 to a glow discharge at −78°C. (*24*). In contrast to the polyoxygen fluorides and krypton difluoride, NF_4AsF_6 is stable and nonvolatile at 25°C.

The synthesis of a rare gas fluoride ordinarily involves the use of elementary fluorine and the concomitant special equipment used in handling fluorine. However, Milligan and Sears (*39*) have described a fluorination technique which avoids the use of fluorine and consequently deserves serious consideration as a general method. They passed mixtures of xenon and CF_4 through a microwave discharge and obtained good yields of XeF_2.

Controlled Reactions of Atoms and Radicals

The syntheses discussed in the preceding section are characterized by the reaction of a mixture of species in an electric discharge. This procedure sometimes leads to the formation of unwanted by-products that complicate the isolation of pure products. These side reactions can partially be avoided by allowing a stream of atoms or radicals (prepared in an electric discharge) to impinge on various compounds in the absence of a discharge. This procedure is somewhat inefficient because of inevitable losses of the atoms or radicals while in transit from the discharge

Publication Date: June 1, 1969 | doi: 10.1021/ba-1969-0080.ch012

In Chemical Reactions in Electrical Discharges; Blaustein, B.;
Advances in Chemistry; American Chemical Society: Washington, DC, 1969.

zone, but it affords considerable control over the nature of the products formed.

Atomic Hydrogen. Many reactions of atomic hydrogen with organic compounds have been studied (*55*). It is generally agreed that the primary reaction with saturated hydrocarbons is hydrogen abstraction, whereas with alkyl halides and alkenes halogen atom abstraction and hydrogen atom addition are involved. Relatively few reactions of atomic hydrogen with gaseous inorganic compounds have been studied (*51*). Apparently no controlled reaction of atomic hydrogen with a boron hydride has been studied. Possibly the reported reaction of a mixture of H_2 and B_5H_9 to give $B_{10}H_{16}$ involved the abstraction of the apical H atom from B_5H_9 followed by coupling of two B_5H_8 radicals (*20, 21*). It would be interesting to see if other similar coupling reactions can be effected by atomic hydrogen. In a study of the reaction of atomic hydrogen with PH_3, only H_2 and red phosphorus were observed as products (*62*). However, the reaction was studied only at 73°C. and higher, at which temperatures P_2H_4 is kinetically unstable (*11*). Possibly useful yields of higher phosphines could be obtained by working at lower temperatures.

The reactions of atomic hydrogen with the elements has been reviewed by Siegel (*51*). In many cases hydrides are formed, but the reactions with metals are often complicated by the heat liberated by the surface-catalyzed atom recombination reaction. McTaggart has reported the reaction of atomic hydrogen with various transition metal oxides to form reduced oxides (*37*). In the case of TiO_2 and ZrO_2, hydrogen-containing oxides of empirical composition $H_{0.2}TiO_{1.3}$ and $H_{0.2}ZrO_{1.66}$ were obtained. Zirconium difluoride has been prepared by the action of atomic hydrogen on thin layers of ZrF_4 at elevated temperatures (*38*).

A number of interesting reactions have been studied by passing streams of atomic hydrogen through aqueous solutions (*5, 6*). In a typical procedure, hydrogen gas at 20–30 mm. pressure is pumped through an electric discharge, through the experimental solution (cooled to reduce evaporation), and through a cold trap to retain volatile products. Dissolved atomic hydrogen sometimes acts as an oxidizing agent, by hydrogen abstraction from organic molecules, or together with the aqueous proton as in the oxidation of ferrous ion (*5, 6*),

$$Fe^{2+} + H + H^+ \rightarrow Fe^{3+} + H_2$$

With many inorganic species (such as Co(III) complexes, nitrate ion, and ferricyanide), atomic hydrogen acts as a reducing agent, with formation of the aqueous proton (*40, 41*). For example,

$$Co(NH_3)_6^{3+} + H \rightarrow Co(NH_3)_6^{2+} + H^+$$

Publication Date: June 1, 1969 | doi: 10.1021/ba-1969-0080.ch012

In Chemical Reactions in Electrical Discharges; Blaustein, B.;
Advances in Chemistry; American Chemical Society: Washington, DC, 1969.

Recently it has been recognized that atomic hydrogen and the aqueous electron are two distinct reducing species, interconvertible by adjustment of the pH (*25*):

$$H_{aq} + OH^- \rightleftarrows e_{aq}^- + H_2O$$

The application of these reagents to synthetic problems has not yet been attempted. Possibly the effect of hydrogen atoms on aqueous systems can be studied by using a static ozonizer discharge containing aqueous solutions. It has been demonstrated that ceric ions may be reduced to cerous ions and that ferrous ions are oxidized to ferric ions (with formation of hydrogen peroxide) by simple exposure of the appropriate solutions to a silent electric discharge (*63*, *64*). These reactions are believed to involve the formation of H atoms and OH radicals.

Atomic Nitrogen. Atomic nitrogen, like most atoms and radicals (*42*), acts as an electrophilic reagent which favors attack at polarizable donor atoms. This behavior is apparent from a study of the reaction of atomic nitrogen with various sulfur compounds (*52*). Divalent sulfur compounds (H_2S, CS_2, OCS, S_8, S_2Cl_2, and SCl_2) yield a variety of sulfur-nitrogen compounds. On the other hand, sulfur compounds containing sulfur atoms with a positive formal charge (SO_2, $SOCl_2$, and SO_3) yield no sulfur-nitrogen compounds. The reaction of atomic nitrogen with S_2Cl_2 was found to give good yields of the unusual molecule NSCl.

Recently it has been shown that when atomic nitrogen is passed through aqueous solutions, it can effect a variety of oxidation-reduction reactions (*35*).

Publication Date: June 1, 1969 | doi: 10.1021/ba-1969-0080.ch012

Literature Cited

(1) Abedini, M., MacDiarmid, A. G., *Inorg. Chem.* **5**, 2040 (1966).
(2) Aoyama, S., Sakuraba, S., *J. Chem. Soc. Japan* **59**, 1321 (1938); *C. A.*, **33**, 1576 (1939).
(3) *Ibid.*, **62**, 208 (1941); *C. A.*, **35**, 4699 (1941).
(4) Besson, A., Fournier, L., *Compt. Rend.* **150**, 102 (1910).
(5) Czapski, G., Stein, G., *J. Phys. Chem.* **63**, 850 (1959).
(6) Davis, T. W., Gordon, S., Hart, E. J., *J. Am. Chem. Soc.* **80**, 4487 (1958).
(7) Drake, J. E., Jolly, W. L., *Proc. Chem. Soc.* **1961**, 379.
(8) Drake, J. E., Jolly, W. L., *J. Chem. Soc.* **1962**, 2807.
(9) Drake, J. E., Jolly, W. L., *Chem. Ind. (London)* **1962**, 1470.
(10) Enrione, R. E., Boer, F. P., Lipscomb, W. N., *Inorg. Chem.* **3**, 1659 (1964).
(11) Evers, E. C., Street, E. H. Jr., *J. Am. Chem. Soc.* **78**, 5726 (1956).
(12) Finch, A., *Can. J. Chem.* **37**, 1793 (1959).
(13) Friedman, L. B., Dobrott, R. D., Lipscomb, W. N., *J. Am. Chem. Soc.* **85**, 3505 (1963).
(14) Gibbins, S. G., Shapiro, I., *J. Am. Chem. Soc.* **82**, 2968 (1960).
(15) Gokhale, S. D., Drake, J. E., Jolly, W. L., *J. Inorg. Nucl. Chem.* **27**, 1911 (1965).
(16) Gokhale, S. D., Jolly, W. L., *Inorg. Chem.* **3**, 946 (1964).
(17) *Ibid.*, **3**, 1141 (1964).

In Chemical Reactions in Electrical Discharges; Blaustein, B.;
Advances in Chemistry; American Chemical Society: Washington, DC, 1969.

(18) *Ibid.*, 4, 596 (1965).
(19) Grimes, R. N., *J. Am. Chem. Soc.* **88,** 1895 (1966).
(20) Grimes, R., Wang, F. E., Lewin, R., Lipscomb, W. N., *Proc. Natl. Acad. Sci. U.S.* **47,** 996 (1961).
(21) Grimes, R., Wang, F. E., Lewin, R., Lipscomb, W. N., *Chem. Eng. News* **39,** Aug. 21, 1961, p. 36.
(22) Grosse, A. V., Kirshenbaum, A. D., Streng, A. G., Streng, L. V., *Science* **139,** 1047 (1963).
(23) Grosse, A. V., Streng, A. G., Kirshenbaum, A. D., *J. Am. Chem. Soc.* **83,** 1004 (1961).
(24) Guertin, J. P., Christe, K. O., Pavlath, A. E., *Inorg. Chem.* **5,** 1921 (1966).
(25) Hart, Edwin J., ADVAN. CHEM. SER. **50** (1965).
(26) Ingraham, T. R., Downes, K. W., Marier, P., *Inorg. Synth.* **6,** 52 (1960).
(27) Jolly, W. L., "Synthetic Inorganic Chemistry," p. 113, Prentice-Hall, Englewood Cliffs, N. J., 1960. *Ibid.*, pp. 170-171 (1960).
(28) Jolly, W. L., "Technique of Inorganic Chemistry," Vol. 1, p. 179, H. B. Jonassen, A. Weissberger, eds., Interscience Publishers, New York, 1963.
(29) Jolly, W. L., Lindahl, C. B., Kopp, R. W., *Inorg. Chem.* **1,** 958 (1962).
(30) Kana'an, A. S., Margrave, J. L., *Adv. Inorg. Chem. Radiochem.* **6,** 143 (1964).
(31) Kautsky, H., Kautsky, H. Jr., *Chem. Ber.* **89,** 571 (1956).
(32) Kirshenbaum, A. D., Grosse, A. V., *J. Am. Chem. Soc.* **81,** 1277 (1959).
(33) Kirshenbaum, A. D., Grosse, A. V., Aston, J. G., *J. Am. Chem. Soc.* **81,** 6398 (1959).
(34) Kotlensky, W. V., Schaeffer, R., *J. Am. Chem. Soc.* **80,** 4517 (1958).
(35) Lichtin, N. N., Juknis, S. E., Melucci, R., Backenroth, L., *Chem. Comm.* **1967,** 283.
(36) Massey, A. G., Urch, D. S., *Proc. Chem. Soc.* **1964,** 284.
(37) McTaggart, F. K., *Nature* **199,** 339 (1963).
(38) McTaggart, F. K., Turnbull, A. G., *Australian J. Chem.* **17,** 727 (1964).
(39) Milligan, D. E., Sears, D. R., *J. Am. Chem. Soc.* **85,** 823 (1963).
(40) Navon, G., Stein, G., *J. Phys. Chem.* **69,** 1384 (1965).
(41) *Ibid.*, **69,** 1390 (1965).
(42) Pearson, R. G., *J. Am. Chem. Soc.* **85,** 3533 (1963).
(43) Ruff, O., Menzel, W., *Z. Anorg. Allgem. Chem.* **211,** 204 (1933).
(44) Sandoval, A. A., Moser, H. C., *Inorg. Chem.* **2,** 27 (1963).
(45) Schreiner, F., Malm, J. G., Hindman, J. C., *J. Am. Chem. Soc.* **87,** 25 (1965).
(46) Schumb, W. C., Gamble, E. L., Banus, M. D., *J. Am. Chem. Soc.* **71,** 3225 (1949).
(47) Schumb, W. C., Rogers, H. H., *J. Am. Chem. Soc.* **73,** 5806 (1951).
(48) Shapiro, I., Good, C. D., Williams, R. E., *J. Am. Chem. Soc.* **84,** 3837 (1962).
(49) Shapiro, I., Keilin, B., Williams, R. E., Good, C. D., *J. Am. Chem. Soc.* **85,** 3167 (1963).
(50) Shriver, D., Jolly, W. L., *J. Am. Chem. Soc.* **80,** 6692 (1958).
(51) Siegel, B., *J. Chem. Educ.* **38,** 496 (1961).
(52) Smith, J. J., Jolly, W. L., *Inorg. Chem.* 4, 1006 (1965).
(53) Spanier, E. J., MacDiarmid, A. G., *Inorg. Chem.* **1,** 432 (1962).
(54) *Ibid.*, **2,** 215 (1963).
(55) Steacie, E. W. R., "Atomic and Free Radical Reactions," 2nd ed., Vol. 1, Reinhold, New York, 1954.
(56) Stock, A., Brandt, A., Fischer, H., *Ber.* **58,** 643 (1925).
(57) Streng, A. G., Grosse, A. V., *J. Am. Chem. Soc.* **88,** 169 (1966).

In Chemical Reactions in Electrical Discharges; Blaustein, B.;
Advances in Chemistry; American Chemical Society: Washington, DC, 1969.

(58) Urry, G., Hanson, J. E., Kaczmarczyk, A., *Abstr. Papers 138th Am. Chem. Soc. Meeting, New York, 1960,* p. 23N.
(59) Urry, G., Wartik, T., Schlesinger, H. I., *J. Am. Chem. Soc.* **76,** 5293 (1954).
(60) Wartik, T., Moore, R., Schlesinger, H. I., *J. Am. Chem. Soc.* **71,** 3265 (1949).
(61) Wartik, T., Rosenberg, R., Fox, W. B., *Inorg. Synth.* **10,** 118 (1967).
(62) Wiles, D. M., Winkler, C. A., *J. Phys. Chem.* **61,** 620 (1957).
(63) Yokohata, A., Tsuda, S., *Bull. Chem. Soc. Japan* **39,** 46 (1966).
(64) *Ibid.,* **39,** 53 (1966).

RECEIVED May 15, 1967. This work was supported by the U. S. Atomic Energy Commission.

13

Hydrazine Synthesis in a Silent Electrical Discharge

J. D. THORNTON, W. D. CHARLTON, and P. L. SPEDDING

Department of Chemical Engineering, University of Newcastle Upon Tyne, Merz Court, Claremont Rd., Newcastle Upon Tyne, 2, England

Publication Date: June 1, 1969 | doi: 10.1021/ba-1969-0080.ch013

Hydrazine is synthesized from ammonia in the silent electrical discharge using a series of reactors of differing geometry. The reported effect on the synthesis of power density, pressure, and residence showed that the energy yield rose with a reduction in the magnitude of these variables while the corresponding percentage conversion of ammonia to hydrazine fell. The use of liquid absorbents and pulsed discharge techniques enabled very low residence times corresponding to higher energy yields of hydrazine to be achieved. The maximum reported energy yield of 15 grams/kwh. was obtained with a pulsed discharge. The liquid absorbent gave an intermediate energy yield but the percentage conversion was well above that for the pulsed discharge.

The synthesis of hydrazine from ammonia using the silent electric discharge was first demonstrated by Besson in 1911 (*2*). Subsequent investigation showed that both the electrical energy yield and percentage conversion obtained were very low (*3, 9*) and interest in the process waned. Further work conducted in the early 1950's enabled substantial improvements in yields to be obtained in certain circumstances and a better understanding of the kinetic mechanisms in the discharge to emerge. Devins and Burton (*4*) showed that significant net hydrazine formation took place only in the positive column of a d.c. discharge. Moreover, it was found that yields could be substantially increased if the atomic hydrogen concentration in the discharge could be reduced by recombination. These general observations were later confirmed by Rathsack (*15*). As a result Devins and Burton proposed a mechanism for hydrazine synthesis in which hydrazine was first formed in the discharge and then degraded by back reactions. Ouchi (*11, 12, 13, 14*)

In Chemical Reactions in Electrical Discharges; Blaustein, B.;
Advances in Chemistry; American Chemical Society: Washington, DC, 1969.

showed that yields could be increased by reducing the residence time of the hydrazine in the discharge in agreement with the general premise of hydrazine degradation in the discharge. Subsequent work has not been at variance with this finding (*1, 16*).

Recently, Imperial Chemical Industry, Ltd. (I.C.I.) of the United Kingdom have reported (*5, 6, 7*) that removal of product hydrazine in a liquid absorbent gives a substantial increase in yield and an improvement in percentage conversion. This is, of course, a modification of technique which is in general agreement with the premise of hydrazine degradation in the discharge proposed by Devins and Burton (*4*) and Ouchi (*11, 12, 13, 14*) and others (*8*). I.C.I. apparently was able to achieve even better yields by suitable modification of the waveform characteristics of the discharge. In order to confirm their claim and to help clarify the mechanisms taking place in the discharge, work was commenced on this system at the University of Newcastle upon Tyne in 1965. This is a preliminary statement of the results obtained to date.

Publication Date: June 1, 1969 | doi: 10.1021/ba-1969-0080.ch013

Experimental

The main aim of this work was to attempt to increase hydrazine yields by reducing the residence time of the product in the discharge. A concentric silica barrier discharge reactor was employed with and without the use of a liquid absorbent. Reactant flow rate was increased up to the maximum pumping capacity of the apparatus after which the discharge volume was reduced by changing the electrode area to give a further reduction in product residence time. Finally, a d.c. parallel electrode reactor was used in which the discharge waveform characteristics were altered so that only a short activating pulse was supplied to the reactant in the electrode gap as it passed through the reactor.

The apparatus consisted essentially of a discharge reactor set between measuring and analyzing sections in a flowing gas train. Most parts of the apparatus were of borosilicate glass. Commercially pure ammonia was fed into the measuring section of the apparatus *via* a reduction valve and a regulating needle valve. The flow rate was measured on a rotameter which had been previously calibrated under operating conditions by using a soap film manometer. Gas temperatures and pressures also were measured before the discharge reactor. The pressure was measured on a capillary mercury manometer with silicon oil seals. The hydrazine formed in the discharge was absorbed in ethylene glycol either *in situ* or in a separate absorption train. Hydrazine was determined using the spectrophotometric method of Watt and Chrisp (*17*). Vacuum control was achieved by a cartesian manostat located before the vacuum pump.

The a.c. radiofrequency power (1.2 meg. cycle/sec.) to the A- and B-type reactors was supplied by a modified C-12 Radyne plasma generator of IKW rated output. The modification consisted of placing a secondary winding within the tank coil of the generator. The power output was tapped off from this winding. Measurement of the power dissipated in the discharge was achieved by determining the power factor

In Chemical Reactions in Electrical Discharges; Blaustein, B.;
Advances in Chemistry; American Chemical Society: Washington, DC, 1969.

directly on a suitable double beam oscilloscope. Three standard methods were used. Either the phase angle between the current and voltage was measured directly or the Lissajous figure technique was used. Both these methods are in error because the current trace is not truly sinusoidal in shape. A more accurate way which was used eventually was the graphical integration of the individual waveforms. The resulting power factor in conjunction with the direct readings of an R.M.S. voltmeter (Airmec 314) and a radiofrequency ammeter (Cambridge Unipivot) enabled a reasonably accurate determination of the power in the discharge to be achieved. The d.c. power for the C-type reactor was provided by a specially engineered 8KW generator. Measurement of the actual discharge power was made using a combination of the graphical integration of the recorded oscilloscope trace and the appropriate meter readings.

The various types of discharge reactors used in this work are illustrated schematically in Figure 1. Other essential geometric details of these reactors and their operating data are given in Table I. The A-type series of reactors consisted of a precision silica tube (which acted as the capacitive barrier) with the high tension electrode attached around the outside. The inner electrode was a spinning stainless steel cylinder so constructed that absorbent liquid could be sprayed onto the inside of the tube to flow down through the annular discharge gap. Co-current gas and liquid flow were employed.

Publication Date: June 1, 1969 | doi: 10.1021/ba-1969-0080.ch013

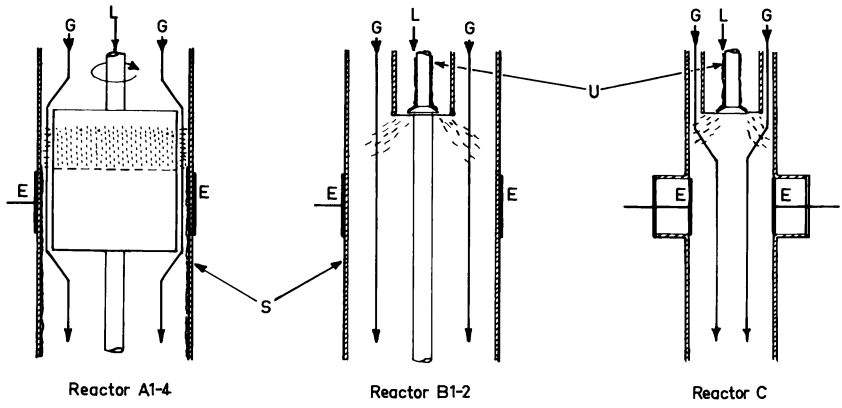

Figure 1. Schematic diagram of reactors used for hydrazine synthesis

E = *Electrodes*, L = *Liquid inlet*, G = *Gas Flow*, S = *Silica Barrier*, U = *Ultrasonic Vibrator*

The B-type series of reactors were of similar construction except that a central wire electrode of stainless steel was used and the absorbent liquid was fed into the incoming gas as a spray. Dispersion of the liquid was achieved ultrasonically using a vibratory generator. The spray was fed into the gas stream through an annular orifice placed at a sufficient distance upstream from the discharge to ensure proper dispersal of spray in the electrode gap. The C-type reactor employed a pair of rectangular

In Chemical Reactions in Electrical Discharges; Blaustein, B.;
Advances in Chemistry; American Chemical Society: Washington, DC, 1969.

electrodes so set in the gas flow as to avoid reactant by-passing. The use of d.c. power necessitated stabilization of the discharge by means of a resistive load in the electrical circuit. Provision was made to admit liquid spray into the inlet gas stream using the same aerosol generator used in the type-B reactors. In all reactors the ammonia flow rate was varied between 60 to 480 cc. N.T.P. per minute. Liquid absorbent flow rate was 45 cc. per minute for all reactors where it was used. The residence time was calculated on the basis of the particular ammonia throughput and the superficial electrode volume for each reactor.

Table I. Reactor Units Employed

Type	*Reactor Code*	*Flow Area sq. cm.*	*Discharge Width cm.*	*Discharge Volume cc.*	*Dielectric Barrier Thickness cm.*
Tubular	A1	2.203	1.270	2.798	0.15875
Centrifugal	A2	2.203	0.254	0.560	0.15875
Film Reactor	A3	2.203	0.127	0.280	0.15875
	A4	2.203	0.040	0.089	0.15875
Tubular	B1	1.089	1.270	1.383	0.15875
Spray Reactor	B2	1.089	0.254	0.277	0.15875
Pulsed Reactor	C1	1.411	0.635	0.896	0

Results

Hydrazine yields for the various reactor geometries and the operating variables employed are given in Figures 2 to 6. From the data presented in Figures 2 to 4, it is evident that the yield varies inversely as an exponential function of the power density at pressures under 100 mm. of mercury. The effect of pressure also follows a negative exponential variation and, therefore, a general equation of the form

$$Y = a \exp(-bP - c\pi)$$

adequately describes the results; where Y = grams of hydrazine per kwh. π = kw. per cc. of reactor volume. Of course this correlation of the results does not in any sense give a complete description of the underlying physical chemistry involved in the synthesis. Ideally, it would have been more preferable to develop separate rate equations in terms of the partial pressures of the various components in the overall hydrazine synthesis. This would have necessitated a complete product analysis and since, in the present case, these data are lacking the phenomenological approach had to be used. The constants in the equation for the various reactors and operating conditions used were evaluated using the method of least squares (*10*). These are tabulated in Table II. It should be noted in the table that certain pressure exponential values are bracketed.

Here the relevant data were lacking for calculation and, therefore, the dependence of energy yield upon pressure for Reactors A2 to A4 and B2 were assumed to be the same as those found experimentally for Reactors A1 and B1. This is a reasonable procedure with any one particular series of reactors, such as A1 to A4, but it is only approximate with differing reactor series—*e.g.*, Reactor series A and B—because of dissimilarities in discharge geometries.

Table II. Derived Constants for the Equation $Y = a \exp(-bP - c\pi)$

Reactor	*a* *gram/kwh.*	*b* *mmHg^{-1}*	*c* *cc./kw.*	*Liquid Absorbent*
A1	13.14	0.0087	73.81	film
A1	6.33	0.0236	118.74	none
A2	10.70	(0.0087)	19.43	film
A3	9.56	(0.0087)	12.93	film
A4	7.28	(0.0087)	3.73	film
B1	12.98	0.0098	73.58	spray
B2	9.26	(0.0098)	13.69	spray
B2	8.88	(0.0236)	35.15	none

Publication Date: June 1, 1969 | doi: 10.1021/ba-1969-0080.ch013

Discussion

The most notable overall feature of the results is the progressive increase in hydrazine yield obtained by the use of a liquid absorbent and by pulsing the discharge. The highest average yield was obtained with the pulsing technique with or without liquid absorbent and was approximately 15 grams of hydrazine per kwh. Isolated values as high as 20 grams/kwh. were obtained but further experimental work is required before reliance can be placed on these values. It is noteworthy that a yield of 15 grams/kwh. is beginning to look commercially attractive. However, it is difficult to forecast costs at this early stage of the gas discharge synthesis route as the final product price will depend to a great extent on the cost of the product purification process downstream of the reactor.

There are several interesting features shown by the results which bear discussion. From an examination of Figures 2 to 4 it is evident that the hydrazine yield decreases with increasing discharge power intensity despite a corresponding increase in the decomposition of ammonia. The only reasonable explanation for these results which has been advanced is that hydrazine is formed in the discharge by a complex reaction mechanism and is subsequently decomposed by electron bombardment or other collision phenomena (*4, 11, 12, 13, 14*).

In Chemical Reactions in Electrical Discharges; Blaustein, B.;
Advances in Chemistry; American Chemical Society: Washington, DC, 1969.

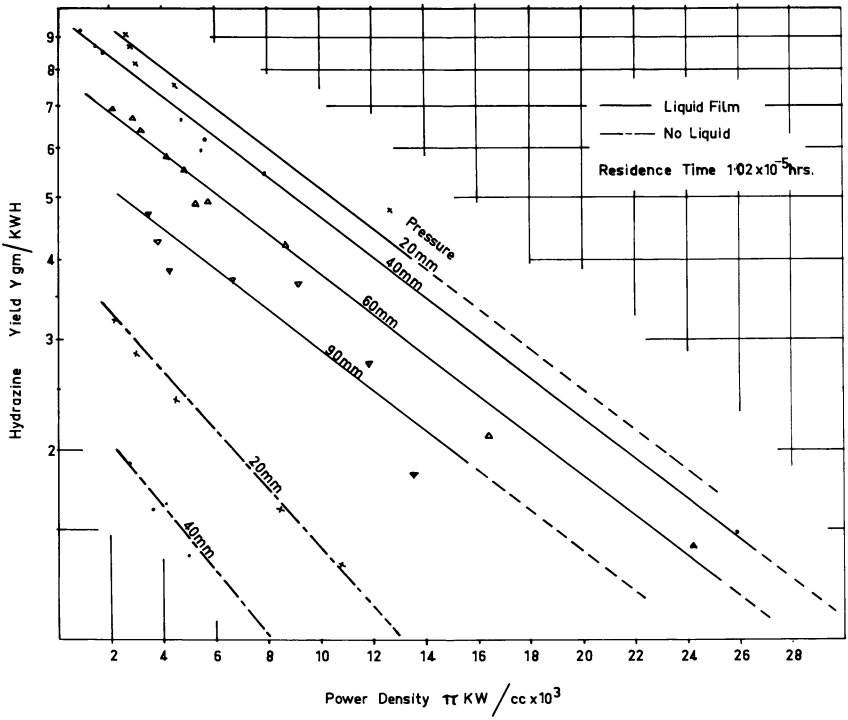

Figure 2. Hydrazine energy yield for the co-axial Reactor A1 with and without liquid film

The use of a liquid absorbent results in a decrease in the slope of the energy yield-power density semi-logarithm plot. The fact is well illustrated in both Figure 2 and Figure 4 by comparing the slope of the plots with and without the use of liquid absorbent. Indications are that hydrazine is being removed from the discharge by the liquid absorbent instead of being degraded. If the hydrazine were completely removed so that degradation did not occur the slope of this plot would depend upon the shape of the reaction activation cross section. The very fact that the slope is still negative with the use of liquid absorbent may indicate that a significant amount of hydrazine is still being degraded in the discharge. Assuming it to be the case, the use of a more efficient absorption process would reasonably be expected to recover more of the hydrazine being degraded and thus increase yields still further. Moreover, the observed decreasing effect of pressure on the yield with the use of liquid absorbent shown in Figure 2 adds weight to the suggested explanation.

As the pressure was decreased below 100 mm. of mercury the yield of hydrazine increased steadily while the slope of the yield-power density

Publication Date: June 1, 1969 | doi: 10.1021/ba-1969-0080.ch013

In Chemical Reactions in Electrical Discharges; Blaustein, B.;
Advances in Chemistry; American Chemical Society: Washington, DC, 1969.

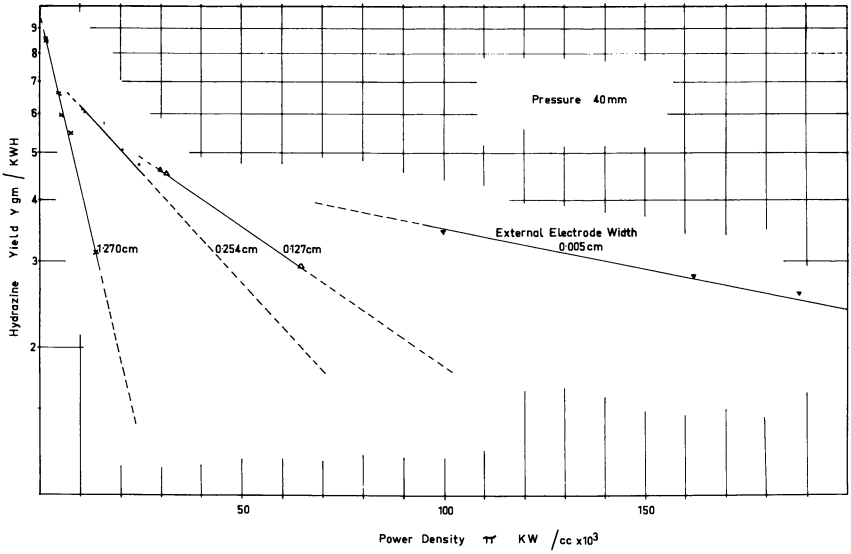

Figure 3. Hydrazine energy yield for the liquid film co-axial Reactors A1 to A4

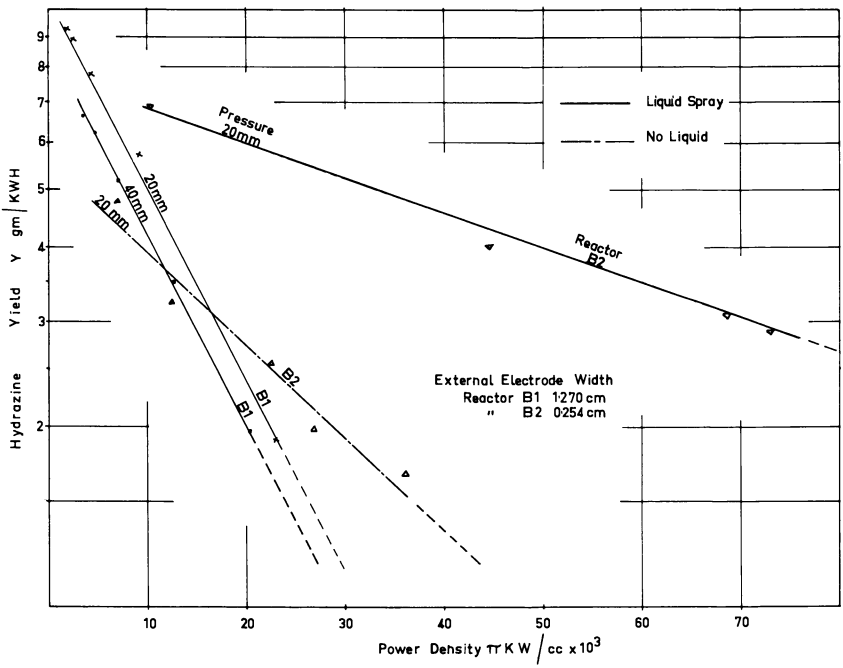

Figure 4. Hydrazine energy yield for the co-axial Reactors B1 and B2 with and without liquid spray

In Chemical Reactions in Electrical Discharges; Blaustein, B.;
Advances in Chemistry; American Chemical Society: Washington, DC, 1969.

curve remained constant for similar reactor operating conditions such as the use of a liquid absorbent. A reasonable explanation for this behavior is that at the lower pressures the electrons passing into the discharge are less likely to suffer collisions in the immediate vicinity of the electrode so that the average energy of the electrons will be high just prior to the required activating collisions. This effect is related to the parameter E/P (where E is the potential drop per unit length of discharge) which has been proposed previously in the interpretation of gas discharge activation phenomena (*4*). Degradation of product by electrons is, by the same argument, more likely under these conditions but other product degrading discharge collisional phenomena—*e.g.*, the reaction with hydrogen atoms —are reduced because of the greater mean free path at the lower operating pressure. The overall result is that hydrazine yields increase. Secondary effects become increasingly important at higher pressures and it is likely that other variations in the effect of pressure on yield may well occur. One such variation is reported to occur at about 5 mm. pressure where the energy yield passes through a maximum (*16*).

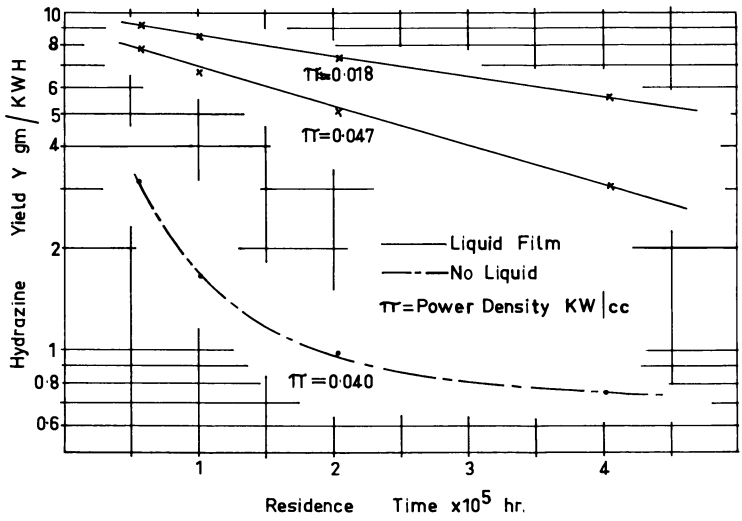

Figure 5. Variation of hydrazine energy yield with flow rate for Reactor A1

Product yields were increased by removing hydrazine in a liquid absorbent film and it was considered that a more efficient absorption technique should lead to even greater yields. The role of the absorbent was viewed solely as a device for reducing the residence time of the hydrazine in the discharge zone. In order to obtain a more intimate gas-liquid dispersion a spray reactor was used of the general design shown

In Chemical Reactions in Electrical Discharges; Blaustein, B.;
Advances in Chemistry; American Chemical Society: Washington, DC, 1969.

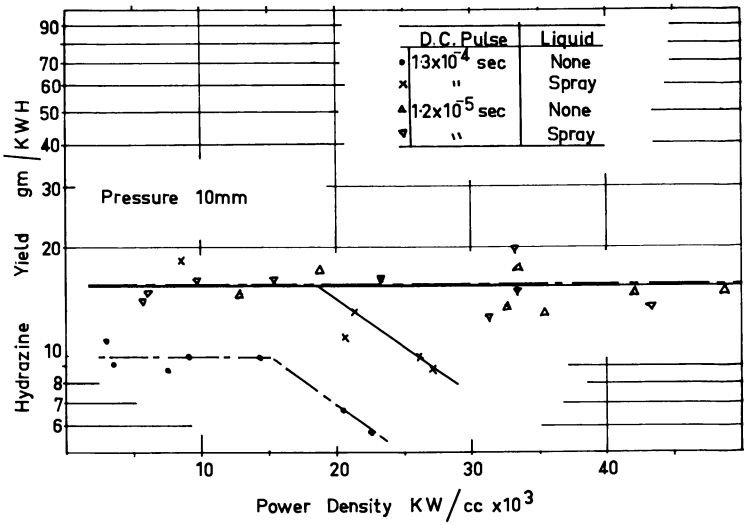

Figure 6. Hydrazine energy yield for the pulsed d.c. Reactor C1

for Reactors B1 and B2 in Figure 1. The results which are presented in Figure 4 show that yields were slightly below that of the film reactor. In practice there were difficulties caused by dissimilarities in the construction of Reactors A and B which led to radically different discharge conditions being obtained. The film reactor (A1) had a more uniform discharge density because it was of an annular construction where the annulus width was small compared with the reactor diameter. The spray reactor (B1), on the other hand, employed a central wire electrode and consequently there was a non-uniform field in the discharge gap with a higher local discharge density in the vicinity of the wire electrode. Because the energy yield is known to depend on an inverse function of the power density, it is only reasonable to expect that the reactor design B1 would give somewhat lower yields than the reactor design A1 under similar operating conditions. This means that the more intimate gas-liquid contact in the spray reactor had no measurable effect on the product yield. On the other hand, if hydrazine is formed and degraded uniformly in the activating section of the discharge this result is difficult to explain. It is suggested from this that, under these conditions, the absorption process is no longer the controlling factor since an increase in the overall potential absorption rate, through an increase in the interfacial area, produces no corresponding rise in hydrazine yields. It may be that liquid surface activation phenomena are taking place and the increased hydrazine yield which is observed with the use of an absorbent liquid is caused by hydrazine formed by other mechanisms in which the liquid surface

Publication Date: June 1, 1969 | doi: 10.1021/ba-1969-0080.ch013

plays an important role. If this were the case the liquid film, which presents a complete barrier to the discharge, would naturally give maximal yield and the spray reactor would only tend to this value in the limit.

It was found experimentally that a decrease in the residence time of the reactant in the discharge was accompanied by an increase in energy yield of hydrazine and a corresponding fall in percentage conversion. The results are detailed in Figure 5 and appear to be in general agreement with those of Ouchi (*11, 12, 13, 14*). When a liquid absorbent is used the logarithm of the yield is a constant function of residence time. In the absence of an absorbent, the yield is very much more dependent upon residence time particularly at low values of the latter. This abnormal behavior suggests that the process resulting in increased hydrazine yields is not just the physical removal of product alone but a change may also be occurring in the basic reaction mechanisms. With the use of a liquid absorbent a further effect on the yield could arise because of changes in the absorption rates caused by increased turbulence and a decrease in the gas liquid contact time accompanying an increase in gas flow. Ouchi (*11, 12, 13, 14*) has concluded from his results that some of the hydrazine formed in the discharge is preserved from degradation by rapid physical removal out of the discharge. This would adequately explain, in general terms, the increase in energy yield with reduced residence time. The concentration of the activated hydrazine species in the discharge must fall as the reactant throughput is increased and, assuming the back reaction to be concentration dependent in the normal way, this would also be associated with a decrease in the back reaction rate.

Another point which must be borne in mind is that physical removal of the product or even the use of the pulsed discharge technique cannot give better conversions than that dictated by the equilibrium concentration of hydrazine for the basic reactions taking place in the discharge (using the term equilibrium in the general overall sense). The use of the liquid absorbent permits higher conversion to be achieved because of the inability of the discharge reaction to reach equilibrium as hydrazine is being continuously removed after it is formed in the discharge.

The negative slope of the energy yield-residence time plot (Figure 5) when liquid absorbent was used, implies that it may be possible to increase yields still further by some other suitable modification of technique.

In an endeavor to reduce the residence time below the level dictated by the capacity of the vacuum system the electrode area was steadily reduced (Reactors A1 to A4). The results obtained are detailed in Figure 3 and show that the yield fell and the discharge itself altered radically because of the increased influence of electrode edge effects.

Publication Date: June 1, 1969 | doi: 10.1021/ba-1969-0080.ch013

In Chemical Reactions in Electrical Discharges; Blaustein, B.;
Advances in Chemistry; American Chemical Society: Washington, DC, 1969.

Discharge pulsing gave a substantial increase in yields over the other methods employed. As the duration of the discharge pulse was shortened the yield was found to rise and become independent of power density. Furthermore, the yield was not affected by the use of a liquid absorbent. Up to this point the usual variations with these two variables were observed. Indications are that hydrazine yields can be increased well beyond 15 grams/kwh. by suitable modification of the pulsed discharge technique.

Conclusion

It is clear from the results that the yield of hydrazine formed from ammonia using the silent discharge can be increased if the residence time of the product in the discharge is reduced by the use of liquid absorbent, physical flowrate of reactant or discharge pulsing. Several aspects of the results seem to imply that the underlying mechanism involved is not simply that of physical removal of product from the degradation of the discharge but other factors, such as changed in the basic reaction mechanisms, also are involved.

Publication Date: June 1, 1969 | doi: 10.1021/ba-1969-0080.ch013

Literature Cited

(1) Andersen, W. H., Zwolinski, B. J., Parlin, R. B., *Ind. Eng. Chem.* **51,** 527 (1959).
(2) Besson, A., *Compt. Rend.* **152,** 1850 (1911).
(3) Bredig, G., Koenig, A., Wagner, O. H., *Z. Phys. Chem.* **193A,** 211 (1928).
(4) Devins, J. C., Burton, M., *J. Am. Chem. Soc.* **76,** 2618 (1954).
(5) Imperial Chemical Industries Ltd., British Patent, **948,772** (Feb. 5, 1964).
(6) *Ibid.*, **958,776**; **958,777**; and **958,778** (May 27, 1964).
(7) *Ibid.*, **966,406** (Aug. 12, 1964).
(8) Jogarao, A., Shastri, B. S. R., *J. Sci. Ind. Res.* (India) **18B,** 38 (1959).
(9) Koenig, A., Wagner, O. H., *Z. Phys. Chem.* **144A,** 213 (1929).
(10) Margenau, H., Murphy, G. M., "The Mathematics of Physics and Chemistry," 2nd ed., p. 519, Van Nostrand, New Jersey, 1957.
(11) Ouchi, K., *J. Electrochem. Soc. (Japan)* **17,** 285 (1949).
(12) *Ibid.*, **20,** 164 (1952).
(13) *Ibid.*, **20,** 168 (1952).
(14) *Ibid.*, **20,** 378 (1952).
(15) Rathsack, H. A., *Z. Phys. Chem. (Leipzig)* **214,** 101 (1960).
(16) Skorokhodov, I. I. *et al.*, *Russ. J. Phys. Chem.* **35,** 503 (1961).
(17) Watt, G. W., Chrisp, J. D., *Anal. Chem.* **24,** 2006 (1952).

RECEIVED June 9, 1967. Financial support for this work was provided by the Science Research Council of the United Kingdom.

14

The Dissociation of Metal Halides in Electrical Discharges

F. K. McTAGGART

Division of Mineral Chemistry, C.S.I.R.O., Box 124, Port Melbourne, Victoria, Australia

Publication Date: June 1, 1969 | doi: 10.1021/ba-1969-0080.ch014

Halides of the Group I and II metals are dissociated in microwave discharges to metals and halogens, and to unstable monohalides (which disproportionate to metals and dihalides) and halogens, respectively. Inert gases may be used as carriers, and if H_2 is employed hydrogen halides instead of halogens result. Up to 70% yields of metal have been obtained. Group III and rare earth halides give metals in good yields only when hydrogen is present, probably via *disproportionation of lower halides. The apparatus is described briefly. Relative reaction rates for the lithium group compounds are given and the effect of power, partial pressure of halide, and pressure of carrier gas are shown.*

The effect of the energetic electrons produced in electrical discharges in dissociating gas molecules is well known, and is the basis of the chemical reactions that are observed in plasma systems. Since gases such as O_2, N_2, H_2, and Cl_2, as well as vapors of organic and other compounds have been dissociated to atoms and/or radicals, it appears logical to suppose that many other molecules would behave similarly. This paper describes the dissociation of the halides of the Group I, II, and III, and rare earth metals.

Experimental

Ideally, the halides should be introduced into the discharge tube in the form of vapors at suitable pressures. Because of the wide range of volatilities occurring in the above compounds and to other experimental difficulties it proved more convenient to use carrier gases, and to volatilize the halides from small boats contained within the reaction tube by heating these boats to suitable temperatures. It was usually possible to

In Chemical Reactions in Electrical Discharges; Blaustein, B.;
Advances in Chemistry; American Chemical Society: Washington, DC, 1969.

make use of the heat generated in the plasma itself for this purpose. Samples were placed upstream from, or within the central plasma region, in positions where heat sufficient to give the desired rate of volatilization was produced. Since heating of solids because of atomic recombination is largely a surface effect, it was also possible to vary the sublimation rate of samples by changing the surface area exposed to the plasma.

Both inert gases (in particular He and N_2) and hydrogen have been used and certain reactions which are discussed below appear to involve H atoms as well as dissociative effects. These gases were of commercial purity, the He and H_2 being purified by passing them over zirconium powder heated to 800°C.; although no essential differences between the cylinder gases and the purified gases were observed. Pressures of the carrier gases were varied between 0.5 and 2.3 mm. Halides used were of A. R. grade, but in certain cases impure compounds were deliberately used to determine the effects of impurities on the dissociation and on the purity of the metal obtained.

Extensive use was made of a 2450 MHz. magnetron generator (Mullard JN2/2.5A) which although capable of an output in excess of 2 kw. continuous wave power, was seldom operated at inputs higher than 600 watts. Radiofrequency energy from the magnetron was fed *via* a 50 ohm air dielectric coaxial line, to a section of waveguide operated as a resonant cavity by means of a sliding plunger inserted into the open end. The discharge tube passed transversely through the guide at a point of maximum electrostatic field. Some investigations, involving the chlorides of Li, Be, and Al, which dissociate very readily, were made using an "RF." generator consisting of a 4-125A vacuum tube at a frequency of 30 MHz., the power of which could be varied from close to zero to about 400 watts. In these cases the reaction tube passed through the "tank coil" of the output circuit.

Conventional methods of analysis were used to determine (a) the amount of metal deposited, (b) the undissociated halide sublimed onto the reaction tube, and (c) the halogen or hydrogen halide collected in the liquid air trap which followed the reaction tube in the flow system.

Publication Date: June 1, 1969 | doi: 10.1021/ba-1969-0080.ch014

Results

From all the halides studied it was possible to separate metals, often in good yields.

The Lithium Group Compounds. These compounds dissociated in both inert carrier gases and in H_2 to give metals and the relative reaction rates were determined for the iodides, bromides, chlorides and fluorides of Li, Na, K, and Cs (*2, 3*). Some of these are shown in Table I. It will be noted that for any one metal the rate is greatest for the iodide and least for the fluoride as might be expected from the bond energies (also quoted). However, in going from one metal to another it is seen that bond energy is not the main factor involved since, for example, the rates for LiI and NaI are 232.5 and 26.0 while the bond energies are 82 and 72 respectively. The rates presumably depend largely on the energy

In Chemical Reactions in Electrical Discharges; Blaustein, B.;
Advances in Chemistry; American Chemical Society: Washington, DC, 1969.

levels to which the molecules must be raised before dissociation will occur. Not a great deal is known about these energies and they appear to depend more on the nature of the metal atom present than on the halogen.

Table I. Relative Reaction Rates for the Halides of Li and Na

Compound	*Bond Energy*	*Rel. React.*	*Compound*	*Bond Energy*	*Rel. React.*
LiI	82	232.5	NaI	72	26.0
LiBr	102	101.5	NaBr	89	15.0
LiCl	115	66.5	NaCl	99	10.0
LiF	138	19.0	NaF	108	5.0

Publication Date: June 1, 1969 | doi: 10.1021/ba-1969-0080.ch014

The effect of variation of sublimation rate (partial pressure) for NaCl is shown in Figure 1 for several input powers. All the Group I halides gave curves of similar shape. As the sublimation rate decreased the percentage dissociation increased to a maximum beyond which there were insufficient halide molecules to "use up" the electrons having sufficient energy to dissociate them. For any one power the amount of halide dissociated was almost independent of sublimation rate (*see* Table II). As expected, an increase in power resulted in increased dissociation and an empirical relationship Rate = $KP^{1.7}$ was found to apply throughout. The highest yield of metal obtained during the experiments was 70% lithium from LiI.

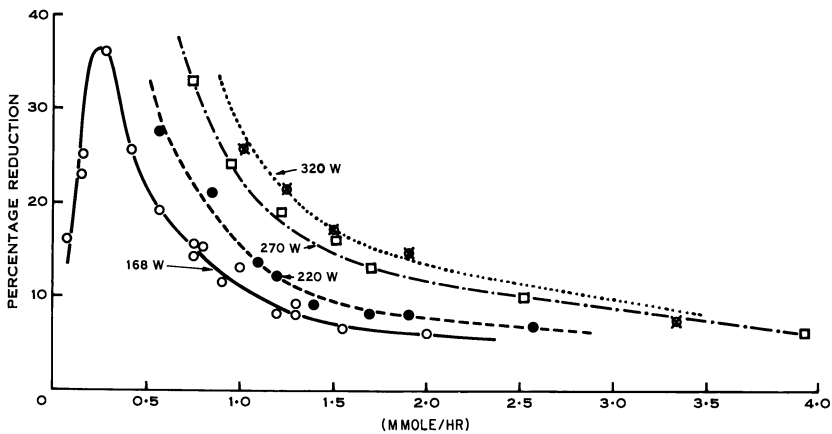

Figure 1. Sodium chloride sublimation rate (mmole/hr.)

Figure 2 shows the effect of carrier gas pressure at constant power. A maximum in metal production occurred at about 1.5 mm. pressure.

For H_2 this pressure coincides closely with the highest concentration of H atoms, and is probably related to the concentration of electrons having sufficient energy to cause dissociation. The reaction rates appeared to be substantially independent of the nature of the carrier gas.

Table II. Dissociation of NaCl in H_2 at 1.0 mm. for Various Input Powers

Sublm. Rate mmole/hour	*mmole/hour Na produced*			
	168W	*220W*	*270W*	*320W*
0.5	0.11	0.160	—	—
1.0	0.11	0.158	0.225	0.280
1.5	0.105	0.145	0.223	0.255
2.0	0.12	0.156	0.230	0.270
2.5	—	0.175	0.250	0.287
3.0	—	—	0.264	0.291
4.0	—	—	0.240	0.280
Mean	0.111	0.159	0.239	0.277

The fact that considerable quantities of highly reactive metals are deposited in atmospheres of even more highly reactive gases, namely halogen atoms, suggests that these halogen species may be in the form of negatively charged ions. Such ions, having a complete outer shell of eight electrons, would be non-reactive chemically, and if neutralization of their charges is delayed until they are swept clear of the metal deposit, an explanation of the apparent absence of appreciable back reaction would be afforded. Mass spectroscopic studies are being made on the nature of the species in these discharges to elucidate this matter.

The Group II Compounds. The majority of the halides of Be, Mg, Ca, Sr, and Ba were investigated. Rates of dissociation did not appear to vary as widely as those of Group I. As optimum conditions were approached for each compound, all the halide vaporized was dissociated and deposits were formed on the walls of the reaction tube in which metals and dihalides were found in equi-molar proportions. This points strongly to the formation of unstable monohalide molecules in the discharge, which disproportionate to yield the observed products. Again the dissociations were not dependent on the carrier gas employed. $BeCl_2$, one of the more volatile halides in this group, and one of the most easily dissociated of all the compounds studied, may be broken down in the lower frequency apparatus mentioned previously.

Metals could be separated from the dihalides in the deposits by means of suitable solvents for the latter, or in some cases by vacuum sublimation of the dihalide.

Publication Date: June 1, 1969 | doi: 10.1021/ba-1969-0080.ch014

In Chemical Reactions in Electrical Discharges; Blaustein, B.;
Advances in Chemistry; American Chemical Society: Washington, DC, 1969.

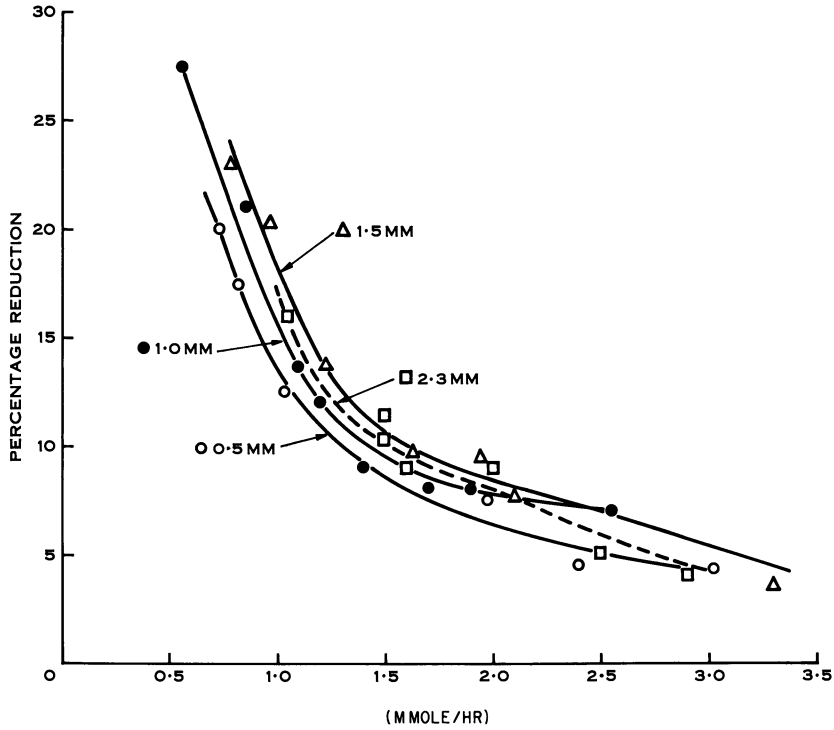

Figure 2. Sodium chloride sublimation rate (mmole/hr.) at 220 watts

The Group III Compounds. No investigations have yet been made on the compounds of boron. Markovskii *et al.* (*1*) reported in 1958 that BCl_3 was reduced to elemental boron by H atoms, but it is by no means certain that the type of discharge used in the present work will yield boron. B_2H_6 may be the major product.

When inert carrier gases were used there was a very limited deposition of metal from Al and Sc halides amounting to only a few percent of the vapor passed through the discharge, but when hydrogen was employed much higher yields of metals were obtained. It would appear, therefore, that at least one step in the decomposition involves an H atom reaction, and the process may be, for $AlCl_3$: initial dissociation of $AlCl_3$ to $AlCl_2$: H atom reduction of $AlCl_2$ to AlCl : disproportionation of AlCl to Al and $AlCl_3$. A mass spectrometric examination of the species present in the discharge revealed AlCl in readily detectable quantities but no $AlCl_2$ was observed. Yields of up to 55% Al metal have been obtained from $AlCl_3$ in a single pass through a 2450 MHz. plasma. In a typical experiment using H_2 at 1.0 mm. pressure, 0.5 gram of $AlCl_3$ was vaporized from an alundum tube placed a short distance upstream from the plasma

Publication Date: June 1, 1969 | doi: 10.1021/ba-1969-0080.ch014

region, during a period of 20 minutes, the input power to the magnetron being 120 watts. 0.055 gram Al metal deposited in the reaction tube. During such experiments, if a second discharge was produced downstream more Al deposited. The rate at which $AlCl_3$ decomposes, with comparatively low power, and with its intense blue plasma makes this reaction one of the most spectacular of those studied. The relatively involatile AlF_3 also dissociated quite readily to give the metal, although it is not easily handled in the experimental apparatus described. The chloride and fluoride of scandium behaved like the corresponding aluminum compounds.

$AlCl_3$ also dissociated readily in the lower frequency apparatus. It should be mentioned here that the chief difference between the waveguide and the coil-coupled apparatus appears to be that in the former the electrons are accelerated to higher energies since the electrostatic field is concentrated between the resonator walls where a high potential gradient exists in a direction axial to the discharge tube. By comparison the E field in a coil is much more randomly distributed.

Rare Earth Compounds. We have not as yet had an opportunity of studying these halides systematically, but preliminary experiments have shown that they behave in a manner similar to $AlCl_3$. That is, there is only limited dissociation to metal in an inert carrier gas, but with hydrogen satisfactory yields of metals are obtained. Thus, Ce and La result from CeF_3, $CeCl_3$, LaF_3, and $LaCl_3$. If, for example, chlorides containing appreciable quantities of oxychloride are used for the dissociation this impurity is left in the sample boat and a highly pure metal is deposited. Such reactions may therefore prove of use in the preparation of certain metals.

Literature Cited

(1) Markovskii, L. V., Lvova, V. I., Kondrashev, Y. D., *Ber.Tr.Konf. po Khim. Bora i Ego Svedin* **36** (1958).
(2) McTaggart, F. K., *Australian J. Chem.* **18**, 936, 949 (1965).
(3) *Ibid.*, **18**, 949 (1965).

RECEIVED June 1, 1967.

15

Glow Discharge Deposition of Boron

A. E. HULTQUIST and M. E. SIBERT

Materials Sciences Laboratory, Lockheed Palo Alto Research Laboratory, Palo Alto, Calif. 94304

Publication Date: June 1, 1969 | doi: 10.1021/ba-1969-0080.ch015

The conventional "hot wire" vapor deposition technique deposits boron from a halide by use of thermal energy to decompose the boron compound at the hot wire surface. Use of a glow discharge substitutes electrical energy for this thermal energy resulting in a high degree of ionization/activation of the boron species present, culminating in deposition of elemental boron on all substrate areas within the glow. Use of this technique enables the process to take place at essentially room temperature. This program demonstrated feasibility of glow discharge as a deposition approach. A thorough study of process variables is described together with nature of the filament produced. Behavior of metallic and non-metallic substrates is discussed.

This study is concerned with investigation of the deposition of boron in an electrodeless glow discharge. Basically a high-voltage, low-amperage, high-frequency RF. current is imposed across a boron-containing gas, resulting in a high degree of ionization/activation of the ions present. Boron then deposits out in elemental form on all surfaces within the glow discharge area. Use of proper deposition conditions confines the glow largely to the filament substrate. By passage of the filamentary substrate continuously through the discharge, the approach is potentially capable of high-rate filament formation with excellent uniformity and reliability. Variation of current input can result in deposition at any point from room temperature up to 800°–1000°C. Both metallic and non-metallic substrates can be employed. Deposition is achieved at low pressures of the order of a few mm..

The glow discharge of boron trichloride has been studied by several workers (*1, 2, 3, 8, 10, 11, 12, 13, 14, 15, 16*) in the field, and their results should indicate the deposit to be expected at high ratios of boron trichloride to hydrogen. Holzmann and Morris (*3*) analyzed the light

In Chemical Reactions in Electrical Discharges; Blaustein, B.;
Advances in Chemistry; American Chemical Society: Washington, DC, 1969.

from glows of boron trichloride at 1 mm. of Hg pressure. The glow discharges were caused by a 2.4 to 2.5 $\times$ 10^9 Hz. field (2,400 to 2,500 Mc.). They observed bands caused by boron monochloride and lines caused by atomic boron and atomic chlorine. Frazer and Holzmann (2) have used this technique to prepare laboratory quantities of B_2Cl_4, which is the primary product under these conditions.

The compound B_2Cl_4 can be decomposed under a variety of conditions. Rosenberg (8) used 60-Hz. 10-kv. discharges in B_2Cl_4 and obtained $BCl_{3(g)}$ and $(BCl)_n$, which he described as a light brown or yellow film which is hydrolyzed by water to form B_2O_3, hydrochloric acid, and hydrogen. From the rather incomplete data on this system and from other authors, it appears that a $(BCl)_n$ phase can be obtained at compositions down to $BCl_{0.9}$ and a material which analyzes as $BCl_{0.6}$ has been reported. At the present time the $(BCl)_n$ material is considered to be a polymer, and a series of higher unit structures other than B_2Cl_4 (such as B_4Cl_4) can also be obtained.

Publication Date: June 1, 1969 | doi: 10.1021/ba-1969-0080.ch015

Experimental

Apparatus. The basic apparatus utilized for parametric studies employing a fixed substrate is shown in Figure 1. The reaction vessel is a 9 mm. borosilicate glass tube with the substrate filament suspended down the central axis and suitably sealed at each end. The reactant gases are admitted at one end of the tube and exit at the opposite end. Electrodes are simple concentric copper strips which may be moved along the tube for optimum positioning. The glow discharge then forms between these electrodes. Both horizontal and vertical reactor configurations have been employed; the vertical system is preferred since substrate alignment is better controlled. The vertical arrangement is also more amenable to moving filament systems for continuous filament preparation. Both air and water cooled reaction vessels have been evaluated. Water cooling was originally instituted to minimize sidewall deposition; later work demonstrated that this could be accomplished by regulation of gas composition and current input so as to confine the glow area to the central area of the 9 mm. tube. A three compartment chamber, each 38 mm. long, was used so three experiments could be performed before the system was opened for examination.

The balance of the system is largely a gas flow system. Hydrogen is passed through a catalytic cartridge and a liquid nitrogen trap for removal of oxygen and water impurities. Boron trichloride is fed into the hydrogen stream. Both lines have appropriate flowmeter devices. The boron trichloride is controlled at the cylinder valve; satisfactory control with respect to potential condensation is obtained by bleeding the gas into a flowmeter operating at reduced pressure. Hydrogen flow is regulated by a stainless steel needle valve just downstream from the flowmeter. The combined hydrogen-boron trichloride stream then passes into the reaction chamber. Exit gases from the reactor pass successively through a trap for condensation of unused boron trichloride, past a

In Chemical Reactions in Electrical Discharges; Blaustein, B.;
Advances in Chemistry; American Chemical Society: Washington, DC, 1969.

manometer, through a Cartesian manostat, and thence to a mechanical vacuum pump.

The power supply is a Lockheed-designed 3 Mc. oscillator capable of about 30 watts output; however, only a portion of this output is available as RF. power, about 20 watts at 14–1500 volts.

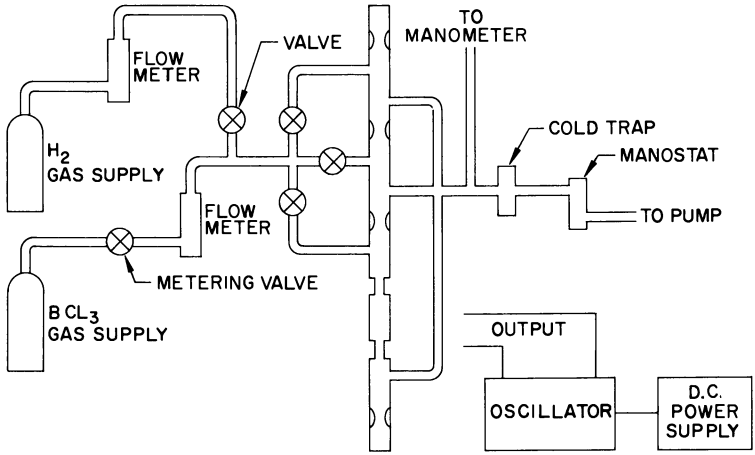

Figure 1. Process Apparatus

Materials. The boron trichloride used was electronic grade supplied by American Potash and Chemical Co. Hydrogen was a high purity laboratory grade (BB-H-886) supplied by Air Reduction Co. Quartz monofilament utilized as a substrate for most of the work was obtained from the General Electric Co. Glass filaments were drawn from borosilicate glass rods by the LMSC glass shop.

General Procedure. Experiments were started by evacuating the assembled apparatus to 1 mm. Hg pressure. The leak rate was determined by turning off the pump and noting the increase in pressure over extended time periods. A leak rate of less than 0.05 mm. Hg/min. was found necessary to avoid boron oxide formation (Figure 2). When the system was determined to be essentially leak free, a flow of hydrogen was introduced and allowed to sweep through the apparatus for 15 to 30 min. The gases were then introduced into the reactor and the power supply for the oscillator turned on. The glow was initiated by adjusting the variable capacitor on the oscillator. At the end of the experiment, the glow discharge and the boron trichloride flow were turned off and hydrogen allowed to sweep through the apparatus for 10 min. to remove unreacted boron trichloride. The pump was turned off and the apparatus returned to ambient pressure using hydrogen. The apparatus was then dismounted and the sample removed.

Results

Preliminary Experiments. Glows were maintained in the presence of both dielectric and conductor filaments to determine their respective

Publication Date: June 1, 1969 | doi: 10.1021/ba-1969-0080.ch015

effects on glow characteristics. The presence of a strand of quartz, QYF-150 to 204 end, 1/0, with oil starch finish, d = 0.004 in., did not affect the operating characteristics of the glow. However, the presence of a 5-mil. tungsten wire resulted in considerable changes in the glow. The tungsten wire acted as a ground connection, and the ground lead from the oscillator could be disconnected without affecting the glow. The glow was concentrated at and spread out along the wire. This system used much higher currents and, as a result, considerable heat was generated. A mirror was deposited on the reaction tube walls.

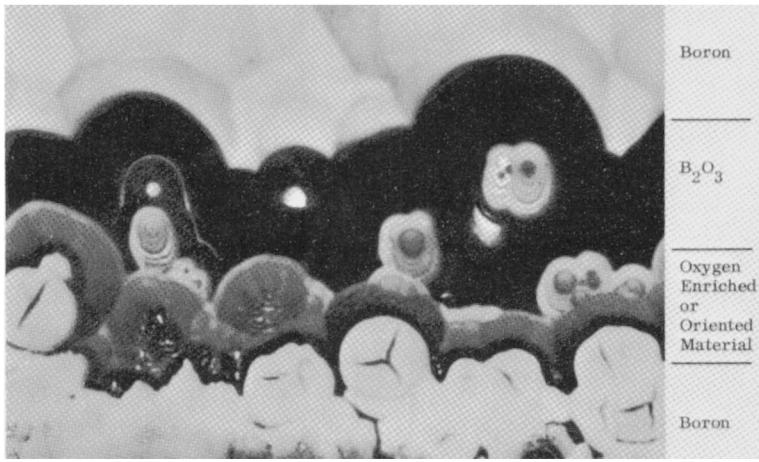

Figure 2. Boron on glass, longitudinal section (1800×)

Following these preliminary experiments, flowmeters were calibrated and a study was then initiated on effects of the various process parameters.

Parametric Study. A study of the effect of process parameters on the deposition of boron using the static filament apparatus was conducted. The parameters studied include system pressure, reactant gas flow, ratios, electrode separation, and configurations, and field strengths. The evaluation of certain parameters has been quantitative and was based on the weight of boron deposited or on the thickness of the deposit at the midpoint of the filament. Other parameters were evaluated by a qualitative description of the deposit.

This study is only an approximation of the moving filament system. The movement of the filament in a continuous system averages the effects of all the parameters so that the filament sample is prepared in a uniform manner. The edge effects noted on the filament situated under the electrodes would not be evident in a continuous system. A typical deposit is shown in Figure 3.

Publication Date: June 1, 1969 | doi: 10.1021/ba-1969-0080.ch015

In Chemical Reactions in Electrical Discharges; Blaustein, B.;
Advances in Chemistry; American Chemical Society: Washington, DC, 1969.

Material efficiencies are based on the amount of boron produced from the total amount of boron passed through the reactor. The electrical efficiency is based on the amount of boron produced divided by the theoretical amount that could be produced by the total charge passed using the reduction equation $B^{3+} \rightarrow B^{\circ} + 3e$. The current was measured by an RF. ammeter placed in the electrical circuit.

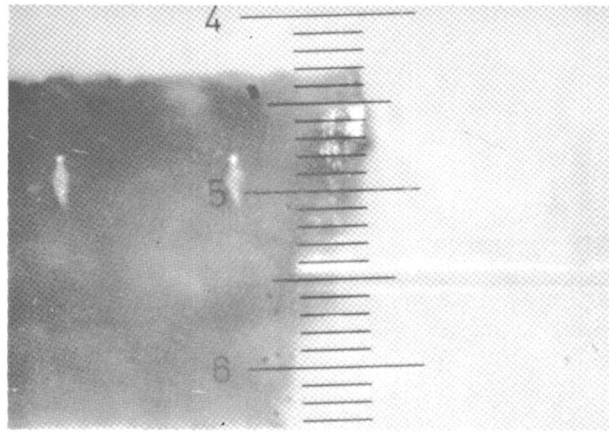

Figure 3a. Boron on quartz; filament emerging from broken end (165×)

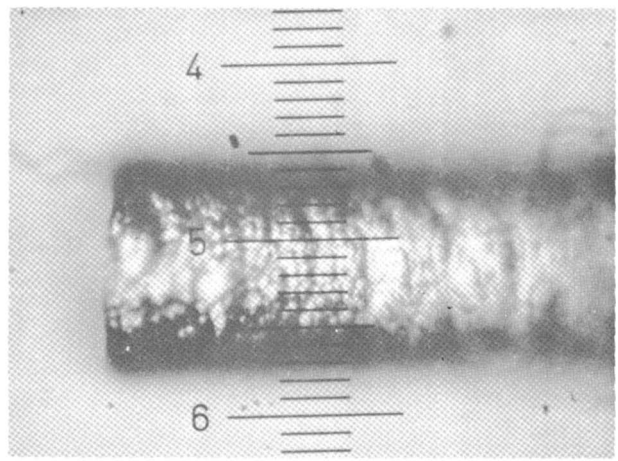

Figure 3b. Boron on quartz; surface of deposit at broken end (165×)

ELECTRODE CONFIGURATION. The preliminary experiments performed used electrodes made from copper foil. The electrodes are shown in

Publication Date: June 1, 1969 | doi: 10.1021/ba-1969-0080.ch015

Figure 4a. It was the purpose of one of the series of experiments conducted to determine if other electrode configurations would be desirable. The configurations shown in Figures 4b, 4c, 4d, and 4e were used. The qualitative observations were sufficient to determine that electrodes, using No. 16 copper wire, hooked up as in Figure 4a produce a minimal amount of sidewall deposition, and influence of the electrodes on the deposit underneath is also reduced; Figure 4a was therefore selected as the best electrode configuration.

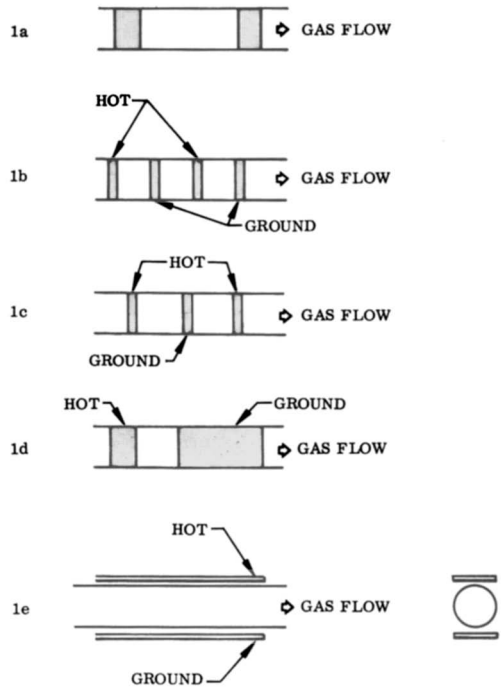

Figure 4. Electrode configuration

ELECTRODE SEPARATION. The effect of electrode separation on the deposition of boron is shown in Table I. The gas flow, reactor pressure, and electrical parameters were the same in all cases. The data show a rise in efficiency as the electrode separation is increased, but the rate of increase decreases with the electrode distance. Increasing the distance beyond approximately 3 cm. does not increase the efficiencies or the length of substrate upon which deposition occurs. The last experiment shown in Table I indicates considerable improvement in efficiencies at 2.5 cm. electrode distances. The reactor is indented at the electrode

Publication Date: June 1, 1969 | doi: 10.1021/ba-1969-0080.ch015

positions in this section so that the distance from the electrodes to the filament is less than the filament-electrode distances of the other sections. This results in considerable improvement in efficiencies.

Table I. Effect of Electrode Separation[a]

Electrode distance (cm.)	*Deposit length (cm.)*	*Deposit weight (μgm./cm.)*	*Total thickness (mils)*	*Material efficiency % per pass*	*Electrical efficiency % per pass*
0.62	0.85	35.3	1.8	0.34	0.76
2.22	2.15	23.4	1.67	0.59	1.52
3.16	2.22	25.3	1.72	0.66	1.41
2.54[b]	2.15	46.5	2.22	1.15	2.55

[a] H_2 flow rate 10 cc./min.; BCl_3 flow rate 18 cc./min.; pressure 20 mm. Hg.
[b] Reactor walls grooved at electrode positions.

Ratio of BCl_3 to Hydrogen. The ratio of BCl_3 to hydrogen in the range of 0.08 to 0.22 has very little effect on the efficiency of the reaction. This is shown in Table II. The increase in efficiency at the very low ratio is probably because of the use of the pinched electrode positions in the reactor walls. The efficiencies are low, the quantities measured are quite small and the material efficiencies shown are not significantly different. No efficiencies were measured at higher ratios. In keeping with this observation, the electrical energy is primarily used in activating atoms or molecules and producing electrons which then react with the other gases. Since hydrogen is the predominant gas it can be presumed that the particular frequency employed in the system results in ionization of the hydrogen.

Table II. Effect of Flow Ratio[a]

Mole ratio BCl_3/H_2	*Reaction time (min.)*	*Material efficiency % per pass*	*Electrical efficiency % per pass*
0.22	7.80	0.046	1.2
0.19	5.0	0.044	1.1
0.12	10.0	0.06	1.1
0.08	20.0	0.14	1.2

[a] Pressure 20 mm. Hg; electrode distance 2.5 cm.

As the mole ratio of BCl_3 to hydrogen is increased from 0.22 to 0.66 (near stoichiometric) and by reducing the hydrogen gas flow, the appearance of the glow and the character of the deposit are changed significantly. The hydrogen flow rate is an estimated value because the calibration curve does not extend to these low flowmeter readings. However, by

In Chemical Reactions in Electrical Discharges; Blaustein, B.;
Advances in Chemistry; American Chemical Society: Washington, DC, 1969.

cutting the hydrogen flow rate in half, making the flow ratio near stoichiometric for the reaction while maintaining a constant pressure, the glow is intensified around the filament substrate and will migrate along the substrate beyond the RF. electrodes. The deposit character produced by this procedure is shown in Figure 5. Varying types of deposits are illustrated which are formed at different points on the substrate under near stoichiometric flow conditions.

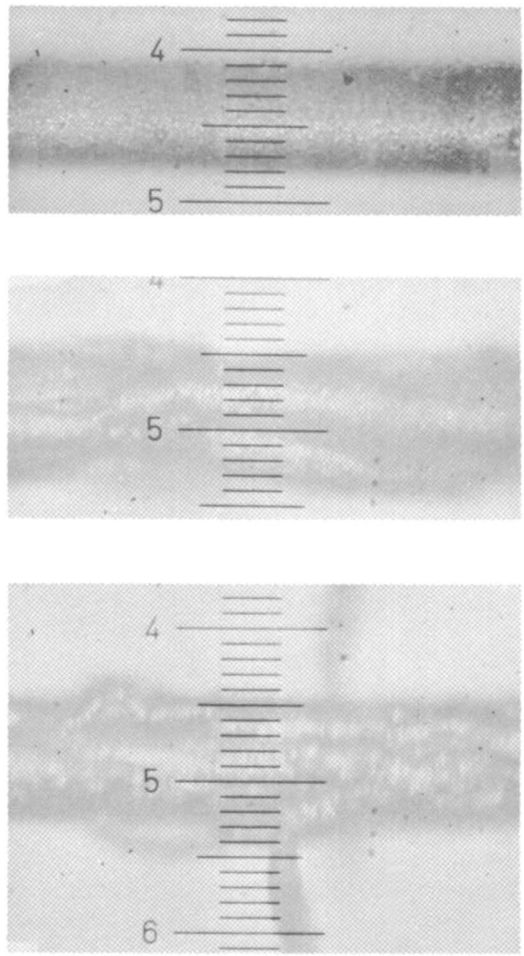

Figure 5. Filaments produced at near stoichiometric flow ratios (143×)

The deposition rate is significantly affected by the flow ratio as shown in Table III.

Publication Date: June 1, 1969 | doi: 10.1021/ba-1969-0080.ch015

In Chemical Reactions in Electrical Discharges; Blaustein, B.;
Advances in Chemistry; American Chemical Society: Washington, DC, 1969.

Table III. Effect of Flow Ratio on Deposition Rate[a]

Mole flow ratio BCl_3/H_2	*Deposition rate (mils./min.)*
0.22	0.05
0.33	0.04
0.66 (est.)	0.19

[a] Pressure 20 mm. Hg; electrode separation 19 mm.

EFFECT OF SYSTEM PRESSURE. The effect of system pressure on deposit characteristics is shown in Table IV.

Table IV. Effects of System Pressure[a]

Pressure (mm. Hg)	*Type of deposit*
5	Needles, trees, and dendrites Exploded from substrate if run was long
20	Thick, fairly uniform, some craters or knobs
30	Thick, small mounds, no craters

[a] H_2 flow rate 10 cc./min.; BCl_3 flow rate 18 cc./min.

EFFECT OF POWER INPUT. At all pressures and flow rates employed, a reduction in RF. current by capacitance control, or a reduction in d.c. voltage to oscillator results in a non-metallic, hydrolyzable material which is clear with a yellow tinge in appearance.

INTERACTION OF PARAMETERS. The gas phase being ionized is an integral part of the electrical circuit. Thus, as gas composition, pressure, or electrode spacing is varied, the impedance of the gas phase is also changed. The necessary voltage and RF. current are thus changed. These changes are reflected in the type of deposit obtained.

Discussion

General. The results of these experiments show that boron can be deposited on a dielectric substrate in a glow discharge (*see* Figure 3). There is no limit on the coating thickness inherent in the process. Complete control of the process parameters has not been achieved, but there is no reason to believe that control cannot be achieved. The results obtained so far indicate that gas purity, gas composition, and RF. power input are among the most important factors.

Gas Purity. The deposit obtained can be considered to be in chemical equilibrium with the gas composition. The introduction of certain impurities such as oxygen or water will result in certain amounts of oxygen in the deposit (*see* Figure 2). The solid solubility of oxygen in

In Chemical Reactions in Electrical Discharges; Blaustein, B.;
Advances in Chemistry; American Chemical Society: Washington, DC, 1969.

boron is probably not great. If an appreciable concentration of oxygen or water is present, the equilibrium solid phase resulting from the processing will logically be the oxide and not the element. Experimental experience has shown that this concentration value is probably not very great, and a tight process system must be used with the reduced pressure process—*i.e.*, a leak rate < 0.05 mm. Hg/min.

Gas Composition. The effect of gas composition—*i.e.*, the ratio of hydrogen to boron trichloride—will influence the type of reaction that occurs and the type of product formed. It has been observed that the amount of (1) sidewall deposition and (2) fine particles that fall out of the gas downstream of the glow increase with increasing hydrogen concentrations. This indicates that reduction in the gas phase increases with the higher hydrogen to boron trichloride ratios. With increasing hydrogen ratios, the glow is more uniform over the space and the formation of fine particles is encouraged.

Increasing the ratio of boron trichloride to hydrogen causes the glow to concentrate toward the center around the substrate. This concentration of the glow toward the center discourages the formation of small particles by the boron atoms directly on the substrate. As the flow ratio approaches the stoichiometric value of 1.5 moles of H_2 per mole BCl_3, the glow concentrates very close to the substrate and migrates along the filament beyond the electrode rings. At the same time the deposition rate increases about fourfold or more. Post-treatment of the deposit in a hydrogen glow modifies the surface character as shown by the cross section in Figure 6.

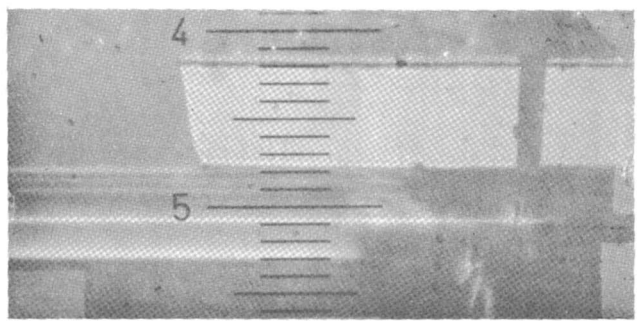

Figure 6. Longitudinal cross section of deposit after exposure to H_2 glow discharge

The resistance of the filament decreases as the boron coating is formed, which allows more current to flow. This increases the filament temperature, which encourages more rapid deposition of boron. Under

Publication Date: June 1, 1969 | doi: 10.1021/ba-1969-0080.ch015

In Chemical Reactions in Electrical Discharges; Blaustein, B.;
Advances in Chemistry; American Chemical Society: Washington, DC, 1969.

these conditions, the reaction goes out of control and the filament heats to a general red-orange glow with brighter spots and finally breaks.

Careful adjustment of the reactant gas concentration and the rf power input to the coil will minimize the gas phase reaction, sidewall deposition, and fine-particle formation.

Power Input. The power input to the glow is of great importance in determining the product and character of the product. The RF. voltage at any gas composition and electrode geometry must be a value greater than the breakdown potential of the gases at that pressure. The RF. current is a direct measurement of the ionization of the gases to produce electrons and positive ions, respectively. At higher currents, a faster coating rate will be attained, but changes in deposit characteristics will occur as a result of such changes in plating rate. Perhaps part of the nonuniformity of the deposit can be attributed to a nonuniform plating rate. The uniformity should be improved by moving the filament substrate through the glow.

In addition to these considerations, experiments have shown that, by operating at reduced RF. currents, a deposit similar in appearance to that of $(BCl)_n$ can be obtained with gas compositions that would normally deposit elemental boron.

Pressure. Since pressure is a concentration function, it may be expected to influence the type of deposit and the rate of deposition. At low pressures, needle-like deposits are observed. As the pressure is increased, the type of deposit changes and a coating or continuous layer is formed. Increasing the pressure further provides a smoother deposit. However, as the pressure is increased the voltage necessary to maintain a glow discharge is increased.

In summarizing the results and literature survey, it is possible by glow-discharge techniques to obtain a variety of products from boron trichloride and hydrogen gas streams. These products can range from a polymer-type $(BCl)_n$, a liquid B_2Cl_4, or a solid $BCl_{0.6}$ to the boranes. In between these gas compositions that will give the foregoing products is the gas-composition range that will give boron as a product. In addition to the gas composition, the amount of RF. power used will also determine the product. It is fortunate that the gas composition obtainable with our experimental apparatus is in the range for boron deposition; otherwise selection of gas composition from present information would be impossible.

Filament Evaluation

Density. The density of filaments produced by this process has been measured by two techniques. A direct measurement was made by drop-

Publication Date: June 1, 1969 | doi: 10.1021/ba-1969-0080.ch015

ping a boron-coated borosilicate glass rod in a density gradient tube, and an indirect measurement made by microscopic-geometric technique. The average density was 2.24 gram/cc., which agrees satisfactorily with the value estimated from the density of boron, 2.35 gram/cc., and the quartz substrate, 2.24 gram/cc.

X-ray Identification. A typical x-ray analysis is shown in Table V. The diffuse lines observed in the x-ray pattern correspond to the alpha rhombohedral structure. This is the low-temperature form of boron. However, the structure is not well developed as indicated by the broad lines. The boron may have been in the process of changing from an amorphous boron.

Other samples of boron-coated 1.0-mil quartz filament show only two broad diffuse halos. No lines indicating B_2O_3 were seen. No positive identification of the material was possible from the data.

Table V. X-ray data of Deposit

X-ray data		*Deposited boron coating*			
d	*Unknown density*	B_2O_3		*Boron*[a]	
		d	I/I_o	*d*	I/I_o
6.0	Medium	6.08	35		
4.1	Strong (broad)			4.07	100
3.2	Medium	3.21	100		
2.55	Strong (broad)			2.55	70
1.95	Weak	1.98	8		
1.40	Very weak (broad)				

[a] Alpha rhombohedral form.

Chemical analysis of the deposited boron was not made. However, the distinctive characteristics of the material formed at non-optimum conditions coincides with the description of the solid subchlorides. Characterization of the deposit in regard to subhydride formation is much more difficult as identification of these materials is not well established for hydrides higher than the dodecaborane.

The product formed at the conditions used in this study has only been characterized by preliminary tests; these tests do indicate that the deposit is in the alpha rhombohedral form., Complete characterization must be performed during future studies.

Coating Evaluation. A typical sample cross section prepared during the process study is shown in Figure 7, demonstrating that a continuous coating can be successfully deposited. In the longitudinal cross section two mounds are fortuitously shown and it can be seen that the growth originates at the substrate surface, possibly as a microcrack or particle of

Publication Date: June 1, 1969 | doi: 10.1021/ba-1969-0080.ch015

In Chemical Reactions in Electrical Discharges; Blaustein, B.;
Advances in Chemistry; American Chemical Society: Washington, DC, 1969.

dust. The bond between the coating and the substrate is essentially mechanical in nature.

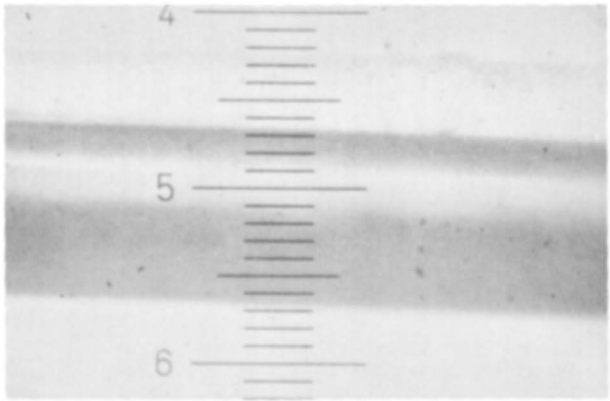

Figure 7a. Longitudinal section of boron-coated quartz monofilament (165×)

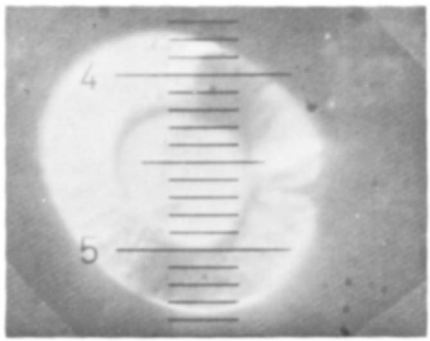

Figure 7b. Cross section of boron-coated quartz monofilament (165×)

The pictures in Figure 8 are typical of what is occasionally seen on samples. The chip and hole in the top and middle picture were not measured, but the rather deep cut made indicates that the quartz monofilament possesses weak portions. The hole and ball shown in the bottom figure have been measured during the microscopic examination. The ball was about 1.0 mil in diameter, the hole was observed to 0.8 mil, while the filament cross section averaged 1.8 mils. The coating thickness can be only 0.4 mil, so that the hole must have been formed by the loss of 0.4 mil of the quartz substrate.

Complete evaluation of the product in terms of physical and mechanical properties could not be made on the small samples produced in a static system of this size. Serious end effects observed and described

Publication Date: June 1, 1969 | doi: 10.1021/ba-1969-0080.ch015

earlier compromise any mechanical or physical measurement. These end effects can probably be averaged out over the whole filament and reduced in intensity by processing the filament continuously. By doing this the uniformity of the deposit is increased and thus any measurement performed becomes meaningful.

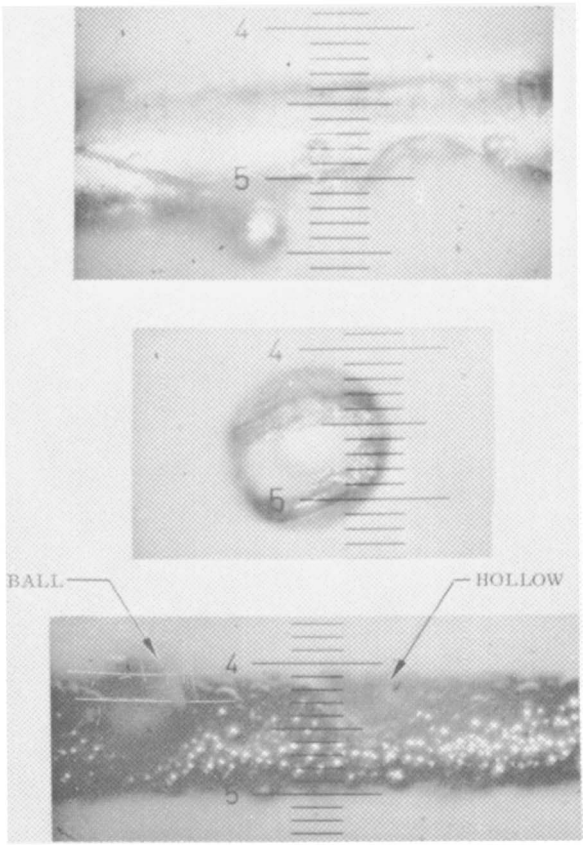

Figure 8. Boron-coated quartz monofilament (221×)

TOP—Hollow in boron-coated quartz monofilament
MIDDLE—Material from hole
BOTTOM—Ball and hollow in thick coating on quartz monofilament

Conclusions

This paper basically represents a feasibility study of the deposition of boron from a glow discharge system produced in a boron trichloride-hydrogen medium. Feasibility of the basic concept has been conclusively

Publication Date: June 1, 1969 | doi: 10.1021/ba-1969-0080.ch015

demonstrated for dielectric or insulating substrates. It is probable that conditions can be adjusted to provide for deposition on metallic or conductive substrates as well. The following secondary conclusions can also be drawn from this work:

(1) Glow discharges can be initiated and sustained in hydrogen-boron trichloride mixtures at pressures of 5–100 mm.

(2) There is no apparent limit on coating thickness which can be deposited.

(3) The deposited boron is amorphous with a partial alpha rhombohedral crystalline character.

(4) Deposition rate is of the order of 5×10^{-5} gram/sec.

(5) Filament resistance decreases with thickness; temperature in turn increases resulting in a higher deposition rate; this also results in increased bonding to the substrate by chemical or diffusive action.

(6) The process is quite sensitive to small amounts of impurities in the gas stream, particularly oxygen and moisture.

(7) The ratio of hydrogen to boron trichloride has a major effect on nature of the deposit; both sidewall deposition and downstream particle fallout increase with hydrogen concentration. However, the glow is more uniform at high hydrogen values, so these factors must be balanced for optimum performance.

(8) An increase in the boron trichloride-to-hydrogen ratio tends to concentrate the glow around the substrate, promoting efficiency and minimizing the extraneous deposition.

Publication Date: June 1, 1969 | doi: 10.1021/ba-1969-0080.ch015

Acknowledgment

This work was sponsored by the U. S. Air Force under Contract AF 33(615)-2130. Acknowledgment is given to J. G. Bjeletich, W. C. Coons, J. Robinson, B. A. Traina, R. N. Varney, and R. D. Wales for assistance on photographic and experimental portions of the program. All are members of the Lockheed Palo Alto Research Laboratory. Further acknowledgment is made to R. M. Neff of the Air Force Materials Laboratory for continuing consultation on progress of the program.

Literature Cited

(1) Apple, F. F., PhD Thesis, Pennsylvania State University (1955).
(2) Frazer, J. W., Holzmann, R. T., *J. Am. Chem. Soc.* **80,** 2907 (1958).
(3) Holzmann, R. T., Morris, W. F., *J. Chem. Phys.* **29,** 677 (1958).
(4) Kotlensky, W. V., Schaeffer, R., *J. Am. Chem. Soc.* **80,** 4517 (1958).
(5) Kroll, W., *Z. Anorg. Allgem. Chem.* **101,** 1 (1918).
(6) Markovskii, L. Ya., L'viva, V. I., Kondrashev, Yu. D., *Bor. Tr. Konf. po. Khim. Bora; Ego Soedin.* (**1958**) 36; *cf.* FTD-MT-64-427, Foreign Technol. Div., AF System Command, 1965.
(7) *Rept. Intern. Symp. Electrical Discharges in Gases, Delft, Netherlands,* April, 1955; The Hague (1955).
(8) Rosenberg, R. M., PhD Thesis, Pennsylvania State University (1959).

(9) Rosenberg, R. M., *Dissertation Abst.* **20,** 526 (1959).
(10) Schlesinger, H. I., Bing, A. B., *J. Am. Chem. Soc.* **53,** 4321 (1931).
(12) Stock, A., Brandt, A., Fischer, H., *Ber. Deut. Chem. Ges.* **58B,** 653 (1925).
(13) Stock, A., Martin, H., Sutterlin, W., *Ber. Deut. Chem. Ges.* **67,** 396 (1934).
(14) Urry, G., Wartik, T., Schlesinger, H. I., *J. Am. Chem. Soc.* **76,** 4293 (1954).
(15) Wartik, T., Moore, R., Schlesinger, H. I., *J. Am. Chem. Soc.* **71,** 3265 (1949).
(16) Weintraub, F., *Trans. Am. Electrochem. Soc.* **21,** 165 (1909).

RECEIVED May 22, 1967.

16

Plating in a Corona Discharge

R. D. WALES

Materials Sciences Laboratory, Lockheed Palo Alto Research Laboratory, Palo Alto, Calif. 94304

Publication Date: June 1, 1969 | doi: 10.1021/ba-1969-0080.ch016

It has been demonstrated that boron can be deposited on tungsten in a corona discharge. Application of high voltage electrical energy across a gaseous hydrogen-boron halide mixture forms ionized/activated states, resulting in the deposition of metallic boron. The deposition process is electrochemical in nature, the boron being deposited cathodically. The morphology of the deposit is essentially the same as that of the substrate. There is no interaction of the boron with the tungsten and there is apparently some anisotropy of the deposit. Like a corona discharge in an inert gas, the coefficient of electron emission and the ability of the electrons to diffuse along the wire are most important in obtaining a uniform corona, and thus a uniform deposit, on the substrate.

Most of the extensive literature on electric discharges (*1, 4, 6, 10*) concerns the nature and properties of discharges taking place in stable gas systems. Relatively little information is available concerning chemical reactions initiated and sustained by electrical discharges, particularly those reactions in which a solid product is formed. Arc reactions are basically thermally initiated reactions deriving their thermal energy from the arc. Glow discharges have been utilized for the polymerization of organic materials and the deposition of oxide films. The formation of pure boron powder (*11*) and the decomposition of diborane (*7*) and boron trichloride (*5*) have been studied in a glow discharge. No references have been located concerning chemical reactions initiated and sustained by a corona discharge.

Those references (*2, 3, 9*) which refer to the utilization of a corona discharge to catalyze, or cause, a chemical reaction are not in fact concerned with a corona discharge, or a glow discharge, but rather a suppressed spark. The discharge goes through the phenomena of spark

In Chemical Reactions in Electrical Discharges; Blaustein, B.;
Advances in Chemistry; American Chemical Society: Washington, DC, 1969.

buildup without generating a spark. Direct current cannot be used since the buildup of charge at the insulated electrodes quenches the discharge, and a reverse cycle is necessary to remove this charge and reinitiate the discharge.

A corona discharge is, essentially, intermediate between a glow and an arc discharge being, however, a low-current phenomenon. Glow discharges are usually generated at low pressures with the gas ionized fairly uniformly throughout the system. An arc is obtained when a narrow path of ionized particles is generated between two electrodes, resulting in a low-resistance path in which extremely energetic particles exist. A corona discharge is obtained at a small electrode opposed by a much larger one. There is a very large change in field through the corona, but very little change over the remaining distance to the opposing electrode. Most studies of corona discharges have been in inert gas systems, where discharges have been generated at a point electrode.

The object of this study was the deposition of a coating of boron on a tungsten substrate in a corona discharge, determination of certain critical parameters, and determination of the mechanism and characteristics of this technique for coating the substrate material.

Publication Date: June 1, 1969 | doi: 10.1021/ba-1969-0080.ch016

Experimental

Figure 1 is a schematic diagram of the system used in this study. The system pressure was controlled with a Cartesian Manostat 6A (Manostat Corporation) and a Welch mechanical pump Model 1402 (W. M. Welch Manufacturing Company). The discharge was initiated and sustained with a 7,000/12,000 volt Jefferson luminous tube outdoor-type transformer (Jefferson Electric Company) connected to a 60-c.p.s. 110-volt power source through a Variac variable transformer.

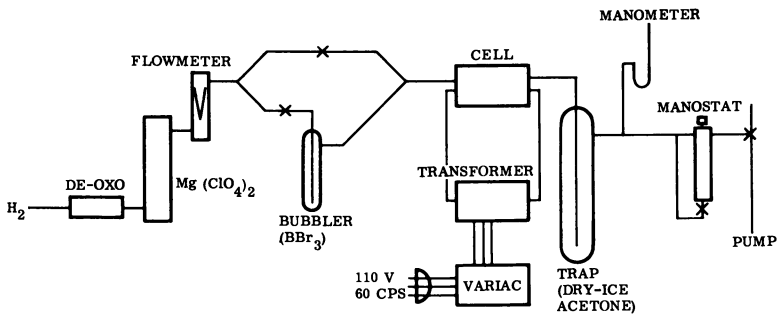

Figure 1. Schematic of system utilized for plating in a corona discharge

To determine the effect of alternating and direct current, an RCA CR 212 half-wave rectifier was added to the circuit, plus a resistance

bridge, a current-measuring resistor, and an ammeter. A schematic of the circuit is presented in Figure 2.

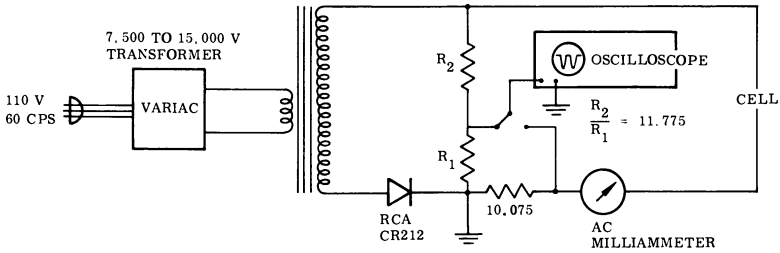

Figure 2. Schematic of power input and measuring circuit used with the corona discharge plating apparatus

The reactants were hydrogen, helium, or argon, and boron tribromide. The hydrogen was passed through a "De-oxo" unit (Engelhard), a drying column of magnesium perchlorate, and a flow meter. After the flow meter, the hydrogen was split into two streams, one of which was bubbled through the boron tribromide, and then recombined into one stream before entering the reaction chamber or cell.

The temperature of the bubbler, the cell, and the associated gas lines, was controlled by wrapping each with heating tape and controlling the power input with a Variac variable transformer. The system was maintained at or below atmospheric pressure for this study, with most of the data being obtained at 2 to 3 in. of mercury below atmospheric pressure (2 to 3 in. of mercury vacuum).

Tungsten wire, the substrate material, was cleaned by being passed successively through a train of concentrated nitric acid, a distilled water rinse, and an acetone rinse.

Using the hydrogen-boron tribromide reactant system and 60-c.p.s. alternating current to develop a corona, approximately a dozen cell designs were tried. The most satisfactory cell design (Figure 3) consists of a 2-in.-long borosilicate glass tube with a neoprene o-ring inside each end. The tube is wrapped with eight turns of 3-mil tungsten wire such that the wire is parallel and concentric to the tube's axis. The wire is 0.9 cm. from the axis. This assembly is then inserted in a 5-in.-long borosilicate glass tube 1.5-in. in diameter and supported such that the tubes are concentric. A tungsten wire lead is extended out of the tube, and neoprene rubber stoppers inserted in each end. Each stopper has a capillary tube through its center such that there are approximately 3 in. between the capillaries, and the filament enters and leaves the cell through these capillaries. The reactants also enter (and leave) the cell through the stoppers.

Primary Variable Considerations

Deposition Utilizing Alternating Current. Hydrogen and boron tribromide vapors were used to obtain a coating of boron on 1-mil tungsten wire in a corona developed with 60-c.p.s. alternating current. At

Publication Date: June 1, 1969 | doi: 10.1021/ba-1969-0080.ch016

~70 and 350 ma./sq. cm., no coating was obtained when the cell (and reactants) were at room temperature, while a coating of boron was obtained if the temperature was raised to approximately 100°C. At higher current densities, the coating is concentrated in nodules. If enough power is supplied to heat the filament to a dull red glow, a good coating is obtained in the hot zone. At lower current densities, a more uniform coating is obtained, depending upon the reactant ratios and flow rates. Thus, hydrogen was bubbled through boron tribromide at ~400 ml./min., and the system was maintained at approximately atmospheric pressure. When the boron tribromide was maintained at room temperature and at a total hydrogen flow rate of ~1.5 liter/min., the corona was discontinuous along the wire, and boron deposited in the area of the coronas to give discrete coated and uncoated areas. With a hydrogen flow rate of ~400 ml./min. and a plating time of ~10 min., a much smoother coating was obtained. There was some tendency for the corona to break into discontinuous sections, which resulted in a nonuniform buildup of boron.

Publication Date: June 1, 1969 | doi: 10.1021/ba-1969-0080.ch016

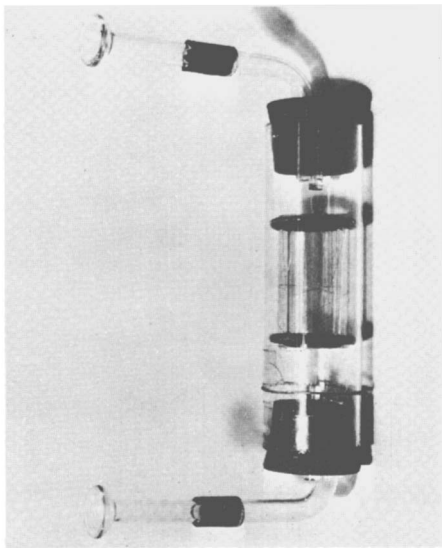

Figure 3. Reaction cell used for plating in a corona discharge

When the boron tribromide was heated to ~30°C. and the hydrogen flow rate was maintained at 400 ml./min., the corona was more continuous and the coating nearly uniform. However, the coating was not nearly as smooth as in the previous example.

Corona points tended to form on the opposing electrode system with a resulting deposition of boron under the corona.

In Chemical Reactions in Electrical Discharges; Blaustein, B.;
Advances in Chemistry; American Chemical Society: Washington, DC, 1969.

Deposition Utilizing Direct Current. Using hydrogen and boron tribromide as reactants to obtain a deposit of boron on 1-mil tungsten wire in a corona developed with half-wave rectified 60-c.p.s. alternating current, no deposit was obtained when the 1-mil wire was the anode. However, a coating was obtained when the 1-mil wire was the cathode. Good, continuous corona and boron deposits were obtained when the corona was initiated in a large excess of hydrogen (the hydrogen flow was then decreased to the desired amount after about 5 min.).

The coating is quite uniform and has an orange peel appearance at 2,000× magnification. Some of the morphology of the substrate is apparent at high magnification—*e.g.*, die marks. The voltage requirements for a particular current increased as the hydrogen flow decreased, increasing from more than 1,000 volt peak to about 7,000 volt peak as the excess hydrogen was decreased in these runs.

Attempts to utilize pure d.c. power were unsuccessful. The power supplies available were designed to deliver several hundred milliamperes and had relatively coarse controls which did not permit sufficient control, resulting in "runaway" or burning in two of the substrate wire.

Deposition Utilizing Argon and Helium. Using helium instead of hydrogen, a coating was obtained, but arcing was more troublesome and thus lower current (and lower flow rates) were necessary. Peak voltages of 7,000 to 8,000 volts were used.

Using argon instead of hydrogen required higher voltage (with lower currents) and resulted in the formation of corona points under which boron was deposited to give whiskers. Peak voltages of ~9,000 volts were used. Whiskers greater than 6 mils long and ~0.5 mil in diameter were obtained before discontinuing these experiments.

Bromine was a product when helium or argon was used; hydrogen caused the formation of hydrogen bromide.

Discussion. (1) CELL DESIGN. The reaction cell should be designed so that the concentration of reactants and products is essentially constant throughout the cell to give a more uniform corona and deposit. The electrode geometry and separation are partially dependent upon the power requirements, which are in turn dependent upon the resistance heating effects in the filament and upon the arcing probability. Thus, in practice, the current in the filament should not be great enough to heat the filament excessively. With this current limitation, the electrode separation is dependent upon the arcing probability and should be great enough to level out any small variations in electrode separation which could cause the current to concentrate in a small region. Furthermore, to obtain a uniform corona around the filament, the opposing electrode should be concentric around the filament. If the power input is not pure direct current, a "motoring" effect results if the opposing electrode is a

Publication Date: June 1, 1969 | doi: 10.1021/ba-1969-0080.ch016

In Chemical Reactions in Electrical Discharges; Blaustein, B.;
Advances in Chemistry; American Chemical Society: Washington, DC, 1969.

wire coiled around the filament, and a vibration or circular oscillation is induced. Therefore, the opposing electrode has been made up of a group of connected electrodes arranged concentrically around the filament and parallel to it to minimize this condition. The opposing electrode could also have been a metal cylinder or screen, but in order both to observe the filament and be able to operate at reasonable electrode separations (reasonable voltages), interconnected parallel wire electrodes were selected.

(2) MECHANISM OF DEPOSITION. The results obtained indicate that the mechanism of boron deposition in a corona discharge is cathodic. In this type of system, electrons are generated and repelled from the cathode while positive ions are drawn to it. At the anode, positive ions are generated, or electrons are drawn to it. Thus, the boron radical is positively charged and drawn to the cathode where it is deposited as elemental boron.

Helium and argon were used to determine if the boron tribromide was ionized directly, or if its ionization was a secondary reaction (Table I). Helium in a corona discharge has only one or two potential (or ionization) levels, and these are quite high. However, helium is ionized at lower applied voltages than most gases because the electrons generated at the cathode have only elastic collisions with helium atoms until they acquire enough kinetic energy from the field to ionize the helium. Argon has a potential (or ionization) level which is relatively low (about half that of helium) but higher than the ionization levels for hydrogen. In helium, the system was very susceptible to arcing, while in argon higher voltages were required with some susceptibility to arcing. In hydrogen, arcing was not such a problem because of the many types of inelastic collisions possible and the consequent tendency to decrease the electron energy and concentration. Boron was deposited in all three systems. However, in hydrogen, hydrogen bromide was obtained while bromine was obtained in both argon and helium. Deposition was easier and there was a slightly increased rate of deposition of boron with an increased tendency to arcing in helium and argon. The difference, however, was not sufficient to be attributed to direct reaction with the free electron, and indicates that the boron tribromide is ionized by collision with ionized particles rather than electrons or through the effect of the field. Thus, the mechanism includes: (a) the ionization (or activation) or the hydrogen (helium or argon), (b) the collision or exchange of energy of the ionized particle with boron tribromide to result in (c) the formation of a positively charged boron radical and hydrogen bromide (or bromine), (d) the transport of the charged boron radical to the cathode in the field, and (e) the electrochemical deposition of boron on the cathode.

Publication Date: June 1, 1969 | doi: 10.1021/ba-1969-0080.ch016

In Chemical Reactions in Electrical Discharges; Blaustein, B.;
Advances in Chemistry; American Chemical Society: Washington, DC, 1969.

Table I. Ionization Levels for Helium, Argon, and Hydrogen (*1*, *8*)

Gas	First Excitation Potential, e.v.	Ionization Potential e.v.			Metastable Level e.v.
		I	*II*	*III*	
He	20.5	24.5	54.1		19.7
A	11.6	15.7	27.7	40.7	11.5
H_2	11.5	15.4			11.9
H	10.2	13.5			10.15

It is apparently necessary to add a small amount of kinetic (thermal) energy to aid the deposition in hydrogen. However, this reactant system offers certain advantages over helium or argon systems. That is, with hydrogen, there are apparently more ionized or activated particles with fewer electrons and consequently less likelihood of creating conditions conducive to arcing.

(3) The Corona. In the high field region near the substrate wire positive ions can attain high energies and the secondary electron emission process is quite efficient. These secondary electrons will start electron avalanches, which will in turn produce many positive ions, which produce more avalanches, etc. At low pressures, diffusion of the electron avalanches spreads the glow and distributes the positive space charge so that the discharge is not quenched. Diffusion does not take place at higher pressure, and a localized dense space charge extinguishes the corona. The extinction lasts until the positive space charge diffuses to the electrode and the last ions reinitiate the discharge, resulting in a periodic corona with a frequency dependent upon the field and the velocity of the positive ions.

With the negative wire (cathode), the ionization increases first with distance from the wire, reaches a peak, then drops sharply. That is, the electrons move out from the wire and produce relatively stationary positive ions between themselves and the wire, thus weakening the field at greater distances. The maximum ionization occurs at several ionizing free paths from the wire, and there is a dark space between the wire and the luminous glow. Furthermore, as mentioned, at low pressures the lateral diffusion of electron avalanches spreads the corona over the wire surface. Since the value of the coefficient of electron emission is important, and since the glow will not be uniform if the coefficient of electron emission varies over the surface of the wire, the glow may settle in patches of greater or lesser luminosity and at high pressures will appear as a single small area of corona. The corona may exhibit a marked flickering near threshold, since the positive ion bombardment may change the effective coefficient of electron emission by denuding the surface of its gas film. The discharge thus decreases or ceases in that region, re-

Publication Date: June 1, 1969 | doi: 10.1021/ba-1969-0080.ch016

In Chemical Reactions in Electrical Discharges; Blaustein, B.;
Advances in Chemistry; American Chemical Society: Washington, DC, 1969.

suming again when the surface has recovered. At low pressures and voltages well above the threshold value, the corona is fairly steady.

It was necessary to clean the substrate wire so that there were no variations in the coefficient of electron emission along the wire, and thus a localization of the corona into points. During deposition the corona was distributed over the substrate wire in a uniform manner. However, the discharge was periodic; the sheath (of light) along the wire not being of a uniform brightness but consisting of brighter and darker areas which seemed to move randomly along the wire and which appeared periodic in nature at a given point on the wire.

Secondary Variable Considerations

Publication Date: June 1, 1969 | doi: 10.1021/ba-1969-0080.ch016

Experimental. The deposition system was previously described. The tungsten wire was cleaned as before, then placed in the cell. The corona was initiated in excess hydrogen and maintained for about 5 min., or until continuous or nearly continuous along the substrate electrode, before the conditions were changed to give boron deposition. This initial "cleaning" process was effected with hydrogen flowing at ~160 cc./min. through the boron tribromide at ~26°C. and with hydrogen flowing through the bypass line at ~270 cc./min. The electrical input during this time was ~17 ma. peak and ~4,700 volts peak for 1-mil tungsten wire and ~5,600 volt peak and 4.5 and 11.0 ma. peak for 0.5-mil tungsten wire.

Results. (1) DEPOSITION ON 1-MIL TUNGSTEN WIRE. Some of the results obtained are presented in Table II. The corona was maintained continuously in all runs. In Run 28-1 the current fell from an approximate initial value of 12.3 ma. peak to a 3.5 ma. peak in 9 min., after which it was nearly constant. The peak voltage changed from 6,900 to 13,190 volts. The filament obtained in this run is apparently the desired type, although not of optimum thickness.

The data obtained in the experiments presented, and in other similar experiments, indicate that:

(a) The voltage requirements increase as the boron tribromide to hydrogen ratio increases.

(b) The voltage requirements increase as the system pressure increases.

(c) The substrate is etched with little or no boron deposited as the boron tribromide to hydrogen ratio decreases.

(d) The corona tends to break up into points at high flow rates, resulting in nonuniform boron deposits.

Good coatings were obtained at high boron tribromide to hydrogen ratios and relatively low currents.

In Chemical Reactions in Electrical Discharges; Blaustein, B.;
Advances in Chemistry; American Chemical Society: Washington, DC, 1969.

Table II. Some Effects of Varying Process

Run	Vacuum (in. Hg)	H_2 Flow Bubbler (cc./min.)	H_2 Flow Bypass (cc./min.)	Current Peak (ma.)	Voltage Peak (volts)
17-3	2.3	160	—	14.2	6,800
23-1	1.2	40	35	16	6,700
23-3	1.4	80	—	13.6	8,100
25-1	2.3	50	40	14.2	6,100
		50	—	13	7,900
28-1	2.6	50	40	12.3	6,900
		50	—	3.5	13,200

(2) Deposition on 0.5-mil Tungsten Wire. The corona was maintained continuously in Runs 30-1 and 30-2. The power input was discontinued in all remaining runs until the boron tribromide and the cell had attained the desired temperature. The currents and voltages indicated for all runs below 35 are approximate since no adjustments were made once the run had begun.

The effects of operating conditions are similar to those observed for deposition on 1.0-mil tungsten wire. However, the decreased heating effects of the 0.5-mil wire necessitated heating the cell to about 200°C. to prevent condensation of the boron tribromide.

In run 31-1, an apparently desirable coating was obtained at the ends of the reaction zone while the central portion of the filament was quite nodular. In Run 31-1 the peak current was 6.2 ma., falling to about 1.8 ma. at the end of the run. During this time the peak voltage changed from 12,480 volts to about 15,780 volts.

Runs 35-1 and 35-2 yielded filaments having uniform coatings of boron. The coating, as shown in Figure 4, had ridges along its surface resembling die marks on wire. Figure 5 shows a cross section of filament from Run 35-1 in normal and in polarized light. The higher magnifications indicate that the markings on the surface correspond to the markings on the substrate. Furthermore, there is no indication of boride formation. However, polarized light indicates some anisotropic properties similar to pyrolytic graphite. The material seems softer and much darker than that grown by gas plating techniques. Although there are some unidentified lines, x-ray data indicate that the coating is amorphous boron with no borides in the filament.

Publication Date: June 1, 1969 | doi: 10.1021/ba-1969-0080.ch016

In Chemical Reactions in Electrical Discharges; Blaustein, B.;
Advances in Chemistry; American Chemical Society: Washington, DC, 1969.

Conditions With 1-mil Tungsten Wire Substrate

Time (min.)	*Temp. BBr_3 (°C.)*	*Comments*
40	26	Corona uniform for about 6 min. then broke up. Coating not uniform, large nodules formed, because of discontinuous corona.
30	26	Corona fairly uniform, substrate etched, no coating.
58	26	Corona fairly uniform, coating fairly uniform, final diameter of about 1.2 mil.
7	—	To attain 47°C.
42	47	Overheated substrate in areas. Coating thick and mostly rough.
5	—	To attain 70°C.
78	70	Good coating, final diameter 1.33 mil.

(3) EFFECT OF MORPHOLOGY OF THE SUBSTRATE. The 0.5-mil tungsten substrate wire has been examined after various stages in the process.

It has been determined that the liquid cleaning train cleans and slightly etches the wire, and the high hydrogen corona etches the wire. At low peak currents the die marks were etched away, but the surface has a very rough orange peel finish. Using both high and low currents consecutively, a much smoother orange peel finish is obtained.

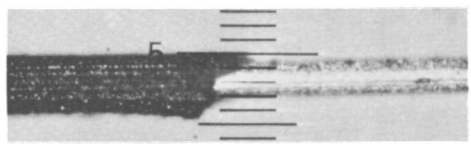

Figure 4. Boron deposit on 0.5-mil tungsten wire, Run No. 35-1 (270×)

Boron deposited on wire etched to an orange peel finish gives a coating similar to that pictured in Figure 6.

Examination of boron deposited on variously etched wire indicates that the coating morphology and growth structure are directly dependent upon the morphology of the substrate.

(4) VARIATION OF PLATING CONDITIONS. Combining the information obtained in the previous tests, several runs were made using variations of the plating conditions. The current-time and voltage-time characteristics for two runs are indicated in Figure 7. The filament obtained in Run 73-1 (final diameter 0.75 mil) was evenly and uniformly coated similar to the filament pictured in Figure 6. The filament obtained from Run 74-1

Publication Date: June 1, 1969 | doi: 10.1021/ba-1969-0080.ch016

(final diameter 1.0 mil) except for one defect was evenly and uniformly coated similar to the filament pictured in Figure 6. As indicated in Figure 7, the defect probably occurred after an elapsed time of about 21 min. at a cell voltage of about 23,600 volts.

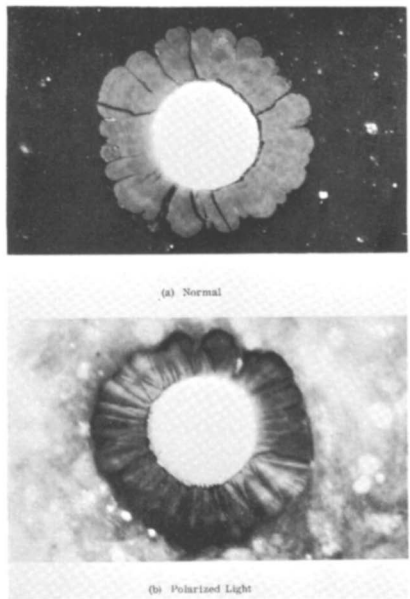

Figure 5. Cross section of filament obtained by plating in a corona discharge, cf. *Figure 4 (1080×)*

The results obtained indicate that the best process conditions and plating procedure for boron deposition on a stationary 0.5-mil tungsten wire are as indicated in Figure 7.

Discussion. The morphology of the deposit obtained reflects, in general, the morphology of the substrate. The coating is essentially amorphous in nature although there is indication of anisotropy.

One set of operating conditions giving a satisfactory coating of boron on tungsten is presently graphically in Figure 7. In general, good coatings have been obtained at high boron tribromide to hydrogen ratios and relatively low currents. Furthermore, if the flow rate is too great, the corona tends to break up into points, resulting in nonuniform deposits.

Continuous Boron Deposition on a Moving Filament

Experimental. Figure 8 is a schematic of the apparatus designed, assembled, and tested for continuous boron deposition on a moving fila-

Publication Date: June 1, 1969 | doi: 10.1021/ba-1969-0080.ch016

ment. The design resembles that for the batch plating process (Figure 1). The filament is pulled through the system with a Graham constant speed motor. The spool is mounted on a shaft and suspended in such a manner as to offer minimum friction. In the unique seal and electrical contact arrangement, the filament moves through the seal in a vertical direction without breaking the seal.

The power obtained for the cells had induced a considerable problem with 60-cycle pickup in the measurement system. Shielding and grounding at various critical positions were necessary to eliminate this problem.

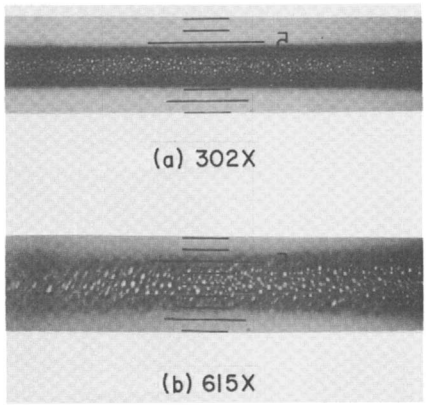

Figure 6. Boron deposit on 0.5-mil tungsten wire, Run No. 52-1

Hydrogen-boron trichloride was chosen as the reactant mixture and was obtained by bubbling hydrogen through boron trichloride maintained at about −20°C. The reaction cells have not been heated externally, and the vapor flow was split between all three cells.

The etching cell was not utilized as such, and was eventually converted to use for cleaning the substrate filament by the hot-wire technique, thus eliminating the chemical cleaning train. Hydrogen only was passed through the cleaning cell and the substrate heated to a red heat in this cell using d.c. power. Tests performed in this system have utilized both 0.5-mil and 0.15-mil tungsten substrates.

Results. (1) A.C. PICKUP. The use of shielded leads and wire cages around the transformers has, with the use of 1,000-ohm current measuring resistors, virtually eliminated the a.c. pickup.

(2) DEPOSITION ON 0.5-MIL TUNGSTEN WIRE. Satisfactory results have been obtained at a hydrogen flow rate through the bubbler of ~100 cc./min. and additional hydrogen at a flow rate of ~350 cc./min. Hydrogen is flowing through the cleaning cell at ~140 cc./min. and the

Publication Date: June 1, 1969 | doi: 10.1021/ba-1969-0080.ch016

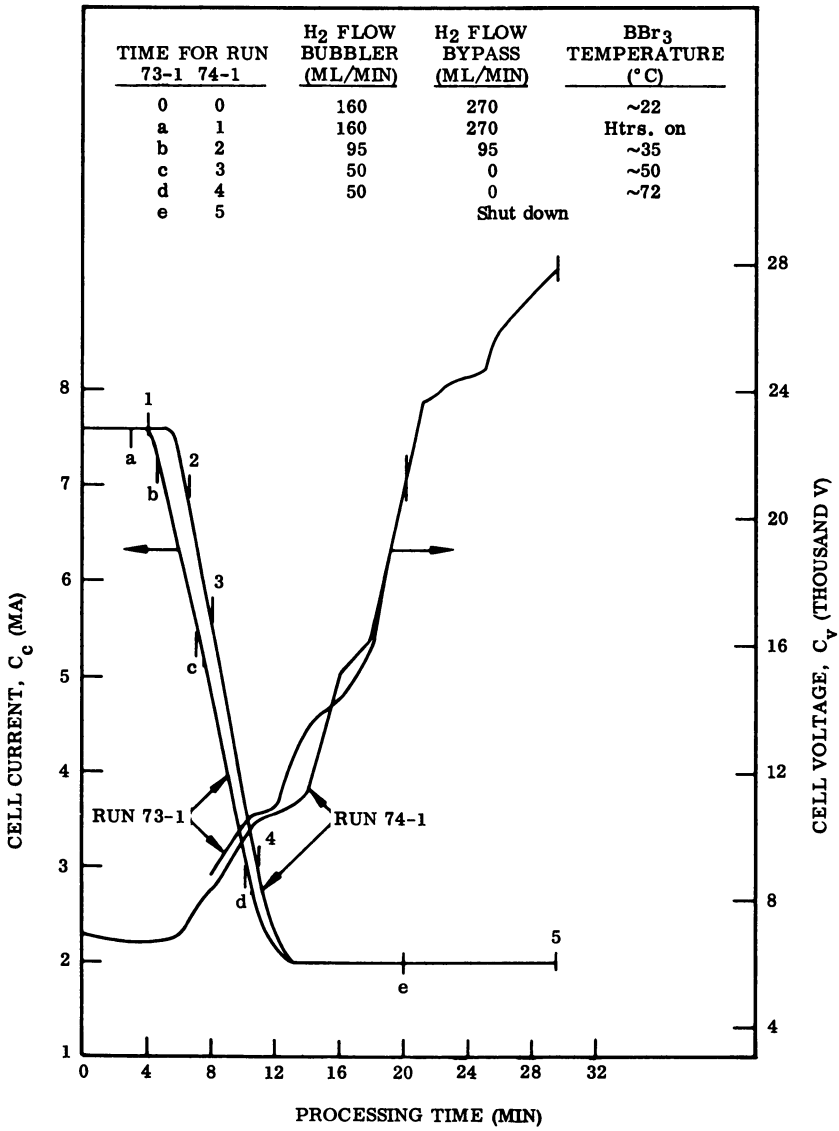

Figure 7. Electrical characteristics during deposition of boron on 0.5-mil tungsten wire in a corona discharge

wire is cleaned by resistance heating as a d.c. voltage of about 70 volts and a d.c. current of about 320 milliamperes.

Using only one cell, at a filament speed of 3.6 in./min. a 0.25-mil thick coating was obtained; at a filament speed of 14.4 in./min., a 0.05-mil thick coating was obtained.

Using two cells, there was some problem in maintaining the corona in the second cell. At a filament speed of 3.6 in./min. a 0.7-mil thick coating was obtained in the areas where a good corona was maintained. At a filament speed of 14.4 in./min. and a current input to the second cell of about half that to the first cell, a 0.07-mil thick coating was obtained.

(3) DEPOSITION ON 0.15-MIL TUNGSTEN WIRE. The 0.15-mil tungsten substrate wire was cleaned by the hot-wire technique at hydrogen flow rate of 140 cc./min. and at a d.c. power input of 208 volts and 90 milliamperes. While the input vapors were split between the three plating cells, only one cell was utilized for plating studies.

The best results were obtained at a filament speed of 5 in./min. with a hydrogen flow rate through the bubbler of 70 cc./min., and additional hydrogen at a flow rate of 350 cc./min. To maintain a uniform corona, it was necessary to switch the power on and off relatively slowly during the run. Under these conditions a 0.17-mil coating thickness was obtained.

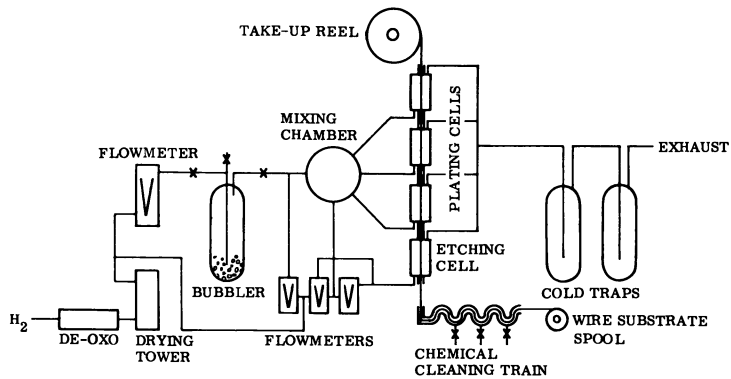

Figure 8. Schematic of continuous system for plating in a corona discharge

Discussion. An apparatus has been presented, and tests performed, indicating the feasibility of depositing boron on a continuously moving substrate in a corona discharge.

Although no tests were made for verification, the results obtained with the 0.15-mil substrate indicate that the substrate diameter also affects the operating conditions, probably through buildup of the positive ion sheath to such an extent that the corona cannot recover after being quenched. This effect is possibly related to the similar effect of high flow rates on larger substrates, noted in the previous section. The effects might be explained by postulating a higher concentration of boron radicals around the smaller substrate, simply through volume considerations, and around the larger substrate through an increased concentration re-

Publication Date: June 1, 1969 | doi: 10.1021/ba-1969-0080.ch016

In Chemical Reactions in Electrical Discharges; Blaustein, B.;
Advances in Chemistry; American Chemical Society: Washington, DC, 1969.

sulting from increased availability due to higher flow rates. The charged species would tend to remain in the volume near the substrate because of the greater effect of the electrical field.

Conclusions

Chemical reactions can be initiated and sustained by a corona discharge. Boron has been deposited on a tungsten wire substrate in a corona discharge at relatively low temperatures. The deposition process is electrochemical in nature, the boron being deposited cathodically, and the mechanism for the reaction is indicated to be of the form:

(1) Emission of electrons from the cathode.

(2) Ionization (or activation) of hydrogen, argon, or helium, and production of secondary electrons, which in turn ionize more hydrogen, etc.

(3) Collision of ionized hydrogen, argon, or helium with boron tribromide and exchange of energy.

(4) Formation of positive boron radicals and hydrogen bromide or bromine.

(5) Transfer of the positive boron radical to the cathode.

(6) Electrochemical reaction of the boron radical to form an essentially amorphous deposit of boron.

The morphology of the deposit is essentially the same as the morphology of the substrate. There is no interaction of the boron with the tungsten and there is apparently some anisotropy of the deposit.

The corona discharge during deposition is not essentially different from a corona discharge developed in an inert gas system, and the same criteria and properties are extant. Like a corona discharge in an inert gas, the coefficient of electron emission and the ability of the electrons to diffuse along the wire are most important in obtaining a uniform corona, and thus a uniform deposit, on the substrate. Furthermore, if the sheath of positively charged boron radicals becomes too dense, the corona is quenched and will not recover fast enough to prevent the breakup of the corona into points.

Acknowledgment

This work was supported by the U.S. Air Force Contract AF 33(615)-2130, and was based upon an idea presented by J. B. Story. The filament cross-sections were prepared by W. C. Coons and the continuous system was operated by Barbara Traina. Grateful acknowledgment is also made to R. N. Varney, M. E. Sibert, and A. E. Hultquist for many helpful discussions of gas discharges in general and of corona discharges in particular.

In Chemical Reactions in Electrical Discharges; Blaustein, B.;
Advances in Chemistry; American Chemical Society: Washington, DC, 1969.

Literature Cited

(1) Brown, S. C., "Basic Data of Plasma Physics," The Technology Press of M.I.T. and John Wiley and Sons, Inc., New York, 1959.
(2) Coffman, J. A., Browne, W. R., *Sci. Am.* **212,** No. 6, 90 (1965).
(3) Dibelius, N. R., Fraser, J. C., Kawahata, M., Doyle, C. D., *Chem. Eng. Progr.* **60,** No. 6, 41 (1964).
(4) Helland, E. J., "The Plasma State," Reinhold Publishing Corporation, New York, 1961.
(5) Holzmann, R. T., Morris, W. F., *J. Chem. Phys.* **29,** 677 (1958).
(6) Kapzow, N. A., "Elelstrische Vorgange in Gasen und in Vakuum," Veb Deutscher Verlog de Wissenschaften, Berlin, 1955.
(7) Kotlensky, W. V., Schaeffer, R., *J. Am. Chem. Soc.* **80,** 4517 (1958).
(8) Lange, N. A., Ed., "Handbook of Chemistry," 10th Ed., p. 111, McGraw-Hill Book Company, Inc., New York, 1961.
(9) Lawrence, S. J., *Chem. Eng. Progr.* **60,** No. 6, 45 (1964).
(10) Loeb, L. B., "Electrical Coronas," Univ. of Calif. Press, 1965.
(11) Markovskii, L. Ya., L'vova, V. I., Kondrashev, Yu. D., *Bor. Tr. Konf. po Khim, Borai Ego Soedin.* **1958,** 36; *cf.* **FTD-MT-64-427,** Foreign Technol. Division, A.F. Systems Command, 1965.

RECEIVED May 29, 1967.

17

The Effect of a Siemens Ozonizer Discharge on the Reaction of Carbon Monoxide and Steam

T. C. RUPPEL, P. F. MOSSBAUER, and D. BIENSTOCK

U. S. Bureau of Mines, Pittsburgh Coal Research Center, Pittsburgh, Pa.

Publication Date: June 1, 1969 | doi: 10.1021/ba-1969-0080.ch017

The gas-phase reaction of carbon monoxide and steam to produce carbon dioxide and hydrogen has been studied in the presence of a Siemens ozonizer discharge. A factorial design was used to determine the effect of input electrical power, pressure, space velocity, and temperature on the conversion of carbon monoxide. With the aid of an empirical equation, derived from the factorial design data, the region of maximum conversion of carbon monoxide within the limits of the factors was determined. The rate of approach to thermodynamic equilibrium was investigated for one set of experimental conditions and was compared with previous work. The effect of changing the surface-to-volume ratio of the reactor upon carbon monoxide conversion was also determined.

The water-gas shift reaction was chosen for study in a Siemens type ozonizer discharge with the aim of establishing the important variables associated with the conversion of carbon monoxide.

The reaction was carried out in a quartz ozonizer having an electrode length of 12 inches and an electrode separation of 8 mm. The electrodes consisted of fired-silver paint—one electrode coating the inside of the inner (high voltage) tube, and the other coating the outside of the outer (ground) tube.

The reaction was studied by means of a four-factor, two-level, factorially designed set of experiments. This consisted of input power levels of 60 and 90 watts, pressures of 1/2 and 1 atm., hourly space velocities (*SV*) of 200 and 800, and reactor temperatures of 127° and

In Chemical Reactions in Electrical Discharges; Blaustein, B.;
Advances in Chemistry; American Chemical Society: Washington, DC, 1969.

527°C. (400° and 800°K.). Although voltage was not a controlled factor, the voltage ranged from 3,100 to 11,000 r.m.s. (root mean square) volts.

The prediction equation resulting from the statistical analysis of the data indicates that carbon monoxide conversion increases with pressure, temperature, and power input, and decreases with space velocity. Practically no reaction occurred in the absence of a discharge.

The maximum conversion of carbon monoxide within the factorial region studied was 16.7% (water-free basis). An extra-factorial region indicating more favorable conversion was explored and 71% was obtained.

At 800°K. and one atm. pressure, the water gas shift reaction approaches thermodynamic equilibrium, rather than an experimental steady-state.

No change in carbon monoxide conversion was found when the surface-to-volume ratio of the quartz reactor was changed by 33% from 4.85 $cm.^2/cm.^3$ to 6.45 $cm.^2/cm.^3$ by packing the reactor annulus with quartz wool.

Novel techniques are being investigated by the Bureau of Mines in an effort to find new uses for coal, or products from coal and its derivatives. One technique under study involves chemical reactions in an ozonizer discharge. Initially the gas-phase reaction of carbon monoxide and steam to produce carbon dioxide and hydrogen has been investigated from an engineering viewpoint.

The immediate aim of this study was to establish the important variables associated with the conversion of carbon monoxide in the water-gas shift reaction. As knowledge is gained on the effect of ozonizer discharge in several simple chemical reactions, more complex reactions involving coal and its products will be studied.

The water-gas shift reaction, which is usually carried out industrially over an Fe_2O_3-Cr_2O_3 catalyst at 300°–500°C. and 100–300 p.s.i.g., has been discussed at length in the literature (*2, 3, 4, 9, 21, 26*). It is almost certainly a surface reaction (*10, 22*).

The physics (*5, 11, 14, 16, 19*) and chemistry (*12, 13, 28*) of electrical discharges have been surveyed by several authors. A bibliography of chemical reactions in electrical discharges over a thirty-year period, 1920–50, has been compiled (*1*).

The water-gas shift reaction has been studied specifically by Lunt (*15*). Similar reactions have been studied by others. Wendt and Evans (*29*) investigated the mixture carbon monoxide plus hydrogen in a corona discharge at atmospheric pressure and 60 Hz. Peters and Kuster (*23*) studied the reaction of carbon dioxide and hydrogen; Peters and Pranschke (*24*) studied the mixture methane, carbon dioxide, and water vapor; while Fischer and Peters (*7*) studied carbon monoxide and hydro-

Publication Date: June 1, 1969 | doi: 10.1021/ba-1969-0080.ch017

gen. Peters and co-workers above used a glow discharge at 20-60 torr and 50 Hz. McTaggart (*18*) studied the reactions of carbon monoxide in a microwave discharge and Sahasrabudhey and Deshpande (*25*) studied mixtures of carbon monoxide and hydrogen at 500 Hz. in a silent discharge.

The above citations were largely laboratory scale investigations, made with a view to increasing the understanding of the chemistry involved. Little work has been done on the engineering aspects of discharge chemistry. A notable exception is the work of Spedding (*27*) who is studying chemical synthesis by gas-phase discharge from an engineering viewpoint.

Equipment and Procedure

Publication Date: June 1, 1969 | doi: 10.1021/ba-1969-0080.ch017

The operational scheme of the discharge unit can be seen in the flow diagram, Figure 1. Carbon monoxide from a compressed gas cylinder (1) is passed through an activated carbon adsorption trap (5). The metered flow (7) passes through a flow control valve (9); a second stream of gas may be blended here if desired. The carbon monoxide at the pressure of the system passes through a steam generator (11). The thermocouple immediately above the reflux condenser (17) controls the steam flow rate *via* a time-proportionating temperature controller (not shown). The carbon monoxide and water flow rates may be individually varied between 0.2 and 3 ft^3/hr. by adjusting the flow controller (9) and temperature controller settings. The carbon monoxide-steam mixture then enters the Siemens-type reactor through preheaters (18) and (21). The reactor is enclosed in a tube furnace (23). The product gases pass through a series of three cold traps (25, one shown) at −80°C. Bypass cold traps (26) are available if required. The noncondensable gases pass through a sample train (28, 29) and then through a flow meter (30) which is at system pressure. On leaving the flow meter the non-condensable gases pass through the system-pressure regulator (31), vacuum pump (33), and finally a wet test meter (34). The system is designed to operate from 1/4 to 2 atm.

The electrical system is shown in Figure 2. It consists of 60 Hz. a.c. frequency 115 volt constant voltage supplying 60 Hz. or 10,000 Hz. circuits. All of the work described in this paper was performed at a frequency of 60 Hz. The equipment required for 10,000 Hz. operation is mentioned briefly here, since it is an integral part of our discharge unit. Experiments are now being performed at 10,000 Hz. The 60 Hz. circuit simply involves the corresponding stepup transformer and the discharge cell. The 10,000 Hz. circuit is slightly more complicated by the insertion of frequency conversion components. These consist of an audio-oscillator for low power 60 to 10,000 Hz. frequency conversion and two amplifiers in parallel for boosting power. A specially designed stepup transformer operating at 10,000 Hz. and the reactor follow the frequency conversion components.

The discharge is monitored with an oscilloscope. Typical oscillographs are shown in Figure 3. The waveforms on the left show the voltage trace above the current trace. The current trace is distorted by

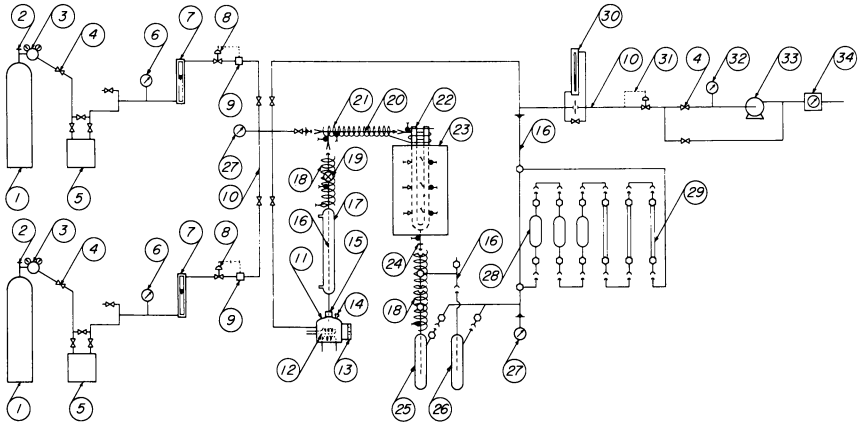

Figure 1. Physical system for reaction of gases in an ozonizer discharge

1 *Feed gas (2)**
2 *Valves (2)*
3 *Reducing regulators (2)*
4 *Valves, 1/8 in., brass (18)*
5 *Activated carbon traps, to remove carbonyls (2)*
6 *Gages, 0-30 psig (2)*
7 *Flowmeters, 0.1-5 scfh (2)*
8 *Valve, 1/8 in., needle, brass*
9 *Flow controllers, 0.1-5 scfh (2)*
10 *Tubing, soft copper, 1/4 in.*
11 *Steam generator*
12 *Internal water heaters (2)*
13 *Distilled water level sight glass*
14 *Water filler cap*
15 *O-ring compression seal*
16 *Tubing, borosilicate glass, 8mm.*
17 *Reflux condenser for room-air or constant-temperature-oil circulation*
18 *Pre- and postheater electrical heating tapes (2)*
19 *Stopcock, borosilicate glass, Teflon clad plug, 3 mm. bore*
20 *Tubing, 96% silica glass, 7 mm.*
21 *Preheater, ceramic-bead-covered wire*
22 *Corona cell, quartz or 96% silica glass*
23 *Furnace, combustion tube type, hinged, 3-element, 25°-1000°C.*
24 *Quartz-borosilicate glass graded junction*
25 *Cold traps, 3 in series (2 not shown)*
26 *Bypass cold traps, 3 in series (2 not shown)*
27 *Gages, 30 in Hg. vacuum to 30 psig (2)*
28 *Gas sampling tubes, 250 CC (3)*
29 *Gas sampling tubes, 10 CC., 8 mm. OD borosilicate glass tubing (3)*
30 *Flowmeter, well type manometer, 0.1-5 scfh*
31 *Regulator, 30 in hg vacuum to 30 psig*
32 *Gage, 0-30 in hg vacuum*
33 *Vacuum pump, 0-25 in hg, explosion proof motor, airtight chamber, uncontaminated gases*
34 *Wet test meter*
*(18)*12/5 joints, ball, borosilicate glass, with Teflon O-ring*
(1) 12/5 joint, ball, 96% silica glass
(16) 12/5 joints, socket, borosilicate glass
(3) 12/5 joints, socket, 96% silica glass
(3) Borosilicate glass-Kovar junctions
(3) Thermocouples, to floating millivoltmeters
(3) Thermocouples, furnace sectional heater control
(1) Thermocouple, for internal water heater control
(9) Thermocouples, to multipoint recorder
(3) Stopcocks, borosilicate glass, 3 mm. bore, 3 way
(17) Stopcocks, borosilicate glass, 3 mm. straight bore

* Number in parentheses indicates number of items in system.

Publication Date: June 1, 1969 | doi: 10.1021/ba-1969-0080.ch017

the discharge, which can be seen as a brush effect at the peak of each voltage cycle. The area enclosed by the Lissajous figure on the right is a measure of the true power dissipated in the discharge. Unfortunately this fact is rather academic since the black area in the Lissajous figure is less than the total area swept out by the electron gun of the oscilloscope. The brush effect consists of hundreds of short-lived breakdowns. If the intensity of the oscilloscope tracing is increased, it is seen that the brush effect extends beyond the grid lines. The area swept out by a single breakdown trace is practically negligible. The integral of these areas may be sizable.

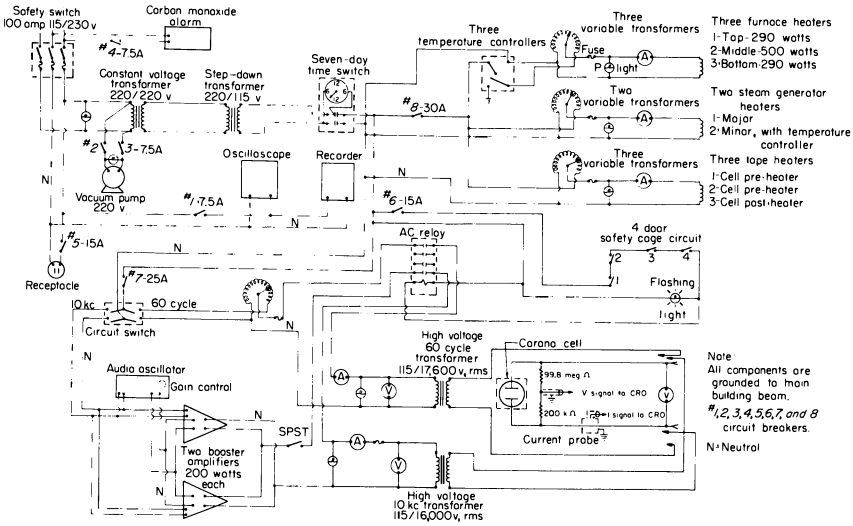

Figure 2. Electrical system for reaction of gases in an ozonizer discharge at 60 and 10,000 Hz.

A measurement of power dissipated in the discharge can be obtained calorimetrically or electronically by the parallelogram method. The calorimetric method is described by Lunt (*15*) and the parallelogram method by Manley (*17*) and others (*8, 11*). We chose to determine the effect of input power on CO conversion, since we felt this gives a better idea of power scaleup requirements.

The oscilloscope probe circuit is shown near the reactor in Figure 2. By proper changes of settings on the oscilloscope, it is possible to measure cell voltage, cell current, cell power, or frequency. For comparison purposes, we have added an electrostatic voltmeter to measure ozonizer voltage.

Four access doors to the high voltage area control micro-switches. If any door is opened while a potential is impressed across the reactor, the circuit is deactivated. The power lines to all components, including the heating elements of the system, are also shown in Figure 2.

The Siemens type reactor, shown in Figure 4, consists of two concentric quartz tubes, 51 and 38 mm. o.d., having a 4 mm. annular space.

Publication Date: June 1, 1969 | doi: 10.1021/ba-1969-0080.ch017

The electrode length is 14 inches, and there is an 8 mm. electrode-to-electrode separation. The electrodes consist of fired-silver paint—one electrode coating the inside of the inner (high voltage) quartz tube, and the other coating the outside of the outer (ground) tube. Tungsten (or optionally copper) wires are attached to the outside and inside of the reactor with two or three coatings of fired-silver paint. The ozonizer shown in Figure 4 is designed so that the annulus may be packed with glass wool, or some other packing material, if desired. Experiments with an open annulus reactor and with the reactor packed with quartz wool (Arthur H. Thomas Co., Philadelphia, Pa., or equivalent) are described in this paper. Using an impedance bridge, the capacitance of the open annulus reactor was measured as 85 picofarad (pf) and that of the packed reactor was found to be 90 pf. The open annulus volume between the electrodes was measured as 200 cc.

For the packed annulus experiments, a known weight of quartz wool was manually distributed around the outside of the inner quartz tube of the disassembled reactor as evenly as possible. It was then bound to the tube by a tight winding of acetate thread. The reactor was then reassembled and the acetate thread was dissolved and removed by washing with acetone.

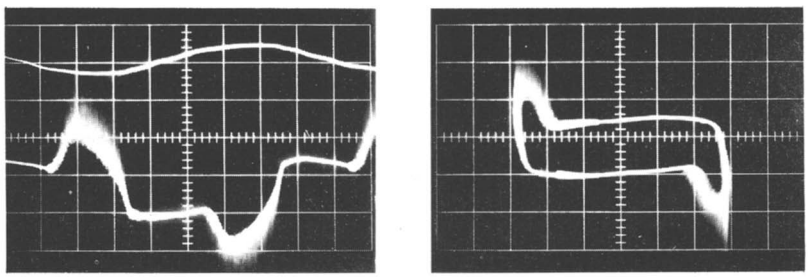

Figure 3. Typical oscillographs of same ozonizer discharge

LEFT: Voltage (above) and current waveforms
RIGHT: Lissajous figure

Borosilicate glass wool was packed tightly into the inside of the spherical joint, shown in Figure 4, to reduce dead volume.

The average wall temperature was used as a measure of the temperature of the system. Three thermocouples were equally spaced vertically along the inside wall of the reactor (Figure 1) and three along the outside wall. The inside wall thermocouples were at the discharge potential and thus were isolated from ground. A millivoltmeter was connected in series to each of the inside wall couples, and thus was similarly "floated." To simplify the electrically hot thermocouple circuits, no compensating ice junction was included; the room temperature correction was added to each millivoltmeter reading. The discharge potential had a slight positive effect on the millivoltmeter readings in the hot circuit. Therefore, the millivoltmeters were read before the discharge potential was impressed on the system. The system temperature was taken as the average of all six thermocouple measurements.

Publication Date: June 1, 1969 | doi: 10.1021/ba-1969-0080.ch017

In Chemical Reactions in Electrical Discharges; Blaustein, B.;
Advances in Chemistry; American Chemical Society: Washington, DC, 1969.

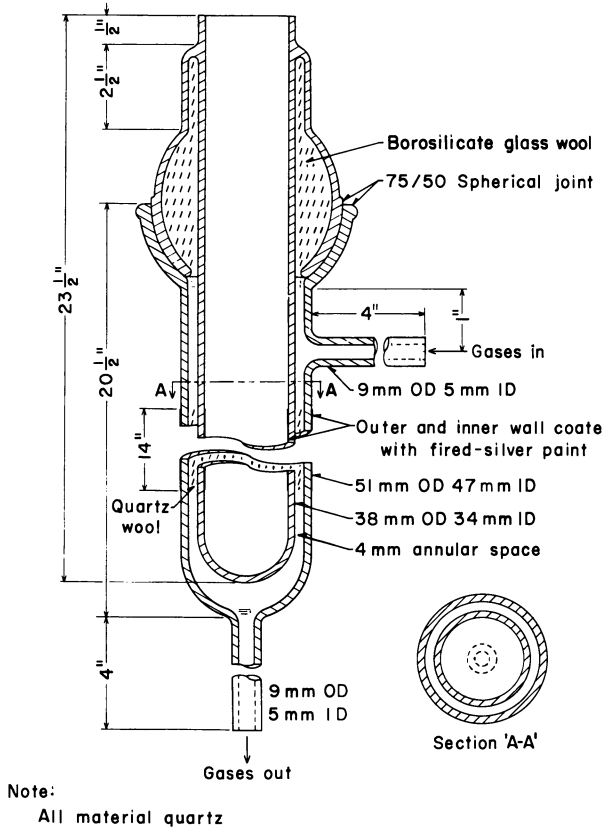

Figure 4. Siemens ozonizer

Input power was measured by multiplying values for input current and voltage. Secondary voltage was measured directly with a Singer a.c.-d.c. electrostatic voltmeter (Singer Co., Metrics Div., Bridgeport, Conn.).

After the desired carbon monoxide and steam flow rates were obtained and stabilized, the discharge was initiated. Operation of the unit was continued until product concentration in all six sample bottles (Figure 1) was uniform. The sample bottles were then isolated from the flow system and removed for analysis. The water-free product gases were analyzed by gas chromatography.

A factorial design was used to determine the effect of pressure, space velocity, temperature, and imput electrical power on the conversion of carbon monoxide. This was a four factor, two level set of experiments as shown in Table I.

These four factors were chosen intuitively because of their expected effect on chemical reactions in an electrical discharge. A two level design was chosen (a) as a factor screening procedure, (b) to obtain positive or negative effects of factors, and (c) to obtain these effects efficiently. A

Publication Date: June 1, 1969 | doi: 10.1021/ba-1969-0080.ch017

three or higher level design would have been given nonlinear effects of factors, but would have required 81 or more experiments. Since a factor screening procedure to obtain positive or negative effects within the factorial region was desired, the two level design was chosen. Sixteen

Table I. Factorial Design of the Experiments

2 level, 4 factor (full factorial)
1:1 molar mixture, H_2O:CO

	Level	
	Low	*High*
Pressure, atm.	0.5	1.0
Space velocity, hr.$^{-1}$	200	800
Temperature, °K.	400	800
Input power, total circuit power, watts	60	90

combinations of high and low levels are possible. Each combination contains one level of each of the four factors. Thus, sixteen experiments were performed, each experiment yielding one figure for carbon monoxide conversion.

Results and Discussion

Experimental results are given in Table II. Within the factorial region studied, carbon monoxide conversions ranged between 0% and 16.7% by volume. An extra-factorial region of interest, also shown in Table II, was investigated and is discussed below.

The factorial design data were analyzed by use of a linear hypothesis statistical model (*20*). By this it is assumed that the conversion of carbon monoxide is dependent on all of the factors to the first power only. The following empirical regression equation for the percent of carbon monoxide converted resulted from this model:

$$\text{Percent CO converted} = -3.57 - 7.88\,P + 0.0146\,SV + 0.0121\,T - 0.0709\,W + 0\,0183\,P \cdot T - 0.0000377\,T \cdot SV + 0.000167\,T \cdot W$$

(Note: T = temperature, °K.; P = pressure, atmospheres; W = input power, total circuit power, watts; and SV = space velocity, flow rate/reactor volume, hr.$^{-1}$) The standard error of estimate of the above equation is 0.59.

According to Table II, maximum conversion of carbon monoxide within the range studied was found to be at 1 atm., 200 hourly space velocity, 800°K., and 90 watts input. The experimental value of 16.7% by volume compares with a value of 15.7 obtained by calculations. The extra-factorial regions of interest suggested by the equation would be

Publication Date: June 1, 1969 | doi: 10.1021/ba-1969-0080.ch017

In Chemical Reactions in Electrical Discharges; Blaustein, B.;
Advances in Chemistry; American Chemical Society: Washington, DC, 1969.

Table II. Experimental Results

Run No.[a]	Percent CO Conversion[b]	Pressure, atm.	Space Velocity, hr.$^{-1}$	Temperature,[c] °K.	Input Power,[d] watts	Secondary Voltage,[e] r.m.s. volts	Input Energy kwh./lb. CO Converted
			Open Annulus Reactor				
161	16.7	1.0	200.	810.	90.0	4450	6.8
162	0.1	0.5	800.	399.	60.0	9450	190.
163	0.3	0.5	200.	401.	89.7	10900	379.
164	0.1	1.0	800.	402.	91.1	10900	288.
165	2.7	0.5	800.	789.	90.2	3340	10.6
166	0.0	1.0	200.	397.	60.0	9400	∞
167	9.6	0.5	200.	795.	60.0	3100	7.9
168	3.9	1.0	800.	801.	60.9	4650	4.9
169	5.4	1.0	800.	801.	90.0	4650	5.3
170	1.0	0.5	200.	398.	60.0	9600	76.0
171	0.2	0.5	800.	398.	89.7	11050	142.
172	13.2	1.0	200.	794.	60.9	4450	5.8
173	0.2	1.0	200.	398.	90.3	10950	572.
174	1.5	0.5	800.	796.	60.0	3250	12.7
175	0.1	1.0	800.	400.	60.0	9450	190.
176	11.6	0.5	200.	805.	90.3	3450	9.9
186	32.1	2.0	100.	800.	104.0	5800	8.2
188′	37.6	2.0	24.	791.	93.0	7600	26.1
220′	52.5	1.0	18.	772.	90.0	5000	24.1
221′	63.7	1.0	3.3	772.	90.0	4800	108.
255	41.9	1.0	25.	798.	91.0	6050	16.7
256	37.4	1.0	51.	799.	90.0	6150	9.1
257	43.8	1.0	10.	798.	90.6	6000	39.8
258′	57.5	1.0	7.5	798.	89.3	5900	39.8
259′	54.1	1.0	5.0	798.	90.5	6030	64.4
260′	69.4	1.0	0.5	796.	90.0	5950	500.
261′	71.0	1.0	1.0	800.	90.7	5820	246.
262	2.4	1.0	1200.	799.	89.7	6130	6.0
			Reactor Annulus Packed with Quartz Wool Pressure = 1 atmosphere				
222	25.6		200.	789.	91.0	5600	3.4
244′	60.4		3.3	795.	88.0	5160	85.0
245′	52.2		6.0	795.	89.7	5100	55.1
246′	58.9		10.	795.	89.5	5150	29.3
247′	46.5		30.	795.	92.1	5150	12.7
248′	59.0		4.6	799.	90.7	5200	64.4
249′	60.6		3.8	799.	89.7	5360	75.0
250	51.2		25.	809.	90.0	5800	13.5
251	34.6		51.	812.	91.2	5975	10.0
252	48.3		10.	812.	91.0	5875	36.3
253	48.4		14.	804.	89.7	6150	25.5
254	39.6		19.	803.	90.0	6300	23.0

Publication Date: June 1, 1969 | doi: 10.1021/ba-1969-0080.ch017

Table II. (continued)

[a] Factorial design data are given from Runs 161 through 176.
[b] Percent conversion = 100 minus the percent in product gas (water-free basis).
[c] Standard deviation of each temperature = ±16°K. at the 400°K. level and ±70°K. at the 800°K. level.
[d] Standard deviation of each power value = ±2.6 watts.
[e] Accuracy of electrostatic voltmeter = ±50 volts below 5000 volts, ±100 volts below 10,000 volts, and ±200 volts above 10,000 volts.
[f] Batch run; equivalent space velocity calculated as reciprocal of measured residence time.

higher pressures, temperatures, and power inputs, and lower space velocities. Within the present limitations of our equipment, and operating on a flow basis, this was $P = 2$, $SV = 100$, $T = 800$, and $W = 100$. The carbon monoxide conversion increased to 32%. The linear hypothesis statistical model predicts 24%. With static conditions, carbon monoxide conversions ranged from 38% to 71%, depending on residence time and pressure. It can be seen that continued increase in pressure has a positive effect upon carbon monoxide conversion. Thus, the effect of pressure at 800°K. as indicated by the prediction equation is real and positive. However, extrapolation of an empirical equation must be done cautiously.

After numerical values of the experimental variables were inserted into the equation, an inspection of the terms showed the following relative importance of the variables: $T > P > W > SV$. However, all variables plus interaction terms shown are important. A poor correlation resulted when the interaction terms were omitted in a determination of the coefficients.

It would also be desirable to correlate the experimental data *via* dimensional analysis, by the Rayleigh method or the Buckingham Pi theorem. This powerful empirical correlational technique could possibly be employed in the field of discharge chemistry as a means of confirming or even discovering pertinent variables associated with chemical reaction in discharges. We chose the linear hypothesis statistical empirical model for correlating our factorial design data, since it is a good first approach empirical model to determine positive or negative effect of independent variables upon a process.

Energy requirements were calculated and are given in the last column in Table II. These values are based upon input power.

It was found that less than 1% carbon monoxide was converted to carbon dioxide and hydrogen in the absence of a discharge, irrespective of secondary voltage (up to breakdown), space velocity, temperature, and pressure. Thus, curves, similar to Paschen's Law curves, were developed for the open annulus reactor. These are shown in Figure 5 and were developed to insure a discharge at the low power level in all cases. These differ from Paschen's Law curves in that Figure 5 shows discharge-sustaining potential whereas Paschen's Law applies to discharge-initiating

Publication Date: June 1, 1969 | doi: 10.1021/ba-1969-0080.ch017

In Chemical Reactions in Electrical Discharges; Blaustein, B.;
Advances in Chemistry; American Chemical Society: Washington, DC, 1969.

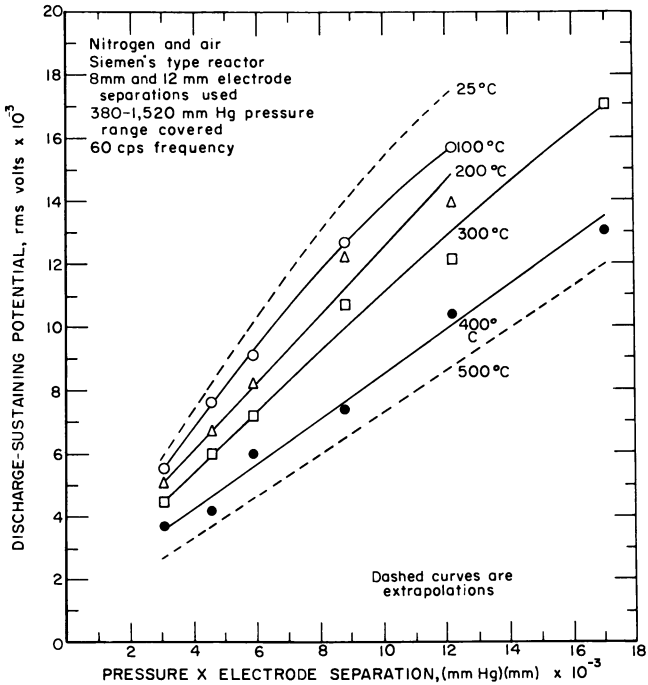

Figure 5. Discharge characteristics of ozonizer annulus

potential. A second reactor with 12 mm. electrode separation was also used to obtain these curves.

Initially it was intended to include secondary voltage, rather than input power as a factor. However, it was not possible to set a high and low level without losing the discharge at low temperatures or drawing too high a current at high temperatures. At high currents an arc would form and puncture the quartz reactor. Maintaining a discharge in some cases and not others would introduce a very significant uncontrolled qualitative variable, discharge *vs.* no discharge, into the design. While it might be possible to include discharge *vs.* no discharge as a factor, it was known that little carbon monoxide would be converted in the absence of a discharge, regardless of the potential across the cell electrodes.

Input power was factorialized since the voltage and amperage required for a chosen power level are determined by the discharge and therefore need not meet set requirements of a factorial design.

Role of Reactor Surface in Reaction. Essentially no reaction occurs between water and carbon monoxide at 600°C. and one atm. pressure in the absence of a discharge. Thus, the quartz walls of the reactor do not catalyze a thermal reaction. Since the reaction in the presence of a dis-

Publication Date: June 1, 1969 | doi: 10.1021/ba-1969-0080.ch017

charge almost certainly proceeds *via* a different mechanism than a thermal reaction, the reactor walls might be involved in the discharge reaction.

This possibility was studied further by packing the annular space of the reactor with 6μ diameter quartz wool to a bulk density of 0.070 gram/cc. The reactor packed in this manner is shown in Figure 4. This packing density was about the limit since further packing could break the reactor. Even so, this corresponded to about 98% void space. The purpose of this procedure was to increase the surface-to-volume ratio of the reactor, which was increased from 4.85 $cm.^2/cm.^3$ to 6.45 $cm.^2/cm.^3$.

If the reactor walls are involved in the discharge reaction, an increase or decrease in carbon monoxide conversion should be observed. The experiments performed with the packed annulus reactor are compared with those of the open annulus reactor in Figure 6 and the experimental data are given in Table II. Within experimental error, no effect of increased reactor surface can be detected. Thus, it appears that the water-gas shift reaction in an ozonizer discharge proceeds *via* a purely gas phase mechanism. It appears to be a homogeneous reaction.

Comparison with Other Work. Lunt (*15*) has studied the water-gas shift reaction in an electrical discharge from the $H_2O + CO$ side. His data were obtained at 15 MHz. whereas the results of this work were obtained at 60 Hz. A comparison of his results with those of this paper is given in Table III. Because of Lunt's voltage limitations (2000 r.m.s.) he could not maintain a discharge at pressures above 0.4 atm. Thus, his work was done at lower pressures. The present work shows that while significant carbon monoxide conversions can be obtained at higher pressures also, continued pressure increase does not appear to result in proportional conversion; the carbon monoxide conversions at 2 atm. are less than expected.

One of the reasons for presenting Table III is to compare the approach with thermodynamic equilibrium observed in the two investigations. A figure presented in Lunt's paper indicates that an experimental steady-state is reached in about seven minutes at 0.4 atm. pressure and in about 18 minutes at 0.074 atm. pressure. From the equivalent temperatures of 1260° and 830°K. given by him, it can be calculated that his systems were at 25 and 87% of thermodynamic equilibrium respectively.

There is evidence from our Figure 6 to support the conclusion that thermodynamic equilibrium is attained at zero space velocity (infinite residence time). This also indicates that the discharge and wall temperatures are equal. The wall temperature of 800°K. was the average of six thermocouple measurements, three on the inside wall and three on the outside wall. The thermodynamic limit conversion value of 80% in

Publication Date: June 1, 1969 | doi: 10.1021/ba-1969-0080.ch017

Table III. Comparison of the Results of Two Reaction in a Siemens Ozonizer Type

Investigator	*Fixed Experimental Conditions*	*Run No.*	*Percent Conversion of CO*[a]		*Percent of Thermodynamic Equilibrium*
			Experimental	*Theoretical*	
Lunt (*15*)	15 MHz.	—	15	61	25
	3.2 mm. annulus	—	15	61	25
	3.44 in length	—	11	61	18
	31.7 cc. reactor	—	3	61	5
	volume	—	68	78	87
		—	68	78	87
		—	46	78	59
		—	12	78	15
This Work	60 Hz.	188	38	81	47
	4.0 mm. annulus	186	32	80	40
	14 in length	[c]	—	80	100
	200 cc. reactor	260	69	80	87
	volume	261	71	80	89
		221	63	82	77
		220	52	82	63
		161	17	80	21
		176	12	80	15

[a] Percent conversion = 100 minus the percent in product gas (water-free basis).
[c] *Calculated.*

Figure 6 resulted from an equilibrium conversion calculation using the thermodynamic equilibrium constant for 800°K. This was obtained from Figure 7. The fact that the experimental percent CO conversion curve in Figure 6 approaches 80% conversion as an asymptote is evidence of the approach to thermodynamic equilibrium, rather than to an experimental steady-state.

However, some further discussion is in order. In spite of Figure 6, it should not yet be generalized that the water gas shift reaction, under the influence of an ozonizer discharge, approaches thermodynamic equilibrium. Lunt has indicated that the equilibrium constant numbers calculated from his steady-state compositions vary with pressure. Our runs 176, 161, and 186 in Table III, while not at steady-state, indicate that this is possible. Further conversion *vs.* time experiments at various pressures are required.

The data in Table III indicate that frequency does not appear to have much effect on the reaction of carbon monoxide and steam in an ozonizer discharge. In spite of the large difference in frequency used in the two investigations, the results are strikingly similar. The same

Publication Date: June 1, 1969 | doi: 10.1021/ba-1969-0080.ch017

Investigators Who studied the Water-Gas Shift Discharge: $H_2O + CO = H_2 + CO_2$

Equivalent Temp., °K. Based on Equil. Const. Calc'd. from Prod. Gas Compositions	*Equilibrium Constant Calc'd. from Product Gas Compositions*[b]	*Measured Wall Temp., °K.*	*Initial Pressure CO, Atm.*	*Residence Time, Min.*	*Input Power, Watts*	*Secondary Voltage, r.m.s. Volts*
1260	0.59	—	0.40	14	150	760
1260	0.59	—	0.40	7	150	760
1260	0.59	—	0.40	2.5	150	760
1260	0.59	—	0.40	0.3	150	760
830	3.21	—	0.074	26	150	520
830	3.21	—	0.074	18	150	520
830	3.21	—	0.074	2.5	150	520
830	3.21	—	0.074	0.3	150	520
—	—	791	2.0	2.5	93	7600
—	—	800	2.0	0.6	104	5800
800	4.04	—	1.0	∞	90	—
961	1.61	796	1.0	120	90	5950
866	2.61	800	1.0	60	90	5820
1050	1.11	772	1.0	18	90	4800
—	—	772	1.0	3.3	90	5000
—	—	810	1.0	0.3	90	4450
—	—	805	0.5	0.3	90	3450

[b] $K = N(H_2) \cdot N(CO_2)/[N(H_2O) \cdot N(CO)]$; N = volume or mole percent.

products are formed and the yields are comparable. As previously mentioned, experiments using a frequency of 10,000 Hz. are being carried out in this laboratory to detect any frequency effect on carbon monoxide conversion. Preliminary experiments using an equimolar mixture of steam and carbon monoxide indicate that the reaction carried out with a frequency of 10,000 Hz. gives results which are very similar to the 60 Hz. results.

The voltage applied to the reactor (secondary voltage) reported by Lunt is lower than expected by a factor of about two, based on our Figure 5. This disagreement cannot be explained.

The prediction equation indicates that input power has a positive effect on carbon monoxide conversion. More power was used by Lunt for comparable conversions than in this work. Possibly there were more extraneous paths for energy dissipation in Lunt's apparatus.

Further Thermodynamic Considerations. The change in equilibrium constant of the water-gas shift reaction with temperature is shown in Figure 7. At equilibrium carbon monoxide conversion decreases with temperature. From the data in Table II and from the prediction equation

Publication Date: June 1, 1969 | doi: 10.1021/ba-1969-0080.ch017

In Chemical Reactions in Electrical Discharges; Blaustein, B.;
Advances in Chemistry; American Chemical Society: Washington, DC, 1969.

it will be noticed that carbon monoxide conversion increased with temperature in the region of investigation. Thus, under the experimental conditions of the factorial design, thermodynamic equilibrium was not attained; the reaction was kinetically controlled.

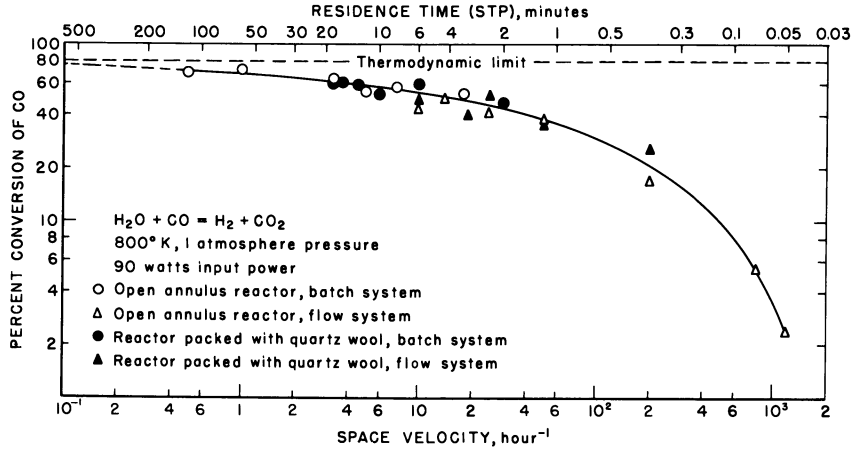

Figure 6. Rate of attainment of thermodynamic equilibrium in the water-gas shift reaction under the influence of an ozonizer discharge

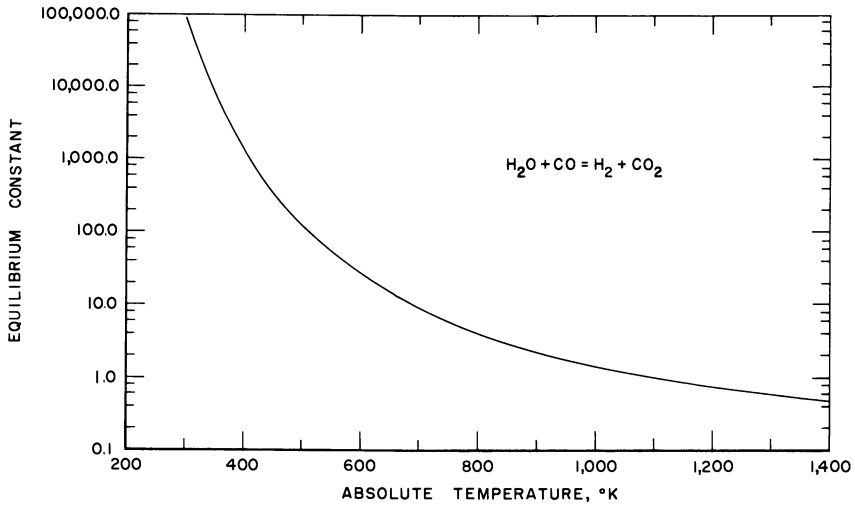

Figure 7. Change in equilibrium constant of the water-gas shift reaction with temperature

Economic Considerations. It is too early in this stage of the discharge work to draw meaningful economic figures. A modification in reactor design or flow regime, while maintaining long residence time, may sig-

Publication Date: June 1, 1969 | doi: 10.1021/ba-1969-0080.ch017

nificantly change the present economic figures. However, for present perspective, input electrical energy requirements to the reactor were calculated as a function of carbon monoxide conversion for a high conversion region found by the previously mentioned factorial design. These results are given in the last column of Table II and are plotted in Figure 8. The ordinate in Figure 8 consists of the energy used by the ozonizer discharge only. Energy values of 0.3 kwh./lb., required to vaporize liquid water at 90°C., and two to three kwh./hr., required to maintain temperatures in the system, are not included.

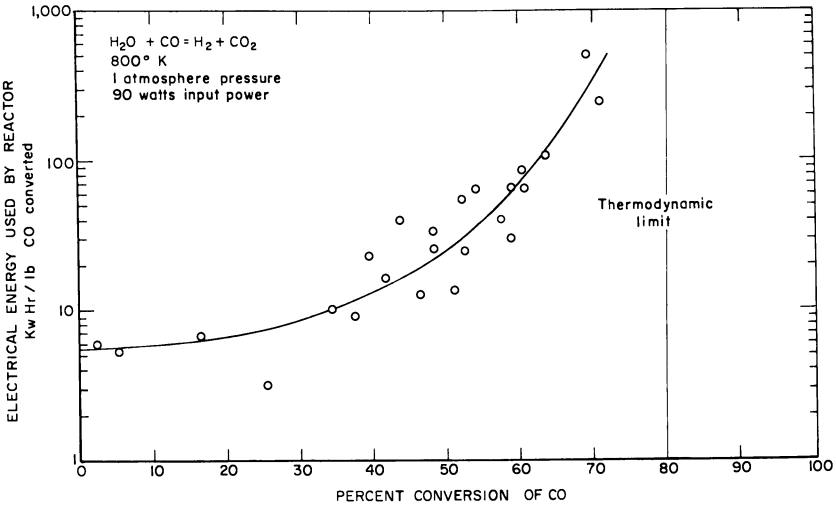

Figure 8. Electrical energy requirements of reactor

Since electrical power is at present a relatively expensive form of power and since the carbon monoxide conversions shown here are less than those achieved industrially (*6*.) by catalytic means, the energy requirements are probably high. What is of more interest is the empirical determination of the functional dependence of the yield of a given product on the several independent variables in an ozonizer discharge. This information is a prelude to future experiments where powdered coal or coal volatiles will be treated with selected gases in an ozonizer discharge.

Conclusions

Within the limits of this investigation, the conclusions that can be drawn are:

(1) The prediction equation arising from the statistical analysis of the data indicates that in the region of interest carbon monoxide con-

Publication Date: June 1, 1969 | doi: 10.1021/ba-1969-0080.ch017

In Chemical Reactions in Electrical Discharges; Blaustein, B.;
Advances in Chemistry; American Chemical Society: Washington, DC, 1969.

version is higher at higher pressures, temperatures, and power inputs, and lower space velocities.

(2) The following relative importance of variables was found: temperature > pressure > input power > space velocity.

(3) Under the experimental conditions employed for most of the experiments in this paper, steady-state conditions were not obtained and the reaction was kinetically controlled.

(4) Essentially no carbon monoxide is converted to hydrogen and carbon dioxide in the absence of a discharge, regardless of the values of temperature, pressure, potential, or space velocity.

(5) The water-gas shift reaction, under the influence of an ozonizer discharge, is a homogeneous gas phase reaction.

Publication Date: June 1, 1969 | doi: 10.1021/ba-1969-0080.ch017

Literature Cited

(1) Akerlof, G. C., Wills, E., "Bibliography of Chemical Reactions in Electric Discharges," Office of Technical Services, Dept. of Commerce, Washington, D. C., 1951.
(2) Blackwood, J. D., *Ind. Chem.* **36,** 55 (1960).
(3) *Ibid.*, **36,** 129 (1960).
(4) *Ibid.*, **36,** 171 (1960).
(5) Brown, S. C., "Basic Data of Plasma Physics," p. 258-273, Mass. Inst. of Tech. Press, Cambridge, Mass. and John Wiley and Sons, Inc., New York, N. Y., 1959.
(6) Christain, D. C., Boyd, P. B., Jr., *Chem. Eng.* **56** (5), 148 (1949).
(7) Fischer, F., Peters, K., *Brennstoff-Chem.* **12,** 268 (1931).
(8) Fraser, J. C., *"Abstracts of Papers," 153rd Meeting, ACS, Miami Beach, Fla., April 1967,* **197.**
(9) Fredersdorff, C. G. von, Elliott, M. A., "Chemistry of Coal Utilization," Supplementary Volume, Chapter 20, H. H. Lowry, Ed., John Wiley & Sons, Inc., New York, N. Y., 1963.
(10) *Ibid.*, p. 893.
(11) Fuji, S., Takemura, N., ADVAN. CHEM. SER. **21,** 334 (1959).
(12) Glockler, G., Lind, S. C., "The Electrochemistry of Gases and Other Dielectrics," John Wiley & Sons, Inc., New York, N. Y., 1939.
(13) Jolly, W. L., "Technique of Inorganic Chemistry," Vol. 1, pp. 179-208, H. B. Jonassen, A. Weissberger, Eds., Interscience Div. of John Wiley & Sons, Inc., New York, N. Y., 1963.
(14) Loeb, L. B., "Electrical Coronas, Their Basic Physical Mechanisms," Univ. of Calif. Press, Berkeley and Los Angeles, 1965.
(15) Lunt, R. W., *Proc. Royal Soc. (London)* **108A,** 172 (1925).
(16) Lunt, R. W., ADVAN. CHEM. SER. **21,** 286 (1959).
(17) Manley, T. C., *Trans. Electrochem. Soc.* 84, 83 (1943).
(18) McTaggart, F. K., *Australian J. Chem.* **17,** 1182 (1964).
(19) Meek, J. M., Craggs, J. D., "Electrical Breakdown of Gases," pp. 148-176, Oxford Univ. Press, England, 1953.
(20) Mendenhall, W., "Introduction to Linear Models and the Design and Analysis of Experiments," Wadsworth Pub. Co., Inc., Belmont, Calif., 1968.
(21) Morgan, J. J., *in* "Chemistry of Coal Utilization," Vol. 2, pp. 1673-1749, H. H. Lowry, Ed., John Wiley & Sons, Inc., New York, N. Y., 1945.
(22) *Ibid.*, p. 1704.
(23) Peters, K., Kuster, H., *Zeit. Physik. Chem.* **148A,** 284 (1930).

(24) Peters, K., Pranschke, A., *Brenn stoff-Chem.* **11,** 473 (1930).
(25) Sahasrabudhey, R. H., Deshpande, S. M., *Proc. Ind. Acad. Sci.* **31A,** 317 (1950).
(26) Sherwood, P. W., *Petroleum (London)* **24,** 338 (1961).
(27) Spedding, P. L., *Nature* **214,** 124 (1967).
(28) Thomas, C. L., Egloff, G., Morrell, J. C., *Chem. Rev.* **28** (1), 1 (1941).
(29) Wendt, G. L., Evans, G. M., *J. Am. Chem. Soc.* **50,** 2610 (1928).

RECEIVED August 10, 1967.

18

The Reaction of Oxygen with Carbonaceous Compounds and Trace Mineral Constituents in an Inductive Electrodeless Discharge

CHESTER E. GLEIT

North Carolina State University, Raleigh, North Carolina 27607

Publication Date: June 1, 1969 | doi: 10.1021/ba-1969-0080.ch018

The relationship between oxidation rate and sample temperature of graphite in a low pressure oxygen plasma was studied. Energy was supplied from an inductively coupled, 13.56-MHz., 250-watt generator. The apparent activation energy of graphite was 6.5 kcal./mole in the temperature range 100° to 300°C. and zero at higher temperatures. The activation energy of both impure graphite and sucrose were slightly lower. Graphite did not react with a CO_2 plasma below 120°C. and yielded an apparent activation energy of 3.2 kcal./mole between 150° and 300°C. Oxidation rate was dependent on electrical field configuration. Increasing the temperature of the reaction tube's walls decreased oxidation rate. Trace elements were generally converted to their highest stable oxidation states. Volatility was not strongly temperature dependent.

In 1962 a method was reported for the decomposition of organic substances based on reaction with an oxygen plasma, which was produced by passing molecular gas through a radiofrequency electrodeless discharge (*5*). This method has found use in a variety of chemical studies. Loss of trace elements through volatilization and diffusion is less than in conventional dry ashing. Destruction of mineral structure is reduced. Since a small quantity of purified oxygen is the only reagent, the possibility of chemical contamination is diminished. Applications of this method include: microincineration of biological specimens (*13*), the ashing of coal (*6*) and filter paper (*4*), and the recovery of mineral fibers from tissue (*1*). Several reviews of analytical applications have been published (*9, 14*).

In Chemical Reactions in Electrical Discharges; Blaustein, B.;
Advances in Chemistry; American Chemical Society: Washington, DC, 1969.

In conventional ashing both reaction rate and retention of volatile components are strongly temperature dependent. However, disagreement exists as to the effect of temperature in plasma ashing. In part, this is attributed to difficulty in applying conventional temperature measuring techniques to solids immersed in a strong radiofrequency field. The question is further complicated by the fact that a single temperature cannot be assigned to the system. Electrons in the low pressure plasma are not in thermal equilibrium with the ions and neutral species. Furthermore, the temperature of the specimen and the surrounding vessel may differ considerably. In this study the effects of temperature on oxidation rate, recombination of active gaseous species, and volatility of inorganic reaction products are considered.

Publication Date: June 1, 1969 | doi: 10.1021/ba-1969-0080.ch018

Experimental

The reaction system employed in these studies (Figure 1) consisted of a 100-cm. long, 3.5-cm. i.d., borosilicate cylinder (Pyrex No. 7740). Specimens were placed on the principal axis 43 cm. from the gas inlet. A 0.6-cm. tube, *C*, passed diametrically through the cylinder and held the specimen on a central projection. Sample temperature was regulated, in part, by circulating liquids between this tube and a constant temperature bath. With the exception of those measurements in which wall temperature was intentionally altered the external temperature of the reaction vessel was maintained between 20° and 25°C. Forced air cooling was employed. Radio-frequency excitation was supplied from a 250-watt, crystal controlled 13.56-MHz. generator, described previously (3). Except as otherwise noted, an output of 115 watts was employed. Power was transferred to the gas by means of an impedance matching network terminating in a 10-turn coil of 1/4-inch o.d. copper tubing tapped two turns from ground. The coil, *B*, which had an inside diameter of 4.5 cm. and was 12.5 cm. long, was coaxial with the reaction tube and placed 10 cm. from the gas inlet.

After passage through a rotometer, molecular gas entered the reaction system through a capillary orifice, *A*. Pressure was monitored by a McCloud gauge attached to side arm *E*, located 50 cm. beyond the gas inlet. Pressure was maintained at 1.2 torr; and flow rates at 150 cc. per minute, S.T.P. U.S.P. grade oxygen and instrument grade carbon dioxide were used.

The temperature of solid specimens in the plasma was determined by means of an infrared radiation thermometer (Infrascope Model 3-1C00, Huggins Laboratories Inc., Sunnyvale, Calif.) attached to a chart recorder. This device employs a lead sulfide detector and suitable filters to permit remote measurement of 1.2 to 2.5μ radiation emitted by the specimen. Line filters and electrostatic shielding were employed to minimize interaction of the radiofrequency field with the infrared thermometer. To compensate for variations in emissivity and inhomogeneity in the optical field, empirical calibration curves were constructed based on measurements of new and partially oxidized graphite pellets in a con-

In Chemical Reactions in Electrical Discharges; Blaustein, B.;
Advances in Chemistry; American Chemical Society: Washington, DC, 1969.

ventional oven. Thermocouples were employed to determine cylinder-wall temperatures. To eliminate interaction with the radiofrequency field, the transmitter was inactivated during the latter measurements. Sequential measurements of both sample and wall temperatures indicated that an extrapolation to generator-on conditions was not required, as cooling rate was low.

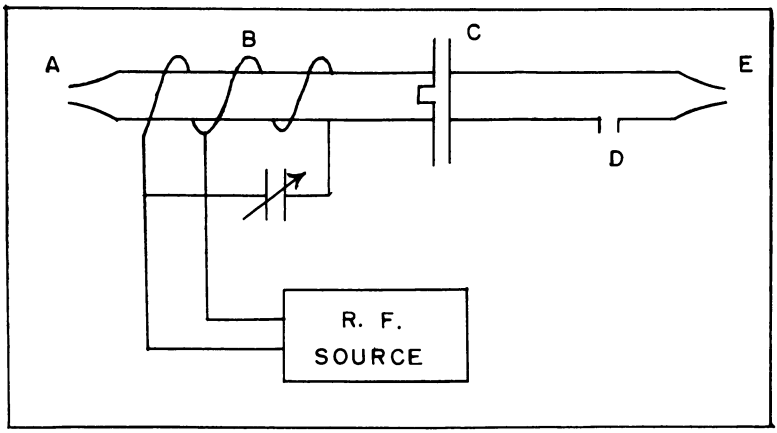

Figure 1. Experimental Apparatus

A = *Capillary inlet;* B = *Power coil;* C = *Specimen mounting tube;* D = *Sidearm to manometer; and* E = *Outlet to vacuum pump*

High purity graphite rods (National Carbon Co., Grade AGKSP) were employed as standard specimens. These rods were 0.61 cm. in diameter and had a cavity machined into their base to affix them to the cooling tube. Pellets of sucrose and carbon containing small quantities of cupric acetate were also employed. The latter were produced by heating and then pressing a slurry of the salt solution and 200-mesh graphite powder. Oxidation rate was determined by weighing the residual solid after 15 minutes. Measurements were usually continued for one hour.

Results and Discussion

Sample Temperature. The temperature variation of oxidation rate of graphite exposed to the oxygen plasma is shown in Figure 2. Over the range 120° to 300°C., the Arrhenius equation, $K = Ce^{-E_a/RT}$, fits the data well and yields a value of 6.5 kcal./mole for the apparent activation energy, E_a. Between 300° and 450°C., the highest temperature studied, oxidation rate is not dependent on temperature. The oxidation of graphite by molecular oxygen at high temperature is strongly dependent on the purity of the graphite. To determine if a similar effect occurs in plasma oxidation, pellets composed of pure graphite powder

Publication Date: June 1, 1969 | doi: 10.1021/ba-1969-0080.ch018

and inorganic salts were utilized. The results of the addition of 0.01*M* cupric acetate are shown in Figure 2. At low temperature the change in oxidation rate of pure and impure graphite with temperature is similar. However, the rate of oxidation of the impure graphite becomes independent of temperature at a lower temperature. Measurements performed with specimens containing lower concentrations of cupric acetate led to results which fell between the illustrated curves.

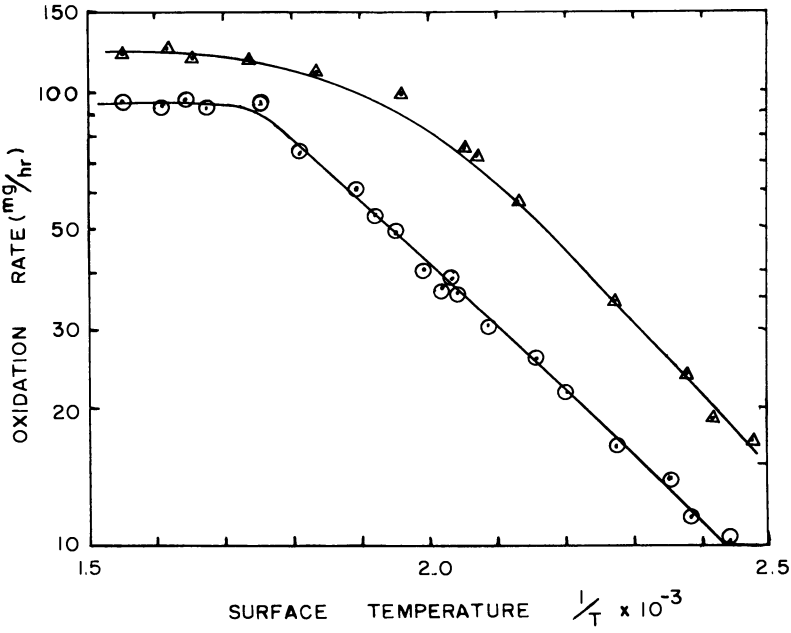

Figure 2. Rate of oxidation vs. *surface temperature for graphite rods and graphite pellets containing 0.01*M *cupric acetate*

⊙—*Graphite rods*
△—*Graphite pellets*

The apparent activation energies are based on the experimentally measured sample surface temperatures. Although this empirically provides a satisfactory means of describing the variation in oxidation rate, its theoretical significance must be qualified. The gas in the low pressure electrodeless discharge is chemically similar to that in the positive column of a low pressure arc. Molecule-molecule and ion-molecule collisions are frequent. The ions and neutral species are, therefore, nearly in translational equilibrium, with the ions having the greater kinetic energy. Elastic collisions between these species and electrons are less frequent. At low pressure electron temperatures are quite high. In addition, spectroscopic measurements indicate that rotational and vibrational modes are not

Publication Date: June 1, 1969 | doi: 10.1021/ba-1969-0080.ch018

equilibrated with translational energy. Therefore, no single experimental temperature can describe correctly the reaction system. Furthermore, the number of active gas species is unknown. In the oxygen discharge atomic oxygen (^3P) is believed to be the most abundant active species. Higher energy states of atomic oxygen, positive and negative ions, and electronically excited states of molecular oxygen are also present.

It is instructive to compare these results with the studies of graphite with atomic oxygen removed from the luminous discharge (*2*). An early study indicated a value of zero for the activation energy of this reaction (*16*). Hennig (*8*) observed no dependence on temperature at a pressure of 1.0 torr and a value of 7 kcal./mole at 10 torr. This difference was attributed to ozone formation. In a recent detailed study of the atomic oxygen-graphite reaction, Marsh *et al.* (*11*) reported an activation energy of 10 kcal./mole between 14° and 200°C., which approached zero at 350°C. Although the rate of oxidation in these studies was considerably lower than that obtained in the plasma, their values are consistent with the belief that atomic oxygen is a major reactant within the discharge. Of a variety of specimens, only graphite exhibited an abrupt change in activation energy near 300°C. For example, the apparent activation energy in the decomposition of sucrose is approximately 4 kcal./mole over the entire measurement range. The independence of oxidation rate for graphite at high temperatures is ascribed to the formation of surface oxides. Numerous studies of graphite combustion have shown that such surface compounds control rate at elevated temperatures in excess oxygen. As anticipated, increasing radiofrequency power to the discharge does not measurably increase the rate of graphite oxidation at high sample temperature.

The exhaust gas of the oxygen-graphite reaction contains both carbon monoxide and carbon dioxide, with the latter more abundant. In the luminous discharge region these gases react with graphite. The results of measurements in which carbon dioxide was passed through the radio-frequency field and then exposed to graphite rods activated are shown in Figure 3. Between 150° and 400°C. the Arhennius equation fits well, yielding an apparent activation energy of 3.2 kcal./mole. Below 120°C. less than one mg. per hour of carbon was removed. This small weight loss is attributed to ion and electron bombardment.

Wall Conditions. In a number of experiments, increasing power beyond an optimum value led to the anomolous result of reducing ashing rate. Earlier it was noted that placing a dry ice-acetone trap in the exhaust stream extended the length of the luminous discharge (*5*). To study this effect, wall temperatures were varied while the carbon rod was maintained at 200°C. The results of a series of measurements are shown in Figure 4. Assuming that the decrease in oxidation rate at increased

Publication Date: June 1, 1969 | doi: 10.1021/ba-1969-0080.ch018

In Chemical Reactions in Electrical Discharges; Blaustein, B.;
Advances in Chemistry; American Chemical Society: Washington, DC, 1969.

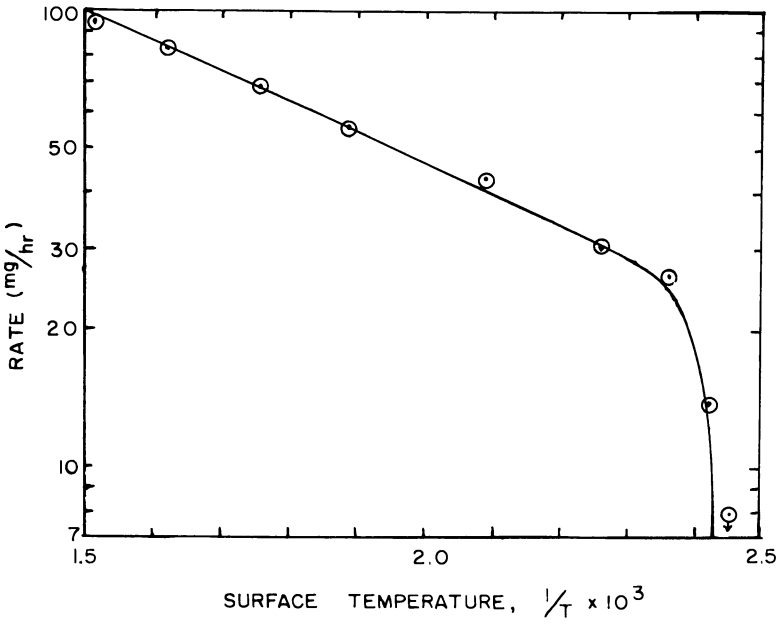

Figure 3. Rate of gasification vs. *temperature for graphite rods exposed to carbon dioxide discharge*

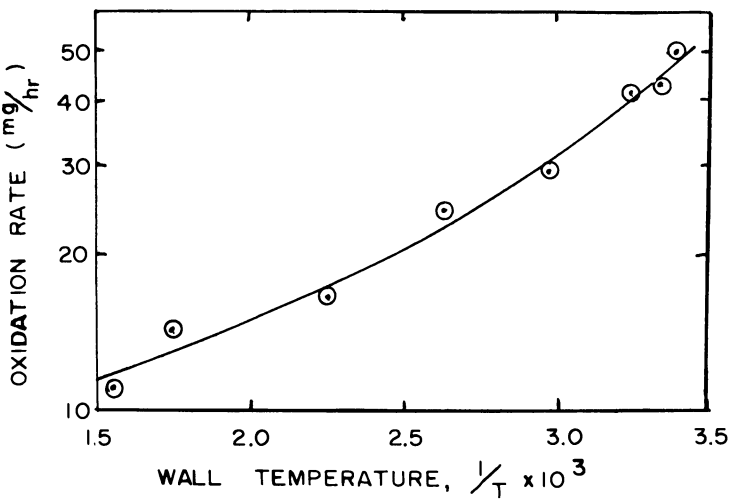

Figure 4. Effect of wall temperature on the oxidation rate of graphite

wall temperature is caused by recombination of active species at the wall, the overall activation energy at low temperatures for this process is approximately 2 kcal./mole.

Publication Date: June 1, 1969 | doi: 10.1021/ba-1969-0080.ch018

The major sources leading to loss of active oxygen species are recombination of atomic oxygen and ions at the walls of the vessel. The recombination of discharged oxygen on glass surfaces has been investigated. Linnett and Marsden (*10*) reported that the recombination coefficient of atomic oxygen on clean borosilicate glass was independent of temperature. However, positive values were observed on contaminated surfaces. In a later series of papers Greaves and Linnett (*7*) studied a number of oxide surfaces, in all cases the recombination coefficient was temperature dependent. For silica apparent activation energies were 1 to 13 kcal./mole over the temperature range 15° to 300°C. The exceptional nature of borosilicate glass was noted.

The second major source of loss of active species results from electron-ion recombination at the chamber walls. The electric field restricts the drift of ions to the chamber walls. Rate of recombination is controlled by ambipolar diffusion, but is limited by the presence of negatively charged oxygen ions in the discharge (*15*). Although diffusion is not dependent on wall temperature, a distortion of the axially symmetric electrical field will enhance wall recombination, producing an increase in wall temperature and a reduction of oxidation rate. This effect is noted in Table I. The presence of a 6-cm. wide metallic ring on the exterior wall of the reaction vessel reduced oxidation rate by more than 10%. Grounding the ring in common with the output coil further reduced the oxidation rate. This is a local effect, in that oxidation rate beyond the ring was not greatly reduced. Distortion of the field can also be introduced by changing the angle between the end of the output coil and the reaction tube. Variations from axial symmetry led to reduced rates and decreased the length of the luminous discharge. Similar effects have been observed in electrodeless discharges at higher pressure (*12*).

Publication Date: June 1, 1969 | doi: 10.1021/ba-1969-0080.ch018

Table I. Effect of Field Distortion on Carbon Oxidation Rate

	Angle	*Oxidation Rate mg./hr.*
Borosilicate glass tube	0°	79
Borosilicate glass tube and ungrounded copper ring	0°	70
Borosilicate glass tube and grounded copper ring	0°	62
Borosilicate glass tube	1°	71
Borosilicate glass tube	3°	63

Effect on Mineral Constituents. It has been reported that there is no appreciable loss of a number of metal ions in plasma oxidation (*4, 5*). Non-volatile species include Na(I), Cs(II), Cu(II), Zn(II), Mn(II),

Pb(II), Cd(II), Co(II), Ho(III), Er(III), Fe(III), Cr(III), As(III), Sb(III), and Mo(VI). The effect of ashing temperature, the reason for the surprisingly low volatility, and the final oxidation state of the product were not previously explored. As part of the present study, 20 to 100 mg. of compounds containing radioactive tracers were deposited on Whatman cellulose filters. After exposure to ashing for a sufficient period to remove the filter paper, generally 30 minutes, the activity of the ash was measured and the oxidation state of the element determined. Specimen temperature was adjusted during ashing by altering input power.

These measurements are summarized in Table II. In general, temperature has little effect on retention. These results and earlier observations indicating complete retention of metals in compounds such as arseneous chloride and metalloporphyrins (5) are believed to be caused by competition between volatilization and oxidation to less volatile compounds. Unlike the other elements studied, the highest valence oxide of osmium, OsO_4, is the most volatile. Therefore, this element is volatilized in the plasma oxidation process.

Publication Date: June 1, 1969 | doi: 10.1021/ba-1969-0080.ch018

Table II. Recovery of Trace Elements from Ashed Filter Paper

Tracer	*Compound*	*Max. Sample Temperature*	*Percent Recovered*	*Highest Oxidation State*	*Percent in Highest Oxidation State*
^{59}Fe	$Fe(OH)_2$	120	100	III	95
^{59}Fe	$Fe(OH)_3$	120	100	III	100
^{75}Se	Na_2SeO_3	110	99	V	91
^{75}Se	Na_2SeO_2	250	100	V	93
^{75}Se	Na_2SeO_4	110	100	V	100
^{75}Se	Na_2SeO_4	250	100	V	100
^{110m}Ag	AgCl	110	89(99) [a]	I	—
^{110m}Ag	AgCl	250	79(100) [a]	I	—
^{191}Os	OsO_2	120	<1	VIII	—
^{191}Os	Na_2OsO_4	150	<1	VIII	—

[a] Recovered after rinsing tube with $HF–HNO_3$.

The volatility of iodide, shown in Figure 5, is also consistent with the hypothesis of competition between volatilization and oxidation. During these measurements, ashing was stopped at 5 minute intervals. It is seen that loss of ^{131}I closely follows the curve for filter paper gasification. No loss of ^{131}I occurs after the filter paper is removed. Loss of ^{131}I varied between 15 and 35%. However, none of the residual ^{131}I could be precipitated with silver nitrate, indicating that the iodide had been oxidized.

In Chemical Reactions in Electrical Discharges; Blaustein, B.;
Advances in Chemistry; American Chemical Society: Washington, DC, 1969.

When the ^{131}I tracer was converted to $NaIO_3$ before ashing, all of the iodine activity was retained.

The behavior of silver ion represents a different type of ashing loss. As opposed to the other metals in this study, only 75 to 90% of the ^{110m}Ag could be recovered from the borosilicate sample holder by rinsing with dilute nitric acid. To recover the remainder of the ^{110m}Ag, the glassware had to be repeatedly rinsed with a warm mixture of nitric and hydrofluoric acids. By maintaining the system at low temperature this difficulty was ameliorated, but not eliminated.

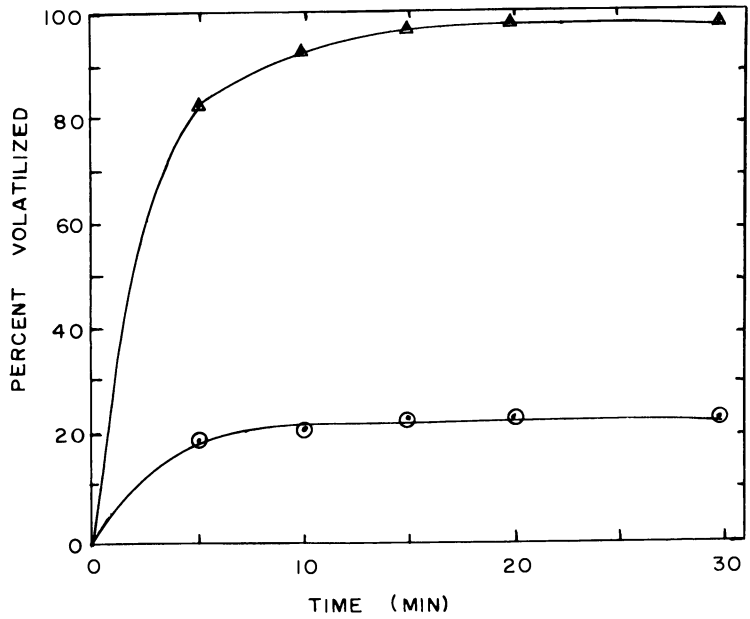

Figure 5. Loss of sample weight and loss of ^{131}I tracer during ashing of filter paper in an oxygen plasma

△—*Sample weight*
⊙—^{131}I *tracer*

Conclusion. A number of active species are known to be present in the luminous electrodeless discharge. Although a similarity between reactions in the plasma and those of discharged oxygen is noted, it cannot be concluded that within the plasma only the reactions of atomic oxygen are significant. The present study indicates appropriate conditions for the application of the electrodeless discharge to decompose carbonaceous materials prior to elemental analysis. Specifically, increasing sample temperature to 200°–300°C. leads to an improvement in ashing rate without appreciably increasing volatility losses.

Publication Date: June 1, 1969 | doi: 10.1021/ba-1969-0080.ch018

Acknowledgment

The electrical apparatus used in this study was constructed by James Breitmeier. The assistance of Juan Wong and Daniel Silvers is appreciated. Walter Holland, Harvey Beaudry and Robert Reinhart assisted in preliminary studies performed under a contract between Union Carbide Chemical Corporation and the Laboratory for Electronics. This study was supported by grants from the North Carolina Engineering Foundation and North Carolina State University Professional Development Fund.

Literature Cited

(1) Berkley, C., Churg, J., Selikoff, I. J., Smith, W. E., *Ann. New York Acad. Sci.* **132,** 48 (1965).
(2) Blackwood, J. D., McTaggart, F. K., *Australian J. Chem.* **12,** 114 (1959).
(3) Gleit, C. E., *Microchem. J.* **10,** 7 (1966).
(4) Gleit, C. E., Benson, P. A., Holland, W. D., Russell, I. J., *Anal. Chem.* **36,** 2067 (1964).
(5) Gleit, C. E., Holland, W. D., *Anal. Chem.* **34,** 1454 (1962).
(6) Gluskoter, H. J., *Fuel* **44,** 285 (1965).
(7) Greaves, J. C., Linnett, J. W., *Trans. Faraday Soc.* **54,** 1355 (1958).
(8) Hennig, G. R., Dienes, G. J., Kosiba, W., *Proc. Second Intern. Conf. Peaceful Uses At. Energy, Geneva* **7,** 301 (1958).
(9) Hollahan, J. R., *J. Chem. Educ.* **43,** A401, A497, 392 (1966).
(10) Linnett, J. W., Marsden, D. G. H., *Proc. Roy. Soc. (London) Ser. A* **234,** 489 (1956).
(11) Marsh, H., O'Hair, T. E., Wynne-Jones, W. F. K., *Trans. Faraday Soc.* **61,** 274 (1965).
(12) Mitin, R. V., Pryadkin, K. K., *Zh. Tekhn. Fiz.* **35,** 1205 (1965).
(13) Thomas, R. S., *J. Cell Biol.* **23,** 113 (1964).
(14) Thomas, R. S., "Subcellular Pathology," J. W. Steiner, H. Z. Morat, A. C. Ritchie, eds., Harper and Row, New York (in press).
(15) Thompson, J. B., *Proc. Phys. Soc. (London)* **73,** 818 (1959).
(16) Turkevich, J., Streznewski, T., *Revue L'Inst. Fran. du Petrole* **13,** 686 (1958).

RECEIVED June 19, 1967.

19

Vapor Phase Formation of Noncrystalline Films by a Microwave Discharge Technique

D. R. SECRIST

International Business Machines Corporation, Poughkeepsie, New York

J. D. MACKENZIE

Rensselaer Polytechnic Institute, Troy, New York

Publication Date: June 1, 1969 | doi: 10.1021/ba-1969-0080.ch019

Noncrystalline films were deposited at low temperatures and pressures by the vapor phase reaction of suitable compounds with the energetic gaseous species generated in a discharge operated at 2,450 megahertz. The decomposition of metal-organic compounds of the type $(R)_x M$ *or* $(RO)_x M$, *where R may be* C_2H_5, C_3H_7, *etc., lead to amorphous oxide films of silicon, germanium, boron, tin, and titanium when an oxygen plasma was maintained. Silica films were also grown* via *an argon plasma. These films were deposited onto metallic or nonmetallic substrates positioned outside the discharge region. Conversely, the oxidation of silicon tetrafluoride to yield a fluorosiloxane polymer of composition* $SiO_{1.5}F$ *was found to occur only within the confines of the plasma.*

Extensive studies have been conducted with crystalline films in regard to film structure, epitaxy, and property variations as a function of the history of a particular deposition process. The nature of glassy films, however, has not been investigated with the same thoroughness. This is owing, in part, to the inability of most materials to form in the glassy state. In general, the approach to film formation has been from the vapor phase. Some methods from the vapor include evaporation, vapor phase hydrolysis, thermal decomposition, and "sputtering." All of these techniques will yield noncrystalline films with the proper conditions. However, with the exception of the later method, relatively high temperatures are required. As a result, most films invariably crystallize immediately after being deposited. The noncrystalline films prepared by these techniques are usually materials which readily form a glass by the conven-

In Chemical Reactions in Electrical Discharges; Blaustein, B.;
Advances in Chemistry; American Chemical Society: Washington, DC, 1969.

tional cooling of a melt—*e.g.*, SiO_2. The method of "sputtering," on the other hand, occasionally leads to the formation of uncommon noncrystalline films when the substrates are maintained at low temperatures (2). In this paper, the low temperature preparation of a wide variety of noncrystalline films is discussed utilizing a microwave discharge method as an alternative to sputtering. With this technique, the rate of film deposition can be carefully controlled by regulation of the reactant flow rates. The quality of any particular film is shown to be a sensitive function of (1) the concentration and type of reaction products, (2) the chemical nature of the substrate, and (3) the reactor (substrate) temperature.

Publication Date: June 1, 1969 | doi: 10.1021/ba-1969-0080.ch019

Apparatus

A schematic of the main flow system employed in this work is shown in Figure 1. A gaseous plasma, in this instance oxygen, could be maintained in a 1 inch o.d. borosilicate glass tube when the system pressure was less than 0.8 torr. The electrodeless discharge was produced with a Raytheon PGM-10 Microwave Generator. This unit could supply 100 watts of microwave energy at a fixed frequency of 2,450 mc./sec. The energized species were allowed to flow into the bell jar through a 0.5 inch diameter borosilicate glass tube. The metal-organic compounds selected for this work were liquids with a vapor pressure of about 0.5 mm. near room temperature and were contained in a graduate cylinder immersed in a constant temperature bath. The metal-organic evaporation rate (flow rate) at any temperature could be altered by adjusting a 1 mm. diameter Teflon stop-cock. The ultimate vacuum achieved in the system was 0.24 torr with a gas flow rate of 1.76 cc./minute. The majority of the studies were performed inside an aluminum furnace 2 1/4 inches in diameter $\times$ 4 inches long. A fused silica cylinder 1 3/8 inches in diameter $\times$ 2 1/2 inches long served as a second furnace core. The constant temperature zones for these furnaces extended one cm. above and below the gas inlet port with a maximum radial temperature variation of $\pm 5°C.$ for points one cm. from the cylinder axes. A fused silica balance having a sensitivity of 1 cm./mg. was employed to determine the rate of film deposition. Details of this apparatus have been previously reported (*4*). In order to provide a secondary work geometry, the basic apparatus was modified as illustrated in Figure 2. This adaptation was used to study the oxidation of silicon tetrafluoride.

Film Deposition and Evaluation

The substrates were positioned in the furnace reaction vessel with their wide dimension perpendicular to the gas inlet tube. The general

cleaning procedure consisted of dipping the specimens into a 48% solution of hydrofluoric acid, followed by a rinse in distilled water. During the period when the furnace temperature was increasing, the system was purged with the gas selected to form the plasma. In all work, the microwave generator was operated at 90% of its rated power output.

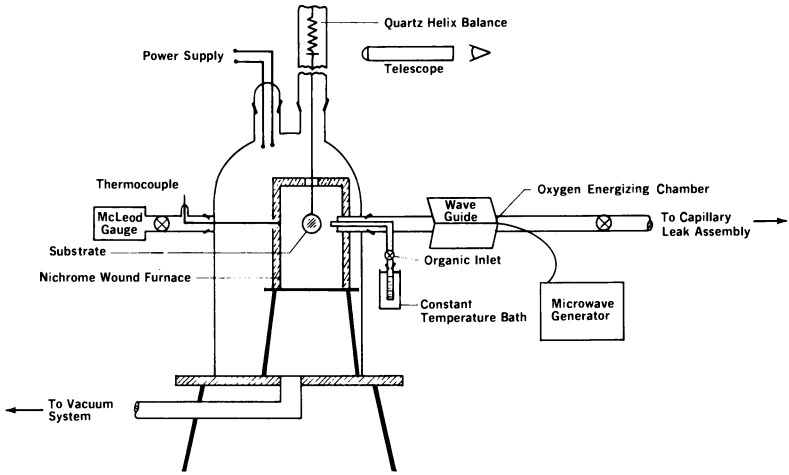

Figure 1. Schematic of microwave discharge apparatus

The films were deposited onto NaCl or KBr discs to facilitate examination by infrared transmission. Substrates of platinum, aluminum, Al_2O_3, and fused SiO_2 approximately one cm. in diameter were prepared for the rate studies. The index of refraction and isotropic character of film specimens obtained from the substrates and/or gas inlet tube were determined with a petrographic microscope. Debye-Scherrer x-ray diffraction powder patterns were made to establish whether the films were amorphous or crystalline.

Results and Discussion

Preliminary studies indicated that extensive water was formed as a reaction product when the metal-organic compounds were decomposed *via* an oxygen discharge. This water could be chemically incorporated into the oxide films when the substrates were held below a certain temperature which depended on the organic evaporation rate and the hygroscopic nature of the substrate. For instance, with NaCl substrates, the silica films were found to be free of water above 180°C. with a tetraethoxysilane evaporation rate of 0.015 cc./hour (5). The presence of silicic acid was detected below 180°C. by infrared transmission studies.

Publication Date: June 1, 1969 | doi: 10.1021/ba-1969-0080.ch019

In Chemical Reactions in Electrical Discharges; Blaustein, B.;
Advances in Chemistry; American Chemical Society: Washington, DC, 1969.

Conversely, with a KBr substrate and similar conditions of temperature and evaporation rate, extensive water was incorporated into the silica film.

The majority of the films prepared in this study were formed at 0.24 torr on NaCl substrates heated to a temperature of 200°C. (deposition rates of about 20 A./minute). The optical properties of some of the films are presented in Table I.

All of the films were isotropic when examined with polarized light and were amorphous by x-ray diffraction. The silica films were formed by (1) decomposing tetraethoxysilane, $(C_2H_5O)_4Si$, in either an oxygen or argon plasma or (2) decomposing tetraethylsilane in an oxygen plasma. The germania and boron oxide films were prepared by decomposing tetraethoxygermane and triethylborate *via* an oxygen discharge. The infrared absorption frequencies and refractive indices of the latter three vapor-formed films are similar to those of the respective fusion-formed glasses, which suggests that a random network structure can be achieved by methods other than the conventional cooling of the melt. The spread in the index of refraction for germania glass was realized by slow-cooling one specimen and quenching another from 1100°C.; the slow-cooled specimen had the larger refractive index. With the exception of the boron oxide film, the films listed in Table I adhered well to the NaCl substrates. The B_2O_3 film was immediately coated with mineral oil after removal from the glow discharge apparatus because of its extreme moisture sensitivity and was only partially adherent.

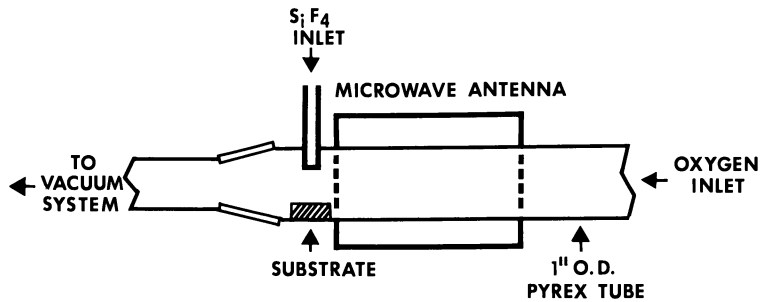

Figure 2. Modified microwave discharge system

The noncrystalline titanium oxide films were prepared from titanium tetraisopropylate while maintaining an oxygen discharge. Since titanium oxide is not a common glass-forming system, one may inquire whether the viscosity of such a film would be similar to that of glass near its transition region—*i.e.*, 10^{13}–10^{14} poises. For many undercooled systems,

In Chemical Reactions in Electrical Discharges; Blaustein, B.;
Advances in Chemistry; American Chemical Society: Washington, DC, 1969.

the growth rate can be described in terms of the reciprocal viscosity (7) as:

$$u = \frac{\Delta H_f(T_f - T)}{3\,T_f \pi(\lambda)^2 \eta N}$$

where u is the rate of growth (cm./sec.), T is the undercooled temperature, η is the viscosity (poises), T_f is the fusion temperature, λ is the mean jump distance (cm.), H_f is the latent heat of fusion (ergs), and N is Avogadro's number. If this relationship is valid for a system, then an approximate estimation of the viscosity at the crystallization temperature can be made if the rate of growth (crystallization) is known. In this study the titanium oxide film exhibited birefringence (crystallized) after 45 minutes at 325°C. An approximate rate of crystallization can be calculated for the film if it is assumed that the particles grew from some arbitrary value, for example, 10 A. to 110 A., before crystallinity was detected. The jump distance λ was taken as 2 A. units. Although TiO_2 dissociates, the heat of fusion has been reported as 15.5 kcal./mole at a melting point of 1840°C. (*1*). The growth rate determined from the rate of crystallization is about 3.7×10^{-10} cm./sec. The corresponding viscosity at 598°K. is 5.5×10^{11} poises, which would classify the film as a highly viscous supercooled liquid since the viscosity value is slightly below 10^{13}–10^{14} poises. Since viscosity is approximately an exponential function of temperature, it is reasonable to conclude that at some slightly lower temperature the viscosity of the film is characteristic of a solid glass—*i.e.*, 10^{13}–10^{14} poises.

Table I. Comparison of the Optical Properties of Vapor-Formed Films and their Respective Glassy or Crystalline Oxides

	Material	*Principal Infrared Frequency (CM^{-1})*	*Index of Refraction*
SiO_2:	vapor-formed film	1,045; 800	1.458 ± 0.002
	fusion-formed glass	1,080; 800	1.458 ± 0.002
GeO_2:	vapor-formed film	850	1.582 ± 0.002
	fusion-formed glass	860	1.534 – 1.607
B_2O_3:	vapor-formed film	1,350	1.470 ± 0.002
	fusion-formed glass	1,370	1.464 (3)
Ti_xO_y:	vapor-formed film	950-700	>1.7
TiO_2:	anatase	1,200-500	>1.7
Sn_xO_y:	vapor-formed film	1,425	1.536 ± 0.002
SnO_2:	cassiterite	850-500	>1.7

An amorphous tin oxide film was formed by decomposing dibutyltin diacetate *via* an oxygen plasma. Preliminary measurements indicated that the electrical resistivity of the film near room temperature was greater than 10^7 ohm-cm. Comparing the infrared spectra of the film and SnO_2,

Publication Date: June 1, 1969 | doi: 10.1021/ba-1969-0080.ch019

it is seen in Table I that the main absorption mode for the amorphous film occurs at a much higher frequency than that of the crystalline modification. This shift can probably be attributed to a large structural variation such as a change in coordination number.

The basic apparatus shown in Figure 1 was modified as illustrated in Figure 2 in order to study the oxidation of SiF_4 *via* an oxygen discharge. Research grade SiF_4 gas was metered into the borosilicate glass chamber at a rate of 1.8 cc./minute. Simultaneously, dry oxygen was admitted at the rate of 5 cc./minute. The electrodeless discharge was maintained at 0.8 torr. Under these conditions, a thick nonadherent film was deposited onto the walls of the borosilicate glass chamber within the boundaries of the plasma in about one hour. The wall temperature in this region was approximately 100°C. The film can be described as a translucent blue-white gel which was amorphous by x-ray diffraction and isotropic when observed with polarized light. The index of refraction of the gel was estimated to be considerably less than 1.400; infrared absorption bands were evidenced at 1080, 920, and 750 $cm.^{-1}$. A microchemical analysis of the film indicated that its composition could be represented as $(SiO_{1.5}F)_n$. It is interesting to note that the film formed only within the confines of the plasma, which suggests that thermal and/or microwave energy are required for the oxidation and/or polymerization processes.

Effect of Pressure, Temperature, and Substrate. An extensive study was made with the silica films with respect to the mechanism and kinetics of film formation (*4*). It is reasonable to suspect that the general conclusions formulated in this work with respect to pressure, temperature, and nature of the substrate are applicable to most of the other oxide films discussed in this report. Support for this viewpoint is also documented in regard to the incorporation of water into the films (*5*).

Basically, the effect of minor pressure fluctuations on the rate of deposition of silica films was found to be negligible. However, above 500 microns pressure, the rate of deposition was rapidly decreased because of (1) an increased atomic oxygen recombination and (2) poisoning effects from the reaction products. The films discussed in the present work were deposited near 0.24 torr. Typical rates of deposition for the silica films ranged from 10 to 80 A./min. by variation of (1) the organic evaporation rate or (2) the substrate temperature. The rate of deposition was constant with time. The relationship between logarithm of the deposition rate and reciprocal temperature is depicted in Figure 3 for various substrates. The data have been spread to show the temperature dependence of deposition with each substrate. With a tetraethoxysilane evaporation rate of 0.15 cc./hour, the silica films were free of water and/or organic inclusions (by infrared transmission studies) above

In Chemical Reactions in Electrical Discharges; Blaustein, B.;
Advances in Chemistry; American Chemical Society: Washington, DC, 1969.

Publication Date: June 1, 1969 | doi: 10.1021/ba-1969-0080.ch019

~290°C. At high temperatures, the rate of deposition decreased with increasing temperature and was ascribed to a process of physical adsorption. The apparent heat of adsorption of silica glass on the fused silica, NaCl, and platinum substrates was calculated to be 12.7 ± 0.2 kcal./mole. For the aluminum or Al_2O_3 substrates, the apparent heat of adsorption of silica was calculated to be 9.5 ± 0.3 kcal./mole. It was concluded that the hygroscopic nature of the Al_2O_3 surface was responsible for the lower heat of adsorption observed. It was postulated that a hydrated surface tends to incorporate further hydroxyl groups into the film structure. With this reasoning, one might surmise that the hygroscopic nature of the KBr substrate discussed earlier would also lead to a decreased heat of adsorption. In conclusion, it is postulated that the rate of deposition of an oxide film with a moisture sensitivity similar to that of silica is most likely affected in the same manner—*i.e.*, physical adsorption controlled below 410°C. The apparent heat of adsorption of an oxide film is, of course, dependent on the molecular structure and chemical nature of both the film and substrate.

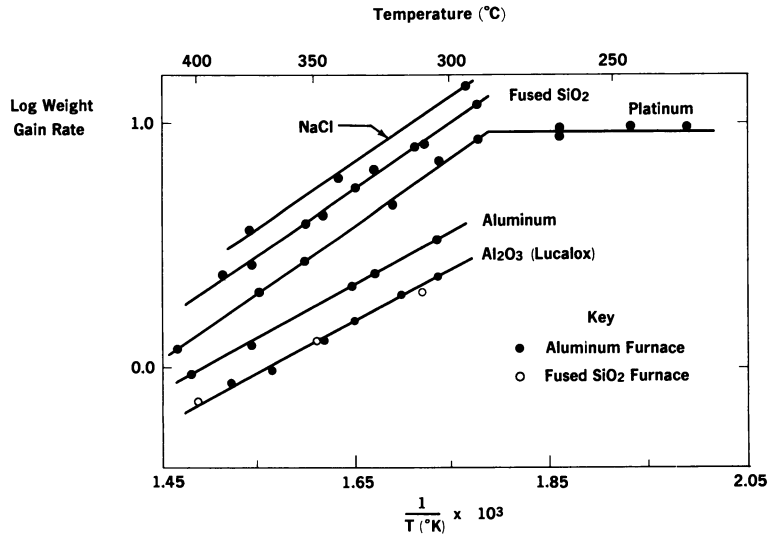

Figure 3. Relationship of logarithm silica deposition rate and reciprocal temperature for deposition on various substrates

Other Systems. The microwave discharge technique can be employed to deposit a variety of thin films at low temperatures. One obvious variation of the technique utilizes gaseous plasmas other than oxygen. For instance, in the work with silica films it was found that $(C_2H_5O)_4Si$ contained sufficient oxygen to facilitate the formation of SiO_2 when the former compound was decomposed with energetic argon species. Sterling

In Chemical Reactions in Electrical Discharges; Blaustein, B.;
Advances in Chemistry; American Chemical Society: Washington, DC, 1969.

and Swann (*6*) have deposited amorphous Si_3N_4 films by the reaction of silane and anhydrous ammonia in an RF discharge. Noncrystalline silicon nitride films have also been prepared at Rensselaer Polytechnic Institute by the decomposition of $(C_2H_5)_4Si$ *via* a nitrogen discharge. The use of a N_2O plasma to form Si_2ON_2 poses another equally interesting possibility. Success to date with the latter reactions has been complicated by the ease of formation of silica. Since metal-organic compounds are now available for a large number of metals, it would seem that the microwave discharge technique could lead to many new and unusual films by a simple variation of the reactant and/or plasma compositions.

Acknowledgment

The authors are grateful to the Pittsburgh Plate Glass Company for the support of a fellowship (D. R. S.).

Literature Cited

(1) Kubachewski, O., Evans, E., "Metallurgical Thermodynamics," p. 306, Pergamon Press, New York, 1958.
(2) Mickelson, R. A., *Sc. D. Thesis, M.I.T.* (1963).
(3) Morey, G. W., "The Properties of Glass," 2nd Ed., Chap. XVI, p. 370, Reinhold Publishing Corp., New York, 1954.
(4) Secrist, D. R., Mackenzie, J. D., *J. Electrochem. Soc.* **113** (9), 914 (1966).
(5) Secrist, D. R., Mackenzie, J. D., *Solid State Electronics* **9**, 180 (1966).
(6) Sterling, H. F., Swann, R. C. G., *Solid State Electronics* **8** (8), 653 (1965).
(7) Turnbull, David, "Solid State Physics," Vol. 3, p. 225, F. Seitz, D. Turnbull, eds., Academic Press, Inc., New York, 1956.

RECEIVED April 27, 1967.

20

Competition of Ethylene and Propane for "Active" Nitrogen

P. TERENCE HINDE and NORMAN N. LICHTIN

Boston University, Boston, Mass., 02215

Publication Date: June 1, 1969 | doi: 10.1021/ba-1969-0080.ch020

Ethylene and propane reacted individually and together with glow discharge-generated "active" nitrogen at autogenous temperature over a wide range of reactant ratios. Consumption data do not correspond to simple competition of ethylene and propane for N(^{4}S) but can be explained by assuming additional attack on each substrate of reactive species generated in the primary reaction. Experiments with mixtures of ^{14}C-labeled ethylene and ordinary propane show that, with N(^{4}S) in molar excess, ethylene is generated at least in part from propane. It is concluded that the specific rate of primary attack of N(^{4}S) on ethylene is more than five times the value for propane. The value of this rate ratio estimated from literature data for the individual compounds is of the order of ten.

The chemical reactions of "active" nitrogen, the luminous, reactive gas produced when molecular nitrogen is passed through an electric discharge at low pressures, have been studied for several decades and the results of these studies have been summarized in a number of reviews, the most recent of which is that of Brocklehurst and Jennings (*2*). The principal chemically reactive species is widely believed to be N(^{4}S) but mechanistic elucidation of the reactions of organic substrates has been frustrated by deep seated molecular disruption and wide diversity of products. For several years work in this laboratory has been devoted to the gas phase reactions of "active" nitrogen with propylene (*8, 11, 12*) and with conjugated dienes (*3, 4, 13*). Experiments involving propylene have employed the three ^{14}C-labeled isomers to identify (*11, 12*) the molecular origins of six products, HCN, C_2H_2, C_2H_4, C_2H_6, C_3H_8, and CH_3CN and to explore (*8*) the resynthesis and molecular rearrangement of propylene under reaction conditions. Experiments employing conju-

In Chemical Reactions in Electrical Discharges; Blaustein, B.;
Advances in Chemistry; American Chemical Society: Washington, DC, 1969.

Table I. Yields of Monomeric[a] Products from 1,3-Butadiene as a Function of Reactant Concentration[b]

$10^4(N_2)$, M	1.6	0.5	1.6	1.5	1.6	1.5
$10^7(N)_o$, M	8.1	27.	8.	8.1	8.	8.1
$(C_4H_6)_o/(N)_o$	6.7	5.	5.	1.0	0.8	0.25
Linear Flow Rate, m.sec.$^{-1}$	7.5	2.3	7.5	5.7	7.5	5.7
	Relative Yields, %					
Pyrrole	23	28	26	22	24	29
cis-Crotononitrile	2	3	2	2	2	3
trans-Crotononitrile	10	15	10	9	8	13
cis-1-Cyanobutadiene-1,3	11	9	11	16	10	3
trans-1-Cyanobutadiene-1,3	14	10	12	20	13	21
3-Cyanobutene	12	7	12	12	10	3
cis-C_5CN	4	3	4	3	4	1
trans-C_5CN	8	6	9	5	8	2
	84	81	86	89	79	75

[a] A monomeric product incorporates one complete butadiene residue in its structure.
[b] Data (3) are relative areas of gas chromatographic peaks.

gated dienes (*3, 4, 13*) have determined yields of as many as 17 (*3*) products as a function of reaction parameters and have provided data amenable to kinetic analysis. Examples of data from these prior studies are presented in Tables I–III. Speculative mechanisms have been proposed (*3, 8, 10*) on the basis of the resulting information—*e.g.*, data for the reaction of 1,3-butadiene can be rationalized by a mechanism the bare elements of which are summarized in Equations 1–7 (*3*). This scheme, in common with others we have proposed (*8, 10*), assumes primary attack

$$C_4H_6 + N \rightarrow C_4H_6N^* \text{ species} \quad (1)$$

$$C_4H_6N^* \rightarrow HCN + NH + C_pH_q \text{ (radicals)} + C_xH_y \text{ (stable molecules)} + \text{pyrrole} + CN + H + \text{etc.} \quad (2)$$

$$C_pH_q + H \text{ or } CN \rightarrow \text{products} \quad (3)$$

$$C_pH_q + N \rightarrow HCN + NH + \text{etc.} \quad (4)$$

$$NH + NH \rightarrow N_2 + H_2 \quad (5)$$

$$NH + N \rightarrow N_2 + H \quad (6)$$

$$C_4H_6 + R' + R \rightarrow \text{adducts} \quad (7)$$

solely by $N(^4S)$ on the organic substrate. Herron has, however, concluded (*6, 7*) from his mass spectrometric studies of the rate of consumption of olefins upon reaction with "active" nitrogen that hydrogen atoms, whether formed as a consequence of primary attack by $N(^4S)$ or present adventitiously, compete with $N(^4S)$ both with respect to primary attack

Publication Date: June 1, 1969 | doi: 10.1021/ba-1969-0080.ch020

on the substrate and with respect to secondary attack on reactive species

$$N + C_2H_4 \rightarrow HCN + CH_3 \quad (8)$$

$$N + CH_3 \rightarrow HCN + 2H \quad (9)$$

$$H + C_2H_4 \rightarrow C_2H_5 \quad (10)$$

$$H + C_2H_5 \rightarrow 2CH_3 \quad (11)$$

$$N + C_2H_5 \rightarrow NH + C_2H_4 \quad (12)$$

$$N + NH \rightarrow N_2 + H \quad (13)$$

formed in the initial attack. Equations 8–14 summarize the mechanism which Herron has proposed (*6, 7*) for the reaction of ethylene.

Table II. Molar Activities of Products from ^{14}C-Labeled Propylenes Relative to Those of Reactant Propylenes[a]

Position of ^{14}C in Propylene	*HCN*	*C_2H_6*	*C_2H_4*	*C_2H_2*	*C_3H_8*	*C_3H_6*	*CH_3CN*
			$(C_3H_6)_o/(N)_o = 10$				
C-1	0.29	0.77	0.66	0.47	0.90	1.02	0.45
C-2	0.32	0.15	0.78	0.86	0.82	1.01	0.99
C-3	0.39	0.95	0.34	0.39	1.00	0.98	0.53
Sum	1.00	1.87	1.78	1.72	2.72	3.01	1.97
			$(C_3H_6)_o/(N)_o = 1.0$				
C-1	0.30	0.69	0.74	0.47	0.98	1.00	0.46
C-2	0.25	0.15	1.00	0.88	1.00	1.03	0.95
C-3	0.39	1.06	0.38	0.56	1.02	1.02	0.48
Sum	0.94	1.90	2.12	1.91	3.00	3.05	1.89
			$(C_3H_6)_o/(N)_o = 0.17$				
C-1	0.33	0.70	0.59	0.47	1.05	0.92[c]	0.48
C-2	0.26	0.02	0.68	0.71	0.89	1.06[c]	0.85
C-3	0.32[b]	0.87	0.36[b]	0.43[b]	0.91[b]	0.96[c]	0.41[b]
Sum	0.91	1.59	1.63	1.61	2.85	2.94	1.74

[a] From Ref. *12* unless otherwise indicated.
[b] Data from Ref. *11*.
[c] Data from Ref. *8*.

The extensive literature of "active" nitrogen chemistry does not appear to record any study of competition between organic substrates. Such an investigation is capable of revealing whether the reactive species produced by attack on one substrate are capable of inducing attack on the second. Such information has some relevance to the role of attack

Publication Date: June 1, 1969 | doi: 10.1021/ba-1969-0080.ch020

on a single substrate by reactive transients produced in primary or later events. Such an investigation also offers the possibility of evaluating the relative reactivity of structurally different substrates with respect to primary attack by $N(^4S)$. This paper reports an investigation of the consumption of hydrocarbons in the competition between an olefin, ethylene, and a paraffin, propane. In addition, ^{14}C-labeled ethylene has been employed to provide information on resynthesis of reactants from reactive species produced in the reaction and, incidentally, on the molecular origin of one of the reaction products. Evidence has been presented (*10, 12*) that, under conditions like those employed in this work, reaction of propylene is completed in the gas phase before trapping. It is assumed that this was also the case in the present work.

Table III. Changes in Activity of ^{14}C-Labeled Propylenes upon Reaction with Active Nitrogen[a]

$(C_3H_6)_o/(N)_o$	Δ(*Total Molar Activity*) %		Δ(*Atomic Activity at C-1*) %
		$C_3H_6 - 1 - {}^{14}C$	
1/6	−7.7		−15.3
1/12	−7.0		−22
		$C_3H_6 - 2 - {}^{14}C$	
1/6	+5.9		+7.0
1/12	+7.6		+9.5
		$C_3H_6 - 3 - {}^{14}C$	
1/6	−3.8		+12.5
1/12	−6.9		—

[a] Ref. 8.

Experimental

The unpoisoned flow system, 2450 MHz. microwave generator, photometer, in-line gas chromatograph and most operating procedures were the same as those described previously (*11*) except that provision was made for introducing a steady flow of the organic substrates without interrupting the discharge. "Active" nitrogen was generated by electrodeless glow discharge supported by 2450 MHz. microwaves at a total pressure of 3 ± 1 torr. Transport rates were 230 cm. $sec.^{-1}$, 150μ mole $sec.^{-1}$ and 1.3 ± 0.2μ mole $sec.^{-1}$ for linear flow, N_2 flow and $N(^4S)$ flow, respectively. The latter was measured by nitric oxide "emission" titration (*5*). Hydrocarbon substrate was introduced countercurrent (*11*) into the "active" nitrogen stream at autogenous temperature (approx. 50°C.) 20 cm. (0.087 sec.) downstream from the glow discharge. The gas stream passed through liquid nitrogen traps 50 cm. (0.22 sec.) downstream from the substrate inlet. Amounts of ethylene and propane recovered in the traps were determined by gas-chromatography on a 4 ft. × 4 mm. i.d.

In Chemical Reactions in Electrical Discharges; Blaustein, B.;
Advances in Chemistry; American Chemical Society: Washington, DC, 1969.

silica gel column employing helium as carrier gas and thermal conductivity as the monitor. Area factors were determined periodically with knowns.

In experiments involving ^{14}C-labeled ethylene the molar radioactivities of products relative to that of reactant ethylene were determined by proportional counting of CO_2 obtained by combustion in O_2 over CuO at 450°C. of products which had been purified by gas-chromatography over silica gel, as has been described previously (8). Bernstein-Ballentein proportional counter tubes filled with P-10 gas at 1 atm. were used with a Tracerlab P30 amplifier and SC72 scaler.

Nitrogen was Matheson's "Pre-Purified" grade further purified by passage over copper wire at 500°C. ^{14}C-labeled ethylene, helium used as carrier in gas chromatography, nitric oxide which was used in titration of "active" nitrogen and was purified by bulb to bulb distillation, P-10 gas used to fill counter tubes, and oxygen used in the combustion of products for assay of radioactivity were also Matheson products. Isotopically normal ethylene and propane were Phillips research grade.

Publication Date: June 1, 1969 | doi: 10.1021/ba-1969-0080.ch020

Data

Table IV summarizes percent consumption of ethylene consequent upon reaction of the pure substrate and three of its mixtures with propane with six different ratios of $N(^4S)$. Table V summarizes analogous data for propane. The data for mixtures given in the two Tables are derived from the same sets of experiments. Table VI summarizes apparent relative specific rates of consumption, "$k_{C_2H_4}/k_{C_3H_8}$." These ratios were calculated by means of Equation 14, the expression which would be appropriate

$$\text{"}k_{C_2H_4}/k_{C_3H_8}\text{"} = \log[(C_2H_4)_o/(C_2H_4)_t]/\log[(C_3H_8)_o/(C_3H_8)_t] \quad (14)$$

if the relative rates of consumption depended entirely on the bimolecular reaction of each of the substrates with the same reagent. Table VII summarizes molar radioactivities of recovered reactants or product ethane relative to that of reactant ethylene for the reaction of equimolar mixtures of ^{14}C-labeled ethylene and ordinary propane.

Discussion

The systematic variation of the ratio "$k_{C_2H_4}/k_{C_3H_8}$" over the range of concentration parameters summarized in Table VI demonstrates that relative consumption of competing hydrocarbons is not determined simply by the relative rates of attack of $N(^4S)$ on ethylene and propane since such determination would lead to constancy of the ratio. A similar conclusion can be drawn from the data of Tables IV and V by comparison of the consumption of a given substrate at a fixed concentration upon reaction with a fixed proportion of $N(^4S)$ in the presence and absence of the competing substrate. Such matched points are designated in

In Chemical Reactions in Electrical Discharges; Blaustein, B.;
Advances in Chemistry; American Chemical Society: Washington, DC, 1969.

Table IV. Percent Consumption of Ethylene[a, b]

$(Total\ Hydrocarbon)_o$ / $(N)_o$	Pure		Average Percent Consumption $(C_2H_4)_o/(C_3H_8)_o$					
	C_2H_4	n[c]	3.0	n[c]	1.0	n[c]	0.33	n[c]
4	19	3	18	3	28[α]	10	—	
2	24[β]	3	27	3	37[+]	10	51	6
1	39[+]	4	45	4	47[×]	16	56	9
2/3	45	2	59	1	—		73°	2
1/2	78[×]	3	87	3	93	10	90	7
1/6	98°	2	—		93	7	84	3

[a] Flow rate of N(^{4}S) was 1.3 ± 0.2μ mole sec.$^{-1}$ throughout.
[b] Pairs of numbers bearing identical superscripts are from experiments in which the ratio $(C_2H_4)_o/(N)_o$ was constant.
[c] Number of independent determinations averaged to give the tabulated figure.

Table V. Percent Consumption of Propane[a, b]

$(Total\ Hydrocarbon)_o$ / $(N)_o$	Pure		Average Percent Consumption $(C_2H_4)_o/(C_3H_8)_o$					
	C_3H_8	n[c]	3.0	n[c]	1.0	n[c]	0.33	n[c]
4	—		25	3	27[α]	10	—	
2	29[β]	1	32	3	32[+]	10	22	6
1	35[+]	2	34	4	32[×]	16	30	9
2/3	—		36°	1	—		32	2
1/2	41[×]	2	39	3	39	10	37	7
1/6	48°	2	—		45	7	44	3

[a] Flow rate of N(^{4}S) was 1.3 ± 0.2μ mole sec.$^{-1}$ throughout.
[b] Pairs of numbers bearing identical superscripts are from experiments in which the ratio $(C_3H_6)_o/(N)_o$ was constant.
[c] Number of independent determinations averaged to give the tabulated figure.

Table VI. Apparent Relative Reactivities

$\Sigma(RH)_o/(N)_o$	$(C_2H_4)_o/(C_3H_8)_o$		
	3.0	1.0	0.33
	"$k_{C_2H_4}/k_{C_3H_8}$"		
4	0.69	1.1	—
2	0.83	1.2	2.9
1	1.5	1.7	2.3
2/3	2.0	—	3.5
1/2	4.1	5.4	5.2
1/6	—	4.5	3.1

Tables IV and V by identical superscripts. If the simple model of the competition from which Equation 14 is derived were correct and, since the degrees of consumption of the pure substrates are similar, addition

Publication Date: June 1, 1969 | doi: 10.1021/ba-1969-0080.ch020

In Chemical Reactions in Electrical Discharges; Blaustein, B.;
Advances in Chemistry; American Chemical Society: Washington, DC, 1969.

of the second substrate should always substantially suppress the consumption of the first and should have the largest effect when substrate is in excess over reagent. In fact, with (reactant hydrocarbon)$_o$/(N)$_o \geq 1$ such suppression is absent or negligible. It becomes significant only when N(^{4}S) is in excess. The complexity of the reaction is also indicated by the shallow dependence of percent consumption of pure hydrocarbon on the ratio, (pure hydrocarbon)$_o$/(N)$_o$, particularly with propane for which a twelvefold decrease in the ratio is associated with increase in percent consumption by a factor of only 1.65. Such behavior is consistent with destruction of the substrate by both attacking reagent and reactive intermediates arising from the primary attack if, as the proportion of N(^{4}S) is raised, these intermediates are increasingly consumed by the reagent before they can attack the substrate. This feature is present with ethylene to a smaller extent.

Except with the largest excess of N(^{4}S), the value of "$k_{C_2H_4}/k_{C_3H_8}$" (Table VI) increases with decrease in the ratio $(C_2H_4)_o/(C_3H_8)_o$ at constant values of (total hydrocarbon)$_o$/(N)$_o$. This systematic change is consistent with occurrence of competition between the two substrates with respect to their destruction by reactive intermediates arising from primary attack of the reagent. More specifically, (*cf.* Tables IV and V) ethylene appears to be more sensitive to consumption by intermediates arising from propane than *vice versa*. Thus, at a constant value of the ratio (Total Hydrocarbon)$_o$/(N)$_o$, the percent consumption of ethylene increases more steeply with decrease in the ratio $(C_2H_4)_o/(C_3H_8)_o$ than the percent consumption of propane decreases. Presumably, the effect of attack by reactive intermediates can be reduced or eliminated by using sufficiently large excesses of N(^{4}S) that the intermediates react with the latter rather than with hydrocarbon. This analysis suggests that the values of "$k_{C_2H_4}/k_{C_3H_8}$" obtained with the largest excess of N(^{4}S) most closely approximate the true value of this ratio for primary attack and indicates that this true value is at least 5. An additional difficulty in estimating the correct value of $k_{C_2H_4}/k_{C_3H_8}$ becomes apparent upon considering the data of Table VII. These data establish that, over a twelvefold range of reagent ratios, synthesis of propane in the reaction mixture from fragments originating at least in part in ethylene is not detectable. However, production of ethylene either by degradation of propane or synthesis at least in part from fragments originating in propane occurs to a detectable extent with a sixfold excess of N(^{4}S) and equal initial concentrations of the hydrocarbons since the relative molar activity of recovered ethylene is significantly lower than that of reactant ethylene. In the absence of excess N(^{4}S) such synthesis was not detected, presumably because of the relatively large amount of unreacted ethylene. The relative molar activity data are supported by the data of Table IV

Publication Date: June 1, 1969 | doi: 10.1021/ba-1969-0080.ch020

In Chemical Reactions in Electrical Discharges; Blaustein, B.;
Advances in Chemistry; American Chemical Society: Washington, DC, 1969.

Table VII. Relative Molar Activities of Recovered Reactants and Product Ethane[a, b]

(Total Hydrocarbon)$_o$ / (N)$_o$	Relative Molar Activity					
	C_2H_4	n^c	C_2H_6	n^c	C_3H_8	n^c
2	0.98	7	—		0.01[d]	1
1	0.98	4	—		—	
1/2	—		0.8	1	0.01[d]	1
1/6	0.89	2	0.5	1	0.01[d]	1

[a] Compared to unreacted ethylene; hydrocarbon reactants equimolar.
[b] Flow rate of N(^{4}S) was 1.3 ± 0.2μ mole sec.$^{-1}$ throughout.
[c] The number of independent experiments.
[d] Indistinguishable from the value found for unreacted propane.

which show that, with hydrocarbons equimolar, percent consumption of ethylene does not change as (Total Hydrocarbon)$_o$/(N)$_o$ decreases from 1/2 to 1/6. With excess propane, the apparent consumption of ethylene actually diminishes over the latter change in (Total Hydrocarbon)$_o$/(N)$_o$. Apparently synthesis of ethylene in whole or in part from propane is even more important when propane is in excess. Such abnormal trends are not found in the consumption data for propane. The values of "$k_{C_2H_4}/k_{C_3H_8}$" obtained with excess N(^{4}S) are, accordingly, reduced by replacement of consumed ethylene to an extent which increases with decrease in both the ratio (Total Hydrocarbon)$_o$/(N)$_o$ and the ratio $(C_2H_4)_o/(C_3H_8)_o$. These reductions are apparent in the data of Table VI for a sixfold excess of N(^{4}S). Reduction with decrease in $(C_2H_4)_o/(C_3H_8)_o$ is also barely detectable with a twofold excess of N(^{4}S).

The synthesis of ethylene during reaction appears to make it impossible to obtain better than a minimum estimate of the value of $k_{C_2H_4}/k_{C_3H_8}$ for primary attack. Excess N(^{4}S) must be used to suppress induced attack on hydrocarbon by reactive transients but with excess N(^{4}S) synthesis of ethylene becomes important. It is conceivable, but by no means certain, that with excesses of N(^{4}S) greater than those used in this work, synthesis of ethylene might be prevented by destruction of transient precursors.

The importance of transient intermediates derived from both of the competitors is further suggested by the relative molar activity of ethane produced in the reaction (*cf.* Table VII). With a sixfold excess of N(^{4}S) this is derived equally from ethylene and from propane. With a twofold excess it derives to a greater extent from ethylene. Extensive data of this sort could be instructive as to the nature and reactions of such transients.

The above discussion tacitly assumes that N(^{4}S) is the only component of "active" nitrogen which is significantly involved. That this is so for ethylene is widely accepted. The work of Jones and Winkler (9)

Publication Date: June 1, 1969 | doi: 10.1021/ba-1969-0080.ch020

In Chemical Reactions in Electrical Discharges; Blaustein, B.;
Advances in Chemistry; American Chemical Society: Washington, DC, 1969.

suggests that it is probably also the case for propane. The latter study provides a value of 1.0×10^6 M^{-1}sec.$^{-1}$ for the rate constant of C_3H_8 at 50°C. and an activation energy of 5.5 kcal. mole^{-1}. Since nitrogen atom concentrations were determined from HCN yields produced by reaction with ethylene, this constant should be adjusted downward 30 to 50%. Since the constant was evaluated from experiments in which propane was in molar excess over N(^{4}S) it is probably also significantly high because it does not correct for the consequences of attack by reactive intermediates arising from initial attack by N(^{4}S). However, the quantity actually measured was the rate of formation of HCN which was assumed to equal three times the rate of consumption of propane. To the extent that significant yields of other products are formed, this procedure will give erroneously low values of the specific rate. Herron has estimated from his elegant mass spectrometric study (7) of the reaction of N(^{4}S) with ethylene that the rate constant for primary attack at 70°C. in the (virtually temperature independent) reaction of N(^{4}S) with ethylene is $1.0 \pm 0.5 \times 10^7$ M^{-1}sec.$^{-1}$. A value of the ratio of specific rates of primary attack by N(^{4}S) on ethylene and propane, respectively, in the vicinity of ten is thus indicated by earlier work. Agreement with the present result is well within the range of the mutual uncertainties. Herron's work further establishes that hydrogen atoms produced in the reaction of N(^{4}S) with ethylene compete with the reagent for the substrate and, in fact, suggests the model upon which interpretation of the present data is based.

Publication Date: June 1, 1969 | doi: 10.1021/ba-1969-0080.ch020

Literature Cited

(1) Bernstein, W., Ballentein, R., *Rev. Sci. Inst.* **21**, 158 (1950).
(2) Brocklehurst, B., Jennings, K. R., "Progress in Reaction Kinetics," G. Porter, Ed., Vol. 4, pp. 1-36, Pergamon Press, New York, 1967.
(3) Fujino, A., Lundsted, S., Lichtin, N. N., *J. Am. Chem. Soc.* **88**, 775 (1966).
(4) Hanafusa, T., Lichtin, N. N., *Can. J. Chem.* 44, 1230 (1966).
(5) Harteck, P., Reeves, R. R., Mannella, G., *J. Chem. Phys.* **29**, 608 (1958).
(6) Herron, J. T., *J. Phys. Chem.* **69**, 2736 (1965).
(7) *Ibid.*, 70, 2803 (1966).
(8) Hinde, P. T., Titani, Y., Lichtin, N. N., *J. Am. Chem. Soc.* **89**, 1411 (1967).
(9) Jones, W. E., Winkler, C. A., *Can. J. Chem.* **42**, 1948 (1964).
(10) Lichtin, N. N., "The Chemistry of Ionization and Excitation," p. 181, G. R. A. Johnson, G. Scholes, Eds., Taylor and Francis, Ltd., London, 1967.
(11) Shinozaki, Y., Shaw, R., Lichtin, N. N., *J. Am. Chem. Soc.* **86**, 341 (1964).
(12) Titani, Y., Lichtin, N. N., *J. Phys. Chem.* **72**, 526 (1968).
(13) Tsukamoto, A. Lichtin, N. N., *J. Am. Chem. Soc.* **84**, 1601 (1962).

RECEIVED April 25, 1967. Paper VI in the series, "Reactions of Active Nitrogen with Organic Substrates." Work was supported in part by a grant from the Graduate School of Boston University.

Hydrocarbons from $H_2 + CO$ and $H_2 + CO_2$ in Microwave Discharges: Le Chatelier's Principle in Discharge Reactions

BERNARD D. BLAUSTEIN and YUAN C. FU

Pittsburgh Coal Research Center, Bureau of Mines, U. S. Department of the Interior, Pittsburgh, Pa. 15213

Publication Date: June 1, 1969 | doi: 10.1021/ba-1969-0080.ch021

In a discharge in a static reactor, initial pressures of mixtures of $H_2 + CO$ of 12 and 50 torr gave conversions of CO to $CH_4 + C_2H_2$ of approximately 20% for reaction times of 1/2 to four minutes. When water was added to the reactants, formation of hydrocarbons was repressed. Conversion of CO was increased to more than 90% when the reaction products were removed by a cold trap as they formed. With $H_2 + CO_2$, no hydrocarbons were formed unless water was frozen out. The different conversions of CO and CO_2 can be explained by assuming that the reaction reaches a stationary state or pseudo-equilibrium. When reaction products are removed from the discharge by being frozen out, the stationary state shifts according to Le Chatelier's principle and more hydrocarbons are formed.

Formation of hydrocarbons from $H_2 + CO$ over metal catalysts is of considerable interest and has been studied at length. Hydrocarbons can also be formed in electrical discharges (*2, 3, 4, 6, 8, 10, 11, 12, 13, 16, 18, 19, 20, 21, 22, 23, 24*), and this offers an interesting alternative for producing hydrocarbons from $H_2 + CO$. Fischer and Peters (*8*) worked with a flow system where the gases at 10 torr pressure circulated through a discharge (50 Hz.) between metal electrodes, then through a mercury vapor pump, a liquid air-cooled trap, and back to the discharge. Conversion of CO to low molecular weight hydrocarbons was very low for one pass through the discharge, but by recirculating the gases for 100 minutes, practically all of the CO would react.

In Chemical Reactions in Electrical Discharges; Blaustein, B.;
Advances in Chemistry; American Chemical Society: Washington, DC, 1969.

Lunt (*13*) and Epple and Apt (*6*) worked with electrodeless radio-frequency (2 to 110 MHz.) discharges in static gas reactors at pressures up to 300 torr. (We define an electrodeless discharge as one in which there are no metal electrodes present in the gas.) Conversions of H_2 + CO and H_2 + CO_2 to CH_4 were quite high for reaction times of several minutes; no other hydrocarbons were formed. McTaggart (*16*), and Vastola *et al.* (*23*), working with electrodeless microwave (2450 MHz.) discharges in flow systems at pressures of a few torr formed only traces of gaseous hydrocarbons from H_2 + CO. Here, the gas passed through the discharge only once, and the residence time was a fraction of a second. However, work in our laboratory has shown that in a static reactor, at initial pressures of 12 and 50 torr and with reaction times of the order of a minute, as much as 90% of the CO or CO_2 originally present can be converted to hydrocarbons in an electrodeless microwave discharge in H_2 + CO or H_2 + CO_2, under conditions where essentially no polymers are formed.

Publication Date: June 1, 1969 | doi: 10.1021/ba-1969-0080.ch021

Experimental Procedures

Reactions were carried out in 11 mm.-i.d. cylindrical 96% silica glass reactors placed in a coaxial cavity [Ophthos Instruments, similar to type 2A described by Fehsenfeld *et al.* (*7*)] connected by a coaxial cable to a Raytheon KV-104A CMD-10 2450 MHz. generator. For a run, the reactors were evacuated to $< 3\ \mu$ and filled with either 5:1 H_2–CO, various H_2–CO–Ar (typically 5.1:1.0:0.4) or 3.5:1 H_2–CO_2 mixtures prepared from tank gases and stored in the vacuum system. Product analyses were made on a CEC 21-103C mass spectrometer. Net power into the discharge, measured with a Microwave Devices model 725.3 meter, was approximately 34 watts, although lower power levels could be used. Air was blown through the cavity to cool the reactor somewhat, but the estimated wall temperature in the discharge was still several hundred degrees C.

Runs with argon gave the same results as in the absence of Ar, and the ratio of total-carbon-to-argon in the product was usually a few percent lower in the product, but did not vary by more than ±10% from its value in the original mixture, indicating that only negligible amounts of polymers were formed in the reaction. For H_2 + CO and H_2 + CO_2 mixtures without Ar it was assumed that polymer formation was negligible, so long as the reaction conditions were similar.

As a precaution against the gradual accumulation of small amounts of polymer in the reactors, they were cleaned before each run by maintaining a discharge in O_2 at about 10 torr for 3 minutes to oxidize any carbonaceous material present. This was repeated twice, with fresh samples of O_2. A discharge in H_2 (about 10 torr) was then maintained for 3 minutes in the reactor. This was also repeated twice, with fresh samples of H_2. Since the reactions studied were to be carried out in a reducing environment, this treatment with H_2 was felt to be desirable after the O_2 discharge.

In Chemical Reactions in Electrical Discharges; Blaustein, B.;
Advances in Chemistry; American Chemical Society: Washington, DC, 1969.

Results

Figure 1 shows the results of experiments made at initial gas pressures of H_2 + CO (5:1) of 12 ± 1 torr in 36 cm.-long by 11 mm. i.d. reactors. The microwave cavity used focuses the electrical energy so that the discharge fills only about 2 cm. in length of the reactor tube. The percent of carbon present in the product as C_2H_2 and as CH_4 + C_2H_2 is plotted *vs.* reaction time. Figure 2 shows the percent of carbon present in the product as CH_4 for the same runs. Water, CO_2, and occasionally slight traces of other hydrocarbons were also present in the product. The conversion of CO to CH_4 + C_2H_2 reaches a maximum of 17–18% for reaction times of 30–120 seconds. Figure 3 shows the results of experiments made at initial gas pressures of 50 ± 3 torr in 20 cm.-long by 11 mm. i.d. reactors. Here, the percent of carbon present as CH_4 + C_2H_2 is at a maximum of 24–25% for reaction times of 3–4 minutes. There is considerable scatter in the data; the dashed curves are intended to show only the general trend.

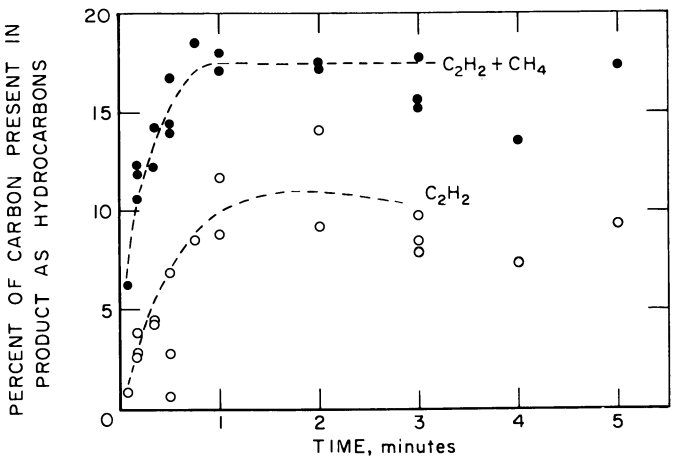

Figure 1. Formation of hydrocarbons from H_2 + CO (5:1) in microwave-generated discharge (Initial gas pressure = 12 ± 1 torr)

○ = *acetylene*
● = *acetylene + methane*

These data show that conversion of CO to hydrocarbons in the discharge under these conditions is limited. The composition of the gases in the reactor approaches a stationary state, for reaction times of the order of 0.5 to 3 minutes, depending upon the pressure. Because of the geometry of the reactors and the volume of a reactor relative to the volume occupied by the discharge, the time required to reach the stationary state

In Chemical Reactions in Electrical Discharges; Blaustein, B.;
Advances in Chemistry; American Chemical Society: Washington, DC, 1969.

appears to be longer than is actually so; this is owing to the relatively long times required for diffusion of gases into and out of the discharge. (The 36 cm.-long reactors were used for the runs made at 12 torr; for the runs made at 50 torr, the shorter 20 cm.-long reactors were used. Preliminary experiments showed that the conversion of CO to $CH_4 + C_2H_2$ at 50 torr in 36 cm.-long reactors were essentially the same as for the 20 cm.-long reactors, but took 1–2 minutes longer to achieve maximum conversions.)

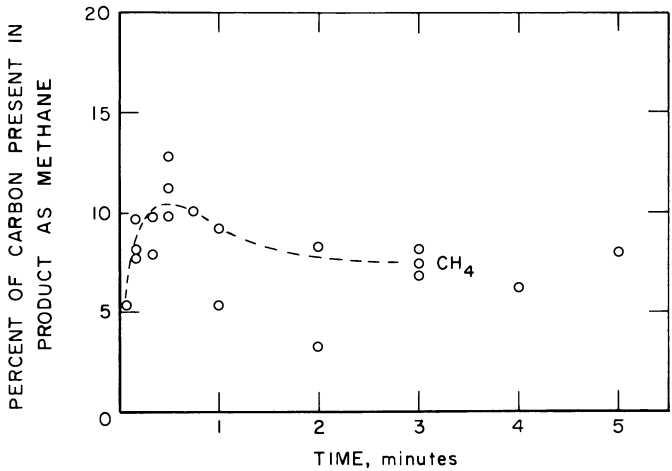

Figure 2. Formation of CH_4 from H_2 + CO (5:1) in microwave-generated discharge (Initial gas pressure = 12 ± 1 torr)

High yields of gaseous hydrocarbons from $H_2 + CO$ have now been shown to occur in low-frequency [50 Hz. (*8*) and 60 Hz. (*24*)] discharges between electrodes, and electrodeless radiofrequency (2–110 MHz.) (*6*) and microwave (2450 MHz.) discharges. However, in all of these cases, the reaction does not appear to be an extremely rapid one, such as is the case for dissociation of diatomic molecules in a discharge, for instance.

As shown in Figures 1, 2, and 3, the conversions appear to decrease for reaction times longer than those needed to reach maximum conversions. This is probably caused by some polymer formation, although the C/Ar ratio did not decrease more than 10%. In fact, several runs at 12 torr (not plotted) of 5 minutes duration, and some longer runs, including one at 50 torr for 10 minutes, gave values of the C/Ar ratio more than 10% below the initial value of the ratio, and this was considered evidence of polymer formation. Here, also, the yields of CH_4 and C_2H_2 were lower.

Conversions of CO could be increased by removing reaction products as they formed, by having a cold trap surround the bottom 5 cm. of the reactor before and during the time that the discharge was maintained

Publication Date: June 1, 1969 | doi: 10.1021/ba-1969-0080.ch021

at a distance of 10 cm. from the bottom. The discharge is localized and extends over a distance of about 2 cm. As shown in Table I, the conversion of CO increased markedly and the product distribution changed.

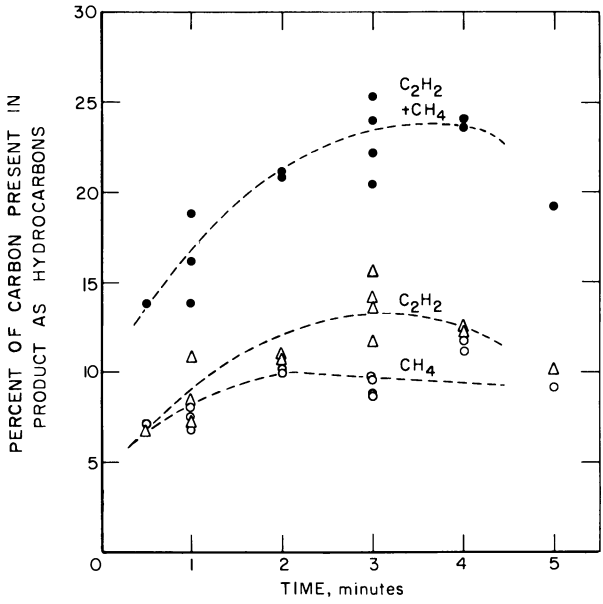

Figure 3. Formation of hydrocarbons from H_2 + CO (5:1) in microwave-generated discharge (Initial gas pressure = 50 ± 3 torr)

○ = *methane*
△ = *acetylene*
● = *acetylene + methane*

Values for the C/Ar ratio indicated that polymers were not formed. Also, there is no indication that the product distribution is any different in the presence of Ar than in its absence. The first three columns in Table I are for the 3-minute runs shown in Figures 1 and 2. When the discharge was maintained for 3 minutes or longer, with Dry Ice (−78°C.) surrounding the end of the reactor, the percent of carbon present in the final product as CH_4 is 51%; C_2H_2, 17%; C_2H_6, 10%. At this temperature, the only reaction product frozen out is H_2O. Apparently, the removal of this is sufficient to increase the conversion of CO to hydrocarbons to approximately 78%.

The next six columns in Table I show that with liquid N_2 cooling (−196°C.), the percent of carbon in the product as CH_4 is only 4%; C_2H_2 + C_2H_6 (with the latter predominating) 82%; C_3 + C_4 hydro-

Publication Date: June 1, 1969 | doi: 10.1021/ba-1969-0080.ch021

Table I. Conversion of CO to Hydrocarbons in a Microwave

Conditions *Run:*	*6294*	*10252*	*10253*	*9232*	*11012*	*7154*
Cooling bath	None	None	None	−78	−78	−78
Time, min.	3	3	3	3	3	5
Pressure, torr	12.0	12.8	12.0	12.6	12.4	12.0
H_2/CO	5.1	5.1	5.1	5.0	5.1	5.1
Argon	Yes	Yes	Yes	No	Yes	Yes
Percent carbon present in product as						
CH_4	6.8	8.1	7.4	52.0	50	51.0
C_2H_2	8.5	9.7	7.9	19.9	15	17.2
C_2H_6	—	—	—	7.8	9	12.6
$C_3 + C_4$	—	—	—	trace	trace	trace
CO_2	2.1	1.4	2.1	trace	—	—
Hydrocarbons	15	18	15	80	74	81

carbons, 5%; more H_2O and CO_2 are also formed. The mass spectrometric analyses indicated that traces of oxygenates were also present in the products of these runs, but in such small amounts that no identification could be attempted. For some unknown reason, C_2H_4 is not formed under these conditions. (Several runs were analyzed by gas chromatography for C_2H_4 and none was found. The sensitivity of these analyses was such that certainly less than 1%, and more likely, less than 0.5% of the CO was converted to C_2H_4.) At a temperature of −196°C., the only noncondensables present in the mixture are H_2, CO, and CH_4; all the other products are frozen out. One can speculate that the high yield of C_2H_6 is caused either by a recombination of CH_3 radicals at the cold surface, or hydrogenation of C_2H_2, but the mechanism of formation of any of the hydrocarbon products is not known.

The next-to-last pair of columns in Table I show that very high conversions of CO to C_2- and higher hydrocarbons can be obtained using a 2.2:1 H_2 + CO mixture. Here, also, the CO_2 production is higher, and the CH_4 lower, than when compared with the more hydrogen-rich reactant mixture. The last pair of columns, giving data for runs made at 50 torr, indicate that C_2H_2 was by far the predominant product in these runs.

The almost complete conversion of CO to hydrocarbons, H_2O, and CO_2, obtained by cooling the bottom of the reactor, is reversible. Several additional experiments (at 12 torr), where the gases reacted for 3 minutes while the bottom of the reactor was cooled with liquid nitrogen, the reactor then warmed to room temperature in a few seconds with a water bath, and the gases reacted for 2 more minutes, gave essentially the same product compositions as for the runs shown in Figures 1 and 2.

Publication Date: June 1, 1969 | doi: 10.1021/ba-1969-0080.ch021

In Chemical Reactions in Electrical Discharges; Blaustein, B.;
Advances in Chemistry; American Chemical Society: Washington, DC, 1969.

Discharge: No Cooling *vs.* Cooling the Bottom of the Reactor

7153	*2072*	*10213*	*11011*	*2222*	*9233*	*9025*	*8192*	*10211*	*7071*
−196	−196	−196	−196	−196	−196	−196	−196	−196	−196
3	3	3	3	3	3	2	3	3	5
11.2	12.8	11.9	13.0	12.2	12.0	12.4	12.6	51	52
5.1	5.1	5.1	5.1	5.1	5.0	2.2	2.2	5.1	5.1
Yes	Yes	Yes	Yes	Yes	No	No	No	Yes	Yes
3.4	5.6	4.0	3.9	2.3	3.4	1.0	.6	3.9	3.7
5.7	33.9	2.9	19.7	4.3	4.8	46.3	32.9	61.8	55.6
79.2	45.0	75.7	63.6	80.1	75.8	35.6	46.6	.4	.5
3.6	2.2	8.9	2.0	7.3	8.7	3.2	10.0	—	—
4.2	5.3	4.1	5.3	3.8	4.3	9.4	9.6	2.4	2.5
92	87	92	89	94	93	86	90	66	60

Figure 4 gives the results of some experiments where water vapor was added to the $H_2 + CO + Ar$ (5.1:1.0:0.4) mixture before reaction. The water vapor was added to the previously evacuated reactor and a portion of the vacuum system connected to a Pace Engineering Company Model P7 pressure transducer containing a ±1 p.s.i. diaphragm. The output of this was indicated on a Pace Model CD 25 transducer indicator. After the water vapor partial pressure was measured, the stopcock to the reactor was closed and the water frozen at the bottom of the reactor. The reactor was then filled with the H_2-CO-Ar mixture, the bottom of the reactor warmed slightly, and 3 minutes allowed for mixing of the gases before the discharge was initiated.

These experiments show that addition of water vapor to the reactant mixture has a strong inhibitory effect on the production of hydrocarbons. The CO_2 yield is increased owing to the reaction $H_2O + CO \rightarrow CO_2 + H_2$. When the water vapor partial pressure is approximately equal to the CO partial pressure in the reactant gas mixture, no hydrocarbons are produced at all. The pronounced inhibitory effect of H_2O vapor on hydrocarbon formation in this reaction may explain some of the scatter of the data shown in Figures 1, 2, and 3. If small (and variable) amounts of H_2O vapor were adsorbed on the walls of the reactor tubes, this would decrease the hydrocarbon yield in (some of) the runs by a varying amount which would show up as scatter in the data. However, there are other, as yet unknown, sources of variability in the experimental conditions which also undoubtedly contribute to the scatter in the data.

Table II gives the results of a series of experiments on the reaction of a $H_2 + CO_2$ (3.5 : 1) mixture in the discharge for 3 minutes at 34

Publication Date: June 1, 1969 | doi: 10.1021/ba-1969-0080.ch021

watts net power input. The data in each column are the average of two or three runs.

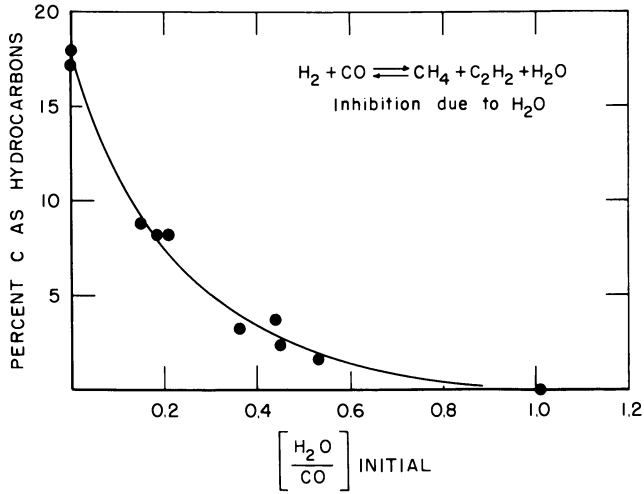

Figure 4. Addition of H_2O vapor to the H_2-CO-Ar (5.1:1.0:0.4) mixture represses hydrocarbon formation in the microwave discharge (Initial pressure of H_2-CO-Ar mixture = 12 torr)

Table II. Reaction of $H_2 + CO_2$ (3.5:1) in a Microwave Discharge

Cooling	*None*	*None*	*−78°C.*	*−78°C.*	*−78°C., −196°C.*[a]
Pressure, torr	12	50	12	50	12
Percent of carbon present in product as					
CH_4	0.1	0.1	25	9	1
C_2H_2	0.1	0.1	15	33	46
C_2H_6	0	0	8	3	40
C_3-	0	0	1	2	4
CO	84	90	46	48	3

[a] The discharge was maintained for 3 minutes, except for the runs in the last column. Here, the discharge was on for 4 minutes; the bottom of the reactor was cooled for two minutes at −78°C. and then for 2 minutes at −196°C.

Discussion

Conversion of CO and CO_2 to Hydrocarbons in a Microwave Discharge. All results of the experimental runs on $H_2 + CO$ can be explained by assuming that the reaction without cooling the bottom of the reactor reaches a stationary state or pseudo-equilibrium where the production of CH_4 and C_2H_2 in the discharge is limited by the back reaction of these

Publication Date: June 1, 1969 | doi: 10.1021/ba-1969-0080.ch021

hydrocarbons with H_2O and CO_2 to form $H_2 + CO$. The data in Figure 3, by comparison with Figures 1 and 2, indicate that conversion of CO to hydrocarbons is increased at higher pressures, as would be expected for a reaction where the volume of the products is less than the reactants. When one or more of the reaction products are removed from the discharge zone by being frozen out, the stationary state shifts and more CO reacts to form hydrocarbons. When the frozen-out hydrocarbons are reintroduced into the discharge, they react very readily to re-form the initial stationary state composition. If, on the other hand, water vapor is added to the initial reactant gas mixture, the conversion of CO to hydrocarbons is repressed.

The different conversions of CO_2, as shown in Table II, can be explained on the basis of the inhibitory effect of water vapor. Without cooling, $H_2 + CO_2$ react in the discharge to form $CO + H_2O$; the H_2O then inhibits any further reaction to form hydrocarbons. When the bottom of the reactor is cooled to −78°C., H_2O is frozen out, and approximately 48% of the CO_2 is converted to C_1-, C_2-, and C_3-hydrocarbons. The last column in Table II lists results of runs where, with the discharge on, the bottom of the reactor was cooled at −78°C. for 2 minutes, followed immediately by 2 minutes at −196°C. Apparently, little or no CO_2 is present at the end of the first 2 minutes (it has been converted to CO and hydrocarbons), or the long times needed for the CO_2 to diffuse to the cold wall and be frozen out at −196°C. allow the CO_2 to remain in the discharge long enough to react. Under these conditions, the conversion of CO_2 to hydrocarbons is approximately 90%, similar to the conversions obtained for CO in Table I.

Stationary State in the Discharge. APPLICATION OF LE CHATELIER'S PRINCIPLE. These experimental observations can be summed up by discussing the reaction $H_2 + CO \rightarrow CH_4 + H_2O$ in terms of a stationary state in the discharge which can shift in the direction that would be predicted by applying Le Chatelier's principle. Actually, in this respect, the system behaves as if it were in chemical equilibrium. As long ago as 1873 (*22*), it was shown that the conversion of $3H_2 + N_2 \rightarrow 2NH_3$ in an electrical discharge could be increased quite markedly by removing the NH_3 with acid as it formed. Fischer and Peters (*8*), Wendt and Evans (*24*), Lunt (*13*), and Epple and Apt (*6*) have all discussed the production of hydrocarbons from $H_2 + CO$ in terms of equilibria in the discharge. Howèver, simple arguments show that any discussion of equilibria in discharges is not a straightforward one because of the absence of temperature equilibria among the various species—electrons, ions, and molecules—in the discharge (*1*).

For an electrically-excited steady-state system such as this, Manes (*14*) has assumed a model chemical reaction system, "in which energy

Publication Date: June 1, 1969 | doi: 10.1021/ba-1969-0080.ch021

is separately conserved within each degree of freedom of each molecular species, each such degree of freedom therefore having in effect its own 'temperature.' A statistical mechanical treatment of this model shows that the composition behavior at any fixed set of 'temperatures' is the same as for an equilibrium system—*i.e.*, the conventional expression for the equilibrium constant is retained—although the expressions for the magnitude and temperature dependence of the equilibrium constant become quite complex and no attempt is made to evaluate them. It is suggested that the model may simulate the behavior of chemical reactions in non-equilibrium steady-state electrical discharges, and therefore that such systems may resemble equilibrium systems in their responses to composition perturbations from the steady state."

That is, given the existence of this "equilibrium" constant for (some) reactions occurring in a discharge, we would then expect Le Chatelier's principle to apply. In fact, the "constant" need be only approximately so, as conditions change over a certain range, for the system to exhibit qualitative changes in accordance with Le Chatelier's principle.

Formation of Hydrocarbons in a Radiofrequency Discharge. CHEMICAL DIFFERENCES BETWEEN DISCHARGES. Lunt (*13*) and Epple and Apt (*6*) have shown that $H_2 + CO_2$ or $H_2 + CO$ react in a radiofrequency discharge to produce CH_4 in high yield as the sole hydrocarbon. Even though CH_4 is present in the discharge for minutes, no C_2H_2 is produced. We have repeated their experiments (using a 400 KHz. generator) and can confirm this finding, as well as their high conversions of CO to CH_4; our conversions of CO_2 to CH_4 were a little lower than they had obtained.

Thus, there are at least two important chemical differences between these reactions in (a) the radiofrequency discharge in an annular ozonizer-type reactor at pressures near 200 torr, and (b) the microwave discharge in a cylindrical reactor at pressures of 12 or 50 torr. Under the microwave conditions, C_2H_2 is always produced (together with CH_4) from $H_2 + CO$; and $H_2 + CO_2$ (without cooling) form CO but no hydrocarbons. Obviously, it would be extremely useful to understand these phenomena. We have explored this situation a bit further, in the following manner.

In the derivation of an equilibrium constant expression for a reaction in an electrically-excited steady-state system (*14*), it was assumed that equilibrium between the individual degrees of freedom for each molecular species does not exist. Therefore, such an equilibrium constant expression no longer has the classical thermodynamic temperature dependence. However, we decided to use the analytical data for the gas composition at the steady-state and the value of K, the thermodynamic equilibrium

Publication Date: June 1, 1969 | doi: 10.1021/ba-1969-0080.ch021

constant, to calculate a temperature "number" for the discharge system. Epple and Apt (*6*) did this for the equilibria

$$K_{1(\text{atm})} = \frac{P_{CO} \times P_{H_2O}}{P_{CO_2} \times P_{H_2}}$$

and

$$K_{2(\text{atm})} = \frac{P_{CH_4} \times P_{H_2O}}{P_{CO} \times P^3_{H_2}}$$

and used values obtained for K_1 and K_2 to define a "chemically equivalent temperature." Lunt (*13*) also calculated values for K_1 and "equivalent absolute temperature," and found that these increased with increasing pressure. These are listed in Table III. For purposes of comparison, the data used to generate Figure 4 were used to calculate values of K_1 and K_2 and the corresponding temperature numbers in our microwave discharge runs. Our temperature number corresponding to the average value of K_2 is essentially the same as Epple and Apt. However, the temperature numbers calculated from K_1 from the three sets of data are not capable of being reconciled.

We have also calculated values for

$$K_{3(\text{atm})} = \frac{P_{C_2H_2} \times P^3_{H_2}}{P^2_{CH_4}}$$

and

$$K_{4(\text{atm})} = \frac{P_{C_2H_2} \times P^2_{H_2O}}{P^2_{CO} \times P^3_{H_2}}$$

Table III. Values of Equilibrium "Constants" and "Temperature Numbers"

	Equilibrium "Constant"		*"Temperature Number"*		
	Average	*Range*	*This Work*	*Epple and Apt*	*Lunt*
K_1	1.4	0.6–1.9	1250	750	830–1270[a]
K_2	16	10–33	800	850	
$K_3 \times 10^3$	12	2–22	1300		
K_4	2.4	0.5–6.9			

[a] The "temperature number" increased with increasing pressure.

From the average value for K_3, one can calculate a temperature number for this reaction of approximately 1300°K. The values for K_4 ($K_4 = K_2^2 \times K_3$) are much higher than there is any reason to expect, since for this reaction, log $K = -4.6$ at 300°K. and decreases with increasing temperature. The values calculated for K_4 indicate that the reaction

$$3H_2 + 2CO \rightarrow C_2H_2 + 2H_2O$$

Publication Date: June 1, 1969 | doi: 10.1021/ba-1969-0080.ch021

In Chemical Reactions in Electrical Discharges; Blaustein, B.;
Advances in Chemistry; American Chemical Society: Washington, DC, 1969.

is not even remotely near any sort of equilibrium in the discharge; the amount of C_2H_2 formed is far greater than can be accounted for at equilibrium.

The significance, if any, of the values calculated for K_1, K_2, etc., and the temperature numbers is not known. However, there are chemical differences between the reactions under microwave and radiofrequency conditions, and perhaps this is reflected in the difference between these numbers for different discharges.

In summary, it is helpful to discuss on a qualitative basis at least some reactions in discharges from the point of view of stationary states or pseudo-equilibria, which can shift according to Le Chatelier's principle. Other workers (*5*) are also attempting to discuss the situation where the active species in a discharge, once the energizing power is removed, tend toward a state of equilibrium, and it will be of interest to see how useful these ideas prove to be in interpreting chemical reactions in discharges.

Publication Date: June 1, 1969 | doi: 10.1021/ba-1969-0080.ch021

Acknowledgment

The authors wish to thank Gus Pantages, Waldo A. Steiner, and Paul Golden for their technical assistance; A. G. Sharkey, Jr. and Janet L. Shultz for the mass-spectrometric analyses; and Irving Wender, Frederick Kaufman, Milton Manes, and R. W. Lunt for their valuable discussions. Reference to a company name is made to facilitate understanding and does not imply endorsement by the U. S. Bureau of Mines.

Note

Another example of the use of equilibrium considerations in discussing reactions in discharges is by Ruppel, *et al.*, for the reaction of CO and steam in an ozonizer at atmospheric pressure (*17*). In a flow system, as the space velocity is decreased, the percent conversion of CO tends toward the thermodynamic limit for this reaction, as determined by the external reactor wall temperature.

The reaction of H_2 + CO in a discharge under our experimental conditions is a relatively slow reaction; however, if C-atoms are generated by passing C_3O_2 through a discharge, and if H_2 is also passing through the discharge, up to 38% of the available carbon reacts to form products, the major ones being acetylene and methane (*15*).

As another example of the effect of water vapor on hydrocarbon formation in discharge, in a paper on the formation of hydrocarbons in model primitive earth atmospheres containing methane and helium (*9*), the authors state that "the presence of water or ammonia decreased the

total yield of hydrocarbons and affected the product composition in interesting ways, which cannot be explained at present."

Literature Cited

(1) Arzimovich, L. A., "Elementary Plasma Physics," p. 5, Blaisdel Pub. Co., New York, N. Y., 1965.
(2) Berthelot, M., *Ann. Chim. et Phys.* **[7] 16,** 21 (1899).
(3) *Ibid.*, **[7] 23,** 433 (1901).
(4) Caress, A., Rideal, E. K., *Proc. Roy. Soc. (London)* **A120,** 370 (1928).
(5) Eck, R. V., Lippincott, E. O., Dayhoff, M. O., Pratt, Y. T., *Science* **153,** 628 (1966).
(6) Epple, R. P., Apt, C. M., "The Formation of Methane from Synthesis Gas by High-Frequency Radiation," p. 47, Gas Operations Research Project PF-27 (ext.), Am. Gas Assoc. Catalog No. 59/OR, Am. Gas Assoc., Inc. (July 1962).
(7) Fehsenfeld, F. C., Evenson, K. M., Broida, H. P., *Rev. Sci. Instruments* **36,** 294 (1965).
(8) Fischer, F., Peters, K., *Brennstoff-Chem.* **12,** 268 (1931).
(9) Irving, C. S., Petterson, R. C., *J. Org. Chem.* **32,** 3714 (1967).
(10) Lefebvre, H., van Overbeke, M., *Chim. Ind.* Special No., p. 338 (April 1934).
(11) Lefebvre, H., van Overbeke, M., *Compt. rend.* **198,** 736 (1934).
(12) Losanitsch, and Jovitschitsch, "The Conversion of Coal into Oils," Chap. IV, F. Fischer, ed., E. Benn, Ltd., London, 1925.
(13) Lunt, R. W., *Proc. Roy. Soc. (London)* **108A,** 172 (1925).
(14) Manes, M., ADVAN. CHEM. SER. **80,** 133 (1969).
(15) Martinotti, F. F., Welch, M. J., Wolf, A. P., *Chem. Communs.* **1968,** 115.
(16) McTaggart, F. K., *Australian J. Chem.* **17,** 1182 (1964).
(17) Ruppel, T. C., Mossbauer, P. F., Bienstock, D., ADVAN. CHEM. SER. **80,** 214 (1969).
(18) Sahasrabudhey, R. H., Deshpande, S. M., *Proc. Indian Acad. Sci.* **31A,** 317 (1950).
(19) Sahasrabudhey, R. H., Deshpande, S. M., *J. Indian Chem. Soc.* **27,** 361 (1950).
(20) *Ibid.*, **28,** 377 (1951).
(21) Sahasrabudhey, R. H., Kalyanasundaram, A., *Proc. Indian Acad. Sci.* **27A,** 366 (1948),
(22) Thenard, P., Thenard, A., *Compt. rend.* **76,** 983 (1873).
(23) Vastola, F. J., Walker, P. L., Jr., Wightman, J. P., *Carbon* **1,** 11 (1963).
(24) Wendt, G. L., Evans, G. M., *J. Am. Chem. Soc.* **50,** 2610 (1928).

RECEIVED June 6, 1967.

22

Radiofrequency Electrodeless Synthesis of Polymers: Reaction of CO, N_2, and H_2

JOHN R. HOLLAHAN[1] and RICHARD P. MC KEEVER

Excited Gas Technology Division, Tracerlab, A Division of LFE, 2030 Wright Avenue, Richmond, Calif. 94804

Publication Date: June 1, 1969 | doi: 10.1021/ba-1969-0080.ch022

Employing RF. electrodeless excitation at 13.56 MHz. products undoubtedly polymeric in nature were synthesized with the simple inorganic gas reactants CO, H_2, and N_2. Syntheses carried out at about 300 watts net radiofrequency (RF.) power, and from 0.3–2.5 torr system pressures, indicate controllable percent nitrogen incorporation into the polymer by regulation of the nitrogen flow rate, other gas flow rates being held constant. The experimental discharge conditions and apparatus configuration were examined with respect to polymer synthesis. Internal reflectance and transmission infrared spectroscopy (2.5–16μ) revealed structural entities similar to polyacrylamides and proteins of some types. Elemental analyses for C, H, O, and N vs. run conditions were determined.

A certain amount of the large literature concerning the synthesis of compounds in electrical discharges relates to the synthesis of polymeric materials, and many industrial patents exist in this category. Most of these syntheses have employed (1) hydrocarbon reactant(s) or (2) discharge apparatuses involving internal electrode configurations as the source of excitation, and the glow discharge or "cold plasma" was initiated by a.c. or d.c. fields of several hundred volts between the internal electrodes (2).

We wish to report an electrodeless discharge synthesis involving the simple inorganic gases CO, N_2, and H_2 of a material having the spectral and physical characteristics of a polymer. The advantages of the elec-

[1] Present address: Boeing Scientific Research Laboratories, Seattle, Wash. 98124.

In Chemical Reactions in Electrical Discharges; Blaustein, B.;
Advances in Chemistry; American Chemical Society: Washington, DC, 1969.

trodeless technique are principally avoidance of electrode erosion or kinetic interaction of the electrodes with the reacting gas mixtures, the capability of filling uniformly a plasma reactor with a volume of excited gas, and engineering advantages of radiofrequency excitation.

Experimental

Run Procedure. An apparatus for precision metering of several gases into plasma reactors was designed and constructed for this work. Figure 1 shows the system design. Up to four different gases may be metered individually at known flowmeter pressures. Since the gases were non-corrosive, mercury manometers adequately served as the flowmeter pressure measurement device. Flows of gases in cc. $min.^{-1}$ NTP were calculated from the gas viscosity at the operating temperature, the gas density at the operating pressure and temperature, and the flowmeter scale reading. The flowmeter operating pressure P_{FM} was calculated from $P_{FM} = \Delta P + P_{SYS}$ where P_{SYS} is the system pressure measured at Point A and ΔP is the differential pressure across the manometer.

The accuracy of flow rates are taken to be $\pm 2\%$ to $\pm 10\%$ depending on flow meter condition and flow rate. In nearly every case, the $\pm 2\%$ accuracy was maintained. The reagent gases, sources, and statement of purity are as follows:

Gas	*Grade*	*Source*	*Purity*
CO	C.P.	Matheson	99.5%
N_2	Extra Dry	Matheson	99.7%
H_2	Pre-Purified	Matheson	99.95%
CO_2	Coleman	Matheson	99.99%

After calculations of the desired flow rates and consequent required flow conditions, the entire gas line is purged by alternate pumping and filling with the desired gases. The metering valve V(2) and the flow meter pressure regulating valve V(3) are adjusted to provide the conditions of flow meter pressure P_{FM} and flow meter indication necessary to produce with accuracy the desired flow rates. Leak checks with a helium mass spectrometer leak detector are made before and after the experimental run. Valve V(1) is a gas flow on-off valve.

With the flow rates accurately adjusted, the RF. generator/RFG-600 (*see* below) connected to the capacitive exciter is energized and the activator tuned while bringing the generator to maximum power, ~300 watts. Trap T(1), which is filled with 3 mm. diameter glass beads and some borosilicate glass wool to assure efficient trapping, is chilled with liquid nitrogen. Traps T(2) and T(3) are chilled respectively with a dry ice isopropyl alcohol slurry and liquid nitrogen. T(3) contains 5 mm. glass beads again to assure efficient trapping and to assure non-interference from vapors originating from the pump. Next, the second RF. generator/RFG-600 connected to the inductive excited is energized and the activator tuned while bringing the generator to maximum power, ~ 300 watts.

Publication Date: June 1, 1969 | doi: 10.1021/ba-1969-0080.ch022

In Chemical Reactions in Electrical Discharges; Blaustein, B.;
Advances in Chemistry; American Chemical Society: Washington, DC, 1969.

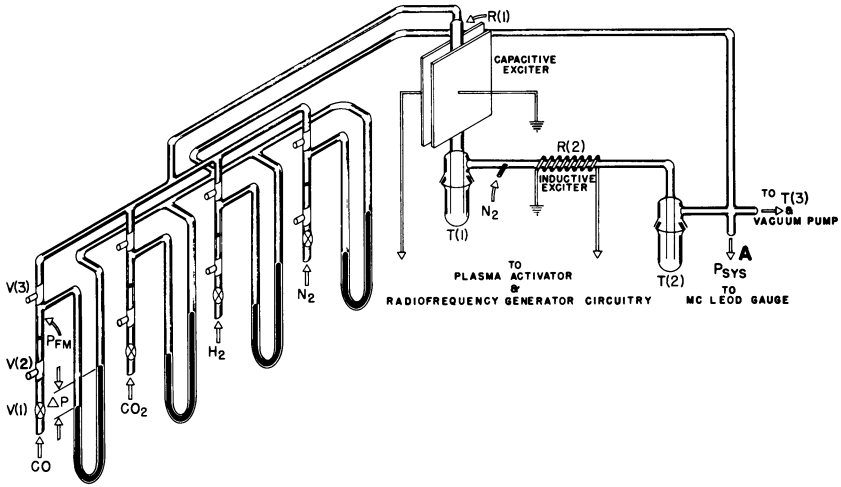

Figure 1. Schematic of flow discharge apparatus and gas monitoring system

With the gases and flows selected for the experiment, the reaction proceeds and the polymer is allowed to accumulate along with the other products. After running a length of time, the generators and gas flows are turned off and the traps allowed to warm up. The pump is then valved off and the system let up to atmosphere with argon. The product of interest is removed from the inner surface of the center tube of T(2) and retained for analysis.

Radiofrequency Equipment. The two plasma reactors were each activated either capacitively or inductively with RF. generators (RFG-600, Tracerlab, Inc.) with deliverable power from minimum up to 300 watts. The generators consist of an RF. section composed of a two stage system utilizing a crystal controlled oscillator, and a Class C power amplifier stage. The second part is a power supply producing plate, screen, bias, and filament power. The details of the electronic requirements for generation and transmission of RF. energy have been described elsewhere (*4*, *5*).

Energy from the generator is transmitted to the exciter plates R(1), or coil, R(2) *via* a plasma activator, the circuitry of which allows maximization of the RF. energy to the gas load and minimization of the reflected power back to the generator. A great experimental advantage of this means of power delivery and measurement is the ability the operator realizes in being able to reproduce his discharge conditions for the different experiments or from run to run. The net power delivered by the generator is a function of gas type and concentrations, which in turn are related to system pressures and flow rates. Each time an excited gas parameter is changed, there is a concomitant change in the intrinsic impedance of the gas load, which must be rematched to the impedance of the secondary activator circuits. Thus, the convenience of simply being able to achieve this matching by the power meter on the generator, which reads forward and reflected power, is a decided advantage.

Publication Date: June 1, 1969 | doi: 10.1021/ba-1969-0080.ch022

In Chemical Reactions in Electrical Discharges; Blaustein, B.;
Advances in Chemistry; American Chemical Society: Washington, DC, 1969.

All experiments were carried out at a radiofrequency of 13.56 MHz. ± 6.87 KHz., an FCC approved non-interference band. The choice of inductive *vs.* capacitive exciters for R(1) and R(2) was rather arbitrary, both were employed to test any significant differences in the reactions induced. The conclusion is that the chemistry is independent of the mode of excitation. There are, however, definite advantages either configuration offers in certain systems, such as gas-solid reactions. This has been described in References 4 and 5.

Observations and Discussion

Synthesis. The polymers to be described below can be produced either of two ways: (1) the reaction directly of CO, H_2, and N_2, or (2) the reaction first of CO_2 and H_2 to produce CO, *via* the water gas reaction, and then subsequent reaction of the produced CO, with excess H_2, and N_2 admitted either downstream of T(1), as indicated in Figure 1, or in the manifold system. The latter experiment was believed to be a purer source of CO and was employed for most of the preparations. The liquid nitrogen temperature of T(1) and its packing trapped all significant water produced in the water-gas reaction, as well as remaining CO_2. It became apparent that if T(1) does not trap all the significant water, that no polymer forms at T(2), owing either to a reaction of H_2O or discharge products therefrom (*3, 6*) with polymer precursors, or to the interference of water to the deposition of the polymer as a film on the cold inner tube of T(2).

The production of the polymer under the flow conditions listed in Table I appears critically dependent on the system pressure. In the experiments, the flows of CO or CO_2 and H_2 were maintained at nearly constant values while the nitrogen flow rate was varied. The very low flow rates of N_2 resulted from permeation through a very short segment of Tygon tubing initially connecting R(1) to the manifold outlet. These rates of permeation were measured by observing rates of system pressure increases with time, and checked by He permeation with the mass spectrometer at the same point. In Run 861, the uncertainty is probably an order of magnitude; in Runs 631 and 291, the uncertainties are half that. In any case, the low flows of N_2 in the initial experiments were much less than measured flow rates in subsequent experiments, which indicate (Table II) that less and less polymer is produced (other gases fixed) as the N_2 flow rate increases. At a very high N_2 flow, *ca.* 107 cc. $min.^{-1}$, no polymer was observed to form at all.

Why no polymer forms at high system pressures, *ca.* 1.0 mm. Hg pressure, is perhaps owing to competing gas phase processes (*1*). The same types of polymers no doubt may be arrived at by substitution of ammonia for the N_2–H_2 mixture, since one often achieves many similar

Publication Date: June 1, 1969 | doi: 10.1021/ba-1969-0080.ch022

In Chemical Reactions in Electrical Discharges; Blaustein, B.;
Advances in Chemistry; American Chemical Society: Washington, DC, 1969.

results irrespective of whether one uses $N_2 + H_2$, or NH_3. Little molecular or atomic oxygen, as such, should be produced in these discharge reactions producing the polymer film. If any appreciable amount were present, this would readily oxidize the polymer, since we typically clean up our system of all organic products using an oxygen discharge.

Table I. Flow Conditions for Several Sample Preparations

	Flow Rates, cc. min.$^{-1}$				P_{SYS}	*Power, Watts*		*Run Time,*
Run	CO_2	CO	N_2	H_2	*torr*	*R(1)*	*R(2)*	*Mins.*
861	1.18	—	$\sim 3.1 \times 10^{-6}$	3.65	.310	330	335	680
631	1.43	—	3.9×10^{-3}	3.95	.320	—	280	414
291	—	2.18	$\sim 2.5 \times 10^{-2}$	4.43	.36	300	—	720
931	1.25	—	1.26	3.60	.45	320	350	463
991	1.36	—	9.88	3.83	.75	320	410	460
890	1.36	—	107	3.74	2.47	320	360	273

Characterization. The polymers at low N_2 flows are transparent, yellow, tightly adherent films. At higher N_2 flows, the transparency decreases, and film strength appears to decrease, indicating perhaps lower molecular weight materials being formed. The films are stable on standing at atmospheric conditions, stable to light, slightly soluble in acetone, and insoluble in water and a variety of other organic solvents.

Table II indicates elemental analyses for C, H, N, and O for several runs. The percent nitrogen is found to increase as the flow of N_2 increases. This suggests, up to a certain point, that one can produce in this experiment tailored polymers containing a controllable amount of a given constituent by controlling its flow rate. The dependence of percent nitrogen found in the polymer on flow rate is given in Figure 2.

Table II. Elemental Analysis for Several Typical Preparations

	% Element Found				
Run	*C*	*H*	*O*	*N*	*Total*
861	80.51	10.31	8.06	0.2	99.1
631	75.0	9.5	12.7	2.8	100.0
291	68.19	9.12	13.23	8.84	99.38
931	55.90	7.77	18.40	17.64	99.71
991	very little formed				
890	no polymer formed				

The transmission infrared (Figure 3) and internal reflectance, ATR (Figure 4) spectra for samples 291 and 633, respectively, show nearly

Publication Date: June 1, 1969 | doi: 10.1021/ba-1969-0080.ch022

identical features for the principal bands. Structural moieties such as

$$C{=}N{-}\overset{\overset{O}{\|}}{C}{-},\ {-}\overset{\overset{O}{\|}}{C}{-}NH_2,\ {=}CH{-},\ {-}CH_2{-},\ {-}CH_3,\ C{-}N,\ C{=}N,\ \text{and}\ {-}OH$$

in organic compounds give the best comparative infrared spectral features to those observed for the synthesized polymer. Spectra of polyacrylamides, and proteins (*9, 10*) of some types, give quite similar spectra. Carbon-nitrogen double or single bonds may exist in the synthesized polymer, but there is no evidence for the strong —C≡N frequency at *ca.* 2240–2260 cm.$^{-1}$ (*9, 10*).

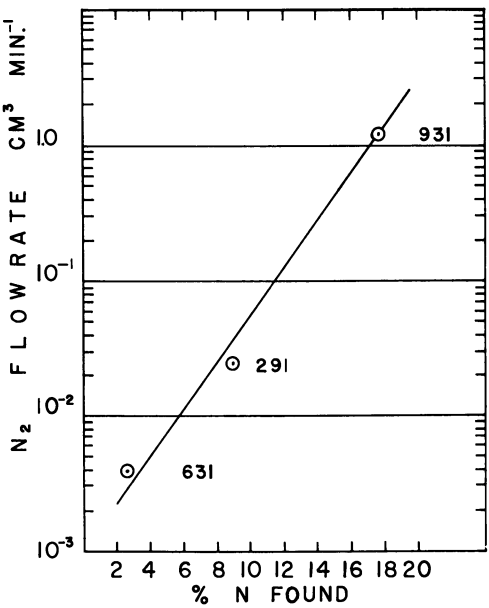

Figure 2. Dependence of nitrogen found in polymer on nitrogen flow rate

Analysis by an automatic amino acid analyzer shows aspartic acid, glutamic acid, glycine, and alanine to be products of the hydrolysis of the polymer in Run 931 (*8*). For high nitrogen flows the H/C, O/C, and N/C ratios approach the ratios found in polyacrylamide.

Nicholls and Krishnamachari (*7*) found in microwave electrodeless discharges at 2450 MHz. emission bands of NCO formed at cryogenic temperatures from the reaction

$$N(^2P) + CO(X^1\Sigma^+) \rightarrow NCO \begin{cases} A^2\Sigma^+ \\ B^2\pi_i \end{cases}$$

Publication Date: June 1, 1969 | doi: 10.1021/ba-1969-0080.ch022

at the cold surface. Thus, an NCO species may enter into the polymer as an important structural entity in the present case.

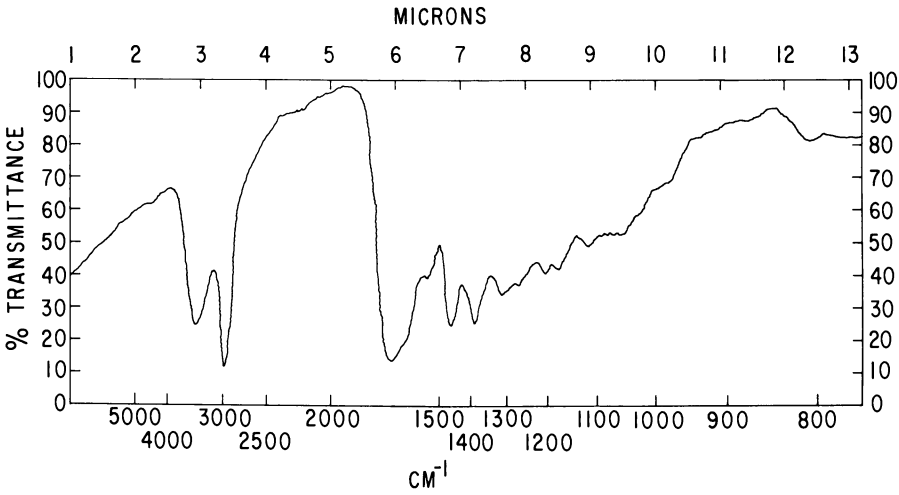

Figure 3. Infrared transmission spectrum of polymer, Run 291

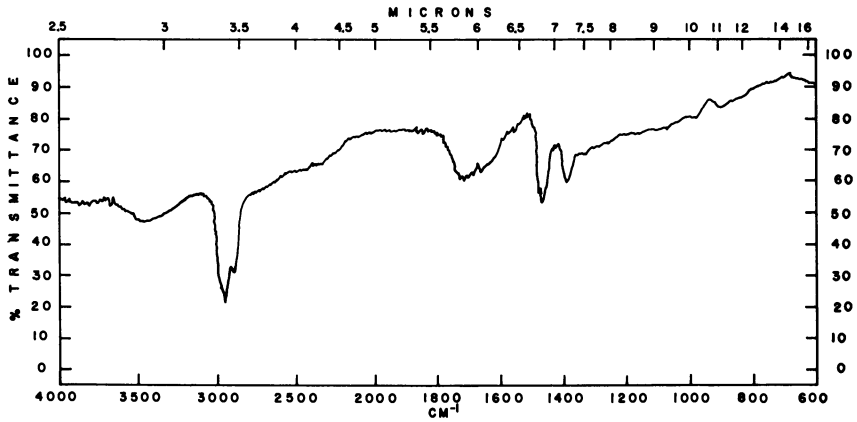

Figure 4. Infrared ATR spectrum of polymer, Run 663

Conclusions

Under the flow discharge conditions of this study, the RF. electrodeless method appears to offer interesting synthetic possibilities with the simple inorganic gases. One might better understand the mechanism of origin of some more complex polymers as a function of simple excited

Publication Date: June 1, 1969 | doi: 10.1021/ba-1969-0080.ch022

molecular, atomic, or free radical precursors, generated in the discharge. The ability to tailor the resulting discharge product with respect to the elemental composition is also a decided advantage of the electrodeless discharge approach.

Acknowledgment

The authors are pleased to acknowledge the analytical assistance of Robert Rinehart of Huffman Laboratories, of Wheatridge, Colorado. Jim Beaudry engineered all the RF. generator and activator circuitry, and for whose assistance we are deeply indebted. Cyril Ponnamperuma of NASA, Ames Research Center, kindly provided the amino acid hydrolysis results on our material. Finally, technical discussions with Richard Bersin were most helpful.

Literature Cited

(1) Blaustein, B. D., U. S. Bureau of Mines, Pittsburgh, Pa. (personal communication).
(2) Goodman, J., *J. Polymer. Sci.* 44, 551 (1960).
(3) Hata, N., Giguere, P. A., *Can. J. Chem.* 44, 869 (1966).
(4) Hollahan, J. R., *J. Chem. Ed.* **43**, A401 (1966).
(5) *Ibid.*, **43**, A497 (1966).
(6) Kaufman, F., *Ann. de Geophys.* **20**, 106 (1964).
(7) Nicholls, R. W., Krishnamachari, S. L. N. G., *Can. J. Chem.* **38**, 1652 (1960).
(8) Ponnamperuma, Cyril, NASA Ames Research Center (private communication).
(9) Schurz, J., Bayzer, H., Sturchen, H., *Makromol. Chem.* **23**, 152 (1957).
(10) Wilks, P. A., Iszard, M. R., paper presented at *Fifteenth Mid-America Spectroscopy Symp., Chicago, Ill.* (June 2-5, 1964).

RECEIVED May 2, 1967.

23

Synthesis of Organic Compounds by the Action of Electric Discharges in Simulated Primitive Atmospheres

C. PONNAMPERUMA, F. WOELLER, J. FLORES, M. ROMIEZ, and W. ALLEN

Exobiology Division, National Aeronautics and Space Administration, Ames Research Center, Moffett Field, Calif.

Publication Date: June 1, 1969 | doi: 10.1021/ba-1969-0080.ch023

In the study of chemical evolution we are interested in the path by which molecules of biological significance could have been formed on the earth before the appearance of life. We have therefore examined the action of electric discharges on the presumed primitive atomsphere of the earth. Three different sets of experiments were performed: (1) with methane, ammonia, and water; (2) with methane and ammonia; (3) with methane alone. Several molecules of biological significance have been synthesized. In some instances polymerization appears to have taken place. These results may be relevant to the Oparin-Haldane hypothesis of chemical evolution.

In the study of chemical evolution we are interested in the path by which molecules of biological significance could have been formed on the primitive earth in the absence of life. It is generally accepted that the primitive atmosphere of the earth consisted mainly of methane, ammonia, and water. Various forms of energy such as ultraviolet light from the sun, electrical discharges, heat, and ionizing radiation acting on this atmosphere must have given rise to a wide variety of organic substances.

Table I gives a summary of the sources of energy on the earth's surface today (7). It is probable, therefore, that solar energy must have made the principal contribution to the synthesis of organic compounds in primordial times. Next in importance are electric discharges, such as lighting and corona discharges from pointed objects. These occur closer to the earth's surface and, hence, would have more effectively transferred

In Chemical Reactions in Electrical Discharges; Blaustein, B.;
Advances in Chemistry; American Chemical Society: Washington, DC, 1969.

the organic matter synthesized to the primitive oceans. This paper describes attempts to simulate some of the reactions which may have taken place on the prebiotic earth, through the action of electric discharges.

While extensive work has been done on the effect of electric discharges on various organic molecules, relatively few experiments have been performed to elucidate its role in chemical evolution. Some of the earliest such investigations were carried out by the chemist Haber. Beutner, in his book entitled "Life's Beginning on the Earth," recalls how Haber performed numerous experiments in which electrical discharges were sent through carbon containing gases like methane, carbon dioxide, etc., with the aim of obtaining sugars (2). Although traces of some sugars were formed, a large number of various other substances were also synthesized. Haber thus came to the conclusion that by means of electrical discharges through carbon containing gases, "practically any substance known to organic chemistry can be found."

Publication Date: June 1, 1969 | doi: 10.1021/ba-1969-0080.ch023

Table I.

Source	*Energy (in cal cm.$^{-2}$ yr^{-1})*
Ultraviolet light (2500 A.)	570
Electric discharges	4
Radioactivity	0.8
Volcanoes	0.13

Perhaps the most celebrated experiment in this field was performed by Stanley Miller in Urey's laboratory in 1953 (5). Miller submitted a mixture of methane, ammonia, and water in the presence of hydrogen to electrical discharges from tesla coils. A large number of organic compounds were formed, four were amino acids commonly found in proteins. Miller postulated two alternative possibilities for the mechanism of synthesis of amino acids. According to the first, aldehydes and hydrogen cyanide are synthesized in the gas phase by the spark. These aldehydes and hydrogen cyanide react in the aqueous phase to give amino- and hydroxynitriles. These nitriles are, in turn, hydrolyzed to amino and hydroxy acids. The mechanism is essentially a Strecker synthesis. A second suggestion made was the amino and hydroxy acids were synthesized in the gas phase by ions and radicals produced in the electrical discharge. Miller's subsequent work has shown that the first mechanism is the one most likely to have produced the amino acids (6). The rate of production of aldehydes and hydrogen cyanide by the spark and the rate of hydrolysis of the aminonitriles were sufficient to account for the total yield of amino acids.

In Chemical Reactions in Electrical Discharges; Blaustein, B.;
Advances in Chemistry; American Chemical Society: Washington, DC, 1969.

In our experimental work, we have endeavored to study the pathways by which various molecules of biological interest could have been formed by the action of electrical discharges. A series of experiments was outlined in which the starting materials were varied. Four different classes of experiments have been performed: with methane; with methane and ammonia; with methane, ammonia, and water; and with methane and water.

The effect of a semi-corona discharge, a low intensity arc discharge, and a high intensity arc discharge on gaseous methane was first investigated. The apparatus used for these studies has been described previously (8). The current through the discharge was measured by the voltage drop across a resistor in series with the cell. For the semi-corona discharge, the cell current was 0.4–0.5 ma. for the low arc, and 10 ma. for the high arc discharge. Gas chromatography and mass spectrometry were used for the analysis of the end products. Comparative results of the analysis of hydrocarbons up to C_5 are shown in Table II. In the semi-corona about half the methane remained unreacted after a 24-hour discharge. Some ethane and propane were formed. There were small amounts of ethene, propene, and substituted paraffins. In the case of the low and high arcs, ethylene and acetylene were also present.

Table II.

	High Arc	*Low Arc*	*Semi-Corona*
Total hours of current flow	1.5	40	48
Electrode voltage	1400	2500	9400
Cell current (ma.)	4.0	0.5	0.3
% Loss CH_4/h	13.5	1.8	0.9
Volatile end products (mole % of hydrocarbon fraction)			
Methane	90.5	59.1	69.8
Ethane	3.2	8.3	19.3
Propane	0.2	2.2	6.6
Ethene	3.2	10.7	0.5
Propene	—	0.8	0.6
Acetylene	2.7	18.5	0.0

The analysis of the hydrocarbons from C_6–C_9 reveals that the semi-corona gave saturated substances while the arc discharges gave rise to aromatic compounds. The semi-corona cell yielded a colorless distillate, the gas chromatogram of which was poorly resolved. The high intensity arc gave a yellow fluid, the chromatogram of which had well spaced peaks. Benzene was the most abundant with toluene next in order of magnitude. Principal peaks from the semi-corona chromatogram were identified by the use of mass spectrometry as: 2,2-dimethylbutane, 2-methylpentane, 3-methylpentane, 2,4-dimethylhexane, 3,4-dimethylhexane. In Figure 1

In Chemical Reactions in Electrical Discharges; Blaustein, B.;
Advances in Chemistry; American Chemical Society: Washington, DC, 1969.

the chromatogram of the semi-corona discharge products (low) has been superimposed on that from the high intensity arc (high). The results presented here show that the character of compounds in the range of interest appears to be determined by the type of discharge more than by any other factor (*8*).

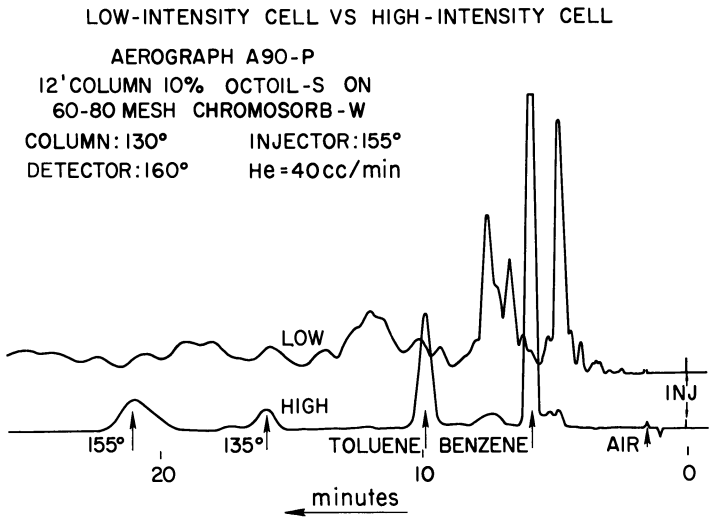

Figure 1. Gas chromatograms of semi-corona and arc discharge products C_6–C_9

We have also examined the composition of the hydrocarbons above C_9 in the products of the semi-corona discharge. The gas chromatogram is very unresolved (Figure 2). No normals or branched-chain isoprenoid hydrocarbons were identified. The preponderance of normal hydrocarbons and the presence of the isoprenoids, pristane, and pythane are considered to be indicative of biological origin. Analysis of the mixture by mass spectrometry shows that the compounds are possibly cyclic in structure (*9*).

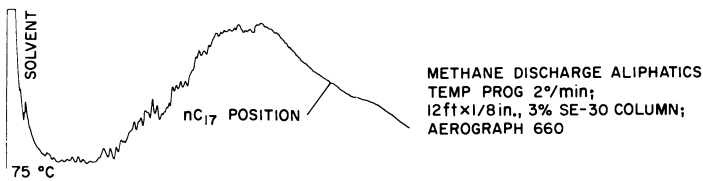

Figure 2. Gas chromatogram of semi-corona discharge products above C_9

Publication Date: June 1, 1969 | doi: 10.1021/ba-1969-0080.ch023

The effect of an arc discharge on anhydrous methane and ammonia was next investigated for two reasons. Firstly, such a study would help us to understand the pathways by which some organic compounds such as amino acids can be synthesized. Secondly, reactions of this type would simulate, to some extent, conditions which may exist on the planet Jupiter.

In this investigation, we have used reaction vessels of about a liter in volume containing an equimolar mixture anhydrous methane and ammonia up to a pressure of 0.5 atm. The electrodes consisted of gold wires about 1 cm. apart. A typical reaction lasted for about 15 hours. The current passing through the system was about 0.5 ma. The end products consisted of: (1) gases, (2) colorless distillate, and (3) a ruby colored residue.

Publication Date: June 1, 1969 | doi: 10.1021/ba-1969-0080.ch023

In the present study, our attention was primarily directed to the colorless distillate. The volatile products were vacuum distilled into a U-trap at −78°C. and analyzed by gas chromatography (Figure 3). The fractions corresponding to each peak were collected for subsequent mass spectrometric analysis. The GLC retention time, the mass spectrometric fragmentation pattern, and the NMR spectrum established the identity of each of the fractions separated by gas chromatography. Ammonium cyanide, methyl cyanide, ethyl cyanide, α-aminoacetonitrile and its C-methyl and *N*-methyl homologues were identified. The α-aminonitriles on hydrolysis give rise to α-amino acids. These nitriles may provide a reasonable pathway for the origin of amino acids under prebiological conditions. Some analyses of the polymeric material generated in an experiment of this type has been recently reported (*4*).

In some of our discharge experiments, we turned to the question of the origin of monocarboxylic acids under prebiotic conditions. If we assume that pre-existing abiotically synthesized fatty acids were necessary for the functioning of selective membranes, some mechanism must have existed for their formation. The reaction between methane and water appears to provide such a pathway. When a mixture of methane and water was exposed to a semi-corona discharge and the end products examined after saponification, the monocarboxylic acids from C_2–C_{12} were identified (*1*).

The volatile acids C_1–C_8 were examined as their free acids by gas chromatography. A resulting chromatogram is illustrated in Figure 4. The individual peaks were then trapped and their identity confirmed by mass spectrometry. Acids containing seven or more carbon atoms were analyzed as methyl esters. The methyl esters, after chromatography, were examined by mass spectrometry. Of eleven major peaks obtained by gas chromatography (Figure 5) only one appears as the normal methyl ester. Presumably, the remaining peaks represented branched-chain isomers.

In Chemical Reactions in Electrical Discharges; Blaustein, B.;
Advances in Chemistry; American Chemical Society: Washington, DC, 1969.

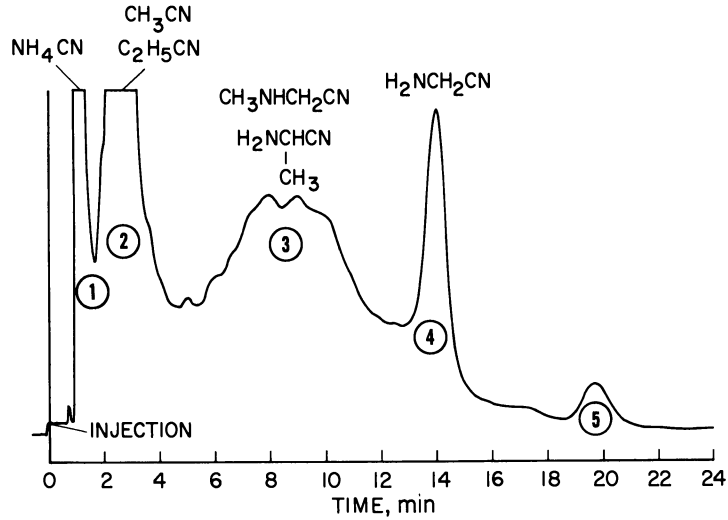

Figure 3. Gas chromatogram of colorless distillate from arc discharge through methane and ammonia

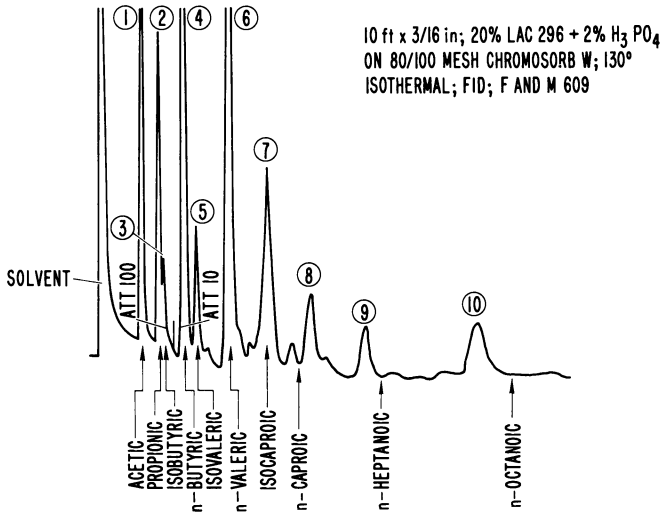

Figure 4. Gas chromatogram of volatile fatty acids from a semi-corona discharge through methane and water

While it is clear that in the case of the longer chain fatty acids several isomers have been produced, only a few of the innumerable possible compounds are realized. A preferential synthesis of some type appears to be favored. Theoretically, the branching of carbon chains, which is favored in free radical reactions, may be repressed by steric

Publication Date: June 1, 1969 | doi: 10.1021/ba-1969-0080.ch023

restrictions when the lengthening carbon chains are absorbed on monolayers. An attempt to favor the formation of straight chain acids by placing the aqueous phase in close proximity with the discharge zone did not produce any change in our results.

In the study of prebiotic organic synthesis, perhaps the most relevant experiments involve the use of all the main consituents of the presumed primitive earth atmosphere. We have therefore exposed a mixture of methane, ammonia, and water to a discharge from tesla coils simulating lightning on the primitive earth. At the end of a 24-hour discharge, the gas phase analysis has shown that over 90% of the starting methane has been converted into organic compounds. Of this, about 45% is found in the water fraction. 18% of the water soluble material is in the form of cyanide. The formation of cyanide in this reaction is significant in the light of the multiple role played by hydrogen cyanide in organic synthesis (*10*).

Publication Date: June 1, 1969 | doi: 10.1021/ba-1969-0080.ch023

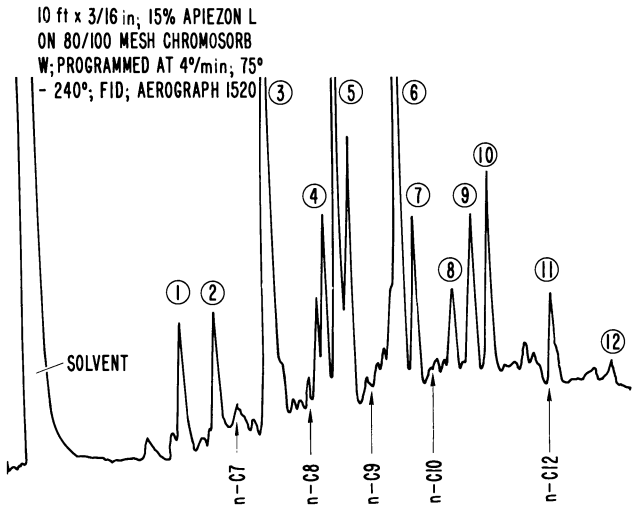

Figure 5. Gas chromatogram of methyl esters of higher fatty acids from a semi-corona discharge through methane and water

The analysis of the end products of this reaction by paper chromatography reveals that a large number of organic compounds were formed but none of these corresponded to the commonly occurring amino acids. A certain amount of material appeared at the origin. However, when the reaction products were hydrolyzed with 6*N* HCl for 24 hours and then analyzed, a large number of amino acids were formed (Figure 6). Among those identified are nine which are commonly found in biological materials: glycine, alanine, aspartic, glutamic, threonine, serine, isoleu-

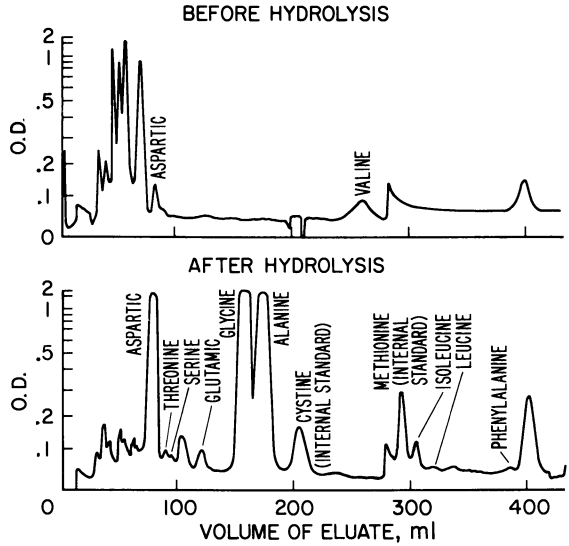

Figure 6. Ion exchange separation of amino acids from a spark discharge through methane, ammonia, and water

cine, and phyenylalanine. The results obtained by ion exchange analysis were confirmed by gas chromatography (Figure 7). The evidence suggests that the amino acids may have been polymerized in the solution of end products. Separation by the use of a biogel-P column gave us a fraction having a molecular weight in the range 186 to about 2,000 and whose 1-dimethylaminonaphthalene-5 sulfonyl chloride (DNS) derivative showed a single band on electrophoresis. When an aliquot from the biogel-P eluate was hydrolyzed, the amino acids aspartic, serine, glutamic, glycine, and alanine were obtained. Until the presence of the peptide bond is definitely established by infrared analysis and enzymatic hydrolysis, some caution is required in interpreting these results as suggestive of polypeptides. Some results similar to our findings have been reported previously by Lowe, Rees, and Marcon (3).

This result is significant in the context of chemical evolution. It has generally been thought that amino acids had first to be synthesized and then condensed together into a polymer. If a suitable condensation agent is present a polymer may be formed as soon as the acids are synthesized. In our case, the condensation agent could be hydrogen cyanide. The presence of 18% hydrogen cyanide in the reaction mixture combined with the fact that in previous experiments we have been able to condense bases and sugars with cyanide support this hypothesis.

The different experiments that have been described so far reveal that important biological molecules can be synthesized by the use of a form

Publication Date: June 1, 1969 | doi: 10.1021/ba-1969-0080.ch023

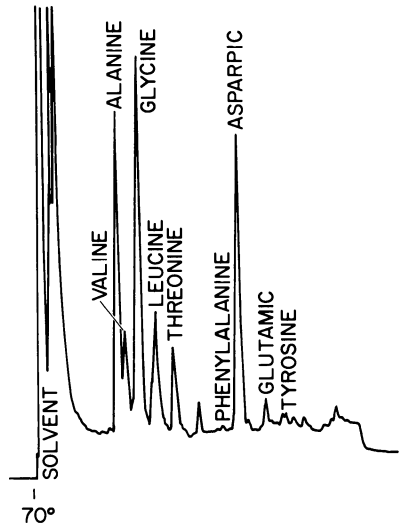

Figure 7. Ion exchange analyses (Amino acids from spark discharge methane, ammonia, and water)

Temperature programmed at 6° min. on a 1.5 m; 1/8 inch H1 EFF 8BP Column

of energy which existed on the primitive earth. These conditions may be considered to be genuinely abiotic since the materials used are the constituents of the presumed primitive earth atmosphere, the conditions are aqueous, and the form of energy is one that is likely to have occurred on the earth before the appearance of life.

Literature Cited

(1) Allen, W. A., Ponnamperuma, C., "Currents in Modern Biology," in press, 1967.
(2) Beutner, R., "Life's Beginning on the Earth," Williams and Wilkins, Baltimore, 1938.
(3) Lowe, C. U., Rees, M. W., Marcom, R., *Nature* **199,** 222 (1963).
(4) Matthews, C. N., Moser, R. E., *Proc. Natl. Acad. Sci.* **56,** 1087 (1966).
(5) Miller, S. L., *J. Am. Chem. Soc.* **77,** 2351 (1955).
(6) Miller, S. L., *Bichim. et Biophys. Acta.* **23,** 480, (1957).
(7) Miller, S. L., Urey, H. C., *Science* **130,** 245 (1959).
(8) Ponnamperuma, C., Woeller, F., *Nature* **203,** 272 (1964).
(9) Ponnamperuma, C., Pering, K., *Nature* **209,** 979 (1966).
(10) Sanchez, R., Ferris, J., Orgel, L. E., *Science* **153,** 72 (1966).

RECEIVED June 13, 1967.

The Dissociation of Toluene Vapor in a Radiofrequency Discharge

FRANK J. DINAN, SHERRILL FRIDMANN, and PETER J. SCHIRMANN

Canisius College, Buffalo, N. Y.

Publication Date: June 1, 1969 | doi: 10.1021/ba-1969-0080.ch024

The excitation of organic vapors in arcs and discharges is widely assumed to involve free radical intermediates. There is often, however, little experimental data to support this conclusion. This study has demonstrated radicals to be of dominant importance in a 28 MHz. radiofrequency (RF.) discharge. The quantity and nature of the condensable products formed in the RF. discharge are consistent with radical precursors. However, the polymeric product formed in the discharge has been shown to result from a different mechanism which cannot involve radical intermediates. Thus, the quantity and nature of the products obtained appears to be a result of two or more competing processes.

The emission spectra resulting from the excitation of toluene vapor in electrode discharges have been investigated by Schüler as a part of his extensive work dealing with the behavior of molecules in discharges (*8*). He found that two distinctly different spectra were emitted. One, the normal toluene emission spectrum, was centered in the 2600–3000 A. region and was related to the forbidden benzenoid absorption band of toluene in the crude mirror image relationship which characterizes fluorescence emission. In addition to this ultraviolet emission, Schüler also observed a visible emission spectrum from toluene which appeared in the 4300 to 5000 A. region. This spectrum was designated the "blue spectrum" and was assigned to the benzyl radical.

In a subsequent study of the reaction of toluene vapor in a high voltage electrode discharge, Kraaijveld and Waterman (*4*) investigated the formation of the bibenzyl molecule from toluene and found that, under optimum conditions in a 2400 volts arc, 40% of the toluene vapor could be converted to bibenzyl. This result, as well as those obtained by

In Chemical Reactions in Electrical Discharges; Blaustein, B.;
Advances in Chemistry; American Chemical Society: Washington, DC, 1969.

Schüler, imply the existence of benzyl radicals as the major species present in electrode induced toluene discharges.

More recently, Streitwieser and Ward conducted the first comprehensive study which was concerned with the full range of condensable products formed from the electrodeless microwave excitation of toluene vapor (9). In this study, flowing toluene vapor in a helium carrier gas stream was excited by a 3 KMHz. microwave generator. The spectrum of the light emitted was not investigated, however the products were carefully determined. The composition of the mixture of products obtained is shown in Table I.

Table I. Condensable Products from Toluene Vapor in a 3 KMHz. Powered Discharge

Product	% [a]
Benzene	55
Ethylbenzene	33
Phenylacetylene	8
Styrene	3
Xylene Isomers	Trace
Bibenzyl	~0.6
Diphenylmethane	~0.2
Biphenyl	~0.1

[a] Normalized to exclude recovered toluene, polymeric, and non-condensable products.

The very minor amounts of dimer biaryls which were formed in this discharge suggested that radical intermediates were not of dominant importance. The lack of formation of the xylene isomers was also interpreted as supporting the absence of methyl radicals in the plasma.

Two other possibilities, the molecular cation and anion were considered as likely intermediates in the microwave discharge. Results obtained from labeling experiments ruled out consideration of the cation, and it was tentatively concluded that anion intermediates remained as the most likely possibility.

This result interestingly contrasted with the conclusions which had been previously drawn regarding the dominance of radicals in toluene discharges and cast some doubt on these conclusions. However, work which had been done in W. D. Cooke's laboratory at Cornell University suggested that significant differences might be anticipated between the products resulting from the excitation of organic vapors in a microwave powered discharge and the excitation of these vapors with a radiofrequency source (2, 5). It was, therefore, decided to investigate both the spectra emitted and the products obtained when toluene vapor was excited in a 28 MHz. radiofrequency discharge.

Publication Date: June 1, 1969 | doi: 10.1021/ba-1969-0080.ch024

The apparatus used in this study is shown in block diagram form in Figure 1. Flowing toluene vapor was passed through a discharge powered by an RF. transmitter operating at 28 megacycles and 100 watts output. The wall temperature of the discharge tube was only slightly above room temperature. The pressure of the vapor was maintained constant at 0.10 to 0.15 mm. at a flow rate of approximately 0.01 mole/hr. Materials formed in the plasma were collected in traps maintained at 0°C. and −80°C. and were subsequently investigated by gas chromatographic and spectroscopic techniques. The light emitted from the discharge was focused into a scanning monochromator and detected by a IP-28 photomultiplier tube. The amplified output of the photomultiplier was recorded electronically. Under the conditions used in these experiments, toluene was converted to products in 12 to 16% yield with 75 to 82% of the toluene being recovered unchanged. Liquid products formed in the discharge were analyzed by gas chromatography. SE-30 and Bentone-3,4 with Apiezon-L columns were used. Percentages were determined from peak area comparisons with working curves.

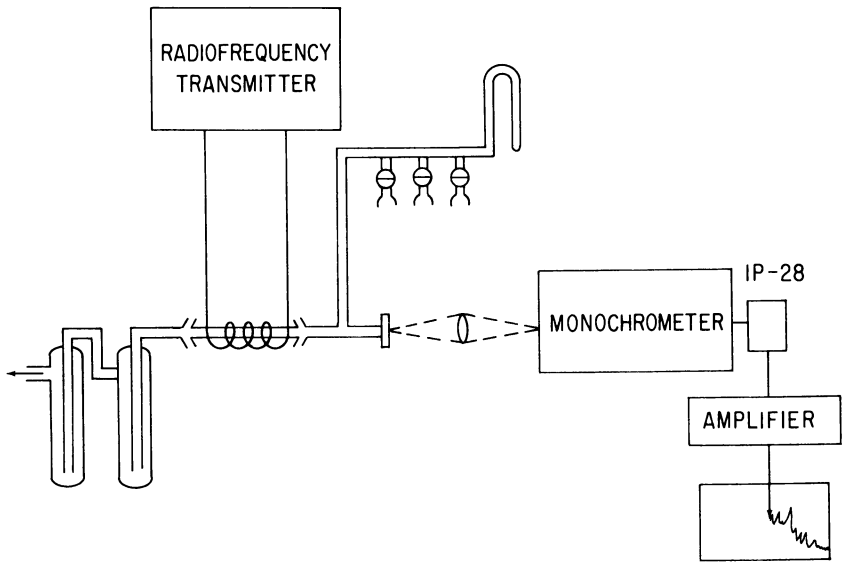

Figure 1. Block diagram of apparatus

A summary of the condensable products formed in the RF. powered discharge is presented in Table II. It should be noted that these results are normalized to exclude recovered toluene. Non-condensable gases and polymeric materials in combination accounted for 6 to 16% of the original toluene vapor. The amount of polymer formed was found to vary, unaccountably over a wide range.

In Chemical Reactions in Electrical Discharges; Blaustein, B.;
Advances in Chemistry; American Chemical Society: Washington, DC, 1969.

Table II. Condensable Products from a 28 MHz. Discharge in Toluene

Product	% [a]
Benzene	35
Ethylbenzene	40
Bibenzyl	16
Diphenylmethane	7
Biphenyl	2
Xylene Isomers	<1

[a] Normalized to exclude recovered toluene, polymeric, and non-condensable products.

The formation of substantial amounts of dimer biaryls; bibenzyl, diphenylmethane and biphenyl is of particular significance since, as noted above, the formation of only trace amounts of these dimer biaryls was observed in the microwave discharge. Additional experiments were conducted in which a helium carrier gas was used, and no substantial difference in the nature and amounts of products formed was noted. The change in product ratios, therefore, appears to reflect a change in mechanism which results from the use of an RF. powered discharge.

The products formed in this study, in particular the large amounts of biaryls, indicate that free radicals are the major intermediates leading to the formation of condensable products. The compounds formed can be readily explained by a series of radical combination and hydrogen abstraction reactions involving benzyl, phenyl, and methyl radicals such as those outlined in Figure 2.

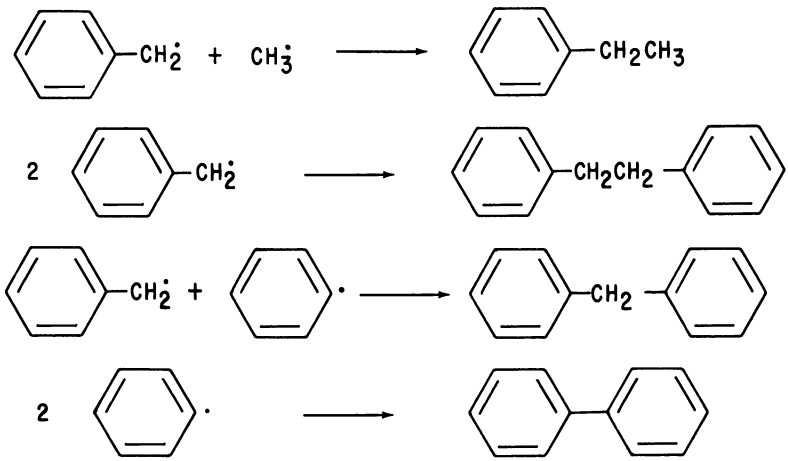

Figure 2. Product formation reactions

It should be noted that minor, but definite amounts of the three xylene isomers were formed in the radiofrequency discharge. The obser-

Publication Date: June 1, 1969 | doi: 10.1021/ba-1969-0080.ch024

vation that the dissociation of toluene vapor in a microwave powered discharge produced only trace amounts of these isomers has been used as an argument against the presence of methyl radicals in the microwave discharge (*9*). It has been demonstrated, however, that methyl radicals react with toluene vapor with a hundred-fold preference for the side chain rather than the ring positions (*1*). It is, therefore, entirely consistent with the presence of methyl radicals in the RF. discharge that reaction should take place predominantly with the toluene side chain to form ethylbenzene rather than with the ring positions to yield xylene isomers, although the formation of small amounts of xylene should be anticipated.

Experiments in which specifically labeled deuteriotoluene was passed through the RF. discharge afforded additional experimental data which supported the importance of radical intermediates leading to condensable products. The materials formed from the labeled toluene were collected, separated by chromatographic techniques, and the distribution of the deuterium label determined by infrared and nuclear magnetic resonance spectroscopy and mass spectrometry.

The side chain of the recovered ethylbenzene was found to be heavily deuterated. The partial mass spectrum of the recovered ethylbenzene compared with the mass spectrum of un-deuterated material is shown in Figure 3. The parent peak of the recovered material is five mass units higher than the corresponding peak in the un-deuterated material, and demonstrates the inclusion of five deuterium atoms in the molecule. The base peak of the unlabeled ethylbenzene molecule results from a P–15 cleavage corresponding to the loss of a methyl group. In the spectrum of the recovered material, the base peak results from P–18 cleavage and clearly demonstrates the methyl group of the side chain to be fully deuterated. This molecule presumably forms from the combination of $C_7H_5D_2$ radical with a CD_3 radical.

The distribution of the deuterium label in the benzyl fragment can be demonstrated by considering the NMR spectrum of the recovered bibenzyl. Comparison of the proton magnetic resonance spectrum of un-deuterated bibenzyl with that of the recovered material disclosed that the 5:2 ratio of aromatic to methylene protons observed in the non-deuterated material is not observed in the recovered bibenzyl. Integration of the spectrum of this material affords an aromatic to aliphatic proton ratio of 40:1. The greatly diminished methylene proton peak in the spectrum of the recovered bibenzyl clearly demonstrates that the label remains localized in the side chain of the benzyl fragment and is not distributed throughout the ring.

This result is entirely consistent with the presence of free radical intermediates in the discharge since it has been demonstrated that the

Publication Date: June 1, 1969 | doi: 10.1021/ba-1969-0080.ch024

In Chemical Reactions in Electrical Discharges; Blaustein, B.;
Advances in Chemistry; American Chemical Society: Washington, DC, 1969.

un-ionized benzyl radical does not undergo any type of rearrangement which would result in the randomization of a label, such as the formation of the tropylium radical (*6*). By contrast, the benzyl cation does undergo an immediate rearrangement to the tropylium ion, which would result in uniform distribution of the deuterium label (*7*). Since this is not observed, the benzyl cation can be ruled out as a significant reaction intermediate leading to the formation of condensable products.

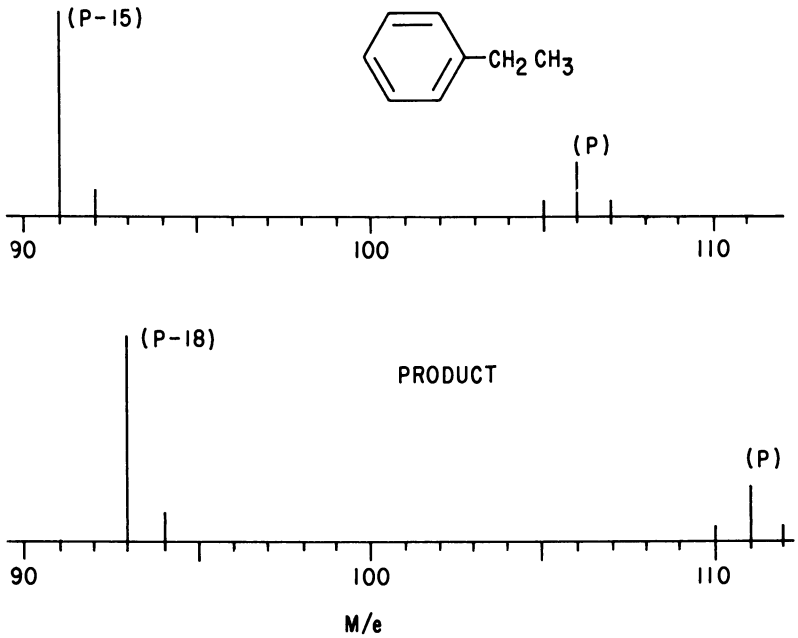

Figure 3. Partial mass spectrum of ethyl benzene

Additional experiments were conducted in which toluene and iodine vapors were passed through the RF. discharge together. Table III shows the composition of the condensable products formed in this experiment. In view of the known affinity of iodine for free radicals (*3*), the formation of benzyl iodide, iodobenzene, and methyl iodide together with greatly reduced amounts of the previously observed products argues for the presence of benzyl, phenyl, and methyl radicals in the discharge.

It should also be noted that the visible emission spectrum which is shown in Figure 4 was obtained from the 28 MHz. toluene discharge. This spectrum is similar to that which Schuler had previously observed from electrode toluene discharges and assigned to the benzyl radical. Its presence adds additional support to the view that this radical is a major intermediate in the electrodeless radiofrequency powered discharge.

Publication Date: June 1, 1969 | doi: 10.1021/ba-1969-0080.ch024

Table III. Condensable Products from Iodine and Toluene Vapor in a 28 MHz. Discharge

Product	% [a]
Benzyl Iodide	47
Iodobenzene	14
Ethylbenzene	11
Benzene	13
Methyl Iodide	6
Unidentified	9

[a] Normalized to exclude recovered toluene, polymeric, and non-condensable products.

Preliminary studies dealing with the nature of the polymeric materials formed from toluene in the 28 MHz. discharge indicate that these products form by a completely different mechanism from that which leads to the formation of condensable products. The polymeric products appear to be low molecular weight substituted polystyrene of varying chain length and degree of cross-linking. This identification is based on proton magnetic resonance, infrared, and ultraviolet spectroscopic data. The exact structure of the polymeric material is, as yet, not completely defined. However, deuterium labeling studies, similar to those described above, have unequivocally established that this material forms by a mechanism which results in nearly complete randomization of the side chain deuterium label of α,α,α-trideuteriotoluene. This is shown by the presence of aromatic deuterium and aliphatic proton atoms in the recovered polymer.

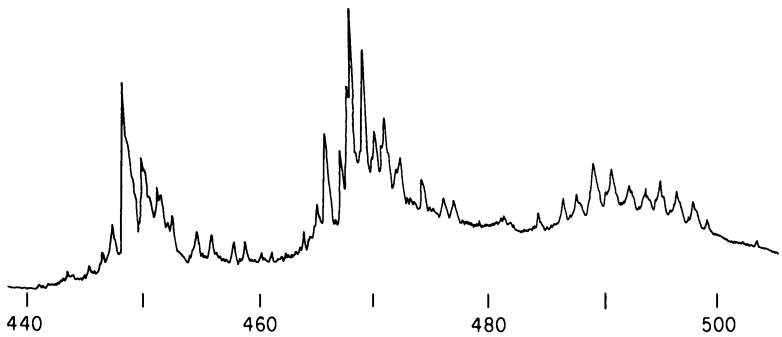

Figure 4. Toluene visible emission

The structural details and mechanism of formation of this polymer are currently being studied. However, the significance of the scrambling of the deuterium label has already been established; namely, that polymer from the reaction of toluene in the 28 MHz. discharge is formed by a mechanism which is entirely different from that leading to condensable

In Chemical Reactions in Electrical Discharges; Blaustein, B.;
Advances in Chemistry; American Chemical Society: Washington, DC, 1969.

products. The products from this discharge must therefore be the result of competing mechanisms, since no single mechanism can account for all products. This balance between two or more competing mechanisms may be the factor which distinguishes the products formed in various types of related discharges.

Summary

The different products and intermediates formed in this work as contrasted to Streitwieser and Ward's study indicates that significant differences are to be anticipated between RF. and microwave powered discharges and unequivocally establish the importance of radical intermediates in the formation of condensable products in the toluene RF. discharge. The formation of polymeric products *via* a different mechanism demonstrates that no single mechanism can account for all of the materials formed in this discharge. The hazards involved in the generalization of data obtained in a specific type of discharge are readily apparent from the observations.

Publication Date: June 1, 1969 | doi: 10.1021/ba-1969-0080.ch024

Acknowledgment

Acknowledgment is made to the donors of the Petroleum Research Fund, administered by the American Chemical Society, for partial support of this work. Additional support for this investigation was received from National Science Foundation Grant GY-704.

Literature Cited

(1) Berezin, I. V., Kazankaya, N. F., Martinek, K., *Zh. Obshch. Khim.* **30,** 4093 (1960); *C.A.* **55,** 27153b.
(2) Dinan, F. J., Cooke, W. D., *J. Org. Chem.* **31,** 3025 (1966).
(3) Garst, J. F., Cole, R. S., *Tetrahedron Letters* **No. 11,** 679 (1963).
(4) Kraaijveld, H. J., Waterman, H. I., *Brenstoff-Chem.* **43,** 33 (1962); *C.A.* **57,** 10627f.
(5) McCormack, A. J., Tong, S. C., Cooke, W. D., *Anal. Chem.* **37,** 1470 (1965).
(6) Pottie, R. F., Lossing, F. P., *J. Am. Chem. Soc.* **83,** 2634 (1961).
(7) Rylander, P. N., Meyerson, S., Grubb, H. M., *J. Am. Chem. Soc.* **79,** 842 (1957).
(8) Schüler, H., Michel, A., *Z. Naturforsch.* **10a,** 495 (1955).
(9) Streitwieser, A., Ward, H. R., *J. Am. Chem. Soc.* **85,** 539 (1963).

RECEIVED June 12, 1967.

25

Chemical Reactions in a Corona Discharge I. Benzene

M. W. RANNEY[1] and WILLIAM F. O'CONNOR

Fordham University, Bronx, N. Y.

Publication Date: June 1, 1969 | doi: 10.1021/ba-1969-0080.ch025

Excitation of benzene vapor in a 15 kv. corona discharge reactor at atmospheric pressure and 45°C. gives an 8.5% conversion to identifiable products. This over-all yield is comparable to that reported for the glow discharge reactions of benzene initiated by radiofrequency and microwave energy sources. Low molecular weight products (up to C_{18}) which have been quantitatively determined in this study include biphenyl, o-, m-, *and* p-*terphenyl, phenylbenzylcycloalkenes, fulvene, 1,3 and 1,4-cyclohexadiene, cyclohexene, and acetylene. Approximately 80% of the product yield is a yellow polymeric material, largely soluble in benzene, with a major fraction having a molecular weight of 4,000. A phenyl and/or benzyl substituted cyclopentene system is indicated as the average repeating unit.*

Corona discharges (silent) have been used to initiate chemical reactions for well over 150 years with much of the early work being confined to inorganic gases (*10*). However, the only commercially significant development over the years has been the process for synthesizing ozone (*17*) by subjecting oxygen to a corona discharge (ozonizer). Most early investigators encountered serious difficulties in studying the interaction of high voltage electricity with organic molecules. Equipment was unreliable and dangerous, and the complexity of the reaction product mass precluded definitive performance evaluation. Since World War II, technology has advanced to the point where high frequency power can be generated and controlled at reasonable cost and many new dielectric materials such as fused quartz, alumina, and mica mat are available (*5*).

[1] Present address: Tarrytown Technical Center, Union Carbide Chemicals and Plastics, Tarrytown, New York.

In Chemical Reactions in Electrical Discharges; Blaustein, B.;
Advances in Chemistry; American Chemical Society: Washington, DC, 1969.

Modern analytical techniques afford the opportunity to determine the composition of the product mix.

Corona electrons are accelerated by the applied voltage to an energy level of 10-20 electron volts, which is sufficient to break the covalent bond. This represents a very efficient approach when compared with high energy radiolysis (Mev. range) where the actual chemical work is effected by secondary electrons with an energy of 10-25 e.v., formed after a series of energy-dissipating steps. Potentially, corona energy can deliver electrons to the reaction site at the desired energy level to give products which are not readily obtainable by more conventional means. The energy available in the corona discharge is somewhat above that commonly encountered in photochemistry (up to 6 e.v.).

In 1876, Bertholot (*2*) reduced benzene to C_6H_8 in what appears to be the first exposure of an aromatic compound to the corona discharge. Losanitsch (*14*) obtained the following products from benzene in an electrical discharge: $(C_6H_6)_2$, biphenyl, $(C_{72}H_{96})$, and $(C_6H_6)_{90}$. Benzene vapor treated at 300°C. in an ozonizer tube gave resinous products with a 6/4 carbon-hydrogen ratio (*7*). Linder and Davis (*13*) exposed benzene vapor to 37,000 volts and found biphenyl, gaseous products, and evidence of polymerization. The early work with benzene reactions in various types of electrical discharges is reviewed in considerable detail by Glocker and Lind (*10*). Brown and Rippere (*4*) investigated the hydrogenation of benzene flowing down the walls of an ozonizer tube and found 1,3- and 1,4-cyclohexadiene, biphenyl, and a resinous mass which gave an infrared spectrum consistent with polystyrene.

In recent years, benzene has been subjected to direct electrode discharge (*20*) and glow discharges induced by microwave (*22, 23*) and radiofrequency (*21*) energy. In this paper, we report some of our observations for the reaction of benzene in a corona discharge.

Publication Date: June 1, 1969 | doi: 10.1021/ba-1969-0080.ch025

Apparatus

The corona reactor system used in this study is shown in Figure 1 and the reactor details are given in Figure 2. The system is designed to run at atmospheric or reduced pressure and, with slight modification, under recycle conditions. The use of the threaded rod center electrode affords a more uniform and higher treating potential than is obtained with a cylindrical electrode (*25*). The electrode threads concentrate surface irregularities thereby eliminating severe discharge points. The copper electrode serves as a cooling coil and affords direct observation of the corona. In a typical run, the benzene reservoir temperature is set at 55°C., the helium is adjusted to 100 ml./min. and after a two minute purge, an electrical potential of 15,000 volts is applied. A brilliant blue corona is established, the intensity being a function of helium flow, pressure, benzene content, and the applied voltage. Benzene traverses the

In Chemical Reactions in Electrical Discharges; Blaustein, B.;
Advances in Chemistry; American Chemical Society: Washington, DC, 1969.

corona reactor as a vapor and is condensed by the cold water trap and collected. Yellow solids gradually deposit in the flask at the bottom of the reactor and eventually adhere to the dielectric surfaces in the reactor. Some benzene and the more volatile reaction products are condensed in the −70° and −195° traps. (*See Experimental* Section for further details.)

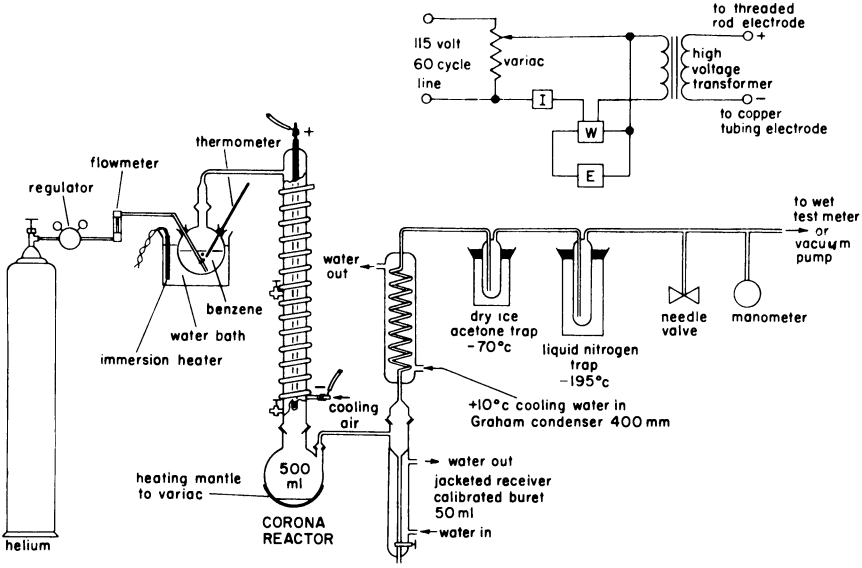

Figure 1. Corona reactor system

Results and Discussion

The excitation of benzene vapor in a corona discharge under the given experimental conditions provides an 8.5% conversion to identifiable products. The major products are a benzene soluble polymer (6%), a benzene insoluble polymer (0.7%), biphenyl (0.3%), and acetylene (1%). The composition of the product mix is given in Table I. The overall yield is similar to that produced in a radiofrequency (*21*) glow discharge (10%, with longer residence time) and somewhat higher than Streitwieser (*22, 23*) obtained using a microwave induced glow discharge (5%). The corona discharge gives a considerably higher proportion of polymer than is obtained from these other energy sources. Benzene substitution products such as toluene, phenylacetylene, and ethylbenzene were observed in the microwave discharge but were not noted in this study or in the radiofrequency investigation. The high yield of fulvene in the radiofrequency discharge is surprising in view of its tendency to polymerize or add oxygen under rather mild conditions. The sum of the carbon and hydrogen analyses for the polymeric fraction obtained by

Publication Date: June 1, 1969 | doi: 10.1021/ba-1969-0080.ch025

Stille (*21*) in the glow discharge of benzene (86–94%) suggests some fixation of oxygen and/or nitrogen during discharge or product work-up. The pressure for these electrodeless glow discharge studies was of the order of 20 mm. or less, while the corona reactor was operated at atmospheric pressure. Schüler (*20*), using a direct electrode discharge in benzene, obtained products similar to those produced in the microwave glow discharge.

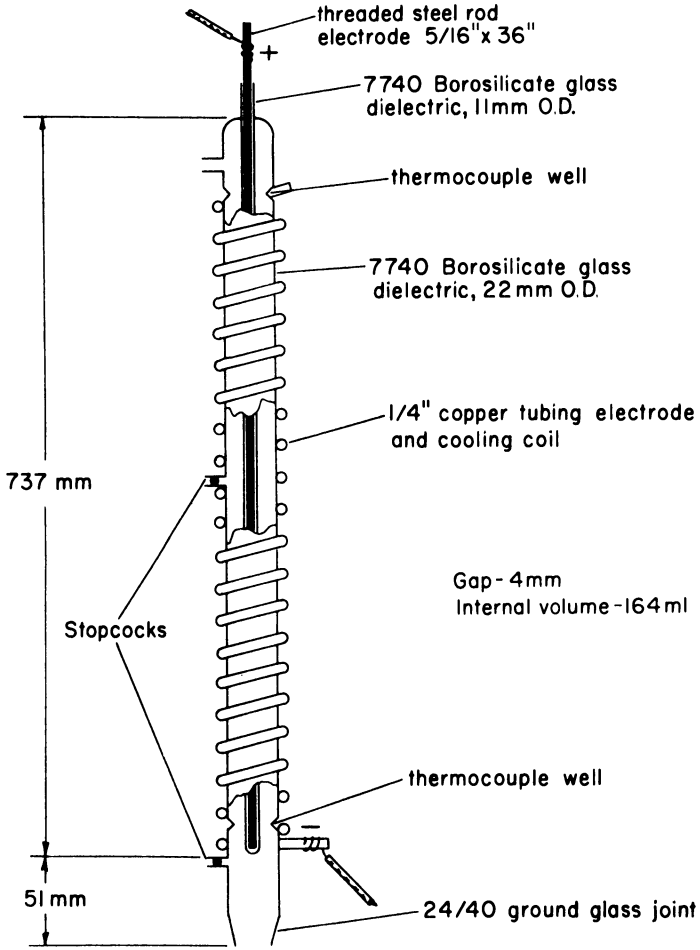

Figure 2. Detail of corona reactor

The reaction products obtained in this study are roughly categorized as the benzene fraction, biphenyl fraction and polymeric material for purposes of discussion. After initial studies indicated that the components of the −70° and −195°C. traps were similar to those in the benzene

Publication Date: June 1, 1969 | doi: 10.1021/ba-1969-0080.ch025

trap, these samples were combined. The acetylene content of the low temperature traps was estimated by weight loss prior to the mixing of these traps with the recovered benzene.

Benzene Fraction. The recovered benzene, as collected in the cold traps, is bright yellow. The following reaction products have been identified in this fraction: 1,3-cyclohexadiene, 1,4-cyclohexadiene, fulvene, and cyclohexene. The approximate percent yield for each of these constituents is given in Table II. The data were determined using a 100 foot support-coated open tubular column with a squalane liquid phase and appropriate calibration standards (Figure 3). No significant change is noted in the cyclohexane content when compared with starting benzene. An increase in the methyl cyclopentane peak may be ascribed to its higher vapor pressure, thus affording some accumulation of this material in the benzene distillate and a concomitant depletion in the benzene feed stock, although some ring contraction cannot be ruled out. Cyclohexene is produced in very low yield, as expected, because of the degree of hydrogenation required during its short residence time in this single pass reactor.

Table I. Product Distribution in the Corona Discharge of Benzene, 15kv.

	Yield-Percent Exposed Benzene	*Yield-Percent of Product Mix*	*Radiofrequency[c] Yield, Percent*
Benzene insoluble polymer	0.7	8.2	N.D.[d]
Benzene soluble polymer[a]	6.0	70.5	5.0[e]
Biphenyl	0.3	3.5	2.0
o-, *m*-, and *p*-Terphenyl	0.1	1.2	N.D.
Phenyl, benzyl substituted cyclopentenes[b]	0.3	3.5	N.D.
1,3- and 1,4-Cyclohexadiene	0.1	1.2	N.D.
Fulvene	0.01	0.1	1.0
Acetylene	1.0	11.8	2.0[f]
TOTAL	8.5	100.0	10.0

[a] Polymer fraction includes materials from 250 molecular weight and up.
[b] Includes several phenyl and benzyl substituted cyclopentenes similar to biphenyl and *o*-terphenyl in vapor pressure. *See Discussion.*
[c] *See* Reference *21*.
[d] N.D.—not determined.
[e] Benzene and toluene soluble polymer.
[f] Acetylene 1%, allene 1%.

The reduction of benzene to the cyclohexadienes is interesting as 1,3-cyclohexadiene is thermodynamically unstable with respect to benzene, cyclohexene, and cyclohexane (*12*). The synthesis of 1,3-cyclohexadiene under these conditions is analogous to the conversion of oxygen to ozone which also represents an eneregtically unfavorable process. The

In Chemical Reactions in Electrical Discharges; Blaustein, B.;
Advances in Chemistry; American Chemical Society: Washington, DC, 1969.

momentary energy input and the rapid removal of the activated species from the reaction zone affords this material in low yield. As expected, the more stable 1,4-cyclohexadiene is produced in higher yield (3/1). Additionally, 1,3-cyclohexadiene would be expected to polymerize at a rapid rate under these conditions. The thermodynamic instability of 1,3-cylohexadiene is demonstrated by its gradual disappearance from the sample after a few days standing at room temperature. The yields of both the 1,4- and 1,3-cyclohexadiene are somewhat higher than previously reported by Brown and Rippere (*4*). The yields reported by these workers after 24 hours exposure to a 15 kv. corona discharge in a counter-current hydrogen stream were 0.02 and 0.01%, respectively. The major variable in technique which likely accounts for this difference in yields is the use of benzene vapor in our work, *vs.* the hydrogenation of a thin liquid benzene film flowing down the annular dielectric surface by Brown and Rippere.

Table II. Product Distribution in Recovered Benzene Fraction[a]

Product	*Yield % Benzene Exposed*
1,3-Cyclohexadiene	0.03
1,4-Cyclohexadiene	0.09
Fulvene	0.01
Cyclohexene	0.01
Unidentified	0.02

[a] Quantitative data obtained by GLC using squalane column and appropriate calibration standards.

The ultraviolet spectrum for the benzene fraction was obtained by running differentially against pure benzene in isooctane. A broad absorption band with a maximum at 258 mμ is ascribed to the 1,3-cyclohexadiene. An additional absorption at 242 mμ and a tailing into the visible region with a broad maximum at 360-370 mμ is also observed. These spectral features are consistent with those reported for fulvene, the non-aromatic isomer of benzene (*24*). Blair and Bryce-Smith (*3*) found fulvene in the photochemical irradiation of benzene in what appears to be the first direct conversion of an aromatic hydrocarbon to a non-aromatic hydrocarbon. In our study, fulvene co-distilled with benzene, but could be separated from benzene using the 100 ft. squalane column (Figure 3). Fulvene prepared by the method of Meuche (*15*) gave the same retention time and spectral features. Additional evidence for assignment of the fulvene peak included its disappearance from the chromatogram after the sample was refluxed with maleic anhydride (color disappears) or exposure to a free radical catalyst. The Diels-Alder reaction product with maleic anhydride was isolated and hydrolyzed to give the adduct, 7-methylene-5-norbornene-2,3-dicarboxylic acid. The melting point and

In Chemical Reactions in Electrical Discharges; Blaustein, B.;
Advances in Chemistry; American Chemical Society: Washington, DC, 1969.

infrared data for this adduct were identical with the sample prepared using fulvene synthesized from cyclopentadiene and formaldehyde (*21*).

The formation of the 1,3,5-hexatrienyl diradical has been suggested as an intermediate in the photochemical decomposition (*9*) and in the radiofrequency discharge (*21*) of benzene. Material isolated in the photochemical excitation gave an ultraviolet spectrum similar to 1,3,5-hexatriene, but displaced by 7.5 mμ and, more disturbing, the investigators were able to separate the material from benzene by fractional distillation. In our work 1,3,5-hexatriene, a possible hydrogenation product of the diradical, could not be detected (less than 100 p.p.m.) in the benzene fraction using the squalane column. No spectral evidence was noted in the ultraviolet although the region of interest is complicated by the presence of 1,3-cyclohexadiene (*27*).

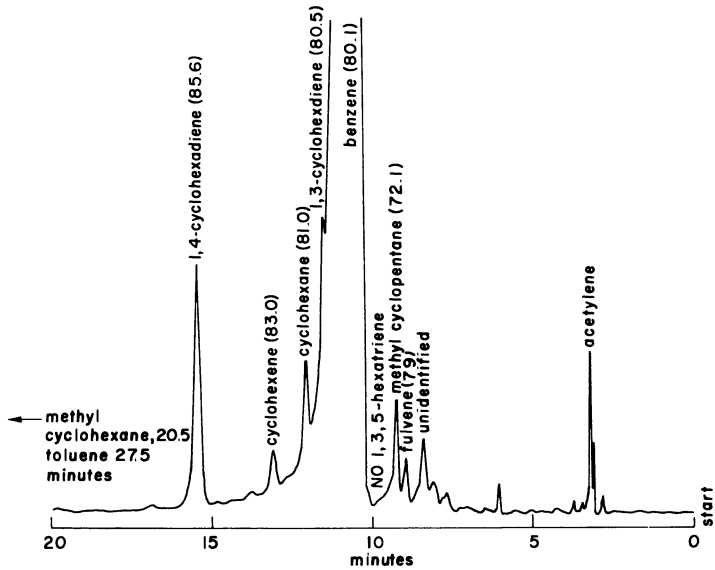

Figure 3. Gas-liquid chromatographic analysis of benzene fraction

Column, 100 ft. × 0.020 inches i.d., support-coated open tubular with squalane liquid phase, temperature 45°C. isothermal

The unidentified peak in the chromatogram (Figure 3) gives a negative test for an acetylenic hydrogen (ammoniacal cuprous chloride solution) and does not disappear after the sample is subjected to free radical catalysis for several hours. Thus, the open chain acetylenic isomers of benzene, hexa-1,3-diene-5-yne, 1,4-hexadiyne, 1,5-hexadiyne, and 1,5-hexadien-3-yne do not appear to account for this peak. The possibility of valence isomers of benzene such as bicyclo (2.2.0) hexa-2, 5-diene,

"Dewar benzene," were considered, but must be generally excluded based on the observation that the peak was stable to prolonged heating at 100°C. The valence isomers would be expected to convert to benzene under such conditions (*26*).

Biphenyl Fraction. The low molecular weight compounds, soluble in isooctane and hot methanol, were primarily biphenyl and *o*-, *m*-, and *p*-terphenyl. These products were identified by gas-liquid chromatography using a silicone gum rubber column (Figure 4) and a Carbowax 20M column with appropriate standards. The components were trapped and analyzed by infrared and NMR spectroscopy for confirmation. Biphenyl was present in sufficient quantity to be readily detected in the initial infrared spectrum and was isolated by sublimation. Quantitative data, obtained using the silicone column with appropriate calibration curves are presented in Table III. With the possible exception of biphenyl, the yields are very low considering the overall conversion noted. The *o*-, *m*-, and *p*-terphenyl ratio (1/0.4/1) indicates a preference for the *para* position beyond that expected for random attack.

Publication Date: June 1, 1969 | doi: 10.1021/ba-1969-0080.ch025

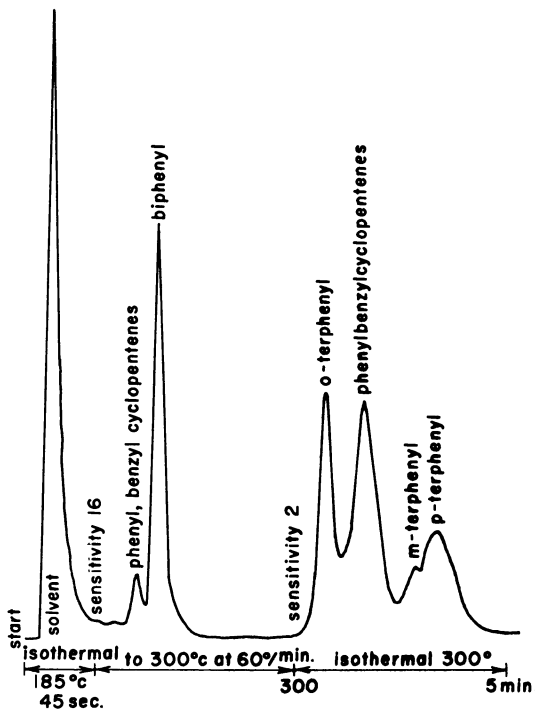

Figure 4. Gas-liquid chromatographic analysis of biphenyl fraction

Silicone gum rubber column

Table III. Biphenyl Fraction[a]

	Yield % Exposed Benzene	*Yield % Reaction Products*
Biphenyl	0.30	3.5
o-Terphenyl	0.05	0.6
m-Terphenyl	0.02	0.2
p-Terphenyl	0.05	0.6
Benzyl and phenyl cyclopentenes (C_{12})	0.05	0.6
Phenylbenzylcyclopentenes (C_{18})	0.25	2.9
TOTAL	0.72	8.4

[a] Quantitative data were obtained by GLC, using a silicone gum rubber column with appropriate standard calibration curves based on peak height.

If hydrogenation of the polyphenyls by hydrogen radicals generated *in situ* is to be considered a primary reaction mechanism, one would expect to see components corresponding to the possible hydrogenated species of biphenyl and the terphenyls. This does not appear to be the case, however, as no significant peak can be ascribed to a hydrogenated *o*-terphenyl compound. The small peaks before biphenyl and after *o*-terphenyl in the chromatogram (Figure 4) actually include four or more components present in small proportions which have not been completely identified. The first peak (eluted before biphenyl), amounting to less than 0.1% of the total yield, was initially ascribed to a mixture of the possible hydrogenation products of biphenyl. On the Carbowax column at lower temperatures, this peak appears between phenylcyclohexane and 1-phenylcyclohexene. Initial infrared examination of this peak after trapping indicated an intriguing similarity with the peak(s) noted after *o*-terphenyl and with the polymer fractions. The possibility that this component was a low molecular weight precursor to polymer formation prompted further study. Infrared indicates a phenyl substituted aliphatic compound containing some olefinic unsaturation, and the spectrum is not consistent with the expected phenylcyclohexenes. Careful examination of the spectrum indicates that the following phenyl substituted compounds are not present on the basis of the indicated missing absorptions—phenylcyclohexane (1010, 1000, 888, 865 $cm.^{-1}$), 1-phenylcyclohexene (922, 805 $cm.^{-1}$), and 3-phenylcyclohexene (855, 788, 675 $cm.^{-1}$) (8). The spectrum is consistent with a non-conjugated benzylcyclopentene system with absorptions at 1070, 1030, and 960 $cm.^{-1}$ and the expected aromatic substitution bands (8). Two additional absorptions are noted, one at 850 $cm.^{-1}$ which may be attributed to vinyl protons and a phenyl substitution band at 730 $cm.^{-1}$. This likely results from biphenyl contamination, but it is interesting to note that benzylidenecyclopentane has an absorption at 732 $cm.^{-1}$ with the remainder of the spectrum being similar to the benzylcyclopentenes.

In Chemical Reactions in Electrical Discharges; Blaustein, B.;
Advances in Chemistry; American Chemical Society: Washington, DC, 1969.

NMR data provides strong evidence for a mixture of compounds containing a ring system (non-olefinic protons poorly resolved 1-3 p.p.m.), non-conjugated olefinic protons at 5.7 p.p.m. and phenyl protons at 7.1 p.p.m. The olefinic protons are complex, giving a closely-spaced doublet superimposed on a broad absorption, suggesting the presence of both ring and exocyclic unsaturation. Additional sharp proton resonances are noted at 1.2 p.p.m. (methyl) and a doublet at 2.7 p.p.m. which is attributed to benzylic protons. The lack of olefinic protons downfield from 5.7 p.p.m. would rule out the benzylidene compounds and likely any similar structures wherein the unsaturation is conjugated with the phenyl moiety. The olefinic protons in cyclopentadiene are found at 6.42 p.p.m. and were not obvious in this fraction. However, absorptions owing to a minor component could have escaped detection because of limited sample size. The difficulty encountered in isolating the components of this peak precludes definite structural assignments, but a mixture of phenyl and benzyl substituted cyclopentenes is clearly indicated. This following reaction products are consistent with the experimental observations:

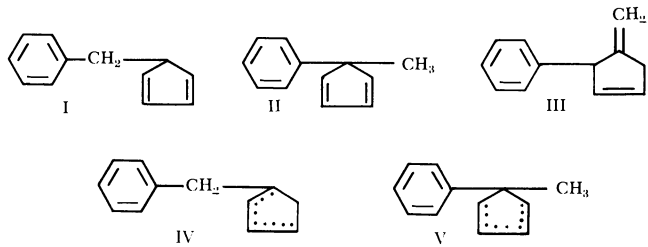

(1)

The inherent complexity of the product mix is illustrated by IV above which could be 1-, 2-, and 4-benzylcyclopentene. NMR data indicate that the average structure contains a single double bond as presented in IV and V. Mass spectral data for this sample, as isolated from the chromatographic separation, indicate *m/e* values of 156 and 158, corresponding to the cyclopentadienes I, II and the cyclopentenes IV, V. Ring substituted compounds such as III would also have a mass of 156. Mass 91, corresponding to the benzyl radical is prominent as is mass 77, the phenyl radical, although this would be expected to arise from the biphenyl contamination. The low yield is reasonable in view of the limited probability for radical termination and hydrogenation compared with the high reactivity of these olefins (or the diene precursors) under the reaction conditions. The glow discharge work of Schüler (*20*) indicates the absence of any products with vapor pressure similar to biphenyl and the other related literature generally does not give details beyond biphenyl analysis and gross polymer properties.

The peak after *o*-terphenyl (Figure 4) actually consists of 3-4 components when analyzed by varying the chromatographic conditions. This

Publication Date: June 1, 1969 | doi: 10.1021/ba-1969-0080.ch025

peak has the same retention time as diphenyl fulvene and is in the same general range as noted for a commercially available hydrogenated terphenyl, Monsanto HB-40. This complex peak was trapped (with trace *o*-terphenyl contamination) as a yellow liquid which gave an infrared spectrum identical to the polymer fractions and very similar to the peak before biphenyl. Again, phenylbenzylcyclopentenes are indicated and the spectrum bears little resemblance to the hydrogenated terphenyl spectrum. The NMR spectrum in carbon tetrachloride showed aromatic protons at 7.1 p.p.m., a broadened olefinic proton resonance at 5.7 p.p.m. and non-olefinic resonances are typical of protons in a fixed ring system such as cyclopentene. The integration for these resonances allow approximation of an average structure containing a cyclopentene ring system substituted with one phenyl and one benzyl group. The reactions appear analogous to those responsible for the components of the peak before biphenyl with termination being with a phenyl radical rather than the hydrogen radical. The mass spectrum for this material as trapped from the chromatographic analysis shows prominent peaks at mass values of 232 and 234 corresponding to VI and VII below. The benzyl and phenyl radical peaks are also evident at mass values of 91 and 77 respectively.

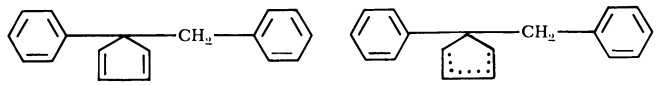

(2)

VI VII

The actual structural definition must await isolation of sufficient quantities of the components for spectroscopic studies under various conditions. The possibility of a hydrogenated *p*-terphenyl was carefully considered, but the only structure even remotely consistent with the infrared and NMR data would require that the center ring of *p*-terphenyl be non-aromatic with mono-substituted phenyl groups attached as in IX. Such a material could be formed by preferential hydrogenation of the center ring of *p*-terphenyl (statistically unlikely) or by the reaction of phenyl radicals and 1,3-cyclohexadiene as follows:

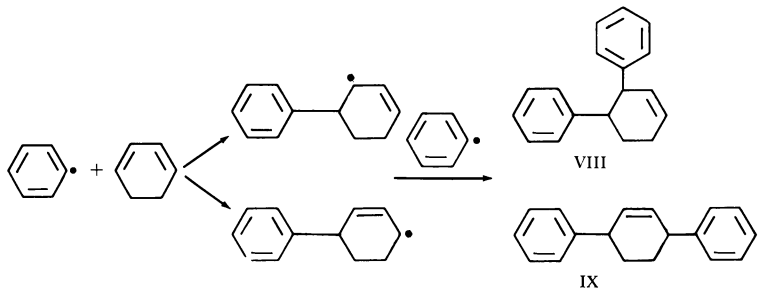

(3)

Publication Date: June 1, 1969 | doi: 10.1021/ba-1969-0080.ch025

In Chemical Reactions in Electrical Discharges; Blaustein, B.;
Advances in Chemistry; American Chemical Society: Washington, DC, 1969.

This mechanism requires the formation of hydrogenated *ortho*-terphenyl derivatives such as VIII, which were not noted by gas-liquid chromatography or infrared.

Polymeric Products. The material which adheres to the glass dielectric surface in the reactor is a high melting solid (>320°C.), insoluble in benzene and all common solvents. The infrared spectrum and the carbon-hydrogen ratio are essentially the same as noted for the benzene soluble material. The benzene soluble polymer was fractionated into three molecular weight ranges based on solubility in isooctane. The polymers are all yellow with the intensity increasing as the molecular weight decreases. The ultraviolet spectrum for the low molecular weight polymer shows a gradual tailing into the visible region. The analytical data for the polymeric fractions are summarized in Table IV.

Publication Date: June 1, 1969 | doi: 10.1021/ba-1969-0080.ch025

Infrared data indicate that the polymeric fractions are structurally similar to the low molecular weight products identified as benzyl and phenyl substituted cyclopentenes. The infrared evidence already presented for the low molecular weight products is applicable to the polymeric products and need not be repeated. The data are consistent with an average repeating unit containing the cyclopentene ring structure substituted with phenyl or benzyl groups. NMR data for the polymers were obtained in carbon tetrachloride at the cell holder temperature (40°C.). The spectrum obtained for the 300 molecular weight polymer fraction is presented in Figure 5. The extreme broadening of the proton resonances is associated with the complex, long range proton coupling in a rigid system and the motional averaging commonly noted in polymers (*19*). Scanning the same sample at 90°C. in tetrachloroethylene did not significantly improve the resolution. The NMR spectrum of the polymer in pyridine (Figure 5) gives some improvement in the high field proton resolution, indicating a doublet at 2.6 p.p.m. (benzylic protons) and a complex methyl proton resonance. The spectra are similar to those obtained for the low molecular weight precursors containing unresolved ring protons. The NMR spectra generally eliminate polymer formation by the way of phenyl and hexatrienyl radicals as suggested for the radiolysis of benzene (*18*). The aliphatic proton portion of the spectrum is very similar to that reported for cyclopentadiene polymers by Davies and Wasermann (*6*). The cyclopentadiene polymers had a molecular weight range of 1200–2300, a λ max. at 320-360 mμ and non-olefinic proton to olefinic proton ratio of approximately 3/1.

The data are consistent with polymer formation by way of phenyl radical reaction with benzene or the fulvene produced to give cyclic radical intermediates which then polymerize to yield a polycyclopentene chain with pendant phenyl and/or benzyl groups. The average non-olefinic to olefinic proton ratio of 2.9 indicates that the many possible

Table IV. Properties of Polymers Produced in Corona Discharge of Benzene

		% C	% H	C/H	M. W.[a]	Infrared cm.$^{-1}$	Protons[b] Aromatic	Olefinic	Non-olefinic
Benzene insol.		86.95	7.17	1.01	—	755,695	—	—	—
Benzene sol.	1	88.32	7.18	1.02	4360	755,695	5	2	5.8
	2	87.26	7.09	1.03	1555	755,695	5	2	5.7
	3	87.23	7.09	1.03	305	755,695	5	2	5.7

[a] Vapor pressure osmometry in benzene solution.
[b] Aromatic proton resonance assigned five protons.

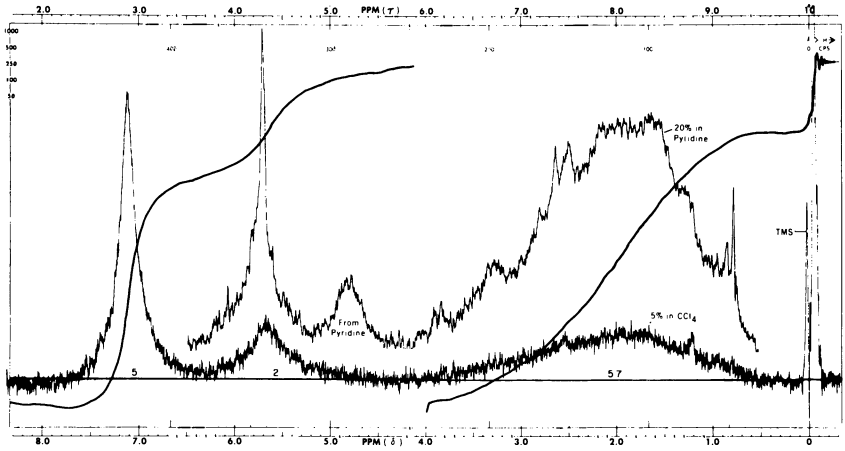

Figure 5. 60MC NMR spectrum for benzene soluble, low molecular weight polymer. Integral applies to CCl_4 sample

structures similar to X (5/2) predominate over the alternate type structures, XI (7/0), assuming our analogy to cyclopentadiene type polymers is valid (*6*).

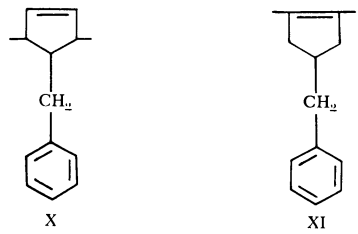

X XI (4)

Many similar structures must be considered, including those derived from phenyl attack on the ring with polymerization through the exocyclic vinyl group of fulvene. NMR evidence does not support any structures wherein the unsaturation is conjugated with the phenyl group. Mass spectral analysis of the 1500 molecular weight fraction indicates the benzyl and phenyl moieties as the predominate fragmentation products.

Mechanism. The available evidence is thus not consistent with the generally proposed mechanism of polymer formation based on the random build-up of a poly(phenylene) chain accompanied by hydrogenation (*4*) or the interaction with the hexatrienyl diradical (*18*). In the radio-frequency discharge of benzene (*21*), evidence was presented which indicated that the polymer contained consecutive para linkages suggesting poly(*p*-phenylenes). Schüler (*20*) observed that the polymer (C/H 1.03, M.W. 503) was a phenyl substituted aliphatic chain based on infrared evidence. Patrick and Burton have demonstrated that hydrogen atoms are not involved to any significant extent in polymer formation when liquid benzene is irradiated with a 1.5 Mev. source (*18*).

In the corona discharge many types of energy transfer are occurring, varying from photolysis (visible corona) to relatively high energy electrons responsible for fragmentation. The low yield of biphenyl in this single pass reactor suggests that phenyl radical production through loss of a hydrogen radical may not be the primary reaction route leading to polymer formation. Considerable energy should be available to excite benzene to relatively high vibrational levels which would be somewhat below that energy required actually to separate the H radical. At any given time the number of these excited benzene molecules should greatly exceed the phenyl radical population. Fulvene (*1*) is produced from benzene by ultraviolet energy (200 mμ, about 112 kcal., or 4.9 e.v.). Thus, the formation of this benzene isomer with a resonance energy (11-12 kcal./mole) intermediate between benzene and 1,3-cyclohexadiene may be energetically favorable in the corona environment. Fulvene has been shown to polymerize rapidly under similar conditions with no reversion to benzene (*1*).

The uniformity of the phenyl(benzyl)-cyclopentene ratio throughout all polymer fractions makes it difficult to accept a mechanism based solely on random attack by phenyl radicals on a growing fulvene polymer. The initial synthesis of a monomeric unit comprised of the benzylcyclopentadienyl system with subsequent diene type polymerization is consistent with all our observations. The phenyl radical produced in the discharge should collide with the nearest benzene molecule which will be excited to a relatively high vibrational energy level. The following reaction sequences are suggested for the phenyl radical:

Publication Date: June 1, 1969 | doi: 10.1021/ba-1969-0080.ch025

In Chemical Reactions in Electrical Discharges; Blaustein, B.;
Advances in Chemistry; American Chemical Society: Washington, DC, 1969.

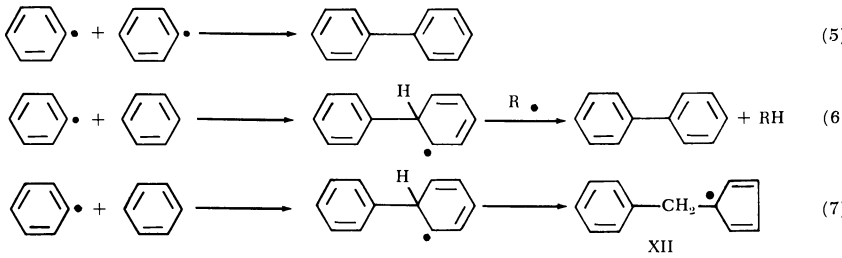

(5)

(6)

(7)

Reaction 5 is the typical termination by radical coupling leading to biphenyl. The intermediate radical in reaction 6 would normally be expected to lose hydrogen more readily than it would add to another benzene molecule to give polymer formation (*16*). The possibility of ring contraction in the excited intermediate, accompanied by an intramolecular shift of a hydrogen atom is suggested in Reaction 7. The benzylcyclopentadienyl radical intermediate XII so obtained would be a very active monomer leading to the polymeric products observed. Although our data support polymer formation by the mechanism indicated, we cannot rule out some participation by the cyclohexadienes and acetylene, both of these being noted in the benzene fraction and the low temperature traps.

The relatively low yield and the complexity of the reaction products does not allow an unequivocal designation of reaction mechanism or of the mode of energy transfer in the corona environment. However, where possible, we have proposed reaction mechanisms which are consistent with our results to date. These mechanisms are summarized in Figure 6. Studies are underway to obtain deuterium exchange data in the corona reactor, and mass spectral data are being evaluated. Investigation of the utility of corona chemistry will be extended to other volatile compounds.

Experimental

Materials. Fisher thiophene-free benzene contained trace quantities of methylcyclopentane, cyclohexane, and toluene. Chromatogram (squalane) of original material was used as reference for irradiated benzene evaluation under the same GLC conditions.

Reference materials for chromatographic identification were generally used as obtained from commercial sources. Most of these materials were of sufficient purity to identify the major peak. However, monophenylfulvene, obtained from Aldrich, gave no peak on the silicone column and infrared indicated extensive hydroxyl and carbonyl absorptions. 1,3,5-hexatriene from Aldrich gave two major and two minor peaks on the squalane column. Infrared (*11*) indicated largely the trans-isomer with only a small cis absorption at 818 $cm.^{-1}$.

Fulvene was prepared by the method of Meuche (*15*). Infrared (1662, 925, 890, 765 $cm.^{-1}$) and ultraviolet ($\lambda_1 = 242$ mμ, $\lambda_2 = 360$ mμ) were in good agreement with literature values (*24*).

In Chemical Reactions in Electrical Discharges; Blaustein, B.;
Advances in Chemistry; American Chemical Society: Washington, DC, 1969.

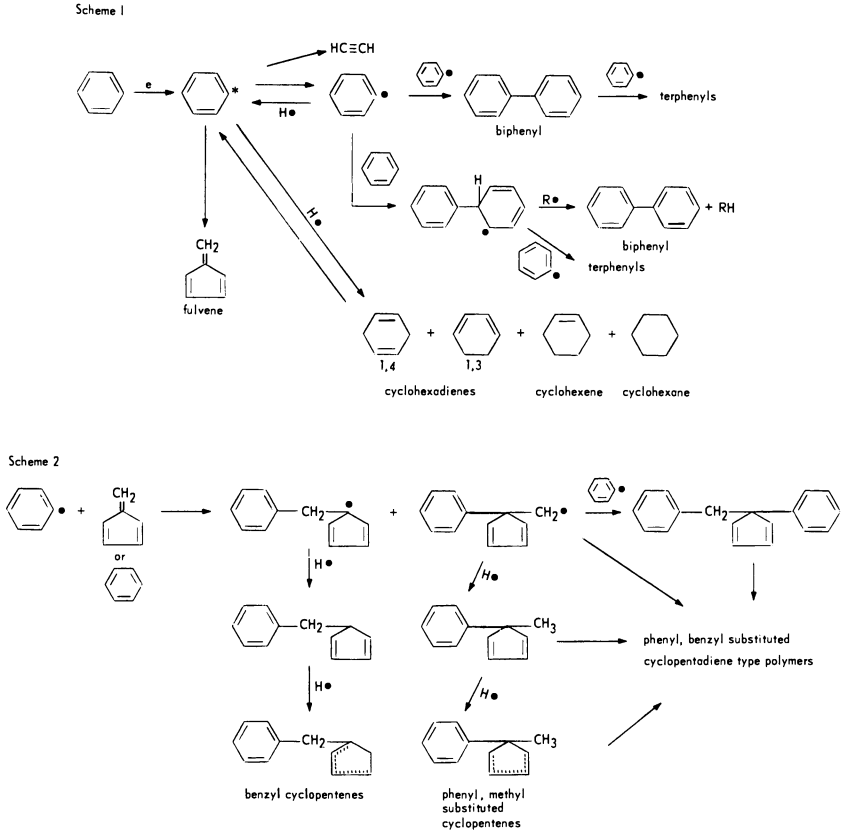

Figure 6. Proposed reaction mechanisms

Reaction Conditions. The equipment used in these experiments was presented in Figures 1 and 2. Helium was bubbled through the benzene reservoir (55°C.) at 100 ml./min. to carry 4.2 grams (0.054 moles) benzene through the corona reactor per hour. The reactor temperature was 45° ± 2°C. A total of 101 grams (1.3 moles) benzene was passed through the 15 kv., 60 cycle, corona discharge in 23.7 hours. A small helium purge was maintained throughout all sampling operations and necessary downtime to limit oxidation.

Product Isolation and Analysis. At the conclusion of the run, the reactor was partially filled with benzene and refluxed on a steam bath for two hours. The benzene soluble material from the column was combined with the yellow brown solid which collected in the lower receiver. The insoluble material was swelled by benzene and generally loosened from the glass dielectric surface. This insoluble material was filtered off, washed several times with chloroform and dried overnight at 70°C. in a vacuum oven. The reactor was cleaned with a 5% hydrofluoric acid solution to remove final traces of polymer after each run. Benzene insoluble polymer—0.7 gram yellow brown color, % C 86.95, %H 7.17, C/H 1.01.

Publication Date: June 1, 1969 | doi: 10.1021/ba-1969-0080.ch025

The benzene containing all solid products from the reactor and pot residue was reduced to 30 ml. volume by vacuum distillation at 50°C. Considerable foaming was encountered, requiring careful control of the distillation. The 30 ml. of brown benzene solution was added to 300 ml. isooctane at room temperature. A yellow solid precipitated immediately and was collected by filtration. After several washings with hot methanol, the material was dried for eight hours at 70°C. in a vacuum oven. Benzene soluble polymer–Fraction 1, 2.3 grams, M.W. 4360, % C 88.32, % H 7.18, C/H 1.02.

The isooctane-methanol solution was reduced to 100 ml. volume (all methanol removed) by vacuum distillation at 60°C. The solution was a brilliant yellow color at this point. On cooling to room temperature, a small proportion of a deep yellow polymeric solid precipitated and was collected by filtration. After washing with hot methanol, this yellow material was dried at 70°C. for eight hours in a vacuum oven. Benzene soluble fraction 2, 0.2 grams, M.W. 1555, % C 87.26, % H 7.09, C/H 1.03.

The isooctane-methanol soluble portion was reduced to 20 grams by vacuum distillation and sufficient benzene added to insure solubility of all components. The percent solids was determined for this sample, being careful to limit sublimation of biphenyl (about two hours at 70°C. in a vacuum oven). This sample contains the low molecular weight products and a yellow resinous polymer. Qualitative analysis for the low molecular weight components was accomplished by gas-liquid chromatography using the following liquid phases: silicone gum rubber, Carbowax 20 M, and Reoplex 400. Quantitative data were obtained on the silicone column (Figure 4) using calibration curves (peak height) prepared from appropriate standards. The concentration of the small peak eluted before biphenyl was estimated using the biphenyl calibration curve and the peak after *o*-terphenyl was estimated using a commercial hydrogenated terphenyl mixture (Monsanto HB-40) as a reference. The F & M Model 500 gas-liquid chromatograph equipped with a standard thermoconductivity detector was used for these analyses. These low molecular weight products (biphenyl, *o*-, *m*-, *p*-terphenyl, and phenylcycloalkenes, M.W. up to ~250) amount to 0.72 grams. (*See* Table III). Peak confirmation was provided by infrared and NMR analysis after fraction collection from the chromatographic separation.

The concentration of the low molecular weight resinous polymer was determined by subtracting the total biphenyl fraction weight from the total isooctane-methanol soluble material. A sample of this material was placed in the vacuum oven at 100°C. until the GLC trace indicated negligible biphenyl content and the molecular weight was determined. Benzene soluble fraction 3, 3.5 grams, M.W. 305, % C 87.23, % H 7.09, C/H 1.03. Prolonged heating at 150°C. in air gives a hard, brittle yellow film. Infrared analysis indicates oxidation is involved in the drying process.

The benzene fraction was initially examined by GLC using 100 ft. support coated open tubular columns containing Carbowax 1540 poly(ethylene glycol) and squalane (Figure 3) as the liquid phases. Quantitative data were obtained at 45°C. on the squalane column with a helium flow of 3.0 ml./min. The Perkin Elmer Model 880 gas-liquid chromatograph, equipped with a stream splitting device and hydrogen flame

Publication Date: June 1, 1969 | doi: 10.1021/ba-1969-0080.ch025

detector was used for these analyses. Peak identification was by comparison with commercial standards and the synthesized fulvene. Additionally, the benzene fraction was refluxed in pressure bottles with maleic anhydride, azobisisobutyronitrile, and ammoniacal cuprous chloride solution prior to chromatographic analysis to note peak changes owing to adduct formation, polymerization, or presence of acetylenic hydrogen. Acetylene content was estimated from weight loss of the −70° and −195°C. traps. The vapor space above those cold traps and the gas stream directly below the corona were analyzed by infrared using an 8 cm. gas cell. Although the study was not exhaustive, several samplings were made and only acetylene was detected. Methylacetylene, allene, and butadiene were not present in sufficient quantity to be detected.

The yellow benzene from several runs (100 ml.) was fractionated and 900 ml. distillate obtained from 79°-80°C. The distillate was refluxed with maleic anhydride until colorless and the benzene removed at reduced pressure. Dilute sodium hydroxide solution was added and the resulting solution was extracted several times with chloroform. After acidification with dilute hydrochloric acid, the solution was extracted with ether. The ether was removed leaving a white solid which, on recrystallization from chloroform and petroleum ether (38°-60°C.), gave the adduct 7-methylene-5-norbornene-2, 3-dicarboxylic acid melting at 146°-150°C. The infrared showed maxima at 1553, 875 and 710 $cm.^{-1}$ (*21*) 1555, 874, 712 $cm.^{-1}$). Fulvene was prepared in low yield (less than 1%) from cyclopentadiene and formaldehyde with sodium ethoxide catalyst (*15*). The adduct was prepared by adding maleic anhydride to the crude fulvene reaction product in Freon 113 (b.p. 47.6°C.) and refluxing until colorless. After removal of the solvent, hydrolysis and recrystallization yielded the adduct, m.p. 147°-150°C., which gave properties identical with the fulvene adduct obtained from the corona discharge. Bryce-Smith obtained a melting range of 105°-110°C. for this adduct which was likely a mixture of the exo and endo isomers (*1*). Stille prepared the fulvene-maleic anhydride adduct with a melting point of 149°-150°C. which may be a single isomer (*21*).

Through the courtesy of the Perkin Elmer Company at Norwalk, Connecticut, the discharged benzene was analyzed by combination of gas-liquid chromatography and mass spectroscopy. The peak attributed to fulvene gave a parent mass of 78 and fragments at *m/e* 77, 52, 51, 50, and 39 in good agreement with literature (*15*). Confirmation of other assignments was obtained by this technique and the one unidentified component on the squalane column gave a parent mass of 78.

Molecular weight and carbon-hydrogen determinations were made by Schwarzkopf Microanalytical Laboratories, New York, New York. Molecular weight was determined in benzene by vapor pressure osmometry.

Literature Cited

(1) Angus, H. J. F., Blair, J. M., Bryce-Smith, D., *J. Chem. Soc.* **1960,** 2003.
(2) Bertholot, M., *Compt. rend.* **82,** 1357 (1876).
(3) Blair, J. M., Bryce-Smith, D., *Proc. Chem. Soc.* **1957,** 1287.

Publication Date: June 1, 1969 | doi: 10.1021/ba-1969-0080.ch025

(4) Brown, G. P., Rippere, R. E., *Am. Chem. Soc., Div. Petrol. Chem., Preprints 2*, **No. 3**, 149-154 (1957).
(5) Coffman, J. A., Browne, W. A., *Sci. Am.* **89**, June (1965).
(6) Davies, A. G., Wassermann, A., *J. Polymer Sci.* 4, 1887 (1966).
(7) Davis, A. P., *J. Phys. Chem.* **35**, 3330 (1931).
(8) Eliel, E. L., McCoy, J. W., Price, C. C., *J. Org. Chem.* **22**, 1533 (1958).
(9) Gibson, G. E., Blake, N., Kalm, M., *J. Chem. Phys.* **21**, 1000 (1953).
(10) Glockler, G., Lind, S. C., "The Electrochemistry of Gases and Other Dielectrics," John Wiley and Sons, New York, 1939.
(11) Hwa, J. C. H., de Bonneville, P. L., Sims, H. J., *J. Am. Chem. Soc.* **82**, 2538 (1960).
(12) Janz, G. J., *J. Chem. Phys.* **22**, 751 (1954).
(13) Karapetoff, V., Trebler, W. H., Linder, E. G., Davis, A. P., *Research Reports, Detroit Edison Company*, Cornell Univ. (1928-32).
(14) Losanitsch, S. M., *Bull. soc. stün. Bucharest* **1914**, 233.
(15) Meuche, D., Neuenschwander, N., Schaltegger, H., Schlunegger, H. V., *Helv. Chim. Acta* **47**, 1211 (1964).
(16) Mortimer, G. A., Arnold, L. C., *J. Am. Chem. Soc.* **84**, 4986 (1962).
(17) "Ozone Chemistry and Technology," ADVAN. CHEM. SER. **21** (1959).
(18) Patrick, W. N., Burton, M., *J. Am. Chem. Soc.* **76**, 2626 (1954).
(19) Powles, J. G., *Polymer* **1**, 219 (1960).
(20) Schüler, H., Prchal, K., Kloppenburg, E., *Z. Naturforsch.* **15a**, 308 (1960).
(21) Stille, J. K., Sung, R. L., Vander Kooi, J., *J. Org. Chem.* **30**, 3116 (1965).
(22) Streitwieser, Jr., A., Ward, H. R., *J. Am. Chem. Soc.* **84**, 1065 (1962).
(23) *Ibid.*, **85**, 539 (1963).
(24) Thiec, J., Wiemann, J., *Bull. Soc. chim., France* **1956**, 177.
(25) U. S. I. Chemicals, Polyolefin News, Feb. (1964).
(26) Van Tamelen, E. E., Pappas, S. P., *J. Am. Chem. Soc.* **85**, 3297 (1963).
(27) Woods, G. F., Schwartzman, L. H., *J. Am. Chem. Soc.* **70**, 3394 (1948).

RECEIVED May 29, 1967.

26

Vapor Phase Decomposition of Aromatic Hydrocarbons by Electric Discharge

MASAYUKI KAWAHATA

Research and Development Center, General Electric Company, Schenectady, N. Y.

Publication Date: June 1, 1969 | doi: 10.1021/ba-1969-0080.ch026

Vapor phase decomposition of aromatic and hydroaromatic hydrocarbons by electric discharge in hydrogen was investigated in electric discharge sustained in a narrow gap between two dielectric barriers. Alternating current, 10,000 hertz, was used as a power source. Hydrogen containing a certain concentration of the organic vapor was preheated and fed into the discharge zone. The reactor temperature was maintained at about 300°C. and the reactor pressure was varied from 70 to 760 mm. Hg. Condensable decomposition products were analyzed by use of mass spectroscopy and vapor phase chromatography.

Decomposition of organic compounds in an electric discharge generally involves fragmentation and polymerization induced by inelastic collision with high energy electrons. When hydrogen is added, active hydrogen atoms produced by electric discharge also participate in the decomposition reactions. The reaction mechanisms are complex involving excited molecules, free radicals, and ions.

In this laboratory hydrocracking of coal, coal volatiles, and related materials by electric discharge in hydrogen was studied. It is postulated by Given (*1*) that coal (vitrinite) molecules contain aromatic and hydroaromatic structures and probably fused aromatic ring nuclei linked together by methylene or ethylene groups forming hydroaromatic rings. Many of the replaceable hydrogens in the structure are substituted by hydroxyl or carbonyl groups. Short alkyl groups and alicyclic rings may also be attached as side chains. In pyrolysis at 500°–600°C., dissociation of hydroxyl groups and dehydrogenation of naphthenic rings take place. These acts lead to formation of OH and H radicals which in turn help to break the linkages between aromatic nuclei, forming smaller, partly

In Chemical Reactions in Electrical Discharges; Blaustein, B.;
Advances in Chemistry; American Chemical Society: Washington, DC, 1969.

aromatic volatile fragments, and at the same time leaving a more aromatic residual structure behind.

On the other hand, high pressure hydrogenation of coal gives partial or complete hydrogenation of the aromatic structure. When this is subsequently cracked, the light products tend to be aliphatic rather than aromatic hydrocarbons. It was thought that hydrocracking of coal by electric discharge might be somewhere between pyrolysis and high pressure hydrocracking. In the course of study this hypothesis was tested by subjecting several aromatic or hydroaromatic compounds to electric discharge in a hydrogen stream for better understanding of the process. Organic compounds selected were *m*-cresol, α-methylnaphthalene, tetrahydronaphthalene, decahydronaphthalene, and 9, 10-dihydrophenanthrene.

Publication Date: June 1, 1969 | doi: 10.1021/ba-1969-0080.ch026

Experimental Apparatus and Procedures

The apparatus consisted of a vaporizer, a preheater, a discharge reactor, and a product collecting system. The organic compounds and hydrogen were fed into the vaporizer at a certain rate and the resultant mixture was then introduced into the reactor through the preheater. The liquid products which condensed in a water cooler were collected in a receiver and the gaseous products were collected in a liquid nitrogen trap. All the condensable products were analyzed by mass spectroscope and vapor phase chromatograph employing a 6 ft. column of 10% silicone rubber, SE-30 on 60-80 Chromosorb P.

The discharge reactor was fabricated with quartz and was of a concentric tube design similar to an ozonizer. The inside of the inner barrier (40 mm. o.d. and 38 mm. i.d.) and the outside of the outer barrier (48 mm. o.d. and 46 mm. i.d.) were coated with conductive tin oxide. The former was connected to the high voltage terminal and the latter to ground. In this arrangement the electric discharge was sustained in an annular space, 46 mm. o.d., 40 mm. i.d., and 200 mm. long. The inside barrier tube was filled with stainless steel wool and a thermometer was placed in the center. Three thermistors were attached to the outside electrode: one located at the middle height of the electrode and the other two located at two ends of the electrode height. The reactor was insulated with glass wool and the reactor temperature indicated by the thermometer and the thermistors was 300° $\pm$ 10°C. for all the runs.

The electric discharge power was supplied by feeding the output of a 10,000 hertz, 30 kilowatt inductor-alternator to the primary of a 50 kilovolt transformer and, in turn, to a tuned circuit, to the reactor and to the high voltage instrumentation. The electric discharge power was determined by measuring the area of parallelogram on the oscilloscope (*3*).

When making the run, hydrogen was fed into the reactor at a definite flow rate and the electric discharge was applied to heat the reactor. When the reactor temperature was stabilized at 300°C., the feed of the organic compound was started. The discharge power sustained for the reaction was in a range from 140 to 170 watts.

In Chemical Reactions in Electrical Discharges; Blaustein, B.;
Advances in Chemistry; American Chemical Society: Washington, DC, 1969.

Experimental Results and Discussions

For cresol-hydrogen mixtures, two runs were made using the empty reactor and three runs were made by filling the reactor space with porous or activated aluminum oxide grains. For all the runs, the reactor pressure maintained at 300 mm. Hg. Experimental results, including product distribution, are listed in Table I. The principle products were phenol, toluene, benzene, aliphatic hydrocarbons, carbon dioxide, and water. Among the aliphatic hydrocarbons acetylene was present in the largest amount and the concentration of unsaturates was about 80%, except for Run 4. In this run the concentration of unsaturates was 55%. This is probably because of a higher hydrogen concentration in the feed causing somewhat more efficient hydrogenation. The bond energies of C_6H_5–CH_3 and C_6H_5–OH are 90 and 73 kcal./mole, respectively. Despite this, it was observed that, in the products, phenol was in higher concentration than toluene.

Table I. Decomposition of *m*-cresol by the Electric Discharge in Hydrogen

			Organic Products Distributions, gram/kwh.					
	m-*cresol*		*Aromatic H/C*				*Energy Yield*	*Unsaturates in*
Exp. No.	*Conc. Vol. %*	*Reactor Packing*	C_6	C_7	*Aliphatic H/C*	*Phenol*	*gram/kwh.*	*Aliphatic %*
1	88.8	No	0.8	2.7	1.4	4.3	9.2	78
2	65.5	No	0.5	2.3	1.0	3.2	7.0	85
3	93.0	Porous Alumina	1.0	4.1	2.2	4.4	11.7	82
4	35.5	Porous Alumina	0.8	2.1	1.5	3.1	7.5	55
5	67.5	Activated Alumina	0.2	0.9	1.4	6.8	9.3	80

Use of aluminum oxide packing in the discharge space was intended to investigate the possibility of increasing the energy yield. Narrowing the gaseous discharge gap with dielectric packings may cause the following two effects on the discharge: (1) increase of discharge current for the same discharge power dissipated, and (2) increase of gaseous space breakdown field strength, if the gap decreases beyond a certain limit. The exact nature of the electric discharge employed in this study is still debatable (2, 5). However, it can be reasonably assumed that the primary reaction rate of the organic vapor with either high energy electrons or active hydrogen atoms may be dependent on discharge current density and field strength, if the system pressure and partial pressure of the

In Chemical Reactions in Electrical Discharges; Blaustein, B.;
Advances in Chemistry; American Chemical Society: Washington, DC, 1969.

reactant are constant. In the ozone production by electric discharge an increase in ozone concentration after filling the discharge gap with packings of various dielectric is reported by Morinaga and Suzuki (*4*). In this study for approximately the same concentration of cresol vapor, the use of aluminum oxide grains in the discharge space appeared to increase the energy yield somewhat, but the results were not conclusive.

In all the runs, the formation of brown solid films was observed on the reactor wall or on the surface of the grains. These solid films were not analyzed but they were insoluble in methyl ethyl ketone or toluene. It is presumed that these films are probably highly cross-linked polymerized products derived from the cresol. The energy yield for film formation was estimated to be in a range from 30 to 50 gram/kwh.; considerably higher than that for the fragmentation products.

Experimental results for the polycyclic compounds are summarized in Table II. Methylnaphthalene vapor in hydrogen was tested under pressures of 760 and 74 mm. Hg. The principal lighter products were aliphatic hydrocarbons, benzene and toluene. At the higher pressure the concentration of the lighter aliphatic hydrocarbons was in the order $C_2 > C_3 > C_4 > C_5$. At the lower pressure, however, this order was reversed. In both cases about 32–35% were unsaturates. The energy yield was approximately doubled by lowering the pressure.

For tetrahydronaphthalene, three experiments were made under different pressures. Among the lighter aliphatic hydrocarbons produced, the C_2 fraction was present in the largest amount, in which ethylene was in highest concentration followed by acetylene and ethane. The total percentage of unsaturates increased as the pressure decreased. This increase was essentially caused by the increase in C_2 and C_3 unsaturates. As observed for methylnaphthalene, the energy yield at 70 mm. Hg was twice as high as that at 760 mm. Hg. A considerably higher energy yield than for the other two runs was observed at the intermediate pressure, 300 mm. Hg.

When decahydronaphthalene was tested, one experiment was made under 760 mm. Hg using 6.7% concentration in hydrogen. Another run was made under 300 mm. Hg using 67% concentration. In the latter run, a higher energy yield and the product distribution richer in the C_2 and C_3 fraction and higher in unsaturate concentration were observed.

One experiment was made to test dihydrophenanthrene in hydrogen. The gaseous products were essentially in the C_2 fraction; about 50% being unsaturated. Vapor phase chromatography of the liquid product showed two peaks. They were not identified but by the combined results of the VPC and mass spectroscope one of the peaks was tentatively identified as butylbenzene. Biphenyl, which is a likely decomposition product, was not found.

Publication Date: June 1, 1969 | doi: 10.1021/ba-1969-0080.ch026

In Chemical Reactions in Electrical Discharges; Blaustein, B.;
Advances in Chemistry; American Chemical Society: Washington, DC, 1969.

Table II. Decomposition of Aromatic Compounds

Exp. No.	*Organic Vapor*	*Vapor Conc. Vol. %*	*Pressure mmHg*	*Energy Yield gram/kwh.*
6	α-methylnaphthalene	4.5	760	0.66
7	α-methylnaphthalene	5.8	74	1.2
8	tetrahydronaphthalene	5.8	760	1.5
9	tetrahydronaphthalene	7.3	300	8.8
10	tetrahydronaphthalene	7.4	70	3.0
11	decahydronaphthalene	6.7	760	3.9
12	decahydronaphthalene	66.7	300	5.4
13[a]	9,10-dihydrophenanthrene	4.5	760	0.69

[a] The balance of the product distribution for this run (61%) was a heavier fraction which was not identified by VPC.

For the polycyclic aromatic and hydroaromatic compounds tested in this study, the energy yield from electric discharge hydrocracking for production of the lighter hydrocarbons was in the following order:

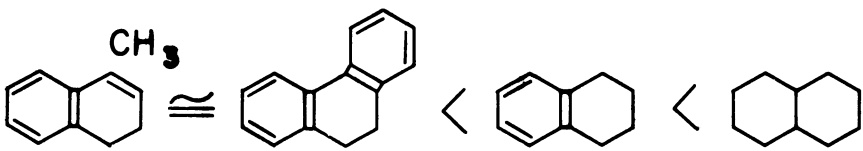

α-methylnaphthalene ≅ 9,10-dihydrophenanthrene < tetrahydronaphthalene < decahydronaphthalene

As observed in cresol runs, solid films were formed on the reactor wall, but they were not analyzed.

The number of experiments are not sufficient to permit drawing a concrete relationship between energy yield and molecular structure. However, it appears that for the same number of rings the extent of the cracking was greater as degree of saturation increased. It is reasonable to assume that the condensed aromatic ring structure absorbs large amounts of energy and requires high energy for cracking. The radiation effect on various polycyclic aromatic compounds were studied by Weiss *et al.* (*6*). They discussed correlations between the radiation stability and various structural factors. These include resonance energy, electron affinity, and ionization constant. Since there is a close similarity between radiation and electric discharge in principle, further information along this line would be helpful for a better understanding of the electric discharge hydrocracking process.

In Chemical Reactions in Electrical Discharges; Blaustein, B.;
Advances in Chemistry; American Chemical Society: Washington, DC, 1969.

by the Electric Discharge in Hydrogen

Product Distribution, Wt. %						
C_1	C_2	C_3	C_4	C_5	C_6–C_9	*Unsaturated*
2	33	24	21	13	7	32
–	5	24	29	40	2	35
5	77	12	3	1	2	74
1	78	16	3	1	2	85
–	74	23	2	.5	.5	90
4	38	20	10	7	21	49
1	56	27	7	2	7	76
3	23	7	3	2	1	71[b]

[b] Percentage of unsaturates in C_1–C_9 fractions.

Elucidation of the reaction scheme in detail is beyond the scope of this study. However, it was indicated that in electric discharge hydrocracking of aromatic or hydroaromatic hydrocarbons, dissociation of the side chains and rupture of the rings are followed by secondary reactions involving the decomposed species; this leads to the formation of aromatic or aliphatic lighter compounds. Energy requirement to form these lighter compounds appear to be too high for practical applications.

The formation of the solid polymerized products, which takes place in parallel with fragmentation, as seen for cresol runs, requires considerably less energy. Study on the formation of polymer films starting with various monomers and using the present discharge system presents an extremely interesting problem which is currently under investigation. The results will be published in the near future.

Acknowledgment

This is a part of the work supported by the Office of Coal Research, U. S. Department of Interior. The author is thankful for their generous support.

Literature Cited

(1) Given, P. H., "Abstracts of Papers, 143rd Meeting, ACS," Cincinnati, Ohio, January, 1963, 4D.
(2) Lunt, R. W., ADVAN. CHEM. SER. **21**, 286 (1959).
(3) Manley, T. C., *Trans. Am. Electro Chem. Soc.* **84**, 83 (1943).
(4) Morinaga, K., Suzuki, M., *Bull. Chem. Soc., Japan* **35**, 429 (1962).
(5) Suzuki, M., Naito, Y., *Proc. Japan Academy* **28**, 469 (1959).
(6) Weiss, J., Collins, C. H., Sucker, J., Carciello, N., *Ind. Eng. Chem., Prod. Res. and Development* **3**, 73 (1964).

RECEIVED July 3, 1967.

27

The Decomposition of Methane and Methyl Chloride in a Microwave Discharge

J. P. WIGHTMAN

Virginia Polytechnic Institute, Blacksburg, Virginia

N. J. JOHNSTON

NASA–Langley Research Center, Hampton, Virginia

Publication Date: June 1, 1969 | doi: 10.1021/ba-1969-0080.ch027

Hydrogen was the major gaseous product of the decomposition of methane in a microwave discharge in the absence of a diluent. Hydrogen chloride, hydrogen, and ethane were observed as gaseous products of the decomposition of methyl chloride. The empirical formulas for the solid polymeric films obtained on decomposition of methane and methyl chloride were $(CH_{1.49}O_{.0363})_X$ *and* $(CH_{.445}Cl_{.293})_X$*, respectively. Thermograms of the films were markedly different and the films differed significantly in free spin concentration. A greater part of the chlorine was displaced to the gas phase but about 30% was incorporated in the film which was hydrogen deficient. It was apparent that for a substituted parent molecule the H/C ratio cannot be used as a guide to predict film properties.*

The decomposition of hydrocarbons in various types of electrical discharges has been widely studied and examples of recent work are cited (*1, 5, 7, 9, 10, 11, 14*). However, the use of the microwave discharge to effect decomposition of hydrocarbons has been limited (*6, 12, 13*). Molecules in a microwave discharge are subjected to a greater degree of fragmentation than in other more commonly used discharges thereby dramatically altering the nature of the decomposition products.

The decomposition of a series of hydrocarbons including methane, in a microwave discharge has been reported (*13*) and from this work, the following postulate could be advanced: if a parent hydrocarbon has a hydrogen to carbon ratio (H/C) greater than about 1.6 a hydrogen saturated solid film will be produced on passage of the hydrocarbon

In Chemical Reactions in Electrical Discharges; Blaustein, B.;
Advances in Chemistry; American Chemical Society: Washington, DC, 1969.

through a microwave discharge in addition to hydrogen. Conversely, if a parent hydrocarbon has a (H/C) ratio less than 1.6 a hydrogen deficient film will be produced and no hydrogen will be observed.

The present work is the first in a series of investigations of the effect of functional groups on the nature of gaseous and solid decomposition products. The results of such measurements should ultimately support a model for decomposition in a microwave discharge. Further, solid polymers produced in various discharges have not in general been the subject of more than the most rudimentary characterization. The present work explores possible avenues of further characterization.

Experimental

Publication Date: June 1, 1969 | doi: 10.1021/ba-1969-0080.ch027

Materials. Methane (ultrahigh purity grade) was obtained from the Matheson Co. and used without further purification. The following analysis was supplied with the methane: CO_2 – 5 p.p.m.; O_2 – 5 p.p.m.; N_2 – 19 p.p.m.; C_2H_6 – 14 p.p.m.; C_3H_8 – 5 p.p.m. Methyl chloride (high purity grade) was obtained from the Matheson Co. and used without further purification.

Apparatus and Procedure. Reactions were carried out in a high vacuum flow system shown schematically in Figure 1. The power source for the microwave discharge was a Raytheon generator (Model KV-104) and was operated at a power level corresponding to about 40 RF. watts at 2450 Mc. The generator was connected to an air-cooled cavity (Raytheon – KV series) by a coaxial cable. Pressures in the discharge region were measured with a thermocouple calibrated against a McLeod gage. A deposition train was used whereby a series of films were deposited sequentially. Two procedures were used depending upon whether an analysis of the gaseous products was being made or whether solid film was being deposited for subsequent analysis. In the former case, the parent gas was passed through a variable leak valve (Veeco – VL). The pressure in a typical experimental run was 0.15 torr at a mass flow rate of 1×10^{-5} moles/min. and a linear flow rate of 20 cm./sec. In the latter case, the parent gas was passed through a Teflon needle valve (Fischer-Porter). Typical pressures in the discharge region were 3 torr for methane and 1 torr for methyl chloride. Film deposition times varied between 5 and 20 min. The volume of the luminous discharge zone was about 4 cc.

The gaseous decomposition products of methane and methyl chloride were determined using a mass spectrometer (Associated Electronics Industries – MS-10). The doser (10 cc.) was located about 140 cm. downstream from the discharge. Gas in the doser was expanded to decrease the pressure prior to introduction into the mass spectrometer.

The solid polymeric films were removed mechanically from the walls of the borosilicate glass tubing. The infrared spectra of the neat films were obtained using a Perkin-Elmer 421 spectrophotometer. The electron spin resonance spectra of the neat films were obtained on a Varian ESR 6 spectrometer. Elemental analyses were made by Galbraith Labs. Ther-

In Chemical Reactions in Electrical Discharges; Blaustein, B.;
Advances in Chemistry; American Chemical Society: Washington, DC, 1969.

mogravimetric analyses were made *in vacuo* using a Cahn RG null type electrobalance and a van der Slice mass spectrometer to monitor volatiles.

Results

Gaseous Products. Selected peaks from the mass spectra of methane and methyl chloride obtained with the discharge on and off are shown in Figure 2 (A and B). The most significant features in the methane spectra (Figure 2A) were the increase in the $m/e = 2$ (H_2^+) peak and the decrease in the $m/e = 15$ (CH_3^+) peak when methane was passed through the discharge. The most significant features of the methyl chloride spectra (Figure 2B) were the increase in the $m/e = 2$ (H_2^+) peak, the decrease in the $m/e = 15$ (CH_3^+) peak, the appearance of the $m/e = 30$ ($C_2H_6^+$) peak and the disappearance of the $m/e = 50$ (CH_3Cl^+) peak.

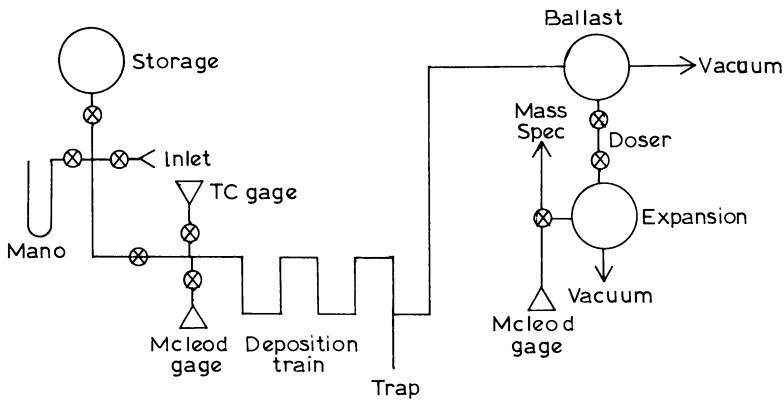

Figure 1. Schematic of microwave discharge apparatus

Results cited below suggest that HCl is a decomposition product yet was not observed in the mass spectra. The disappearance of HCl is presumed to be attributable to the reaction of HCl with stainless steel in the inlet system of the mass spectrometer. The reaction would give hydrogen in addition to that produced in the discharge. Independent evidence for the presence of HCl was obtained by trapping the downstream gases at liquid air temperature, allowing the trap to warm-up and bubbling the gas(es) through water. The resultant solution was titrated with a standardized NaOH solution.

Solid Films. A solid polymeric film was observed to form in the discharge region when either methane or methyl chloride was passed through the discharge. Both films were characterized in several ways.

Publication Date: June 1, 1969 | doi: 10.1021/ba-1969-0080.ch027

In Chemical Reactions in Electrical Discharges; Blaustein, B.;
Advances in Chemistry; American Chemical Society: Washington, DC, 1969.

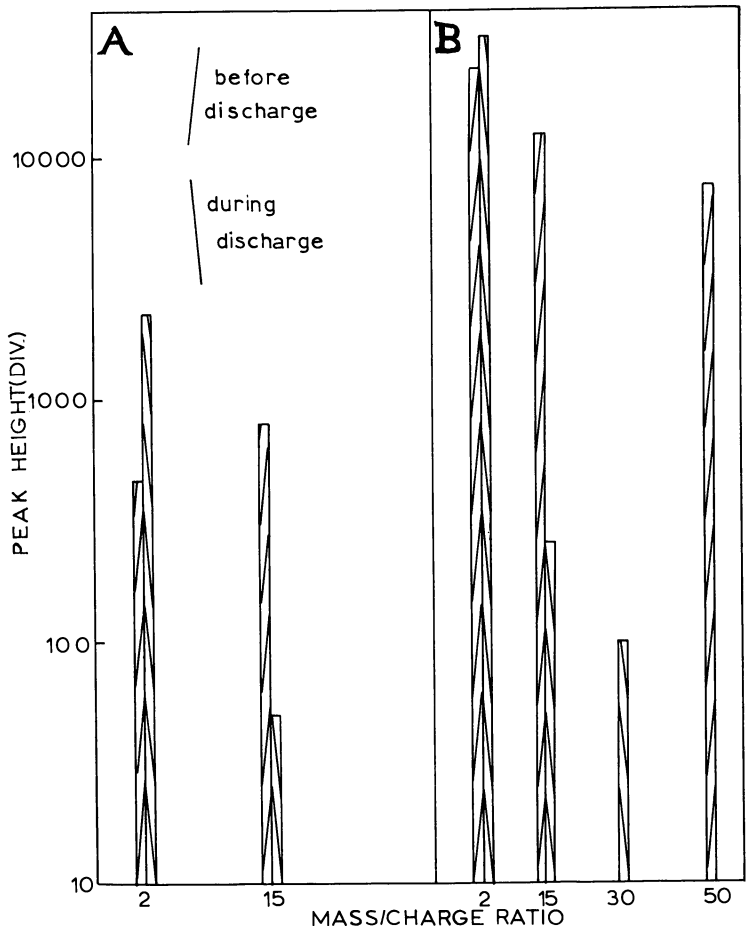

Figure 2. (A) Selected peaks from mass sepectra of methane in a microwave discharge and (B) Selected peaks from mass spectra of methyl chloride in a discharge

The results of elemental analysis of the polymeric films produced from methane and methyl chloride are shown in Table I. Both films were heated at 60°C. under reduced pressure prior to analysis to remove adsorbed water.

Table I

Gas	*% C*	*% H*	*% Cl*	*% O*	*Total*	*Empirical Formula*
Methane	85.35	10.61	—	4.13	100.00	$(CH_{1.49}O_{.0363})_x$
Methyl chloride	53.40	1.98	44.7	None	100.15	$(CH_{.445}Cl_{.293})_x$

Publication Date: June 1, 1969 | doi: 10.1021/ba-1969-0080.ch027

The infrared spectrum of a neat sample of freshly prepared film from methane is shown in Figure 3 and is almost identical to a thin film of polyethylene (2) with one notable exception: the absence of strong absorption bands in the 700-800 cm.$^{-1}$ region characteristic of $(CH_2)_n$ groupings where $n \geqslant 2$. The broad weak absorption centered at 3420 cm.$^{-1}$ is attributed to adsorbed water and not to alcoholic O–H stretching frequencies since the film for infrared analysis, contrasted to elemental analysis, was not handled under anhydrous conditions. The lack of absorption in the 1075–1170 cm.$^{-1}$ region characteristic of the high intensity C–OH stretching vibrations supports the presence of water. The broad absorption at 1700 cm.$^{-1}$ which increases in intensity on aging is assigned to carbonyl groups probably formed by reaction of radical sites with oxygen after the film was removed from the reaction tube. This is consistent with the fact that a small percentage of oxygen was found on analysis of the methane film (Table I). Jesch *et al.* (3) reported similar observations with polymer produced in an ethylene glow discharge.

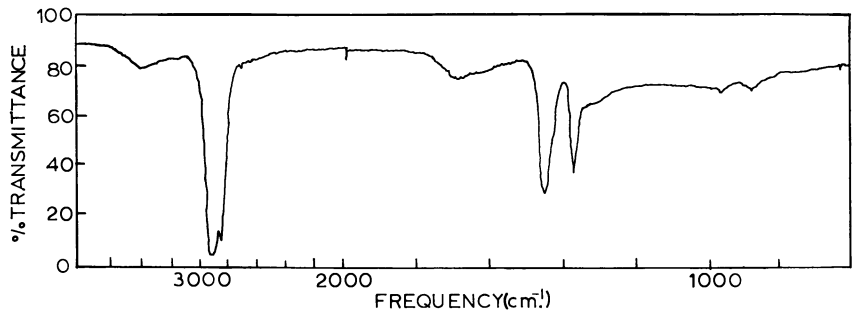

Figure 3. Infrared spectrum of polymer produced from methane

The presence of CH_3 and CH_2 groups is shown by the strong absorptions at 2960 ($\nu_{as}CH_3$), 2930 ($\nu_{as}CH_2$), 2870 (ν_sCH_3, CH_2), 1450 ($\delta_{as}CH_3$, δ_sCH_2), and 1375 (δ_sCH_3) cm.$^{-1}$. This latter band does not appear to be split showing the absence of geminal dimethyl units. The very weak absorption at 1630, 965, and 880 cm.$^{-1}$ can be assigned to di- and trisubstituted alkene moieties. The infrared data indicate that the film produced from methane is comprised mainly of highly branched saturated carbon chains containing pendant and terminal CH_3 groups and little, if any, $(CH_2)_n$ units where $n \geqslant 2$. The highly cross-linked nature of the polymer is consistent with its solubility behavior (*see* below). Tetrasubstituted alkenes are difficult to detect since they possess weak C=C stretching frequencies and no C–H out-of-plane deformations. Thus, the percentage double bond character in the methane film might be somewhat greater than indicated by its spectrum.

Publication Date: June 1, 1969 | doi: 10.1021/ba-1969-0080.ch027

The infrared spectrum of a neat film obtained from methyl chloride is shown in Figure 4a. The spectrum is appreciably less definitive than the methane film spectrum (Figure 3). The spectrum of a more concentrated powdered sample contained in a potassium bromide disc is shown in Figure 4b. The insert at the low frequency end was made with a different interchange.

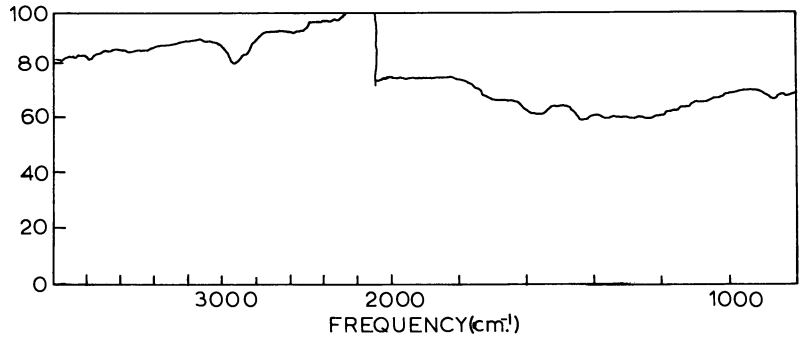

Figure 4a. Infrared spectrum of neat polymer from methyl chloride

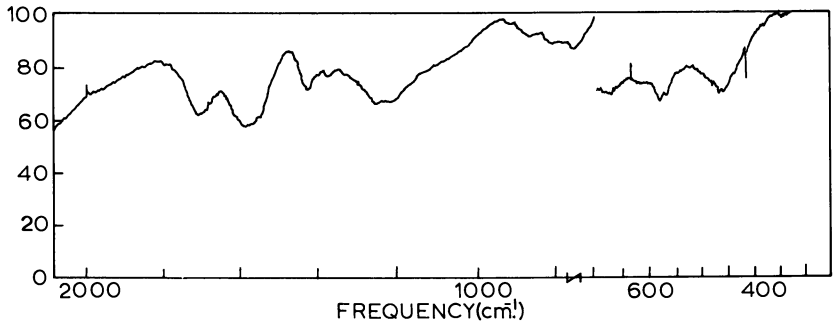

Figure 4b. Infrared spectrum of polymer (in KBr) from methyl chloride

Carbon-hydrogen stretching frequencies are present in the characteristic 2870–2960 cm.$^{-1}$ region; however, the C–H bending mode at 1430 cm.$^{-1}$ is shifted to a lower frequency from its position observed in the methane film spectrum attributable to the influence of adjacent ethylenic bonds (*8*). The weak 1370 cm.$^{-1}$ band is the symmetrical methyl bending vibration and the stronger absorption centered at 1595 cm.$^{-1}$ is assigned to the C=C stretching vibration of a conjugated polyene structure (*8*). The substitution of halogen for ethylenic hydrogen tends to lower the frequency of this vibration (*4*). The relative intensities of these absorptions and the elemental analysis clearly indicate the presence of a high degree of unsaturation and relatively small amounts of CH_3 and CH_2 groups.

In Chemical Reactions in Electrical Discharges; Blaustein, B.;
Advances in Chemistry; American Chemical Society: Washington, DC, 1969.

The lack of strong well resolved absorptions in the fingerprint and far infrared regions make the C–Cl stretching frequency difficult to assign. Most of the chlorine atoms probably are attached to unsaturated carbons; this may result in low intensity C–Cl band and a shift of its frequency to higher wavenumbers than normally observed for saturated C–Cl stretching modes. Consequently, the weak peaks in the 750–870 $cm.^{-1}$ region may be assigned to C–Cl and/or ethylenic absorptions.

The electron spin resonance spectra of the films produced from methane and methyl chloride are shown in Figures 5a and 5b. A significantly larger free spin concentration on the order of one thousand times greater was noted in the case of the methyl chloride film. Thus, the methyl chloride film contains a greater number of unsaturated valences than the methane film. This is consistent with the results obtained from the infrared spectra of both films. No fine structure was observed in the case of the methyl chloride film. The g-values of both films were essentially identical to the value for pitch ($g = 2.000$).

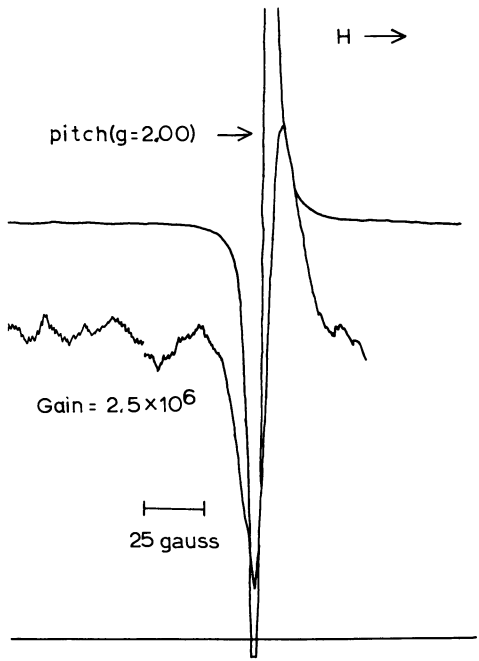

Figure 5a. ESR spectrum of polymer produced from methane

An extensive series of liquids were tested as possible solvents for the films prior to NMR measurements. Partial solubility was noted in hot hexamethylphosphoramide and hot concd. H_2SO_4. Even in these two

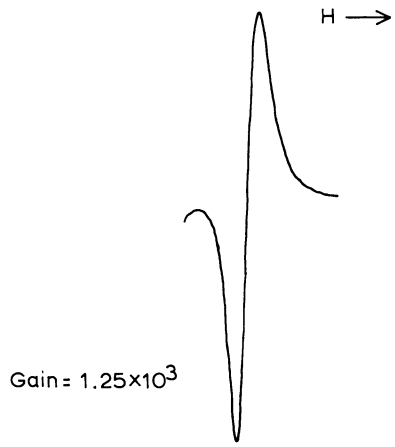

Figure 5b. ESR spectrum of polymer produced from methyl chloride

cases the concentration of the resultant solution was not sufficient to obtain an NMR spectrum.

Thermograms of the methane and methyl chloride films and a commercial sample of polyethylene are shown in Figure 6. The latter is presented for comparative purposes. The differences between the methane and methyl chloride films can be seen readily from their thermal stabilities. The behavior of the methane film is similar to polyethylene, losing weight rapidly above 300°C. The methyl chloride film by contrast loses weight slowly above 300°C. and the loss levels off above 550°C. About 81% of the sample is left at 800°C.

Polyethylene degraded into hydrogen and low molecular weight hydrocarbons ($m/e \leqslant 58$) accounting for 95% of the total pressure. The fragments from the methane film having $m/e \leqslant 58$ accounted for only 55% of the total pressure. Such decomposition behavior would be expected from highly branched cross-linked materials. The methyl chloride film displayed no detectable fragmentation in the $m/e = 30$ to 38 range. This implies that the hydrogen and chlorine atoms in the polymer are stable as in vinyl type compounds with little tendency to form hydrogen chloride during the thermal treatment.

Discussion

The equation for the observed decomposition of methyl chloride in the discharge may be written

$$x\mathrm{CH_3Cl} \rightarrow (\mathrm{CH_{.4}Cl_{.3}})_x + .7x\mathrm{HCl} + .9x\mathrm{H_2}$$

Publication Date: June 1, 1969 | doi: 10.1021/ba-1969-0080.ch027

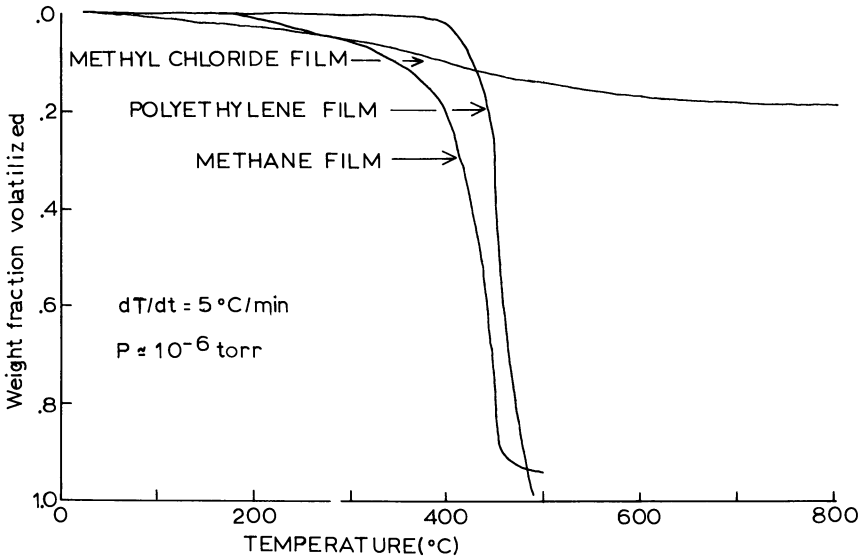

Figure 6. Comparison of thermograms obtained with polyethylene and with polymer films produced from methane and methyl chloride

neglecting ethane which does not subtract from the present argument since it was not formed in high concentrations. Chlorine introduced into the discharge by dissociation of methyl chloride thus appeared in two decomposition products. Approximately 70 mole percent of Cl was accounted for as HCl and the balance is incorporated into the polymer. The inclusion of Cl produced a polymer having characteristics of a hydrogen deficient film similar to the films reported previously on decomposition of acetylene, benzene, and naphthalene in the discharge. The color of the transparent methyl chloride film was dark (brownish-black) characteristic of hydrogen deficient films in contrast to the light yellow methane film characteristic of hydrogen saturated films. The high electron spin concentration of the methyl chloride film had also been observed for the hydrogen deficient film from acetylene.

In conclusion, the (H/C) ratio of a parent molecule will not necessarily be a valid guide to predictions of substituted decomposition products. Extension to other functional groups is expected to determine whether this is a general scheme.

Acknowledgments

The authors would like to acknowledge the help of R. E. Dessy in obtaining the ESR spectra and the experimental assistance of R. O. McGuffin and S. H. Wu. The authors wish to thank R. A. Jewell and

H. D. Burks of NASA – Langley Research Center for the thermograms and the infrared spectra.

Literature Cited

(1) Borisova, E. N., Eremin, E. N., *Zh. Fiz. Khim.* **40,** 2366 (1966).
(2) Haslam, J., Willis, H. A., "Identification and Analysis of Plastics," p. 409, D. van Nostrand Co., Princeton, N. J., 1965.
(3) Jesch, K., Bloor, J. E., Kronick, P. L., *J. Poly. Sci.*, A-1 **4,** 1487 (1966).
(4) Jones, R. N., Sandorfy, C., "Chemical Applications of Spectroscopy," Chap. 4, Vol. IX of "Techniques of Organic Chemistry," A. Weissberger, Ed., Interscience, New York, N. Y., 1956.
(5) Kraaijveld, H. J., Waterman, H. I., *Brennstoff-Chem.* **42,** 369 (1961).
(6) McCarthy, R. L., *J. Chem. Phys.* **22,** 1360 (1954).
(7) Mignonac, G., Miquel, R., Lecouls, H., *Bull. Soc. Chim.* **1966,** 2161.
(8) Nakanishi, K., "Infrared Absorption Spectroscopy—Practical," Holden-Day, San Francisco, Calif., 1962.
(9) Ponnamperuma, C., Woeller, F., *Nature* **203,** 272 (1964).
(10) Schuler, H., Prchal, K., Kloppenburg, E., *Z. Naturforsch.* **15a,** 308 (1960).
(11) Stille, J. K., Sung, R. L., van der Kooi, J., *J. Org. Chem.* **30,** 3116 (1965).
(12) Streitwieser, Jr., A., Ward, H. R., *J. Am. Chem. Soc.* **85,** 539 (1963).
(13) Vastola, F. J., Wightman, J. P., *J. Appl. Chem.* **14,** 69 (1964).
(14) Williams, T., Hayes, M. W., *Nature* **209,** 769 (1966).

RECEIVED May 8, 1967.

28

Reaction of Maleic Anhydride with Aromatic Hydrocarbons under the Influence of Silent Electric Discharge at Atmospheric Pressure

STYLIANOS SIFNIADES, DAVID JEROLAMON, and ROBERT FUHRMANN

Allied Chemical Corporation, Central Research Laboratory, Morristown, N. J.

Publication Date: June 1, 1969 | doi: 10.1021/ba-1969-0080.ch028

Maleic anhydride reacts with alkylbenzenes in the presence of free radicals to form adducts of Type I and with benzene, chlorobenzene, and alkylbenzenes under photochemical excitation to form adducts of Type II. In this study solutions of maleic anhydride in benzene, toluene, ethylbenzene, and cumene were exposed to high frequency (3.6 and 8.0 kc./sec.) electric discharge in an atmosphere of N_2 or He. Adducts of Type II were isolated in yields ranging from 8 to 23% of the converted maleic anhydride. The balance was made up of adducts of Type I together with products of higher condensation with maleic anhydride. The product distribution suggests that most of the active species in the present system are excited molecules and not free radicals.

Maleic anhydride is known to form two classes of adducts with alkylbenzenes, depending on the conditions of excitation. At reflux temperatures and in the presence of catalytic amounts of peroxides adducts of Type I are formed (*3, 4*). A free radical chain reaction is assumed involving abstraction of a benzylic hydrogen. The chain length, based on the ratio of product to added peroxide, is 20 to 100.

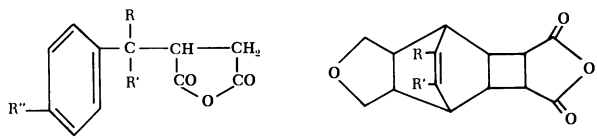

In Chemical Reactions in Electrical Discharges; Blaustein, B.;
Advances in Chemistry; American Chemical Society: Washington, DC, 1969.

At room or somewhat higher temperatures and in the presence of ultraviolet radiation, adducts of Type II are formed (*1, 5, 6, 7, 10, 11, 15*) (The positions of the substituents R and R′ in II have been established by means of NMR studies on the corresponding methyl esters for R=H, R′ = Me, Et, *i*-Pr, *t*-Bu (*5*). For R = R′ = Me the positions were assigned on the basis of steric considerations (*6*).) Excited charge transfer complexes of maleic anhydride with an aromatic molecule are claimed to be the reaction intermediates. The addition is sensitized by benzophenone (*6*) or acetone (*5*) but the adduct can be formed in the absence of a sensitizer, although at a much lower rate. It appears that the presence of a sensitizer is indispensable if sunlight is used as the source of exciting radiation (*8, 9*). It is interesting to note that in this case only benzene forms an adduct II with maleic anhydride, while alkylbenzenes are only partly incorporated in polyanhydride chains which are formed.

Recently formation of the adduct II of benzene and maleic anhydride under the influence of gamma radiation was reported (*14*). The adduct is only a minor product of the reaction, corresponding to about 4% of the maleic anhydride spent. The main product is a mixture of polyanhydrides. These can be considered to arise through a free radical chain similar to the one yielding adducts of Type I.

It is then clear that in the system maleic anhydride-benzene (or alkylbenzene) two types of reactions are prevalent, one by free radical chain yielding adduct I or polyanhydrides, the other by means of excited charge transfer complexes yielding adduct II. It was thought of interest to investigate the influence of silent or corona discharge on this system. This type of discharge was chosen because it is easy to maintain at atmospheric pressure.

Experimental

The discharge apparatus was essentially a modified Siemens ozonizer vertically mounted. It was made of borosilicate glass. A solution of sodium chloride in glycerol circulating in the jacket constituted the ground electrode, while a silver coating in the interior surface of the central tube served as the high voltage electrode. The separation between the dielectric surfaces was 3 mm. and the total discharge volume was 150 ml. The liquid reaction mixture was circulated at the rate of 500 to 800 ml. per minute from top to bottom through the reactor by means of a custom made pulsating membrane pump constructed of Halon (Allied Chemical Corp.) and in such a way that it wetted both the concave and convex surfaces of the ozonizer. An inert gas, nitrogen or helium, was introduced at the top of the reactor and vented at the bottom through a condenser. The temperature of the liquid reaction mixture was measured at the exit of the discharge. Temperature control was ensured by regulating the temperature of the glycerol solution circulating in the jacket.

In Chemical Reactions in Electrical Discharges; Blaustein, B.;
Advances in Chemistry; American Chemical Society: Washington, DC, 1969.

Table I. Condensation of Maleic Anhydride with Benzene and

Run No.		*Frequ. kc./sec.*	*Potentl. kv.*	*Temp. °C.*	*Adduct, Type I & telomers*	*Grams II*
1	350 ml. benzene 50 grams MA, N_2	8.0	10.0	78	25.3	2.12
2	350 ml. benzene 51 grams MA, N_2	3.6	13.0	75	18.0	3.40
3	350 ml. benzene 49 grams MA, N_2	3.6	12.5	37	13.2	2.19[a]
4	380 ml. benzene 12 grams MA, N_2	3.6	13.0	74	14.5	2.77
5	380 ml. benzene 13 grams MA, He	3.6	13.0	75	15.1	4.16
6	380 ml. toluene 13 grams MA, He	3.6	13.0	82	30.0	4.79
7	368 ml. ethylbenzene 29 grams MA, N_2	3.6	13.0	121	25.1	7.35
8	416 ml. cumene 29 grams MA, N_2	3.6	13.0	127	23.0	5.18

[a] The product was brown.

Publication Date: June 1, 1969 | doi: 10.1021/ba-1969-0080.ch028

Current at the desired frequencies was produced by an audio-frequency generator (Heathkit Model IG-72) coupled with a 1000 VA (volt-ampere) custom made power tube amplifier. It was raised to high voltage by means of a 25 kv. transformer. Lower voltages could be obtained by acting on the output of the amplifier. The power input to the system was monitored by means of a watt-meter (Westinghouse Type PY6, specially compensated for high frequency work) at the primary circuit of the transformer.

Eastman White Label chemicals were used without purification. In a typical experiment 29.4 grams of maleic anhydride in 416 ml. of cumene were circulated for two hours in the apparatus while the discharge was maintained at a power level of 400 watts. Nitrogen was supplied at the rate of 50 ml./min. The temperature of the reaction mixture was 127°C. The reaction mixture was cooled to 20°C. and the resulting crystals were filtered and washed with 50 ml. of cold benzene. Additional crystals were obtained after the mother liquor had been condensed to one third of its initial volume by flash evaporation. The combined product was dried at 50°C. in a vacuum oven. It weighed 5.18 grams and had melting point 255°–257°C. The melting point of the photoadduct of cumene and maleic anhydride is 250°–255°C. (5). The neutralization equivalent in aqueous acetone was 79.2, compared with 79.1 expected from a compound of Formula II (R = H, R′ = *i*-Pr). Elementary analysis was consistent with this formula. Flash evaporation of the unreacted cumene and maleic anhydride left 23.0 grams of a viscous residue which had neutralization equivalent corresponding to a mixture of a 1:1 and 2:1 adduct of maleic

In Chemical Reactions in Electrical Discharges; Blaustein, B.;
Advances in Chemistry; American Chemical Society: Washington, DC, 1969.

Alkylbenzenes Under the Influence of Silent Electric Discharge

Yield II	*m.p. of II*		*Neutzn. Equiv. of II*	
mmole/kwh.	*obs.*	*lit.*	*Calcd.*	*Found*
12.0	355-57	350 (*1, 5*)	68.5	68.8
26.5	355-57	350-55 (*15*)	68.5	68.6
15.6	350-55		68.5	68.9
26.2	355-57		68.5	68.2
33.3	355-57		68.5	68.7
30.4	245-60	265-70 (*5*) 250-70 (*15*)	72.0	72.2
36.0	260-61	250-55 (*5*)	75.5	75.3
29.8	255-57	250-55 (*5*)	79.0	79.4

[b] Abbreviation: MA, denotes maleic anhydride.

anhydride and cumene. It was assumed that it contained adduct of Formula I (R = R′ = Me) together with products of further condensation with maleic anhydride. An NMR spectrum revealed the presence of aromatic protons in ratio 4.7:6 to methyl protons indicating that the cumyl group exists largely intact in the resinous material. This is consistent with Formula I.

Similar results were obtained using benzene, toluene, and ethylbenzene as substrates. Chlorobenzene and nitrobenzene failed to yield a crystalline product. The experimental conditions and the results are summarized in Table I.

Discussion

It is apparent from the present results that maleic anhydride forms an adduct of Type II with benzene and alkylbenzenes under the influence of silent discharge. The generally accepted path of formation of II in photochemical (*6*) or gamma-radiation induced (*14*) reaction is the following (benzene is used as substrate for convenience):

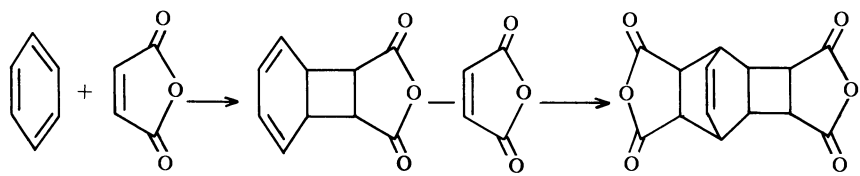

Publication Date: June 1, 1969 | doi: 10.1021/ba-1969-0080.ch028

It is reasonable to expect that the same path is followed also in the present case of discharge excitation. Since the rate of formation of adduct II is independent of the concentration of maleic anhydride (experiments 2 and 4), it is concluded that the formation of the intermediate mono-adduct is the rate determining step. The same conclusion has been reached in the photochemical formation of adduct II (*6, 11*).

Adduct II is not, however, the only product formed in the reaction; a considerably larger amount of resinous material (tabulated as adduct "Type I and telomers") is also formed in all cases. This material is thought to arise from a free radical reaction similar to the one giving rise to adduct I in peroxide initiated reactions. The chain length of these reactions is about 20 to 100, as mentioned earlier. On the other hand, it has been shown that the quantum yield of adduct II formed in photochemical reaction is about 0.1 (*11*). Since in the present experiments adduct II is formed in amounts about one quarter of the amount of "Type I" adduct although about ten excited molecules, or charge transfer complexes, are necessary to produce one molecule of II, while one free radical will produce 20 to 100 molecules of I, it must be concluded that the great majority of active species in the liquid phase in contact with the discharge are excited molecules and not free radicals. In fact, it can be estimated that 98 to 99% of the active species are excited molecules. The absence of free radicals as important reaction intermediates has also been deduced by product analysis in the microwave glow discharge of aromatics in helium (*16*).

In the photochemical reaction, benzene forms an adduct II at a higher rate than the alkylbenzenes, which in turn react in relative rates indicative of steric hindrance. No such effect was observed in the present work, as shown by the power yields in the table. These yields are also measures of the rate of formation of adduct II since roughly equal power levels of discharge were maintained in all cases.

Comparison of Runs 1 and 2 shows that formation of adduct II is favored at the lower frequency with a correspondingly higher potential difference applied across the electrodes. Although the electric field strength between the dielectric surfaces is not necessarily proportional to the externally measured potential difference (*2*), it appears that electrons of higher average energy favor the production of adduct II, as evidenced by the fact that the rate of formation of II is higher in a helium than in a nitrogen atmosphere (Runs 4 and 5). It is known that the average electron energy for equal field strength is quite larger in the former gas (*13*). Of course, the presence of organic vapors modifies the electron energy distribution, but it is reasonable to expect that some difference still exists.

Publication Date: June 1, 1969 | doi: 10.1021/ba-1969-0080.ch028

In Chemical Reactions in Electrical Discharges; Blaustein, B.;
Advances in Chemistry; American Chemical Society: Washington, DC, 1969.

The mechanism of energy transfer cannot be deduced with certainty from the present data. Comparison of yields at two temperatures (Runs 2 and 3) shows higher yield at the higher temperature, a fact which may be interpreted as meaning that benzene vapors in the discharge are excited by collision with electrons: at the higher temperature, the concentration of benzene in the gas phase is higher. While the conclusion may be correct, it is not unambiguous because of mechanical difficulties at the lower temperature, arising from the fact that adduct II was sparingly soluble in benzene at this temperature and quickly coated the dielectric surfaces where it was partly decomposed. Another way of excitation would involve bombardment of the liquid phase with electrons generated in the discharge. This method of excitation has been shown to prevail in the discharge induced oxidation of acidified water and ferrous ion (*17, 18*). Excitation by collision with excited nitrogen or helium cannot be an important process, considering that the first excited state of helium contains 19.81 e.v. of energy (*12*). Collision with such a species would result in extensive fragmentation of an organic molecule, whereas the present results point to the fact that free radical initiation is very limited in this system.

Publication Date: June 1, 1969 | doi: 10.1021/ba-1969-0080.ch028

Literature Cited

(1) Angus, H. J. F., Bryce-Smith, D., *J. Chem. Soc.* **1960,** 4791.
(2) Bartnikas, R., Levi, J. H. E., *Rev. Sci. Instr.* **37,** 1245 (1966).
(3) Beavers, E. M., *Rohm and Haas Co., U. S. Patent* **2,692,270** (1954).
(4) Bickford, W. G., Fisher, G. S., Dollear, F. G., Swift, C. E., *J. Am. Oil Chemists Soc.* **25,** 251 (1948).
(5) Bradshaw, J. S., *J. Org. Chem.* **31,** 3974 (1966).
(6) Bryce-Smith, D., Gilbert, A., *J. Chem. Soc.* **1965,** 918.
(7) Bryce-Smith, D., Lodge, J. E., *J. Chem. Soc.* **1962,** 2675.
(8) Bryce-Smith, D., Gilbert, A., Vickery, B., *Chem. Ind.* **1962,** 2060.
(9) Bryce-Smith, D., Gilbert, A., Vickery, B., *British Patent* **986,348** (1965).
(10) Grovenstein, E., Jr., Rao, D. V., Taylor, J. W., *J. Am. Chem. Soc.* **83,** 1705 (1961).
(11) Hammond, G. S., Hardham, W. M., *Proc. Chem. Soc.* **1963,** 63.
(12) Loeb, L. B., "Electrical Coronas," p. 17, Univ. of Calif. Press, Berkeley, Calif., 1965.
(13) Loeb, L. B., "Basic Processes of Gaseous Electronics," p. 319, Univ. of Calif. Press, Berkeley, Calif., 1961.
(14) Raciszewski, Z., *Chem. Ind.* **1966,** 418.
(15) Schenck, G. O., Steinmetz, R., *Tetrahedron Letters* **No. 21,** 1 (1960).
(16) Streitwieser, A., Jr., Ward, H. R., *J. Am. Chem. Soc.* **85,** 539 (1963).
(17) Yokohata, A., Tsuda, S., *Bull. Chem. Soc., Japan* **39,** 46 (1966).
(18) *Ibid.*, **39,** 1636 (1966).

RECEIVED May 24, 1967.

29

The Polymerization of Benzene in a Radiofrequency Discharge

DAVID D. NEISWENDER

Central Research Division Laboratory, Mobil Research and Development Corporation, Princeton, N. J.

Publication Date: June 1, 1969 | doi: 10.1021/ba-1969-0080.ch029

Benzene vapor has been converted to polymeric materials in a radiofrequency discharge. Depending on conditions employed, the reaction yielded either total conversion to a solid polymer or a low conversion to a liquid polymer and diphenyl. High energy dose and/or low benzene partial pressure favored the former while low dose and high partial pressure favored the latter. The solid is a very intractable material with interesting properties. Infrared, ultraviolet and nuclear magnetic resonance data suggest that both polymer products are similar to polystyrene in structure, the liquid being low molecular weight; the solid being high molecular weight and highly cross-linked. A synthetic route from benzene to polystyrene type polymers is suggested. The effect of several reaction variables is discussed.

The reactions of benzene in various types of electrical discharges have been studied by a number of researchers over a span of nearly 70 years. Reported results vary widely. Several early workers (*3, 4, 5, 9*), using ozonizer tubes, obtained a gummy wax-like substance, along with hydrogen, acetylene, and other light hydrocarbon gases. One of these researchers later obtained a liquid and a solid, both analyzing as $C_{24}H_{25}$ compounds (*10*). In 1930, Austin and Black (*1*) found diphenyl and a solid which they suspected to be a polyphenylene containing phenol groups. Harkins and Gans (*6*), using an electrodeless discharge, got complete conversion to a red-brown insoluble solid analyzing for $(CH)_x$. Davis (*2*), on the other hand, obtained diphenyl, *p*-terphenyl, a resin $(C_6H_4)_x$, hydrogen, acetylene, ethylene, and light paraffins. A 1935 U. S. patent (*8*) describes a discharge apparatus for preparing diphenyl from benzene. More recently, Streitwieser and Ward (*13, 14*) obtained a 5%

In Chemical Reactions in Electrical Discharges; Blaustein, B.;
Advances in Chemistry; American Chemical Society: Washington, DC, 1969.

conversion of benzene in microwave discharge, the products being low molecular weight gases, toluene, ethylbenzene and phenylacetylene. Stille and co-workers (*12*), using a radiofrequency discharge, got a 10% conversion to poly(*p*-phenylenes), diphenyl, fulvene, acetylene, allene, and methylacetylene. Vastola and Wightman (*15*) obtained a solid film and concluded from the infrared spectrum of the film that no aromaticity remained in the polymer. Jesch *et al.* (*7*), on the other hand, also obtained a solid film, but interpreted its infrared spectrum as suggesting the presence of aromatic groups as well as olefinic and acetylenic unsaturation. The wide disparity of the results certainly indicates there is still much to be learned about the chemistry of benzene in electrical discharges. This disparity is probably largely because of widely varying reaction conditions. Especially important are considerations such as the power dissipated in the discharge, the pressure, etc.

The work described here is an attempt to systematize the study of benzene reactions in radiofrequency discharges. The only products isolated in these reactions were diphenyl, a liquid polymer and a solid polymer. The polymers appear to be polystyrenes.

Publication Date: June 1, 1969 | doi: 10.1021/ba-1969-0080.ch029

Experimental

Apparatus and Procedure. The apparatus consisted of a 3.69 MHz. radiofrequency generator capacitively coupled to a cylindrical borosilicate glass flow reactor by means of two external copper electrodes. An inductively coupled tank circuit was used to match the impedances of the generator and the reactor. An approximate measure of the power dissipated in the discharge was determined by measuring the voltage and current during the experiments and making a phase correction for the capacitive component of the reactor current. A simple schematic of the apparatus is shown in Figure 1.

The hydrocarbon or helium-hydrocarbon mixture was metered into the reactor at various rates. Reactor pressures from 1-20 mm. were employed. In most cases, the discharge established itself as soon as the RF. signal was applied. If it did not, it was triggered with a Tesla coil. Products were collected in a series of traps, one at room temperature, one at −78°C. and one at −195°C.

Chemicals. Reagent grade, thiophene free benzene (Baker), and vacuum distilled styrene (Matheson, Coleman and Bell) were used in the discharge experiments. The helium (Matheson) had a reported minimum purity of 99.995%. The acetylene (Matheson) was at least 99.6% pure.

Results

Depending on the conditions employed, the reaction of benzene in the RF. discharge resulted in either a complete conversion to a solid polymer or a lower conversion to a liquid polymer and diphenyl. The

In Chemical Reactions in Electrical Discharges; Blaustein, B.;
Advances in Chemistry; American Chemical Society: Washington, DC, 1969.

solid tends to form under conditions of high power dissipation and/or low partial pressures of benzene in the reactor. Conversely, the liquid polymer and diphenyl result under low power dissipation and/or high partial pressures of benzene.

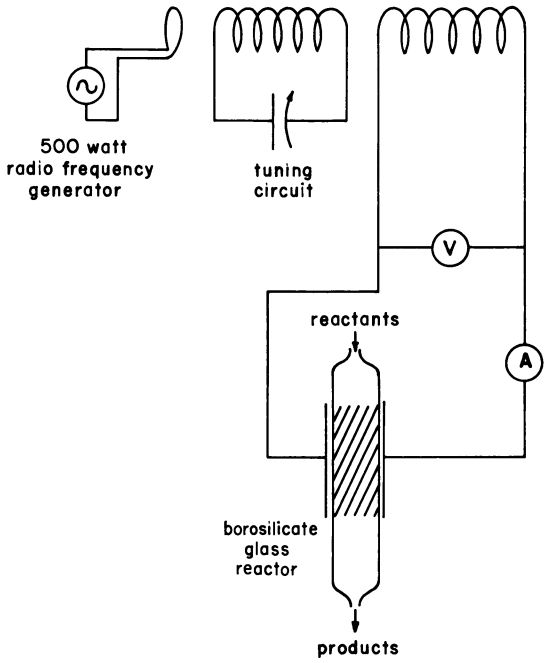

Figure 1. Radiofrequency discharge reactor

The solid polymer, which can sometimes be observed leaving the discharge zone as a fine smoke, deposits throughout the trap system, but principally in the dry ice trap. When collected, it is a very light, fluffy, nearly white powder which picks up a considerable static charge upon handling. Some of the substance's physical and chemical properties are as follows:

1. It is completely insoluble in water and in all organic solvents which were tested.
2. It does not melt up to 435°C. and shows no thermosetting or thermoplastic properties at even higher temperatures.
3. Thermogravimetric analysis shows that the polymer undergoes a stepwise loss in weight, with the loss being complete at 580°C.
4. X-ray diffraction studies show it to be completely amorphous.
5. The density of a pressed pellet is 1.10 gram/cc.
6. A freshly prepared sample was found to have an electron spin density of 2×10^{17} spins/cc.

Publication Date: June 1, 1969 | doi: 10.1021/ba-1969-0080.ch029

7. Its surface area (nitrogen adsorption) is 42 meter^2/gram, a rather high value for an organic substance.

8. It chemisorbs oxygen from the air at room temperature, the adsorption continuing for extended periods of time.

9. The experimentally determined carbon-hydrogen ratios varied from 1.02 to 1.05 for the many polymer samples studied. Thus, the elemental composition is the same as in the starting benzene (ignoring the chemisorbed oxygen in some samples).

In those experiments which did not yield the solid polymer, the conversion of the benzene was of the order of 30%. About 5% of the benzene was converted to diphenyl; the other 25% was converted to a liquid polymer with an average molecular weight of 617. This polymer, a viscous amber liquid, was not characterized as completely as the solid, but infrared spectral data indicate it to be very similar structurally to the solid.

Diphenyl is a commonly reported product of the reaction of benzene in electrical discharges and will not be considered further in this paper. Most authorities suggest that it arises *via* combination of phenyl free radicals.

Publication Date: June 1, 1969 | doi: 10.1021/ba-1969-0080.ch029

Discussion

Polymer Structure. The physical properties of the solid suggest that it is a high molecular weight, highly cross-linked polymer with an irregular structure. The extreme insolubility precludes spectral studies requiring solutions. It was possible to obtain an infrared spectrum by preparing a KBr pellet containing 2% of the solid. The liquid polymer, which was soluble in organic solvents had an infrared spectrum very similar to the solid.

Of several structural possibilities considered, the one which agrees best with the infrared data and seems the most likely from a chemical viewpoint is a polystyrene type structure. In Figure 2, the infrared spectrum of a reference polystyrene film (A) is compared with the spectra of the solid (B), the liquid (C), and a solid polymer obtained when a styrene-helium mixture was passed through the discharge (D). An equimolar mixture of benzene and acetylene in helium also produced a solid polymer whose infrared spectrum was indistinguishable from spectra B and D. All the spectra are similar, the only significant differences being the OH absorptions in the 3300–3400 cm.$^{-1}$ range and the carbonyl absorptions at about 1700 cm.$^{-1}$. These bands in all of the spectra from the discharge-derived polymers are caused by rapid oxidation by molecular oxygen. These bands become quite pronounced if the polymers are allowed to stand in air for a few hours.

In Chemical Reactions in Electrical Discharges; Blaustein, B.;
Advances in Chemistry; American Chemical Society: Washington, DC, 1969.

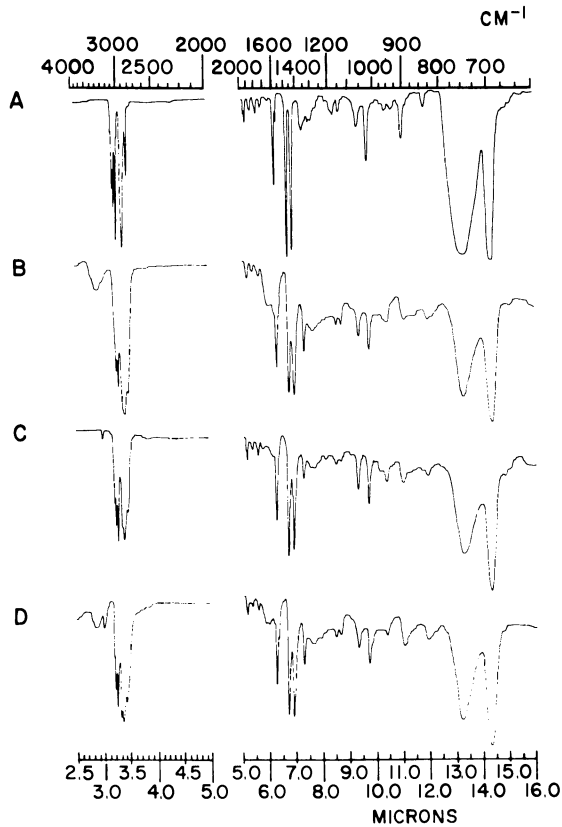

Figure 2. Infrared spectra

A = Polystyrene film
B = Solid polymer from benzene
C = Liquid polymer from benzene
D = Solid polymer from styrene

It is believed that the principal difference between the solid and liquid products is that the liquid is essentially a linear polymer, while the solid is highly cross-linked. Such a highly cross-linked polystyrene would be expected to have a lower ratio of aromatic C–H to aliphatic C–H bonds than would a linear polymer. Comparison of spectrum B or D with C in Figure 2 shows that the intensity of the aromatic and aliphatic C–H stretching vibrations agrees with this expectation.

Unfortunately, the NMR spectrum of the solid polymer could not be obtained owing to its extreme insolubility. However, because the solid and liquid seem to be structurally similar, the NMR spectrum of the later was examined and compared with that of an authentic polystyrene sample (*see* Figure 3). As is generally true with polymeric

Publication Date: June 1, 1969 | doi: 10.1021/ba-1969-0080.ch029

materials, the resolution was quite poor and only broad bands were observed. The polystyrene (10% solution in CCl_4) spectrum simply showed two broad peaks—one centered at $\delta = 1.50$ owing to aliphatic protons and one at $\delta = 7.08$ (with a small companion peak at $\delta = 6.58$) owing to aromatic protons. The spectrum of the liquid polymer (10% solution in CCl_4) was quite similar to the peaks appearing at $\delta = 1.60$ and 7.04 (no peak at $\delta = 6.58$). In addition, a very small peak at $\delta = 5.70$ was observed. This is probably because of protons on olefinic double bonds, and suggests either that some unsaturation is present in the polymer backbone, or that some unpolymerized vinyl groups are present. An attempt was made to increase the resolution of the NMR spectra by using a time averaging computer on very dilute solutions of the polymers, but the resolution was unchanged.

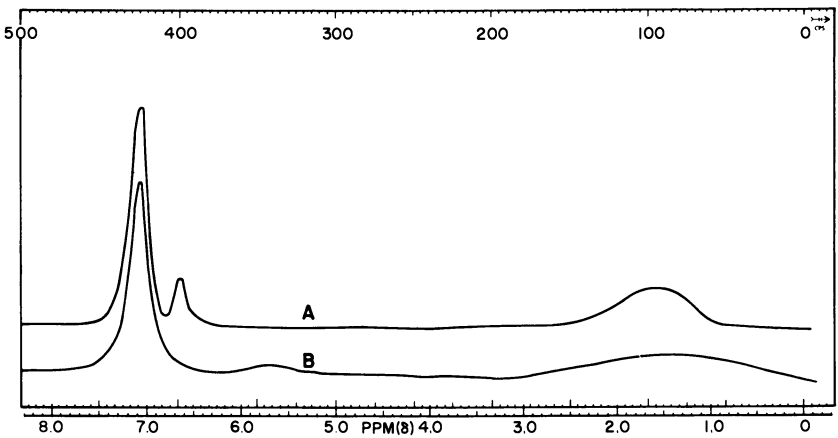

Figure 3. NMR spectra (60MC)
A = Polystyrene (10% solution in CCl_4)
B = Liquid polymer (10% solution in CCl_4)

Since the insolubility of the solid polymer precluded any ultraviolet studies in solution, attempts were made to obtain a diffuse reflectance spectrum of the solid. Meaningful data could not be obtained. Again, however, the liquid polymer could be compared with authentic polystyrene. Figure 4 shows the ultraviolet spectra of the two materials. Although the resolution is poor for the liquid polymer, its spectrum generally agrees with that of polystyrene.

Thus, although they are of limited value, the NMR and ultraviolet data do support a polystyrene type structure and, when coupled with the infrared data, strongly suggest that the polymers are both polystyrenes.

In Chemical Reactions in Electrical Discharges; Blaustein, B.;
Advances in Chemistry; American Chemical Society: Washington, DC, 1969.

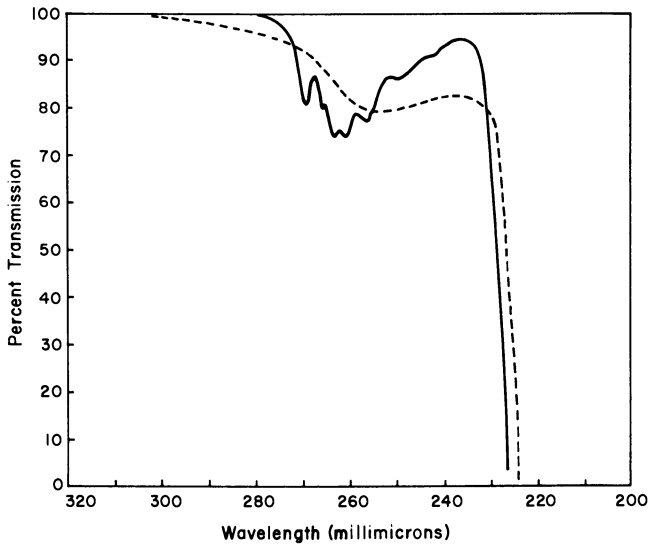

Figure 4. Ultraviolet spectra
——— = Polystyrene in cyclohexane
– – – = Liquid polymer in cyclohexane

Mode of Formation of Polymer. The most likely route from benzene to polystyrene involves several steps, the first of which is the establishment of an equilibrium between benzene and acetylene:

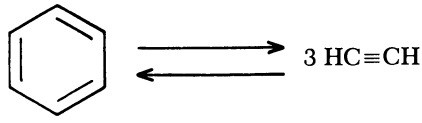

This interconversion has been observed in many high energy systems including electrical discharges. In the next step, the benzene and acetylene, one or both of which may be in a reactive state, combine to give styrene which then polymerizes:

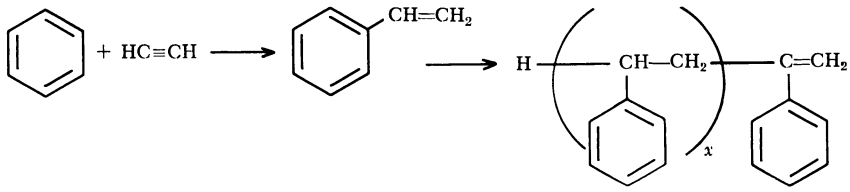

The simple linear polymer thus formed, limited to small chains such as pentamers, hexamers, etc., would explain the liquid polymer product.

Publication Date: June 1, 1969 | doi: 10.1021/ba-1969-0080.ch029

The formation of the highly cross-linked solid polymer can be explained by postulating the formation of benzenes substituted with more than one vinyl group which, when polymerized, would yield an extensive, irregular structure.

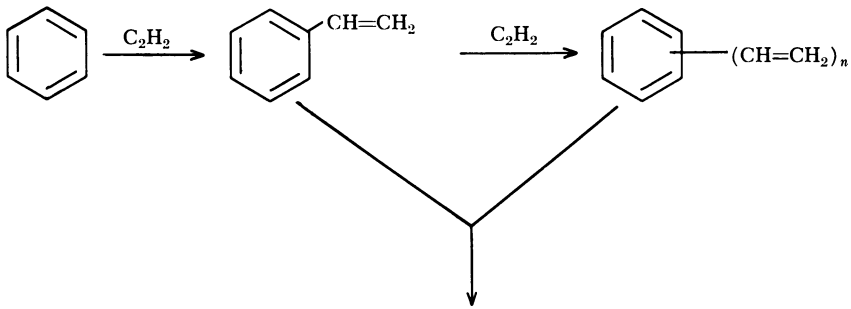

Highly cross-linked polystyrene

Both ionic and free radical mechanisms can be written to explain the foregoing reactions in more detail, but these would be strictly speculative, since no definitive experimental evidence has been obtained. Some sort of benzene ion must form as a result of inelastic collisions between the electrons and benzene molecules in the plasma, but whether these ions or some derivative species are the reactive intermediates is not known. Recently, Potter *et al.* (*11*) have shown that styrene, when perfectly dry, does polymerize *via* an ionic mechanism when irradiated with gamma rays. One can picture a similar mechanism occurring in the electrical discharge.

On the other hand, the fact that the polymer has a high electron spin density suggests free radical involvement. However, it can be questioned whether the unpaired electrons arose during or after the polymerization reaction. An attempt was made to induce a spin signal in a finely divided polystyrene sample by passing the solid through a helium discharge. No signal was detected after this treatment.

The question of mechanism must await the results of more fundamental studies of the phenomena occurring within the discharge.

Effect of Reaction Variables. Correlations between the types of product obtained and several reaction variables were studied briefly, and are discussed in the following paragraphs.

A. Energy Dose. An obvious variable to examine for a correlation is the amount of energy absorbed per mole of benzene. This quantity,

Publication Date: June 1, 1969 | doi: 10.1021/ba-1969-0080.ch029

calculated from experimental data for more than fifty experiments, was obtained by using the equation,

$$E = \frac{PT}{B}$$

where E = energy dose (joules/mole or watt seconds/mole)
P = power (watts)
T = residence time in the reaction zone (seconds)
B = quantity of benzene treated in time T (moles)

Table I summarizes the data obtained from these calculations.

Table I. Effect of Energy Dose (joules/mole)

Conversion and Product	*Lowest Dose*	*Highest Dose*	*Average Dose*
Complete conversion to solid polymer	8.9×10^6	5.2×10^7	1.9×10^7
Low conversion to liquid polymer and diphenyl	1.5×10^6	1.3×10^7	7.0×10^6

Although there is an overlapping dose range (8.9×10^6–1.3×10^7) where either type product can be obtained, there was an indication that high doses favored solid formation and low doses favored liquid. This seemed reasonable since more energy would be required to furnish the additional acetylene necessary for cross–linking and to gain the complete conversion.

This suggested correlation was tested by performing several experiments under conditions that had always produced solid (10% benzene in helium; 10 mm. pressure; 2.6 second residence time), except the energy dose was kept low by detuning the tank circuit used to couple the RF. generator to the reactor. Doses as low as 4.9×10^6 joules/mole produced the solid polymer, but the conversions dropped from 100% to about 30%. Therefore, while the energy dose appears to correlate well with the conversion obtained, it alone does not seem to determine the type product.

Since the energy dose and the dissipated power are directly proportional, a similar correlation arises when the variation of products with power is studied.

B. Residence Time. Very limited data are available to study the effect of residence time because nearly all the experiments were performed using 2.6–3.0 second times. Table II shows two experiments using pure benzene vapor at 2 mm. pressure.

Publication Date: June 1, 1969 | doi: 10.1021/ba-1969-0080.ch029

Table II. Effect of Residence Time

E *(joules/mole)*	P *(watts)*	T *(seconds)*	*Results*
4.3×10^6	63	0.6	Low conversion to liquid
1.2×10^7	40	2.6	High conversion to liquid

This limited data suggests that decreasing the residence time, even at high power levels, causes low conversion to liquid polymer. Such a correlation would make sense since the solid polymer, being more highly cross-linked, would probably require more time for formation.

C. BENZENE CONCENTRATION. The quantity B in $E = PT/B$ can best be studied by varying the partial pressure of the benzene while holding the power and residence time constant. The partial pressure can be varied either by adjustment of the total pressure of pure benzene vapor or by dilution with a rare gas. Table III shows some data obtained at various total pressures and benzene partial pressures.

Table III. Effect of Benzene Partial Pressure (Res. Time = 3.0 sec.)

Partial Press. ϕH (mm.)	*Total Press. (mm.)*	*Power (watts)*	*Energy Dose (joules/mole)*	*Reactant*	*Result*
1.0	10	70	4.5×10^7	10% ϕH in He	[a]
1.8	18	34	1.2×10^7	10% ϕH in He	[a]
2.0	2	40	1.2×10^7	ϕH	[a]
2.0	10	30	9.6×10^6	20% ϕH in He	[a]
3.0	10	45	1.0×10^7	30% ϕH in He	[a]
3.6	18	35	6.2×10^6	20% ϕH in He	[b]
4.0	10	32	5.5×10^6	40% ϕH in He	[b]
5.0	10	41	5.8×10^6	50% ϕH in He	[b]

[a] High conversion to solid polymer.
[b] Low conversion to liquid polymer.

Similar series of experiments with benzene in argon and benzene in neon gave the same results. Low partial pressures of benzene—*ca.* 3.0 mm. or lower—always seem to give the solid polymer while higher partial pressures yield liquid polymer.

One possible explanation of this observation lies in the fact that the energy distribution of the electrons changes with benzene partial pressure. (The rare gas probably has little effect compared with benzene because of the much lower ionization potential of the latter.) At higher partial pressures of benzene, the electron-benzene collision rate increases and the mean free path of the electrons decreases. These changes would cause a limitation of the energy which electrons could gain in the alternating

In Chemical Reactions in Electrical Discharges; Blaustein, B.;
Advances in Chemistry; American Chemical Society: Washington, DC, 1969.

field. Less energetic reactions (such as linear polystyrene formation) would be expected to predominate over more energetic reactions (such as formation of cross-linked polystyrene).

It must also be pointed out that Table III shows a general decrease in energy dose as the partial pressure of benzene increases. This suggests a cause and effect relationship between the benzene partial pressure and the energy capable of being absorbed by the system. Because of this possible relationship, it is difficult to say whether the energy dose or partial pressure is more important in determining the type of product.

D. Involvement of Rare Gas. Although the solid polymer can form in the absence of rare gas, some experiments suggest that the rare gas may be involved mechanistically, perhaps as an energy transfer agent. Experiments have not supplied any definitive answers.

It is obvious from the above considerations, that it is difficult to study one variable at a time, since they interplay with each other. As in the question of mechanism, a better understanding of the effect of reaction variables will have to await more fundamental studies involving plasma probing, etc.

Particle Size Studies. Electron microscopy studies of the solid polymer show it to be composed of spherical particles which tend to agglomerate in chains and clumps. The average sphere diameter of one sample was 0.12 microns. Using this value and a density of 1.10 gram/cc., the surface area of the sample was calculated to be 45 meter^2/gram. The experimentally determined area of the sample (nitrogen adsorption) was 42 meter^2/gram. Thus, the available surface is entirely on the outside of the spheres. Apparently, the cross-linking is so extensive that even nitrogen gas cannot enter into the polymer matrix.

A few experiments were performed to see whether the particle size could be regulated by changing the residence time. Table IV summarizes the data obtained.

Table IV. Particle Size and Residence Time

Res. Time (sec.)	*Range of Particle Sizes (microns)*	*Average Particle Size (microns)*	*Relative Particle Volume*
1	0.1-0.5	[a]	—
3	0.09-0.6	0.12	3.00
~5	0.06-0.5	0.14	4.76

[a] Not enough good particles for a meaningful average. Most of the exposures showed only cloudy blotches rather than discrete particles.

Although the particle size range shows no correlation with residence time, the volumes of the average particles in the 3 and 5 sec. experiments

Publication Date: June 1, 1969 | doi: 10.1021/ba-1969-0080.ch029

correlate well. The 5 sec. experiment was designed to give a 10 sec. residence time, but the discharge filled only about one-half of the reactor volume (thus, the residence time of *ca.* 5 sec.), suggesting that the particle size may have been limited by the exhaustion of the reactants. If fresh reactants could be continually supplied, the particles might grow larger. Of course, there may also be a natural limit caused by a precipitation phenomenon.

Literature Cited

(1) Austin, J. B., Black, I. A., *J. Am. Chem. Soc.* **52,** 4552 (1930).
(2) Davis, A. P. *J. Phys. Chem.* **35,** 3330 (1931).
(3) DeHemptinne, A., *Bull. Sci. acad. roy. Belg.* (3) **34,** 269 (1897).
(4) DeHemptinne, A., *Z. physik. Chem.* **22,** 358 (1897).
(5) *Ibid.*, **25,** 284 (1898).
(6) Harkins, W. D., Gans, D. M., *J. Am. Chem. Soc.* **52,** 5165 (1930).
(7) Jesch, K., Bloor, J. E., Kronick, P. L., *J. Polymer Sci.* 4, 1487 (1966).
(8) Kleinschmidt, R. V., *U. S. Patent* **2,023,637** (1930).
(9) Losanitsch, S. M., Jovitschitsch, M. Z., *Ber.* **30,** 135 (1897).
(10) Losanitsch, S. M., *Ber.* **41,** 2683 (1908).
(11) Potter, R. C., Bretton, R. H., Metz, D. J., *J. Polymer Sci.* 4, 2295 (1966).
(12) Stille, J. K., Sung, R. L., Vander Kooi, J., *J. Org. Chem.* **30,** 3116 (1965).
(13) Streitwieser, A., Ward, H. R., *J. Am. Chem. Soc.* **84,** 1065 (1962).
(14) *Ibid.*, **85,** 539 (1963).
(15) Vastola, F. J., Wightman, J. P., *J. Appl. Chem.* **14,** 69 (1964).

RECEIVED May 2, 1967.

Publication Date: June 1, 1969 | doi: 10.1021/ba-1969-0080.ch029

30

Chemistry of Electrical Discharge Polymerization

PETER M. HAY[1]

Central Research Laboratories, J. P. Stevens & Co., Inc., Garfield, N. J.

Publication Date: June 1, 1969 | doi: 10.1021/ba-1969-0080.ch030

Organic compounds were polymerized by a Tesla discharge acting on a mixture of nitrogen and the vapor of the organic compound at one atmosphere. The polymer was collected as a deposit on a moving plastic film passing between the electrodes. Easy solubility of most coatings indicated little cross-linking. Elemental analysis of the coatings found carbon, hydrogen, and nitrogen. Infrared spectra of polymers from benzene, toluene, and styrene were all similar and indicated the presence of oxygenated or nitrogenated groups in addition to an aromatic structure. It was tentatively concluded that the mechanism of reaction is fragmentation of the monomer by the electrical discharge followed by a complex recombination reaction.

The conversion of volatile organic compounds into liquid and solid products by the action of a high-voltage gas discharge has been observed by many people over the past 100 years or more (*5*). The literature of the past 40 years contains a large number of references to the effects of electric discharge on organic compounds and a complete review of all of these is beyond the scope of this paper. Many of the investigators were interested in the synthesis of derivatives having about the same molecular weight as the starting compounds and a few (*2, 4, 11, 18*) mentioned high-boiling liquid or solid by-products. Other investigators collected and analyzed solid products formed in electric discharge from butane (*2*), benzene (*10, 14, 18*), and tetrabromomethane (*6*) and other compounds, but little has been reported on the molecular structure of such products. Even in the older references the solid products have been referred to as polymers.

[1] Present address: Sandoz Inc., Hanover, N. J.

In Chemical Reactions in Electrical Discharges; Blaustein, B.;
Advances in Chemistry; American Chemical Society: Washington, DC, 1969.

In a few instances solid polymers have been made by electric discharge from vinyl monomers which are commonly polymerized by other means. Thus, styrene (*8, 13, 16*), vinyl acetate (*15*), methyl methacrylate (*8*), and numerous alkenes have been polymerized by exposure to discharge. The products usually were compared with polymers made from the same monomers by conventional catalysis and the close similarity of infrared spectra was used as evidence for similar molecular structure.

Recently some companies have been reported to be working on the application of electric discharge polymerization to coating of containers (*3*), steel strip (*21*), or fabric (*1*). These references all have indicated that the coatings would be formed under vacuum conditions. This imposes severe process limitations. The work described in this paper was carried out at atmospheric pressure, with the electrical discharge taking place in a mixture of nitrogen and volatile organic compounds, some of them vinyl monomers. One expectation was that the ionization of a vinyl monomer would start a vinyl polymerization reaction by an ionic mechanism or that an organic ion would decompose to a free radical and start a free-radical vinyl polymerization. The function of the nitrogen was merely for dilution of the organic monomer so that the reaction could be carried out in simple equipment at atmospheric pressure. The basic scheme was to lead a strip of fabric through a discharge polymer-polymerization zone and thereby coat it with deposit of polymer.

It was expected that the rate of polymerization would be small and for this reason some attention was paid to additives which might have the effect of increasing the yield of polymer. Brominated and chlorinated compounds were tried in view of their known influence on the course of other polymerization reactions (*17, 20*).

Experimental Methods

All polymerizations were carried out at room temperature in a mixture of organic vapors and nitrogen at a total pressure of one atmosphere. The gases were delivered to the reaction zone through the system shown schematically in Figure 1. Nitrogen passed through liquid monomer in one bubble tube and through additive in another tube. The nitrogen and entrained vapors entered the enclosed reaction chamber at one corner and exited to the atmosphere at the opposite corner. The ratio of monomer to additive was determined by weighing the tubes before and after the experiment.

Details of the reaction chamber are shown in Figure 2. Polymerization was initiated by corona discharge between two cylindrical, parallel, insulated electrodes (A) made by lining the inner surfaces of borosilicate glass tubing with aluminum foil. The glass tubing had a wall thickness of 2.5 mm. and an outside diameter of 62 mm. The two glass surfaces were separated by a gap of 4 mm. The alternating current high voltage was supplied by a Tesla generator, manufactured by Lepel High Fre-

Publication Date: June 1, 1969 | doi: 10.1021/ba-1969-0080.ch030

quency Laboratories, Inc. (Model HFSG-2). The peak voltage, as estimated by spark length in air, was about 20,000 volts. Because of the irregular wave-form in a Tesla circuit it was not considered practical to determine instrumentally the power consumed in the corona gap so no observations of chemical efficiency were possible. A moving strip of flexible substrate, (B) was positioned in the electrode gap. As shown in Figure 2, this substrate, which in most cases was 2-mil (50 microns) poly(ethylene terephthalate) film, was formed into a closed loop 47 cm.

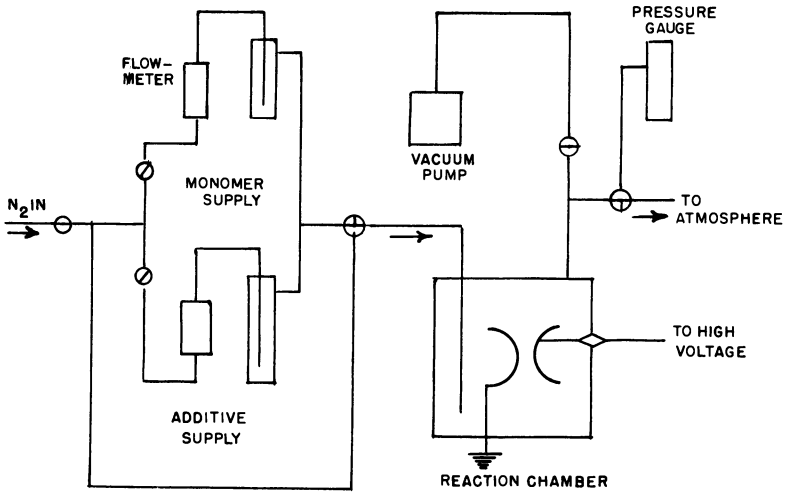

Figure 1. Vapor polymerization-schematic layout

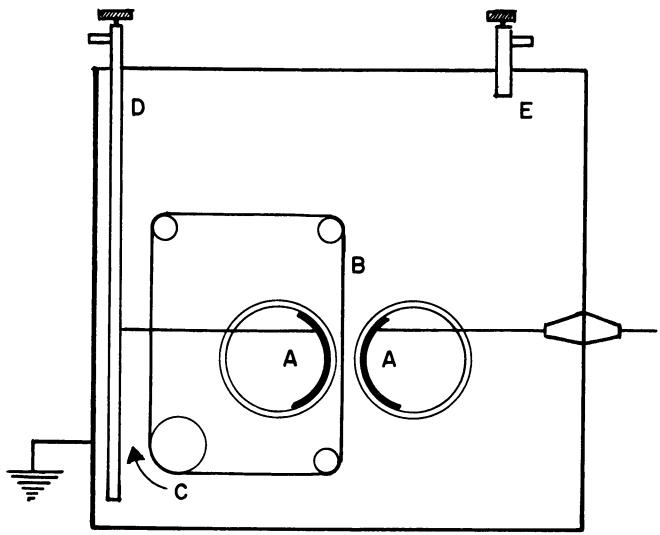

Figure 2. Vapor polymerization on moving substrate

Publication Date: June 1, 1969 | doi: 10.1021/ba-1969-0080.ch030

long and 5 cm. wide and was moved by the rotating roller, C. Vapors entered through D and exited through E.

Polymer which formed in the corona zone deposited both on the glass electrode coverings and on the moving substrates. The substrate strip was dried and weighed before and after the polymerization. The coated strips were also baked in a circulating air oven and reweighed. The final weight gain was taken as the yield. In some cases polymer was removed from the glass surfaces by solvent and recovered for infrared or chemical analysis.

Results

Survey of Polymerizable Compounds. A number of volatile organic compounds were subjected to corona discharge with a wide variety of results. In almost all cases a deposit of oily or solid brown material formed on the substrate strip. The weight gain resulting from 15 minutes of corona polymerization ranged from tenths of a milligram to over 30 milligrams. When the coated strips were heated at 150°C. for 10 minutes, part of the added weight was lost. Some of this loss is thought to be unreacted monomer which was absorbed by the substrate and coating. Another part of it could be very low molecular weight products of the corona reaction or be the result of thermal decomposition of the coating.

The compounds which gave the heaviest coatings after heating (taking into account the amount of monomer volatilized), included triallylamine, acrylonitrile, toluene, and styrene. As the list in Table I shows it is not necessary for the monomer to be a vinyl compound in the strict sense of the word for a non-volatile polymer product to form in corona discharge. Toluene, benzene, benzotrifluoride, and even acetone gave measurable yields. There seemed to be no pattern of relationship between the structure of a monomer and its yield in corona polymerization.

Table I. Corona-Polymerizable Compounds

Acetone	Ethyl Acrylate
Acrylic Acid	1-Octene
Acrylonitrile	Styrene
Allylamine	Toluene
Benzene	Vinyl Acetate
Benzotrifluoride	4-Vinylcyclohexene

Effect of Additives. It was found that many halogenated organic compounds, when added to the monomer being volatilized, had the effect of giving a higher yield. Chloroform, bromoform, and iodoform were more effective in increasing polymer yields from styrene than some other additives. The yields after oven heating are given in Table II, expressed as percent of styrene vaporized. It is interesting to note that the yield

Publication Date: June 1, 1969 | doi: 10.1021/ba-1969-0080.ch030

In Chemical Reactions in Electrical Discharges; Blaustein, B.;
Advances in Chemistry; American Chemical Society: Washington, DC, 1969.

is usually increased more by a moderate amount of additive and not so much by a larger amount. Bromine itself reacted immediately with the styrene in the bubble tube but produced the largest yield of all additives tested. Chlorine and iodine seemed to have the reverse or no effect.

Table II. Effect of Halogenated Additives on Corona Polymerization of Styrene Yield of Polymer as a Percent of Styrene Used

Additive	*Percent Added*	*Yield*	*Additive*	*Percent Added*	*Yield*
Chloroform	0.5	2.24	Chlorine	7	0.56
Bromoform	0.5	1.16	Bromine	1	1.90
Bromoform	1.0	1.42	Bromine	5	3.20
Bromoform	2.5	1.97	Bromine	10	1.67
Bromoform	5.0	1.92	Iodine	5	0.97
Bromoform	10.0	1.20	None	0	1.07
Iodoform	5.0	2.12	—	—	—

Other additives that enhanced the yields of styrene polymer were carbon tetrachloride, 1,2-dibromo-1,1,2,2-tetrafluoroethane, 1-bromobutane and 2-bromobutane. Yields from monomers other than styrene were not all increased by halogenated additives; some even were decreased. It was impossible to develop any rational relationship between monomer structure and susceptibility of the monomer to yield enhancement by halogenated additive.

The results given above were all derived from experiments in which the additive and the monomer were mixed and volatilized from a single bubble tube. Thus, the exact composition of the vapor was not known. A new set of experiments was carried out using separate bubble tubes for monomer and additive. The weight changes of the tubes during a run were used to calculate mole ratios of additive to styrene. The results of experiments with four additives are shown in Figure 3. The conversion to polymer of styrene without additives was 0.75 to 0.9%. As increasing amounts of bromoform, 1-bromobutane or 2-bromobutane were added, the conversion increased and then fell off again. The pattern of points in the case of 1-bromobutane was widely scattered but most of the points lay well above the level for styrene itself. With 2-bromo-2-methylpropane as an additive there was no significant increase in conversion. The weight gain from the additives alone, with no styrene, were all low compared with styrene.

In considering chemical explanations for corona polymerization, both free radical and ionic intermediates are possibilities. Experiments were run with various additives to styrene that might be expected to inhibit each kind of reaction through combination with the active intermediate but no clear-cut reduction in yield was observed. Benzoquinone at 1 and 2 mole % gave normal yields. Water and butylamine were extensively

Publication Date: June 1, 1969 | doi: 10.1021/ba-1969-0080.ch030

studied but, as Figure 4 demonstrates, the tendency for these supposed cation scavengers to depress the conversion is slight and not clear-cut. Butylamine by itself gave a surprisingly high yield. Ammonia, triethylamine, acetone, and carbon dioxide as additives had no substantial effect on yield.

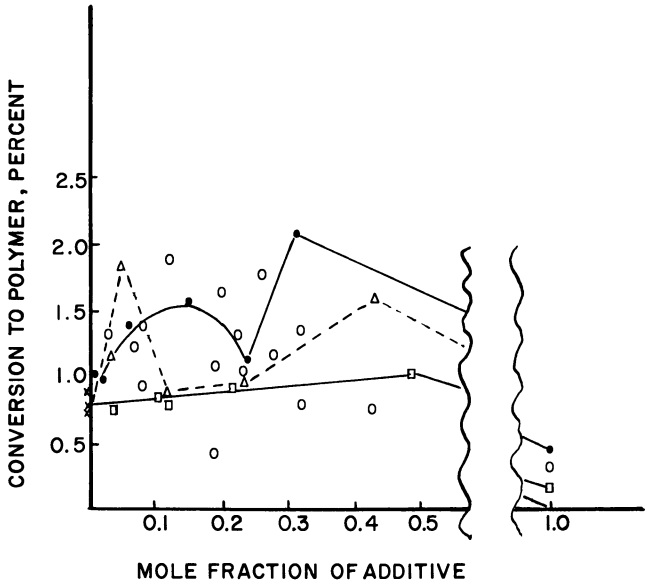

Figure 3. Effect of brominated additives on styrene polymerization

○ *Styrene with 1-bromobutane*
△ *Styrene with 2-bromobutane*
□ *Styrene with 2-bromo-2-methylpropane*
● *Styrene with bromoform*

Analytical Results

Some evidence was collected on the chemical nature of some of the products. The products deposited on the moving film and on the glass electrode covers were usually easily dissolved in common solvents like acetone, chloroform, and benzene, indicating low molecular weight and that there was little cross-linking. Infrared spectra were obtained of polymers made from benzene, toluene, styrene, and styrene mixed with 1-bromobutane.

The electrode deposits were dissolved in chloroform and films were cast on salt plates by evaporating the solvent. All the transmission spectra were similar to one another, as can be seen in Figures 5 and 6, and they

Publication Date: June 1, 1969 | doi: 10.1021/ba-1969-0080.ch030

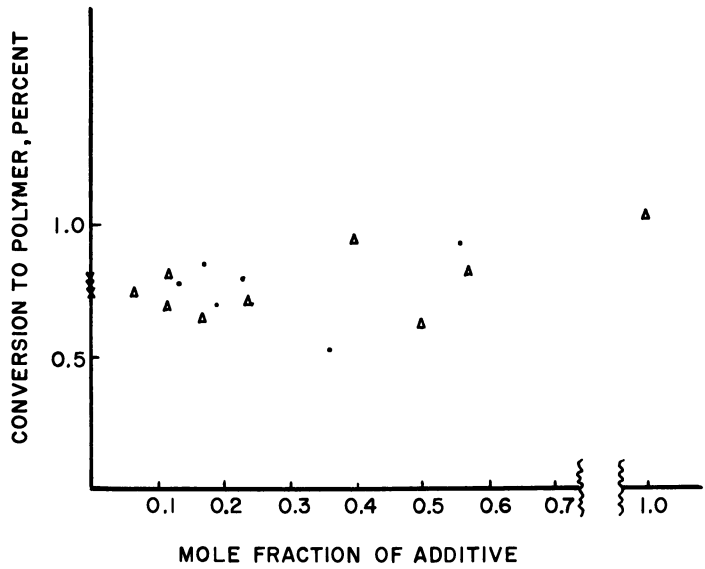

Figure 4. Effect of potential inhibitors on styrene polymerization

● *Styrene with water*
△ *Styrene with butylamine*

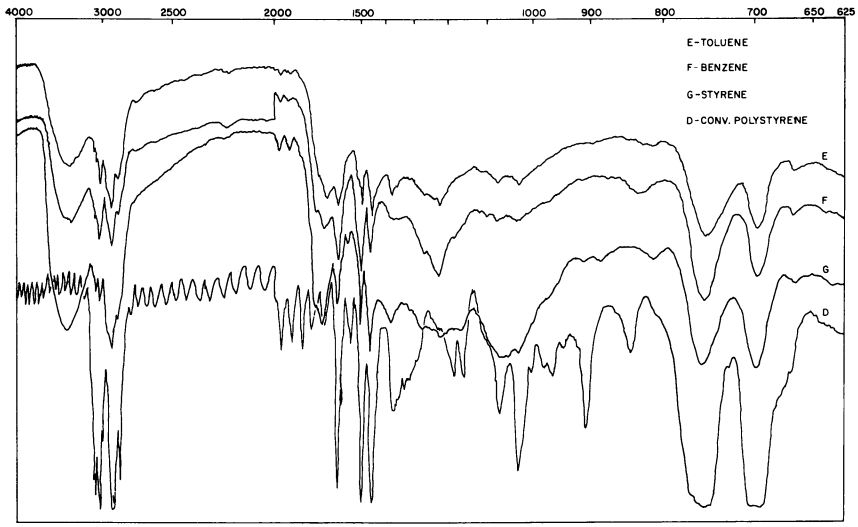

Figure 5. Infrared spectra of corona discharge polymers

had many of the same general features as the spectra published by Jesch, Bloor, and Kronick (*13*) and by Williams (*21*) for spectra of the insoluble coatings formed by glow discharge at low pressure.

Publication Date: June 1, 1969 | doi: 10.1021/ba-1969-0080.ch030

When compared with the spectrum of conventional polystyrene all the spectra show many of the same strong absorbances (two in the range 700–770 cm.$^{-1}$, three in the range 1400–1650 cm.$^{-1}$, and two in the range 2800–3000 cm.$^{-1}$) but, at the same time, lack the distinct absorption patterns of polystyrene found in the regions from 850 to 1400 cm.$^{-1}$ and 1800 to 1950 cm.$^{-1}$. In addition, all of the experimental spectra contain absorption bands not found in polystyrene—*e.g.*, 1220-1250 cm.$^{-1}$, 1700 cm.$^{-1}$, 3400–3500 cm.$^{-1}$. It is likely that these additional bands come from oxygen and nitrogen groups such as hydroxyl, amino, acid, ester, and amide.

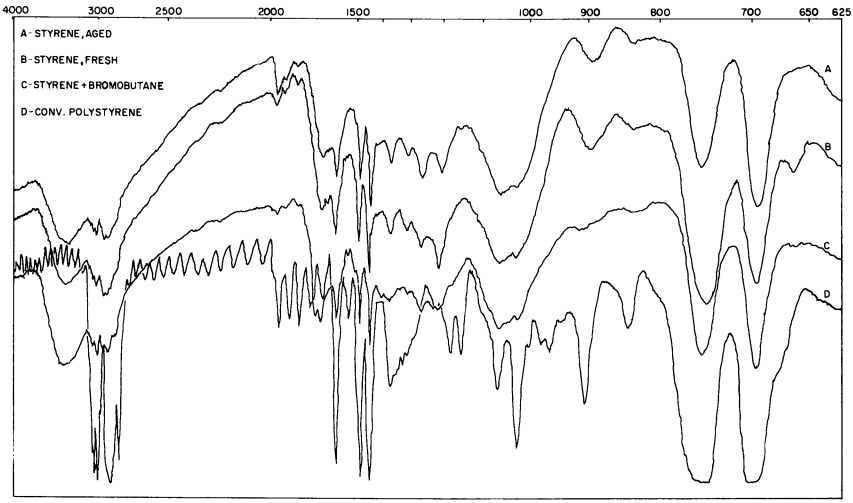

Figure 6. Infrared spectra of corona discharge polymers

The nitrogen-containing groups can arise from the reaction of active nitrogen in the discharge whereas the oxygen-containing groups may be formed by reaction of traces of water or oxygen in the discharge or they may result from combination of water and oxygen of the air with reactive groups left in the discharge polymers. An attempt to obtain spectroscopic evidence of such a post-reaction was not successful. As shown in Figure 6, there was little alteration in the spectrum of a styrene polymer upon aging overnight in the air.

The structure of the product from a mixture of styrene and 1-bromobutane, as far as is shown by the infrared spectrum of Figure 6, is the same as that from styrene alone.

The infrared spectra give evidence that substituted aromatic rings are a major component of these solids, along with various groups containing nitrogen or oxygen. Although a polystyrene structure (a long

Publication Date: June 1, 1969 | doi: 10.1021/ba-1969-0080.ch030

In Chemical Reactions in Electrical Discharges; Blaustein, B.;
Advances in Chemistry; American Chemical Society: Washington, DC, 1969.

carbon chain with pendant phenyl groups on alternate carbons) is a possibility, there is no direct evidence that this is the chemical structure of these products. The close similarity between spectra of products of benzene, toluene, and styrene suggests that all are of similar structure, possibly recombination products of fragments from a relatively severe breakdown of the respective monomers.

Other evidence of chemical composition was found in elemental analysis. The styrene product had considerably less carbon than styrene itself, as seen in Table III. It also contained a significant amount of nitrogen and, as determined by difference, a large amount of oxygen. Heating the polymer in air did not change the composition significantly. Styrene polymer made in the presence of 25 to 30 weight–% 1-bromobutane had almost the same analysis plus a significant bromine content.

Table III. Elemental Analysis of Corona Polymers

Monomer	*C*	*H*	*N*	*Br*	*O (by difference)*
Styrene, unheated product	72.23	6.86	3.2	—	17.71
Styrene, oven-heated	73.46	6.68	3.39	—	16.47
Styrene plus bromobutane					
unheated product	73.74	6.95	3.59	6.08	9.64
oven-heated product	73.29	6.69	3.56	6.97	9.49
Styrene, calculated	92.26	7.74	—	—	—
Bromobutane, calculated	35.06	6.62	—	58.32	—

Discussion

The salient features of the information presented above might be summarized as follows. In a mixture of organic vapor and nitrogen subjected to high-frequency, high-voltage, electrodeless discharge, the nitrogen, the organic compound, and trace amounts of oxygen and water are activated and combine chemically to yield products of higher molecular weight than the starting materials. These products condense on any solid surface available and may even undergo further chemical reaction within themselves and with more monomeric material which is not electrically activated.

The chemical mechanism of this series of reactions must be complex, possibly initiated by simple ionization through collision with a rapidly-moving electron followed by expulsion of two secondary electrons:

$$N_2 + e^- \rightarrow N_2^+ + 2e^- \text{ or}$$
$$RH + e^- \rightarrow RH^+ + 2e^-$$

These are the products ordinarily found in mass spectrometry and on exposure to gamma or beta radiation. These activated cationic products might activate vinyl polymerization or undergo other secondary

In Chemical Reactions in Electrical Discharges; Blaustein, B.;
Advances in Chemistry; American Chemical Society: Washington, DC, 1969.

reactions, yielding neutral free radicals or even anions, either of similar structure or in the form of fragments and combination or rearrangement products. In the present case there exists the further possibility that reaction products become reactivated, since they are formed in the presence of the high-voltage field, and undergo further reaction.

The simplest mechanism to consider would be polymerization of the vinyl monomers to long-chain products after initiation by some active species. The fact that non-vinyl compounds gave good yields may be explained through a mechanism involving some fragmentation of every monomer molecule and combination of the fragments to products of higher molecular weight. This leads to the likelihood that vinyl monomers are polymerized by this non-vinyl mechanism, rather than by an ionic or free-radical polymerization reaction.

The effect of various additives on a styrene polymerization reinforces the tentative conclusion that vinyl polymerization is not taking place. Even though yields were increased by halogenated additives they were not decreased by additives expected to act as scavengers for free-radical species (benzophenone) or ionic species (butylamine or water). Under an assumed mechanism of fragmentation and rapid recombination to condensed products, halogenated compounds additives may serve to increase the efficiency of energy transfer from the electric field to the monomer.

The fact that nitrogen is found in these discharge polymers might have been expected from previous reports on the chemistry of active nitrogen (*7, 9, 12*), some of which referred to solid products containing nitrogen that were formed by mixing electrically-activated nitrogen with unactivated organic molecules. In the case of the present report, the situation is complicated by the possibility of having both the nitrogen and the organic molecule be activated by the corona discharge.

It must be said that the chemical system reported here is sufficiently complex not to allow complete analysis. In addition, although the apparatus and conditions used in the experiments reported here proved adequate for coating a moving substrate, the properties and usefulness of the coatings were not suitable for practical use. Perhaps further research work on the complex chemical mechanism will lead to the means for improving the properties of the coatings.

Acknowledgments

The able assistance of Roger Kolsky and Walter Miner and the helpful analytical interpretations of Elliot Baum are gratefully acknowledged. Special thanks are due Paul Stam for his interest in and support of this research.

In Chemical Reactions in Electrical Discharges; Blaustein, B.;
Advances in Chemistry; American Chemical Society: Washington, DC, 1969.

Literature Cited

(1) Anon., *Manmade Textiles*, p. 58 (July, 1965).
(2) Badareu, E., Popovici, C., *Comun. acad. rep. populare Romine* **9**, 1249 (1959). *CA* **54**, 21952 (1960).
(3) Brick, R. M., Knox, J. R., *Modern Packaging*, p. 123 (January, 1965).
(4) Brown, G. P., Rippere, R. E., *Am. Chem. Soc., Div. Petrol. Chem.*, Preprints **2**, No. 3, 149 (1957). *C.A.* **54**, 24533 (1960).
(5) Charlesby, A., "Atomic Radiation and Polymers," p. 1, Pergamon Press, Oxford, 1960.
(6) Durie, R. A., Iredale, T., *Trans. Faraday Soc.* 44, 806 (1948). *C.A.* **43**, 3723 (1949).
(7) Evans, H. G. V., Winkler, C. A., *Can. J. Chem.* **34**, 1217 (1956). *C.A.* **51**, 1855 (1957).
(8) Goodman, J., *J. Polymer Sci.* 44, 551 (1960).
(9) Hanafusa, T., Lichtin, N. N., *J. Am. Chem. Soc.* **82**, 3798 (1960).
(10) Harkins, W. D., Gans, D. M., *J. Am. Chem. Soc.* **52**, 2578 (1930).
(11) Hiedemann, E., *Ann. Physik* (5) **2**, 221 (1929). *C.A.* **23**, 4858 (1929).
(12) Howard, L. B., Hilbert, G. E., *J. Am. Chem. Soc.* **60**, 1918 (1938).
(13) Jesch, K., Bloor, J. E., Kronick, P. L., *J. Polymer Sci.* A-1, **4**, 1487 (1966).
(14) Jovicic, M. Z., *Bull. Sci. acad. roy. Belg.* **13**, 365 (1927). *C.A.* **22**, 2114 (1928).
(15) Kikuchi, Y., *J. Sci. Hiroshima Univ.*, **Ser. A-11 25**, 319 (1961). *C.A.* **57**, 2400 (1962).
(16) Liechti, A., *Helv. Phys. Acta* **11**, 477 (1938). *C.A.* **33**, 6727 (1939).
(17) Potter, R. C., Bretton, R. H., Metz, D. J., *J. Polymer Sci.* **A-1**, 2295 (1966).
(18) Schuler, H., Prchal, K., Kloppenburg, E., *Z. Naturforsch.* **15a**, 308 (1960). *C.A.* **54**, 22012 (1960).
(19) Steinman, G. D., Lillevik, H. A., *Arch. Biochem. Biophys.* **105** (2), 303 (1964). *C.A.* **61**, 4198 (1964).
(20) Ueno, K., Hayashi, K., Okamura, S., *J. Polymer Sci.* **B3**, 363 (1965).
(21) Williams, T., *J. Oil & Colour Chemist's Assoc.* **48**, 936 (1965).

RECEIVED May 25, 1967.

Generation and Measurement of Audio-frequency Power for Chemical-Electrical Discharge Processes

JAMES C. FRASER

Research and Development Center, General Electric Company, Schenectady, N. Y.

Publication Date: June 1, 1969 | doi: 10.1021/ba-1969-0080.ch031

Various factors are involved in the design of an audiofrequency power supply for chemical-electrical discharge processes. Types of equipment include the inductor-alternator with step-up transformer and parallel-resonant tuned circuit, the SCR inverter with step-up transformer, and the vacuum tube high-power amplifier. The ratings of the major components of this equipment depend on, and are affected by, matching the discharge reactor load to the power supply operating characteristics. Electrical power consumed in the reactor is measured by the parallelogram-oscilloscope technique. Selecting the best combination of power supplies for a particular application depends upon the chemical requirements and the design of the corona reactor.

In developing equipment for use in high voltage, high frequency chemical-electrical processing, we have built a number of different types of "corona" power supplies. At the start, from the standpoint of the electrical equipment, let us use "corona" in this particular sense. We will define a "corona" discharge as an electric discharge produced by capacitively exciting a gaseous medium lying between two spaced electrodes, at least one of which is insulated from the gaseous medium by a dielectric barrier. This corona discharge may be maintained over wide ranges of pressure and frequency, although atmospheric pressure and frequencies in the audio range substantially above power transmission values are typically employed (*1*).

Since the power which can be dissipated in a corona reactor or cell is a function of the supply frequency, we have settled arbitrarily on the

In Chemical Reactions in Electrical Discharges; Blaustein, B.;
Advances in Chemistry; American Chemical Society: Washington, DC, 1969.

audio range (3,000 to 10,000 Hz.) as a desirable compromise. It is within the limits of rotating machinery and solid state components, presents no undue corona reactor heat dissipation problems, and provides a happy compromise between operating voltages, reactor size, and economy of operation (2).

The ratings for the basic electrical components are dependent upon the characteristics of the corona reactor and the impedance load which it represents to the power supply. Corona reactor values which affect these ratings are:

a. The corona power required
b. The electrode corona power density and, thereby, the electrode cooling or heat dissipation capability
c. The gaseous atmosphere present
d. The gaseous gap spacing
e. The barrier material and dielectric constant

From these values we can determine:

a. Peak voltage required to initiate corona
b. Barrier thickness required to withstand the total voltage across the barrier in the event of an arc across the gap
c. Barrier, gaseous gap, and total reactor capacitance
d. Maximum operating voltage
e. Capacitive charging, or displacement, current drawn by the reactor
f. Corona resistive current
g. Resultant load current
h. Power factor of the corona reactor load

The objectives which we attempted to meet in the design of our equipment were:

a. Suitability for use with a wide variety of corona reactors
b. Operation over a wide range of breakdown voltages
c. Flexibility over a wide range of operating conditions
d. Maximum electrical efficiency
e. Trouble-free operation and minimum maintenance over long periods of operation

Among the types of equipment built were the inductor-alternator with step-up transformer and parallel-resonant tuned circuit, the SCR inverter with step-up transformer, and the mobile vacuum tube high power-amplifier. In the discussion of this equipment which follows, it is intended only to consider some of the major components of a corona power supply and to outline to the chemist and the chemical engineer a general approach to audiofrequency power generation. Without the full details of a particular application, it is impossible to select the most

Publication Date: June 1, 1969 | doi: 10.1021/ba-1969-0080.ch031

In Chemical Reactions in Electrical Discharges; Blaustein, B.;
Advances in Chemistry; American Chemical Society: Washington, DC, 1969.

suitable equipment. The design of any corona power supply must start with the corona reactor specifications.

Motor-Alternator Set

A typical power supply based on rotating equipment consists of the following major components: an inductor-alternator, by means of which 60 cycle power is converted to 10,000 cycles, at 500 volts. This output is fed to the primary of a high voltage, high frequency transformer rated for 25 or 50 kv. at 10,000 cycles. The output of this transformer is fed, in turn, to a parallel resonant tuned circuit, the discharge reactor, and the high voltage instrumentation.

The KVA rating of the M-G Set (inductor-alternator) is determined by the product of the corona operating voltage and the resultant load current (or the corona power divided by the power factor). Since the corona power generated in a gaseous gap in series with a dielectric is directly proportional to frequency, and the upper limit for frequency for commercially available rotating equipment is about 10,000 Hz., this has generally been considered the optimum frequency. Also, the use of lower frequencies would require higher voltages or increased corona reactor capacitance for any given power level. The output voltage of the alternator can be any value consistent with usual generator practice and with the transformer primary voltage.

The KVA rating of the transformer will usually be the same as that of the inductor-alternator. Its secondary voltage will be determined by the corona reactor requirements for voltage breakdown of the gaseous gap. Secondary or load current will be the vector sum of charging, or displacement, current and resistive, or corona, current. Primary voltage must be consistent with alternator output voltage. If experimental flexibility is required, the transformer primary should be arranged for series-parallel connection.

The corona reactor represents a capacitive load on the major items of the power supply equipment, up to the time of corona initiation. Since this generally results in a poor power factor, there are two possible means of solution:

a. The motor-alternator set must be built with sufficient KVA capacity to meet the power factor and corona power requirements.

b. The transformer secondary and the corona reactor can be tuned with a parallel resonant circuit consisting of a choke and high voltage, vacuum capacitors. This provides power-factor correction so that the high voltage transformer secondary sees mainly the resistive load represented by the corona power.

The parallel-resonant circuit must be tuned to give maximum transformer output voltage for some arbitrarily selected value of alternator

Publication Date: June 1, 1969 | doi: 10.1021/ba-1969-0080.ch031

In Chemical Reactions in Electrical Discharges; Blaustein, B.;
Advances in Chemistry; American Chemical Society: Washington, DC, 1969.

field current. With a 0.16 henry choke, for example, the capacitance required for tuning at 10,000 cycles can be found from the expression—

$$f = \frac{1}{2\pi\sqrt{LC}}, \text{ or } C = \frac{1}{4\pi^2 f^2 L} \cong 1580 \text{ picofarads}$$

However, this value is reduced by the capacitance of the discharge reactor itself, by that of any instrumentation voltage dividers, and by stray capacitances, so that the actual tuning capacitance used is somewhat lower and must be determined experimentally.

The decision as to whether the motor-alternator should be built with increased KVA capacity or whether the secondary circuit should be tuned depends on the experimental versatility required, and on economic considerations. In general, the dollars per KVA for high frequency motor-alternator sets are considerably higher than for tuning circuit components.

An alternator field-control chassis supplies and regulates the current for the alternator field windings, and has a feedback system designed to meet varying conditions of high voltage output. Alternator output voltage and, thus, transformer high voltage are raised and lowered by changing alternator field current. A magnetic amplifier stabilizer circuit maintains constant high voltage output. In the event of a decrease in high voltage, it calls for an increase in alternator field current, with a corresponding output voltage increase.

Control devices and instrumentation for a corona power supply based on rotating equipment includes at least the following:

a. Provision for varying the transformer output high voltage from zero to maximum by varying alternator field current, and a means of measuring the field current.

b. Provision for measuring transformer primary voltage, current, and power.

c. Provision for measuring the peak voltage applied to the corona reactor.

d. Provision for measuring the power dissipated in the corona reactor.

e. Some form of protective current overload relay, for removing high voltage from the corona reactor in the event of a short circuit in the reactor, or a low voltage, high current arc between the electrodes. This will prevent exceeding the current rating of the transformer secondary.

Since the use of this equipment involves working with high voltage, the control circuit includes provision for test area safety interlocks and flasher-warning lights.

Figure 1 shows the basic power and instrumentation circuit for a typical power supply based on the M-G (motor-generator) set.

Publication Date: June 1, 1969 | doi: 10.1021/ba-1969-0080.ch031

In Chemical Reactions in Electrical Discharges; Blaustein, B.;
Advances in Chemistry; American Chemical Society: Washington, DC, 1969.

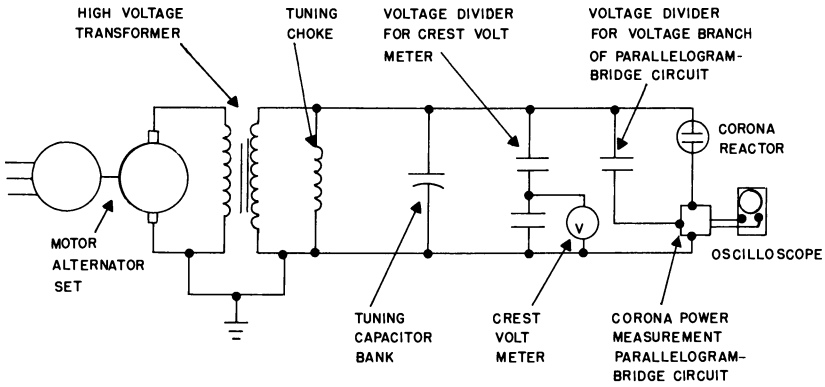

Figure 1. Basic power and instrumentation circuit

Inverter

The solid state corona generator consists of a 3,000 cycle inverter utilizing silicon controlled rectifiers feeding a step-up transformer. A rectifier is a device or circuit for changing alternating current to direct current. The inverter may be thought of as a rectifier operating in reverse, changing d.c. to a.c. A combination of the two achieves a change from 60 cycle a.c. to approximately 3,000 cycle a.c.

Rectifier circuits occur in several configurations such as half-wave, full wave, bridge, etc. Inverter circuits may be grouped in a similar manner. The key feature of an SCR (silicon controlled rectifier) as used in an inverter circuit is that a small current from its "gate" element to the cathode can fire or trigger the SCR so that it changes from being an open circuit into being a rectifier.

The inverter operates from a single phase, 220 volt, 60 cycle source, and by means of a full-wave bridge rectifier, rectifies it to 187 volts d.c. which in turn is changed to 150 volts, 3,000 cycles, approximate sine wave through SCR's. Variac control of the 220 volt input provides a variable supply output.

The inverter output is fed to a step-up transformer delivering up to 12,000 volts r.m.s. This transformer is a dry type, potted with silicone rubber, with integral high voltage terminals. The particular transformer used was built as a compromise between low cost, size, and electrical capability. Rated at 3 KVA, the transformer was only 6 inches $\times$ 6 inches $\times$ 7 inches high overall.

What is noteworthy with this equipment is that the inverter, transformer, and corona reactor are not independently operating components. The concentric cylinder corona reactor was so designed that its capacitance, reflected to the primary of the transformer, formed a part of the

In Chemical Reactions in Electrical Discharges; Blaustein, B.;
Advances in Chemistry; American Chemical Society: Washington, DC, 1969.

inverter LC circuit, as did the inductance of the high voltage transformer. The reactor gaseous gap conductance forms a part of the inverter load circuit.

Since this is an untuned high voltage circuit, the inverter and the transformer were designed to carry the power factor loss current.

Advantages of the inverter supply over the motor-alternator are the absence of moving parts, ease of mounting and installation, and the "module" or building block concept whereby units can be stacked to increase voltage and current capability.

Figure 2 shows the basic inverter circuit. In operation as a corona generator, capacitor C is replaced by the step-up transformer and corona reactor.

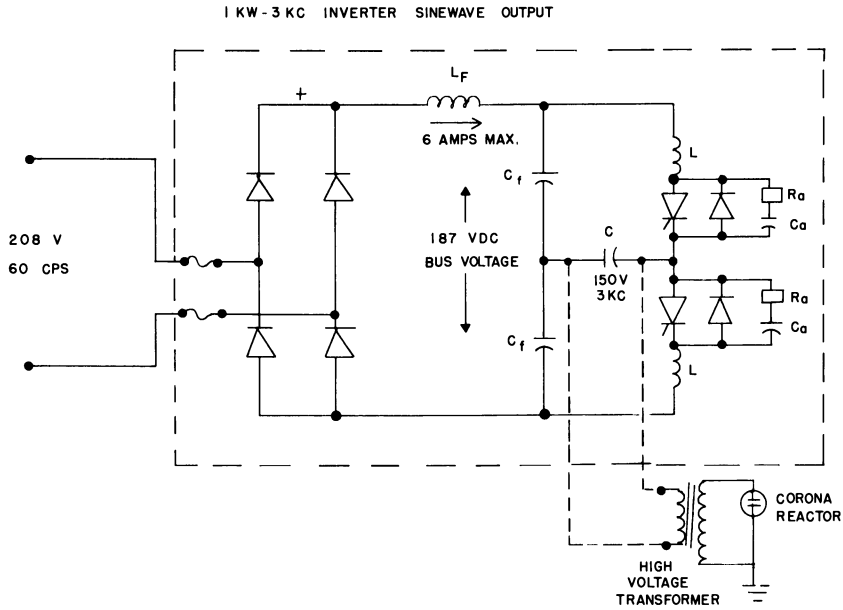

Figure 2. Basic inverter circuit

Vacuum-Tube Amplifier

The mobile corona generating equipment was designed for operation over a wide range of frequency and voltage. Corona power is generated by a vacuum tube, high-power amplifier driven by a stable low-power, audiofrequency sine-wave oscillator. Power is taken from the secondary winding of a high-voltage step-up transformer, with one end at ground potential.

The corona output voltage may be varied from zero to 50,000 volts, depending on the impedance of the applied load, and on the settings of

In Chemical Reactions in Electrical Discharges; Blaustein, B.;
Advances in Chemistry; American Chemical Society: Washington, DC, 1969.

the frequency and amplitude controls located on the master sine-wave oscillator panel. The frequency of the output voltage is determined by the master oscillator and is independent of load impedance or output voltage level. The frequency may be varied instantaneously between the rated limits of 3 to 10 kilocycles per second.

The a.c. power from the 60 c.p.s. line is converted into the high voltage variable frequency output as follows:

A master oscillator feeds a driver amplifier. This in turn drives a tetrode power amplifier stage and the output step-up transformer. A d.c. plate supply source, a screen grid voltage supply, a control grid bias supply, and an a.c. filament supply feed power at appropriate voltage levels to the tetrode amplifier stage. The power line control circuitry incorporates on-off switching, circuit breakers, and starting contactors for the power amplifier supplies.

Power amplification is produced by four tetrode vacuum tubes connected in pushpull-parallel as a Class AB_2 amplifier. Control of the master audio oscillator signal amplitude is provided by a potentiometer on the master control panel. The output voltage of the equipment may be reduced to zero even when full voltage is applied to the plates of the power tetrodes.

Power delivered by the tetrodes to the output transformer, and thence to the corona reactor load, is controlled by the oscillator and the variable autotransformer in the tetrode plate power supply. The autotransformer control keeps the total power consumed by the equipment during an experiment as low as possible, to minimize heat developed in the cabinet and to extend tube life.

The corona cell impedance, which is mainly capacitive before corona breakdown, acquires a resistive component after breakdown which depends on the rate of production of ionized and electrically conducting chemical entities. The a.c. voltage at the plates of the power tetrodes will lag the plate current by a large angle before power is consumed, and the plate current will be collected at a high rather than a low value of plate voltage. Thus, the power dissipated by the tetrodes will be high under no-load conditions.

The high voltage transformer has an effective primary to secondary step-up ratio of 11 to 1. The maximum a.c. current that can be drawn from the secondary winding of the transformer is 60 milliamperes r.m.s.

Figure 3 is a block diagram of the vacuum-tube amplifier equipment.

Reactor

The corona reactor or cell represents a capacitive load to the power supply equipment up to the time of initiation of the electrical discharge.

Publication Date: June 1, 1969 | doi: 10.1021/ba-1969-0080.ch031

In Chemical Reactions in Electrical Discharges; Blaustein, B.;
Advances in Chemistry; American Chemical Society: Washington, DC, 1969.

The total reactor capacitance consists of the series combination of dielectric barrier and gaseous gap capacitance. The voltages appearing across the barrier and the gap divide inversely as their capacitance.

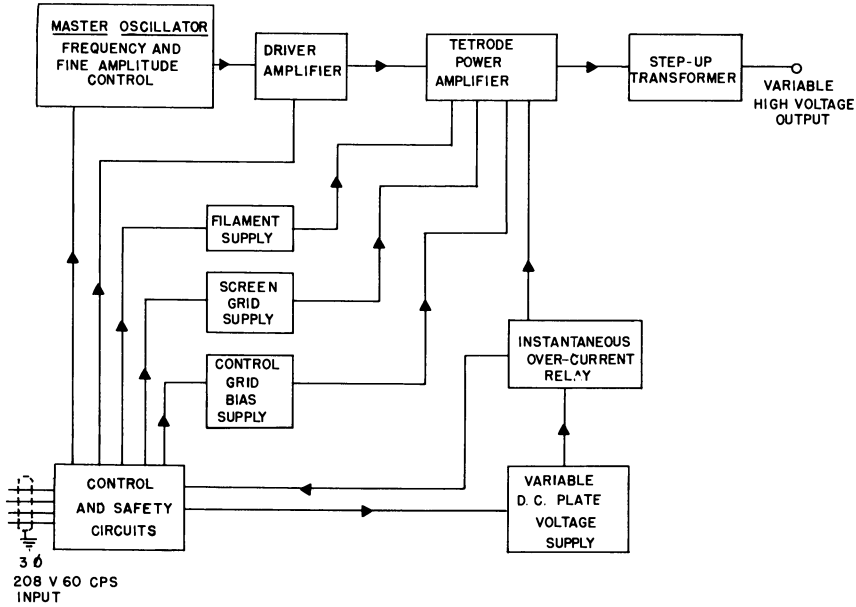

Figure 3. Vacuum-tube amplifier equipment

Before corona starts, the reactor current consists of the charging, or displacement, current which is proportional to the applied voltage, frequency, and cell capacitance. After the start of corona, the cell acts as an impedance load consisting of a conductance across the gaseous gap, in addition to the gap capacitance. The total current drawn by the reactor then is the vector sum of charging plus resistive currents.

If the corona reactor power supply has a tuned circuit in the transformer high voltage secondary, for power factor correction, the corona reactor capacitance functions as part of the tuning capacitance, and the reactor charging current is a part of the circulating current in the parallel resonant circuit. The total load current through the transformer secondary winding then consists chiefly of corona current plus whatever capacitive current might be present as a result of tuning unbalance.

If the power supply is untuned, the total power available for chemical processing is the product of supply volt-amperes times the power factor of the load, and in this case the transformer secondary winding must carry the full reactor impedance current.

Publication Date: June 1, 1969 | doi: 10.1021/ba-1969-0080.ch031

In Chemical Reactions in Electrical Discharges; Blaustein, B.;
Advances in Chemistry; American Chemical Society: Washington, DC, 1969.

The dielectric barrier in the corona reactor serves as a built-in current-limiting device, or ballast in the event of a short circuit or arc between the cell electrodes, so that the stored energy is dissipated in the barrier at breakdown.

The maximum power density at which a corona reactor can be operated without puncturing the barrier is a function of the dielectric strength of the barrier material, the total thickness of the barrier, the ambient temperature in which it is operated, and the gap spacing between barriers. The dielectric constant of the barrier affects both the voltage gradient across the barrier, and the corona power which can be dissipated in the reactor. The dissipation factor is a measure of the electric losses which produce heating of the barrier.

The voltage at which breakdown will occur between a set of electrodes in a corona reactor depends upon the gaseous atmosphere present, the density (pressure, temperature) of the gas between the electrodes, and the gap length.

The corona power dissipated in a gaseous gap in series with one or more dielectric barriers can be calculated from the expression (*3, 4*)

$$P = 4fC_bV_{gas}\left(V_{max} - \frac{C_{gas}}{C_t}V_{gas}\right), \text{ where}$$

P = Corona power in watts
f = Power supply frequency in cycles/second
C_b = Dielectric barrier capacitance
C_{gas} = Capacitance of corona cell gas gap
C_t = Total corona cell capacitance
V_{gas} = Peak voltage across the gaseous gap at the time of corona initiation
V_{max} = Total operating voltage applied to the corona cell

This can be re-written as:

$$P = 4fC_bV_{gas}(V_{max} - V_t), \text{ where}$$

$$V_t = \frac{C_{gas}}{C_t}V_{gas} = \text{voltage across the corona cell at the instant of corona initiation}$$

An item of concern to all, in evaluating an experiment, or in scaling up for pilot plant operation, is the electrical efficiency of a process. Care must be taken not to confuse equipment power factor with what might be called "electrical efficiency of conversion," though both may contribute to the same end result. Power factor relates to ability to convert equipment input volt-amperes (not necessarily in phase) to available chemical-result-producing "watts." This is a function of electrical equipment and electrical circuit design.

"Electrical efficiency of conversion" may be considered as the effectiveness in utilizing all or most of the available wattage in the corona reactor. This is a function of reactor design, with particular emphasis

Publication Date: June 1, 1969 | doi: 10.1021/ba-1969-0080.ch031

In Chemical Reactions in Electrical Discharges; Blaustein, B.;
Advances in Chemistry; American Chemical Society: Washington, DC, 1969.

on relative barrier and gap capacitance and gap spacing. As a matter of practical design, the cell geometry and gap spacing present limits to the power which can be dissipated in any given cell.

Power Measurement

The power consumed in the discharge cell is determined by means of the parallelogram-oscilloscope technique which shows the relationship between the voltage on the cell electrodes at any instant, and the charge flow in the circuit up to that instant. Before corona initiation, the corona null value is seen on the oscilloscope as a closed figure, or slant line. With the initiation of the electrical discharge, the figure opens up into a parallelogram, and the discharge power is represented by the area of the parallelogram.

The bridge circuit for power measurement consists of two branches between the high voltage terminal of the reactor and ground, called "Voltage" and "Charge." The "Voltage" branch consists of a capacitance voltage divider giving an approximate 10^4 to 1 voltage division. The "Charge" branch consists of the corona reactor in series with some value of capacitance such that a voltage division of 10^4 or 10^3 to 1 will be obtained across the divider. The outputs from the low voltage ends of these dividers are fed to the X and Y axes of the oscilloscope. A variable potentiometer across the lower end of the "Charge" divider provides phase shift control to bring the "Voltage" and "Charge" branch outputs into phase for a null reading on the scope.

It should be noted that two signals, of equal amplitude, in phase, fed to the X and Y axes of a scope, give a 45-degree line on the scope. Any variation of relative amplitude shifts the angle of the line.

The area of the parallelogram represents the total power dissipated in the cell when the parallelogram bridge circuit and the oscilloscope are calibrated in the following manner:

The X-axis deflection is calibrated with a peak reading voltmeter so that reactor voltage (peak-to-peak) is presented as volts per cm. of scope deflection.

The Y-axis deflection is calibrated with the known value of capacitance in the grounded end of the "Charge' 'branch so that the charge flowing through the reactor is presented as coulombs per cm. of scope deflection.

The $X - Y$ product, then, is—

$$\left(\frac{\text{volts}}{\text{cm.}}\right)\left(\frac{\text{coulombs}}{\text{cm.}}\right) = \frac{\text{volts} - \text{coulombs}}{\text{cm.}^2}, \text{ or } \frac{\text{watt-seconds}}{\text{cm.}^2}$$

Publication Date: June 1, 1969 | doi: 10.1021/ba-1969-0080.ch031

In Chemical Reactions in Electrical Discharges; Blaustein, B.;
Advances in Chemistry; American Chemical Society: Washington, DC, 1969.

Since this is the energy per cm.^{2} in one cycle, the power per cm.^{2} of parellelogram area is obtained by multiplying the energy per cycle by the frequency in reciprocal seconds. The parallelogram area can be determined by planimeter measurement of a Polaroid picture, or by direct measurement.

With a dual beam oscilloscope it is also possible to view the voltage and charge waveforms simultaneously.

Figure 4 shows the parallelogram-oscilloscope bridge circuit for corona power measurement.

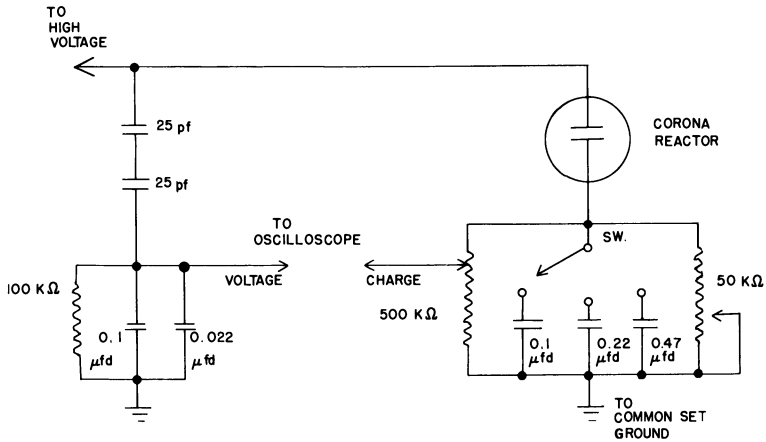

Figure 4. Corona power measurement (parallelogram-oscilloscope bridge circuit)

Literature Cited

(1) Coffman, John A., Browne, William R., *Sci. Am.* **212 (No. 6)**, 91 (June, 1965).
(2) Dibelius, N. R., Fraser, J. C., Kawahata, M., Doyle, C. D., *Chem. Eng. Progr.* **(No. 6)**, 41 (June, 1964).
(3) Manley, T. C., *Trans. Electrochem. Soc.* **84**, 83 (1943).
(4) Parker, E. J., *Marconi Instr.* **8 (No. 7)**, 157 (Sept., 1962).

RECEIVED June 12, 1967.

32

Chemical Engineering Aspects of Chemical Synthesis in Electrical Discharges

J. D. THORNTON

Department of Chemical Engineering, Merz Court, The University, Newcastle Upon Tyne, 2, England

Publication Date: June 1, 1969 | doi: 10.1021/ba-1969-0080.ch032

A basis for the classification of gaseous electrical discharge (G.E.D.) reactors is proposed and the requirements for economic synthesis outlined. Possible methods of increasing the yields of products by reducing the rate of reverse and degradative reactions are discussed and illustrated by reference to hydrazine synthesis from gaseous ammonia. A promising approach is to reduce the residence time of the product in the discharge zone either by selective absorption with an inert liquid absorbent or by the use of pulsed discharge techniques. Although it is not yet possible to predict quantitatively the effects of reactor scale-up upon the course of chemical reactions, it is possible that the problems of handling commercial scale reactant flow rates might be solved more economically by stepping-up procedures.

Although numerous investigations have been published dealing with the effects of electrical discharges upon chemical reactions, most of the work is fragmentary in the sense that even now no clear picture has emerged of the relative importance of discharge characteristics and reactor geometry upon the reaction yield. This is largely because no systematic studies have been undertaken with a fixed reaction system covering a reasonably wide range of discharge conditions and reactor configurations. Furthermore most of the published work has been concerned with laboratory-scale investigations so that, with the possible exception of ozone synthesis, little or no attention has been paid to the chemical engineering problems involved in gas phase electrosynthesis. This is no doubt consequent upon the low yields obtained in many laboratory studies and is unfortunate insofar as a proper application of the engineering factors affecting the reactor efficiency could, in many cases, lead to considerably improved reaction yields.

In Chemical Reactions in Electrical Discharges; Blaustein, B.;
Advances in Chemistry; American Chemical Society: Washington, DC, 1969.

Whereas physical chemistry is usually concerned with the individual kinetic steps contributing to a particular reaction scheme, chemical engineering is concerned with the translation of the laboratory reaction to a full scale continuous process wherein the desired reaction product is produced at the lowest capital and operating costs. Chemical engineering is therefore concerned with optimization with respect to economic factors and operating conditions must be chosen so that the maximum product yield is obtained for the lowest energy expenditure. In the context of gaseous electrical discharge (G.E.D.) reactors, this implies that conditions should be chosen such that both the energy yield (expressed as grams product per kilowatt-hour) and the percentage conversion of reactant per pass should be high. Unfortunately, at the present time, little is known about the way in which either of these factors depend upon operational parameters and it is therefore necessary to undertake extensive laboratory studies for each system of interest.

Publication Date: June 1, 1969 | doi: 10.1021/ba-1969-0080.ch032

In principle it might be expected that the energy yield and the conversion per pass would depend upon such factors as:

(a) Operating pressure
(b) Gas flow rate
(c) Electrical Discharge characteristics
(d) Reactor, including electrode, geometry
(e) Surface properties of the reactor and electrodes
(f) Reactor size

If, therefore, the effects of such variables were studied for a single system much useful information would be obtained which would help to put the whole subject on a more fundamental basis. In practical terms, it is not necessary to have a detailed step by step knowledge of the reaction kinetics in order to design the reactor so long as an empirically determined rate equation is available which describes adequately the influence of the operational variables upon the net rate of reaction. Clearly a more informed approach to the design problem is possible when fundamental data are available but this is seldom the case at the design stage.

Types of Reactors

In the case of gas discharge synthesis, an economically acceptable reactor should fulfill three requirements:

(a) High energy yield (grams per kilowatt-hour).
(b) High percentage conversion per pass.
(c) High degree of selectivity for the desired product—*i.e.*, side reactions with their consequent wastage of material and energy should be reduced to a minimum.

In Chemical Reactions in Electrical Discharges; Blaustein, B.;
Advances in Chemistry; American Chemical Society: Washington, DC, 1969.

These criteria in turn imply that four conditions must be observed which relate to the reactor geometry as well as the mode of operation.

(a) Care must be taken to ensure that unsuitable reactor geometries are not employed in which a sizeable fraction of the reactant by-passes the discharge zone.

(b) The type of discharge employed must be associated with a high level of activation with respect to the desired reaction.

(c) The residence time distributions of the reactant and product should be such that the reaction reaches equilibrium without subsequent degradation of the products.

(d) Steps must be taken to eliminate parallel reactions which compete for the reactant and reverse or degradative reactions which consume the product.

Publication Date: June 1, 1969 | doi: 10.1021/ba-1969-0080.ch032

While (a) above is purely a question of engineering design, conditions (b), (c), and (d) are influenced by the chemical system employed. Although no generalized picture has yet emerged of the ways in which discharge characteristics and residence time distributions affect reactor performance, some specific comments can be made in relation to hydrazine synthesis from ammonia, based on studies currently being carried out in this department. Furthermore, it is possible to indicate some promising techniques for the minimization of unwanted reactions such as those mentioned in (d) above.

First of all, it is useful to consider the basic electrode geometries that can be employed in G.E.D. reactors. Although no formal reactor classification has been proposed hitherto, the electrode configuration and the direction of gas flow in relation to the discharge can be made the basis of a convenient system of classification. Thus, the electrodes may consist of parallel plates, co-axial cylinders or a pair of points while the gas flow may be parallel or at right angles to the plane of the discharge. Figure 1 shows in diagrammatic form the seven various electrode and flow arrangements on the basis of this classification. Parallel flow in parallel plate and co-axial electrode reactors necessitates the use of porous electrodes through which the gas phase flows as shown in Figures 1.1 and 1.2. On the other hand, the commoner cross-flow arrangements shown in Figures 1.4, 1.5, and 1.6 usually employ impervious metal electrodes, there being no necessity for the reactants to flow through the electrodes themselves. The usual parallel/point and cross-flow/point reactors are depicted in Figures 1.3 and 1.7 respectively.

The distinction between parallel-flow and cross-flow is not an academic one by reason of the non-uniform nature of the electric field in many of these reactor arrangements. In most of the laboratory investigations reported in the literature, the areas of the electrodes are small and little or no attempt has been made to minimize edge effects by the use

In Chemical Reactions in Electrical Discharges; Blaustein, B.;
Advances in Chemistry; American Chemical Society: Washington, DC, 1969.

of suitable electrode profiles. The field intensity is therefore a function of position in the inter-electrode gap. Furthermore, the use of co-axial geometries where the respective electrode radii are very different also give rise to highly non-uniform fields in the vicinity of the central electrode. It follows, therefore, that the overall activation effects might well be different in the parallel/parallel (Figure 1.1) and cross-flow/parallel systems (Figures 1.4 and 1.5). In the former case, molecules traversing a center-line path will encounter electrons of different energies to molecules following a peripheral path while, in a cross-flow reactor, all the molecules encounter electrons with a wide spectrum of energies. In co-axial reactors, the position is further complicated by virtue of the non-uniform field associated with the central electrode. Thus, in Figures 1.2 and 1.6 not only is there a transverse field variation but there is also an axial variation as the molecules approach the bottom and top planes of the outer electrode.

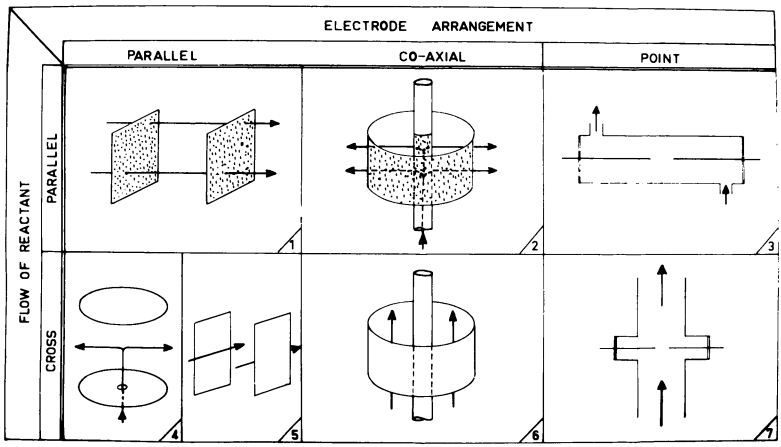

Figure 1. Basic reactor geometries

Such considerations are purely speculative at the present time because no experimental data are available which would enable a direct comparison of reactant conversion for parallel and cross-flow systems to be made for the same reactants under similar conditions. Nevertheless, these factors must be borne in mind when interpreting the influence of reactor geometry on a quantitative basis.

Co-axial electrode systems in which the reactant flows through the annular space between the two electrodes have an advantage in that all the reactant molecules must pass through the discharge. There is, therefore, no by-passing and subject to suitable electron energies, there will be a high level of activation in the gas phase. Such conditions are difficult

In Chemical Reactions in Electrical Discharges; Blaustein, B.;
Advances in Chemistry; American Chemical Society: Washington, DC, 1969.

to achieve in parallel plate arrangements unless the reactant is introduced at the center of one of the electrodes as in Figure 1.4. Much work has been reported with point electrode systems such as those illustrated in Figures 1.3 and 1.7, and here it is difficult to see how by-passing of the discharge can be avoided. Furthermore, the flow pattern within the reactor is also dependent upon the turbulence level so that changes in the gas flow rate will almost certainly be accompanied by corresponding changes in the fraction of the gas stream by-passing the discharge zone.

All the reactor systems discussed so far can be described as homogeneous in the sense that only a single, gaseous phase is present in the reactor. In many instances, however, it is advantageous to remove one or more products of reaction as rapidly as possible in order to minimize subsequent reactions which would adversely affect the primary reaction yield. A convenient method of achieving this involves the introduction of a second phase into the discharge zone in the form of a liquid absorbent (*12, 13, 14, 15, 16*) or fluidized adsorbent (*23*). In principle, a second phase can be introduced between any of the electrode arrangements shown in Figure 1. This modification gives rise to a second series of reactor systems which will be referred to subsequently as heterogeneous reactors.

Publication Date: June 1, 1969 | doi: 10.1021/ba-1969-0080.ch032

Discharge Characteristics and Electrode Arrangement

For optimum performance it is necessary to ensure that the reactants have suitable residence times in that part of the discharge zone where activation is most favored. In this connection it will be recalled that the relative rate of ammonia synthesis from its elements has been shown to be greatest in the region of the cathode potential drop (*2, 3*), while in the case of hydrazine synthesis from ammonia, the significant fraction of the discharge is the positive column region (*7*). In theory, it is desirable to be able to predict the discharge conditions necessary for optimum conversion in any particular reaction; in practice, however, this is not yet possible. This is because in the past it has been customary to describe discharges in general terms such as glow, arc, or silent discharges without regard to the local or point properties existing in different parts of the discharge zone. Since there is a gradual transition between one regime and the next, qualitative descriptions of this type are not of great value in interpreting reaction rate data. Any fundamental correlation of rate data with discharge characteristics would involve not only a knowledge of the concentrations and energy distributions of the various species present in the discharge space, including electrons, but also an understanding of the way in which the probability of excitation varied with electron energy. A typical example of the way in which the degree of

In Chemical Reactions in Electrical Discharges; Blaustein, B.;
Advances in Chemistry; American Chemical Society: Washington, DC, 1969.

excitation is dependent upon electron energy is shown in Figure 3 which depicts total cross section curves for argon and neon (*11*). The cross section to an *mn* type transition by electron collision is zero when the electron energy is less than the energy required to raise a valency electron of an atom from the m^{th} to the n^{th} level, but increases with electron energy to a maximum after which any further increase in electron energy is accompanied by a decrease in the value of the total cross section. There is, therefore, an optimum value of the electron energy corresponding to the maximum cross section for the process under consideration. It is the lack of data of this type together with a knowledge of the reactive species present in the discharge that makes it difficult to correlate reaction rates with discharge parameters for systems of engineering interest.

Nevertheless, despite the absence of fundamental information relating to the activation characteristics of discharges, one or two general observations can be made with regard to the nature of the discharges commonly employed. All the reactor geometries discussed so far, and illustrated diagrammatically in Figure 1, employ the same type of discharge in the sense that both electrodes are located within the reactor and are, therefore, in contact with the reactant gas. This class of discharge in which electrons pass freely between the two electrodes is represented schematically in Figure 2a. An alternative type of discharge which has been used frequently is the so called barrier discharge shown diagrammatically in Figure 2c. Here one of the electrodes is separated from the gas phase by means of a dielectric barrier such as quartz so that the reactor may be looked upon as a combination of capacitive and resistive loads. In practice, a dielectric barrier may be employed in conjunction with any of the reactor geometries shown in Figure 1. This arrangement has the advantage of providing a more uniform type of discharge which is current limited so that the build up of spark or arc type discharges is avoided. If this principle is carried to its logical conclusion, both electrodes may be isolated from the reactant gas and molecular excitation set up by applying a high frequency potential to the external electrodes or by induction from an external conductor carrying a high frequency current (Figure 2d). This type of "electrodeless" reactor has not been mentioned in the classification discussed above but is of interest since in the absence of metal electrodes in the gas phase, the degree of dissociation of the gas and therefore the concentration of atoms would be expected to be high (*20*). The high concentration of atomic species in such discharges is evidenced by the after glow phenomena frequently encountered in electrodeless systems.

One type of electrodeless system which might well prove of interest in electrosynthesis is the microwave discharge. Here the degree of activation can be high (*19*) and it has been reported that the atomic yields in

Publication Date: June 1, 1969 | doi: 10.1021/ba-1969-0080.ch032

In Chemical Reactions in Electrical Discharges; Blaustein, B.;
Advances in Chemistry; American Chemical Society: Washington, DC, 1969.

hydrogen, nitrogen, and oxygen are approximately ten times greater than the yields of atoms and radicals in low frequency and direct current discharges at the same field strength and pressures. From the engineering point of view, microwave systems have the added advantage that they can be sustained at higher pressures but on the other hand the detailed economics still require evaluation.

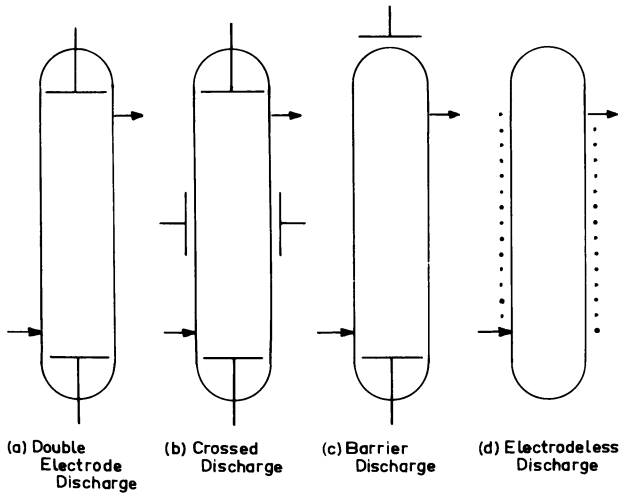

Figure 2. Diagrammatic electrode arrangements for various discharge conditions

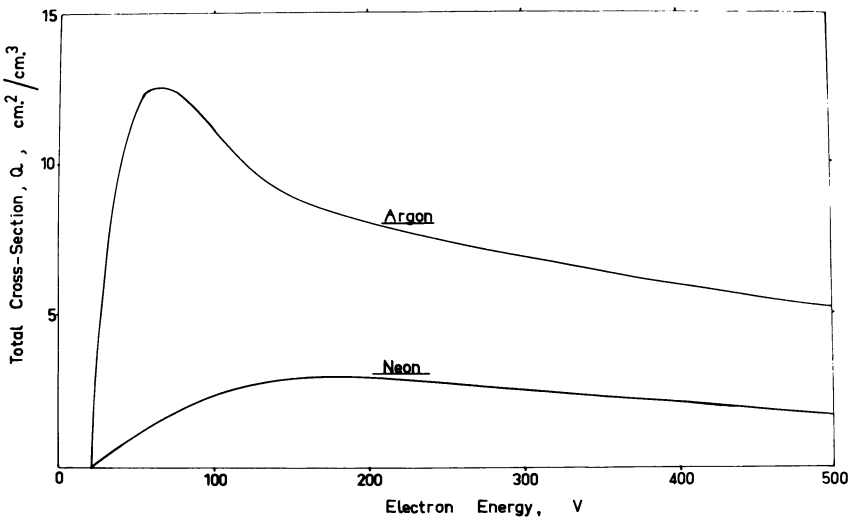

Figure 3. Typical cross section vs. *electron energy curves*

Publication Date: June 1, 1969 | doi: 10.1021/ba-1969-0080.ch032

The crossed discharge arrangement shown in Figure 2b comprises a low frequency discharge at right angles to one of high frequency. The discharge zone itself is said to be characterized by a low energy density and to result in unexpectedly high activation of the reactants and relatively high yields of the reaction products (*5*, *6*). These claims have not, however, been confirmed by recent work in these laboratories in which methane was subjected to a crossed discharge at 31 mm. Hg pressure. The reactor shown in Figure 4 consisted of a 15 mm. internal diameter glass tube fitted with two pairs of 3 mm. diameter stainless steel electrodes arranged at right angles. The percentage decomposition of methane was observed using a 0.91 MHz. high frequency discharge, a 50 Hz. low frequency discharge and combinations of high and low frequency discharges simultaneously. Figure 5 shows some typical data plotted in the form % methane decomposed *vs.* % H.F. power for a series of runs at constant total power. The methane flowrate was constant throughout at 93 cc./minute at N.T.P. These results confirm the general trend whereby an increase in discharge power is accompanied by an increase in the percentage decomposition of the methane but on the other hand do not substantiate the claim made for the higher activating effect of the crossed discharge. Had this been the case, the curves shown in Figure 5 would have exhibited maxima whereas, in fact, the observed methane decomposition at constant total power increased steadily with increasing percentage of H.F. power. In this particular case, there is, therefore, no advantage in the use of crossed discharges and the characteristics claimed by Cotton still remain to be confirmed.

Publication Date: June 1, 1969 | doi: 10.1021/ba-1969-0080.ch032

Mean Residence Time and Residence Time Distribution

In the simple plug flow reactor, the conversion (x) obtained is related to the residence time τ by the expression:

$$\tau = \int_0^x \frac{dx}{v_F r}$$

d = Electrode spacing
x = Fractional conversion of reactant
v_f = Molal volume of the reacting mixture
r = Reaction rate
τ = Residence time in the discharge

If the reaction is one which can only take place under the influence of an electrical discharge, then the residence time refers to the time spent by the reactants in the discharge zone itself. If, however, subsequent reactions involving the primary reaction products are possible outside the discharge zone, these will usually proceed at a different rate and

In Chemical Reactions in Electrical Discharges; Blaustein, B.;
Advances in Chemistry; American Chemical Society: Washington, DC, 1969.

must be taken into account separately in analyzing the overall performance of the reactor system.

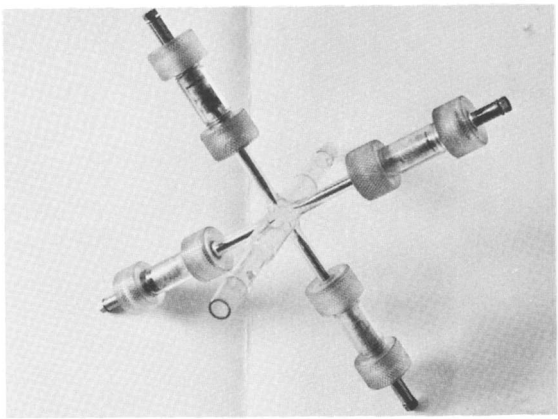

Figure 4. Crossed discharge reactor

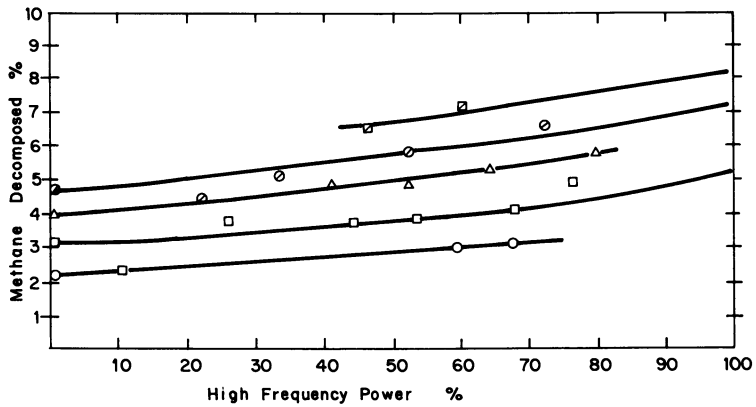

Figure 5. Effect of a crossed discharge on % methane-decomposition

○ = *10.3 watts*
□ = *13.5 watts*
△ = *16.8 watts*
⊘ = *19.6 watts*
⊠ = *23.7 watts*

If the reaction rate (r) could be written in terms of the concentrations of the reactants and a rate constant (k) which in turn was dependent upon the discharge characteristics, then in principle it would be possible to integrate the above expression for any set of discharge conditions and compute the residence time for any desired conversion. In practice, however, this is seldom possible because the functional rela-

Publication Date: June 1, 1969 | doi: 10.1021/ba-1969-0080.ch032

tionship between the reaction rate and the discharge characteristics is unknown.

The concept of plug flow is only an approximation at the best of times and in many practical situations considerable divergences are observed between the residence time (τ) calculated from the above expression and that observed in practice for the same conversion. Such discrepancies result from the velocity profile of the gas as it passes through the reactor; molecules adjacent to the wall have a lower velocity than molecules travelling along an axial path and as a result there is a distribution of residence times. The effect of such a distribution can be serious in the case of polymerization-type reactions where a wide spread in residence times is often accompanied by a corresponding spread in the molecular weights of the products. If, therefore, a product is required with a relatively narrow molecular weight distribution, steps must be taken to ensure that the distribution of residence times is correspondingly small. One way of achieving this is to promote rapid mixing in the reactor by the use of suitably designed baffles so that each element of gas spends approximately the same time in the discharge.

From what has been said above with regard to polymerization reactions, it will be clear that the mean residence time of the gas molecules in the discharge zone will exert an important influence on both the composition and yield of the products. Thus, for example, when methane is subjected to discharge activation, the molecular weight range of the products is dependent upon the mean residence time, other factors remaining constant. This is illustrated in Figure 6 which shows how the propane–ethane ratio increases with a corresponding increase in the mean residence time (*22*). On the other hand when the product is likely to be degraded by a prolonged residence time in the discharge, it is clearly advantageous to work with as short a residence time as is compatible with the forward reaction. This is the case in the synthesis of hydrazine from ammonia and Figure 7 shows how the energy yield of hydrazine varies as an inverse function of the mean residence time. Figure 7 also shows the effect upon the yield of decreasing the hydrazine residence time in the gas phase by rapid absorption with an inert liquid absorbent; this is an important innovation and is discussed in detail below.

Reaction Selectivity

Discharge reactions are frequently complicated by reason of the interactions between the atomic, molecular, ionic, and free radical species present. Moreover, because of the wide range of species present, reactions are rarely simple in the sense that only one primary reaction product is produced. Competing parallel, consecutive, and degradation reactions

Publication Date: June 1, 1969 | doi: 10.1021/ba-1969-0080.ch032

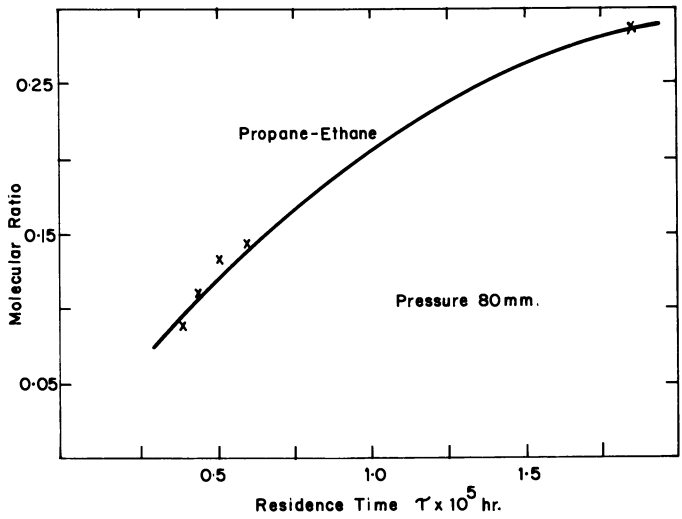

Figure 6. Effect of residence time on propane-ethane ratio

are often present, the net result of which is to produce a wide spectrum of reaction products. At the present time one of the key problems is how to design reactors in which unwanted side reactions are reduced to a minimum. There is no clear-cut answer to this problem as yet, but an examination of some of the more elementary types of reactions such as those listed in Table I indicates a promising method of approach.

Table I. Examples of Elementary Reactions

Consecutive Reactions	$A + B \rightarrow C$ $A + C \rightarrow D$
Polymerization Reactions	$A + A \rightarrow B$ $A + B \rightarrow C$ $A + C \rightarrow D$
Parallel Reactions	$A + B \rightleftharpoons \begin{matrix} C \\ D \end{matrix}$
Reversible Reactions	$A + B \rightleftharpoons C + D$
Degradative Reactions	$A + B \rightarrow C \rightarrow D \rightarrow E$

In all the reactions listed in Table I it is assumed that C is the preferred product. Intermediate steps involving excited species are omitted so that the equations merely represented the overall stoichiometry of the various situations. If, therefore, product C is being produced from reactants A and B and a second (consecutive) reaction is present which destroys C, then the rate of the second reaction can be reduced by main-

Publication Date: June 1, 1969 | doi: 10.1021/ba-1969-0080.ch032

taining the concentration of C at a low value. Since the primary reaction responsible for the formation of C should, on economic grounds, proceed as rapidly as possible, the only way of maintaining a low product concentration is to remove C from the discharge zone as rapidly as it is formed. The methods by which this can be achieved will be discussed further below.

The same principles apply to the other reactions in Table I. Thus, for polymerization reactions, the molecular weight of the product can be controlled by selective removal of certain constituents from the discharge. If product B is preferred, then further polymerization can be minimized by rapid removal of B. If, on the other hand, the higher molecular weight product C is required, B is allowed to remain in the discharge and C is selectively removed. It frequently happens that the product yield is limited by reverse and parallel reactions. In the latter case, C can be produced in preference to D by selective removal of C. In the former instance, any yield limitations imposed by equilibrium considerations can be overcome by rapid removal of C so that the equilibrium is displaced almost entirely in favor of products.

Similar reasoning shows that for degradative reactions, product C can be produced in preference to D or E provided that C is removed rapidly enough from the activating influence of the discharge.

A number of methods are available for the rapid removal of a particular component from the discharge zone, namely:

(1) Quenching the reaction at low temperatures and freezing out the product (*2, 3, 4, 10, 25*).

(2) Absorbing the desired product selectively in an inert liquid absorbent (*12, 13, 14, 15, 16, 24*).

(3) Adsorbing the desired product in a fluidized bed of solid adsorbent (*23*).

(4) By using a low residence time in the discharge zone. This may be achieved either by high gas flow rates or by using a pulsed discharge technique.

These are all devices which reduce both the product concentration and residence time in the gas phase and so minimize product losses through subsequent reactions. Methods (1), (2), and (3) are means of controlling selectively the residence time and concentrations of certain specific products in the discharge and a choice can only be made between them in the light of the physical properties of the various constituents of the gas phase. The fourth method, which does not discriminate between the concentrations or residence times of reactants and products, can only be evaluated when the relative rates of the competing reactions are known. Of the various techniques available, simultaneous reaction and absorption in a heterogeneous reactor (Method 2) opens up interesting

Publication Date: June 1, 1969 | doi: 10.1021/ba-1969-0080.ch032

possibilities for producing economic yields of many chemical products where hitherto the overall yield has been restricted by decomposition reactions. The theoretical analysis of such systems is, however, extremely complex and even if the kinetics of the process were fully understood, it is doubtful if the absorption rate into the liquid phase could be predicted with any degree of certainty because of the complications arising from dielectrophoretic stirring of the liquid. If the liquid phase is polarizable, the electrical forces in a non-homogeneous field will cause polar molecules to move toward regions of maximum non-homogenity. Any turbulence thereby set up within the liquid phase will enhance the rate of gas absorption but at the same time render the prediction of mass transfer coefficients extremely uncertain. From a practical point of view, such effects are desirable insofar as it is important that the rate of absorption of the product should be high compared with its rate of production by synthesis.

Some illustrations of the effects of mean residence time on reaction yield are of interest at this stage and reference has already been made to the dependence of the propane-ethane ratio on τ when methane is subjected to discharge activation. The data shown in Figure 6 were obtained at 80 mm. Hg pressure in a cross-flow/coaxial reactor using 1.60 mm. thick quartz barrier adjacent to the inside surface of the outer electrode. The outer and inner electrode diameter were 17 mm. and 3 mm. respectively and the power density was 0.05 kw./cc. throughout. Similar effects have been reported by other workers and the trends toward higher molecular weight fractions at longer residence times are well known (*17*).

In the discharge synthesis of hydrazine from ammonia, it has been suggested (*1*, *7*) that the hydrazine can be subsequently destroyed by further electron excitation or by reaction with atomic hydrogen produced in the primary electron bombardment of ammonia. If, therefore, the concentration and residence time of the hydrazine in the gas phase can be reduced, degradative reactions should be minimized and the yield increased correspondingly. A convenient way of achieving this is by absorption of the hydrazine from the discharge zone by means of a spray of ethylene glycol which is itself substantially inert at low power densities. A suitable type of reactor for combined reaction and absorption which has been developed in these laboratories is shown diagrammatically in Figure 8. The outer tube of the reactor was 28.6 mm. o.d. and was made from quartz with a wall thickness of 1.60 mm. An outer band of copper served as one electrode while the inner electrode consisted of a perforated stainless steel drum 19 mm. o.d., mounted on a co-axial hollow shaft so that it could be rotated at high speed. During operation, ethylene glycol was fed to the drum so that as the latter rotated, the glycol was forced through the drum perforations into the discharge zone in the form

Publication Date: June 1, 1969 | doi: 10.1021/ba-1969-0080.ch032

of a fine spray. The liquid and gaseous phases, therefore, flowed co-currently through the discharge and were removed from the bottom of the reactor. Typical data shown in Figure 7 were obtained at an average power density of 0.044 kw./cc. and illustrate the fact that not only can the energy yield of hydrazine be increased by reducing the gas residence time—*i.e.*, increasing the gas flow rate—but that a further substantial increase in yield can be obtained if the hydrazine is rapidly removed from the discharge by selective absorption (*24*). This effect cannot be attributed to the slightly different power densities used in the two sets of experiments (*24*). On the other hand, the grams N_2H_4 produced per gram NH_3 (X′) is also reduced at lower residence times and so from a practical standpoint a balance has to be achieved between energy yield and reactant conversion per pass. This problem is of great importance in the design of industrial G.E.D. reactors and a detailed discussion of this topic will be deferred until a later paper.

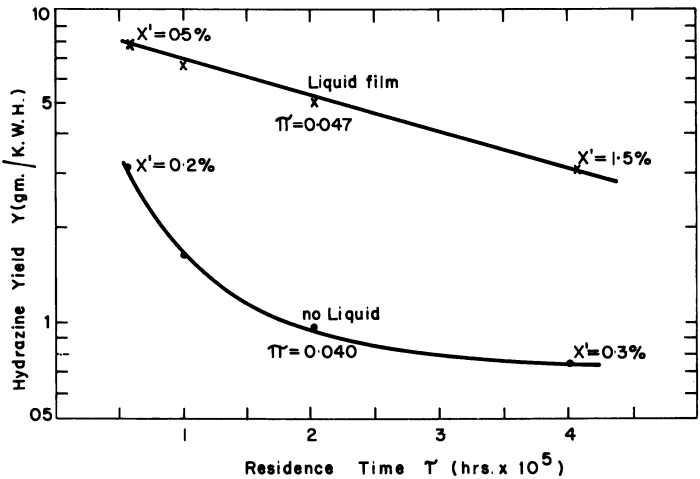

Figure 7. The effect of residence time and an inert liquid absorbent on hydrazine yield from ammonia

In certain situations in which it is impracticable to use selective absorption or high gas flow rates as a means of securing low residence times and product concentrations, a possible alternative is to use a pulsed discharge in which the effective residence time of the gas molecules is dictated by the pulse duration and the time interval between successive pulses. By this means, very short effective residence times can be achieved and typical data, again for the ammonia–hydrazine reaction, are shown in Figure 9, in which the energy yield of hydrazine is plotted *vs.* the discharge duration for a constant gas flow rate. The reactor was

In Chemical Reactions in Electrical Discharges; Blaustein, B.;
Advances in Chemistry; American Chemical Society: Washington, DC, 1969.

a cross-flow/parallel plate unit in which the two electrodes were 11 mm. apart, each measuring 12.5 × 6.3 mm. In these runs the average power density was 0.01 kw./cc. using a pulsed d.c. discharge. Again the results follow the previous pattern in that the lower effective residence times favor higher energy yields because of the smaller loss of hydrazine through unwanted side reactions. In these experiments the gas flow rate was constant at 150 cc./minute measured at 20°C. and 760 mm. Hg pressure while the pulse on-time ranged from 12 to 130 microseconds at a constant off-time of 10^{-2} seconds. In this case, however, the fractional conversion of the reactant was low because of the short activation time.

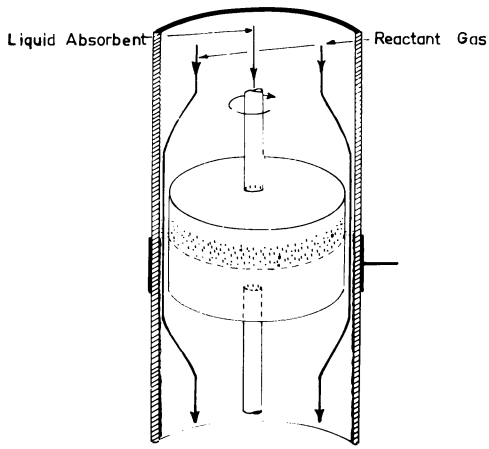

Figure 8. Arrangement of differential reactor with liquid absorption for hydrazine synthesis from ammonia

It has already been pointed out that hydrazine is probably subject to attack by atomic hydrogen and in this connection it is interesting to note that an alternative technique in which atomic hydrogen is converted to the less reactive molecular form through the agency of a platinum catalyst has also shown increased yields of hydrazine (7).

When two or more reactants participate in a reaction the problem of obtaining a high yield of the desired product with the minimum contamination from secondary reactions is considerably more difficult. In certain cases a partial solution to the problem may well lie in activating one reactant only and mixing the active species so obtained with the second reactant. This is only possible, however, in cases where the mixing time is less than the average lifetime of the activated species. In an interesting application of this principle, Fenn (9) has expanded the discharge plasma through a nozzle and shown that its characteristic properties can be preserved downstream of the discharge where mixing with

Publication Date: June 1, 1969 | doi: 10.1021/ba-1969-0080.ch032

a second reactant can take place. Another interesting possibility aimed at obtaining better selectivity is to allow the gas to flow through a suitably designed venturi nozzle so that the particular conditions of pressure, temperature and residence time favoring reaction optimization are approached in the discharge (*21*).

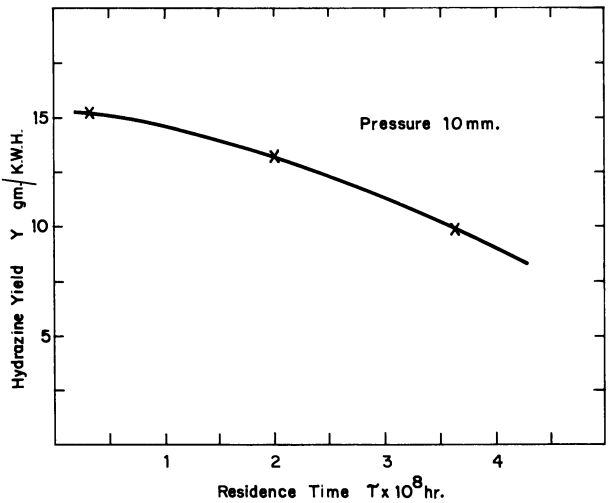

Figure 9. Effect of short residence times on hydrazine yield when the effective residence time is dictated by the pulsed discharge characteristics

The extent to which such techniques are likely to be of value in practice still remains to be confirmed but nevertheless they do offer possibilities worthy of further investigation.

Scale-up of G.E.D. Reactors

Once a satisfactory design of reactor has been developed on the laboratory scale, the next question to consider is how the unit can be scaled up to handle the larger gas throughput commensurate with industrial scale operation. Although the applications of similarity principles to gas discharge phenomena have been discussed at length elsewhere (*8*, *18*), two basic problems still preclude the application of similarity concepts to discharges in which chemical reactions are taking place:

(a) It is not yet clear which discharge parameters are primarily responsible for activation and hence reaction initiation.

(b) The influence of solid surfaces adjacent to the reaction zone is still undetermined. This is important in that the ratio of surface area per unit volume varies with scale in geometrically similar units.

Publication Date: June 1, 1969 | doi: 10.1021/ba-1969-0080.ch032

In Chemical Reactions in Electrical Discharges; Blaustein, B.;
Advances in Chemistry; American Chemical Society: Washington, DC, 1969.

Nevertheless, despite the fact that no quantitative predictions can yet be made with regard to reactor scale-up, it is of interest to consider some possible implications in the simplest case of a parallel plate reactor in which the field is considered to be perfectly uniform. Furthermore, if it is assumed that solid surfaces play no part in the chemical processes and that the reaction rates are only dependent upon the reduced field (E/p), then for a reactor having an electrode spacing d and operating at a voltage V and pressure p,

$$(E/p) = (V/d \cdot p)$$

(E = Field strength)

It follows, therefore, that if the reactor is scaled up by a factor n, the electrode spacing will become equal to nd and the only way in which (E/p), and hence the reaction rate, can be kept constant is either by reducing the pressure to a value (p/n) or by using n times the voltage in the larger unit. Either way, the conclusions are unacceptable from an engineering point of view since very small pressures result in large equipment and inordinately high voltages pose safety problems as well as necessitating expensive transmission and control gear.

This analysis is, of course, oversimplified in the sense that uniform fields are not normally attainable in discharge reactors so that (E/p) varies over the electrode gap. Furthermore in cases where the field is extremely non-uniform, ionization can be so high locally that the resultant space change distorts the field to such an extent that a proper mathematical treatment becomes difficult. Again the surface/volume ratio becomes smaller as the reactor is scaled up and this effect would clearly become an important consideration in cases where free surfaces play an important part in the reaction kinetics. If, however, the need for higher voltages or lower pressures was subsequently substantiated in respect of a particular reaction, it is doubtful whether direct scale-up would prove to be economically attractive. A far more attractive possibility might be to step-up the laboratory reactor until the desired throughput was achieved. In principle, this involves putting a sufficient number of small-scale reactors in parallel to handle the required gas flow rate. In practical terms, however, there is much scope for ingenuity here as all that is required is that the appropriate number of laboratory scale discharges be housed in a common shell of the appropriate dimensions.

Acknowledgments

The author is indebted to a number of his colleagues and to C. A. Walley of the Department of Electrical Engineering for many helpful discussions.

Literature Cited

(1) Andersen, W. H., Zwolinski, B. J., Parlin, R. B., *Ind. Eng. Chem.* **51** (4), 527 (1959).
(2) Brewer, A. K., Westhaver, J. W., *J. Phys. Chem.* **33**, 883 (1929).
(3) *Ibid.*, **34**, 153 (1930).
(4) Broida, H. P., Pellam, J. R., *U. S. Patent* **2892766** (June 30, 1959).
(5) Cotton, W. J., *Trans. Electrochem. Soc.* **91**, 407 (1947).
(6) *Ibid.*, **91**, 419 (1947).
(7) Devins, J. C., Burton, M., *J. Am. Chem. Soc.* **76**, 2618 (1954).
(8) von Engel, A., "Ionized Gases," 2nd ed., Oxford Univ. Press, England, 1965.
(9) Fenn, J. B., *U. S. Patent* **3005762** (Oct. 24, 1961).
(10) Golden, S., *U. S. Patent* **2924562** (Feb. 9, 1960).
(11) Howatson, A. M., "Introduction to Gas Discharges," Pergamon Press, London, England, 1965.
(12) Imperial Chemical Industries, *U. K. Patent* **948,772** (1964).
(13) *Ibid.*, **958,776** (1964).
(14) *Ibid.*, **958,777** (1964).
(15) *Ibid.*, **958,778** (1964).
(16) *Ibid.*, **966,406** (1964).
(17) Kraaijveld, Von H. J., Waterman, J. I., *Brennstoff-Chemie.* **42** (**12**), 369 (1961).
(18) Llewellyn-Jones, F., "Ionization and Breakdown in Gases," Methuen and Co., Ltd., London, 1966.
(19) McCarthy, R. L., *J. Chem. Phys.* **22**, 1360 (1954).
(20) Miyazaki, Takahashi, *Nippon Kagaku Zasshi* **78**, 553 (1958).
(21) Rouy, A. L. M. A., Peterson, C. H., Glasscock, G. B., *U. S. Patent* **3003939** (Oct. 10, 1961).
(22) Sergio, R., Univ. of Newcastle Upon Tyne, England (unpublished work).
(23) Thornton, J. D., *Chem. Processing* **XII** (**3**), S6 (1966).
(24) Thornton, J. D., Charlton, W. D., Spedding, P. L., ADVAN. CHEM. SER. **80**, 165 (1969).
(25) Thorp, C. E., *U. S. Patent* **2876188** (March 3, 1959).

RECEIVED May 24, 1967.

33

Chemistry in High Temperature Plasma Jets

CHARLES S. STOKES

Research Institute of Temple University, Philadelphia, Pa.

Publication Date: June 1, 1969 | doi: 10.1021/ba-1969-0080.ch033

The high temperatures attainable with plasma jets can be used to produce chemical reactions of substances introduced into the jet. This opens an entirely new field of investigation in the area of chemical synthesis. Since the jet can be operated using several different gases—helium, argon, nitrogen, hydrogen, or mixtures thereof—and gases, liquids, or solids, can be introduced into the jet, many reaction schemes may be carried out. Acetylene, hydrogen cyanide, the oxides of nitrogen, cyanogen, inorganic nitrides, inorganic carbides, and several other compounds, including some complex organic materials, have been successfully prepared. Various methods of material entry have been used including liquid spraying, powder and rod feeding, and direct mixing of reactants with the plasma gas.

Plasma generators, in general, have been found suitable for a variety of uses. They generally provide an electric arc which is condensed or constricted into a smaller circular cross section than would ordinarily exist in an open arc type device. This constriction generates a very high temperature (8,000°-20,000°K.) so that a superheated-plasma working fluid can be ejected through the nozzle and the composition of the plasma determines the use to which the plasma generator is put. Plasma generators have been used for cutting, welding, metal spraying, and chemical processing. For chemical processing, plasma generators have provided the possibility of the production of new alloys and compounds and the processing of less commonly used materials, as well as the preparation of certain common chemicals.

Plasma Jet Equipment

Two types of plasma generators are possible: the nontransferred and the transferred arc. A nontransferred arc consists of a cathode and

In Chemical Reactions in Electrical Discharges; Blaustein, B.;
Advances in Chemistry; American Chemical Society: Washington, DC, 1969.

a hollow anode where the arc is struck between the electrodes and the flame emerges through the orifice in the anode. In the transferred arc, the cathode is placed some distance away from the anode and an arc is passed between the electrodes. The nontransferred arc is the most popular in the chemical studies made to date. A plasma jet used in chemical synthesis can have varied designs to meet special requirements, such as the introduction of a reactant material into the flame path at a particular point.

Consumable cathodes have been used in experiments in which carbon was one of the reactants. Carbon, vaporized from a graphite cathode, was used in the synthesis of cyanogen and hydrogen cyanide. Powdered carbon introduced in a gas stream or as a constituent of a gas has also been used as the source of carbon in a plasma flame.

Electrodes of 2%-thoriated tungsten are the most frequently used water-cooled nonconsumable electrodes. Water-cooled copper anodes have been widely used in experimental work. Figure 1 shows a typical plasma jet assembly. A reactor chamber may be of any configuration desired to accommodate different feeding and quenching devices.

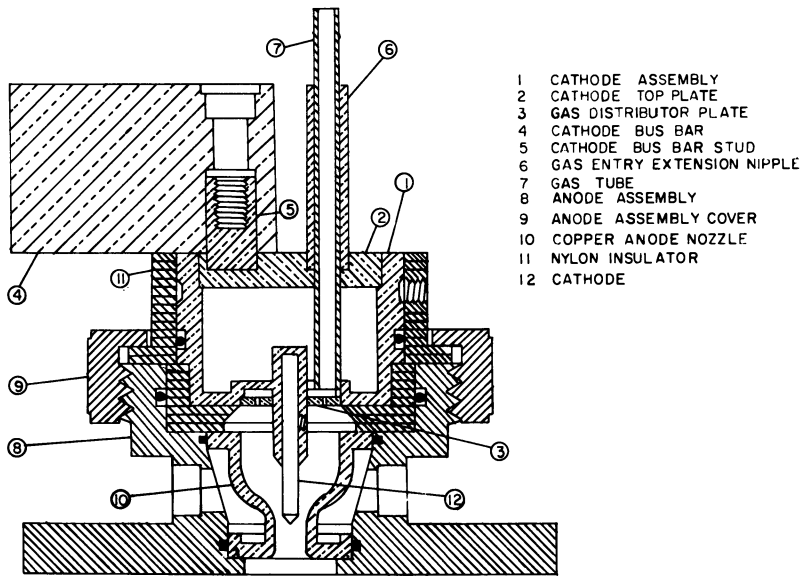

Figure 1. Typical plasma jet assembly

Plasma Jet Reactions

Gas-Gas Reactions to Produce a Gas and Gas Decomposition Reactions to Produce a Gas. A considerable amount of research has been done by a number of people in the area of plasma jet gas-gas reactions.

Publication Date: June 1, 1969 | doi: 10.1021/ba-1969-0080.ch033

The following are the gas reactions producing gases that have been investigated:

$$CH_4 \text{ (or other hydrocarbons)} \xrightarrow[\text{Ar Jet}]{H_2 \text{ Jet}} C_2H_2 \quad (1)$$

$$CH_4 + N_2 \xrightarrow[\text{Ar} + N_2 \text{ Jet}]{\text{Ar Jet}} HCN + C_2H_2 \quad (2)$$

$$CH_4 + NH_3 \xrightarrow[\text{Ar} + N_2 \text{ Jet}]{\text{Ar Jet}} HCN + C_2H_2 \quad (3)$$

$$CH_4 + H_2O \text{ (Gas)} \rightarrow CO + 3H_2 \quad (4)$$

$$N_2 + O_2 \xrightarrow{N_2 \text{ Jet}} 2NO \quad (5)$$

$$CF_4 + N_2 \rightarrow NF_3 + CF_3NF_2 \quad (6)$$

$$SF_6 + N_2 \rightarrow NF_3 \quad (7)$$

NH_3 or CH_4 cracking rate studies (8)

In the past several years, considerable effort has been directed to the investigation of the production of acetylene from hydrocarbons (Reaction 1).

The production of acetylene by the reaction of methane in the flame of an argon plasma jet yielded an 80% conversion to acetylene (*12*). Most of the methane was converted to acetylene and hydrogen with little formation of soot. Figure 2 shows the power consumption *vs.* the feed ratio of argon to methane. This ratio is the most important parameter in the acetylene yield. The minimum power consumption, 60 kwh./100 cu. ft. acetylene produced, corresponded to a ratio of argon to acetylene of 0.3. Arc conditions for a typical run were, CH_4 10 liter/min. Ar 10 liter/min., power, 5.40 kw. Damon and White (*3*) selected the manufacture of acetylene as an application for plasma processing which might be of interest to the petroleum industry. Methane was one of the gases proposed with the use of recycle procedure. Anderson and Case (*1*) studied the methane decomposition reaction and compared it with available thermodynamic data. In these experiments a hydrogen plasma torch was used, coupled to a reaction chamber and water quench system. The hot hydrogen stream emitted from the plasma jet, entered the reaction chamber and mixed with a methane feed. The gas mixture was analyzed after exiting

Publication Date: June 1, 1969 | doi: 10.1021/ba-1969-0080.ch033

In Chemical Reactions in Electrical Discharges; Blaustein, B.;
Advances in Chemistry; American Chemical Society: Washington, DC, 1969.

from the reaction chamber and water quench system. The optimum cracking conditions for methane produced a 76% yield of acetylene.

In a report of the National Academy of Sciences (*13*) the investigation by the Linde Company of the production of acetylene using a plasma jet and natural gas was reported. This process is said to have a more efficient transfer energy to the feed stream than does the open arc process used in Germany.

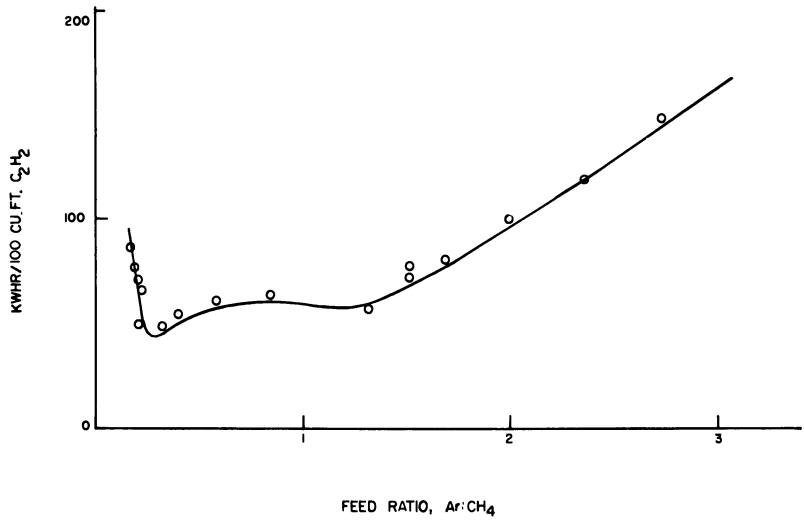

Figure 2. Power consumption vs. *the feed ratio of argon to methane*

Considerable research has been done on the methane-nitrogen and methane-ammonia reactions (Reactions 2 and 3) to produce hydrogen cyanide and as a by-product acetylene. Leutner (*7*, *11*) reported up to 50% conversions were obtained based on the carbon input (as methane) by using either nitrogen, argon, or nitrogen-argon mixtures as the plasma gas. Figure 3 shows a schematic of the apparatus used in these studies. These experiments showed that up to 75% of the carbon input as methane was converted into HCN and acetylene for Reaction 3 and 90% for Reaction 2 where a power level of 12 kw. was used. Flow rates of methane were varied from 2 to 8 liter/min. with the other reactant gases fed at ratios of 1:1 to 1:8 of the methane flow. No other hydrocarbons besides acetylene were found and cyanogen was present in only trace amounts.

Damon and White (*4*) proposed the production of reducer gas by Reaction 4 using natural gas or propane as a hydrocarbon source. The proposed process for steam-methane reforming would operate at a tem-

Publication Date: June 1, 1969 | doi: 10.1021/ba-1969-0080.ch033

perature of 3000° to 6000°F. and provide a high temperature reducing gas for metals and other high temperature processes.

The fixation of nitrogen (Reaction 5) has been one of the major applications for arc induced reactions in the past. During the past several years, direct fixation of oxygen-nitrogen mixtures has been investigated; however, only 2% of the total nitrogen input has been converted to NO (*7*, *17*). The use of a liquid oxygen and/or liquid nitrogen quench system with a nitrogen plasma jet has shown no improvement on the above yield (*8*).

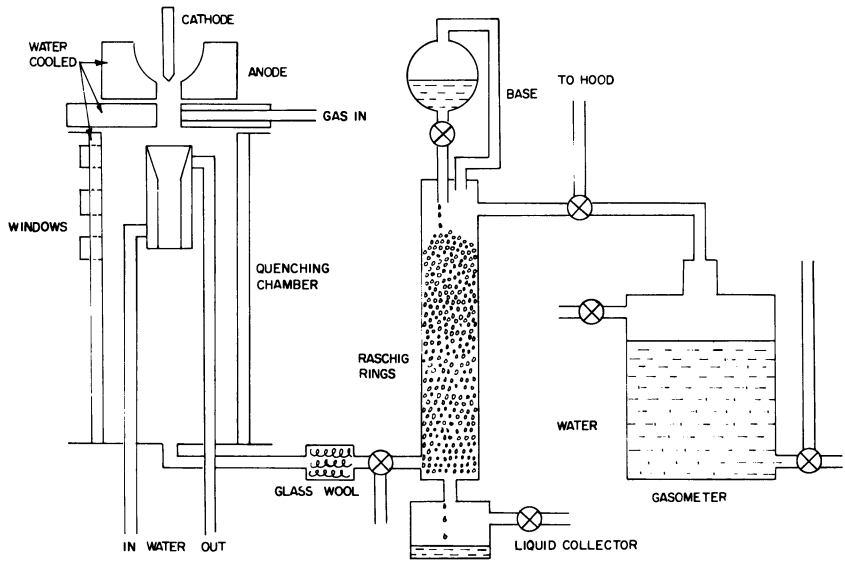

Figure 3. Scheme of apparatus used in the research on methane-nitrogen and methane-ammonia reactions to produce hydrogen cyanide with acetylene as a by-product

Bronfin and Hazlett (*2*) have experimented with the introduction of CF_4 and SF_6 into a nitrogen plasma jet. Small yields of NF_3, N_2F_4 and CF_3NF_3 (Reactions 6 and 7) were produced. The yield of fixed nitrogen compounds was of the order of 1% of the nitrogen inlet. The yield of these compounds increased with both increased power input and F/N ratio.

Freeman and Skrivan (*5*) have studied the decomposition rate of ammonia and methane in a plasma jet (Reaction 8) and have shown it to be rate limited by a diffusion process. The apparatus used has been fully characterized and shown to be a very good fit for a diffusional model.

Publication Date: June 1, 1969 | doi: 10.1021/ba-1969-0080.ch033

Gas-Solid Reactions to Produce a Gas.

$$H_2 + S \rightarrow H_2S \quad (9)$$

$$C + H_2 \rightarrow C_2H_2 \quad (10)$$

$$C + H_2 + N_2 \rightarrow HCN + C_2H_2 \quad (11)$$

$$C + NH_3 \rightarrow HCN + C_2H_2 \quad (12)$$

$$C + N_2 \rightarrow C_2N_2 \quad (13)$$

Recent investigations at the Research Institute of Temple University have shown that hydrogen sulfide can be synthesized from its elements, hydrogen, and sulfur powder, fed in a helium plasma jet (*14*). Typical arc conditions were—He, 17.7 liter/min.; H_2, 4 liter/min.; S, 0.5 gram/min.—with power at 7.75 kw. Conversions as high as 37% based on the sulfur input have been obtained. Figure 4 shows both the percent con-

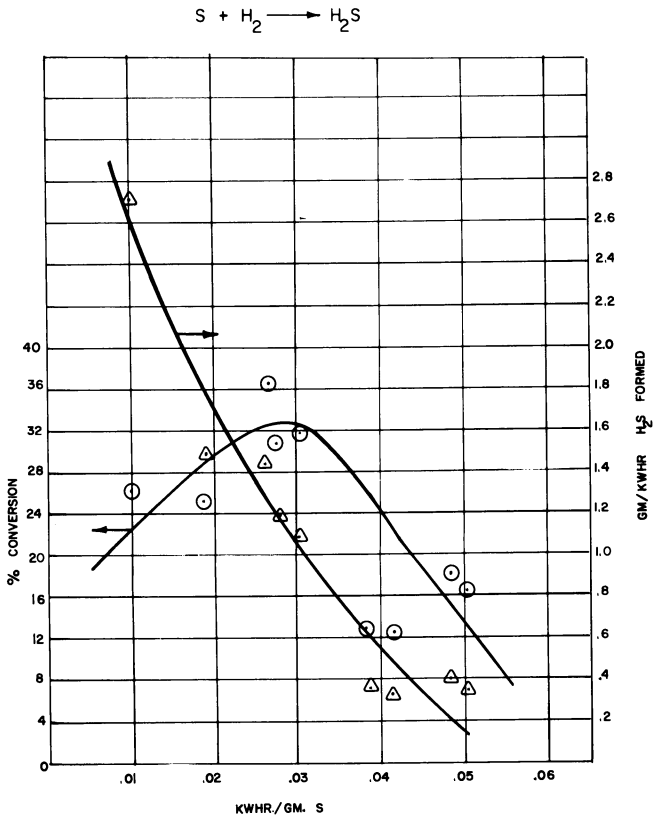

Figure 4. Percent conversion and the gram/kwh. of hydrogen sulfide formed vs. *kwh./gram of sulfur input*

Publication Date: June 1, 1969 | doi: 10.1021/ba-1969-0080.ch033

version and the gram/kwh. of hydrogen sulfide formed *vs.* kwh./gram of sulfur input. As seen from Figure 4, the maximum conversion percent does not necessarily have the maximum production efficiency.

A considerable number of syntheses have been carried out using solid carbon powder or graphite elements as a carbon source for reactions with various materials including hydrogen, nitrogen, hydrogen-nitrogen, and ammonia. Reactions 10 through 13 show the various products obtained by these reactions. In the case of acetylene synthesis (Reaction 10) the highest yield obtained by direct synthesis from the elements was 33% (*12*). Hydrogen cyanide yields up to 51% for Reaction 11 and up to 39% for Reaction 12 have been obtained (*11*). A complete study of the synthesis of cyanogen from its elements was made by Leutner (*7*, *10*) and this reaction gave 15% conversion based on the carbon input at the optimum reaction conditions.

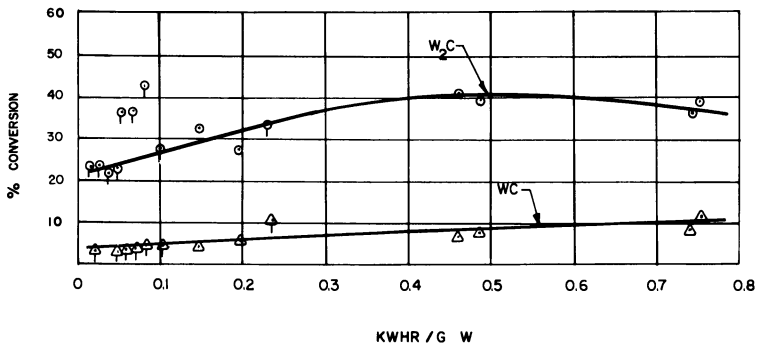

Figure 5. Percent conversion vs. kwh./gram tungsten input for Reaction 19

⊙ △ *micron size W*
⊙ △ *—325 mesh W*

5 inch quench distance

Graves, Kawa, and Hiteshue (*6*) reported investigations using bituminous coal fed into an argon plasma jet. Acetylene, the principle product, was obtained in yields of 15 wt. percent. This work studied the effects of coal feed rate, particle size and plasma temperature on yields and products formed.

Gas-Gas Reactions to Produce a Solid.

$$TiCl_4\ (gas) + NH_3 \text{ or } N_2 + H_2 \rightarrow TiN \qquad (14)$$

$$\text{Hydrocarbons} \rightarrow C \qquad (15)$$

Harnisch, Keymer, and Schallus (*9*) reported the preparation of titanium nitride (Reaction 14) from titanium tetrachloride gas with either plasma jet heated ammonia or nitrogen/hydrogen mixtures. The reaction produced very finely divided black titanium nitride up to 95% pure. The Thermodynamics Corporation (*19*) has reported the possibility of producing carbon blacks from hydrocarbons using a plasma jet. Methane or other hydrocarbons which would be introduced into the plasma flame, would be cracked using hydrogen as the operating gas and producing carbon black. Liquid as well as gaseous hydrocarbons can be used as a source for carbon, and the Vitro Laboratories (*13*) have experimented with carbon black production from liquid hydrocarbons.

Gas-Solid Reactions Producing a Solid.

$$Ti + N_2 \rightarrow TiN \quad (16)$$

$$Mg + N_2 \rightarrow Mg_3N_2 \quad (17)$$

$$W + N_2 \rightarrow WN \quad (18)$$

$$W + CH_4 \rightarrow WC + W_2C \quad (19)$$

$$WO_3 + CH_4 \rightarrow WC + W_2C \quad (20)$$

$$Ta + CH_4 \rightarrow TaC + Ta_2C \quad (21)$$

$$Ta_2O_5 + CH_4 \rightarrow TaC + Ta_2C \quad (22)$$

$$Ta_2O_5 + H_2 \rightarrow Ta \quad (23)$$

$$WO_3 + H_2 \rightarrow W \quad (24)$$

$$Al_2O_3 + H_2/CH_4 \rightarrow Al \quad (25)$$

$$FeO + H_2 \rightarrow Fe \quad (26)$$

The production of metal nitrides (*16*, *17*) from the elements has been investigated for three elements: titanium, magnesium, and tungsten (Reactions 16 to 18). The production of titanium nitride in 100% yield was accomplished by using 200 mesh titanium powder fed into a nitrogen plasma jet. The titanium nitride particle size was found to be 0.75 to 7.5 microns. The product was also formed in large, compact, golden yellow crystals. In like manner, tungsten nitride was formed in 25% yield. Forty percent conversion to magnesium nitride was obtained when magnesium was fed into a nitrogen plasma jet.

The preparation of metal carbides has also been reported (*14*, *16*). Figure 5 shows the percent conversion *vs.* kwh./gram tungsten input for Reaction 19. As can be seen, the WC conversion is directly proportional to the power input level. The highest conversions obtained were 43% for W_2C and 11% for WC. Reaction 20 is shown in Figure 6 where

Publication Date: June 1, 1969 | doi: 10.1021/ba-1969-0080.ch033

percent conversion is plotted *vs.* kwh./gram WO_3 input. The three products of the reaction, tungsten (43 to 81% conversion), tungsten carbide (4 to 11% conversion) and ditungsten carbide (9 to 35% conversion), are formed in a total conversion of 81 to 94%. The major product is tungsten, which is favored at higher kwh./gram WO_3 inputs.

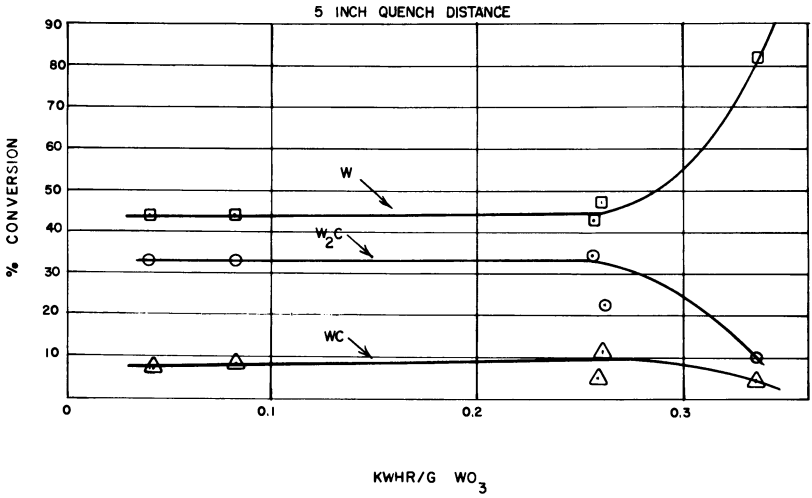

Figure 6. Percent conversion vs. *kwh./gram WO_3 for Reaction 20*

The reaction of tantalum and methane in a helium plasma jet is shown in Figure 7, where a water-cooled quenching probe was placed at 1/2 inch and 5 inches below the plasma jet. The effect of the quenching distance is dramatic. The amount of Ta_2C formed is not appreciably different in either case. However, the TaC yield changed considerably by the placement of the quenching device. Conversions up to 72% TaC have been produced by this reaction. Figure 8 shows a plot of the tantalum pentoxide plus methane reaction carried out in a helium plasma jet. The percent conversion is plotted *vs.* kwh./gram tantalum pentoxide input for two different quenching probe distances from the plasma jet. In the case where the quencher was 1/2 inch below the jet, the production of TaC went up linearly with the kwh./gram input. Where the quenching distance was 5 inches, a peak was obtained, which shows that adequate quenching does not take place beyond a value of 0.4 for kwh./ then falls off rapidly, in contrast to the 1/2 inch distance. Tantalum metal is the favored product in the 5 inch case. Maximum conversions are 24% TaC, 17% Ta_2C, and 18% Ta for both cases.

Publication Date: June 1, 1969 | doi: 10.1021/ba-1969-0080.ch033

In Chemical Reactions in Electrical Discharges; Blaustein, B.;
Advances in Chemistry; American Chemical Society: Washington, DC, 1969.

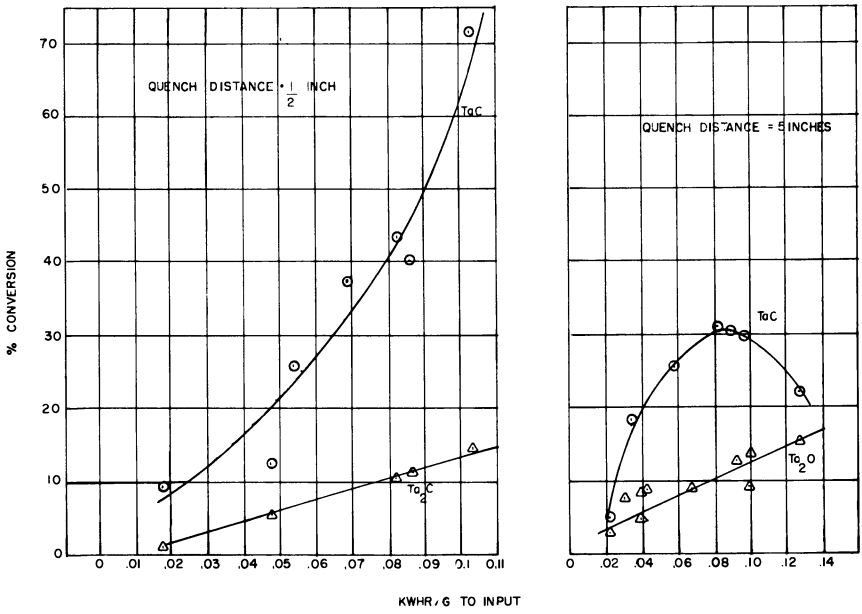

Figure 7. Reaction of tantalum and methane in a helium plasma jet

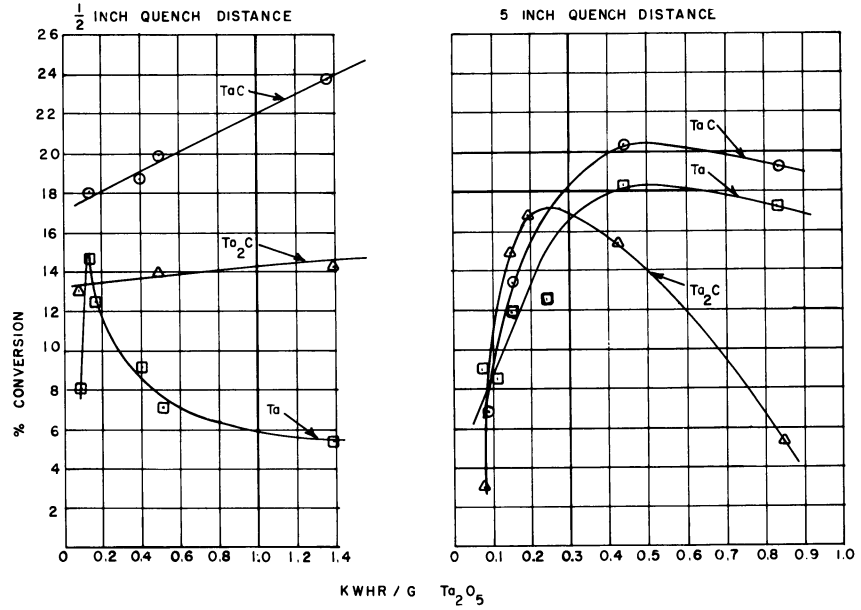

Figure 8. Plot of the tantalum pentoxide plus methane reaction carried out in a helium plasma jet

Publication Date: June 1, 1969 | doi: 10.1021/ba-1969-0080.ch033

The reduction of tantalum pentoxide with hydrogen (*14*) in a helium plasma jet to produce tantalum metal (Reaction 23) is shown in Figure 9. Again the percent conversion is plotted *vs.* kwh./gram Ta_2O_5 input for two different quenching distances. As can be seen, the more rapid quenching (1/2 inch case) gives the maximum conversion (42%), which peaks at 0.35 kwh./gram Ta_2O_5.

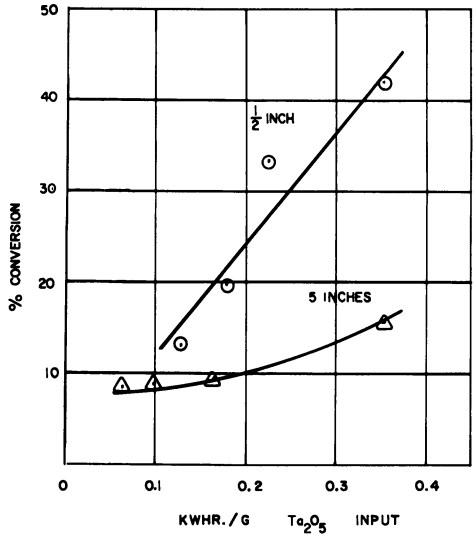

Figure 9. Reduction of tantalum pentoxide with hydrogen in a helium plasma jet to produce tantalum metal

In a similar manner, the reduction of tungsten trioxide was carried out in a helium plasma jet (*16*) with the quenching device 5 inches below the plasma jet. Conversions as high as 95% were obtained carrying the tungsten trioxide in hydrogen into the flame of the jet. The reduction of other metal oxides has also been experimentally investigated (*16*). Ferric oxide was reduced to iron metal in a 100% conversion using a helium plasma jet and carrying the ferric oxide in hydrogen (Reaction 26). Titanium dioxide and zirconium dioxide reductions were also attempted by the same method. However, no reduction was obtained in either case. The reduction of aluminum oxide with hydrogen in a helium plasma jet produced only a 2 to 5% conversion to aluminum metal using several different quenching methods. In the above experiments, powder feed rates were in the gram/min. range with the arc gas flow at 30 to 40 liter/min. and power levels of 9 to 16 kw.

Publication Date: June 1, 1969 | doi: 10.1021/ba-1969-0080.ch033

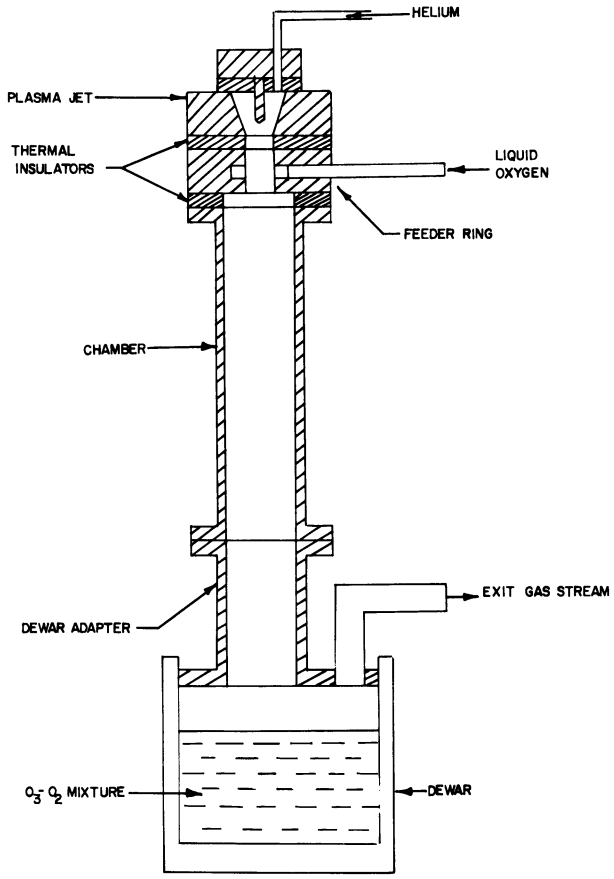

Figure 10. Scheme of apparatus used in the production of ozone by means of a plasma jet

Liquid-Gas Reactions Producing a Gas.

$$\text{Liq. } O_2 \xrightarrow{\text{He plasma}} O_3 \qquad (27)$$

$$\text{Hydrocarbons} \rightarrow C_2H_2 \qquad (28)$$

The production of ozone by means of a plasma jet was accomplished by feeding liquid oxygen into a helium jet (*18*). Figure 10 shows the scheme of the apparatus used. Figure 11 shows the effect of liquid oxygen flow on ozone production under constant arc conditions of 27 kw. with He flow at 16 liter/min. The liquid oxygen acts as both a reactant and quenching medium.

Another example of this type of reaction is the decomposition of hydrocarbons into acetylene by use of a plasma jet device. Thermody-

In Chemical Reactions in Electrical Discharges; Blaustein, B.;
Advances in Chemistry; American Chemical Society: Washington, DC, 1969.

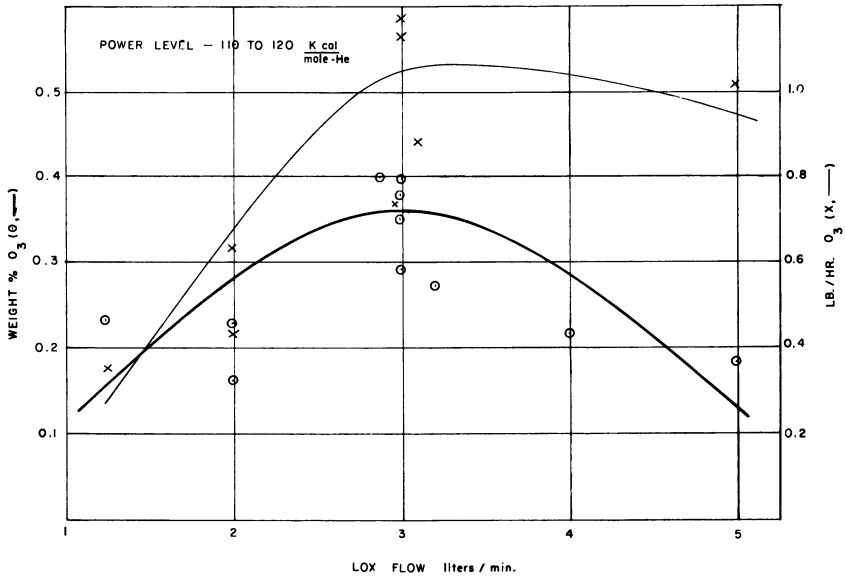

Figure 11. Effect of liquid oxygen flow on ozone production under constant arc conditions of 27 kw. with He flow at 16 liter/min.

namics Corporation (*20*) has proved the feasibility of producing acetylene from kerosene using a plasma torch. Preliminary runs gave yields of 18% acetylene.

Liquid-Gas Reactions to Produce a Liquid

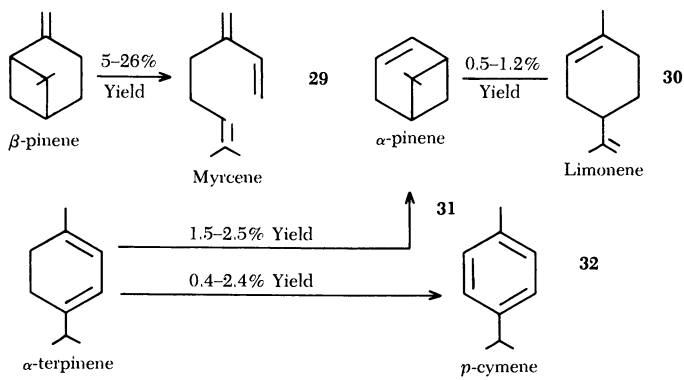

Under a program carried on at the Research Institute of Temple University for the Glidden Company, the reactions of terpenes in a plasma jet were studied (*15*). The reactions shown above were investigated by use of the apparatus shown schematically in Figure 12. All experimental

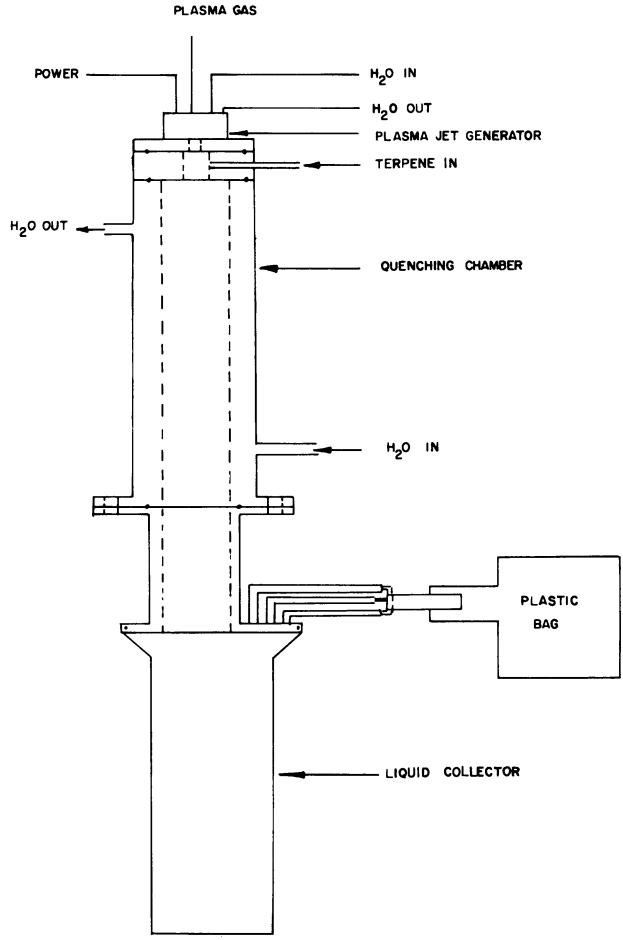

Figure 12. Scheme of apparatus used in the study of the reactions of terpenes in a plasma jet

data were obtained using a helium plasma jet where the terpene was added in a liquid state into the helium plasma flame. Typical arc conditions for these experiments were He flow, 25 to 30 liter/min., terpene flow 600–1400 cc./min. with power at 6 to 18 kw. The products were analyzed by means of chromatographic absorption. The most productive synthesis was the conversion of β-pinene to myrcene in 26% yield (Reaction 29). Although this is a normal pyrolysis product of β-pinene, it is the first time that a complicated molecule has been produced by means of a plasma jet. Other reactions included the preparation of limonene

In Chemical Reactions in Electrical Discharges; Blaustein, B.;
Advances in Chemistry; American Chemical Society: Washington, DC, 1969.

from α-pinene in 1% conversion and *p*-cymene in 2 1/2% yield and α-pinene in 2 1/2% yield from α-terpinene (Reactions 30 to 32).

Summary

The chemical reactions discussed herein summarize the syntheses that have been accomplished thus far using a plasma jet device and are by no means all the syntheses studied using a plasma jet. The plasma jet has shown itself to be a useful tool in the area of synthesis of compounds and recently has moved from the preparation of simple materials to more complex ones. With the ever increasing number of investigations being carried out by private industry, there is no doubt that the plasma jet will become a commercial chemical process device. Its potential has just been touched and with each new use a whole field of investigation is opened.

Publication Date: June 1, 1969 | doi: 10.1021/ba-1969-0080.ch033

Literature Cited

(1) Anderson, J. E., Case, L. K., *Ind. Eng. Chem., Process Design Develop.* **1**, 161 (1962).
(2) Bronfin, D. R., Hazlett, R. N., *Ind. Eng. Chem. Fundamentals* **5**, 472 (1966).
(3) Damon, R. A., White, D. H., "Proposed Plasma Chemical Processes of Interest to the Petroleum Industry," **Report No. PLR-115,** Plasmadyne Corp., Santa Ana, Calif., Feb. 8, 1962.
(4) Damon, R. A., White, D. H., "Typical Inorganic and Inorganic High Temperature Plasma Jet Reactions," **Report No. PLR-119,** Plasmadyne Corp., Santa Ana, Calif., September 20, 1962.
(5) Freeman, M. P., Skrivan, J. P., *Am. Inst. Chem. Eng. J.* **8**, 450 (1962).
(6) Graves, R. D., Kawa, W., Kiteshue, R. W., *Ind. Eng. Chem., Process Design Develop.* **5**, 59 (1966).
(7) Grosse, A. V., Leutner, H. W., Stokes, C. S., *First Ann. Rept. Office of Naval Research* **Contract NONR-3085(02),** *Res. Inst. Temple Univ.,* Philadelphia, Pa. (December 31, 1961).
(8) Grosse, A. V., Stokes, C. S., Cahill, J. A., Correa, J. J., Plasma Jet Chemistry, *Final Rept. Office of Naval Research* **Contract NONR-3085(02),** *Res. Inst. Temple Univ.,* Philadelphia, Pa. (June 30, 1963).
(9) Harnisch, H., Keymer, G., Schallus, E., *Angew. Chem.* **2**, 238 (1963).
(10) Leutner, H. W., *Ind. Eng. Chem., Process Design Develop.* **1**, 166 (1962).
(11) *Ibid.*, **2**, 315 (1963).
(12) Leutner, H. W., Stokes, C. S., *Ind. Eng. Chem.* **53**, 341 (1961).
(13) *Nat. Acad. Sci., Nat. Res. Council, Washington, D. C.,* **Report MAB-167-M,** Div. Eng. Ind. Res. (August 30, 1960).
(14) Stokes, C. S., Cahill, J. A., *Final Rept., Air Force Office of Scientific Research* **Grant 775-65,** *Res. Inst. Temple Univ.,* Philadelphia, Pa. (December, 1965).
(15) Stokes, C. S., Correa, J. J., *Final Rept. for Glidden Co., Res. Inst. Temple Univ.,* Philadelphia, Pa. (December, 1964).

(16) Stokes, C. S., Cahill, J. A., Correa, J. J., Grosse, A. V., *Final Rept., Air Force Office of Scientific Research* **Grant 62-196,** *Res. Inst. Temple Univ.*, Philadelphia, Pa. (December, 1964).
(17) Stokes, C. S., Knipe, W. W., *Ind. Eng. Chem.* **52,** 287 (1960).
(18) Stokes, C. S., Streng, L. A., *Ind. Eng. Chem., Product Res. Develop.* 4, 36 (1965).
(19) Thermal Dynamics Corp., Lebanon, N. H., *Plasma Fax Bulletin* **PF-3** (October, 1960).
(20) *Ibid.*, **Bulletin PF-2** (October, 1960).

RECEIVED May 24, 1967.

34

Production of Hydrogen Cyanide from Methane in a Nitrogen Plasma Jet

I. Reactive Species Titration; Further Quantitative Studies

MARK P. FREEMAN[1]

Central Research Division, American Cyanamid Co., Stamford, Conn.

Publication Date: June 1, 1969 | doi: 10.1021/ba-1969-0080.ch034

Results from recent work in which the reactor configuration is systematically varied, presented together with some previous experimental work and theoretical calculations, unambiguously establish that the formation of HCN through the admixing of methane to a nitrogen plasma jet is titration in the true meaning of the word. No attempt is made to establish an exact mechanism but the titration of either the heat flow or alternatively of nitrogen atomic ions is seen quantitatively to account for the observed rate of production of HCN.

The reaction of methane with a nitrogen plasma to make hydrogen cyanide and acetylene is of considerable interest. Conversions are high enough to be of commercial interest on the one hand (*8, 11*), while the formation of HCN in particular proceeds in such an interesting and reproducible way that clarification of the details of the reaction should considerably advance the use of the plasma jet in synthetic chemistry, and further might be expected to contribute significantly to basic chemical knowledge.

The formally identical synthesis of HCN from "active nitrogen" and methane has been extensively studied (*4, 9, 12*) for more than a half century. That the systems are different is apparent, for the high-voltage discharge is a high excitation device, whereas the plasma jet is thought to be nearly in local thermal equilibrium and hence a low excitation

[1] Temporary address: Department of Chemical Engineering, Massachusetts Institute of Technology, Cambridge, Mass.

In Chemical Reactions in Electrical Discharges; Blaustein, B.;
Advances in Chemistry; American Chemical Society: Washington, DC, 1969.

device (spectroscopically speaking, intermediate between arc and spark (*10*)). Furthermore, the plasma jet experiments are performed at one-half atmosphere (as opposed to about 1 torr) and at an average temperature twenty times as high on the absolute scale as room temperature, where the bulk of active nitrogen experiments have been performed. Finally, in the plasma jet the carbonaceous species reacting is evidently not methane. That is, the products other than HCN are acetylene and higher acetylenes with various degrees of saturation. These are the same products that would form if the jet were, say, argon. It has been shown elsewhere (*7*) that the precursors for these products form rapidly compared to the time for mixing of the methane with the jet.

There is no question that the plasma jet provides a difficult environment in which to do "good work" in the usual sense. The enormous temperature gradients and consequent inhomogeneities are generally thought of as being a sort of physical chemical bar sinister. On the other hand, perhaps because of their extreme magnitude, the effects owing to the temperature gradients are found to be sufficiently reproducible to allow systematic investigation of the jet as a whole, which in its hotter parts represents in a steady state flow situation a chemically unique environment found only in high intensity arc devices. As compensation for tackling this difficult environment, the investigator need not work with trace quantities, but instead with partial pressures and relative conversions at least two orders of magnitude higher than those encountered in active nitrogen research.

The work reported here represents a systematic continuation of a study performed some time ago (*5*). The procedure followed then as now is to add methane through an annular slot to a confined nitrogen jet of precisely defined average enthalpy—*i.e.*, a calibrated flow rate and a measured heat flow. It has been shown that under these conditions mixing is very rapid, as is the drop in temperature defined from average enthalpy (*7*). After about one millisecond the resulting flow of high temperature species is further chilled by the entrainment of cold product gas (the fastest of several quench methods investigated on the basis of its efficacy in quenching the ammonia decomposition reaction) (*7*) and the flow of HCN in the product gas is chemically determined. Except as noted, the data are taken at 350 ± 20 torr chamber pressure, as this pressure is found to reduce the formation of solid product to an insignificant level. As the methane is added at various flow rates, the corresponding rate of production of HCN is noted. Just as in *e.g.*, Winkler's work with active nitrogen, a plateau is observed which seems to indicate that some active species is indeed being titrated (Figure 1). Of utmost interest in the older study was the provocatively simple dependence of the plateau level on jet power level (Figure 2). Because this may in turn

Publication Date: June 1, 1969 | doi: 10.1021/ba-1969-0080.ch034

In Chemical Reactions in Electrical Discharges; Blaustein, B.;
Advances in Chemistry; American Chemical Society: Washington, DC, 1969.

be shown to correlate with the rate of production of ions in the arc process (*5*), it raised the question, still unresolved, as to whether the ions might not in some way be responsible for the chemistry. As a direct consequence, there is a long-term quantitative spectroscopic study of plasma jets (*6*) currently in progress that is expected ultimately to yield information on the nature and quantity of ions, atoms, and high temperature molecular species flowing in jets of common plasma materials.

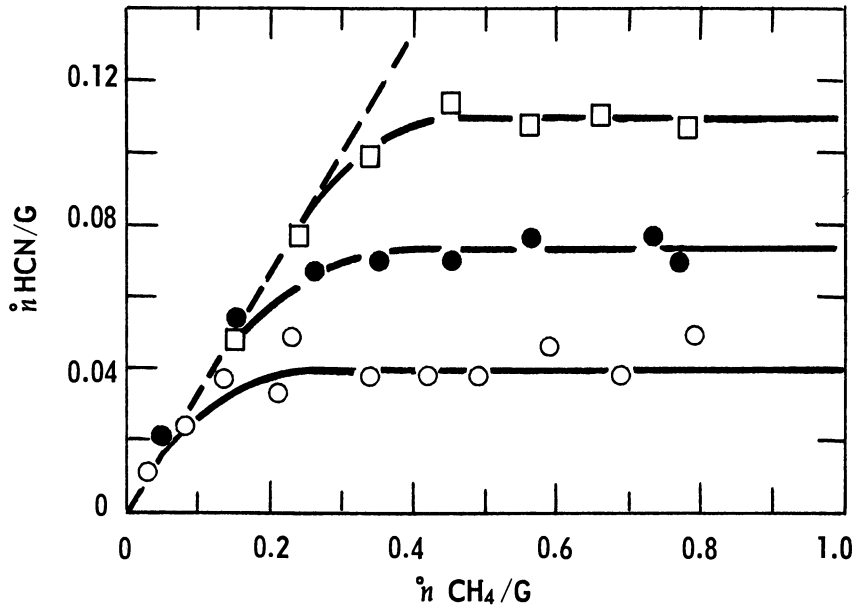

Figure 1. Absolute production rate of HCN vs. *feed rate of methane (both normalized by dividing by G, the most common flow rate of nitrogen. G = 0.0171 gram moles/sec. = 0.383 liter (STP)/sec.) at three net power levels: 3522 watts—○; 6992 watts—●; and 9782 watts—□. Old data, reactor configuration of Figure 5, (0 inch; 2 inch)*

Although thermodynamic calculations had previously been performed for the nitrogen-carbon-hydrogen system (*14*), they were not in a form easy to compare with plasma jet results obtained under normal operating constraints. The calculations were therefore reproduced (*1*) with the pertinent parameters varied to conform to the exigencies of plasma jet operation. Figures 3 and 4 show the results obtained when solid carbon is suppressed in the calculations to be consistent with its absence in the observed products. An important fact immediately emerges. Neither at any experimentally attained average enthalpy, nor at any experimentally used ratio of methane to nitrogen, has the thermodynamically expected yield of HCN for a well-mixed system been exceeded. (Note that the

Publication Date: June 1, 1969 | doi: 10.1021/ba-1969-0080.ch034

apparent fall-off in calculated yield at high power levels and/or low methane flow rates is owing to the competitive formation of cyano, CN, which may be presumed to be an HCN precursor.)

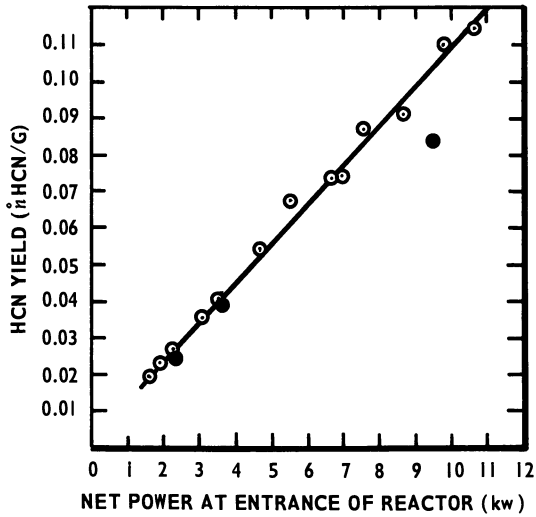

Figure 2. Absolute production rate of HCN (normalized) vs. net power flowing in gas at entrance to reactor. CH_4: N_2::1: 2. Filled data points were taken at substantially reduced nitrogen flow, 0.0125 gram moles/sec.

The relationship between the observed and calculated equilibrium yields for the CH_4-N_2 system is strikingly similar to that recently reported for the F-C-N system by Bronfin (2), who thereupon advanced the plausible hypothesis that in either case the observed yield is in some way a consequence of equilibrium considerations. Now, from earlier work on the acetylene system (7), it would seem that the composition and enthalpy dependence are not what one would expect for mixing and subsequent freezing of a reaction in a confining tube and further for the shorter reactors the enthalpy at the exit is still very high. We shall therefore disregard this possibility here. (B. R. Bronfin and L. S. Cohen (United Aircraft Laboratories) are currently testing this model by means of computer simulation.) The expected way in which equilibrium could control the reaction is for the product distribution to be a function of the enthalpy and composition profiles at the exit of the reactor where there is an onset of rapid quenching. The calculations indicate that composition is only of secondary importance in the "plateau" region so that presumably the enthalpy profile would be controlling. This differs from true titration in the important respect that in titration one in effect irreversibly consumes a certain potential of the nitrogen jet to form HCN

Publication Date: June 1, 1969 | doi: 10.1021/ba-1969-0080.ch034

In Chemical Reactions in Electrical Discharges; Blaustein, B.;
Advances in Chemistry; American Chemical Society: Washington, DC, 1969.

that is clearly a function only of the temperature and/or composition and velocity profile in the nitrogen at the point of mixing but before mixing occurs. If we assume the velocity profile of a plasma jet is uniquely determined by the enthalpy profile (*6*), then the reacting potential as a consequence would in turn be uniquely related to the heat flow in the gas.

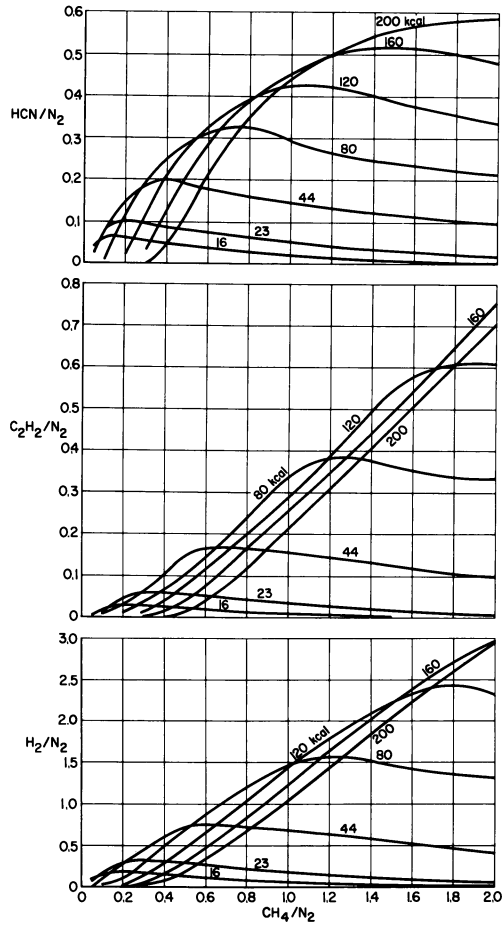

Figure 3. Calculated yields of HCN, acetylene, and hydrogen relative to initial nitrogen resulting from the indicated nitrogen-methane mixtures. The methane is initially cold and the nitrogen initially at the indicated enthalpy. Solid carbon has been suppressed as a species in this calculation

Despite this difference, there is no way to distinguish unambiguously between these two possibilities using but one reactor. This is because fractional heat loss from a plasma in a particular reactor type has been

Publication Date: June 1, 1969 | doi: 10.1021/ba-1969-0080.ch034

shown to be primarily a function of reactor length and arc unit design (*15*), so that the ratio of exit heat flow to inlet heat flow is nearly constant. The primary objective of the work reported here was therefore to distinguish carefully between these possibilities by performing identical titration experiments in two or more reactors that differ significantly in length in order to determine unambiguously whether inlet or exit heat flow controls the reaction.

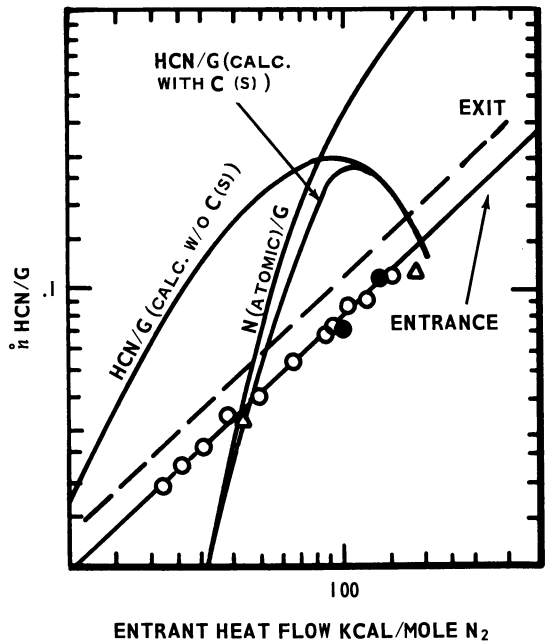

Figure 4. Old HCN plateau yield data plotted vs. *initial nitrogen heat flow. Also shown are the appropriate theoretically calculated curves for HCN (full equilibrium), HCN (carbon suppressed) and N atoms. The dashed line indicates where the somewhat more scattered experimental data would have fallen if plotted* vs. *2 inch reactor exit heat flow*

It had been inferred from the earlier work by rather incomplete evidence that somehow the capacity to make HCN is primarily dependent on arc conditions no matter how far removed the injection point is from the arc unit itself. A further objective of this experiment was therefore systematically to check this tentative conclusion by careful control and variation of the injection point on a long reactor. From the standpoint of the titration hypothesis, if the arc unit conditions are indeed controlling,

Publication Date: June 1, 1969 | doi: 10.1021/ba-1969-0080.ch034

then a very long-lived reactive species is implied; such a species is hardly to be expected under these experimental conditions.

Finally, at the same time the older work was being done, Leutner (*11*), using a very short tubular reactor of otherwise the same design, found he was able to work at atmospheric pressure and achieve a nitrogen fixation of 12.5% (erroneously reported as 21.9%) (*16*) in a nitrogen (62%)-argon jet (erroneously reported as pure nitrogen) with a total flow of 5.0 l(STP)/min. and a power flowing in the gas of 11.5 kw. × 55% (16) = 6.32 kw. It was deemed desirable to reproduce his reactor as nearly as possible to attempt to see if the two sets of results were consistent. Such comparison will be made in a subsequent paper (Part II), where the effect of argon dilution of the plasma will be discussed in some detail. The contribution such a reactor makes to the present work is of course to extend the range of reactor lengths studied.

Publication Date: June 1, 1969 | doi: 10.1021/ba-1969-0080.ch034

Experimental

Apparatus. Plasma-jet reactors consist of three parts, head or arc unit, intermediate section, and quenching section. The plasma-jet head unit used for this study is a Thermal Dynamics L-40 Plasma-jet with "turbulent nitrogen" electrodes, powered by two 12 kw. welding power supplies, open circuit voltage 160 volts, connected in parallel but with opposite phase rotations on their 3ϕ input so as to minimize line frequency ripple in the output. The intermediate sections (Figure 5) are made of copper and are fully water-cooled, as is the head. The three intermediate sections are themselves modular. Of length 2 inches, 2 inches, and 4 inches, they are mutually compatible and can be joined in any order to make a reactor of length 2, 4, 6, or 8 inches with a feed port at any multiple of 2 inches. Note that the feed rings are not exactly reproducible in that there are residual gaps left when the surrounding gaskets are tightly compressed by the joining threaded parts. The "Leutner reactor" is a standard Thermal Dynamics spray nozzle with the solids injection port, which is about 1/4 inch from the nozzle exit, opened up to a 180° slot. The spray nozzle and the turbulent nitrogen electrode used with the intermediate reactors has a 7/32 inch diameter as do the intermediate reactors. Insofar as the various reactor configurations vary only in length and feed point, it will suffice to distinguish between them with a bracket specifying first the distance from the point of heat balance to the point of methane feed, and second the distance from the point of heat balance to the exit of the reactor. Thus, the 8 inch reactor fed at the 2 inch point would be designated (2 inches; 8 inches), while the Leutner reactor is (−1/4 inches; 0 inches).

The quenching section where the hot stream of plasma and reaction products are quenched by entrainment of cold product gas is simply a stainless steel pot 11 inches long and 11 inches in diameter sparsely wound with soldered-on copper tubing. All parts subject to heat damage are well-cooled, but between the windings the pot may get hot enough to cause flesh burns. At the outlet of the quenching section is six feet of

In Chemical Reactions in Electrical Discharges; Blaustein, B.;
Advances in Chemistry; American Chemical Society: Washington, DC, 1969.

1 inch thick rubberized acid hose. This in turn is fastened to the bottom of a vertical mixing section consisting of a three foot long 2 inch diameter pipe loosely packed with glass wool. The carbon dioxide is mixed with the product stream at the inlet to the mixing section. The top of the mixing section is connected to a high capacity steam vacuum jet with an automatic control valve for maintaining desired pressures.

A Toeppler pump is arranged to withdraw 522 ml. of gas from the top of the mixing section at room temperature and at the reactor pressure. This aliquot is then collected for analysis in a suitable gas collection system.

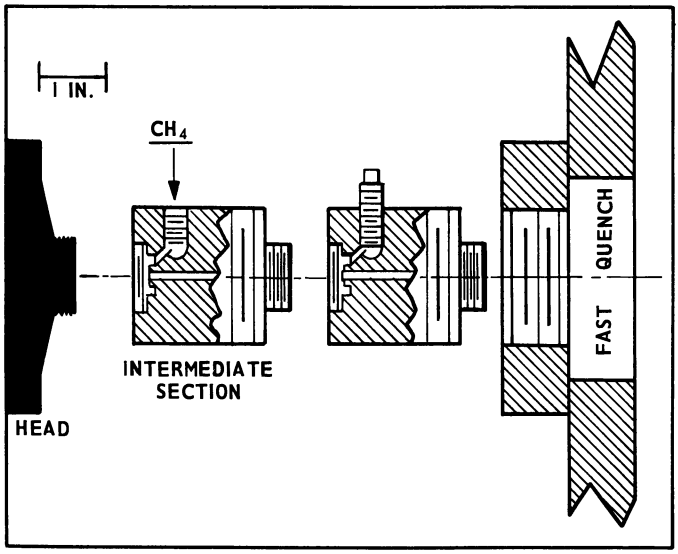

Figure 5. Schematic representation of modular plasma jet reactor showing but two two-inch intermediate sections

Gas flows except for methane are metered by orifice gages calibrated by water displacement to within 1% for CO_2 and N_2, respectively. Methane flow, much less critical, is determined by a Rotameter calibrated by calculation. All cooling water flows are determined by experimentally calibrated Rotameters. Cooling water temperature rise is determined by suitably graduated, interconsistent mercury thermometers.

Procedure. Heat flow in the nitrogen plasma at the point of methane introduction is determined by subtracting from the voltage-current product in the arc the heat lost to all cooling water supplies up to that point. For the most part, just the heat flowing at the exit of the head is required. For data taken at a particular heat flow an attempt is made to keep the heat flow constant. In this endeavor the relatively great intrinsic stability of plasma jets made by this manufacturer help, but especially in runs lasting for several hours it is necessary continually to introduce small corrections. This control is greatly facilitated through use of an analog computer that continuously monitors voltage, current, and cooling water temperature rise and either directly controls the rectifiers or displays the

Publication Date: June 1, 1969 | doi: 10.1021/ba-1969-0080.ch034

In Chemical Reactions in Electrical Discharges; Blaustein, B.;
Advances in Chemistry; American Chemical Society: Washington, DC, 1969.

net heat flow in kilowatts continuously on a recorder chart so that manual corrections may be introduced as needed. Heat levels given are generally correct to within ±5%.

Except where noted, the pressure in the quenching chamber is kept at 350 ± 20 torr. The actual pressure of each sample is known to ±1 torr but that is not a significant datum in the analysis and is used only as a consistency check. Quench section pressure measures intermediate section pressures fairly well, but probably not the arc pressures because of the pressure drop through the front orifice of the plasma jet. These arc units are not instrumented to measure the pressure inside the head.

Whenever methane flow rate, power level, and/or pressure conditions are changed, the system is operated for eight minutes before taking a sample. This is found to be sufficient time to establish a constant composition.

The collected gas aliquot is slowly bubbled through 200 ml. of ice-cold caustic containing 12.5 millimoles of base. The half liter space over the caustic is initially evacuated so that the entire sample, together with the air used to flush the lines, might be collected in the caustic and the space over it. This is followed by one minute of vigorous shaking. This procedure has been found satisfactory for the quantitative recovery of CO_2 and HCN. Total acid in the gas is then determined by back-titration with 0.500*N* HCl until all the carbonate has been converted to bicarbonate (pH = 8.3). Ammoniacal KI is then added as an indicator and cyanide determined by precipitometric titration with 0.0100*N* silver ion. This permits the initial ratio of HCN to CO_2 to be determined. Because the absolute flow rate of CO_2 is known, the absolute production rate of HCN follows directly. Note that for convenience in presentation the flow rate of HCN is always presented as some fraction of 0.383 liter (STP)/sec. (0.0171 gram moles $sec.^{-1}$) so that it may conveniently be compared with the most often used flow rate of nitrogen. In the figures this "standard" flow rate is represented as G.

Accounting for the various sources of uncertainty, the actual HCN flow rate is estimated to be within about 10% of the reported value, and the heat flow to within 5%. Air leakage into the system, a potential source of error, is held below 0.05% of the total gas flow.

The upper limits of operation are fixed by the onset of plugging. For all but the Leutner reactor, solids formation is otherwise negligible though not nonexistent. At high power levels the Leutner reactor does not plug, the heat of the jet evidently serves to clear incipient plugs, but a fair quantity of a low density brown solid is produced that is about 14% polymerized HCN. Its quantity is estimated to be small compared with the total methane utilized.

Although temperatures are not quoted, the temperatures corresponding to the extremes of the eightfold average enthalpy range are 3250-7000°K.

Results

Composition Dependence. Figure 6 shows typical "titration" curves for the different situations of interest. In every case a plot of HCN produced *vs.* methane added (both normalized to the "standard flow rate"

Publication Date: June 1, 1969 | doi: 10.1021/ba-1969-0080.ch034

of 0.0171 mole/sec.) divides cleanly into two regimes separated by a break to which we refer as the "equivalence point." To the left of the equivalence point, the yield is simply dependent on methane feed rate but not on the power level. Lines of slope 1/3 and 2/3 are included on the graph to facilitate intercomparison in this region. Although the data are too scattered to draw firm conclusions, it is clear that the break quite generally occurs along the line corresponding to a slope of 1/3. In this region it is as though the nitrogen were somehow present in excess. To the right of the break the HCN throughput is seen to depend only weakly on methane but, as is demonstrated below, is a strong and simple function of heat flow in the nitrogen before mixing. Excluding for the moment the (−1/4 inch; 0 inch) data (Figure 6-d), the methane dependence on the right shows a real linear increase with methane flow rate in every case, but this slope is not found to be particularly reproducible since it is apt to change slightly when the apparatus is demounted and reassembled. Hence, the scale has been chosen to emphasize the plateau-like character of the curve. Note that the data excepted may be explained by the fact that in this case the exit rather than the entrant heat flow is regulated. Because of the small heat loss in this short section only a second order effect of this magnitude would be expected.

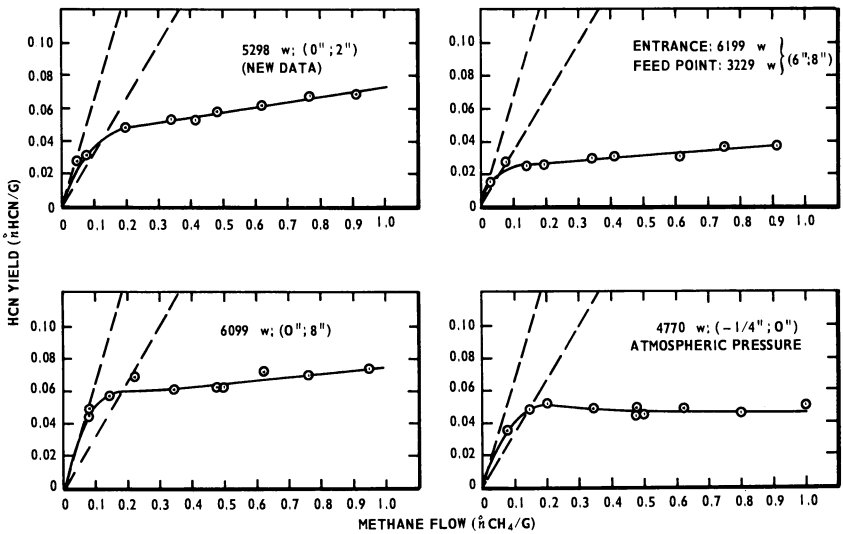

Figure 6. Typical titration curves for the case noted. Normalized production rate of HCN vs. flow rate of methane. Dashed lines of slope 1/3 and 2/3 are included for reference

Power Level Dependence. To take account of the residual slope of the "titration" curves, intercomparison of power-level-dependence studies is done at the same methane flow rate corresponding to one half the

"standard" flow whether it is an interpolated point taken from a full titration curve as shown in Figure 6 (filled points)or an isolated measurement (open points). The best line through the old data (Figure 2) appears in Figures 7 through 9 as a reference to aid in intercomparison. Note that Figure 6-a should be exactly consistent with the older data of Figure 1 while the data of Figure 7-b should exactly reproduce Figure 2. The extent that they fail to do this is a fair measure of the nonreproducibility of this experiment when performed in different laboratories, with different equipment, with the chemical analyses performed by different persons.

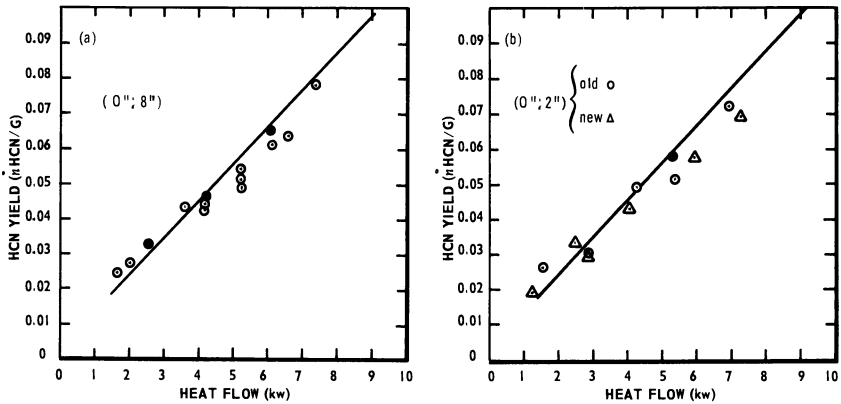

Figure 7. Normalized HCN vs. heat flow (head exit power) for the eight inch reactor (left) and the two inch reactor (right). Triangles and circles indicate two different 2 inch reactors. Filled points were interpolated from full titration curves; open points were isolated runs. The "normal" line of Figure 2 is included in either case for reference

In Figure 7-b data from two different 2 inch reactors are intermingled as shown. This is to be compared with the (0 inch; 8 inch) data of Figure 7-a. It is quite clear that within the experimental scatter it would indeed be difficult to improve the agreement. Now the heat leaving the 8 inch reactor for a given input is only about one half that leaving a 2 inch reactor for the same input, so that there can be no question but that the HCN production depends only on the heat flow at the point of mixing (or at the exit of the head) and not at all on that at the exit of the reactor.

Mixing Point Dependence. Figure 8 demonstrates clearly that the ability of the nitrogen to make HCN does not persist down the tube at its high initial level, but rather decays as the heat flowing in the gas decays. Shown are a particular set of (6 inch; 8 inch) data plotted on the left *vs.* heat flow at the exit of the head, and on the right as a function

Publication Date: June 1, 1969 | doi: 10.1021/ba-1969-0080.ch034

of the heat flowing at the point of mixing, the 6 inch point. Hence, that part of the earlier work indicating the existence of a "long-lived" reactive species is wrong.

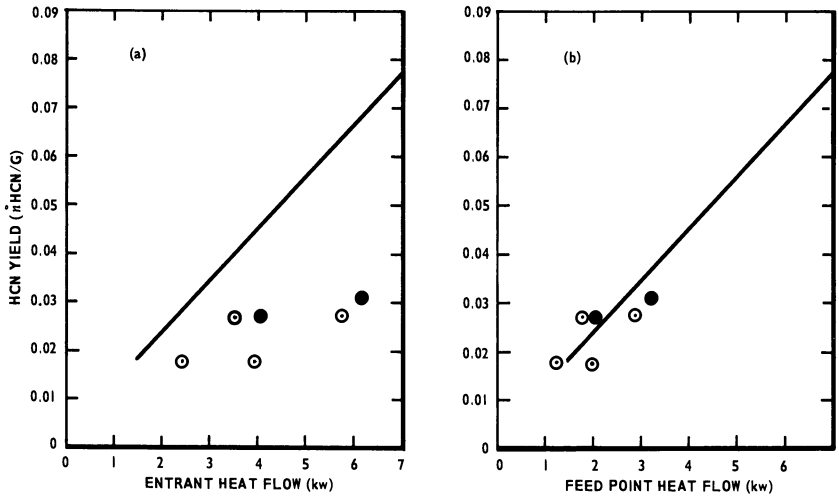

Figure 8. Normalized production rate of HCN for the eight inch reactor fed methane at the six inch point, (6 inch; 8 inch) data, vs. *heat flow at (a) the exit of the head and (b) at the 6 inch feed point. Filled points were interpolated from full titration curves. The "normal" line of Figure 2 is included in either case for reference*

Leutner Reactor. Data for the simulated Leutner reactor are shown in Figure 9. Despite the fact that these data were taken at atmospheric pressure it is clear that the results are completely consistent with those of the other reactors. This agrees with an observation made in the earlier work that there is but slight pressure dependence for this reaction. Of significance here is the fact that reactors from 1/4 inch to 8 inches in length give the same result, dependent only on entrant heat flow. (Actually for the 1/4 inch reactor the exit heat flow is measured, but presumably in this case there is a nearly negligible difference.)

Product Distribution. PLATEAU REGION. Mass spectrometer checks made on product formed in the "plateau" region show N_2, H_2, HCN, C_2H_2, and CH_4 together with some small quantities of higher acetylenes to be the only species present to any appreciable extent. The N_2 is of course present in large excess while the H_2 is simply the balance of the hydrogen. The HCN is apparently formed by some sort of irreversible process to be discussed further below while the relative amounts of methane and acetylene seem to conform to considerations investigated previously (7) for the cracking of methane in an argon jet.

Publication Date: June 1, 1969 | doi: 10.1021/ba-1969-0080.ch034

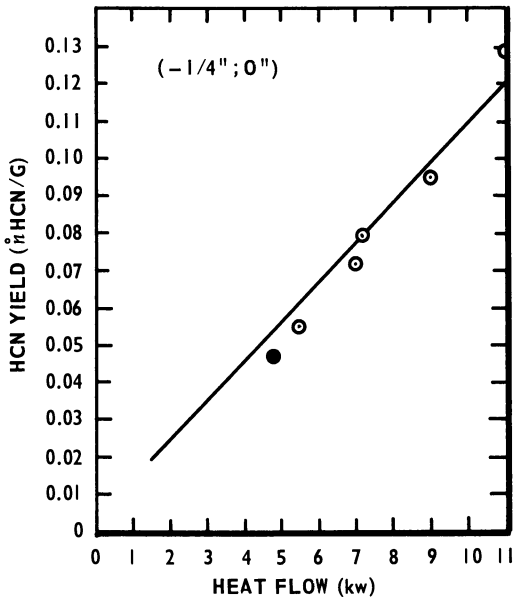

Figure 9. Normalized production rate of HCN in the Leutner reactor vs. heat flow at the exit of the reactor. The "normal" curve of Figure 2 is included for reference

INITIAL REGION. To the left of the break region where the potential of the nitrogen jet to react is in excess, one might expect all or most of the methane to be converted to HCN, *i.e.*, an initial straight line of unit slope, but such is not the case. Earlier work seemed to favor an initial slope of 1/3 for all titration curves. This would imply that one mole of acetylene is formed for each mole of HCN produced. At the time, however, admittedly crude mass spectrometer checks showed no more than two-thirds to three quarters mole of acetylene to each mole of HCN. The work reported here indicates an initial slope corresponding to one quarter to one half mole of acetylene for each mole of HCN. At the breakpoint, however, equimolar quantities of HCN and acetylene would still seem to be the rule. The analytical and sampling apparatuses were neither designed for accuracy nor high precision in this low yield region and it is possible that the differences in the low HCN yield region might have reflected some small change in analytical procedure. It seems more probable, though, that this region is indeed not reproducible and that product distribution here reflects some intangible of the process such as "mixing efficiency," etc. (Note that the reactors are constructed so that the widths of the slots through which the methane flows are not precisely reproducible.)

Publication Date: June 1, 1969 | doi: 10.1021/ba-1969-0080.ch034

Discussion

The Titration Curve. It is clear that the reactor length and hence the heat flow at the onset of sudden quenching is irrelevant; the heat flow at the mixing point evidently governs the extent of reaction. It is further seen that the ability of the nitrogen jet to react with the methane decreases as the nitrogen flows down the reactor in such a way that its potential to react with methane, at least with this reactor geometry, is a function only of heat flow in the nitrogen before mixing.

INITIAL REGION. From a different perspective, with no methane flowing in a long tube the reactive potential of the nitrogen jet is seen to persist to some appreciable extent almost indefinitely, but decays as the heat flow decays, presumably through heat conduction processes. As the methane flow is introduced, some of this "potential to react" (PR for brevity) is now used up by the methane, while the balance decays by the heat conduction process. This gives rise to the "initial region."

EQUIVALENCE POINT. As the methane flow is increased, more of the PR of the nitrogen jet is used by the methane until the equivalence point is reached. At this point none of the PR survives the mixing of the jet with the methane and the break in the curve occurs.

PLATEAU REGION. Because mixing is not instantaneous at the point of mixing, some of the PR is still used up by heat conduction processes at the equivalence point. As the methane flow is further increased, the equivalent amount mixes closer and closer to the slot so that less of the residual PR is lost to heat conduction. This latter process probably gives rise to the observed residual slope in the "plateau region" of the titration curves.

The Potential to React. It remains to propose an explanation for the "PR." Although something is being titrated, it is by no means clear just what it is. Nor, as of the present time, has anyone experimentally characterized a nitrogen jet sufficiently well to distinguish clearly between likely alternatives. Nonetheless, it is instructive to examine some of these possibilities for their heuristic value.

HEAT BALANCE. From Figure 2 a fairly constant heat requirement of 1280 kcal. mole^{-1} may be obtained. This corresponds very nicely (and probably fortuitously) to the endothermic heat of the most probable reaction at 6000°K. (3):

$$3\,CH_{4(298^\circ K.)} + 1/2\,N_{2(6000^\circ K.)} = CN_{(6000^\circ K.)} + C_{2(6000^\circ K.)} + 12\,H_{(6000^\circ K.)}$$
$$\Delta H = 1281 \text{ kcal.}$$

or that of the equally probable reaction at 4500°K.:

$$3\,CH_{4(298^\circ K.)} + 1/2\,N_{2(4500^\circ K.)} = CN_{(4500^\circ K.)} + 2/3\,C_{3(4500^\circ K.)} + 12\,H_{(4500^\circ K.)}$$
$$\Delta H = 1225 \text{ kcal.}$$

In Chemical Reactions in Electrical Discharges; Blaustein, B.;
Advances in Chemistry; American Chemical Society: Washington, DC, 1969.

Each of these equations correspond to the correct stoichiometry for the most probable precursors of the observed product at the equivalence point. The heat for the reaction endotherm is carried mainly by the heat of the dissociation and ionization of the large excess of diluent nitrogen, not included in the equations, which is assumed to go to molecular nitrogen at 6000°K. respectively 4500°K. in the course of the reaction. Because the enthalpy of molecular nitrogen at these temperatures is comparatively negligible, virtually the entire heat flow of the jet prior to mixing is available for the reaction endotherm and thus from this point of view it would appear that the heat of the jet is in some way being "titrated" by the methane.

Active Species. One might well ask, however, if it is just the heat being titrated why does the reaction apparently stop when the core of the jet is still 4000°–6000°K.? And why is the amount of cyano (CN) formed so sharply limited and constrained so far below the equilibrium value? Note that below 4000°K. strong exothermic reactions occur that delay further cooling, so that fast quenching cannot be the answer. The most ready answer to these questions is that the HCN reaction is far too slow to equilibrate in jet residence times. Of the manifold complex of forward reaction paths leading to equilibrium, only a few of them will be fast enough to produce HCN in the time available. But these fast reaction paths might well involve nitrogenous species which at thermal equilibrium corresponding to the average enthalpy of the jet would flow in trace amounts but which, as a consequence of the hot core, are present in the plasma jet at many orders of magnitude higher throughout. Thus we are led naturally to consider this as the titration of some sort of especially reactive species in the jet.

Consider for example a jet producing 0.00171 moles sec.$^{-1}$ of HCN. From Figure 2, we can see that this requires about 9 kw. of heat flowing in the gas. If we assume there is a small core to the jet at 12,000°K. (enthalpy at one-half atmosphere = 500 kcal./mole) (*13*), then the heat flow can be accounted for by assuming the hot core occupies about half the diameter of the jet (one fourth the area) and that the nitrogen flowing outside this core carries negligibly enthalpy. In this calculation is the unproved assumption carried over from the argon jet (*6*) that the mass flux of nitrogen is constant over the entire cross section. Under the assumed core conditions the jet is 100% dissociated and the atoms 17% ionized. The fluxes are then:

$$\text{atom flow: } 1/4 \times 2 \times (1 - 0.17) \times 0.0171 = 0.0071 \text{ moles (N atoms) sec.}^{-1}$$

$$\text{ion flow: } 1/4 \times 2 \times 0.17 \times 0.0171 = 0.00145 \text{ moles (N ions) sec.}^{-1}$$

Publication Date: June 1, 1969 | doi: 10.1021/ba-1969-0080.ch034

The ion flow is thus seen to be in excellent agreement with the 0.00171 moles sec.$^{-1}$ production rate of HCN. To some extent this may be caused by a fortunate choice of hot core temperature but is nevertheless a promising possibility.

On the other hand there seems to be no good way to account for the reaction on the basis of nitrogen atoms, in this case present in large excess, suggesting that the nitrogen atoms are somehow deactivated before the carbonaceous species enters the hot core. Insofar as the hydrogen from the dissociation of methane must completely fill the reactor in a very short while, it seems probable that the nitrogen atoms are deactivated from this initial infusion, and that the carbonaceous species react with the nitrogen ions (which might well be molecular ions by this time) or some other species sometime later.

Conclusion

By systematic variation of reactor geometry it has been conclusively demonstrated that methane added through a peripheral slot to a nitrogen jet titrates, apparently in the true meaning of the word, some potential of the nitrogen jet to react with the thermal decomposition products of methane to form HCN. It is further demonstrated that the potential to react is simply related to heat flow even far down the reactor and is therefore probably the consequence of some steady-state temperature and/or composition profile in a flow with local thermal equilibrium.

For their heuristic value, two superficially different explanations are proposed to explain the "potential to react." On the one hand, the experimental endotherm of the reaction at the equivalence point is shown to be quite consistent with the heat flowing in the hot core of the jet, for a jet model consistent with what we might expect. On the other hand, for the same heat flow and jet model, the yield is shown to be consistent with the flow rate of *e.g.*, ions at the point of mixing and it may equally well be postulated that the ions or some other identifiable species are in fact an active ingredient being titrated.

Acknowledgment

Many people have contributed in some way to the success of this work, but in particular the author wishes to express his appreciation to Charles Mentzer (Chemical Engineering Department, Princeton University) who helped perform some of the experiments, and to Hugh Hulburt (Chemical Engineering Department, Northwestern University) and Barry R. Bronfin (United Aircraft Laboratory) for their invaluable discussions and continuing interest.

In Chemical Reactions in Electrical Discharges; Blaustein, B.;
Advances in Chemistry; American Chemical Society: Washington, DC, 1969.

Literature Cited

(1) Bronfin, B. R., DiStefano, V. N., Freeman, M. P., Hazlett, R. N., *Proc. 15th CIC Chem. Engr. Conf., Quebec City, Quebec* (Oct. 25-27, 1965).
(2) Bronfin, B. R., Hazlett, R. N., *Ind. Eng. Chem. Fundamentals* **5,** 472 (1966).
(3) Dow Chemical Company, "Janaf Thermochemical Tables," Midland, Michigan (December 31, 196υ).
(4) Evans, N. E. V., Freeman, G. R., Winkler, C. A., *Can. J. Chem.* **34,** 1271 (1956).
(5) Freeman, M. P., "Abstracts of Papers," 147th Meeting, ACS, Philadelphia, Pa., April 5-10, 1964, I9.
(6) Freeman, M. P., *Quant. Spectrosc. Radiat. Transfer* **8,** 435 (1968).
(7) Freeman, M. P., Skrivan, J. F., *Am. Inst. Chem. Eng. J.* **8,** 450 (1962).
(8) Hulburt, H. M., Freeman, M. P., *Trans. N.Y. Acad. Sci.* **2,** No. 25, 770 (1963).
(9) Jennings, K. R., Linnett, J. W., *Quart. Rev. (London)* **12,** 116 (1958).
(10) Kovolev, F. A., Kvaratskheli, Yu. K., *Opt. Spectr., (USSR)* (English Transl.) **10,** 200 (1961).
(11) Leutner, H. W., *Ind. Eng. Chem. Process Design Develop.* **2,** 315 (1963).
(12) Manella, G. G., *Chem. Rev.* **63,** 1 (1963).
(13) Martinek, F., "Thermodynamic and Transport Properties of Gases, Liquids and Solids," p. 130, McGraw-Hill Book Co., Inc., New York, N. Y., 1959.
(14) Marynowski, C. W., Phillips, R. C., Phillips, J. C., Hiester, N. K., *Ind. Eng. Chem. Fundamentals* **1,** 52 (1962).
(15) Skrivan, J. F., VonJaskowsky, W., *Ind. Eng. Chem. Process Design Develop.* **4,** 371 (1965).
(16) Stokes, C. S. (personal communication).

RECEIVED June 15, 1967.

Hydrogen Cyanide Synthesis in a Thermal Radiofrequency Induction Plasma

BARRY R. BRONFIN

United Aircraft Research Laboratories, United Aircraft Corp.,
East Hartford, Conn.

Publication Date: June 1, 1969 | doi: 10.1021/ba-1969-0080.ch035

Methane-nitrogen mixtures were fed into a thermal argon plasma stabilized at 1/2 atm. by radiofrequency induction coupling. A rapid quench of the resulting high temperature (typically 10,000°K.) plasma mixture yielded hydrogen cyanide, acetylene, and hydrogen. The yield of HCN, expressed as a fraction of the nitrogen input converted, was found to be a function of input stoichiometry and to range up to 70%. A model based upon thermochemical equilibrium in the plasma and freezing during quench is suggested which predicts observed product compositions.

Gas temperatures above 15,000°K. have been observed in plasma generated by radiofrequency induction coupling (*32*). This high thermal energy regime becomes of interest to the chemist for the investigation of highly endothermic reactions. In particular, this paper will report reactions between methane and nitrogen fed to a thermal induction plasma and subsequently quenched to yield hydrogen cyanide, acetylene and hydrogen.

Previous Studies of the H–C–N System

Low Pressure Discharges. Winkler and his co-workers (*8, 9, 13, 15*) have systematically studied the reactions of nitrogen, activated by passage through a high-voltage discharge, with various hydrocarbons. These studies were carried out at pressures near 1 torr with very low reagent flow rates. Gas temperatures were also low, typically 300°C. In this non-equilibrium system the reaction between methane and "active" nitrogen yielded hydrogen cyanide, acetylene, and hydrogen (*13*).

In Chemical Reactions in Electrical Discharges; Blaustein, B.;
Advances in Chemistry; American Chemical Society: Washington, DC, 1969.

High Pressure Arcs. More recently high-power thermal arcs were used for the study of the H–C–N system near atmospheric pressure. Leutner (*21*) operated a nitrogen plasma jet into which methane was mixed. In his briefly reported results, up to 10% conversion of the nitrogen to HCN was found. In this volume Freeman (*10*) has reported an extensive study of the synthesis of HCN from a nitrogen plasma jet intermixed with methane. Typically, a 7% conversion of N_2 to HCN was observed. In both studies H_2, C_2H_2, and unreacted CH_4 were also identified as major consituents in the cooled product stream.

The Thermal Induction Plasma Study

The present study was undertaken to attempt higher nitrogen fixation levels in a reactor system markedly different from the previous investigations. Specifically, the thermal induction plasma reactor was chosen to provide very high average gas temperatures and to allow premixing of feed reagents. These factors were somewhat limiting in the previous investigations.

Dissociating Plasmas. Upon considering the various species possible in the H–C–N system, the strongest bond found is N≡N (226 kcal./gram mole). Thermal dissociation of N_2 is essentially complete at temperatures in excess of 8000°K. (*6*). One can envision a high-pressure, stable plasma fed with any of a variety of carbon, hydrogen, or nitrogen compounds and supplied with sufficient enthalpy to reach this high temperature range. The constituent species of such a plasma would be primarily atomic nitrogen, atomic hydrogen, and atomic carbon near 10^{17} cm.$^{-3}$ concentration. The result of rapidly quenching such a highly reactive atom mixture has been generally unexplored. Ammann and Timmins (*1*, *37*), however, did study the rapid quenching of simpler atomic-nitrogen/atomic-oxygen mixtures at 10,000°K. and 1 atm., which were generated by a constricted d.c. arc. The study which is reported in this paper was undertaken to explore the chemical composition of mixtures formed by the rapid quench of atomic-nitrogen/atomic-carbon/atomic-hydrogen mixtures.

Plasma Reactor

Radiofrequency Induction Plasma. One convenient approach to achieve the required temperatures in excess of 10,000°K. at atmospheric pressure is generation of a thermal plasma by radiofrequency induction heating. The techniques for generating and containing a stable high-temperature induction plasma have been described in detail by Reed (*32*, *33*), Mironer (*25*), Marynowski and Monroe (*24*), Freeman and

Publication Date: June 1, 1969 | doi: 10.1021/ba-1969-0080.ch035

Chase (*11*), and Thorpe (*36*). Figure 1 presents a diagram of the plasma generator used. A few turns of copper tubing were wound around the outside of a water-cooled quartz reactor tube. This coil inductively coupled the supplied RF. power into the gaseous reactants sent through the reactor. A water-cooled sampling tube with very small internal diameter which served to quench rapidly the reactive plasma species is shown. Efficient cooling allowed the entrance tip of the quench tube to be placed directly into the plasma core.

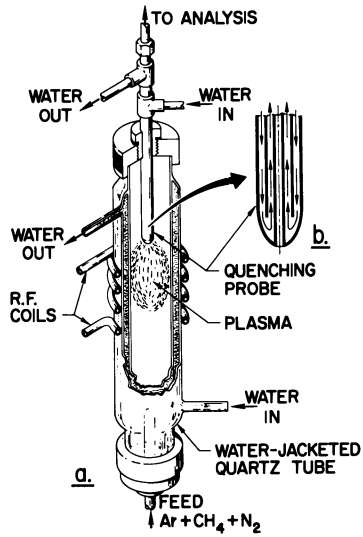

Figure 1. (a) Diagram of radiofrequency induction plasma reactor. (b) Cross section of water-cooled quenching probe

A cross-sectional diagram of the reactor is presented in Figure 2. The isotherms indicated are those determined spectroscopically by Reed (*32*), and are representative of conditions in this study. Eckert and coworkers (*7*) have extended this work to spectroscopic observations of induction-coupled plasmas in both air and argon. Conditions of local thermodynamic equilibrium were approached and temperatures above 6000°K. were measured. No direct temperature measurements were attempted in the present study.

The Induction Plasma as a Chemical Reactor. Several characteristics of this system can be exploited for chemical synthesis:

(1) Average temperatures in excess of 10,000°K. allow essentially complete molecular dissociation. (Lower power input can reduce the specific enthalpy to preserve desired free radicals.)

Publication Date: June 1, 1969 | doi: 10.1021/ba-1969-0080.ch035

(2) Plasma stability is maintained while operating at very low gas velocities ($<$ 1 cm./sec.). Thus, long residence times and efficient mixing are achieved.

(3) The power coupling involves no contact of electrodes with the plasma. Therefore, electrode corrosion and contamination are eliminated, and with sufficient input power, thermal plasmas of any stoichiometry can be stabilized.

(4) Quenching rates on the order of 10^7 K./sec. can be achieved in the sampling probe. Thus, the high heat of reaction released as the plasma species recombine i. efficiently absorbed.

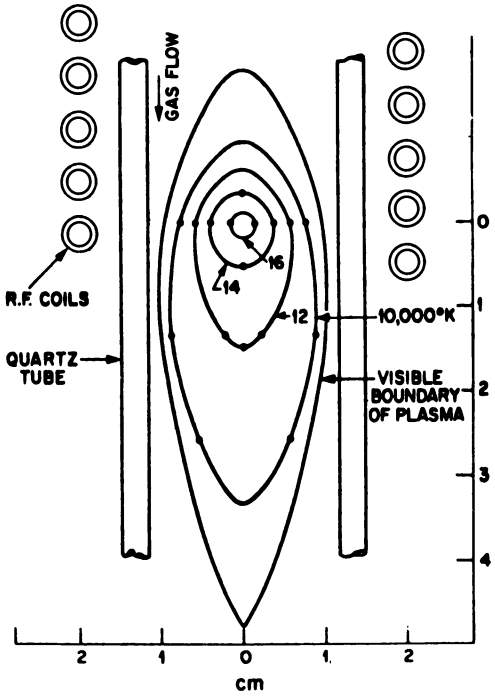

Figure 2. Isotherms in pure argon at 1 atm.
(32)

The system actually is comprised of two reactors in series: I. the plasma reactor, wherein high-temperature transient species are generated, followed by II. the quench reactor, wherein the plasma precursors are rapidly cooled within the cold-walled sampling tube to yield room-temperature stable products.

Plasma Composition

Thermochemical Equilibrium. One of the unique features of the thermal induction plasma is stable operation with low gas flow. Since

Publication Date: June 1, 1969 | doi: 10.1021/ba-1969-0080.ch035

flow velocities in the plasma zone are typically a few centimeters per second, residence times on the order of a second are associated with plasma species. In a plasma near atmospheric pressure the particle mean free path is very short and the collision rate very high. At plasma temperatures (*ca.* 10,000°K.) gas phase reactions can be expected to proceed quite rapidly. These facts lead to the initial assumption that local plasma composition approaches thermodynamic equilibrium.

The H–C–N System. The theoretical compositions of hydrogen–carbon–nitrogen mixtures at thermodynamic equilibrium have been computed by Kroepelin, *et al.* (*18, 19*). Marynowski, *et al.* (*23*), and Bronfin, *et al.* (*4*), for a variety of conditions. Computations were based on free energy minimization using tabulated thermochemical data (*17*). Figure 3 presents calculated equilibrium composition data for a typical stoichiometry: H:C:N = 4:1:2, (CH_4/N_2 = 1), at 1/2 atm. (380 torr). Only

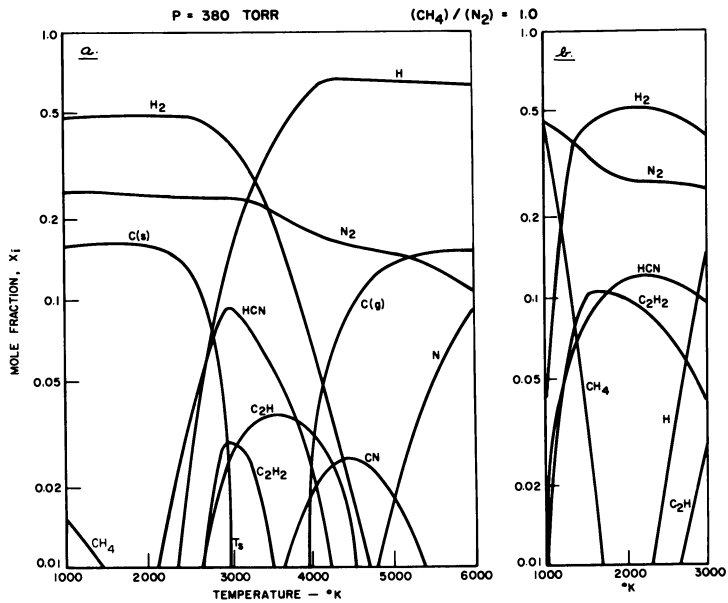

Figure 3. Equilibrium composition of equimolar CH_4–N_2 mixture. (a) Including solid carbon; (b) Excluding solid carbon. Region above T_s common

species whose concentration is greater than 1.0 mole-percent are shown on this plot; however, twenty-one different chemical species were considered. In Figure 3a, full equilibrium was considered for a two-phase system which included graphite. Figure 3b shows that temperature segment which is altered by the exclusion of the solid-phase, C(s).

Publication Date: June 1, 1969 | doi: 10.1021/ba-1969-0080.ch035

Molecular nitrogen, N_2, is a major constituent over a broad range up to 8000°K.; thereafter, thermal dissociation results in the predominance of atomic nitrogen, N. As mentioned above, at temperatures over 8000°K., not shown of the graph, the system becomes completely dissociated into a simple three-component atomic state: H, C, N. At temperatures greater than 7000°K. significant thermal ionization occurs, generating significant concentrations of singly-ionized atoms—*e.g.*, C^+, H^+, and N^+. As noted in both plots, CH_4 dissociation is well underway at 1000°K., resulting in the formation of H_2 and C(s) in the two-phase system (a); but the formation of HCN and C_2H_2 in the single-phase system (b). At temperatures above 3000°K., C_2H_2 begins to fragment to C_2H and H, and with increasing temperature, to the atomic species. At temperatures above 3800°K., HCN begins to fragment to CN and H, and with increasing temperature, to the atomic species. Nitrogen-hydrogen species—*e.g.*, NH_2, occur at concentrations below 0.01 mole-percent over the entire range plotted.

In comparing the common temperature segments of the single-phase and two-phase composition diagrams, important differences are noted in that: (1) higher concentrations of species like HCN and C_2H_2 are preserved at lower temperatures in the single-phase case, and (2) the maximum concentration of these species is somewhat higher in the single-phase case. Hence, in the lower temperature range, the predicted yield of HCN and C_2H_2 is enhanced by retarding carbon nucleation. This kinetic limitation acts to freeze the mixture composition at around 2700°K. so that negligible composition change is predicted over a fairly broad temperature interval, down to 1500°K.

Composition of the Plasma. No direct determination of the plasma composition was attempted in the present study. Only a few efforts in this direction have appeared in the literature. O'Halloran *et al.* (*26*), have directly sampled an argon plasma jet using a specially designed entrance cone opening to a time-of-flight mass spectrometer. Raisen *et al.* (*30*), have made spectroscopic identifications of species in an air plasma. Unlike the mass spectrometer measurements, however, emission spectroscopy is difficult to quantify because of the wide variance in the oscillator-strengths of the likely emitters.

Faced with the difficulty of determining plasma composition directly, one is prone to apply equilibrium predictions as a guide to local plasma composition. Referring both to Figures 2 and 3, a highly dissociated composition can be expected in most of the plasma region. Temperatures in excess of 10,000°K., expected over most of the central region of the plasma, would dictate that the atomic species H, C, and N, and their ions would predominate.

In Chemical Reactions in Electrical Discharges; Blaustein, B.;
Advances in Chemistry; American Chemical Society: Washington, DC, 1969.

Quenching

At this juncture it is important to ask what changes in composition would be encountered on cooling the H–C–N atom plasma. A slow, gradual cooling of the labile intermediates resident in the plasma zone may well allow the system to revert to the original reactants along an equilibrium path. Kroepelin and Kipping (*18, 19*) found this effect in their study of a 10 amp., 40 volt d.c. arc burning in a hydrocarbon-nitrogen atmosphere. The composition of the slowly cooled arc-heated gases was found to be mainly N_2, H_2, and C_1 and C_2 hydrocarbons. No HCN was observed. Under extremely rapid cooling, however, kinetic limitations can interpose along the reaction path to yield different, more interesting or valuable products.

The Cold-Wall Tube. A small-diameter, water-cooled tube was selected from the variety of available high-cooling-rate devices, to provide rapid and convenient quenching of the plasma species. Figure 1b shows a diagram of the simple design of the three-concentric tube arrangement of the quenching probe (*28*). The overall outside diameter of the probe was 3/8 inch. The surfaces of the inner tube were stainless steel; other parts were fabricated from copper. The effect of a variation in the composition of the cold surface was not studied.

Cooling Rate. Because of the high rate of heat transfer from plasma to adjacent cold wall, rapid cooling occurs in the quenching tube. Freeman and Skrivan (*12, 35*) have measured an initial temperature decay rate of 5×10^7 °K./sec. in water-cooled tubes. In their model of the heat-transfer process occurring in very small tubes, Ammann and Timmins (*1*) have calculated cooling rates greater than 10^9 °K./sec. Probably quenching rates in this range were associated with the quenching tube used in this study.

Reaction Path During Quench. Unfortunately, there is a sparsity of high-temperature kinetic data for the H–C–N system. Hence, one is unable to predict with certainty the reaction path followed as the atomic species H, C, and N, are cooled from 15,000°K. to 500°K. in 10 msec., for example. After an examination of the experimental results in the succeeding sections, it may be possible to infer the important steps in the reaction sequence.

Experimental Conditions

Radiofrequency Supply. A commercially available (*20*) 12 kw. (nominal) induction heater, oscillating at 4 MHz., was the power source for the experiment. The load coil, shown in Figure 1, consisted of five turns of 1/4-inch o.d., water-cooled, copper tubing wound tightly around

Publication Date: June 1, 1969 | doi: 10.1021/ba-1969-0080.ch035

In Chemical Reactions in Electrical Discharges; Blaustein, B.;
Advances in Chemistry; American Chemical Society: Washington, DC, 1969.

the quartz reaction tube. The overall height of the coil was 1 1/2 inches, with a central diameter of 3 inches.

Reactor. Containment of the plasma was accomplished within a 35 cm. long, 47 mm. i.d. quartz tube, mounted vertically. The high-power loadings necessitated cooling which was afforded by causing 1/3 gallon per minute of water to flow into a cooling jacket surrounding the central reaction tube. The plasma-forming gases were premixed and sent into the tube through a brass fitting sealed onto the tube base. Gas flow rates were monitored with calibrated Rotameters. Plasma-heated gases left the reaction tube through a second brass fitting sealed onto the top of the tube. This cap, which was of approximately 1 liter volume, was water-cooled. In this configuration the top fitting functioned as a cooling chamber to reduce the average gas temperature to within a few degrees of ambient. The system pressure was controlled by a high-capacity regulated vacuum line attached to the upper cap.

A sliding O-ring seal was provided at the center of the upper cap for positioning of the 3/8-inch o.d. by 0.032-inch i.d. quench probe along the central axis of the reaction tube. Cooling water was supplied to the quench probe at a metered rate of 1/3 g.p.m. The entrance tip of the probe was typically located at the center of the uppermost winding of the load coil.

The flow rate through each cooling water line was metered with calibrated Rotameters which were placed downstream of liquid pressure regulators. Interconsistent mercury thermometers were mounted at each cooling water line inlet and outlet. By measurement of the temperature rise and flow rate in each cooling line, total enthalpy delivery rates could be determined.

Chemical Analysis. The gas stream withdrawn through the quench probe was sent to an on-line gas chromatograph for quantitative analysis. A triacetin column, recommended by Isbell (*15*), followed by a molecular sieve column, recommended by Purnell (*28*), was used for resolution of chromatogram peaks. This configuration allowed the detection of the following compounds with a thermal conductivity cell: HCN, H_2, Ar, N_2, CH_4; and various higher hydrocarbons. A parallel flame-ionization detector was useful for detecting low concentrations of hydrocarbons—*e.g.*, CH_4 and C_2H_2.

Experimental Variables. Total pressure in the plasma reactor was typically 380 torr; some data were also acquired in a range from 160 to 760 torr. For the data reported here the argon feed rate was 42 std. cc./sec. (6.5 gram-mole/hr.). This flow rate insured good plasma stability for the available RF. power and remained within the capacity of the subatmospheric pressure regulating equipment. Added reagent gases were fed at 1/50th to 1/10th that rate, with the molal ratio varied over a broad range: $0.1 \leqslant CH_4/N_2 \leqslant 25$. The power coupled into the gas mixtures was ~3.5 kw. maximum, as determined from the summation of cooling water heating rates.

In the later stages of the experiment various nitrogen-substituted hydrocarbon liquids were fed to the argon plasma, namely: CH_3CN, CH_3CH_2CN, and CH_2CHCN. Special modifications to the gas-flow system were made to insure injection of these nitriles into the plasma. A part

Publication Date: June 1, 1969 | doi: 10.1021/ba-1969-0080.ch035

In Chemical Reactions in Electrical Discharges; Blaustein, B.;
Advances in Chemistry; American Chemical Society: Washington, DC, 1969.

of the argon feed stream was split off to a sealed gas-liquid bubbler containing warmed reagent. Since the low-molecular-weight nitriles are all relatively volatile, a substantial amount of nitrile vapor entrainment occurred. Rather than introduce the nitrile-laden argon stream into the relatively cool gas region at the base of the reaction tube, a special injection probe was provided to introduce the stream into the hot plasma region. This second water-cooled probe was positioned through an O-ring seal in the base cap. The probe design was identical to that previously described for quenching (*cf.* Figure 1b). The tip of the injector probe was placed at the center of the lowermost winding of the load coil. Material exiting the injector thus was assured of entering the plasma zone.

Experimental Results

Plasma Stability. Over the entire range of experimental variables the plasma was stable and brightly luminous. The luminous region of the plasma appeared to fill about 90% of the cross-sectional area of the cooled quartz tube and extended from the bottom to about 3 inches above the RF. load coil. With high hydrocarbon flow rates a gradual build up of soot occurred on the quartz tube walls.

Methane-Nitrogen Reactions. PRODUCTS OF REACTION. A quantitative analysis of the gas stream withdrawn through the quenching probe was made for each run. Over the entire range of stoichiometries studied, the methane fed to the plasma reacted completely; no methane was detected in the quenched gas stream. The following major reaction products were identified: HCN, C_2H_2, H_2. Also present were Ar and unreacted N_2.

NITROGEN CONVERSION. Since essentially complete conversion of methane was observed for each run, the varying conversion of nitrogen was selected as an important datum. If the mole fraction of a species i found in the quenched product stream is defined as x_i, then the conversion of nitrogen, defined as α, is given by:

$$\alpha = \frac{\frac{1}{2}x_{HCN}}{x_{N_2} + \frac{1}{2}x_{HCN}}$$

Figure 4 shows the percent conversion of nitrogen as a function of feed stoichiometry, CH_4/N_2. The argon feed rate for these runs was fixed at 42 std. cc./sec. The total flow rate of the reactant mixture was typically 2 std. cc./sec. The key at the bottom right of the figure identifies the reactor pressure for each data point.

The measured conversion of nitrogen varied from 3% at the lowest stoichiometry considered, $CH_4/N_2 = 0.1$, to a maximum of 70% at a methane-rich stoichiometry, $CH_4/N_2 = 25$. This high value of nitrogen fixation is considerably in excess of previously reported nitrogen conversion levels observed in thermal plasma reactions. So long as the brilliant

Publication Date: June 1, 1969 | doi: 10.1021/ba-1969-0080.ch035

In Chemical Reactions in Electrical Discharges; Blaustein, B.;
Advances in Chemistry; American Chemical Society: Washington, DC, 1969.

thermal plasma was maintained, pressure variations, made over a range from 250 to 760 torr, had no significant effect on fixation levels.

Typical Product Composition. Table I, below, presents the composition of the product stream produced under typical conditions.

Table I. Typical Product Composition

Reactor Pressure—380 torr *Net Power Input—3.5 kw.*

Input	*Feed Rate (std. cc./sec.)*	*Feed Composition (mole-percent)*
Ar	41.8	97.6
N_2	0.5	1.2
CH_4	0.5	1.2
Total	42.8	100.0

Product	*Composition (mole-percent)*	*(mole-percent, Ar-free)*
Ar	96.5	—
H_2	2.0[a]	57
N_2	1.0	29
HCN	0.3	9
C_2H_2	0.2	5
CH_4	trace	—
Total	100.0	100

[a] Compositions determined from gas chromatograms; ±10%.

As was seen in Figure 4, Table I shows that about 12% of the nitrogen fed at this stoichiometry was converted to hydrogen cyanide. Ninety-nine percent of the methane fed was converted to the gaseous products hydrogen and acetylene and also to an unmeasured small quantity of solid product which deposited on the wall. The minor disparity between the nitrogen and carbon material balances indicates the small fraction of material which was lost from the reaction zone to deposition on the reactor walls.

Nitrile Reactions. PRODUCTS OF REACTION. Small quantities of nitriles could be continuously fed to the argon plasma by using the modified injection arrangement (described in the previous section). Mixed plasma which was quenched by withdrawal through the water-cooled probe was analyzed with no change in the gas chromatograph. Essentially complete conversion of the lower molecular weight compounds, acetonitrile, CH_3CN, and acrylonitrile, CH_2CHCN, was observed. A minor amount (~10%) of propionitrile, CH_3CH_2CN, was observed in the quenched gas stream, perhaps owing to a bypassing of the plasma core. Each of

Publication Date: June 1, 1969 | doi: 10.1021/ba-1969-0080.ch035

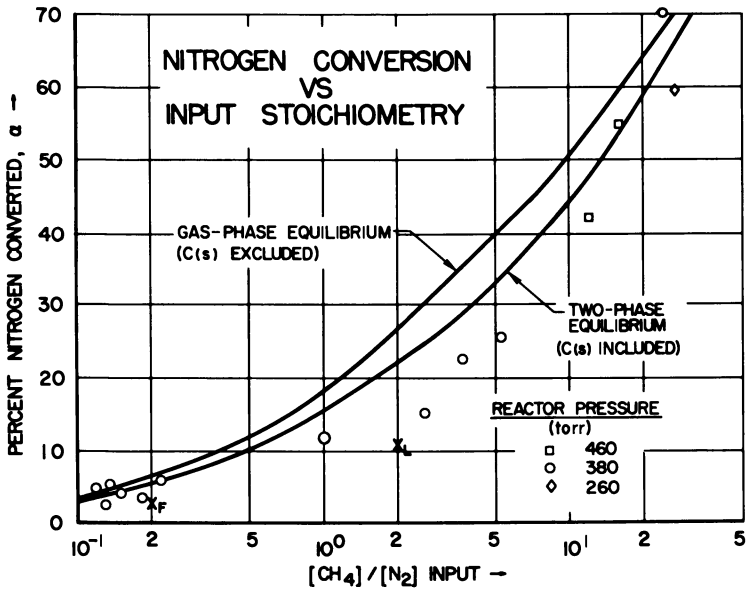

Figure 4. Yield of HCN, expressed as percent N_2 converted, as a function of input stoichiometry. Solid lines show maximum yield predicted by thermodynamic equilibrium. Data points show experimental results from the plasma reactor: Ar flow rate 42 std. cc./sec., total reagent flow rate 2 std. cc./sec., net power ~3.5 kw. Reactor pressure identified with key. Points labeled × from plasma jet studies (10, 21)

the nitriles produced the same reaction products, a repeat of those produced in the methane-nitrogen study. High concentrations of HCN, C_2H_2, H_2, and N_2 were observed along with the argon diluent. A complete quantitative chemical analysis of these nitrile runs has not, as yet, been performed.

Discussion of Results

Variance in the Conversion Percentage. Considerable variance in the fraction of nitrogen converted was observed among repetitions of runs with constant stoichiometry, net power input, and pressure. The data points plotted in Figure 4 include the maximum observed conversion levels for each stoichiometry. Sources of error in the experimental procedure which could have scattered the data down from maximum conversion were:

(1) Improper adjustment of RF. supply controls so as to mismatch the supply and plasma impedance, perhaps generating plasma irregularities,

Publication Date: June 1, 1969 | doi: 10.1021/ba-1969-0080.ch035

(2) Minor air leaks which would add additional nitrogen to the plasma to alter the stoichiometry from preset values,

(3) Deposition of carbon or hydrocarbon material on the reactor walls or, the reverse, significant vaporization of carbon from the walls, to alter the preset stoichiometry.

Thermochemical Equilibrium Predictions. As described in the *Plasma Composition* section, above, a full range of composition calculations were made assuming thermochemical equilibrium. These calculations predicted that the plasma composition within the RF. coil would be dominated by atomic species for the specific power input used in this study. Perhaps the following additional consideration of these theoretical predictions can elucidate the processes occurring during rapid quench.

Freezing. Hypothesize that equilibrium is followed during the initial stages of cooling within the quench tube. For heuristic purposes, assume that equilibrium is obeyed during temperature decay to approximately 3000°K. or more specifically, to that temperature where equilibrium predicts that maximum number of moles of HCN be formed. Then assume that all reactions involving nitrogen species are frozen at that point, so that even as cooling continues, negligible decomposition of the HCN occurs. By choosing to freeze the nitrogen fixation reactions at the point of maximum conversion, the hypothesis becomes biased toward the most optimistic yield predictions. Note that no comment has been made concerning the freezing temperature applicable to other quench reactions which do not involve nitrogen-containing species (however, *see* Reference 9).

Chemical Reaction Kinetics. In making this series of seemingly unwarranted assumptions, some specific reaction rates have been implied to be very fast, while others, very slow. Focusing on nitrogen-containing species, the following types of reaction have been assumed to be rapid under the conditions developed in the quenching tube:

$$N^+ + e^- \overset{M}{\rightleftarrows} N \quad (1)$$

$$C + N \overset{M}{\rightleftarrows} CN \quad (2)$$

$$N + N \overset{M}{\rightleftarrows} N_2 \quad (3)$$

$$H + CN \overset{M}{\rightleftarrows} HCN \quad (4)$$

Further, the following have been assumed to be very slow:

$$HCN \rightarrow \text{many steps} \rightarrow H_2 + N_2 + C \quad (5)$$

$$C(g) \overset{\text{wall}}{\rightarrow} C(s) \quad (6)$$

Publication Date: June 1, 1969 | doi: 10.1021/ba-1969-0080.ch035

To date a full description of the reaction kinetics of the H–C–N system, even at moderate temperatures, is unavailable. In the shock tube study by Marshall, Jeffers, and Bauer (*22*), preliminary results indicate that the equilibrium in Reaction 4 may be achieved rapidly at elevated temperatures. However, the evidence points to a rather complex reaction mechanism for the thermal dissociation of HCN, wherein many more steps are involved than mentioned here. In another recent shock tube study, Rao, Mackay, and Trass (*31*) present a detailed consideration of possible reaction steps in the formation of HCN from hydrocarbon-nitrogen mixtures, which augment the above list. Their experimental data show HCN formation to be favored by temperatures in excess of 2500°K., followed by a rapid quench, in agreement with the present hypothesis concerning the reaction path in the plasma system. The complexity of the reaction kinetics in the H–C–N system was encountered in the earlier study of Robertson and Pease (*34*), and in similar systems explored by Goy, Shaw, and Pritchard (*14*). Paraskevopoulos and Winkler (*27*) have obtained evidence that nitrogen atom/hydrocarbon reactions proceed very rapidly.

Rapid dissociation/recombination rates have been determined for nitrogen, Reaction 3, by Wray (*38*). Reaction rate data is not available for Reaction 2, nor for other reactions likely to be quite important in the H–C–N system. Atomic-ion/electron recombination reactions for each of the three atoms in the plasma are likely to be rapid (*3*) relative to the quenching time.

In summary, existing reaction rate data is far from sufficient to check the assumptions made about the reaction mechanisms appropriate to this H–C–N system. Additional kinetic studies which generate presently unknown reaction rates are needed before an accurate reaction path can be predicted theoretically for the reacting H–C–N system.

Composition at the Assumed Freezing Point. The validity of this freezing approach can be found by comparing the predicted composition the freezing temperature with the observed composition of the quenched gas stream. The following variables are defined for Table II, which facilitates the comparison.

For the equilibrium calculations, let the input stoichiometry be characterized by the molar ratio $[CH_4]/[N_2]$, set equal to ϕ; let n_{N_2} be the number of moles of N_2 introduced; and let n_i^* be the number of moles of species i present at equilibrium at a pressure, P, and a temperature, T. If the optimistic freezing point hypothesis is followed, T_f is established for a given ϕ and P, as the temperature at which equilibrium predicts the quantity n^*_{HCN}/n_{N_2} is a maximum.

Table II shows the mole fraction of the predominant species for a T_f value found in an equimolar input stoichiometry. As mentioned in the

Publication Date: June 1, 1969 | doi: 10.1021/ba-1969-0080.ch035

Plasma Composition section, above, solid-carbon formation may be retarded in this system. Therefore, a second set of mole fraction data have been presented for comparison in Table II which excludes the species C(s) from the calculation.

Table II. Calculated Equilibrium Composition at the Temperature where HCN Yield is Maximized

Pressure—380 torr $\phi \equiv [CH_4]/[N_2] = 1.0$

Mole Fractions

	Including C(s) $T_f = 3050$ *K.*		*Excluding C(s)* $T_f = 2500$ *K.*	
	x_i	x_i' [a]	x_i	x_i' [a]
H_2	0.421	0.543	0.497	0.522
N_2	0.252	0.283	0.266	0.274
HCN	0.097	0.109	0.120	0.124
C_2H_2	0.038	0.065	0.073	0.080
H	0.144	—	0.025	—
C_2H	0.020	—	0.005	—
others	0.030	—	0.014	—
	$\frac{n^*_{HCN}}{n_{N_2}} = \alpha_{max\text{-}1} = 0.161$		$\alpha_{max\text{-}2} = 0.185$	

[a] Adjusted to allow for the reactions: $C_2H + H \rightarrow C_2H_2$; $2H \rightarrow H_2$.

Frozen Composition Calculation *vs.* Experimentally Observed Composition. If, indeed, the original assumption that important reactions occurring in the gas withdrawn from the plasma into the cold quenching tube are frozen in the vicinity of 3000°K. is valid, then agreement should be found between the compositions listed in Tables I and II. In comparing the argon-free composition listed in Table I with Column 2 in Table II, relatively good agreement is found.

This comparison has been extended to the full range of stoichiometries studied. On Figure 4, the maximum nitrogen conversion values, $\alpha_{max\text{-}1}$, and $\alpha_{max\text{-}2}$, have been plotted against input CH_4/N_2-mole ratio, ϕ. The subscript 1 refers to calculations including C(s); subscript 2, to those excluding C(s). Agreement between the freezing model and observed results is very good over more than a two-decade range in stoichiometry variation. These results strongly support the freezing model in the overall reaction path. With the existing scatter of the data, a delineation between the single-phase and two-phase equilibrium predictions of composition at T_f is not impossible. Additional experimental runs may lessen this ambiguity. The retardation of carbon solid formation, however, accounts for less than a 10% change in predicted maximum nitrogen conversion, on the average.

Publication Date: June 1, 1969 | doi: 10.1021/ba-1969-0080.ch035

Freezing Temperature. The data do not allow an exact determination of a freezing temperature appropriate to the quenching process. Referring back to Figure 3a, a change of a few hundred degrees in the assumed T_f could account for the data points which indicate 10 to 20% less than the two-phase equilibrium predictions of maximum nitrogen conversion. Figure 3b shows the HCN concentration plateaus to be quite broad. Hence, the nitrogen conversion prediction would be relatively insensitive to variation in freezing temperature over the range from 2000° to 3000°K. Nevertheless, the original optimistic assumption that T_f existed in the vicinity of 3000°K. seems to be borne out by the present data and also is supported by the results reported by Rao, Mackay, and Trass (*31*) referred to above. Future experimental refinements may allow a more exact determination of T_f.

Observed Compositions in Nitrile Experiments. An analysis of the maximum nitrogen conversion predicted by thermochemical equilibrium has not been made for the different nitrile inputs described in the *Experimental Conditions* section. The similarity of product distribution and of the ratio of HCN to N_2 in the product points to the same reaction mechanisms as in the CH_4/N_2 studies.

Correlation with Studies by Other Investigators. If the proposed reaction mechanism is correct, then the yields found in other studies of the synthesis of HCN by thermal reactions of hydrocarbons with nitrogen should not exceed the predicted values of α. Some results of the production of HCN in plasma jets have been reported, as were mentioned in the *Previous Studies* section. While the differences in design between the plasma jet and induction plasma reactors are not detailed here, sample results from these other studies are plotted on Figure 4. The maximum nitrogen conversion values observed in the nitrogen plasma jet experiments of Leutner (*21*) (designated x_L) and Freeman (*10*) (designated x_F) appear. These experimental data points are seen to lie below the maximum nitrogen conversion prediction.

The phenomena in the plasma jet experiments which lead to nitrogen conversion levels lower than the maximum predicted by the freezing model are thought to be linked to mixing limitations, (CH_4 and N_2 were not premixed in the plasma jet experiments). The influence of mixing rate on yield in plasma jet reactors is the subject of a separate theoretical analysis by the author (*5*).

The Reaction Sequence

The experimental data support the following description of the overall reaction sequence:

Publication Date: June 1, 1969 | doi: 10.1021/ba-1969-0080.ch035

In Chemical Reactions in Electrical Discharges; Blaustein, B.;
Advances in Chemistry; American Chemical Society: Washington, DC, 1969.

Plasma Reactions. Feed reagents are dissociated to their atomic constituents in a thermal plasma. Some thermal ionization occurs at sufficiently high temperatures.

$$CH_4 + N_2 \rightarrow C + H + N + C^+ + H^+ + N^+ + e^-$$

Initial Cooling. Plasma taken into a small-diameter cold tube rapidly cools with chemical reactions following equilibrium.

$$C + H + N + \text{ions} \rightarrow H + CN + C_2H + N_2 \rightarrow HCN + H_2 + N_2 + C_2H_2$$

Frozen Reaction Kinetics. Rapid cooling continues, but at a rate much greater than the progress of the apparently complex reaction sequence necessary to destroy the species HCN, C_2H_2, and H_2. Hence, the composition of the cooling gas is frozen at the end of Step 2.

Evidence for the Freezing Model in Other Reacting Systems. The freezing model likely is applicable to a wide variety of reacting thermal plasma systems which employ a rapid quench. Ammann and Timmins (*1*) found a mechanism involving the freezing of equilibrating reactions to be applicable to their study of the quenching of nitrogen-oxygen plasma. Aided by a wealth of published rate data on chemical reactions in air, they were able to model the time-temperature-composition history of N–O plasma cooling within small-diameter tubes. A quite similar freezing temperature, T_f, was found at 3500°K. for that system. The equilibrium composition of nitric oxide, NO, at T_f was preserved during continued rapid cooling.

Conclusions

Mixtures of methane and nitrogen can be fed continuously to a thermal argon induction plasma maintained above 10,000 K. A rapid quench of the heated plasma mixture produces HCN, C_2H_2, and H_2. Final yields of HCN, expressed as a fraction of the nitrogen converted, range between 3 and 70%, a function of the input stoichiometry.

The reaction is thought to proceed by the complete dissociation of the feed reactants in the plasma to yield a mixture of H, C, and N. As this mixture is quenched, the reaction initially proceeds along an equilibrium path, forming HCN, C_2H_2, H_2, and N_2. Below the temperature where the equilibrium yield of HCN is maximized, the slower rearrangement reactions and carbon nucleation are frozen by the rapid cooling, so that negligible alteration in the gas composition occurs upon further cooling.

Publication Date: June 1, 1969 | doi: 10.1021/ba-1969-0080.ch035

In Chemical Reactions in Electrical Discharges; Blaustein, B.;
Advances in Chemistry; American Chemical Society: Washington, DC, 1969.

Acknowledgment

The author thanks William McLaughlin for his diligent assistance in performing these experiments. Thanks are also extended to M. P. Freeman, of American Cyanamid's Central Research Laboratory, and W. G. Burwell, at these laboratories, for many clarifying discussions.

Literature Cited

(1) Ammann, P. R., Timmins, R. S., *A.I.Ch.E.J.* **17,** 956 (1966).
(2) Baddour, R. F., Blanchet, J. L., *Ind. Eng. Chem. Proc. Design Devel.* **3,** 258 (1964).
(3) Bates, D. R., Kingston, A. E., McWhirter, R. W. P., *Proc. Roy. Soc. A.* **267,** 297 (1962).
(4) Bronfin, B. R., *et al., 15th Chem. Inst. Canada Chem. Eng. Conf., Universite Laval, Quebec,* Oct. 25-27, 1965.
(5) Bronfin, B. R., Cohen, L. S., *3rd Intern. Symp. High Temp. Tech., Pacific Grove, Calif.,* September, 1967 (in press).
(6) Busz, G., Finkelnburg, W., *Z. Physik* **139,** 218 (1954).
(7) Eckert, H. U., Kelly, F. L., Olsen, H. N., *J. Appl. Phys.* **39,** 1846 (1968).
(8) Forst, W., Evans, H. G. V., Winkler, C. A., *J. Phys. Chem.* **61,** 320 (1957).
(9) Forst, W., Winkler, C. A., *J. Phys. Chem.* **60,** 1424 (1956).
(10) Freeman, M. P., ADVAN. CHEM. SER. **80,** 406 (1969).
(11) Freeman, M. P., Chase, J. D., *130th Meeting, Electrochem. Soc., Philadelphia, Pa.,* Oct. 12, 1966.
(12) Freeman, M. P., Skrivan, J. F., *A.I.Ch.E.J.* **8,** 450 (1962).
(13) Gartaganis, P. A., Winkler, C. A., *Can. J. Chem.* **34,** 1457 (1956).
(14) Goy, C. A., Shaw, D. H., Pritchard, H. O., *J. Phys. Chem.* **69,** 1504 (1965).
(15) Haggart, C., Winkler, C. A., *Can. J. Chem.* **38,** 329 (1960).
(16) Isbell, R. E., *Anal. Chem.* **35,** 255 (1963).
(17) JANAF Tables of Thermochemical Data, Dow Chemical Co., Midland, Mich., Dec. 31, 1964.
(18) Kroepelin, H., Kipping, D. E., "Progress in International Research on Thermodynamic and Transport Properties," p. 649, J. F. Masi, D. H. Tsai, eds., Amer. Soc. Mech. Eng., Academic Press, New York, 1962.
(19) Kroepelin, H., Kipping, D. E., Pietruck, H., "Progress in International Research on Thermodynamic and Transport Properties," p. 628, J. F. Masi, D. M. Tsai, eds., Amer. Soc. Mech. Eng., Academic Press, New York, 1962.
(20) Lepel High Frequency Labs, Inc., New York, N. Y., **Model T-5-3.**
(21) Leutner, H. W., *Ind. Eng. Chem. Proc. Design Devel.* **2,** 315 (1963).
(22) Marshall, D., Jeffers, P., Bauer, S. H., Chemistry Dept., Cornell Univ., Ithaca, N. Y. (personal communication, Nov., 1966).
(23) Marynowski, C. W., *et al., Ind. Eng. Chem. Fund.* **1,** 52 (1962).
(24) Marynowski, C. W., Monroe, A. G., "High Temperature Technology," pp. 67-83, Butterworths, Washington, 1964.
(25) Mironer, A., *A.I.A.A.J.* **1,** 2638 (1963).
(26) O'Halloran, G. J., *et al., Bendix Corp. Research Laboratories, Southfield, Mich.,* **Report No. ASD-TDR-62-644** (1964).

(27) Paraskevopoulos, G., Winkler, C. A., *J. Phys. Chem.* **71,** 947 (1967).
(28) Plooster, M. N., Reed, T. B., *J. Chem. Phys.* **31,** 66 (1959).
(29) Purnell, H., "Gas Chromatography," pp. 371-373, John Wiley, New York, 1962.
(30) Raisen, E., *et al.*, *Appl. Spectr.* **19,** 41 (1965).
(31) Rao, V. V., Mackay, D., Trass, O., *Can. J. Chem. Eng.* **45,** 61 (1967).
(32) Reed, T. B., *J. Appl. Phys.* **32,** 821 (1961).
(33) Reed, T. B., *J. Appl. Phys.* **34,** 3146 (1963).
(34) Robertson, N. C., Pease, R. N., *J. Am. Chem. Soc.* **64,** 1880 (1942).
(35) Skrivan, J. F., Von Jaskowsky, W., *Ind. Eng. Chem. Proc. Design Devel.* **4,** 371 (1965).
(36) Thorpe, M. L., *Research/Development* **17**(1), 28 (Jan. 1966).
(37) Timmins, R. S., Ammann, P. R., *A.I.Ch.E. Meeting, Boston, Mass.*, Dec. 7, 1964.
(38) Wray, K. L., "Progress in Astronautics and Rocketry," Vol. 7, p. 181, F. R. Kiddell, Ed., Academic Press, New York, 1962.

RECEIVED July 18, 1967.

36

A Viewpoint on Electrical Discharge Devices and Their Application as Chemical Reactors

JAMES E. FLINN and WILLIAM M. GOLDBERGER

Columbus Laboratories, Battelle Memorial Institute, Columbus, Ohio

Publication Date: June 1, 1969 | doi: 10.1021/ba-1969-0080.ch036

Discharge devices of many types are available for study and use in connection with chemical reactions of commercial significance. In such studies it is the reaction rather than the device which usually receives the major attention of the experimenter. Consequently, any attempt to compare results from more than one study is usually frustrated through lack of an adequate knowledge of the similarities and differences among the large number of devices in use. This paper attempts to show in a limited way that such interrelationships do exist—e.g., *between a low pressure glow discharge and a high pressure high temperature plasma arc. Also factors of importance in selecting and evaluating devices for process use are discussed.*

There are many long-established and well-known chemical processes based on electrical discharge phenomena. The subject of discharge chemistry certainly is not new. However, the relatively recent development of new types of reliable discharge devices has stimulated interest in their use as chemical reactors. The extent of research in discharge chemistry is rapidly increasing and it is of value, therefore, to establish bases for comparing the results of these various investigators.

For the most part, the ultimate objective of this research is the production of new and useful products or the production of known products at less cost. Thus, the essential background of information already developed by the physicist, electrochemist, chemical and electrical engineer must be brought together in a manner that is readily understood by each. The papers presented in this volume reflect this diversity of interest in discharge chemistry.

This paper attempts to provide a perspective showing the interrelationships existing among a few types of discharge devices of interest in

In Chemical Reactions in Electrical Discharges; Blaustein, B.;
Advances in Chemistry; American Chemical Society: Washington, DC, 1969.

discharge chemistry and chemical processing research. In doing so no new theories are presented, nor are existing theories discussed. Rather phenomenological descriptions of various discharge modes are used to achieve the desired purpose.

Depending on the chemical system of interest and the ultimate objective of the study or process, there will probably be one mode of discharge and one type of discharge device that will be best suited. Thus, advanced consideration of both the differences and similarities of various discharge modes and devices can prove extremely valuable.

Discharge Devices

Some of the more common names for a variety of electrical discharge devices are listed in Table I. These names and others not listed, when conceived, were meant to be descriptive: (1) of the physical aspect of a given device, (2) of the plasma environment formed in a device, or (3) of an individual who was closely associated with the study of a particular discharge device or phenomena. Thus, one can readily visualize a glow discharge as a type of discharge whose plasma environment "glows"; an ozonizer as one in which ozone is produced; a brush cathode discharge (*10*) as one whose cathode has the appearance of a wire brush; etc. This method of identifying specific discharges or devices has led to confusion in the literature. It is, for instance, not uncommon to see the words "glow discharge" used to describe the phenomena observable in a number of distinctly different discharge devices.

Table I. Names for a Variety of Electrical Discharge Devices

Induction plasma	Spark
Plasma jet (or torch)	Glow
Silent	Arc
Ozonizer ozonator	Ring
Electrodeless	Corona
Electronic torch	Semi-corona
Penning	Microwave
Townsend	Brush cathode plasma
Wood-Bonhoeffer tube	Radio frequency

It will take some time before this collection of terms will fade from usage and a more rational basis for identifying different discharge devices and phenomena is developed. In the meantime these terms will serve, albit imprecisely, their intended purpose. In developing such a basis the interrelationships existing among the various devices will have to be defined more clearly than is presently possible.

Because of this situation a problem arises with respect to a symposium such as this on reactions in electrical discharges. The question is

Publication Date: June 1, 1969 | doi: 10.1021/ba-1969-0080.ch036

In Chemical Reactions in Electrical Discharges; Blaustein, B.;
Advances in Chemistry; American Chemical Society: Washington, DC, 1969.

asked: what is an electrical discharge? Is an arc or a plasma jet to be considered in the same vein as a glow or corona discharge?

An examination of the numerous types of electrical discharges mentioned in this collection of symposium papers revealed that each almost without exception has the three elements illustrated in Figure 1. That is, they are sustained by a source of electrical power (1), this power being delivered by means of a coupling mechanism (2), to a plasma environment (3), associated with the particular device. This simplified picture is rapidly obfuscated when one realizes that the number of combinations of power sources, coupling mechanisms, and plasma environments can be quite large, not to mention the variety of device geometries and modes of operation that are possible.

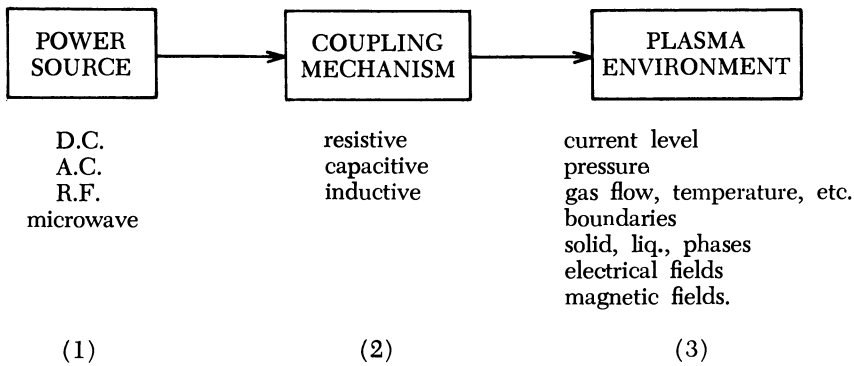

Figure 1. Elements of an electrical discharge device

Perhaps the most meaningful of the three elements in Figure 1 with respect to a classification scheme for discharge devices is the method by which electrical energy is coupled into a given plasma environment. Kunkel (9) has discussed such a scheme.

The mode of coupling is resistive for those devices which have electrodes in direct contact with the ionized gas or plasma environment. In these devices the electrical field necessary to sustain the plasma is caused by positive and negative charge accumulations both within and at the boundaries (walls, electrodes, etc.) of the plasma region. A finite potential difference at the gas-electrode boundary always exists as a consequence of the accumulated charges. This potential supports a number of collision processes (ionization, excitation, electron emission or collection, etc.) which act to sustain the discharge.

Inductively or capacitively coupled discharges on the other hand do not have electrodes in direct contact with the gaseous plasma region and hence are frequently referred to—sometimes without adequate distinction—as "electrodeless" discharges. The electric field is generated

Publication Date: June 1, 1969 | doi: 10.1021/ba-1969-0080.ch036

(induced) in the inductively coupled discharge by a changing magnetic field. Electrons are generated entirely within the discharge device in contrast to resistively coupled discharges where electrons flowing in the external circuitry enter and leave at the electrode boundaries. Thus, current flowing in an inductively coupled discharge flows in closed loops. This situation with inductive discharges is analogous to that of a transformer. That is, the plasma environment acts as a one-turn (short circuited) secondary coil.

Capacitively coupled discharges—also known as polarization discharges—are characterized by the fact that the electrodes through which the electrical power is delivered are physically separated from the plasma region by a non-conducting material—*i.e.*, a dielectric barrier. This barrier material is in direct contact with both the electrodes on one side and the plasma region on the other. In contrast to inductive discharges the electrical field in the plasma region of a capacitive discharge is caused by oscillating electrostatic charges at the dielectric barrier surfaces covering each electrode rather than by a changing magnetic field in the plasma region. To obtain such coupling a high voltage oscillating power supply is needed to allow a displacement current to be passed through the dielectric barrier material (*4*).

This general way of classifying electrical discharge devices, while convenient, is not absolute. Discharges having combinations, both inherent and purposeful, of these coupling mechanisms are known (*14*). However, such a categorization is useful as a first step in understanding the interrelationships and differences among the various types.

For a given power source, mode of coupling, and device geometry, a plasma environment can be generated. The properties of this environment are readily altered by any number of externally controlled variables. These include the gas pressure; the gas flow rate, direction, and inlet temperature; the frequency, current, voltage level, and duration of the input power; the presence or absence of a magnetic field, solid or liquid phases, and others. If a chemical reaction is occurring in the plasma environment, it follows that manipulation of any of these variables is apt to affect such a reaction through the changes that would occur in the plasma. These changes include the electron and gas temperatures, degree of gas ionization or excitation, electrical field strengths, gas density, volume of plasma relative to the volume of the device, and other factors which directly or indirectly determine the course of a chemical reaction.

Since very little is known about the true nature of chemical reactions involving ions, electrons, radicals, photons, etc., it is not possible to predict *a priori* what would be expected from one type of device or another under specified conditions. For that matter, in most studies of chemical reactions in electrical discharges, very little is known or reported

Publication Date: June 1, 1969 | doi: 10.1021/ba-1969-0080.ch036

In Chemical Reactions in Electrical Discharges; Blaustein, B.;
Advances in Chemistry; American Chemical Society: Washington, DC, 1969.

about the true state of the plasma environment—*i.e.*, electrical field strengths, geometry, gas flow, temperatures, etc. Thus, meaningful comparisons of experimental results for the same reaction in different devices often cannot be made. Yet we know that the same reaction can be carried out in discharges differing greatly with respect to the state of the plasma environment.

Let us examine just how radically the plasma environment of a given device can be altered by manipulation of a few selected externally controlled variables. Figure 2 shows two routes by which one can, in a device of more or less fixed geometry, alter the plasma environment to form a low intensity arc roughly at atmospheric pressure beginning with a glow discharge at a much lower pressure. Since each device in the series can be initiated by resistive coupling to a d.c. power supply, the transitions from one type of discharge to another can be made (in principle) by varying only the current, pressure, and possibly the electrode spacing. Other transitions from the low intensity arc are possible and will be briefly discussed. One of them (plasma jet) involves the introduction of yet another variable, namely, gas flow.

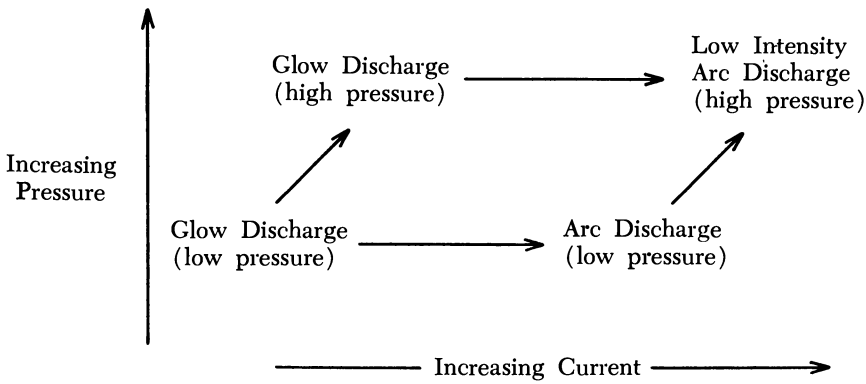

Figure 2. Two routes of transitions from glow to arc

The physical aspects of each of these type discharges have been described in detail in the literature. Our only purpose here is to emphasize the interrelationships among these devices which in themselves are usually studied as separate entities.

The low pressure glow discharge (a few cm. of Hg) can be formed by a transition from a Townsend discharge (5), as is typically shown by means of a V-I plot of the type shown in Figure 3. It is characterized by a high potential drop at the cathode of several hundred volts. Because of this high potential drop, ions are accelerated toward the cathode at high velocities. Thus, the emission of electrons from the cathode is largely caused by positive-ion bombardment in this type of discharge. As with

Publication Date: June 1, 1969 | doi: 10.1021/ba-1969-0080.ch036

In Chemical Reactions in Electrical Discharges; Blaustein, B.;
Advances in Chemistry; American Chemical Society: Washington, DC, 1969.

most discharges at low pressure the electron temperature is much higher than that of the heavier ions or neutral gas atoms, which themselves are at a moderate temperature level of 300°–500°K. (even lower if the discharge is externally cooled). This is because at these pressures the electron has more time between collisions (a longer mean free path) to gain energy from the electrical field. Likewise, the moderate temperatures are because of the fewer elastic collisions which occur between electrons and neutral gas atoms at the lower gas densities prevailing.

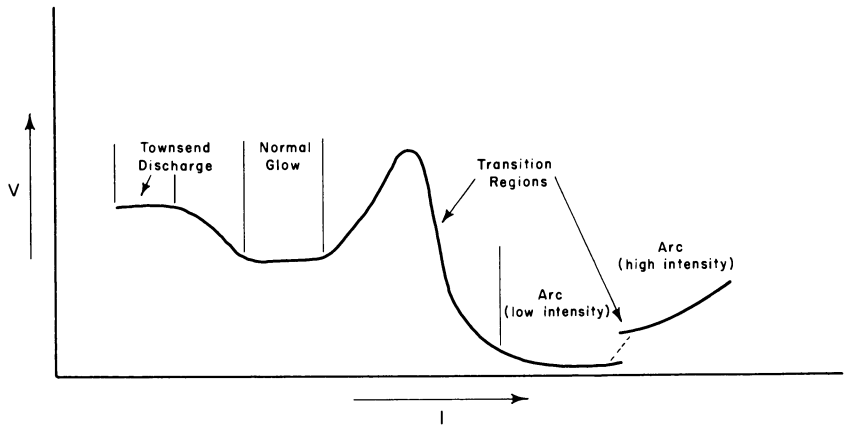

Figure 3. Typical voltage-current diagram for electrical discharges

As a consequence of the high electron temperatures, ionization will be low, on the order of 10^{-4} percent of the neutral particle density. The current is typically at the milliamp to hundreds of milliamps level. Because of the low gas densities, electron-ion recombination at the discharge boundaries predominates rather than in the gas volume. The discharge will be diffuse—*i.e.*, will fill the device with its glow.

Now it is possible, in raising the pressure of a glow discharge to the atmospheric level and above, to maintain the essential characteristics associated with the low pressure glow. These so-called high pressure glows (*7*, *13*) differ from low pressure glows in that the positive column is no longer diffuse but rather is constricted; appearing as a streamer between the electrodes. A discussion of some parameters causing constriction is given by Phelps (*11*). The temperature of the ions and neutral gas in the streamer is much higher and the electron temperature much lower relative to the low pressure glow. The high potential drop at the cathode, however, is essentially preserved as is the process of emission of electrons by ion-bombardment of the cathode.

By increasing the current flow through this high pressure glow a point is reached where a transition to a low intensity arc discharge can be made to occur. This transition is characterized by a considerable re-

Publication Date: June 1, 1969 | doi: 10.1021/ba-1969-0080.ch036

In Chemical Reactions in Electrical Discharges; Blaustein, B.;
Advances in Chemistry; American Chemical Society: Washington, DC, 1969.

duction in the potential drop at the cathode and an increase in the current density along the discharge length. Typical operating current levels for this type of discharge are in the 1 to 20 ampere range. Other essential changes in the glow to arc transition are compared in Tables II and III. Notable in these tables are the decreased potential drops both at the cathode and along the positive column for the arc type discharge. This implies that different and perhaps more efficient electron emission and ionization processes are operating in these regions. In contrast to the glow discharge the mechanism for electron emission from either a low or high pressure arc cathode is believed to be thermionic for electrodes which are not readily vaporizable and by field emission for vaporizable electrodes (*3*). The temperature necessary to cause thermionic emission is still the result of ion-bombardment of the cathode; however, the bombardment occurs at much higher current densities than in the glow discharge regions. Similarly, there is considerable thermal ionization in addition to ionization by electron impact in the positive column of the arc as a result of the much higher temperatures. The electron, ion, and neutral particle temperatures in arcs at atmospheric pressure are nearly equal owing to the greater frequency of collisions at the prevailing particle densities. Temperatures of the low intensity arc column at atmospheric pressure are roughly in the 4000° to 7000°K. range.

Publication Date: June 1, 1969 | doi: 10.1021/ba-1969-0080.ch036

Table II. Comparison of Glow and Arc Discharges at One Atmosphere in Air with Tungsten Electrodes[a]

	Glow	*Arc*
Power input, watts	60	60
Discharge current, amps	0.1	0.6
Cathode drop, volts	425	45
Positive column gradient, volts/cm.	350	~90
Discharge length, mm.	5	5

[a] *See* Reference 7.

Table III. Comparison of Glow and Arc Discharges at One Atmosphere in Hydrogen with Carbon Electrodes[a]

	Glow	*Arc*
Current, amps	2	2
Positive column gradient, volts/cm.	530	280
Change in total voltage across discharge, volts	+96	—
Appearance of discharge	less intense, striated	highly luminous, homogeneous along axis

[a] *See* Reference *13*.

The alternate route shown in Figure 2 to an arc at atmospheric pressure is *via* transition from a low pressure glow to a low pressure arc. This low pressure transition is likewise made by an increase in the discharge current (Figure 3). Cobine (3) discusses this transition in detail. The cathode emission and voltage phenomena discussed for the high pressure glow to arc transition are in general the same here. However, the luminous positive column for a low pressure arc is similar to the low pressure glow, differing only in the higher degree of ionization that usually prevails. Electron temperatures are much higher than the neutral gas temperature which itself is moderate. Ionization is by electron impact. The low pressure arc is also diffuse, and electron loss by recombination at the discharge boundaries predominates.

From the low intensity arc at near atmospheric pressure additional transitions can be made—*e.g.*, either to a plasma jet or a high intensity arc. The term "jet" ("torch" is sometimes used) is again descriptive, in that a stream of glowing hot plasma issues from these devices. Until now, little mention has been made of gas flow in connection with the glow or arc, because gas flow was not necessarily needed for electrode cooling and, therefore, the maintenance of the discharge. In the plasma jet, however, the flow of gas is an essential element. It serves to cool the discharge at the boundaries of the device, inducing a thermal pinch effect which is not present in the arc or glow. This thermal pinch is a constriction of the plasma toward the axis of the device that occurs because of the boundary cooling. The net result is an increase in current density, degree of ionization, and plasma temperature in the axial plasma core. Further increases in current to the discharge of fixed geometry results in higher current densities and plasma temperature. At even higher currents (hundreds of amperes) the magnetic field of force induced by the electron flow begins to exert a second pinch effect causing even further increases in current density and gas temperatures (so that temperatures up to 20,000°K. become possible). This magnetic pinch effect is not peculiar to the plasma jet device but occurs in other plasmas where the current becomes sufficiently high. The flow of gas acting to cool the boundaries of the plasma jet, combined with magnetohydrodynamic (MHD) forces, act to force the core of hot plasma gas out of the discharge region—in most designs usually through a hole created in the cathode. This jet of gas carries away by convection to the surroundings much of the heat generated in the discharge. Other heat transfer mechanisms operating are radiation and transfer by convection/conduction to and through the device boundary walls.

The transition from a low intensity to a high intensity arc is simpler and can be achieved primarily by increasing the current flow to an arc. As shown in Figure 3, one manifestation of the transition is an abrupt

Publication Date: June 1, 1969 | doi: 10.1021/ba-1969-0080.ch036

In Chemical Reactions in Electrical Discharges; Blaustein, B.;
Advances in Chemistry; American Chemical Society: Washington, DC, 1969.

change in the V-I characteristic from a negative to a positive slope. Accompanying this change is an increase in the rate of vaporization of the anode, and (at sufficiently high currents), the appearance of a high velocity jet of superheated vapor issuing at an angle from the anode crater. This jet or "tail flame" is the means by which heat is convected away. Operating currents for high intensity arcs can range upwards to several thousand amperes.

Thus, we see that by manipulation of pressure, current, and gas flow that various transitions from a glow type plasma environment to a high intensity arc can be made. New phenomena occur as these variables are manipulated, namely, thermal ionization, thermionic emission, thermal and magnetic pinch effects, etc. These phenomena change the nature of the plasma environment, generally toward higher degrees of ionization, and higher gas temperatures.

With reference to chemical reactions in such devices, the mechanism by which a given product is produced would certainly be a function of the specific plasma environment established. Not enough is known at present about reaction mechanisms or the control of plasma environments to select the best device for a desired product. However, some general comments regarding the problems of selection and use of plasma devices for chemical processing applications can be made.

Publication Date: June 1, 1969 | doi: 10.1021/ba-1969-0080.ch036

Chemical Processing

The possibilities of extremely rapid processing and the production of useful new products stimulates interest in the development of plasma reactors for the chemical process industries. Categories for potential near-term application of the discharge reactor include (8):

Highly endothermic reactions such as acetylene formation by pyrolysis.

Reactions that are extremely slow at ordinary temperatures; many reactions of this type involve high melting point solids.

Reactions dependent on excited species.

The step of evaluating the technical and economic merit of a proposed process requires selection of the type of equipment and processing conditions to be employed. However, too little is known about the factors controlling the plasma reaction to apply kinetic theory to aid in the selection. As a result, reaction studies have been empirical. However, as this series of papers shows, there is extensive research being undertaken. What is needed is a means of correlating the results reported for the various discharge reactor systems used so as to guide future research and to obtain answers for the many questions yet unresolved.

In Chemical Reactions in Electrical Discharges; Blaustein, B.;
Advances in Chemistry; American Chemical Society: Washington, DC, 1969.

A major factor in the economics of any electrothermal chemical process will be the operating pressure on the process. Generally it is easiest and less costly to operate a process at atmospheric pressure or slightly higher. A first consideration in the development of a process should be the possibility of conducting the discharge reaction at atmospheric pressure. The higher the pressure, the more thermally stable the product must be to withstand the plasma environment. As for production of high endothermic compounds such as acetylene or HCN, major attention has been given to the plasma jet which can operate at pressures well above atmospheric and at extremely high throughput. Conversely, for production of compounds of low thermal stability or for generation of excited species that rapidly recombine and revert to less excited states, the low pressure plasma environment may be the only possible one of practical interest.

Publication Date: June 1, 1969 | doi: 10.1021/ba-1969-0080.ch036

It is one thing to demonstrate conclusively in the laboratory that a desired product can be made at high yield by plasma processing. It is by far another to design the discharge reactor system for commercial operation. If this latter phase of a development is to be done in a systematic way, information is needed relative to the factors controlling the rate of the reaction and the influence of the geometry of the device on the results. The research results included in this compilation of papers relate to studies of chemical synthesis and reaction mechanism and also to studies concerned more with reaction kinetics, the latter being the most meaningful at the process development stage. The kinetic data required for process reactor design will differ from those needed to elucidate the reaction mechanism. Design data will be concerned mainly with the effect of the process variables, such as flow rates, power input, pressure, and reactor geometry on the conversion and yield. Attempts will be made to determine if the process rate is controlled by chemical kinetics or by mass or heat transfer factors.

The work of Ruppel, Mossbauer, and Bienstock (*12*) on the water-gas shift reaction in a corona discharge is a good example of a process kinetic study which provides reactor design data. The experimental data were correlated empirically to show the dependence of hydrogen yield as a function of pressure, flow rate, wall temperature, and input power. Thornton, Charleton, and Spedding (*15*) show the importance of reactor geometry in accomplishing hydrazine synthesis. Use of enthalpy rather than temperature has been shown to be a means for correlating process rate data for the high pressure, high flow reactor systems in which extreme temperature gradients exist (*1, 6*). The influence of the kinetics of quenching the plasma mixture on the product yield is of extreme importance as illustrated again by the paper of Bronfin (*2*).

In Chemical Reactions in Electrical Discharges; Blaustein, B.;
Advances in Chemistry; American Chemical Society: Washington, DC, 1969.

Too often in the literature the details of a device used in a kinetic study are only vaguely recorded. Discharge parameters, common to all devices, need to be identified and measured in the course of such studies. In this way the results of various investigators can be properly compared and used to advantage in the selection of a device for chemical processing. Phelps (*11*) has discussed some parameters of particular importance. However, to date very little correlation of these parameters against chemical reaction results in discharges has been reported.

Summary

Despite apparent gross physical differences between a low pressure, low temperature d.c. glow discharge and a high pressure, high temperature d.c. plasma jet, it was shown that the two extremes are interrelated. An understanding of the interrelationships between various types of devices appears to be important from the standpoint of selecting the best device for either research or process applications. Greater effort needs to be exerted in identifying the specific type device being used for a given chemical reaction study. Research is needed which compares the results obtained with the same chemical reaction in different types of devices.

Publication Date: June 1, 1969 | doi: 10.1021/ba-1969-0080.ch036

Literature Cited

(1) Ammann, P. R., Timmons, R. S., Krukonis, V., "Abstracts of Papers," 153rd Meeting, ACS, April 9-14, 1967, I101.
(2) Bronfin, B. R., ADVAN. CHEM. SER. **80,** 423 (1969).
(3) Cobine, J. D., "Gaseous Conductors," Dover, 1958.
(4) Coffman, J. A., Browne, W. A., *Sci. Am.* 91-97 (June 1965).
(5) Francis, G., "Handbuch der Physik," Springer-Verlag, Berlin, 1956.
(6) Freeman, M. P., ADVAN. CHEM. SER. **80,** 406 (1969).
(7) Bamblin, W. A., *et al., Brit. J. Appl. Phys.* **5,** 36 (January 1954).
(8) Goldberger, W. M., *Chem. Eng.* (March 14, 1966).
(9) Kunkel, W. B., "Plasma Physics in Theory and Application," Chap. 10, McGraw-Hill, New York, 1966.
(10) Persson, Karl-Birger, *J. Appl. Phys.* **36** (10), 3086 (1965).
(11) Phelps, A. V., ADVAN. CHEM. SER. **80,** 18 (1969).
(12) Ruppel, T. C., Mossbauer, P. F., Bienstock, D., ADVAN. CHEM. SER. **80,** 214 (1969).
(13) Suits, C. G., *Phys. Rev.* **53,** 609 (1938).
(14) Thornton, J. D., *Chem. Processing* **12** (2), S6 (1966).
(15) Thornton, J. D., Charlton, W. D., Spedding, P. L., ADVAN. CHEM. SER. **80,** 165 (1969).

RECEIVED October 9, 1967.

37

Some Problems of the Kinetics of Discharge Reactions

ROBERT LUNT

Department of Physics, University College, London, England

Publication Date: June 1, 1969 | doi: 10.1021/ba-1969-0080.ch037

The 1936 statistical theory of discharge reaction is recalled in respect to uniform-field zones, together with Kirkby's 1907 and 1911 data for positive column reaction to illustrate the lacunae in information that still impede the exploitation of the theory in tracing the detailed mechanism of a discharge reaction. These lacunae relate to single collisions, ion and electron motion in discharges, and the accompanying radiation from excited species, dependent on grosser and more easily measured parameters. Another group of problems relates to the generality and to the physical significance of Becker's parameter of 1920, devised to coordinate rate coefficients for reaction in streaming gas. The estimation of rate coefficients and criteria for selecting discharge parameters to advantage are outlined.

The kinetics of reaction in a gas through which an electrical discharge is maintained is concerned with the quantitative relation between the rate of formation of a new species from a reactant or parent species and an appropriate or convenient measure of the state of partial ionization of the gas. The usual meaning of 'discharge' in this connection is: any variant of a partially ionized gas for which there is a distribution in velocity, and hence in energy, of the charged particles. The concentration or particle number density for species in collision is common to the kinetics of thermal and of discharge reaction. In thermal reaction temperature is used as an index of the mean kinetic energy of the reactants and is associated with a Maxwell-Boltzmann distribution. The kinetics of discharge reaction also takes into account ions and electrons for each

In Chemical Reactions in Electrical Discharges; Blaustein, B.;
Advances in Chemistry; American Chemical Society: Washington, DC, 1969.

of which the mean kinetic energy and the energy distribution are specific to the composition of the reactant gas and to the kind of discharge.

Measurements of concentration for the reactant species in relation to the rate of reaction are customarily used in describing the kinetics of thermal reaction between uncharged atoms and molecules. For discharge reaction effecting chemical change, measurement of concentration and of distribution in energy for ions and electrons can be said to have scarcely begun. This difference springs partly from the relative simplicity of measuring charge transported between electrodes and energy absorbed in maintaining a discharge compared with the inconvenience of measuring, simultaneously with reaction rate, concentration and distribution in energy for the charged particles. These circumstances have led to differences more apparent than real between the rate coefficients of experiment, and between the formal statements of theory, in these two fields of reaction kinetics.

Of many investigations on the kinetics of chemical change in discharges since those of Warburg (*95*), few experiments were designed appropriately for tracing the mechanism of reaction. The corresponding experimental investigations on physical change, such as the generation of radiative excited molecules, since those of Wiedemann (*100*) and of Naccari and Bellati (*68*) led to an early recognition that the phenomena of discharge reaction are attributable mainly to collisions between a molecule of the parent species and an electron.

Townsend (*85, 86, 87, 88*) contributed the first analytical statement of the kinetics of discharge reactions; this is based on single collisions between reactant molecules and electrons occurring in a weakly ionized gas pervaded by a uniform electric field. Kirkby (*46*) extended the theory to discharge chemistry and designed experiments that showed that the predictions of theory were consistent with measurements of reaction rate coefficients with respect to charge transport. Imperfections in the Kirkby-Townsend theory were redressed in a restatement of some generality by Emeléus and Lunt (*23*). For uniform-field discharges the amended theory traces a precise connection between the rate of reaction and the rates of charge transport and of energy consumption.

Even for uniform-field discharges carrying an unvarying current, problems arise in applying the revised theory to the interpretation of experiment on chemical change. These problems are largely connected with a lack of auxiliary information such as would be available from simultaneous measurement of rates of reaction and emission of radiation, and of electron concentration and distribution in energy.

The kinetics of discharge reaction effecting chemical change are more amenable to investigation when the mean energy of the reactant

Publication Date: June 1, 1969 | doi: 10.1021/ba-1969-0080.ch037

In Chemical Reactions in Electrical Discharges; Blaustein, B.;
Advances in Chemistry; American Chemical Society: Washington, DC, 1969.

molecules is too small to initiate reaction, and when the gas consists mainly of reactant molecules at a constant concentration. This account deals with some problems of interpretation for chemical change in stationary and in streaming gas, and arising within these restrictions. For stationary gas the problems are outlined in discussing the interpretation of the pioneer experiments of Kirkby for uniform positive column reaction in which electrolytic gas is converted to water. For a reactant streamed through a discharge, problems have appeared in exploring the validity of Becker's (3) empirical procedure devised only for coordinating data for the rate coefficient with respect to energy consumption for the synthesis of ozone by the silent electric discharge in oxygen.

List of Symbols and of Their Meanings

The symbols used largely follow accepted usage in the physics of electrical discharges, astrophysics, spectroscopy, chemistry, and electrical engineering. Some compromises have been made to meet the special requirements for discussing the kinetics of discharge reactions; the aim is to use the least practicable number of primary symbols and to indicate variants of meaning by suffices. Because only the accepted symbols of spectroscopy for light atoms and diatomic molecules have been used, none of these are listed.

Comment is appropriate in a few cases. For concentration, or particle number density, n is used, usually with a suffix to identify the species concerned. X is used, as in spectroscopy, to denote the ground state, and, by extension, any reactant or parent species unchanged by a discharge. E is used only to denote an energy, and usually with a distinguishing suffix. Compromise between the claims for the diverse symbols that have been used for the Townsend parameter has led to the adoption of $\bar{X}/n$. The following symbols are not in common usage although some have been used in discussing the reaction kinetics of discharges:

z: position in inter-electrode space, relative to cathode,
uc: unit (electronic) charge irrespective of sign,
P_z: Kirkby's 'activity' of a discharge at a position z,
B_z: $\int_0^z P_z dz$,
$E(\mathrm{X})$: the variant of Becker's parameter now adopted, and
$a(\mathrm{K}), m(\mathrm{K})$: atoms, or molecules, of the species K.

The symbols and suffices are listed under four main groups: I, General; II, Processes and Species; III, Electrical and Energy Quantities; and IV, Reaction Rate Coefficients and Related Factors.

In Chemical Reactions in Electrical Discharges; Blaustein, B.;
Advances in Chemistry; American Chemical Society: Washington, DC, 1969.

(I) General.

Symbol	*Unit*	*Meaning and Comments*
a(X), a(K*) m(X), m(X*d*)	atom molecule	Atom of the species X, of the excited species K* Molecule of the species X, of the species X that is dissociated
n, n_X	a(X) cm.$^{-3}$	Total concentration or particle number density, of the atomic or molecular species specified by the suffix
f_X, f_{FP}		Fractional concentration of the species specified by the suffix
n_0, $f_{X,0}$		Initial values at some specified time, t = 0
ν	cm.^{3} sec.$^{-1}$	Volume rate at entry of gas streaming through a region in which a discharge is maintained
v_X	m(X) sec.$^{-1}$	Rate at which molecules of the species X enter a region in which a discharge is maintained
$(f_{FP})_\infty$		Limiting value of f_{FP} associated with indefinitely large values of ν or of E(X)
$f_{c;XK}$		Fractional conversion of the species X to the species K
$f_{c;XK;FP}$		Fractional conversion of the species X to a specified final product, the first intermediate in the reaction mechanism being the species K
T_g	°K.	Gas temperature
T_w	°K.	Temperature of the outer surface of the wall or envelope containing a discharge

The following relate more particularly to a d.c. cold-cathode glow discharge maintained within a cylindical tube

CDS, NG, NZ		Cathode dark space, negative glow, negative zones
FDS, PC		Faraday dark space, positive column
R, r	cm.	Radius of the inner wall surface, radial distance (from axis)
ca		Cathode-to-anode; used only as a suffix
z, z_{ca}	cm.	Position in the inter-electrode space relative to the cathode surface, distance of anode from cathode
z_{cds}, z_{ng}, z_{fds}	cm.	Distance (axial) from cathode surface to: *CDS-NG* boundary, *NG-FDS* boundary, and *FDS-PC* boundary

Publication Date: June 1, 1969 | doi: 10.1021/ba-1969-0080.ch037

In Chemical Reactions in Electrical Discharges; Blaustein, B.;
Advances in Chemistry; American Chemical Society: Washington, DC, 1969.

(II) Processes and Species.

Process or Species	*Suffix*	*Meaning and Comments*
X	X	Parent or reactant species; ground state
K	K	Immediate product of electron-impact reaction
J	J	A species to which the species K decays, or is changed, radiatively or by a collision of a specified kind
FP	FP	Final product of a reaction mechanism
I^+	I^+	Positive ion, species unspecified
X^+	X^+	Positive ion derived from the parent species
XK	XK	Process converting species X to species K
KJ	KJ	Process converting species K to species J
Xd	Xd	Process dissociating species X, unspecified
Xd:HH	Xd:HH	Process dissociating species X to H and H
Xi	Xi	Process ionizing X, unspecified products
XX^+	XX^+	Process ionizing X, products X^+ and e
D	D	Mixture of species characteristic of a discharge
		The following relate to species in the ground state
H	H	Hydrogen atom
H_2	hy	Hydrogen
O	O	Oxygen atom
O_2	ox	Oxygen
O_3	oz	Ozone
H_2O	wa	Water, usually as vapor
NH_3	am	Ammonia
N_2H_4	hyz	Hydrazine, usually as vapor
CO	cmx	Carbon monoxide
CO_2	cdx	Carbon dioxide
H_2 diss.	Xd	Molecule of H_2 dissociated
CO_2 dcp.	cdx:dcp	Molecule of CO_2 decomposed
NH_3 dcp.	am:dcp	Molecule of NH_3 decomposed
H^+	H^+	Positive ion derived from H
O^+	O^+	Positive ion derived from O
H_2^+		Positive ion derived from hydrogen
O_2^+		Positive ion derived from oxygen

(III) Electrical Quantities and Energies.

Symbol	*Unit*	*Meaning and Comments*
e	electron	Electron (negative), used mainly as a suffix
uc	unit charge	Electronic charge irrespective of sign
i	unspecified	Total current carried by a discharge between the electrodes
i_{uc}	uc $sec.^{-1}$	i, Current in unit charges per second
i_e	uc $sec.^{-1}$	Electron-borne component of i_{uc}
j_{uc}, j_e	uc $cm.^{-2}$ $sec.^{-1}$	Total, electron-borne, current density
n_e	uc $cm.^{-3}$	Electron concentration

Publication Date: June 1, 1969 | doi: 10.1021/ba-1969-0080.ch037

Symbol	*Unit*	*Meaning and Comments*
V_{ca}	volt	Cathode-to-anode voltage
$\mathcal{X}$	volt cm.$^{-1}$	Electric field in the cathode-to-anode direction, position specified by a suffix
w	e.v. sec.$^{-1}$	Energy per second absorbed in maintaining a discharge
w_r	e.v. cm.$^{-3}$ sec.$^{-1}$	w per unit volume of the space in which a discharge is maintained
W	cm. sec.$^{-1}$	Mean electron drift velocity in the direction of the field $\mathcal{X}$
$E(\mathrm{X})$	e.v. $m(\mathrm{X})^{-1}$	Energy absorbed in maintaining a discharge for some specified period Δt per molecule of reactant, X, exposed to the action of the discharging during Δt; the variant of the Becker parameter
E, E^+	e.v.	Electron, ion, kinetic energy
$\bar{E}$	e.v.	Mean electron energy
$f(E), f_M(E)$		Electron energy distribution function, a particular form of the function specified by the suffix: *M* for Maxwell-Boltzmann, *D* for Davydov-Druyvesteyn, and so on
$\mathcal{X}/n$	volt cm.^{2}	The form of the Townsend parameter adopted here in which n may carry a suffix to specify the species concerned
uc · cm.	uc · cm.	Unit distance of unit charge transport in the cathode-to-anode direction

(IV) Rate Coefficients for Thermal, Ion-Impact and Electron-Impact Reaction, and Related Quantities.

Symbol	*Unit*	*Meaning and Comments*
$k_{XY;K}$	$m(\mathrm{K})$ cm.^{3} sec.$^{-1}$	Rate coefficient for conversion, by collision with a species Y, of the species X to the species K (thermal bimolecular reaction) with respect to the concentrations of X and Y
Q_{XK}	πa_0^2	Cross section for the conversion of X to K by electron-impact reaction and a function of E
Q^+_{XK}	πa_0^2	The counterpart to Q_{XK} for ion-impact reaction
Q_{Xd}	πa_0^2	A variant of Q_{XK} relating to dissociative excitation, and denoting $\sum_K Q_{XK}$ for all the reactions concerned
$Q_{Xd;HH}$	πa_0^2	A variant of Q_{Xd} specifying that the products of the dissociation are two hydrogen atoms
R_{XK}	$m(\mathrm{K})$ cm.$^{-3}$ sec.$^{-1}$	Rate of generation of the species K from the species X by electron-impact reaction

Publication Date: June 1, 1969 | doi: 10.1021/ba-1969-0080.ch037

In Chemical Reactions in Electrical Discharges; Blaustein, B.;
Advances in Chemistry; American Chemical Society: Washington, DC, 1969.

Symbol	*Unit*	*Meaning and Comments*
R^{+}_{XK}	m(K) cm.$^{-3}$ sec.$^{-1}$	The counterpart to R_{XK} for ion-impact reaction
R_{FP}	m(FP) cm.$^{-3}$ sec.$^{-1}$	The rate of formation of a specified final product
α_{XK}	m(K) cm.^{3} sec.$^{-1}$	Rate coefficient for the electron-impact reaction specified by the suffix with respect to the concentrations of the species X and of electrons
α^{+}_{XK}	m(K) cm.^{3} sec.$^{-1}$	The counterpart to α_{XK} for ion-impact reaction
α_{FP}	m(FP) cm.^{3} sec.$^{-1}$	The corresponding rate coefficient for the formation of the specified final product
$B_{z;XK}$	$m(K)$ *uc.*$^{-1}$	Rate coefficient for the reaction specified by the suffix with respect to the rate of transport of charge through the distance z in the inter-electrode space
$B_{z;FP}$	m(FP) uc^{-1}	The corresponding rate coefficient for the specified final product
$P_{z;XK}$	m(K) (uc. cm.)$^{-1}$	Rate coefficient for the specified reaction with respect to unit distance of unit charge transported in the ~~X~~ or inter-electrode direction, the "activity" of Kirkby, in the region specified by z
$P_{z;FP}$	m(FP) (uc. cm.)$^{-1}$	The "activity" for the formation of the specified final product and in the region of the discharge specified by z
η_{XK}	m(K) e.v.$^{-1}$	Rate coefficient for the reaction specified by the suffix with respect to the rate at which energy is consumed in maintaining the discharge, alternatively any particular zone of a discharge which may be specified by an additional suffix—*e.g.*, $\eta_{nz;XK}$, $\eta_{pc;XK}$
η_{FP}	m(FP) e.v.$^{-1}$	The counterpart to η_{XK} for the formation of a specified final product
$(\eta_{FP}^{-1})_o$	e.v. m(FP)$^{-1}$	The inverse of η_{FP} found by extrapolating $\eta_{FP}^{-1} = f[E(X)]$ to $E(X) = 0$
$(\eta_{Xd}^{-1})_o$	e.v. $m(Xd)^{-1}$	The corresponding inverse rate coefficient for the dissociation (or decomposition; suffix: *dcp*) of the parent species
$\Phi_{XK;FP}$		Dimensionless factor taking into account the stoichiometry of the reaction mechanism whereby the species X is converted to the specified final product, and also all losses of species involved in that mechanism other than in the formation of the specified final product together with any loss of that product before it is isolated

In Chemical Reactions in Electrical Discharges; Blaustein, B.;
Advances in Chemistry; American Chemical Society: Washington, DC, 1969.

Symbol	*Unit*	*Meaning and Comments*
ϕ_s		The stoichiometric component of $\Phi_{XK;FP}$
β_{XK}	e.v. cm.^{3} sec.$^{-1}$	Rate coefficient for electron energy consumed in effecting the reaction specified by the suffix; if the reaction involves a super-elastic collision, β_{XK} is negative
F_{XK}		The fractional electron energy absorbed in effecting the reaction specified by the suffix; it is negative when β_{XK} is negative in sign, and $\sum_{X,K}(F_{XK}) = 1$
λ_{XK}		The average fractional electron energy absorbed per collision of all kinds, that is with respect to E, in effecting the reaction specified by the suffix
λ		The total average fractional electron energy absorbed per collision of all kinds—*i.e.*, λ_{XK} summed for all species present including the parent species and for all associated electron-impact reactions, elastic, inelastic and super-elastic
$h\nu_{KJ}$	photon	Photon emitted, or absorbed, in the radiative conversion of the species K to the species J
$E_{h\nu;KJ}$	e.v.	Energy of a photon $h\nu_{KJ}$

The Rate Coefficients for Discharge Reaction

Ambit of Systems Under Consideration. In recalling some of the principal results of the statistical theory of discharge reactions (*23*), attention is restricted mainly to the idealized case of a plasma consisting of a weakly ionized gas in a steady state pervaded by a uniform electric field because this is a system to which many discharges of present interest approximate more or less closely. The implications of the postulate of a plasma in a steady state include identity between the concentrations of positively and negatively charged species and the provision of devices to ensure that n, the total concentration of the particles present, and f, the fractional concentration of each species, are maintained constant together with T_g, the gas temperature. Furthermore, it is supposed that $T_g \gtrsim 300°K.$ so that thermal reaction in the un-ionized reactant occurs to an insignificant extent and the observed change is attributable primarily to the charged particles in the gas. Reaction attributable to collisions between the parent species and electrons appears to be of primary importance in accounting for the results of experiment. It is therefore pertinent to consider first the conversion of a reactant or parent species X to some other species K according to the following equation.

Publication Date: June 1, 1969 | doi: 10.1021/ba-1969-0080.ch037

In Chemical Reactions in Electrical Discharges; Blaustein, B.;
Advances in Chemistry; American Chemical Society: Washington, DC, 1969.

$$e + X = e + K - E_{XK} \qquad (R1)$$

where E_{XK} denotes the electron kinetic energy absorbed in effecting the reaction. The species K may be of three main kinds: (1) different from the parent species only by having acquired translational, rotational or vibrational energy, (2) a radiative or metastable electronically excited species, and (3) a dissociative electronically excited species decomposing 'spontaneously' into two (or more) molecular fragments, one or both of which by subsequent chemical reaction leads to the formation of a final product and exemplified by the dissociation of oxygen to atoms and the subsequent formation of ozone. Consequently, it is appropriate to mention the rate coefficients for primary electron-impact reaction of the type R1 before touching on those for the formation of a final product.

The Primary Reaction Rate Coefficient α_{XK}. What may be called the primary rate coefficient for Reaction R1 occurring in a volume element of an isotropic region pervaded by a uniform electric field, $\mathscr{X}$ volt cm.$^{-1}$, is defined in terms of $R_{G;XK}$, the generation rate of the species K in molecules (m(K)) per unit volume and per unit time, by

$$R_{XK} = \alpha_{XK} n_e n f_X \quad m(K) \text{ cm.}^{-3} \text{ sec.}^{-1} \qquad (1)$$

where n_e denotes the electron concentration and f_X specifies the fractional concentration of the parent species; α_{XK} is related to Q_{XK}, the cross section for the reaction for electrons of energy E e.v., and to $f(E)$, the electron energy distribution function, by

$$\alpha_{XK} = 5.22 \times 10^{-9} \int_0^\infty E^{1/2} Q_{XK} f(E) dE \quad \text{cm.}^3 \text{ sec.}^{-1} \qquad (2)$$

where Q_{XK} is in units of πa_o^2 (0.8806×10^{-16} cm.^{2}); Q_{XK} is a function of E, and except for elastic collisions, Q_{XK} is zero for $E < E_{XK}$. In some cases it may be preferable to discuss in place of R_{XK} the rate of decomposition or dissociation of the parent species, R_{Xd}.

α_{XK} is a formal counterpart to the rate coefficient for thermal homogeneous reaction involving binary collisions and exemplified by reaction between the species X and another species Y leading to the formation of the species K: if $R_{TG;XY;K}$ denotes the volume rate of this thermal reaction, it is customary to write

$$R_{TG;XY;K} = k_{XY;K} n^2 f_X f_Y \quad m(K) \text{ cm.}^{-3} \text{ sec.}^{-1} \qquad (3)$$

where f_Y relates to the species Y. A characteristic of the rate coefficient $k_{XY;K}$ is that it is a function of T_g and in some cases it can be represented to an acceptable approximation by

$$k_{XY;K} = s z_{XY} \exp(-\Delta E_{XY}/kT_g) \quad \text{cm.}^3 \text{ sec.}^{-1} \qquad (4)$$

Publication Date: June 1, 1969 | doi: 10.1021/ba-1969-0080.ch037

In Chemical Reactions in Electrical Discharges; Blaustein, B.;
Advances in Chemistry; American Chemical Society: Washington, DC, 1969.

where the 'collision number' $z_{XY} \approx 3 \times 10^{-10}$, s denotes the steric factor, and where ΔE_{XY} is called the 'activation energy.'

A comparison of Formulae 1 and 3 shows that the product of the concentration terms $n_e n f_X$ for electron-impact reaction corresponds to $n^2 f_X f_Y$ for thermal reaction. For chemical change induced by electrical discharges simultaneous measurements of n_e are largely lacking; consequently, it is rare to find comparisons between the two kinds of rate coefficients. For thermal reaction between uncharged species it is unusual to find values of $k_{XY;K} > 10^{-10}$ cm.^{3} sec.$^{-1}$, but comparable and larger values of α_{XK} are found for some electron-impact reactions.

From Formula 2 it is apparent that α_{XK} depends on the overlap between Q_{XK} and $E^{1/2}f(E)$. For a particular gas, however, $f(E)$ and $\bar{E}$, the mean electron energy, are functions of $\mathbb{X}/n$, the Townsend parameter. The mean electron energy is given by

$$\bar{E} = \int E f(E) dE / \int f(E) dE. \tag{5}$$

The precise form of f(E) for molecular gases remains controversial (*see* References 10, 20, and 25) but there is increasing evidence that the Maxwellian form is a useful approximation (*see* References 24, 29, 52, 53, 55, 57, 61, 92 and 93). It follows that α_{XK} is a function of $\mathbb{X}/n$ which, in principle, is an unrestricted parameter; alternatively, it may be preferred to discuss α_{XK} and related rate coefficients discussed below in terms of $\bar{E}$. For many reactions Q_{XK} is characterized by a major maximum for some value of the electron energy now denoted by $E_{Q,max}$; consequently, it may be expected in such cases that the overlap with $E^{1/2}f(E)$ is small for $\bar{E} << $ or $>> E_{Q,max}$, that is that α_{XK} passes through a maximum when considered as a function of $\mathbb{X}/n$ or $\bar{E}$. This is relevant to the selection of discharge parameters to effect a particular reaction at a conveniently rapid rate.

The Subsidiary Rate Coefficients P_{XK} and η_{XK}. The rate of transport of charge or the total current density in the direction of $\mathbb{X}$, the electric field, is given by the sum of the electron-borne and ion-borne current densities, or in terms of unit (electronic) charge (uc)

$$j_{uc} = j_e + j_+ \quad \text{uc cm.}^{-2} \text{ sec.}^{-1} \tag{6}$$

an additional term being appropriate in the exceptional case when negative ions are present to a significant extent; in many cases the current is carried almost exclusively by electrons, and then to a close approximation $j_{uc} = j_e$. The electron-borne current density is given by

$$j_e = W n_e \quad \text{uc cm.}^{-2} \text{ sec.}^{-1} \tag{7}$$

Publication Date: June 1, 1969 | doi: 10.1021/ba-1969-0080.ch037

In Chemical Reactions in Electrical Discharges; Blaustein, B.;
Advances in Chemistry; American Chemical Society: Washington, DC, 1969.

where W cm. sec.$^{-1}$ denotes the average electron drift velocity in the $\mathscr{X}$ direction. Per unit volume of the partially ionized gas Wn_e also specifies the distance through which unit charge is transported per second and hence it follows that P_{XK}, the number of molecules of the species K formed per unit distance of unit charge transport, is given by

$$P_{XK} = R_{XK}/(Wn_e) \tag{8}$$

so that P_{XK} is a rate coefficient with respect to current density; and from (1) it then follows that

$$P_{XK} = (\alpha_{XK}/W) \cdot nf_X \quad m(K)\ uc^{-1}\ cm.^{-1} \tag{9}$$

or

$$P_{XK}/n = f_X(\alpha_{XK}/W) \quad m(K)\ (uc \cdot cm.)^{-1}\ cm.^3 \tag{10}$$

Because W and E are functions of $\mathscr{X}$/n, it follows that so also is P_{XK}/n. Formulae 8 and 9 provide criteria of an assumed validity of the generation of the species K by reaction involving single electron collision with the parent species: for, when $\mathscr{X}/n$ is constant, the requirements are, respectively, that P_{XK} is independent of the current density and is proportional to nf_X. It is seen later that P_{XK} as given by Formula 9 is the formal counterpart to the 'activity' of Kirkby (*46*) for a uniform-field region.

From Formula 7 it follows that $\mathscr{X}j_c = W\mathscr{X}n_e$ e.v. cm.$^{-3}$ sec.$^{-1}$ specifies the rate at which energy is supplied by the electric field per unit volume of the partially ionized gas. Hence, η_{XK}, the number of molecules of the species K formed by Reaction R1 per unit energy supplied by the field, is given by

$$\begin{aligned}\eta_{XK} &= R_{XK}/(W\mathscr{X}n_e) \\ &= f_X\alpha_{XK}/(W\mathscr{X}/n) \quad m(K)\ e.v.^{-1}\end{aligned} \tag{11}$$

from this it is evident that η_{XK} is also a function of $\mathscr{X}/n$ and that this coefficient passes through a maximum corresponding to that for α_{XK} but occurring for a smaller value of $\mathscr{X}/n$. This characteristic of η_{XK} is relevant to the economics of using a discharge reaction as the basis of an industrial process.

The Energy Rate Coefficients β_{XK} and λ_{XK}. β_{XK}, a rate coefficient analogous to α_{XK} but specifying the rate of absorption of electron energy in effecting any particular Reaction, R1, is given by

$$\beta_{XK} = 5.22 \times 10^{-9} \int_0^\infty E^{1/2}Q_{XK}E_{XK}f(E)dE \quad e.v.\ cm.^3\ sec.^{-1} \tag{12}$$

where for many reactions E_{XK} does not vary with E; F_{XK}, the associated fractional energy consumption, follows as

$$F_{XK} = f_X\beta_{XK}/(W\mathscr{X}n_e) \tag{13}$$

hence, for all reactions of type R1 in which E_{XK} does not vary with E

Publication Date: June 1, 1969 | doi: 10.1021/ba-1969-0080.ch037

In Chemical Reactions in Electrical Discharges; Blaustein, B.;
Advances in Chemistry; American Chemical Society: Washington, DC, 1969.

$$\eta_{XK} = F_{XK}/(f_X E_{XK}). \tag{14}$$

When f_X differs from unity so slightly that all processes involving electron-impact reaction with species other than X occur at negligible rates,

$$\sum_K F_{XK} \simeq 1 \tag{15}$$

where the summation extends over all the possible simultaneous reactions of the type R1.

Because for any gas there are many possible reactions of the type R1, all of which occur simultaneously to some extent, for any single reaction F_{XK} must be less than unity; the experimental evidence for reactions effecting electronic excitation and ionization in a uniform-field region when $f_X \simeq 1$ is that F_{XK} is unlikely to exceed 0.25 ± 0.1. For such reactions it follows from Reaction 14 that there is a corresponding upper limit to η_{XK} given by

$$\eta_{XK;max} \gtrsim 0.25/E_{XK}. \tag{16}$$

This is a useful formula for estimating the maximum attainable value of η_{XK} and the indications from experiment are that this formula has a wide validity. A correspondingly simple procedure for estimating the discharge parameters that are associated with the attainment of $\eta_{XK;max}$ is, however, lacking.

A quantity related to β_{XK} is λ_{XK}, the average fractional electron energy consumed in effecting the specified Reaction R1 per electron collision of all kinds. The average energy is $\bar{E}$ and when $f_X \simeq 1$ the total electron collision rate coefficient is $\sum_K \alpha_{XK}$; hence,

$$\lambda_{XK} = \beta_{XK}/(\bar{E}\sum_K \alpha_{XK}). \tag{17}$$

Values for $\lambda = \sum_K \lambda_{XK}$ for $f_X \simeq 1$ and as a function of $\mathfrak{E}/n$ have been derived from experiment (*cf. e.g.*, Townsend (*88*); Healey and Reed (*33*); Massey and Burhop (*66*)). Townsend (*loc. cit*) (*88*) derived the formula $\lambda = a(W/U)^2$ in which a is a numerical factor depending on $f(E)$, and U denotes the r.m.s. value of the electron random velocity so that $U = 5.93 \times 10^7 \bar{E}^{1/2}$ cm. sec.$^{-1}$. He used this formula to compute values for λ from experimental data for U and W after putting $a = 2.46$, the value found by him to be appropriate when $f(E)$ is of the Maxwellian form. On the other hand Formula 17 relates to a single component of λ, namely λ_{XK}, and is similar to Townsend's formula only in respect of containing $\bar{E}$ in the divisor. A comparison of λ_{XK} with λ provides a criterion of the relative importance of a particular Reaction, R1; and a sharp maximum in the dependence of λ on $\mathfrak{E}/n$ is an indication that a particular

Publication Date: June 1, 1969 | doi: 10.1021/ba-1969-0080.ch037

In Chemical Reactions in Electrical Discharges; Blaustein, B.;
Advances in Chemistry; American Chemical Society: Washington, DC, 1969.

reaction of the type R1 is associated with relatively large values of λ_{XK} in the relevant narrow range of X/n.

The Rate Coefficients for a Final Product. The first group of final products includes radiative and metastable molecules that are excited states of the parent species, and molecular fragments of that species. In the second group, the final product, FP, of a discharge reaction effecting chemical change is usually a species formed by one or more sequential reactions involving the initial generation of a species K as envisaged in Reaction R1 so that that reaction is the rate determining step of the whole reaction mechanism leading to a particular final product. The rate coefficients for the generation of a specified final product are then related to those for the species K by a dimensionless factor $\Phi_{XK;FP}$ that takes into account the stoichiometry, and for the species K and all other species concerned, loss by reactions that do not lead to the specified final product. In place of Formulae 2, 10, and 11 we then have:

$$\alpha_{FP} = \Phi_{XK;FP} f_X \alpha_{XK} \quad m(\text{FP}) \text{ cm.}^3 \text{ sec.}^{-1}, \tag{18}$$

$$P_{FP}/n = \Phi_{XK;FP} f_X (\alpha_{XK}/W) \quad m(\text{FP}) \text{ uc}^{-1} \text{ cm.}^2, \tag{19}$$

and

$$\eta_{FP} = \Phi_{XK;FP} f_X \eta_{XK} \quad m(\text{FP}) \text{ e.v.}^{-1}. \tag{20}$$

Hence, when $\Phi_{KX;FP}$ is constant, each of these three rate coefficients may be expected to be a function of X/n; in principle, the characteristics of this factor may be deduced from the kinetics of the reactions that are sequential to Reaction R1 in leading to the formation of a final product.

Computation of the Rate Coefficients. Formulae 2 to 11 and 18 to 20 provide a basis for the computation of theoretically predicted values for the rate coefficients that can be compared with the corresponding values derived from experiment. Information on some of the quantities concerned in these formulae is far from complete; in such cases recourse may be made to estimates based on approximations.

In experiments on chemical change induced by discharges, measurements are lacking not only for n_e but also for the dependence of $f(E)$ and W on X/n. For a number of the simpler molecular gases, for $T_g \lesssim 300°$K., and for relatively very low values of the current density, data are available for W and $\bar{E}$ as functions of X/n—cf., References 9 and 34. These considerations and the fact that the electron motion in a particular gas may differ from that in a mixture of that gas and a relatively small amount of another species (*see* References 50 and 53) are associated with the restriction $f_X \simeq 1$ in some of the formulae; they also lead to this restriction in specifying the experimental conditions that are to be preferred for measuring rate coefficients that may properly be compared with the predictions of theory. There are extensive data for E_{XK} directly from experiment and from spectroscopic information. But data for Q_{XK}

Publication Date: June 1, 1969 | doi: 10.1021/ba-1969-0080.ch037

for Reaction R1 in molecular gases that lead to chemical change are largely lacking: Corrigan's measurements (*14*) of ΣQ_{XK} for all the reactions of that kind in hydrogen that lead directly and indirectly to dissociation into atoms, and which extend over the range $8.8 < E < 100$ e.v., exemplify the kind of information required.

When the Maxwellian distribution is assumed to be a valid approximation to $f(E)$, Formula 2 is replaced by

$$\alpha_{XK} = 10.9 \times 10^{-9}\, \bar{E}^{-1.5} \int_0^\infty Q_{XK} E \exp(-1.5\, E/\bar{E})\, dE \qquad (2.1)$$

and a similar change provides the replacement for Formula 12. A histogrammic approximation for Q_{XK} is convenient for computation and may be devised from the nature of the transition involved, $X \rightarrow K$; the indications from theory and experiment (*see* Reference *66*) are that $E_{Q,max}$ is likely to vary from *ca.* 1.2 E_{XK} for forbidden transitions to *ca.* 5.5 E_{XK} for allowed transitions. For any specified Reaction, R1, criteria of the acceptability of such estimates for α_{XK}, and for the resulting estimates for the other rate coefficients, are provided by the requirements, when $f_X = 1$, then $F_{XK} < 1$ and $\lambda_{XK} < \lambda$; there is also the requirement that the resulting inequalities provide a margin adequate to allow for the simultaneous occurrence of other reactions of the same general kind.

Electron-Impact Reaction in Other Kinds of Discharge. Although Formulae 1 and 2 remain valid for a volume element of a partially ionized gas, they have not been found to be useful in interpreting reaction rate coefficients except in uniform-field regions. For reaction in the negative glow a formal analysis was developed by Emeléus and Lunt (*23*); it has been used in discussing the data for negative zone reaction in electrolytic gas (*63*).

Ion-Impact Reaction. It has often been suggested that chemical change induced by electrical discharges is attributable to the positive ions present, but an analysis of the reaction kinetics appears to be lacking. For reactions analogous to Reaction R1, and denoting a positive ion by I^+:

$$I^+ + X = I^+ + K - E^+_{XK} \qquad (R2)$$

a formula for the rate coefficient, α^+_{XK}, is available by making the appropriate substitutions for E, $f(E)$ and Q_{XK} in Formula 2. But the known characteristics of such reactions—*e.g.*, Reference *33*—and the fact that $\bar{E}$, the mean ion energy in a uniform-field region, is of the order 1 e.v. or less, make it improbable that reactions of the kind Reaction R2 contribute significantly to the rates of chemical change found by experiment. And a fundamental question is whether the characteristics of P_{FP}/n and η_{FP} as

Publication Date: June 1, 1969 | doi: 10.1021/ba-1969-0080.ch037

derived from experiment require the invocation of a reaction mechanism initiated by positive ions. Reactions such as

$$H_2^+ + H_2 = H_3^+ + H \qquad (R3)$$

involve the prior generation of the species H_2^+ which is known to occur by Reaction R1, the reaction product being $K = H_2^+ + e$. Thus, Reaction R3 is important only in relation to the particular final product under consideration, H or H_3^+, and to the corresponding particular characteristics of $\Phi_{XK;FP}$.

Reaction Rate Coefficients Derived From Experiment

The D.C. Cold-Cathode Glow Discharge. This form of the discharge when realized between plane electrodes, the anode movable so that z_{ca}, the cathode-to-anode spacing can be varied, and contained within a cylindrical glass tube, has advantages as a 'reference standard' for discharge reaction. These advantages derive from the following considerations: the physics of this form of the discharge is relatively well understood; as Kirkby saw (*45, 46*) the zone known as the uniform positive column approximates to the ideal plasma envisaged earlier; and techniques have been developed for the measurement of the quantities concerned in investigating the kinetics of discharge reaction. This form of the discharge has been described so extensively that it may suffice to recall here only some relevant aspects. It is convenient to consider some characteristics of present interest as functions of nz cm.$^{-2}$ where z cm. denotes (axial) distance reckoned from the cathode surface, and to trace the development of the principal zones as z_{ca} is progressively increased. The nature of the discharge and the considerations mentioned earlier restrict the ranges of gas concentration and of current density, broadly speaking, to $10^{15} < n < 5 \times 10^{17}$ m(X) cm.$^{-3}$ and $5 \times 10^{15} < j_{uc} < 5 \times 10^{17}$ uc cm.$^{-2}$ sec.$^{-1}$. (Here and elsewhere 'current' and 'current density' refer to the current transported between the electrodes.)

For particular values of n and of V_{ca}, the cathode-to-anode voltage, there is a least value of the electrode spacing for which a discharge can be maintained and which is roughly specified by $nz_{ca;min} \approx 1.3\ nz_{cds}$ where z_{cds} denotes the axial distance to the boundary between the cathode dark space (*CDS*) and the negative glow (*NG*); for the least, or 'normal' value of V_{cf}, the 'cathode fall,' nz_{cds} usually lies in the range (1 to 3) $\times$ 10^{16} cm.$^{-2}$. As z_{ca} is progressively increased the *NG* attains its maximum anodeward extension and then a Faraday dark space (*FDS*) develops, usually a field-free zone. With further increase in z_{ca} the discharge can be maintained only by correspondingly increasing V_{ca}; this is a regime

Publication Date: June 1, 1969 | doi: 10.1021/ba-1969-0080.ch037

accompanied by the development of a positive column (*PC*) which, when 'uniform' (that is, not striated), is the variant of present interest. In experiments on chemical change it appears that only the two earliest criteria of 'uniformity' have been invoked: visual appearance and measurements of $\bar{\mathbb{X}}$, the average axial field as given by $\Delta V_{ca}/\Delta z_{ca}$. In such investigations, however, it is rare to find a visual description of the discharge and a spectroscopic record of the radiation emitted is more exceptional. It is seen later that the progressive development of the various zones may be associated with corresponding changes in the chemical activity.

The characterization of the 'uniform' positive column is the more complete when n is so small that the luminous region extends radially to the wall of the containing tube except for a thin annulus, the Langmuir sheath (*11*), adjacent to the wall. The electron concentration is a maximum at the tube axis and sensibly zero at the gas-glass interface; consequently measurements of the total current between the electrodes lead only to radial average values of $j_e = Wn_e$ specified by

$$j_e = (\pi R^2)^{-1} \int_0^R 2\pi r j_{e,r} dr \tag{21}$$

where r denotes radial distance and R the tube radius. When no negative ions are present, recombination of positive ions and electrons occurs almost exclusively at the gas-glass interface. (One of the referees has drawn attention to an account by Oskam (*69*) of the more complicated circumstances that may arise when negative ions are present.) That is, for the stationary state, in any volume element $\pi R^2\, dz$ within the *PC*, the rate of generation of ions and electrons, by reactions of type R1, where $K = X^+ + e$, is counterbalanced by the loss rate at an area $2\pi R\, dz$ of gas-glass interface. From Formulae 1 and 2 it can be seen that $f(E)$ is a principal parameter determining the generation rate when n is constant; the loss rate, being determined by radial diffusion, varies in an inverse way with n. These are principal considerations that prescribe the variation of $f(E)$ with n and R so that $\bar{E}$ and $\bar{\mathbb{X}}/n$ decrease as nR is increased, in accordance with approximate theory.

The radial variation of n_e is associated with various processes contributing to radial inhomogeneity of the positive column. The rate of heating of the gas associated with momentum transfer is specified by

$$R_{Xm} = \beta_{Xm} n_e n f_X \tag{1.1}$$

where β_{Xm} is given by Formula 12 when Q_{XK} is identified with Q_{Xm} relating to momentum transfer and $E_{XK} = (2m/M)E$ where M denotes the mass of the species X. The provision of a thermal sink at temperature

Publication Date: June 1, 1969 | doi: 10.1021/ba-1969-0080.ch037

In Chemical Reactions in Electrical Discharges; Blaustein, B.;
Advances in Chemistry; American Chemical Society: Washington, DC, 1969.

T_0 at the outer surface prescribes, but does not eliminate, the consequent radial variation of T_g and hence of n; values for $\overline{T}_g$, the radial average gas temperature, may be computed in terms of $\pi R^2 \overline{X}j_c$ and the thermal conductivities by the procedure of Verweij (*90*). The provision of a chemical sink to remove reaction products from the gas, for example by refrigeration of the discharge tube (*36*) or by absorption on a chemically reactive surface (*41, 42, 43, 44*) is also associated with concentration gradients, that is with the variation with position of the detailed composition of the gas; an analysis of the kinetics of the diffusion processes involved has been given by Emeléus and Beck (*22*).

It is thus apparent that measurements of chemical change relating to a volume element $\pi R^2 \Delta z$ within a uniform positive column are complicated radial averages, and this holds broadly for other zones of the discharge; it can also be seen that restricting the current density to relatively low values conduces to minimize radial inhomogeneity. Furthermore, even when measurements of the axial field in terms of $\Delta V_{ca}/\Delta z_{ca}$, or by probe techniques, indicate apparent uniformity, the evidence about rapidly moving striations casts doubt about the attainment of strict uniformity in the axial direction. The challenge presented by the empirical rate coefficients of experiment is that they conform with the predictions of simple theory for the idealized plasma envisaged earlier in this paper.

The detailed physical characterization of the positive column rests mainly on experimental data for discharges through monatomic gases in which chemical change, such as the formation of He_2 and Hg_2, occurs to an apparently unimportant extent. The phenomena are probably similar but different in detail for discharges through molecular gases that suffer chemical change; and it is remarkable that in many cases the rate coefficient for chemical change is comparable with, or greater than, that for the generation of ions and electrons.

Kirkby's (*45*) data for discharges through electrolytic gas illustrate the trend of V_{ca} with progressive increase in nz_{ca}, the current being maintained constant. For each value of n data are cited for V_{ca} at several values of z_{ca} which were not chosen to provide regular increments of nz_{ca}. Figure 1 shows V_{ca} on a scale of nz for four relatively large values of n which almost certainly correspond to a regime of normal cathode fall; V_{ca} is nearly constant and the range $3.5 < nz \times 10^{-16} < 30$ cm.$^{-2}$ may be inferred to correspond to the progressive development of the *NG*. Figure 2 relates to a lower range of n and to the transition to the regime of abnormal cathode fall, evidenced by the larger values of V_{ca} in the lower range of nz where there are insufficient data to trace the trend of V_{ca} unambiguously. For $nz > ca.\ 25 \times 10^{16}$ cm.$^{-2}$, however, V_{ca} increases linearly, corresponding in Kirkby's account to the development of a

Publication Date: June 1, 1969 | doi: 10.1021/ba-1969-0080.ch037

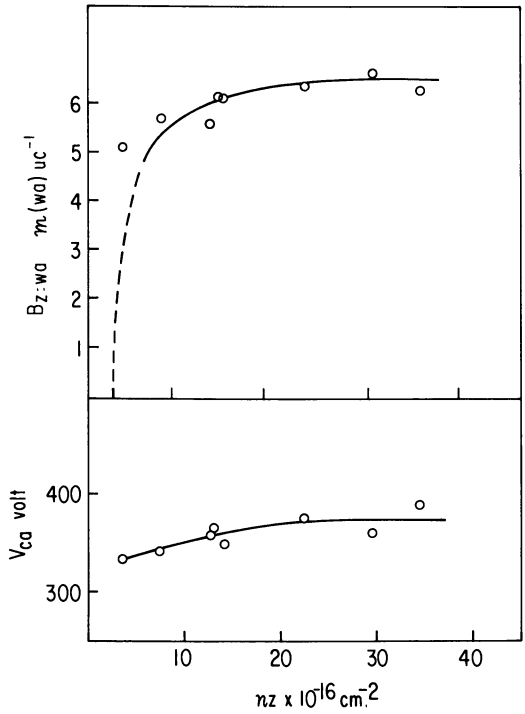

Figure 1. V_{ca} and $B_{z:wa}$ for negative zone reaction in electrolytic gas (Ref. 45)

'uniform' positive column. For these ranges of linear variation the rate of increase is equal to the Townsend parameter since

$$dV_{ca}/d(nz) = \text{Ж}/n \qquad (22)$$

and it can be seen that Ж/n decreases as n is increased.

Rate Coefficients for the D.C. Cold-Cathode Glow Discharge. The quantities now seen to be pertinent to measure in order to derive a detailed understanding of reaction rate coefficients are mentioned earlier. To discuss the measurements that have been made it is convenient to recall some more or less general aspects of the experiments. There are two volumes to consider: τ cm.^{3}, the volume of an enclosed space which includes the region in which the discharge is maintained, and τ_d, the volume of the inter-electrode space. Values for n, the initial gas concentration, have been derived from measurements of the pressure at a region distant from the discharge zone; τn thus specifies the initial amount of the reactant. It appears that no estimates have been made of $\overline{T}_g$ during a

Publication Date: June 1, 1969 | doi: 10.1021/ba-1969-0080.ch037

discharge. No experiments have been traced in which the reactant product is continuously removed from discharge region and, in order to maintain a steady state, the reactant is fed in at a compensating rate. Continuous removal of the final product is associated with concentration gradients for that species and these are accompanied by concentration gradients for the parent species diffusing to the region of the discharge.

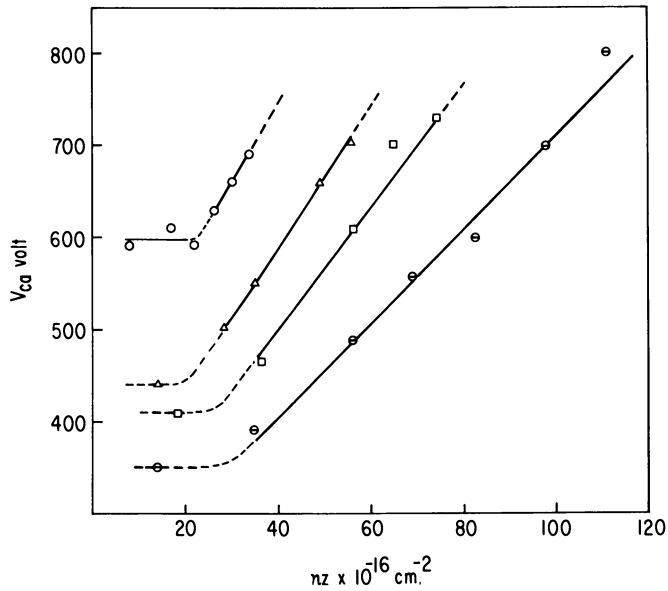

Figure 2. V_{ca} in electrolytic gas (Ref. 45)

Values of n × 10^{-16}*:*

○ = *2.1* □ = *4.6*
△ = *3.5* ⊖ = *6.9*

The procedure adopted by Kirkby and followed in many later investigations is to maintain the discharge for a period Δt for a set of values of n, z_{ca}, V_{ca} and i_{uc}, the total current in unit charges sec.$^{-1}$, and to measure Δn, the resulting decrease in the reactant concentration. The total charge transported between the electrodes is $i_{uc}\Delta t$, and $i_{uc}V_{ca}\Delta t$ e.v. is the corresponding energy absorbed in maintaining the discharge. Hence, $B_{z;Xd}$, the number of molecules of the parent species decomposed or reacted per unit charge transported across the distance $z = z_{ca}$ follows as

$$B_{z;Xd} = \tau\Delta n/(i_{uc}\Delta t) \quad m(Xd)\ uc^{-1}, \tag{23}$$

and the corresponding rate coefficient with respect to energy is

$$\eta_{z;Xd} = \tau\Delta n/(i_{uc}V_{ca}\Delta t) \quad m(Xd)\ e.v.^{-1}. \tag{24}$$

Publication Date: June 1, 1969 | doi: 10.1021/ba-1969-0080.ch037

In Chemical Reactions in Electrical Discharges; Blaustein, B.;
Advances in Chemistry; American Chemical Society: Washington, DC, 1969.

The corresponding rate coefficients for the formation of a specified final product, $B_{z;FP}$ and $\eta_{z;FP}$, may be derived by replacing $\tau\Delta n$ in Formulae 23 and 24 by the measured number of molecules of final product formed, or by introducing into those formulae a stoichiometric factor ϕ_s that specifies the number of product molecules known to be formed per molecule of the parent species decomposed or reacted. B_z and η_z are thus average rate coefficients for the inter-electrode space, and they are measures of the difference between the rate of synthesis of the final product and the sum of the rates of loss of that species by being decomposed in the discharge and by other processes.

For any region z to $z + dz$ in the inter-electrode space Kirkby defined the activity of a discharge for effecting reaction, now denoted by $P_{z;FP}$, as the number of product molecules formed per cm. of unit charge transport between the electrodes; hence, when $B_{z;FP}$ is known as a function of nz for a specified value of n, it follows that

$$P_{z;FP}/n = dB_{z;FP}/d(nz) \tag{25}$$

and the corresponding coefficient for the decomposition of the parent species is related by

$$P_{z;FP} = \phi_s P_{z;Xd}.$$

The qualification remains, however, that each of these rate coefficients is a measure of the net rate of synthesis and decomposition. Uncertainty about the extent of reformation of the parent species and decomposition of the final product can be largely eliminated by showing that $B_{z;Xd}$ as derived from Formula 23 and $B_{z;FP} = \phi_s B_{z;Xd}$ are independent of the current. If z is such that nz corresponds to a region within a uniform positive column, $P_{z;FP}/n$ is the experimental counterpart to the theoretically derived quantity P_{FP}/n in Formula 19; and constancy of $P_{z;FP}/n$ over a range of z is a demonstration of the uniformity of that region in respect of chemical activity.

In some investigations measurements have been made which lead to values for $B_{z;Xd}$ or $B_{z;FP}$ for a single value of z_{ca} and a range of n; although such data can be discussed as functions of nz, they do not provide information about $P_{z;Xd}$ or $P_{z;FP}$.

The Experimental Data of Kirkby. The experiments relate to the conversion of electrolytic gas to water (wa); the final product was removed continuously by absorption on a phosphorus pentoxide surface distant from the inter-electrode space. It is convenient to discuss first the experiments of 1907, mentioned earlier in this section, relating to a single discharge tube, $2R = 2.2$ cm., provision being made to vary z_{ca} up to 16 cm. For the range $6.9 \times 10^{16} < n < 15 \times 10^{16}$ $m(X)$ cm.$^{-3}$, the values found for $B_{z;wa} = \phi_s B_{z;Xd}$ using Formula 23 and $\phi_s = 0.67$

Publication Date: June 1, 1969 | doi: 10.1021/ba-1969-0080.ch037

are shown in the upper part of Figure 1 as functions of nz. The points corresponding to particular values of z_{ca} appear to lie about a smooth curve extrapolating to zero for $nz = ca.\ 2._5 \times 10^{16}$ cm.$^{-2}$, and attaining a constant value for $nz = 20 \times 10^{16}$ cm.$^{-2}$. This lower limit for nz is close the estimate for nz_{cds} in electrolytic gas for normal cathode fall and based on a simple rule of mixtures. It is therefore the more plausible to associate the range up to $nz = ca.\ 20 \times 10^{16}$ cm.$^{-2}$ with the progressive growth of the negative glow in accordance with the consideration of the corresponding values for V_{ca}. Furthermore, in this low range of nz the values found for $B_{z;wa}$ increase linearly with V_{ca} and are nearly independent of n for a particular value of V_{ca}; these are the characteristics of $B_{z;FP}$ for negative zone reaction found in other investigations.

It cannot be excluded that reaction occurs to some extent in the region between the cathode surface and the *CDS-NG* boundary and makes a contribution to $B_{z;wa}$. In similar experiments but with a discharge tube immersed in liquid air Brewer and Westhaver (*5*) found that ammonia formed from ($0.25\ N_2 + 0.75\ H_2$) mixture was deposited as a sharply defined band on the wall surrounding the *NG*, no detectable deposit occurring in the regions surrounding the *CDS* and the *FDS*. The account of the later experiments on electrolytic gas (*7*) states that reaction occurred uniformly over the whole inter-electrode space, now estimated to extend to $nz = ca.\ 3 \times 10^{16}$ cm.$^{-2}$; such uniformity is, however, improbable.

The corresponding data for a lower range of gas concentration, $2 \times 10^{16} < n < 7 \times 10^{16}$ m(X) cm.$^{-3}$, are shown in Figures 2 and 3; for $nz < ca.\ 25 \times 10^{16}$ cm.$^{-2}$ there are not enough observations to trace the trends of V_{ca} and $B_{z;wa}$ unambiguously. For each value of n there is a higher range of nz in which the values found for V_{ca} increase linearly and are thus associated with a constant value of $\mathfrak{X}/n$. The corresponding values of $B_{z;wa}$, shown in Figure 3, exhibit a similar trend. At each value of n there is a range of nz in which $B_{z;wa}$ varies so that $P_{z;wa}/n$, computed from Formula 25, is sensibly constant; and this range of nz coincides approximately with that in which $\mathfrak{X}/n$ is constant. These experiments of 1907 thus provide the first example of chemical change effected by discharge reaction for which $P_{z;FP}/n$ varies with $\mathfrak{X}/n$; this is the expectation from theory embodied in Formula 19 when $\Phi_{XK;FP}$ is constant. It had been the aim of Kirkby to seek evidence of that kind and his discovery that the uniform positive column is a zone where this dependence can be studied led to the design of further experiments.

The subsequent investigation by Kirkby (*46*) is concerned only with *PC* reaction in an extended range of $\mathfrak{X}/n$. The cylindrical discharge tube, $2R = 2.4$ cm., was provided with gold-plated disc electrodes and z_{ca}

Publication Date: June 1, 1969 | doi: 10.1021/ba-1969-0080.ch037

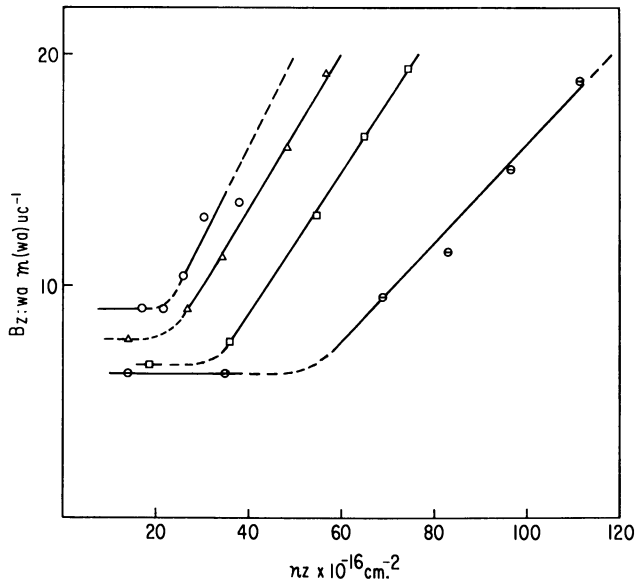

Figure 3. $B_{z;wa}$ for water formed in electrolytic gas as a function of nz (Ref. 45)

Values of n × 10^{-16}*:*

○ = *2.1* □ = *4.6*
△ = *3.5* ⊖ = *6.9*

could be varied up to 32 cm. The range $0.6 \times 10^{16} < n < 7 \times 10^{16}$ $m(X)$ cm.$^{-3}$ partly overlaps that previously explored, and as in the earlier experiments n denotes the mean gas concentration during Δt, the duration of the discharge, or $n = n_0 - 0.5\ \Delta n$; a refinement was to restrict Δt so that $\Delta n/n_0 < 0.03$. The current lay in the range $0.6 \times 10^{15} < i_{uc} < 3 \times 10^{15}$ (uc) sec.$^{-1}$, roughly proportional to n, but much lower than that in the earlier experiments, 1.7×10^{16} (uc) sec.$^{-1}$; this control of the current facilitated the attainment of the restriction on Δn and ensured that the *PC* was free from striations. At each pair of values of n and i_{uc}, the observations relate only to two or three values of z_{ca}. The least value was chosen 1.0 ± 0.5 cm. anodeward of the *FDS-NG* boundary; the largest value lay in the range 24 to 32 cm.; and for some values of n, observations were made also for z_{ca} midway between the two extreme values. The procedure adopted thus provides values of $P_{z;wa}/n$ and of $\bar{X}/n$ that are averages over relatively large ranges of nz but the evidence for uniformity of the positive column is less conclusive than that afforded by the data in Figures 2 and 3. All these values of $P_{z;wa}/n$ together with those derived from the earlier experiments, now denoted

Publication Date: June 1, 1969 | doi: 10.1021/ba-1969-0080.ch037

by P_{wa}/n, are shown in Figure 4 with the associated values of $\mathbb{E}/n$ in the range (2 to 14) $\times$ 10^{-16} volts cm.^{2}.

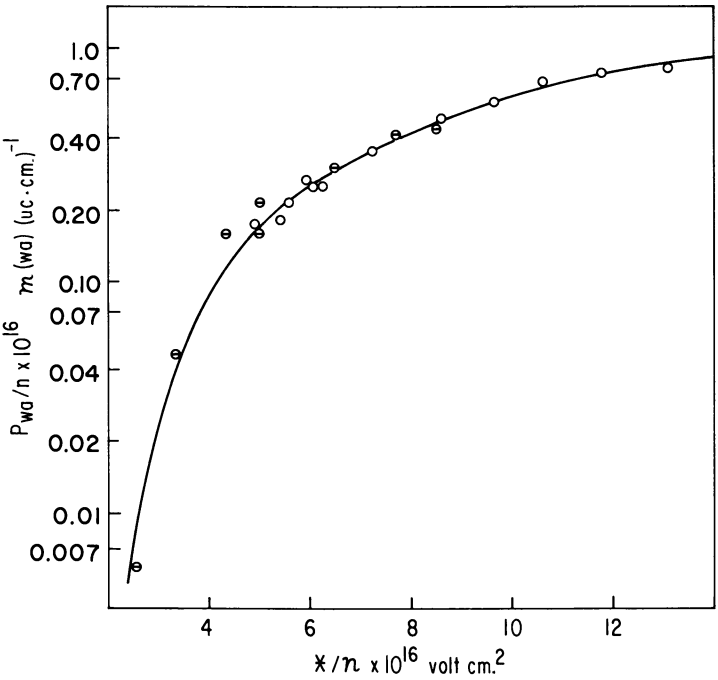

Figure 4. P_{wa}/n for water formed in electrolytic gas by positive column reaction (Refs. 45 and 46)

⊖: *Ref. 45*
○: *Ref. 46*

It can be seen from Figure 4 that the two groups of experimental data are self-consistent and that the rate coefficient for the water formed by reaction in an approximately uniform positive column is a function of $\mathbb{E}/n$. This is explicable in terms of the theory outlined earlier if the formation of water were attributable to an electron-impact reaction of the type R1 when the species X is identified as H_2 or O_2 and if the factor $\Phi_{XK;FP}$ were constant. More detailed consideration of the two groups of data for the common range of $\mathbb{E}/n$ leads to the following conclusions. There is no detectable effect on P_{wa}/n of a large change in the current, sixfold at the lower end of the range and twentyfold at the upper end; but for neither group are there any experiments that directly demonstrate this invariance. Secondly, because the heating of the gas is roughly proportional to the current, it follows that there is no indication of a contribution by thermal reaction to the observed rate of reaction. There

Publication Date: June 1, 1969 | doi: 10.1021/ba-1969-0080.ch037

is, however, no demonstration that, for a specified value of $\bar{X}/n$, the value found for P_{wa}/n is independent of n; to gain such information it is usually necessary to make observations using several discharge tubes of different radii.

The use of Formulae 23 and 25 to derive values for P_{wa}/n may obscure the fact that these values are complicated averages. For $z = z_{ca}$ the amount of water formed in an interval Δt is specified by $\phi_s \tau \Delta n$ and hence $\bar{R}_{wa}$, the volume average rate of water formation in the inter-electrode space, is given by

$$\bar{R}_{wa} = \phi_s \tau \Delta n/(\pi R^2 z \Delta t) \qquad m(H_2O) \text{ cm.}^{-3} \text{ sec.}^{-1}$$

The radial average current density is $\bar{j}_{uc} = i_{uc}/\pi R^2$ and hence the average number of water molecules formed per cm. of unit charge transport follows as

$$\begin{aligned} \bar{P}_{z;wa} &= \bar{R}_{wa}/\bar{j}_{uc} \\ &= B_{z;wa}/z \ , \end{aligned}$$

a result consistent with Formula 25. $\bar{P}_{z;wa}$ is thus an average, axial and radial, over the whole inter-electrode space and also over any change in the gas composition that occurs during the interval Δt. The procedure adopted by Kirkby in his later experiments using two values of the electrode spacing z and $z + \Delta z$, each associated with some development of a positive column, is based on an approximate form of Formula 25 giving an average over Δz, or

$$\bar{P}_{\Delta z;wa}/n = (1/n)\Delta B_{z;wa}/\Delta z. \qquad (25.1)$$

When data for n_e are lacking it is sometimes convenient to derive estimates for α_{FP} from experimentally determined values of P_{FP}/n; when acceptable estimates are available for W this may be done by rearranging Formula 19, and for illustration, now changing the suffices to refer to water formation, to read

$$\alpha_{wa} = WP_{wa}/n = f_X \Phi_{XK;wa} \alpha_{XK}. \qquad (19.1)$$

Rate Coefficients for Other Forms of the Discharge. For other forms of the discharge maintained by a voltage across two electrodes, constant or varying in time, Formulae 23 and 24 remain applicable; the interpretation of the data in terms of Formula 25 largely depends on the information available on the physical characterization of the discharge. If the current varies in time, the transport of charge cannot be deduced from measurements of the rms value of the current; and when external electrodes are used it is necessary to identify the component of the total current that is associated with the transport of charge by the partly

Publication Date: June 1, 1969 | doi: 10.1021/ba-1969-0080.ch037

In Chemical Reactions in Electrical Discharges; Blaustein, B.;
Advances in Chemistry; American Chemical Society: Washington, DC, 1969.

ionized gas. For discharges induced by very high frequency fields, such as 'microwave' discharges, in which the mean electron concentration can be measured, the average value of α_{FP} can be derived from the average volume rate of reaction. The corresponding derivation of the average value of η_{FP} requires only appropriate precision in measuring the rate at which energy is absorbed in maintaining the discharge, which when external electrodes are used, should be distinguished from the energy absorbed by the glass of the discharge tube adjacent to electrodes (*see* References 30, 54, and 56).

The Interpretation of Reaction Rate Coefficients Found by Experiment

The interpretation of rate coefficients for chemical change induced by discharges is hampered by the lack of auxiliary data; these circumstances are illustrated below in discussing Kirkby's data for positive column reaction. Two principal questions are: (1) can the primary and rate-determining step in the reaction mechanism be identified and (2) can a rate coefficient based on that primary step be computed from theory in quantitative agreement with that derived from experiment for the final reaction product.

Information on chemical change induced by the absorption of photons of specified energy by the reactant species provides a guide to the reactions of type R1 that involve allowed transitions. The principal reactions of that kind involving disallowed transitions can be inferred in many cases from spectroscopic data and theory. It may be expected in general that, for a particular reactant, many reactions of type R1 occur simultaneously to some extent in any discharge, the relative extent being determined by the range of electron energy in which Q_{XK}, the cross section for the reaction, is of significant amplitude. For each kind of transition the indications from experiment and theory are that the amplitude of Q_{XK} is largest for the lowest value of E_{XK} and that the range of significant amplitude is shorter for forbidden transitions. These considerations lead to the expectation that, for a single reactant species, there may be more than one product of a discharge reaction and that more than one reaction of type R1 may contribute to the formation of a particular final product. It is therefore the more remarkable that many discharge reactions are known for which the kinetics appear to be characteristic of a single reaction of type R1; this may become explicable when data for Q_{XK} become available for the various reactions of that kind that can lead to chemical change.

For mixtures of molecular gases a rule is lacking to estimate the dependence of the mean electron energy and drift velocity on $\mathfrak{X}/n$. For

Publication Date: June 1, 1969 | doi: 10.1021/ba-1969-0080.ch037

uniform-field discharges in molecular gases in which no significant heating of the gas occurs, a principal uncertainty is the form of $f(E)$, the electron energy distribution function. The Maxwellian form, adopted in Formula 2.1, is widely used in the physical theory of discharges as a convenient approximation. The validity of the approximation in connection with the computation of reaction rate coefficients has been explored mainly for reactions that do not lead to chemical change but to electronically excited species, and exemplified by

$$e + H_2(X\,^1\Sigma_g^+) = 2e + H_2^+(X\,^2\Sigma_g^+) - E_{XX^+} \qquad (R4)$$

and

$$e + H_2(X\,^1\Sigma_g^+) = e + H_2(C\,^1\Pi_u) - E_{XC} \qquad (R5)$$

For Reaction R4 the rate coefficient P_{XX^+}/n computed from Formulae 2.1 and 10 agrees closely with the values found from experiment (usually denoted as α/n or α/p) and long known as the Townsend coefficient of ionization (*24*). For Reaction R5 and for similar reactions generating the radiative species H_2 ($a\,^3\Sigma_g^+$) and N_2 ($C\,^3\Pi_u$), a similar concordance is found between experiment and the predictions of theory (*16, 58, 59, 61, 74*). In discussing possible interpretations of Kirkby's data for positive column reaction, it is assumed that the Maxwellian form for $f(E)$ is a valid approximation to the true distribution.

When an apparently acceptable identification has been made of an electron-impact reaction of the type R1, or of its ion-impact counterpart, it remains to trace the subsequent reactions that lead to the formation of the particular final product, and for that reaction mechanism to derive values of the loss-cum-stoichiometric factor $\Phi_{XK;FP}$ that pertain to the conditions explored by experiment. Procedures for dealing with problems of that kind are outlined in discussing the detailed interpretation of the results of Kirkby's experiments.

The Interpretation of Kirkby's Data: Electron-Impact Reaction. For electrolytic gas in a 'uniform' positive column it is to be expected that reactions of type R1 occur for each component of the reactant; processes of dissociative electronic excitation are known for hydrogen and for oxygen (*see* References 35 and 66). Two species that may contribute to sequential reactions not involving electrons but leading to the formation of water can thus be identified: hydrogen atoms and oxygen atoms; and there may be other species concerned. In principle, in attempting to trace the reaction mechanism, one procedure to pursue is to compute for the relevant range of X/n:

(1) α_{Xd} for the reactions of type R1 that generate the two readily identified species that may be involved in sequential reactions of the kind envisaged; that is, to compute values of $\alpha_{Xd;HH}$ for $X = H_2$ $X\,^1\Sigma_g^+$, $v'' = 0$ and of $\alpha_{Xd;OO}$ for $X = O_2$ $X\,^3\Sigma_g^-$, $v'' = 0$; and

Publication Date: June 1, 1969 | doi: 10.1021/ba-1969-0080.ch037

In Chemical Reactions in Electrical Discharges; Blaustein, B.;
Advances in Chemistry; American Chemical Society: Washington, DC, 1969.

(2) for the range of discharge parameters associated with Kirkby's experiments, values of the corresponding special forms of $\Phi_{XK;FP}$, namely $\Phi_{Xd;HH;wa}$ and $\Phi_{Xd;OO;wa}$, using the data for thermal reaction.

In respect of (1) it can be said that experimental data for Q_{XK}, now denoted by $Q_{Xd;HH}$, as a function of E have been provided recently by Corrigan (*14*); this summed cross section relates to all the reactions of type R1 in hydrogen that generate hydrogen atoms, directly or indirectly. Corresponding data for $Q_{Xd;OO}$ in oxygen are lacking; some consequences of assuming the validity of a rough estimate for $Q_{XA;OO}$, relating to the dissociative excitation of the A $^3\Sigma_u^+$ state of oxygen, are mentioned later.

In respect of (2) it can be said that the gas temperature in Kirkby's experiments may be estimated to lie in the range $290° < T_g < 350°$K., and that the coherence between the data of 1907 and of 1911, shown in Figure 4 and relating to two different discharge tubes, is a strong indication that reaction at the gas-glass interface does not make any significant contribution to the chemical change observed. Secondly, there is no golden road to deriving, or even to estimating, values for $\Phi_{Xd;HH;wa}$ and for $\Phi_{Xd;OO;wa}$. This can be traced to an important difference between the atoms generated in a discharge as the consequence of dissociative excitation and the atoms of hydrogen and of oxygen envisaged in mechanisms of thermal gas-phase reaction, the system being in a stationary state of thermodynamic equilibrium.

For these latter conditions the mean kinetic energy of random motion is about 0.042 e.v. for $T_g = 320° \pm 30°$K., and there are extensive data for the rate coefficients of reactions such as:

$$O + H_2 \rightarrow OH + H, \qquad (R6)$$

$$H + O_2 \rightarrow OH + O, \qquad (R7)$$

and

$$H + O_2 + X \rightarrow HO_2 + X, \qquad (R8)$$

where X may be identified with one or other of the molecular reactant species (*see* References 12, 13, 37, 39, 40, 67, 77, and 91).

In marked contrast, hydrogen atoms resulting from the direct, or indirect, generation by electron-impact from molecules in the X $^1\Sigma_g^+$, $v'' = 0$ state, of molecules in the b $^3\Sigma_u^+$ state, have an initial kinetic energy of *ca.* 2.2 e.v. For the oxygen atoms resulting from the transition X $^3\Sigma_g^-$, $v'' = 0$ to A $^3\Sigma_u^+$ in oxygen, the initial kinetic energy is about 0.25 e.v. And for the corresponding variants of the Reactions R6, R7, and R8 no data for rate coefficients has been traced.

A further impediment to deriving values for the two variants of $\Phi_{XK;wa}$ mentioned above is that it is necessary to take into account the

Publication Date: June 1, 1969 | doi: 10.1021/ba-1969-0080.ch037

In Chemical Reactions in Electrical Discharges; Blaustein, B.;
Advances in Chemistry; American Chemical Society: Washington, DC, 1969.

simultaneous generation of metastable species by electron-impact reaction; the species concerned include:

$$H_2: X\ ^1\Sigma_g^+, v'' > 0 \text{ and } c^3\Pi_u, v = 0;$$

$$O_2: X\ ^3\Sigma_g^-, v'' > 0, a\ ^1\Delta_g, b\ ^1\Sigma_g^+, \text{ and } A\ ^3\Sigma_u^+.$$

Most of these species may be associated with a range of rotational and vibrational levels, and each of all these species may be associated with another set of variants of one or other of the three illustrative reactions mentioned above. To assess the relative of all these possible reactions a primary requirement is a knowledge of the fractional concentration of each metastable species in the quasi-stationary states attained in Kirkby's discharge experiments.

Procedures for estimating such fractional concentrations have been outlined by Lunt and Swindell (*64*), and an example of the utility of such procedures has been provided by Schram, Herman, and Lunt (*78*) when discussing a metastable species generated in a 'uniform' PC through nitrogen. For Kirkby's experiments, however, it appears that the information available on the generation of metastable species is inadequate to make estimates of the associated fractional concentrations.

Hydrogen Atom Generation in Kirkby's Experiments. In order to illustrate in more detail, and in terms of Kirkby's observations for positive column reaction in electrolytic gas, the lacunae of auxiliary information that impede the tracing of the mechanism of discharge reaction, the much simpler procedure now adopted is: to compare the predictions of theory for uniform-field discharges in respect of the dissociative excitation of hydrogen with the results of experiment for an apparently uniform positive column. This procedure is based on Formula 19 and can be seen to be equivalent to enquiring what values must be assigned to $\Phi_{Xd:HH:wa}$, for the ranges of X/n and of other parameters concerned in Kirkby's experiments, in order to provide agreement between $f_X\alpha_{Xd:HH}/W = P_{Xd:HH}/n$ as computed from theory and P_{wa}/n as derived from experiment. For this purpose the following provisional assumptions are made:

(1) that the observed formation of water is attributable mainly to 'sequential' reaction involving hydrogen atoms.

(2) that the Maxwellian form of $f(E)$ is a valid approximation so that Formula 2.1 may be invoked for the computation of $\alpha_{Xd:HH}$.

For hydrogen in electrolytic gas $f_X = 0.67$. The values found for $0.67\ \alpha_{Xd:HH}$ $m(H_2$ diss.) cm.^{3} sec.$^{-1}$ using Formula 2.1 and the data of Corrigan (*14*) for $Q_{Xd:HH}$ in the relevant range of $\bar{E}$ are listed in the following table.

In Chemical Reactions in Electrical Discharges; Blaustein, B.;
Advances in Chemistry; American Chemical Society: Washington, DC, 1969.

Table I. 0.67 $\alpha_{Xd;HH}$ Computed from Formula 2.1

$\overline{E}$ e.v.	$0.67\ \alpha_{Xd;HH} \times 10^9$	$\overline{E}$ e.v.	$0.67\ \alpha_{Xd;HH} \times 10^9$
1.5	0.00153	3.5	0.332
2.0	0.0157	4.0	0.555
2.5	0.0648	4.5	0.830
3.0	0.168	5.0	1.040

In order to make the proposed comparison with experiment, it is necessary, next, to set the values of $\overline{E}$ in Table I on a scale of $\mathfrak{X}/n$ for electrolytic gas and then, by using the associated values of W, to compute $P_{Xd;HH}/n$ as 0.67 $\alpha_{Xd;HH}/W$. Because experimental data are lacking, crude estimates have been made based on the data for the individual gases (*cf.* References 9 and 34) by assuming a simple mixture rule and using for each value of $\mathfrak{X}/n$ the formulae

$$\overline{E} = 0.67\ \overline{E}_1 + 0.33\ \overline{E}_2 \tag{26}$$

and

$$W = 0.67\ W_1 + 0.33\ W_2 \tag{27}$$

where the suffices 1 and 2 relate, respectively, to hydrogen and to oxygen. The values thus found for $P_{Xd;HH}/n$ for a series of integral values of $\mathfrak{X}/n$ are listed in column 2 of Table II. The remarkable result is that the computed values follow closely those derived from experiment which are given in the 3rd column: the ratio $\rho = (P_{wa}/n)/(P_{Xd;HH}/n)$ is nearly constant, about $2._0$.

Table II. The Comparison of $P_{Xd;HH}/n$ with P_{wa}/n

$\mathfrak{X}/n \times 10^{16}$	$P_{Xd;HH}/n \times 10^{16}$	$P_{wa}/n \times 10^{16}$	ρ	$WP_{wa}/n \times 10^9$
3	0.012_5	0.025	2.00	0.010
4	0.038	0.090	2.37	0.047
5	0.073	0.17_5	2.40	0.11
6	0.12	0.26	2.17	0.19
7	0.18_5	0.35	1.89	0.29
8	0.25	0.45	1.80	0.44
9	0.31	0.55	1.77	0.63
10	0.36	0.66	1.83	0.81
11	0.40_5	0.76	1.88	1.03
12	0.44	0.81	1.84	1.20
13	0.47	0.87	1.85	1.42
14	0.49	0.94	1.92	1.69
			mean 1.98	

Reference to Formula 19 which for the reaction mechanism under consideration reads

Publication Date: June 1, 1969 | doi: 10.1021/ba-1969-0080.ch037

$$P_{wa}/n = f_X \Phi_{Xd;HH;wa} \alpha_{Xd;HH}/W, \quad (19.2)$$

where P_{wa}/n denotes the quantity determined by experiment, suggests that ρ may be identified with the loss-cum-stoichiometric factor, or $\Phi_{Xd;HH;wa} \simeq 2$; and at first sight this factor appears to be the only unknown quantity in relation to the data of Table II. But P_{wa}/n is a complicated average shown by experiment to be a function of $\mathfrak{X}/n$; and $\alpha_{Xd;HH}/W$, is a quantity computed from theory for a uniform-field region and it is a function of $\mathfrak{X}/n$ that can be identified if Formulae 2.1, 26, and 27 are valid approximations. It thus appears that $\Phi_{Xd;HH;wa}$ may be regarded not only in the sense already defined but also as a quasi-empirical factor that brings into identity these two functions of $\mathfrak{X}/n$ and that, incidentally, takes into account j_e/j_{uc}, the fraction of the total current carried by the discharge that is electron-borne. Reasons have been given for doubting that the information on thermal reaction suffices to predict the stoichiometrical factor for the particular circumstances in Kirkby's experiments; and the simultaneous occurrence of the dissociative electronic excitation of oxygen may have contributed to the observed formation of water. These considerations indicate that caution is necessary in interpreting the comparison portrayed in Table II and the discovery that ρ is nearly constant.

Apart from those considerations, for the reaction mechanism envisaged, $\Phi_{Xd;HH;wa}$ would be sensibly equal to the stoichiometric yield of water from atomic hydrogen in reaction with oxygen if the fractional loss of water by decomposition while diffusing through the discharge were negligibly small; the provisions of a 'chemical sink' for water vapor ensured that $f_{wa} << f_X$, and although a procedure has been described for estimating the fractional concentration of a final product (*22, 64, 78*), it is not readily adapted to the geometry of Kirby's experiments. If f_{wa} were negligibly small, the significance of $\rho \approx 2.0$ would be that two molecules of water are formed per molecule of hydrogen dissociated into atoms. A yield of 0.9 molecule of water per hydrogen atom of thermal energy reacting at 293°K. with oxygen in the presence of hydrogen at a total concentration of $5 \times 10^{16} < n < 7 \times 10^{16}$ cm.$^{-3}$ has been reported by Clyne and Thrush (*12*). It has been mentioned that reactions of type R1 in hydrogen generate atoms that have an initial kinetic energy of *ca.* 2.2 e.v.: the apparent slight discrepancy between the provisional interpretation of the value found for ρ and the results of experiment for thermal reaction is thus in the sense to be expected.

The balance of evidence thus appears to be that the conversion of electrolytic gas by 'uniform' positive column reaction to water is explicable in terms of a mechanism of which the first step is the electron-impact dissociation of hydrogen to atoms.

Publication Date: June 1, 1969 | doi: 10.1021/ba-1969-0080.ch037

In Chemical Reactions in Electrical Discharges; Blaustein, B.;
Advances in Chemistry; American Chemical Society: Washington, DC, 1969.

From the data for $P_{wa}/n = f(\text{Ж}/n)$ in Figure 4 and Table II, the empirical result of experiment is that $\eta_{wa} = (P_{wa}/n)/(\text{Ж}/n)$, the rate coefficient with respect to the energy consumed in maintaining the positive column, passes through a maximum, *ca.* 0.07 $m(H_2O)$ e.v.$^{-1}$, for $\text{Ж}/n$ = *ca.* 11 $\times$ 10^{-16} volts cm.^{2}. For the group of reactions for which $Q_{Xd;HH}$ has been measured, the weighted average value of E_{XK} is close to 9 e.v. From the estimated stoichiometric yield of water and from Formulae 14 and 20, it follows for the mechanism envisaged that the estimate for the maximum total fractional electron energy loss associated with the reactions concerned of type R1 is $(F_{Xd;HH})_{max} \approx 0.5$. If this estimate were correct, only about half the total electron energy in the discharge would be available for effecting the other simultaneous reactions of that kind. One possibility is that the experimental values for $Q_{Xd;HH}$ should be adjusted by a factor *ca.* 0.7 (*15*), and this would lead to the more plausible estimate $(F_{Xd;HH})_{max} \approx 0.35$. That adjustment would require that the stoichiometrical yield of water per hydrogen atom generated by electron-impact reaction is about 1.4; it appears that the data of thermal gas-phase reaction do not exclude that such a yield may be attained.

Oxygen Atom Generation in Kirkby's Experiments. It has been mentioned that experimental data are lacking for any reaction of type R1 in oxygen that leads to dissociative excitation. For reasons to be discussed elsewhere, it may be assumed that the principal reaction of that kind is the generation of molecules in the A $^3\Sigma_u^+$ state, and that $Q_{XA;OO}$, the cross section for the process, has an average value 0.05 πa_o^2 only in the range $6 < E < 9$ e.v. On inserting this value in Formula 2.1 and using the procedure adopted in deriving the data for Tables I and II, it is found that, for the range of $\text{Ж}/n$ in Table II, $P_{XA;OO}/n$ decreases rapidly from 0.05 $\times$ 10^{-16} to 0.02 $\times$ 10^{-16}, a trend very different from that of P_{wa}/n. Secondly, for T_g = *ca.* 300°K., the rate coefficient for binary thermal reaction of oxygen atoms with hydrogen is less than 10^{-17} cm.^{3} sec.$^{-1}$ according to Clyne and Thrush (*12*) and is thus unimportantly small compared with the values found for $WP_{wa}/n = \alpha_{wa}$ and cited in the 5th column of Table II.

Although the fate of the oxygen atoms generated remains to be identified, the foregoing enquiry may be seen to support the earlier conclusion that Kirkby's experimental data are explicable quantitatively in terms of a reaction mechanism in which the second step involves the interaction of hydrogen atoms with oxygen.

The Role of Oxygen Atoms Envisaged by Kirkby in 1911. It is pertinent to touch briefly on Kirkby's interpretation of his data for positive column reaction in electrolytic gas because of its historical impor-

Publication Date: June 1, 1969 | doi: 10.1021/ba-1969-0080.ch037

tance: it led to the first determination from discharge data subsequent to that of E. Wiedemann (*100*) of the energy necessary to dissociate a molecule into uncharged fragments by electron collision.

Kirkby envisaged the dissociation of oxygen to atoms by electron-impact and subsequent reaction written by him as

$$O + H_2 = H_2O$$

and he gave reasons for dismissing from consideration reaction that involved the initial dissociation of hydrogen to atoms.

In seeking a quantitative interpretation of the rate coefficient for the formation of water, P_{wa}/n, Kirby invoked the theory of electron-impact reaction formulated first by Townsend (*85*, *86*). In terms of the account given earlier in this paper, the formal statement of that early theory can be seen to approach closely Formulae 2 and 12 when the following qualifications are made:

(1) Q_{XK} has a constant value for $E > E_{XK}$ such that every electron-molecule collision effects a reaction of type R1,

(2) at each such collision the loss of electron energy is not E_{XK} but the whole of the energy of the impacting electron, E.

On that basis, subsequently seen to be imperfect (*23*), for the dissociation of oxygen to atoms by electron collision Kirkby deduced that $E_{XK} = 6.1 \times 10^{-12}$ erg or 3.8 e.v.; if the species K is identified with the A state of the molecule, $E_{XA} = ca.$ 5.5 e.v.

Ion-impact and Ion-molecule Reactions in Kirkby's Experiments. A reaction of the type R2, associated with a rate coefficient α^+_{XK}, may be the initial step of a reaction mechanism that contributes a term α^+_{wa} to $\alpha_{wa} = WP_{wa}/n$. By analogy with Formula 18 these quantities are related by

$$\alpha^+_{wa} = f_X \Phi^+_{XK;wa} \alpha^+_{wa} \tag{28}$$

It is convenient to assume provisionally that the total water formation in the positive column, at the volume average rate $\bar{R}_{wa}$ $m(H_2O)$ cm.$^{-3}$ sec.$^{-1}$, is initiated by positive ion reaction. The volume average value of α^+_{wa} would then be practically the same as that of α_{wa} for electron-impact reaction because $n_+ \simeq n_e$, and for any specified value of $\mathbb{X}/n$ may be computed from

$$\alpha^+_{wa} \simeq \bar{R}_{wa}/(n_e n f_X) = \alpha_{wa}, \tag{28.1}$$

or more conveniently from Formula 19.1 which now reads

$$\alpha^+_{wa} \simeq \alpha_{wa} = WP_{wa}/n. \tag{28.2}$$

In each case a knowledge of W is necessary when measurements of n_e are lacking, the radial average value of n_e being $\simeq i_{uc}/(\pi R^2 W)$.

Publication Date: June 1, 1969 | doi: 10.1021/ba-1969-0080.ch037

In Chemical Reactions in Electrical Discharges; Blaustein, B.;
Advances in Chemistry; American Chemical Society: Washington, DC, 1969.

The last column of Table II cites values of WP_{wa}/n computed from the values of P_{wa}/n derived from experiment and from estimates of W based on Formula 27. From Formulae 28 and 28.2 it can be seen that, at each value of $\bar{X}/n$, the estimate for WP_{wa}/n specifies approximately the value of $\Phi^{+}_{XK;wa}\alpha^{+}_{XK}$ which would have to be accounted for by a reaction mechanism in which the primary step is a reaction of type R2.

From the characteristics of the reactions of type R1 effecting ionization in hydrogen and in oxygen, for which E_{XX}^{+}, the energy absorbed, is 15.6 and 12.2 e.v., respectively, estimates of the rate coefficients in electrolytic gas indicate that the predominant reaction for the range of $\bar{X}/n$ concerned is that generating the species O_2^{+}, and the charge transfer reaction

$$H_2^{+} + O_2 = H_2 + O_2^{+} \qquad \text{(R9)}$$

is likely to ensure that the fractional concentration of the species H_2^{+} is relatively very small. Consequently, the mechanism of chemical change requires to be based mainly on an initial reaction of type R2 in which the species I^{+} and X are identified as O_2^{+} and H_2, respectively.

If the energy of drift motion of the species O_2^{+} in electrolytic gas for the range of $\bar{X}/n$ concerned is assumed to be ten times that for positive ions in oxygen (*9, 76*), it would be less than 0.5 e.v. For such values of the ion kinetic energy the characteristics of reactions of type R2 effecting electronic excitation (*see* References 33 and 66) indicate that the rate coefficient for reactions that could lead to chemical change is much too small to make a significant contribution to the observed rate coefficient for water formation.

The Rate Coefficient η_{FP} for Reaction in Streaming Gas

In 1920 Becker (*3*) described empirical procedures to co-ordinate data for rate coefficients with respect to energy for the formation of a final product and for the associated fractional concentrations of the final product when the reactant or parent species is streamed through a region in which a discharge is maintained. This analysis may be regarded as an extension of that of Warburg (*95, 96, 97*) and was evolved to systematize the information for the generation of ozone from oxygen at atmospheric pressure. For this process it had long been known that, as the velocity of streaming is progressively increased, f_{FP}, the fractional concentration of the final product, decreases towards zero, and that η_{FP} increases apparently towards a limiting value $(\eta_{FP})_o$. A procedure had been lacking, however, to determine $(\eta_{FP})_o$, a quantity that could be used to judge the merit of different forms of the discharge. From the examples discussed below it is apparent that Becker's analysis is of considerable generality

Publication Date: June 1, 1969 | doi: 10.1021/ba-1969-0080.ch037

In Chemical Reactions in Electrical Discharges; Blaustein, B.;
Advances in Chemistry; American Chemical Society: Washington, DC, 1969.

but its physical significance remains somewhat obscure. Concerning the examples cited, it is pertinent to mention that, in some contexts, it is convenient to replace η_{FP} by η_{Xd}, the corresponding quantity relating to the dissociation, or to the decomposition, of the parent species, using the relation $\eta_{Xd} = \eta_{FP}/\phi_s$. This procedure ignores any loss of the products of dissociation that are not consumed in making the final product, and thus leads to values for η_{Xd} that may be less than the true values. Secondly, the values of η_{FP} derived from experiment in which the reactant is streamed through a region in which a discharge is maintained, relate to the discharge as a whole except in one investigation in which the gas stream flowed only through a positive column.

In terms of the units preferred here, $w_r\,\Delta t$, the co-ordinating parameter introduced by Becker, is defined by

$$w_r\,\Delta t = (w/\tau_d)/(\tau_d/\nu) = w/\nu \quad \text{e.v. cm.}^{-3} \tag{29}$$

where w e.v. sec.$^{-1}$ denotes the power consumed in maintaining the discharge, τ_d cm.^{3} the volume occupied by the discharge, and where ν cm.^{3} sec.$^{-1}$ specifies the volume rate at which the reactant enters the region in which the discharge is maintained. Becker called $w_r = w/\tau_d$ the 'spacial power density' ("Raumliche Wattdichte"); Δt is a time interval that determines the total amount of energy imparted to the gas and, for streaming gas, is given by τ_d/ν, the time of passage of the gas through the discharge.

In order to take into account the concentration of the reactant that is admitted to the discharge zone, it is convenient to elaborate Becker's parameter by replacing ν in Formula 29 by $v_x = \nu n_X$, the rate at which the reactant species enters the region of discharge. In some cases the volume occupied by the discharge is less than τ, the total volume associated with the 'discharge tube' or, for non-streaming gas, the volume enclosing the initial amount of reactant. It is therefore appropriate to introduce the factor τ_d/τ, and then consistency with Formula 29 requires that Δt is given by τ/τ_d. $\tau_d/\nu = \tau/\nu$. With these elaborations the definition of the Becker parameter reads:

$$E(X) = (\tau_d/\tau)\,(w/\tau_d)\Delta t/n_X \quad \text{e.v. } m(X)^{-1}. \tag{30}$$

In this definition $E(X)$ specifies the energy used to maintain the discharge per molecule of the reactant species that is exposed to the action of the discharge, and it also appears to be applicable to both streaming and to stationary gas. In the first case when $\tau = \tau_d$ and consequently $\Delta t = \tau_d/\nu$, Formula 30 reduces to

$$E(X) = w/(\nu n_X) = w/v_x \tag{30.1}$$

and for the usual case of non-streaming gas with $\tau_d < \tau$, it becomes

$$E(X) = w\Delta t/(\tau n_X) \tag{30.2}$$

Publication Date: June 1, 1969 | doi: 10.1021/ba-1969-0080.ch037

In Chemical Reactions in Electrical Discharges; Blaustein, B.;
Advances in Chemistry; American Chemical Society: Washington, DC, 1969.

In principle the simplest ways of varying $E(X)$ are:

(1) for streaming gas: to maintain constant values of w and of n_X in the stream entering the discharge zone, and to vary ν which in effect is to vary $\Delta t = \tau_d/\nu$; and

(2) for stationary gas at the initial concentration n_X and enclosed in a fixed volume τ: to maintain w constant and to vary Δt, the duration of the discharge.

In each case it is plausible to expect, for relatively large values of Δt, and hence of $E(X)$, that the change in composition of the gas is so extensive that secondary effects become significantly large. There are many investigations on streaming gas that conform more or less closely to the conditions envisaged but relatively few for stationary gas. No investigation has been traced for a reaction effected by a particular discharge in both stationary and streaming gas that provides a link between the phenomena for a common range of $E(X)$.

For both stationary and streaming gas it is evident that $E(X)$ does not take into account many factors that are likely to determine the discharge parameters and their variation with Δt. They include: the heating of the gas by the discharge which is determined partly by the geometry of the discharge tube and by the refrigeration of its outer surface; the variation of the total particle concentration with position which may depend on convection, diffusion, heating of the gas, and the streaming velocity; and the variation with position of the fractional concentration of each species present in the discharge zone. $E(X)$ is likely to be specific to the kind of discharge; Becker made use of data relating only to the silent electric discharge (SED). This name has come to signify, since many years, that form of the discharge which develops when a layer of gas is contained between two layers of dielectric, external to each of which is an electrode, and devised by W. von Siemens in 1857 (*94*) (Fr.: *décharge silencieuse or effleuve;* Ger.: *stille Entladung*).

Becker's discovery was that, for the generation of ozone (oz) from oxygen (ox) streamed at atmospheric pressure through a SED maintained in a particular discharge tube, η_{oz}^{-1} varies linearly with $E(O_2)$ when V_{ca} is held constant; it was found that w did not vary with ν. When generalized for a specified final product from a reactant X, this formula reads

$$\eta_{FP}^{-1} = a + bE(X) \tag{31}$$

where a and b are empirical factors, b being dimensionless. Becker interpreted a, obtained by extrapolating the linear variation of η_{FP}^{-1} to $E(X) = 0$, as $(\eta_{FP}^{-1})_o$, the limiting value corresponding to indefinitely large values of ν; that is, as the inverse of the largest attainable value of η_{FP} for the particular type of discharge and the associated discharge parame-

Publication Date: June 1, 1969 | doi: 10.1021/ba-1969-0080.ch037

In Chemical Reactions in Electrical Discharges; Blaustein, B.;
Advances in Chemistry; American Chemical Society: Washington, DC, 1969.

ters. For a particular discharge tube he concluded that a is independent of V_{ca} and of w; but it is doubtful whether his data are sufficiently precise and extensive to support this conclusion (*see—e.g.*, the two lower curves in Figure 5). Although $(\eta_{FP}^{-1})_o$ as obtained by linear extrapolation of the experimental data was shown to be a useful quantity for coordinating data and for predicting the dependence of η_{FP} on $E(X)$, the validity of this extrapolation to $E(X) = 0$ and the physical significance of the result require to be discussed. For a particular discharge tube it was also found that the factor b increases with V_{ca} and w, but it is doubtful whether any physical significance can be attached to the empirical formulae developed for the dependence of b on V_{ca}.

It is to be expected that a relation similar to Equation 31 holds for η_{Xd}^{-1}, the corresponding inverse rate coefficient for the decomposition of the parent species from which the final product is derived; this is relevant also in those cases in which the loss or decomposition of the parent species is the only process for which a rate coefficient can be derived from the data of experiment.

Three examples are shown in Figure 5 to illustrate the validity of Equation 31 for the decomposition of a parent species. The reaction is the decomposition of oxygen to atoms for which the inverse rate coefficient $\eta_{Xd;OO}^{-1}$ is taken to be $2\eta_{oz}^{-1}$ as derived from experiment; it is assumed that the loss of oxygen atoms in other ways may be neglected because n, the concentration of oxygen molecules is relatively very large. Consequently, if the ordinate scale is reduced by 0.5, Figure 5 portrays the variation of $\eta_{FP}^{-1} = \eta_{oz}^{-1}$ with $E(O_2)$. The two examples drawn from Becker's data relate to the SED developed in a single discharge tube, U.R.1, at two values of V_{ca} of 500 Hz., and to a range of $v = \nu n$ in which w was constant at each value of V_{ca}. The other example is drawn from Manley's (*65*) data for a single discharge tube, TX 22, in which a variant of the SED, now denoted by SED-S, was developed, no dielectric layer separating one of the electrodes from the gas; V_{ca} of 60 Hz. was *ca.* 16 kv. and n was larger than in Becker's experiments by a factor of *ca.* 1.6. For convenience Manley's results are shown in terms of $2\eta_{Xd;OO}^{-1}$.

It appears from Figure 5 that there is a difference in character between Becker's data and Manley's data, the latter are almost certainly the more precise; this may reflect the difference between the two kinds of discharge, SED and SED-S. Becker's data conform closely with a linear dependence on $E(O_2)$ but for Manley's data this holds only for $E(O_2) < 0.7$ e.v. $m(O_2)^{-1}$. From other data cited below it is evident that such a divergence from linearity is not exceptional but the significance of this has not been discerned. Other examples are to be found in Becker's data which support his conclusion that, even for a single type

Publication Date: June 1, 1969 | doi: 10.1021/ba-1969-0080.ch037

In Chemical Reactions in Electrical Discharges; Blaustein, B.;
Advances in Chemistry; American Chemical Society: Washington, DC, 1969.

of discharge, the factor b in Formula 31 increases as w/τ_d is increased. The extrapolations to $E(O_2) = 0$ lead to not very dissimilar values for $(\eta_{Xd;OO}^{-1})_o$: 18.5 (Manley) and 19 and 20 (Becker) e.v. $m(O_2$ diss.$)^{-1}$. Much more extensive data would be necessary to decide whether these small differences exceed the uncertainties in the measurements.

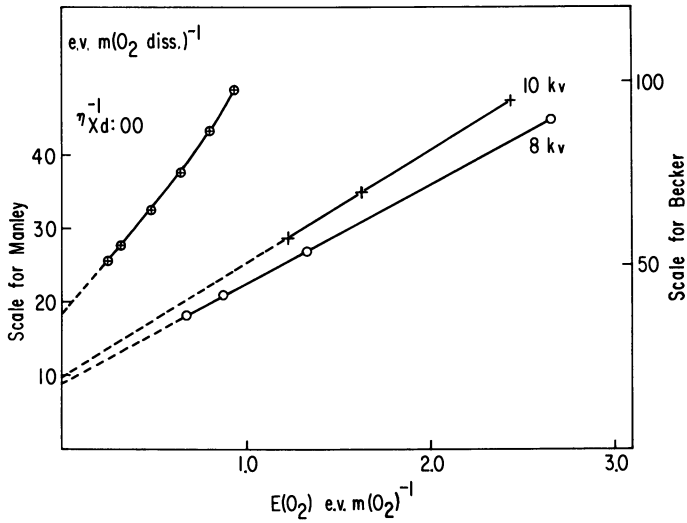

Figure 5. Rate coefficients $\eta_{Xd;OO}^{-1}$ for the dissociation of oxygen

⊕: Manley's data as $2\eta_{Xd;OO}^{-1}$ for SED-S, 60 Hz., n = 3.9 × 10^{19}
○, +: Becker's data for SED, 500 Hz., n = 2.5 × 10^{19} m(O_2) cm.$^{-3}$

The second main part of Becker's analysis deals with the dependence of f_{FP}, the fractional concentration of the final product, on $E(X)$ and with the limiting value $(f_{FP})_\infty$ which is attained, at least for some chemical systems, as ν is progressively decreased towards zero, that is in stationary gas. The restatement of his empirical formulae in the notation used here reads

$$(f_{FP})_\infty = E(X)/(\eta_{FP}^{-1} - (\eta_{FP}^{-1})_o) \tag{32}$$

and

$$f_{FP} = E(X)/[(\eta_{FP}^{-1})_o + bE(X)] \tag{33}$$

from which latter it follows that as $E(X)$ is indefinitely increased ($\nu \to 0$, $w \neq 0$), the predicted limiting value is

$$(f_{FP})_\infty = 1/b. \tag{34}$$

Publication Date: June 1, 1969 | doi: 10.1021/ba-1969-0080.ch037

In Chemical Reactions in Electrical Discharges; Blaustein, B.;
Advances in Chemistry; American Chemical Society: Washington, DC, 1969.

This last result is somewhat surprising but is consistent with the requirement already noted that b is dimensionless; it presents another aspect of Becker's analysis that invites further investigation. Although the general validity of Formula 33 appears not to have been examined, it is illuminating to compare Manley's experimental values for f_{oz} with the predicted values. His data in the preceeding diagram on extrapolation to $E(O_2) = 0$ lead to $(\eta_{oz}^{-1})_o = 9.25$ e.v. $m(O_3)^{-1}$; using his three lowest values for η_{oz}^{-1} $(= 0.5\ \eta_{Xd;OO}^{-1})$, it is found from Formula 32 that $(f_{FP})_\infty = 0.07_0$. The values then found for f_{oz} from Formula 33 are shown by the lower smooth curve in Figure 6 and may be seen to be in close accord with the values derived from experiment. It is interesting to compare this conformity with experiment with that afforded by the earlier analysis of Warburg (*95*) for stationary gas.

Warburg's Formula for f_{FP} in Stationary Gas. Warburg (*95*) was interested in the relation between f_{FP} and $B_{ca;FP}$, the rate coefficient with respect to charge transport $(i_{uc}\Delta t)$ for the total amount of reaction effected by a discharge in stationary gas enclosed within a volume τ. The formula which he developed in 1900 can be restated as

$$f_{FP} = (f_{FP})_\infty\ (1 - e^{-\lambda\tau\Delta t}), \tag{35}$$

where

$$\lambda' = i_{uc}(B_{ca;FP})_o/n(f_{FP})_\infty, \tag{36}$$

in which $(B_{ca;FP})_o$ denotes the initial value of $B_{ca;FP}$ found by extrapolation to $\Delta t = 0$ and hence corresponding to $f_{FP} = 0$. Warburg found that Formula 35 predicted satisfactorily the values found from experiment for f_{FP} at successively larger values of Δt in an investigation on the formation of ozone from oxygen by point-to-plane discharges. Other cases are cited in his review of 1909 (*97*).

It can now be seen that by invoking V_{ca}, the cathode-to-anode voltage, we may write

$$\begin{aligned}\lambda' &= (i_{uc}V_{ca}/\tau n) \cdot (B_{ca;FP})_o/V_{ca} \cdot (f_{FP})_\infty^{-1} \\ &= (w/\tau n) \cdot (\eta_{FP})_o/(f_{FP})_\infty\end{aligned}$$

Hence, by writing

$$\lambda = (\eta_{FP})_o/(f_{FP})_\infty$$

and recalling Formula 30.2 for $E(X)$ for stationary gas, Warburg's relation between f_{FP} and the duration of the discharge can be restated in the form

$$f_{FP} = (f_{FP})_\infty\ (1 - e^{-\lambda E(X)}) \tag{38}$$

which is convenient for comparison with Becker's Formula 33.

Using the values previously derived from Manley's data, $(\eta_{oz})_o = 0.108\ m(O_3)$ e.v.$^{-1}$ and $(f_{oz})_\infty = 0.070$, $\lambda = 1.54\ m(O_3)$ e.v.$^{-1}$ so that the

Publication Date: June 1, 1969 | doi: 10.1021/ba-1969-0080.ch037

In Chemical Reactions in Electrical Discharges; Blaustein, B.;
Advances in Chemistry; American Chemical Society: Washington, DC, 1969.

exponent in Formula 38 is dimensionless. The resulting values for f_{oz} in the range of $E(O_2)$ to which Manley's measurements relate are shown by the upper curve in Figure 6; for the range $0.25 < E(O_2) < 1.0$ e.v. $m(O_2)^{-1}$ they are larger by a factor of about 1.2 than the values predicted by Becker's formula for streaming gas.

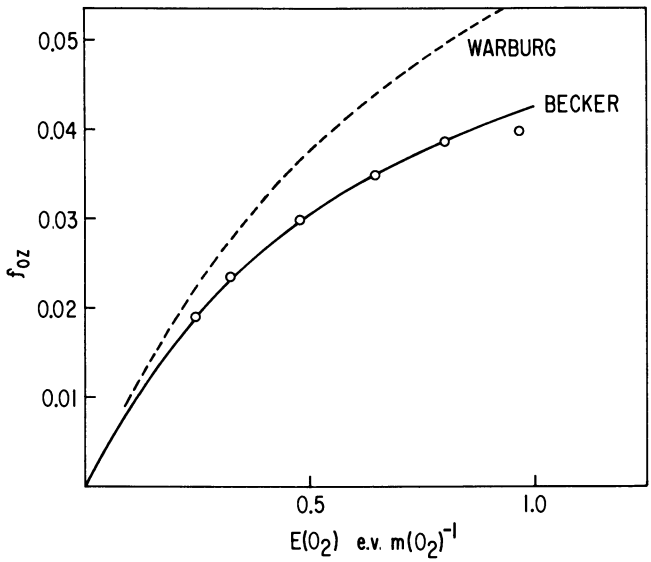

Figure 6. The fractional concentration of ozone, f_{oz}, associated with Manley's data in Figure 5 and computed from the formulae of Becker for streaming gas and of Warburg for stationary gas

The similarity in trend of the two sets of predicted values is remarkable. The discrepancy by a factor of *ca.* 1.2 may be connected with Warburg's analysis for stationary gas being applied to data for streaming gas. His later analysis for streaming gas (*97*) may provide an explanation, but the exploration of the validity of that analysis is inconclusive because it was based on the experimental data of Warburg and Leithhäuser (*98*) for ozone generation in the SED energized by 50 Hz. a.c.; in those experiments the measurements of i_{uc} and w are suspect. (*cf.*—*e.g.*, References 21, 54, and 56).

Alternatively, these results may be construed to signify that by introducing an arbitrary numerical factor, in this case *ca.* 0.8, Warburg's formula of 1900 for stationary gas satisfactorily predicts values for f_{FP} in streaming gas. If this were the correct inference an explanation would

Publication Date: June 1, 1969 | doi: 10.1021/ba-1969-0080.ch037

appear to be at hand for the results reported by Erjemin, Kobosev, and Wassiljew in 1936 (*26, 27*) for a number of reactions in streaming gas; for these conditions a formula similar to that of Warburg (Formula 35) was developed and may be restated as

$$f_{FP} = (k_o/k)(1 - e^{-k\tau_d/\nu}). \quad (39)$$

In this formula k_0 is a constant, k is a rate coefficient for the decomposition of the final product by the discharge such that the rate of the process is specified by knf_{FP} but otherwise undefined; k_0/k was identified with $(f_{FP})_\infty$, the limiting fractional concentration of the final product for $\nu = 0$. It was shown for several reactions that the dependence of f_{FP} on ν^{-1}, the inverse of the streaming velocity, could be accounted for in terms of Equation 39 by appropriate choice of k and k_0. This result would not be surprising if w were constant in each range of ν concerned because when there are no restrictions on the values selected for k and k_0, Equation 39 is indistinguishable from Warburg's (Formula 35) when modified by an arbitrary factor. No more detailed examination can be made because information is lacking about the kinds of discharge concerned and the associated values of i_{uc} and w.

Erjemin and his collaborators dismissed Warburg's analysis because it involves a rate coefficient with respect to charge transport; it appears, however, that k may be regarded as an average over the whole discharge region of $\alpha_{FP,d}n_e$ for final product decomposition. These investigators also dismissed Becker's formula for f_{FP} because of its empirical nature but they later used $n_X E(X) = w/\nu$ as a co-ordinating parameter in discussing some data of Peters and Wagner (72) apparently without having recognized that this parameter had been invoked by Becker.

The Physical Significance of Becker's Analysis. Before considering the consequences of applying this analysis to data for other discharge reactions, it is pertinent to consider what can be said about the physical significance of the quantities concerned: $E(X)$, $(\eta_{FP}^{-1})_0$, and $1/b = (f_{FP})_\infty$ which appears to provide a link between the phenomena in stationary and in streaming gas. On that point it can be said that no investigation has been traced for any type of discharge and for a particular chemical reaction which provides data for these two sets of conditions; that data appear to be lacking that would facilitate a comparison between the value found for $(f_{FP})_\infty$ from Formula 32 for a range of values of $\nu > 0$, and the value found for the stationary state in non-streaming gas for the same set of discharge parameters.

The general formula for $E(X)$ (Formula 30), may be written

$$(\tau/\tau_d)E(X) = w/(n_x\tau_d)\Delta t \quad \text{e.v. } m(X)^{-1}$$

Publication Date: June 1, 1969 | doi: 10.1021/ba-1969-0080.ch037

In Chemical Reactions in Electrical Discharges; Blaustein, B.;
Advances in Chemistry; American Chemical Society: Washington, DC, 1969.

the term $w/(n_X\tau_d)$ e.v. $m(X)^{-1}$ sec.$^{-1}$ specifies the average rate at which energy is absorbed to maintain the discharge per unit volume of the discharge zone and per molecule of the parent species, X, which is admitted to that zone, or exposed to the action of the discharge. For uniform-field discharges within a cylindrical envelope this rate is $Wn_e \cdot (\text{Ж}/n_D)$ e.v. $m(D)^{-1}$ sec.$^{-1}$, the product of the current density, $j_e = Wn_e$, and the Townsend parameter now written as $(\text{Ж}/n_D)$, the suffix recalling that it relates to the various species D present in the discharge not all of which are unchanged molecules of the parent species. By introducing a dimensionless factor u_d we may therefore make the identification

$$(\tau/\tau_d)E(X) = u_d \cdot Wn_e(\text{Ж}/n_D)\Delta t \qquad (40)$$

where, as before, $\Delta t = \tau_d/v$ for streaming gas; u_d takes into account such considerations as the difference between the species X and D, and the difference between the values of n_X and n_D that are associated with the heating of the gas and its streaming velocity; it must also take into account the fact that a particular value of $W\text{Ж}n_e/n_D$, and hence of $E(X)$, may be attained, in principle, by a wide range of pairs of values for Wn_e and for $\text{Ж}/n_D$. It has been seen that for a given reaction effected by a uniform-field discharge, η_{FP} may be expected to depend only on $\text{Ж}/n_D$; consequently on this account it is likely that u_d is specific to a particular set of discharge parameters.

If this identification of a physical significance for $E(X)$ is accepted, there are two principal corrolaries. Firstly, $E(X)$ may be expected to be a useful co-ordinating parameter for all discharges for which the total observed chemical change is mainly attributable to those zones of the discharge that approximate more or less closely to a uniform-field region. Secondly, there are zones of marked chemical activity, such as the *NG*, for which the Townsend parameter largely ceases to be a useful concept; thus, for example, if for a cold-cathode glow discharge, nz_{ca} is restricted so that there is no development of a *FDS* and *PC*, it may be that $E(X)$ fails to correlate the reaction rate coefficients in stationary and in streaming gas. No data have been traced, however, that would illuminate this possibility.

Concerning the dimensionless factor $b = d\eta_{FP}^{-1}/d[E(X)]$ in Formula 31, it can be seen that the analytical form for $E(X)$ given in Formula 40 is too nebulous to be tractable; and for *PC* reaction in streaming gas data are lacking for the dependence of b on $\text{Ж}/n_D$. Becker found, using the SED at 500 Hz. and oxygen at atmospheric pressure, that, for a particular discharge tube, b increases with V_{ca}, the potential across the electrodes (*cf.* Figure 5). If this form of the discharge has characteristics similar to those of the *PC* of a d.c. cold-cathode glow discharge as has been suspected (*cf.* Reference 56), it would be expected

Publication Date: June 1, 1969 | doi: 10.1021/ba-1969-0080.ch037

In Chemical Reactions in Electrical Discharges; Blaustein, B.;
Advances in Chemistry; American Chemical Society: Washington, DC, 1969.

that $\mathbb{X}/n_D$ decreases as V_{ca} is increased; Formula 40 then leads to the expectation that, at a given value of $E(X)$, η_{FP}^{-1} increases with V_{ca} which is conformity with the data of Becker. No explanation has been found for the indication from Formula 34 that $1/b$ should be identified with the limiting value of f_{FP} associated with zero streaming velocity.

To Becker, thinking in terms of streaming gas, it seemed axiomatic that $a = (\eta_{FP}^{-1})_o$ in his Formula 31, which is obtained by extrapolation of experimental data to $E(X) = 0$, should be identified with the inverse of the maximal attainable value for η_{FP} for any particular reaction and kind of discharge. But the following considerations cast doubt on the validity of this simple extrapolation.

For a particular discharge and value of V_{ca}, it is plausible to infer that the discharge parameters remain constant provided that the linear streaming velocity is significantly less than the mean molecular velocity in the discharge zone; for Becker's data shown in Figure 5 the consequence of this consideration would be that the extrapolation may be valid down to $E(X) = ca.$ 0.01 e.v. $m(O_2)^{-1}$ and at this point the difference between η_{oz}^{-1} and the extrapolated value for $E(X) = 0$ would be unimportantly small. According to Formula 30.2, small values of $E(X)$ may be attained in stationary gas by selecting appropriately small values of Δt, the period for which the discharge is maintained; it is therefore pertinent to consider the indications from experiment for stationary gas in relation to small values of $E(X)$ and the associated values of η_{FP}^{-1} although these experiments were not designed to this end.

The design of experiment in stationary gas to derive rate coefficients for *PC* reaction in a cold-cathode glow discharge has involved the selection of two, and preferably of at least three, values of $\tau_d < \tau$ which can be written $\tau_{d,o}$, $\tau_{d,o} + \Delta\tau_d$, and $\tau_{d,o} + 2\Delta\tau_d$; for a discharge having a movable anode there are then corresponding values for the electrode spacing, $z_{ca,o}$, $z_{ca,o} + \Delta z$, and $z_{ca,o} + 2\Delta z$. For the range of n_X investigated $n_X z_{ca,o}$ is such that there is some development of the *PC*. The increments $\Delta\tau_d$ and $2\Delta\tau_d$ then correspond to extensions of the *PC*. For experiments of this kind, first devised by Kirkby (*46*), values for $E(X)$ associated with an increment $\Delta\tau_d$ may be derived from Formula 30.2 in the alternative form

$$E(X) = i_{uc}\Delta V_{ca}/(\tau n_X) \cdot \Delta t \qquad (41)$$

where ΔV_{ca} denotes the corresponding increment in the cathode-to-anode voltage. In many such investigations Δt was not recorded but in some cases it can be inferred from the text.

In Kirkby's (*46*) experiments on the formation of water (wa) from electrolytic gas there are six values of n_X for which observations were

Publication Date: June 1, 1969 | doi: 10.1021/ba-1969-0080.ch037

In Chemical Reactions in Electrical Discharges; Blaustein, B.;
Advances in Chemistry; American Chemical Society: Washington, DC, 1969.

made for the increments $\Delta\tau_d$ and $2\Delta\tau_d$. Δt was restricted, from 5 to 12 sec., and from Kirkby's account it is plausible to associate a value $\Delta t = 5$ to 6 sec. with $2\Delta\tau_d$ and $\Delta t = 10$ to 12 sec. with the smaller increment. It then appears that for each pair of values of n_X and $\mathbb{X}/n_D$, the data relate to a single value of $E(X)$ which can be approximately estimated. For the range $5 \times 10^{-16} < \mathbb{X}/n_D < 12 \times 10^{-16}$ volt cm.^{2} the estimated range of $E(X)$ is 0.35 to 0.2 e.v. $m(X)^{-1}$. The demonstration by Kirkby that P_{wa}/n, and hence η_{wa}, are functions of $\mathbb{X}/n_D$ carries the implication that the values found for these rate coefficients are independent of the values selected for Δt in the experiment—*cf.* the account given earlier in this paper. Kirkby's data relate only to the positive column while those of Becker and of Manley (Figure 5) relate to the whole of the region in which a discharge is maintained. That is, at each value of $\mathbb{X}/n_D$ the inference is that η_{wa}^{-1} remains constant for a range of $E(X)$ extending down from the value estimated for the experiments to a value corresponding to $\Delta t = ca.$ 1 msec.

One group of experiments of Brewer and Westhaver (*6*) on the formation of ozone (oz) from oxygen using a single increment $\Delta\tau_d$ (their Curve 1, Figure 3) lead to the constant value $\eta_{oz}^{-1} = 12$ e.v. $m(O_3)^{-1}$ for the range $0.05 < E(X)/\Delta t < 0.25$ e.v. $m(O_2)^{-1}$ sec.$^{-1}$ for $n_X = 3.5 \times 10^{16}$ $m(O_2)$ cm.$^{-3}$. From the procedure used to derive the values of η_{oz} it is plausible to infer that they should be associated with $\Delta t = ca.$ 6 sec. The estimated range in which η_{oz}^{-1} was constant is then *ca.* $0.3 < E(O_2) < 1.5$ e.v. $m(O_2)^{-1}$. This is a range that overlaps that in Figure 5 in which η_{oz}^{-1} increases with $E(O_2)$. Another aspect of these data for stationary gas is that $\eta_{oz}^{-1} = 12$ e.v. $m(O_3)^{-1}$ and the slightly lower value found in closely similar experiments by Lunt, Mahon-Smith, and Tuffy (*60*), 9.0 ± 0.9 e.v. $m(O_3)^{-1}$, show that the values found for $(\eta_{oz}^{-1})_0$ by extrapolating the experimental data for streaming gas to $E(O_2) = 0$ are realizable, at least in other experimental conditions.

Westhaver's (*99*) experiments on the decomposition of ammonia (am) in the *PC* relate to a single increment $\Delta\tau_d$, $n_X = 28.4 \times 10^{16}$ $m(NH_3)$ cm.$^{-3}$, to $\mathbb{X}/n_D = 1.5_4 \times 10^{-16}$ volts cm.^{2}, and to a tenfold range of *w;* they lead to the constant value $\eta_{am:dcp}^{-1} = 100$ e.v. $m(NH_3$ dcp.$)^{-1}$ for the range $0.01 < E(NH_3)/\Delta t < 0.10$ e.v. $m(NH_3)^{-1}$ sec.$^{-1}$. From the statement that the experimental procedure was the same as that in earlier investigations of the series—*e.g.*, Brewer and Westhaver (*5*)—the least value of Δt appears to be 30 sec. This leads to a lower limit for the range in which $\eta_{am:dcp}^{-1}$ was found to be constant: $0.3 < E(NH_3) < 3.0$ e.v. $m(NH_3)^{-1}$.

Because values for Δt are cited, more definite information is provided by the investigation of Kutszegi (*51*) on the decomposition of carbon

Publication Date: June 1, 1969 | doi: 10.1021/ba-1969-0080.ch037

dioxide (cdx) to carbon monoxide and oxygen by *PC* reaction for single values of the current and of the increment $\Delta\tau_d$. The data are summarized in the following table.

Table III. Ranges of $E(CO_2)$ Associated with Constant Values for $\eta_{cdx;dcp}^{-1}$; the Decomposition of CO_2 by *PC* Reaction

$n_X \times 10^{-16}$ $m(CO_2)$ $cm.^{-3}$	$\mathcal{E}/n_D \times 10^{16}$ *volt* $cm.^2$	$\eta_{cdx;dcp}^{-1}$ *e.v.* $m(CO_2\ dcp)^{-1}$	*Ranges of* Δt *and of* $E(CO_2)$ *in which* $\eta_{cdx;dcp}^{-1}$ *was Constant*	
			Δt *sec.*	$E(CO_2)$ *e.v.* $m(CO_2)^{-1}$
10.9	3.17	$76._8$	2 to 18	0.06 to 0.52
4.35	5.25	$61._6$	1 to 16	0.10 to 1.5
1.10	9.20	$51._5$	2 to 5	0.33 to 0.83

These ranges of $E(CO_2)$ are comparable with those estimated above for the formation of water and of ozone and for the decomposition of ammonia.

It is evident that further experimental investigation is needed to trace the connection between the rate coefficients and $E(X)$ for stationary and for streaming gas. The slight balance of evidence is that, at least for some reactions and when $\mathcal{E}/n_D$ is constant, as $E(X)$ is progressively decreased a range is reached in which η_{FP}^{-1} ceases to diminish and becomes constant. Caution is therefore necessary in regarding values found for $(\eta_{FP}^{-1})_0$ as an index of the maximum attainable value of η_{FP} for a particular set of discharge parameters.

Some Related Investigations. The contribution of Erjemin, Kobosev, and Vasil'ev (*28*) is an elaboration of their analysis already noted (*26, 27*). Poole (*74*) developed a variant of Becker's formula (Formula 31) which is equivalent to replacing the empirical factors a and b by $(\eta_{FP}^{-1})_0 \cdot (1 + c/\nu)$ and $v_X(d/\nu - e)$, respectively, where c, d, and e are empirical factors; η_{FP}^{-1} then appears as a function of w, the power absorbed. In Becker's interpretation of the extrapolation to $E(X) = 0$ no allowance is made for the loss of species involved in the reactions leading to the final product. Poole was concerned to derive rate coefficients for these loss processes, and noted imperfections in the analysis of Steiner (*83, 84*); on that basis he evolved a more elaborate interpretation for the values found for $(\eta_{FP}^{-1})_0$ corresponding to extrapolation to $w = 0$ in place of extrapolation to $E(X) = 0$ envisaged as associated with indefinitely large values of ν in Becker's analysis. It is doubtful, however, whether this replacement carries much advantage, except possibly as an empirical procedure, because extrapolation to $w = 0$ may have no physi-

Publication Date: June 1, 1969 | doi: 10.1021/ba-1969-0080.ch037

In Chemical Reactions in Electrical Discharges; Blaustein, B.;
Advances in Chemistry; American Chemical Society: Washington, DC, 1969.

cal counterpart: for the kind of discharge studied by Poole, progressive decrease in the current density, and hence of w, leads eventually to a transition to another form of the discharge, the 'sub-normal' glow discharge. Deckers and his collaborators (*17, 18, 19*) investigated the generation of radiative species in relation to the discharge parameters for a gas streamed through the *PC* of a glow discharge. And Kobosev, Filanova, Nekrasov, and Skorokhodov (*47*) in discussing the conversion of ammonia to hydrazine refer to a quantity 'proportional to' w/ν as a useful parameter. None of these investigations trace the coherence between the several approaches to the kinetics of reaction in streaming gas and their connection with the data for stationary gas, nor do they refer to the earlier contributions of Warburg and Becker.

It has been noticed earlier in this paper that, for streaming gas, Formula 31 is likely to remain applicable when the rate coefficients derived from experiment relate to a single set of discharge parameters, for example when n_X and w or $\mathfrak{X}/n_D$ are maintained constant and ν is varied; if n_X is varied when ν and w are constant, it is to be expected that $\mathfrak{X}/n_D$ may vary. For the converse case when the streaming velocity is constant and w is varied for a single kind of discharge, the evidence on the validity of Formula 31 is inconclusive. From Elliott's data (*21*) for the dissociation of hydrogen and from those of Peters and Küsten (*70*) for the synthesis of hydrogen cyanide from methane and nitrogen, it is readily shown that the inverse rate coefficient decreases rapidly as $E(X)$ is progressively increased, ν and n_X being constant; on the other hand Poole, using the variant of Formula 31 already mentioned, found $\nu n_X \cdot E(X) = w$ to be a convenient co-ordinating parameter for values of $\eta_{Xd;HH}^{-1}$ relating to a range of n_X and to a series of values of ν at each of which w was varied.

For a number of other reactions in stationary and in streaming gas it has been found that the data for η_{Xd}^{-1} and η_{FP}^{-1} appear to be functions of the same character as is illustrated in Figure 5 (*57*). The reactions for which the data have been examined include the following syntheses: hydrazine from ammonia (*47, 49, 79, 82*); acetylene from methane (*71*); sulfur trioxide from sulfur dioxide and oxygen (*81*); acetylene and methane from carbon monoxide and hydrogen (*4*). Kobosev *et al.* gave a diagram of their results which shows that η_{FP}^{-1} passes through a minimum as w/ν is progressively increased, but no details are given of the experimental observations. Apart from that result, the data in all these investigations are consistent with those shown in Figures 5 to 8 in that small values of η_{Xd}^{-1} and of η_{FP}^{-1} are associated with values of $E(X) \gtrsim 20$ e.v. $m(X)^{-1}$.

The examples mentioned below have been selected to illustrate the range of experimental data for which the Becker parameter serves to co-

Publication Date: June 1, 1969 | doi: 10.1021/ba-1969-0080.ch037

ordinate rate coefficients such as η_{Xd} and η_{FP} and to draw attention to some results the significance of which is obscure.

The Dissociation of Hydrogen to Atoms. The four groups of experimental data shown in Figures 7 and 8 relate to streaming gas and to values of $\eta_{Xd;HH}^{-1}$ given by $2\eta_H^{-1}$ for the observed generation of atoms as measured in the gas leaving the discharge zone; that is, the values shown do not take into account either the fact that the average value of f_H in the discharge zone is less than unity, or the loss of atoms occurring before the gas reaches the sampling point. With the exception of Poole's data, the observations relate to a range of ν and to constant values of w and n_X.

Elliott's data (*21*), shown for convenience as 0.01 $\eta_{Xd;HH}^{-1}$, relate to the SED maintained by 400 Hz a.c. and to $n_X = 1.40 \times 10^{18}$ $m(H_2)$ cm.$^{-3}$; at this concentration it is to be expected that a large fraction of the atoms generated are lost by homogeneous recombination and that, consequently, the value found by extrapolation to $E(H_2) = 0$ may be relatively large, $(\eta_{Xd;HH}^{-1})_0 = 6000$ e.v. $m(H_2$ diss.$)^{-1}$.

Bak and Rastrup-Anderson (*1*) used a mixture (0.96_5 H_2 + 0.03_5 H_2O), $n_X = 1.0 \times 10^{16}$ $m(X)$ cm.$^{-3}$ and an a.c. frequency now estimated to be *ca.* 3 GHz. $w_r = w/\tau_d = 1.4 \times 10^{19}$ e.v. cm.$^{-3}$ sec.$^{-1}$; and $\bar{f}_X$, the average fractional concentration of hydrogen in the discharge zone, varied from *ca.* 0.6_5 to 0.5_5 as $E(X)$ was increased. $\eta_{Xd;HH}^{-1}$ is seen to vary linearly with $E(X)$ and extrapolation to $E(X) = 0$ leads to $(\eta_{Xd.HH}^{-1})_0 = 82$ e.v. $m(H_2$ diss.$)^{-1}$.

Shaw (*80*) used a similar discharge in hydrogen at 3.0 GHz, $n_X = 1.7 \times 10^{16}$ $m(H_2)$ cm.$^{-3}$, and $w_r = 2.5 \times 10^{20}$ e.v. cm.$^{-3}$ sec.$^{-1}$; only two values are cited for ν for which $\bar{f}_X = 0.8$ associated with the lower resulting value for $E(H_2)$ and for the other $\bar{f}_X = 0.5$. If the validity of Formula 31 is assumed, extrapolation to $E(H_2) = 0$ leads to $(\eta_{Xd;HH}^{-1})_0 = 30.5$ e.v. $m(H_2$ diss.$)^{-1}$; that is almost twice the value cited by Shaw, 15.4 e.v. $m(H_2$ diss.$)^{-1}$, and derived by him from experiment by a procedure which is not described in detail.

These last two groups of observations appear to relate to comparable experimental conditions: in Shaw's experiments n_X and w_r were larger by factors of 1.7 and 10.8, respectively. These are circumstances for which it is plausible to infer that the value of $\bar{E}$ was the lower in Shaw's experiments. If that inference were not much in error, the much larger value now found for $(\eta_{Xd;HH}^{-1})_0$ from the data of Bak and Rastrup-Andersen may be explicable in terms of the early analysis of Lunt and Meek (*61*): it may be that the selection of relatively low values of n_X and w_r conduced to the attainment of a value of $\bar{E}$ considerably larger than that for which $\eta_{Xd;HH}$ passes through a maximum for the particular variants of $f(E)$ concerned.

In Chemical Reactions in Electrical Discharges; Blaustein, B.;
Advances in Chemistry; American Chemical Society: Washington, DC, 1969.

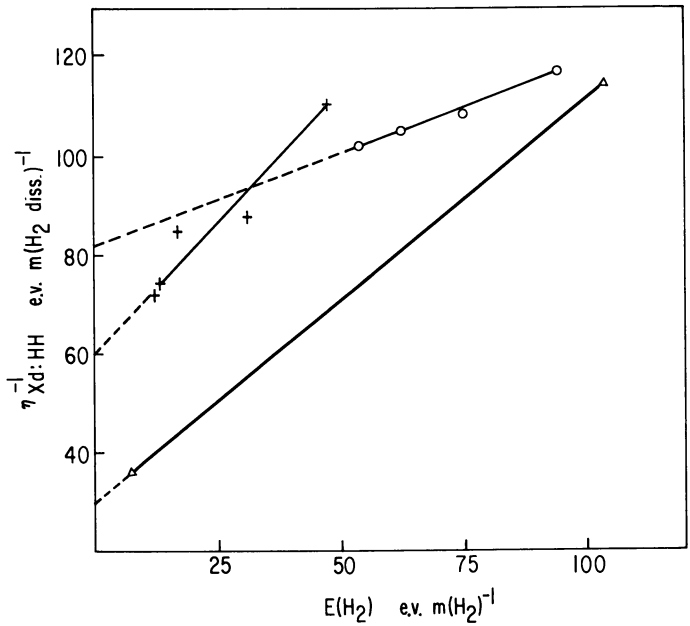

Figure 7. $\eta_{Xd:HH}^{-1}$ *for the dissociation of hydrogen*
+: *Elliott* × *0.01* (21)
○: *Bak and Rastrup-Andersen* (1)
△: *Shaw* (80)

The lack of any record of the spectrum of the discharge in these two investigations provides a further example of an impediment to the interpretation of the data for reaction.

The value of $\bar{f}_X$ prescribes the fraction of electron energy that is expended in collisions with hydrogen molecules, the remainder being absorbed mainly by hydrogen atoms. The values cited above are averages of the value where the gas stream enters the discharge zone, $f_X = 1$, and the value at the sampling point; they are thus no more than crude approximations to the true values. For the experiments in very high frequency discharges $\bar{f}_X$ is thus estimated to lie between 0.5 and 0.8. On that account it is not surprising that the values found for $\eta_{Xd:HH}^{-1}$ are considerably larger than the corresponding rate coefficients for the dissociation of oxygen, $\eta_{Xd:OO}^{-1}$, shown in Figure 5; it may be seen from Figure 6 that these latter are associated with values of $\bar{f}_X = 0.5\ (2 - \bar{f}_{0_2})$ lying in the range 0.98 to 0.99.

For the lowest cited value of $E(X)$ in Shaw's experiments, $\eta_{Xd:HH}^{-1}$ $= 0.027_6\ m(H_2\ \text{diss.})$ e.v.$^{-1}$ and $\bar{f}_X = 0.8$. Taking 9 e.v. as a conservative

Publication Date: June 1, 1969 | doi: 10.1021/ba-1969-0080.ch037

estimate for the average electron energy loss per parent molecule dissociated, for the mixture of atoms and molecules it follows that $F_{Xd:HH} = 0.25$ and would be about 0.3 if referred to the hydrogen content of the gas in the discharge zone. This fractional electron energy loss for a discharge at 3 GHz is about half the maximum predicted for a Maxwellian electron energy distribution. (*See The Primary Reaction Rate Coefficient* α_{XK}.)

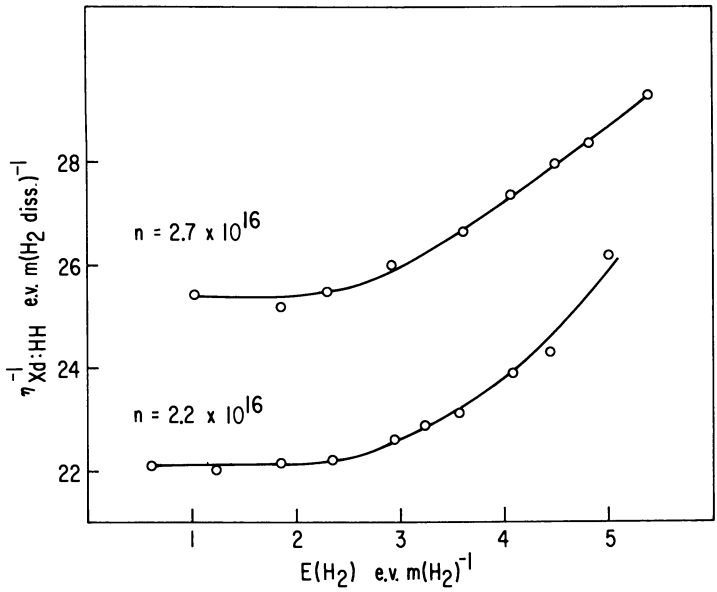

Figure 8. $\eta_{Xd:HH}^{-1}$ *for the dissociation of hydrogen (Ref. 74)*

The experiments of Poole (*74*) relate to hydrogen streamed through a striated *PC* of a cold-cathode glow discharge at a series of values of n_X in the range (1.5 to 4.8) $\times 10^{16}$ $m(H_2)$ cm.$^{-3}$. At each value of n_X a range of ν was explored; for each of the corresponding values of $v_X = \nu n_X$ data are recorded for $\eta_{Xd:HH}^{-1}$ in a range of w, the power absorbed in the *PC*. Poole analyzed these data for rate coefficients considered as functions of w, and he regarded the variant of Formula 31 already described as providing, to an acceptable approximation, a general but empirical statement; the discovery that, for a constant value of n_X, the values found by extrapolation to $w = 0$ varied markedly with ν led to an elaborate investigation of the loss processes. Restatement of the data in terms of $E(H_2) = w/v_X$ does not change the character of the variation of $\eta_{Xd:HH}^{-1}$. Two examples are shown in Figure 8; these relate to $n_X = (2.20 \text{ and } 2.66) \times 10^{16}$ $m(H_2)$ cm.$^{-3}$ and, respectively, to $\nu = (4.45 \text{ and } 3.14) \times 10^3$ cm.^{3}

In Chemical Reactions in Electrical Discharges; Blaustein, B.;
Advances in Chemistry; American Chemical Society: Washington, DC, 1969.

sec.$^{-1}$. The data in Figure 8 illustrate that when w is the only quantity varied, the inverse rate coefficient may vary with $E(X)$ in a way somewhat similar to that seen in Figures 5 and 7. These two examples suggest that $\eta_{Xd;HH}^{-1}$ may be constant in a low range of $E(H_2)$; this would be in accord with the indications for reaction in stationary gas. Whilst the data in Figure 8 are only a small fraction of the whole, they also suggest that the validity of the variant of Becker's formula used by Poole should be re-examined.

If an approximate allowance is made for $\bar{f}_X$ as in discussing the data of Shaw, it is found that $\eta_{Xd;HH}^{-1} = 21.4 \pm 0.4$ e.v. $m(H_2$ diss.$)^{-1}$ for $0.6 < E(H_2) < 4.5$ for the lower value of n_X, and for the higher value of n_x is 24.8 ± 0.6; this is a considerably longer range of $E(H_2)$ than those in Figure 8 for which the inverse rate coefficient appears to be constant. The corresponding values found for $\eta_{Xd;HH}$ are 0.046_8 and 0.040_3 $m(H_2$ diss.$)$ e.v.$^{-1}$; these are smaller by about 0.75 than the values derived by Poole from much more extensive data and after allowing for loss rates, respectively, 0.055_5 and 0.059_5 $m(H_2$ diss.$)$ e.v.$^{-1}$. (One of the referees has drawn attention to the propriety of comparing the predictions of theory (as in Table II for reaction in electrolytic gas) with the values found for $(\eta_{Xd;HH})_o$, by extrapolating to $E(H_2) = 0$, the data of Shaw in Figure 7 and those of Poole in Figure 8. For Poole's data the comparison is of uncertain significance because the experiments relate to a striated *PC*, which the referee has appreciated; but this was recognized by Lunt and Meek in 1936 (*61*) when discussing the matter on the basis of theoretically predicted values computed from Formula 2.1 when Q_{XK} was replaced by the values predicted from wave-mechanical theory by H. S. W. Massey for the principal components of what is here denoted by $Q_{Xd;HH}$. The corresponding comparison can be made using the values for $\alpha_{Xd;HH}$ which are based on Corrigan's experimental data for $Q_{Xd;HH}$ (*cf.* Table I) together with the published data for electron motion in hydrogen which have been mentioned in connection with Formulae 26 and 27. It happens that the resulting predicted values of $\eta_{Xd;HH}$ as $f(X/n)$ are not very different from those of 1936. The significance of the comparison with experiment remains obscure for Poole's data, and it is shadowed further by the uncertainties about the analyses of the experimental data preferred by Poole and later by Shaw; these uncertainties are mentioned above.)

From the point of view of the utilization of discharges to effect chemical change, it may be seen from Figure 8 that for $n_X = 2.2 \times 10^{16}$ $m(H_2)$ cm.$^{-3}$ and for $0.6 < E(H_2) < 2.5$ e.v. $m(H_2)^{-1}$, four determinations of the rate of dissociation lead to the mean value $\eta_{Xd;HH} = 0.045$ $m(H_2$ diss.$)$ e.v.$^{-1}$; it follows that $F_{Xd;HH}$ was not less than 0.40. This

Publication Date: June 1, 1969 | doi: 10.1021/ba-1969-0080.ch037

In Chemical Reactions in Electrical Discharges; Blaustein, B.;
Advances in Chemistry; American Chemical Society: Washington, DC, 1969.

appears to be the largest value derived directly from experiment for a fractional energy loss; consequently, it sets a scale for what may be achieved by the appropriate choice of discharge parameters in using discharges to generate a particular final product.

Some General Considerations Concerning the Utility of Discharges in Relation to the Reaction Rate Coefficients

The problems of the detailed interpretation of the kinetics of discharge reaction do not invalidate the more general and qualitative indications of theory for the selection of discharges to effect chemical synthesis or decomposition. The particular predictions of theory and the indications from experiment for uniform-field discharges concerning the existence of maxima for the rate coefficients P_{FP}/n and η_{FP} are likely to remain valid for a wide variety of discharges in which the negative zones occupy an unimportantly small part of the space in which the discharge is maintained. And the standard techniques for varying $\bar{E}$, the mean electron energy, may be invoked in experiment to identify the ranges of discharge parameters in which, for a specified reactant, either of these two rate coefficients passes through a maximum, circumstances conducive to attaining a large rate of reaction. An indication of the kind of transition involved in the primary reaction step (Reaction R1), may be gained in many cases from a consideration of the changes induced in the same reactant by photon absorption. Such information together with a knowledge of E_{XK}, the energy change involved, provides a guide to the range of $\bar{E}$, or of X/n, in which, for example, η_{FP} passes through its maximum value.

The rate coefficient for the generation of a final product with respect to the energy consumed in maintaining a discharge, η_{FP}, has long been used as a criterion to appraise the economic merit of a discharge reaction considered as the basis of an industrial application. For radiation sources a reaction of type R1 is selected such that the generated species, K, decays or is lost from the system, by conversion to some other species J by a process of the type

$$K \rightarrow J + h\nu_{KJ}; \qquad (R1.1)$$

a well established criterion is the maximum attainable value of η_{XK} or of $\eta_{KJ;h\nu}$ photons-(KJ) e.v.$^{-1}$. When the requirement is a new chemical species, exemplified by the large scale generation of ozone in streaming air or oxygen, the same criterion has been invoked, in this case η_{oz} $m(O_3)$ e.v.$^{-1}$ (*see* References 31, 38, 48, 56, and 75); but it happens that the exploration of the reaction kinetics has been pursued in relation to chemical change less exhaustively than for the generation of radiative species.

Publication Date: June 1, 1969 | doi: 10.1021/ba-1969-0080.ch037

In Chemical Reactions in Electrical Discharges; Blaustein, B.;
Advances in Chemistry; American Chemical Society: Washington, DC, 1969.

Consideration of reaction kinetics and related subjects germane to the industrial uses of discharges lies outside the scope of this paper (*see* Reference 32).

Reasons have been mentioned earlier for thinking that, for any single reaction of type R1, $(F_{XK})_{max}$ is unlikely to exceed 0.25 ± 0.1 when $f_X \simeq 1$. It is therefore pertinent to cite some of the empirical information from experiment that sustains that view, especially because estimates of $(\eta_{FP})_{max}$ can be derived from those for $(F_{XK})_{max}$.

For the generation of radiative species it is now assumed that the measured energy yield of photons KJ suffices to identify F_{XK}. What appears to be an exception has been described by Barnes and Thayer (2) for the generation of the species Hg 6^3P_1 in discharges through mercury vapor, values of F_{XK} up to 0.6 were attained. For the visible radiation from a *PC* in neon, which to a first approximation may be attributed to a single reaction, Uyterhoeven (89) cites as typical of what may be attained $F_{XK} = 0.14$; this relates to the measured parameters n $= 3.5 \times 10^{16}\ a(\text{Ne})$ cm.$^{-3}$, $\bar{X}/n = 0.33 \times 10^{-16}$ volt cm.^{2}, $\bar{E} = ca.$ 4 e.v., $j_{uc} = 2.26 \times 10^{17}$ uc cm.$^{-2}$ sec.$^{-1}$ and $n_e = 1.07 \times 10^{11}$ cm.$^{-3}$. From the experimental data for chemical change to which Figures 5, 7, and 8 relate, it has been seen that for the dissociative excitation of hydrogen and oxygen values of F_{Xd} in the range 0.25 have been attained. Only for Kirkby's *PC* reaction is there evidence that $F_{FP} = F_{wa}$ passes through a maximum considered as $f(\bar{X}/n)$; and if the reaction mechanism involving the dissociation of hydrogen is accepted, it is found that $(F_{Xd:HH})_{max}$ is about $0.4_0 \pm 0.0_5$. But in these cases of dissociative excitation more than one reaction of type R1 is involved (*see* References 56 and 58 for H_2); consequently, it is preferable to regard $(F_{FP})_{max} \approx 0.25$ as a more acceptable value for any single reaction of type R1.

The corresponding estimates for $(\eta_{FP})_{max}$ follow simply from Formulae 20 and 16. It is plausible to associate the maximum attainable value of η_{FP} with negligible loss of all species involved in the reaction mechanism other than in forming the specified final product; then $\Phi_{XK\ FP}$ becomes ϕ_s, the stoichiometric factor. For reactions of type R1 generating radiative species or dissociative species $\phi_s = 1$ in many cases; for the generation of ozone from oxygen $\phi_s = 2$. With these considerations in mind we can write

$$(F_{FP})_{max} \approx \phi_s (F_{XK})_{max}$$

and Formula 16 then leads to

$$(\eta_{FP})_{max} \approx (0.25 \pm 0.1)\phi_s / E_{XK} \quad m(\text{FP})\ \text{e.v.}^{-1} \qquad (16.1)$$

Publication Date: June 1, 1969 | doi: 10.1021/ba-1969-0080.ch037

In Chemical Reactions in Electrical Discharges; Blaustein, B.;
Advances in Chemistry; American Chemical Society: Washington, DC, 1969.

For the dissociative excitation of hydrogen and of oxygen the largest values attained in experiment of η_{Xd} are about 0.05 m(X diss.) e.v.$^{-1}$. For the cited reactions in neon and in mercury, E_{XK} = *ca.* 2 and 4.77 e.v., respectively; hence, the values of F_{XK} found from experiment lead to η_{XK} = *ca.* 0.07 a(Ne*) e.v.$^{-1}$ and to $\eta_{XK} = 0.12_5$ a(Hg 6^3P_1) e.v.$^{-1}$. For uniform-field Townsend discharges Lunt and Corrigan (58) found that, considered as a function of $\mathfrak{X}/n$, $\Sigma\eta_{XK}$ passes through a maximum when this quantity relates to the generation from the ground state of the following groups of radiative species in which all the values of E_{XK} lie in the range 11 to 13 e.v.: H_2, C $^1\Pi_u$ and B $^1\Sigma_u^+$; and N_2, C $^3\Pi_u$, $v = 0, 1, 2$. $(\Sigma\eta_{XK})_{max}$ was found to have the values, respectively, 0.028 $m(H_2^*)$ e.v.$^{-1}$ and 0.012 $m(N_2^*)$ e.v.$^{-1}$; with these values the quasi-empirical Formula 16.1 is in accordance.

The foregoing considerations suggest that, for reactions of type R1 leading to chemical change and for which E_{XK} lies in the range 5 to 10 e.v., the following alternative statements may have a wide validity:

$$\left.\begin{aligned} &(\eta_{FP})_{max} \approx (0.03 \pm 0.01)\phi_s \quad m(\text{FP}) \text{ e.v.}^{-1} \\ \text{and} \quad &(\eta_{Xd})_{max} \approx (0.03 \pm 0.01) \quad m(\text{X diss.}) \text{ e.v.}^{-1} \end{aligned}\right\} \quad (16.2)$$

These relations provide a criterion of the selection of the discharge in relation to any specified final product or dissociative excitation: thus, for example, if $\eta_{FP} < 0.003\ \phi_s\ m$ (FP) e.v.$^{-1}$, there is a strong indication that $\bar{E}$ and $f(E)$ for the particular discharge concerned are ill-chosen to effect the reaction to advantage.

Acknowledgments

It is a pleasure to record my indebtedness to many: to the referees for suggestions that have ensured greater clarity in the text; and for enlivening discussions to B. D. Blaustein, Sandborn Brown, S. J. B. Corrigan, K. G. Emeléus, H. A. v Engel, V. A. Hann, L. S. Harley, L. Herman, F. Kaufman, T. C. Manley, C. A. Meek, L. R. Megill, and to Sir Harrie Massey.

Literature Cited

(1) Bak, G., Rastrup-Andersen, J., *Acta Chem. Scand.* **16,** 111 (1962).
(2) Barnes, B. T., Thayer, R. S., *J. Opt. Soc. Am.* **29,** 131 (1939).
(3) Becker, H., *Wiss. Veröffentl. Siemens-Konzern* **1,** 76 (1920).
(4) Blaustein, B. D., Fu, Y. C., ADVAN. CHEM. SER. **80,** 259 (1969).
(5) Brewer, A. K., Westhaver, J. W., *J. Phys. Chem.* **34,** 153 (1930).
(6) *Ibid.*, **34,** 1280 (1930).

Publication Date: June 1, 1969 | doi: 10.1021/ba-1969-0080.ch037

(7) *Ibid.*, **34**, 2343 (1930).
(8) Brown, Sandborn C., "Introduction to Electrical Discharges in Gases," John Wiley & Sons, New York, 1966.
(9) Brown, Sandborn C., "Basic Data of Plasma Physics," M.I.T., Cambridge, Mass., 1966.
(10) Carleton, N. P., Megill, L. R., *Phys. Rev.* **126**, 82 (1962).
(11) Compton, A. H., Langmuir, I., *Rev. Mod. Phys.* **12**, 123 (1930).
(12) Clyne, M. A. A., Thrush, B. A., *Proc. Roy. Soc. A* **275**, 545 (1963).
(13) *Ibid.*, **275**, 559 (1963).
(14) Corrigan, S. J. B., *J. Chem. Phys.* **43**, 4381 (1965).
(15) Corrigan, S. J. B., private communication (1967).
(16) Corrigan, S. J. B., von Engel, H. A., *Proc. Roy. Soc. A* **245**, 335 (1958).
(17) Deckers, J. M., Bois d'Engien, P. A., *Can. J. Chem.* **42**, 1792 (1964).
(18) Deckers, J. M., Peeters, J. L., Rundle, H. W., *Can. J. Chem.* 44, 1981 (1966).
(19) Deckers, J. M., Gillespie, K. A., Rundle, H. W., Sova, R., Yealland, R. M., *Can. J. Chem.* 44, 2981 (1966).
(20) Druyvesteyn, J. M., Penning, F. M., *Rev. Mod. Phys.* **12**, 87 (1940).
(21) Elliott, G. A., *Trans. Faraday Soc.* **23**, 60 (1927).
(22) Emeléus, K. G., Beck, J. W., *Proc. Roy. Irish Acad.* **46A**, 49 (1940).
(23) Emeléus, K. G., Lunt, R., *Trans. Faraday Soc.* **32**, 1504 (1936).
(24) Emeléus, K. G., Lunt, R., Meek, C. A., *Proc. Roy. Soc. A* **156**, 394 (1936).
(25) Engelhardt, A. G., Phelps, A. V., *Phys. Rev.* **131**, 2115 (1963).
(26) Eremin, E. N., Kobosev, N. I., Wassiljew, S. S., *Acta Physicochim. USSR* **5**, 201 (1936).
(27) Eremin, E. N., Kobosev, N. I., Wassiljew, S. S., *Zhur. Fiz. Khim.* **7**, 619 (1936).
(28) Eremin, E. N., Kobosev, N. I., Wassiljew, S. S., *Phys. Chem. (USSR)* **10**, 543 (1937).
(29) Francis, G., *Handbuch der Physik* **22**, Part II, 53 (1956).
(30) Francis, G., "Ionization Phenomena in Gases," Butterworths, London, 1960.
(31) Haber, F., "Grundriss d. Techn. Elektrochemie," München, 1898.
(32) Hahn, V. A., Harley, L. S., Lurit, R. (in preparation).
(33) Hasted, J. B., "Physics of Atomic Collisions," Butterworth, London, 1964.
(34) Healey, R. H., Reed, J. W., "Behaviour of Slow Electrons in Gases," Amalgamated Wireless (Australia) Ltd., Sydney, Australia, 1941.
(35) Herzberg, G., "Spectra of Diatomic Molecules," Nostrand, New York, 1950.
(36) Hughes, L. A., Skellett, A. M., *Phys. Rev.* **30**, 11 (1927).
(37) Hunt, B. G., *J. Geophys. Res.* **71**, 1385 (1966).
(38) Jellinek, K., "Physikalische Chemie de. Gasreaktionen," Leipzig, 1913.
(39) Kaufman, F., *Ann. Geophys.* **20**, 106 (1964).
(40) Kaufman, F., ADVAN. CHEM. SER. **80**, 29 (1969).
(41) Kirkby, P. J., *Phil. Mag.* **7**, 223 (1904).
(42) *Ibid.*, **7**, 471 (1904).
(43) *Ibid.*, **9**, 171 (1905).
(44) *Ibid.*, **10**, 467 (1905).
(45) *Ibid.*, **13**, 289 (1907).
(46) Kirkby, P. J., *Proc. Roy. Soc. A* **85**, 151 (1910).
(47) Kobosev, N. I., Filanova, A. D., Nekrasov, L. I., Skorokhodov, I. U., *Russ. J. Phys. Chem.* (English Transl.) **35**, 503 (1961).
(48) Kondratieff, V. N., "Chemical Kinetics of Gas Reactions," Addison Wesley, Reading, Mass., 1964.

(49) Koenig, A., Wagner, O. H., *Z. Physik. Chem.* **144A,** 213 (1929).
(50) Kruithof, A. A., *Physica* **7,** 519 (1940).
(51) Kutszegi, K., Thesis, Univ. of Oklahoma (1967).
(52) Llewellyn-Jones, F., "The Glow Discharge," Methuen, London, 1966.
(53) Loeb, L. B., "Basic Processes of Gaseous Electronics," Univ. of Calif., 1955.
(54) Lunt, R., Thesis, Univ. of London (1936).
(55) Lunt, R., *Rept. Progr. Phys.* **8,** 338 (1941).
(56) Lunt, R., ADVAN. CHEM. SER. **21,** 286 (1959).
(57) Lunt, R., unpublished investigations (1966-67).
(58) Lunt, R., Corrigan, S. J. B., **AFCRL-62-1077, AD-298-703** (1962).
(59) Lunt, R., Corrigan, S. J. B., Mahon-Smith, D., Tuffy, E. T., "Atomic Collision Processes," p. 1145, M. R. C. McDowell, ed., Amsterdam, 1964.
(60) Lunt, R., Mahon-Smith, D., Tuffy, E. T., unpublished investigations (1962).
(61) Lunt, R., Meek, C. A., *Proc. Roy. Soc. A* **157,** 146 (1936).
(62) Lunt, R., Meek, C. A., Smith, E. C. W., *Proc. Roy. Soc. A* **158,** 729 (1937).
(63) Lunt, R., Pearson, T. G., Topley, B., *Trans. Faraday Soc.* **36,** 1087 (1940).
(64) Lunt, R., Swindell, G. S., *Trans. Faraday Soc.* **36,** 1072 (1940).
(65) Manley, T. C., *Welsbach Corp. Rept.*, Philadelphia, Pa. (1951).
(66) Massey, H. S. W., Burhop, E. H. S., "Electronic and Ionic Impact Phenomena," Clarendon Press, Oxford, 1952.
(67) McGrath, W. D., McGarvey, J. J., *Planetary Space Sci.* **15,** 427 (1967).
(68) Naccari, A., Ballati, M., *Atti. Ist. Venetzia* 4, 1 (1878).
(69) Oskam, H. J., *Philips Res. Rept.* **13,** 335 (1958).
(70) Peters, K., Küster, H., *Brennstoff-Chem.* **12,** 122 (1931).
(71) Peters, K., Pranschke, A., *Brennstoff-Chem.* **11,** 239 (1930).
(72) Peters, K., Wagner, O. H., *Z. Physik. Chem. A* **153,** 161 (1931).
(74) Poole, H. G., *Proc. Roy. Soc. A* **163,** 404 (1937).
(75) Rummel, Th., "Hochspannungs-Entladungschemie und Ihre Industrielle Anwendung," Verlag von R. Oldenbourg and Hanns Reich Verlag, München, 1951.
(76) Samson, J. A. R., Weissler, G. L., *Phys. Rev.* **137,** 381 (1965).
(77) Schofield, K., *Planetary Space Sci.* **15,** 643 (1967).
(78) Schram, H., Herman, L., Lunt, R., *J. Phys. Rad.* **16,** 59 (1957).
(79) Schüler, H., Degenhart, V., *Z. Naturforsch.* **8a,** 251 (1953).
(80) Shaw, T. M., *J. Chem. Phys.* **30,** 1366 (1959).
(81) Smith, C. R., Thesis, Univ. of London (1964).
(82) Spedding, P. L., Thornton, J. D., Charlton, W. D., ADVAN. CHEM. SER. **80,** 165 (1969).
(83) Steiner, W., *Trans. Faraday Soc.* **31,** 623 (1935).
(84) *Ibid.*, **31,** 962 (1935).
(85) Townsend, J. S. E., *Phil. Mag.* **1,** 198 (1901).
(86) *Ibid.*, **6,** 598 (1903).
(87) Townsend, J. S. E., "Electricity in Gases," Clarendon Press, Oxford, 1915.
(88) Townsend, J. S. E., "The Motion of Electrons in Gases," Clarendon Press, Oxford, 1925.
(89) Uyterhoeven, W., "Elektrische Gasentladungslampen," Springer, Berlin, 1938.
(90) Verweij, W., Thesis, Univ. of Utrecht (1960).
(91) Volman, D. H., *Advan. Photochem.* **1,** 44 (1963).

In Chemical Reactions in Electrical Discharges; Blaustein, B.;
Advances in Chemistry; American Chemical Society: Washington, DC, 1969.

(92) von Engel, A. H., Steenbeck, M., "Elektrische Gasentladungen," Vol. I, Springer, Berlin, 1932.
(93) *Ibid.*, Vol. II, 1934.
(94) von Siemens, W., *Pogg. Ann.* **102,** 66 (1857).
(95) Warburg, E., Sitzungsberichte der Königlich Preussischen Akademie der Wissenschaften zu Berlin, XXXIII, zweiter Halbband, 712 (1900).
(96) Warburg, E., *Ann. Physik.* **28,** 17 (1905).
(97) Warburg, E., *Jahrb. Radioakt.* **6,** 181 (1909).
(98) Warburg, E., Leithauser, G., *Ann. Physik.* **28,** 17 (1909).
(99) Westhaver, J. W., *J. Phys. Chem.* **37,** 897 (1933).
(100) Wiedemann, G., *Pogg. Ann.* **158,** 57 (1876).

RECEIVED November 28, 1967.

INDEX

In Chemical Reactions in Electrical Discharges; Blaustein, B.;
Advances in Chemistry; American Chemical Society: Washington, DC, 1969.

D

E

Publication Date: June 1, 1969 | doi: 10.1021/ba-1969-0080.ix001

In Chemical Reactions in Electrical Discharges; Blaustein, B.;
Advances in Chemistry; American Chemical Society: Washington, DC, 1969.

F

G

H

I

In Chemical Reactions in Electrical Discharges; Blaustein, B.;
Advances in Chemistry; American Chemical Society: Washington, DC, 1969.

K

L

M

N

O

P

Publication Date: June 1, 1969 | doi: 10.1021/ba-1969-0080.ix001

In Chemical Reactions in Electrical Discharges; Blaustein, B.;
Advances in Chemistry; American Chemical Society: Washington, DC, 1969.

Publication Date: June 1, 1969 | doi: 10.1021/ba-1969-0080.ix001

In Chemical Reactions in Electrical Discharges; Blaustein, B.;
Advances in Chemistry; American Chemical Society: Washington, DC, 1969.

V

W

X

Publication Date: June 1, 1969 | doi: 10.1021/ba-1969-0080.ix001